CONVECTIVE HEAT TRANSFER BETWEEN A BUNDLE OF CIRCULAR CYLINDERS AND A POWER LAW FLUID

Thesis Submitted in partial fulfillment of the requirements

for the degree of

Master of Technology

in

Chemical Engineering

By

Narasimha Mangadoddy

DEPARTMENT OF CHEMICAL ENGINEERING

INDIAN INSTITUTE OF TECHNOLOGY, KANPUR

Jan, 2002

CERTIFICATE

It is certified that the work contained in the thesis entitled **CONVECTIVE HEAT TRANSFER BETWEEN A BUNDLE OF CIRCULAR CYLENDERS AND A POWER LAW FLUID** by **Narasimha Mangadoddy, (Roll Number: Y010213),** has been carried out under our supervision and that this work has not been submitted elsewhere for a degree.

Dr. R. P. Chhabra,
Professor and Head,
Department of Chemical Engg.,
Indian Institute of Technology,
Kanpur. 208016.

Dr. V. Eswaran,
Professor,
Department of Mechanical Engg.,
Indian Institute of Technology,
Kanpur. 208016

Jan, 2002

Dedicated to

My teachers and parents

ACKNOWLEDGEMENT

I feel great pleasure in expressing deep sense of gratitude and sincere thanks to my thesis supervisors Dr. R.P. Chhabra and Dr.V.Eswaran for their discerning guidance, constructive advice and constant encouragement throughout the course of thesis work. On the personal front, they have been most liberal in all the aspects, very caring especially whenever, I was having some tough time during my stay at IITK and above all, had immense trust in us. They have taught us the values of Research and independent thinking. Working with them, has been the most exciting phase of my career. I have learnt a lot from them , which would be of great help in future.

I am highly thankful to Dr. Goutham Biswas (Mechanical Engg.) for teaching the basics on CFD (Course ME 640). Special thanks to Mr.Abir Benerji and Mr. Atul Sharma for their helping hands.

I am highly thankful to Mr.T.V. Malleswara Rao, Mr. Sunil Dhole, Miss. Rupali Shukhla for their timely help in the lab. Helping hands of Mr. Siva Ganesh, Mr.P.Srinivasa Rao, Mr.V.Vamsi, Mr. Rama Rao and Mr. V. Laxman, are greatly acknowledged. Thanks to my loving juniors Mr.Nanda Kishore, Mr. B.Ravi Kumar, Mr. Y. Laxman Rao, Mr. M.V.Pavan Kumar and Mr. Brijesh Paliwal for their unforgettable help.

I am fortunate enough to have good associations of my OUCTian friends such as Mr. T.V. Malleswara Rao, Mr. Sravan Kumar Reddy, Mr. Nanda Kishore, Mr. M.V. Pavan Kumar, Miss S.Sujatha and all of my seniors who have made my life easier at IITK.

Finally, I would like to express my heartfelt appreciation to my parents and my family members for their love and support throughout the years. Their blessings have always shown me the right path in the most critical moments of my life. A big thanks to my dear ones.

Narasimha Mangadoddy

Abstract

In this work, the two dimensional axisymmetric, incompressible steady flow and forced convective heat transfer of a non Newtonian power-law fluid across a bank of circular cylinders has been investigated numerically. The inter-cylinder interactions are modelled using the Happel's free surface model. The equations governing fluid flow and convective heat transfer are solved using the finite difference method. Simulations, to obtain the values of the local and average Nusselt number, were carried out over a wide range of physical and kinematic parameters as :$0.40 \le \varepsilon \le 0.60$, $0.5 \le n \le 1$, $1 \le Re \le 500$ and $1 \le Pr \le 500$ for both boundary conditions, i.e., the constant wall temperature and the constant heat flux at the surface of the cylinder. The angular variation of the local Nusselt number on the surface of the cylinder as well as isotherms are shown under varying conditions of porosity, power-law index, Prandtl and Reynolds number to gain useful insights in to the physics of the flow and heat transfer. The results obtained agree well with the results for limiting conditions available in the literature. Limited comparisons with experimental data are also presented.

CONTENTS

LIST OF FIGURES

\

List of Tables

Nomenclature

C_p	-heat capacity of the non-Newtonian fluid
h	-heat transfer coefficient
e	-porosity
i	-index used in θ-direction
j	-index used in r-direction
m(chapter2)	-Power law consistency index
m(chapter3)	-number of cells in θ-direction
n(chapter2)	-Power law index
n(chapter3)	-number of cells in r-direction
p	-pressure
Pr	-Prandtl number
q_w	-heat flux per unit length
r	-radius of cell(i,j)
r_o	-radius of the cylinder
r_s	-radius of the outer cylinder
Re	-Reynolds number based on the diameter for power law fluid
T	-temperature
T_i	-temperature at the surface of cylinder
T_0	-temperature of the fluid

U	-free stream velocity
v_r	-radial velocity
v_θ	-angular velocity

Greek letters

$\varepsilon_{i,j}$	-compnents of deformation tenson
ε	-porosity
Δ	-small change in variable
ψ	-stream function
η	-viscosity
κ	-thermal conductivity of the non-Newtonian fluid
ω	-vorticity
ρ	-density of the non-Newtonain fluid
τ	-shear stress
θ	-angle in radians
Π	-second invariant of rate of strain tensor

Superscripts

$'$	-dimensional variable
n	-time step

Chapter 1

INTRODUCTION AND SCOPE OF THE WORK

1.1 Introduction

The steady, axisymmetric and incompressible flow of non-Newtonian fluids normal to an array of cylinders and heat transfer from a collection of cylinders immersed in moving fluid streams represents an idealisation of many industrially important processes encountered in chemical, mineral and process engineering applications. Typical examples include flow in packed and fluidised beds employed for drying of fibrous materials (coconut shell, rice husk, etc.), in the shell of tubular heat exchangers, in aerosol and cigarette filters and during the transport of sap in plants and trees (Tripathi and Chhabra, 1996). Other examples are to be found in polymer process engineering applications such as the manufacture of fiber –reinforced composites entails the flow of a resin through a bed of fibers (Willians, Morris, &Ennis, 1974; Gupta, 2000). There is no question that the variable of central interest in all these applications is the frictional pressure loss and the rate of heat transfer for a given flow rate and the thermo – physical properties of the fluids. Over the years, several analytical treatments have been performed for the creeping flow of a incompressible Newtonian fluids normal to a bank of cylinders arranged in a variety of geometric configuration, eg., triangular, square, etc. For finite values of the Reynolds number of flow, the governing equations become non-linear and only limited numerical results are available for pressure drop and heat transfer in the intermediate Reynolds number region (Reynolds number up to 100). Limited comparisons suggest that the correspondence between predicted and experimental data is satisfactory for the

flow of Newtonian fluids (Skartsis, 1992). Most of the theoretical developments in this area have been summarised by Drummond and Tahir (1984) whereas the pertinent experimental studies have been reviewed by Skartsis *et al.* (1992).The corresponding studies on heat transfer have been dealt with by Zakuskas (1987) and by Krieth (2000).

The heat transfer from individual circular cylinders oriented normal to the flow has also been the subject of analytical investigations, but these studies have not been as intensive as those involving the flow phenomenon especially for non-Newtonian fluids. The recent work of Mandhani *et al.*(2002) on the heat transfer from an array of circular cylinders in cross flow was the recent numerically simulated in the range of Reynolds number (1-500) and prandtl numbers (0.7 and 7.70) for Newtonian fluids with constant thermo-physical properties, is first extensive study. And also recently Bailer *et al.* (1997) investigated numerically heat transfer and air flow around a single heated cylinder for Reynolds number of 200 and 2000. Similarly, Lange *et al.* (1998) have studied numerically the momentum and heat transfer characteristics of air flow around a single cylinder. Most of these studies have been reviewed recently by Ahmad (1996). From a theoretical standpoint, Sangani and Acrivos (1982) calculated the average temperature difference between the bulk fluid and the uniformly heated cylinders under conditions of small Reynolds number (Re=0) and Peclet numbers. Hsu (1964) analysed the phenomenon of heat transfer to liquid metals (high Prandtl number) in cross flow through rod bundles by invoking the inviscid flow approximation, as under these conditions, the momentum boundary layer would be much thinner than the thermal boundary layer.

In contrast to this, little is known about the flow of non-Newtonian fluids over tube bundles such as that encountered in the production of fiber

reinforced resins using an autoclave process, in heat exchangers employed to heat/cool non-Newtonian fluids in food and biotechnological applications and in enhanced oil recovery operations. Furthermore, this flow configuration has been used to capture some aspects of non-Newtonian fluid flow (such as extensional effects) in porous media. Despite such overwhelming theoretical and pragmatic significance, little research has been directed at the elucidation of the role of non-Newtonian characteristics in this flow configuration. Metzner *et al.* (1960) have investigated the heat transfer to non–Newtonian fluid systems passing though smooth round tubes under laminar conditions. Metzner and Reed (1955) have derived a generalized Reynolds number to correlate the friction factor for power law non–Newtonian fluids in cylindrical conduits. Metzner *et al.*(1957) presented theoretical analyses combined with an experimental study of the variables determining the heat transfer coefficient for laminar flow of non-Newtonian fluids in pipes. Shah *et al.* (1962) obtained analytical solutions and experimental data for free convection heat transfer from a single cylinder to a power law non-Newtonian fluid. The purpose of the work was to determine the feasibility of application of rheological equations of state derived from viscometer data to predict the fluid behaviour in laminar boundary- layer flows. Adams and Bell (1968) investigated the fluid friction and heat transfer for flow of CMC solutions across banks of tubes.

From a theoretical stand point, a mathematical description of inter-cylinder interaction is also required in addition to the usual mass, momentum and energy conservation equations. In the literature, there have been two approaches to model the strong particle interactions. The first approach attempts to solve the field equations for a preconceived geometrical configuration such as triangular or square array in-line or staggered configuration such as that employed by Sangani and Acrivos (1982). Notwithstanding the significance of detailed kinematics, it is generally believed that the macroscopic quantities such as drag on cylinders/ or

pressure drop in fibrous filters and the overall rate of heat transfer are relatively insensitive to the actual arrangement of cylinders and are primarily determined by the value of the porosity of the system and the kinematics conditions (namely, the Reynolds number Prandtl number, porosity, rheology of the flow). Thus the cell model approach which converts a difficult many-body problem into a conceptually much simpler one-body equivalent thereby making it more attractive both analytically as well as numerically affords a reasonable analysis of such extremely complicated flows. This approach will be used in this work to study heat transfer characteristics between a tube bundle and a fluid stream for non-Newtonain fluids.

1.2 Scope of the work

This thesis sets out to solve the mass, momentum and energy equations for the incompressible steady flow and energy equation of non-Newtonian fluids in a collection of cylinders via the so called free surface model. In particular the equations of continuity and momentum together with appropriate boundary conditions have been solved numerically to obtain the detailed kinematics of the flows. In this study, the equation of energy for the Reynolds number (1-500) and Prandtl numbers (1-500) for non-Newtonian fluids with constant thermo physical properties, have been solved numerically. Extensive results on detailed temperature profiles as well as on the local Nusselt number are obtained over wide ranges of physical (Prandtl number, porosity of arrays) and kinematic (Reynolds number) conditions. Furthermore, the role of the usual two types of thermal boundary conditions on the cylinder, constant temperature and constant heat flux, has been elucidated in determining the values of the Nusselt number.

Chapter 2

PROBLEM STATEMENT AND GOVERNING EQUATIONS

In this chapter, the flow problem investigated herein is outlined briefly, followed by the model development. This then leads on to the development of the field equations,namely, the momentum,energy and continuity equations together with the specification of physically possible boundary conditions employed in this study.

2.1 Problem Statement

The steady incompressible flow of a power law fluid past an array of long circular cylinders, which are oriented normal to the direction of flow, as shown schematically in Fig (2.1a) is considered. The rheological equation of state for a fluid obeying power law behavior is given by

$$\eta' = m(2\Pi_\varepsilon)^{(n-1)/2} \tag{2.1}$$

where m is the power law consistency index, n is the power law index and Π_ε is the second invariant of the rate of strain tensor, ε'_{ij}.

In order to complete the problem formulation, it is essential to have a mathematical model of cylinder-cylinder interactions. The spherical and cylindrical free cell models have been successful in predicting the macroscopic flow phenomena in particulate systems(Tripathi and Chhabra,1992). The two most extensively used models are the free surface model (Happel, 1958) and the Kuwabara model (1959).

In this study, the Happel's free surface cylindrical cell model is employed to study the flow behavior around a collection of cylinders. The free surface model consists of a cylinder of radius r_0 surrounded by an imaginary cylindrical envelope of radius r_∞ such that the porosity of each cell is equal to the porosity of the array of cylinders. The cell boundary at r_∞ is frictionless, thereby implying the non-interacting nature of cells. In the Happel free surface model, a zero shear condition is imposed on the outer boundary. Depending on the distance r_∞, one can simulate different porosity conditions which defined by $\varepsilon = 1 - r_\infty^{-2}$. For the limiting case of a single cylinder in the fluid flow, porosity will become 1.

A cylinderical co-ordinate system is chosen for convenience. The angle θ is measured from the front stagnation point of the cylinder as shown in Figure 2.1(b), and r_0 is the radius of inner cylinder and r_∞ that of the outer imaginary cylinder. The Fluid is approaching with a uniform velocity of U and temperature T_0. The components of the velocity in r- and θ- directions are v_r' and v_θ' respectively. It is assumed that the flow is two dimensional and steady. The flow variables do not depend upon the coordinate z.

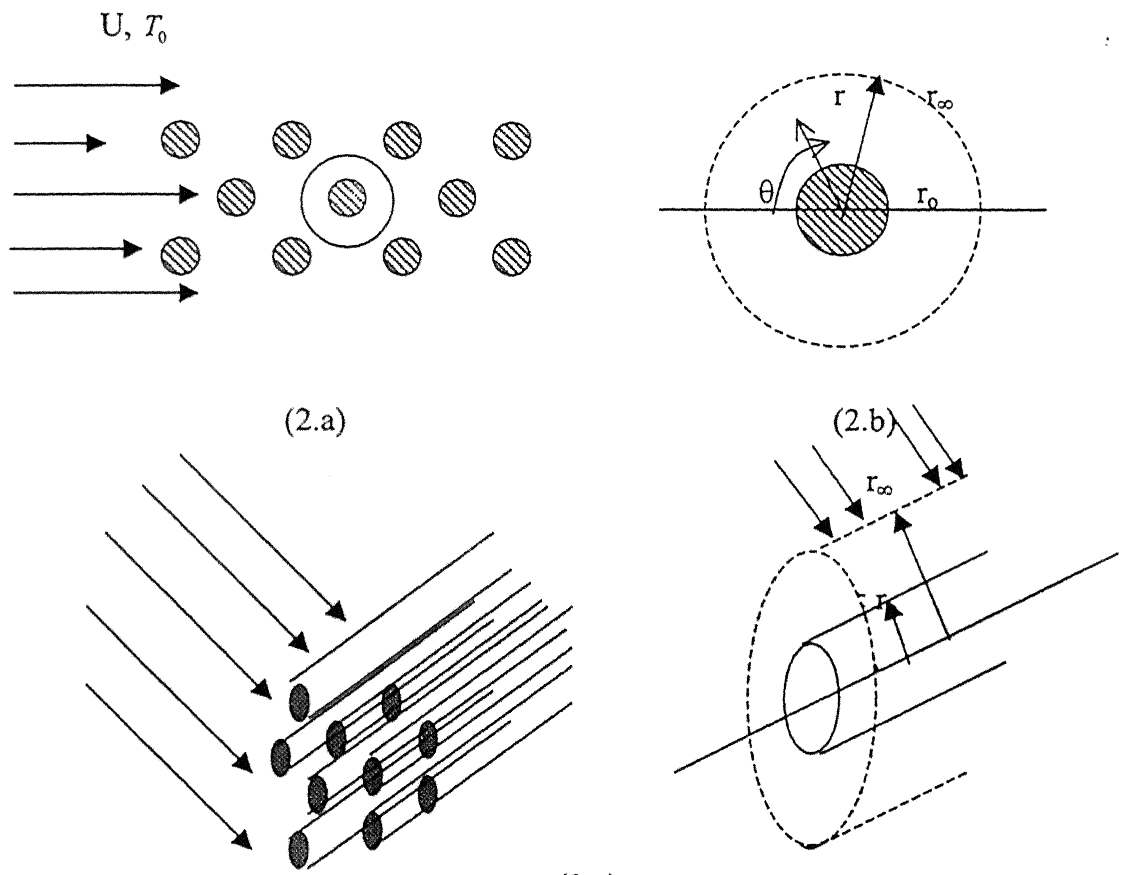

(2.c)

Figure 2.1 Array of infinite long cylinders. b.Cell model idealization. c.Three dimensional view

2.2 Governing Equations for fluid flow

With the above assumptions, the governing equations, namely the equations of continuity , motion and energy in cylindrical coordinates can be written as;

The velocity components in the r, θ, z directions are

$$v_r'=v_r'(r',\theta) \quad v_\theta'=v_\theta'(r',\theta) \quad v_z'=0 \tag{2.2}$$

Similarly, the temperature can also be expressed as $T_{\theta}^{'}(r',\theta)$.

Under these conditions, the equation of continuity for an incompressible fluid is given as ;

$$\frac{1}{r'}\frac{\partial(rv_r')}{\partial r}+\frac{1}{r'}\frac{\partial v_\theta'}{\partial\theta}=0 \tag{2.3}$$

and the components of the equations of motion are written as ;

r'-component :

$$\rho\left(\frac{\partial v_r'}{\partial t'}+\frac{1}{r'}\frac{\partial(rv_r'^2)}{\partial r'}+\frac{1}{r'}\frac{\partial(v'_r v_\theta')}{\partial\theta}-\frac{v'^2_\theta}{r'}\right)=-\frac{\partial p'}{\partial r'}+\left(\frac{1}{r'}\frac{\partial(r'\tau'_{rr})}{\partial r'}+\frac{1}{r'}\frac{\partial\tau'_{r\theta}}{\partial\theta}-\frac{\tau'_{\theta\theta}}{r'}\right) \tag{2.4}$$

θ-component :

$$\rho\left(\frac{\partial v'_\theta}{\partial t'}+\frac{1}{r'}\frac{\partial(v_\theta^2)}{\partial\theta}+\frac{1}{r'}\frac{\partial(rv'_r v'_\theta)}{\partial r'}+\frac{v'_r v'_\theta}{r'}\right)=\frac{1}{r'}\frac{\partial p'}{\partial\theta}+\left(\frac{1}{r'^2}\frac{\partial(r'^2\tau_{r\theta})}{\partial r'}+\frac{1}{r'}\frac{\partial\tau'_{\theta\theta}}{\partial\theta}\right) \tag{2.5}$$

where $\tau'_{ij}=2\,\eta'\varepsilon'_{ij}\quad(i,j=\theta,r)$ (2.6)

where η' is the (non-Newtonian) viscosity

$$\eta'=\eta'(\Pi'_\varepsilon)$$

where $\Pi'_\varepsilon=\varepsilon'^2_{rr}+\varepsilon'^2_{\theta\theta}+\varepsilon'^2_{zz}+2(\varepsilon'^2_{r\theta}+\varepsilon'^2_{\theta z}+\varepsilon'^2_{rz})$

In the above expressions $\varepsilon_{i,j}$ is the rate of strain tensor which is related to the velocity components by

$$\varepsilon'_{rr} = \frac{\partial v_r'}{\partial r} \tag{2.7}$$

$$\varepsilon'_{\theta\theta} = \frac{1}{r'}\frac{\partial v'_\theta}{\partial \theta} + \frac{v_r'}{r'} \tag{2.8}$$

$$\varepsilon'_{r\theta} = \varepsilon'_{\theta r} = \frac{1}{2}\left[r'\frac{\partial}{\partial r}\left(\frac{v'_\theta}{r'}\right) + \frac{1}{r'}\frac{\partial v_r'}{\partial \theta} \right] \tag{2.9}$$

$$\varepsilon'_{zz} = \varepsilon'_{zr} = \varepsilon'_{rz} = \varepsilon'_{\theta z} = \varepsilon'_{z\theta} = 0$$

and for a power law fluid equation (see 2.1) is

$$\eta' \quad = \quad m(2\Pi'_\varepsilon)^{(n-1)/2}$$

Now all the quantities in the above expressions are rewritten in their dimensionless form by using the following transformations.

$$v_r = \frac{v_r'}{U} \qquad v_\theta = \frac{v_\theta'}{U} \qquad r = \frac{r'}{r_o} \qquad t = \frac{t'}{t_0}$$

$$p = \frac{p - p'}{1/2\rho U^2} \qquad \eta = \frac{\eta'}{\eta_o} \qquad \tau = \frac{\tau'}{\eta'\frac{U}{r_o}} \qquad \Pi_\varepsilon = \frac{\Pi_\varepsilon}{\left[\frac{U}{r_o}\right]^2} \tag{2.10}$$

$$\text{where } \eta_o = m\left[\frac{U}{r_o}\right]^{n-1}$$

Then, the continuity equation will remain unchanged and the equations from (2.4) and (2.5) remain unchanged in their form, and become

$$\frac{1}{r}\frac{\partial(rv_r)}{\partial r}+\frac{1}{r}\frac{\partial v_\theta}{\partial \theta}=0 \tag{2.11}$$

$$\left(\frac{\partial v_r}{\partial t}+\frac{1}{r}\frac{\partial(rv_r^2)}{\partial r}+\frac{1}{r}\frac{\partial(v_rv_\theta)}{\partial\theta}-\frac{v_\theta^2}{r}\right)=-\frac{1}{2}\frac{\partial p}{\partial r}+\frac{2^n}{\mathrm{Re}}\left(\frac{1}{r}\frac{\partial(r\tau_{rr})}{\partial r}+\frac{1}{r}\frac{\partial\tau_{r\theta}}{\partial\theta}-\frac{\tau_{\theta\theta}}{r}\right) \tag{2.12}$$

$$\left(\frac{\partial v_\theta}{\partial t}+\frac{1}{r}\frac{\partial(v_\theta^2)}{\partial\theta}+\frac{1}{r}\frac{\partial(rv_rv_\theta)}{\partial r}+\frac{v_rv_\theta}{r}\right)=-\frac{1}{2}\frac{1}{r}\frac{\partial p}{\partial\theta}+\frac{2^n}{\mathrm{Re}}\left(\frac{1}{r^2}\frac{\partial(r^2\tau_{r\theta})}{\partial r}+\frac{1}{r}\frac{\partial\tau_{\theta\theta}}{\partial\theta}\right) \tag{2.13}$$

Substitution of the equations (2.6) through (2.9) into equations (2.12) and (2.13) yields

$$\left(\frac{\partial v_r}{\partial t'}+\frac{1}{r}\frac{\partial(rv_r^2)}{\partial r}+\frac{1}{r}\frac{\partial(v_rv_\theta)}{\partial\theta}-\frac{v_\theta^2}{r}\right)=-\frac{1}{2}\frac{\partial p}{\partial r}+\frac{2^n\eta}{\mathrm{Re}}\left(\frac{\partial}{\partial r}\left(\frac{1}{r}\frac{\partial(rv_r)}{\partial r}\right)+\frac{1}{r^2}\frac{\partial^2 v_r}{\partial\theta^2}-\frac{2}{r^2}\frac{\partial v_\theta}{\partial\theta}\right)+\frac{2^{(n+1)}}{\mathrm{Re}}\left[\varepsilon_{rr}\frac{\partial\eta}{\partial r}+\frac{\varepsilon_{r\theta}}{r}\frac{\partial\eta}{\partial\theta}\right] \tag{2.14}$$

$$\left(\frac{\partial v_\theta}{\partial t}+\frac{1}{r}\frac{\partial(v_\theta^2)}{\partial\theta}+\frac{1}{r}\frac{\partial(rv_rv_\theta)}{\partial r}+\frac{v_rv_\theta}{r}\right)=-\frac{1}{2}\frac{1}{r}\frac{\partial p}{\partial\theta}+\frac{2^n\eta}{\mathrm{Re}}\left(\frac{\partial}{\partial r}\left(\frac{1}{r}\frac{\partial(rv\theta)}{\partial r}\right)+\frac{1}{r^2}\frac{\partial^2 v\theta}{\partial\theta^2}+\frac{2}{r^2}\frac{\partial v_r}{\partial\theta}\right)+\frac{2^{(n+1)}}{\mathrm{Re}}\left[\varepsilon_{r\theta}\frac{\partial\eta}{\partial r}+\frac{\varepsilon_{\theta\theta}}{r}\frac{\partial\eta}{\partial\theta}\right] \tag{2.15}$$

where the Reynolds number, $\mathrm{Re}=\dfrac{\rho U^{(2-n)}(2r_o)^n}{m}$ (2.16)

Equation 2.12 and 2.13 can be solved numerically to obtain the velocity and pressure field.

Furthermore, it is customary to introduce the corresponding vorticity function

as;

$$\omega = \frac{\partial v_\theta}{\partial r} - \frac{1}{r}\frac{\partial v_r}{\partial \theta} + \frac{v_\theta}{r} \tag{2.17}$$

the above equation become

$$\frac{1}{2}\frac{\partial p}{\partial r} = -\frac{\partial}{\partial r}\left(\frac{v_r^2 + v_\theta^2}{2}\right) + v_\theta \omega - \frac{2^n \eta}{\mathrm{Re}}\frac{1}{r}\frac{\partial \omega}{\partial \theta} + \frac{2^{n+1}}{\mathrm{Re}}\left(\varepsilon_{rr}\frac{\partial \eta}{\partial r} + \frac{\varepsilon_{r\theta}}{r}\frac{\partial \eta}{\partial \theta}\right) \tag{2.18}$$

$$\frac{1}{2r}\frac{\partial p}{\partial \theta} = -\frac{1}{r}\frac{\partial}{\partial \theta}\left(\frac{v_r^2 + v_\theta^2}{2}\right) - v_r \omega + \frac{2^n \eta}{\mathrm{Re}}\frac{\partial \omega}{\partial r} + \frac{2^{n+1}}{\mathrm{Re}}\left(\varepsilon_{r\theta}\frac{\partial \eta}{\partial r} + \frac{\varepsilon_{\theta\theta}}{r}\frac{\partial \eta}{\partial \theta}\right) \tag{2.19}$$

These equations can be used to specify the boundary conditions for the pressure.

2.3 Boundary Conditions

In the Happel's free surface model, the fluid is assumed to be stationary and the cylinder as moving. The no-slip boundary condition is employed on the cylinder surface(at r =1). For the cell surface(r = r_∞), the outer radial velocity and the shear stress is taken as zero.

In Kuwabara's model, a zero vorticity is imposed on the outer surface instead of zero shear stress.Thus the boundary conditions are,

at r=1 $\quad v_r$= - cosθ $\quad v_\theta$=sinθ (2.20)

at r=r_∞ $\quad v_r$=0 $\quad \tau_{r\theta}$=0 in Happel Model, $\omega_{r\theta}$=0 in Kuwabara Model. (2.21)

By a Gallilean transformation, we can convert this system to one where the cylinder is stationary and the fluid is moving, i.e.,

at $r=1$ $\quad v_r$=0 $\quad v_\theta$=0 (2.22)

at $r=r_\infty$ $\quad v_r$=-cosθ $\quad \tau_{r\theta}$=0 in Happel Model, $\omega_{r\theta}$=0 in Kuwabara

Model. (2.23)

These latter boundary conditions are used in the flow computations in this work.

Fig 2.2 Cell model

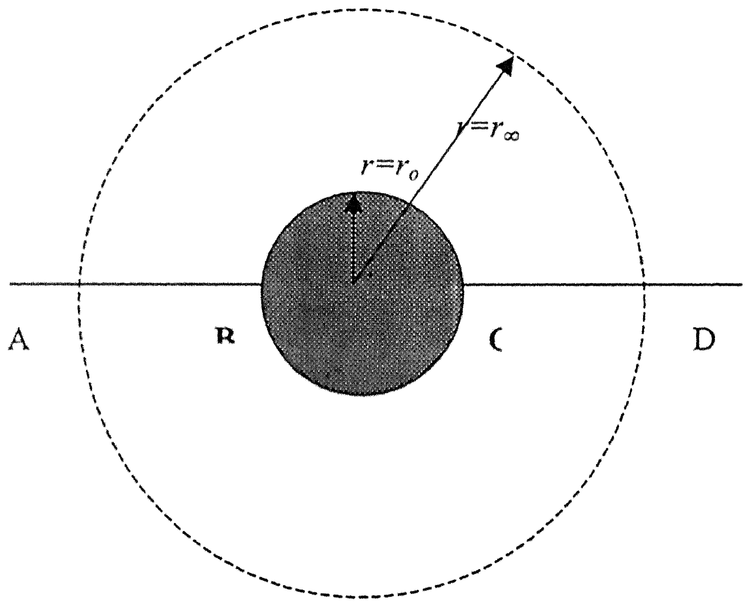

2.3.1 Cell model and boundary conditions

Boundary	Boundary conditions
AB	$v_\theta = \Psi = 0,\ \frac{\partial v_r}{\partial \theta} = 0$
BC	$v_r = v_\theta = \Psi = 0$
CD	$v_\theta = \Psi = 0,\ \frac{\partial v_r}{\partial \theta} = 0$
AD	v_r=-cosθ, Ψ=-rsinθ, $\tau_{r\theta}$ =0 (Free surface cell model) and , $\omega_{r\theta}$=0(Kuwabara model)

IIn addition to the boundary conditions out lined in eq. (2.20) & (2.21), the condition of axisymmetry was used at $\theta = 0$ and $\theta = \pi$ planes.

2.4 Energy equation for Heat Transfer

the equation of energy in terms of the transport properties, for non-Newtonian fluids of constant $\rho, C_p and\ \kappa$, and neglecting the viscous dissipation term, can be written as;

$$\rho C_p\left(\frac{\partial T'}{\partial t'}+\frac{1}{r'}\frac{\partial(rv_r'\ T')}{\partial r'}+\frac{1}{r'}\frac{\partial(\ v_\theta' T')}{\partial \theta}\right)=\kappa\left(\frac{1}{r'}\frac{\partial}{\partial r'}\left(r'\frac{\partial T'}{\partial r'}\right)+\frac{1}{r'^2}\frac{\partial^2 T'}{\partial \theta^2}\right) \quad (2.24)$$

where ρ, C_p and κ are the density, heat capacity and thermal conductivity of the fluid respectively which are assumed to be independent of temperature.

Now all the quantities in the above expressions are rewritten in their dimensionless form by using the transformations as outlined in eq.(2.10) (not for temperature).

In heat transfer applications, it is a common practice to employ two different type of thermal boundary conditions, namely, a constant temperature (T_i) or a constant heat flux(q_w per unit length) at the surface of solid cylinder at r = 1.

Thus, depending upon the type of boundary condition, the non-dimensional temperature can be defined accordingly. Thus ,for the case of a constant temperature at r = 1, one can introduce the following dimensionless

temperature T_i:

$$T = \frac{T^1 - T_0}{T_i - T_0} \tag{2.25}$$

or for the case of a constant heat flux at r = 1,the correspondingly it is given by:

$$T = \frac{T^1 - T_0}{\frac{q_w r_0}{\kappa}} \tag{2.26}$$

Then the energy equation in non-dimensional form becomes

$$\left(\frac{\partial T}{\partial t} + \frac{1}{r}\frac{\partial(rv_r T)}{\partial r} + \frac{1}{r}\frac{\partial(v_\theta T)}{\partial \theta}\right) = \frac{\kappa}{\rho C_p U r_0}\left(\frac{1}{r}\frac{\partial}{\partial r}\left(r\frac{\partial T}{\partial r}\right) + \frac{1}{r^2}\frac{\partial^2 T}{\partial \theta^2}\right) \tag{2.27}$$

where the T_i is the inner surface temperature of the cylinder T_0 is the fluid temperature .

By defining the Reynolds number, $\mathrm{Re} = \dfrac{\rho U^{(2-n)}(2r_o)^n}{m}$ (2.28)

Prandtl number, $\Pr = \dfrac{C_p m}{\kappa}\left(\dfrac{U}{2r_0}\right)^{n-1}$ (2.29)

We can write $\dfrac{\kappa}{\rho C_p U r_0} = \dfrac{2}{\mathrm{Re}\Pr}$ (2.30)

The ultimate energy equation in non-dimensional form becomes

$$\left(\frac{\partial T}{\partial t} + \frac{1}{r}\frac{\partial(rv_r T)}{\partial r} + \frac{1}{r}\frac{\partial(v_\theta T)}{\partial \theta}\right) = \frac{2}{\mathrm{Re}\Pr}\left(\frac{1}{r}\frac{\partial}{\partial r}\left(r\frac{\partial T}{\partial r}\right) + \frac{1}{r^2}\frac{\partial^2 T}{\partial \theta^2}\right) \tag{2.31}$$

The non-dimensionalised energy equation does not depend upon the way the temperature is non-dimensionalised in these two cases. The only difference is that the boundary condition is changed at the cylinder surface i.e. at r = 1.

2.5 Boundary conditions for energy equation

As mentioned previously, two cases are considered here. For the case of uniform temperature at the solid cylinder :

$$\text{at } r = 1;\ T = 1 \tag{2.32}$$

$$\text{at } r = r_\infty;\ T = 0 \tag{2.33}$$

on the otherhand, when a constant heat flux is maintained at inner solid cylinder:

$$\text{at } r = 1;\ \frac{\partial T}{\partial r} = -1 \tag{2.34}$$

$$\text{at } r = r_\infty;\ T = 0 \tag{2.35}$$

Boundary	Boundary condition
AB	$\frac{\partial T}{\partial \theta} = 0$
BC	$\frac{\partial T}{\partial r} = -1$ (for constant heat flux) T = -1 (for constant inner cylinder temperature)
CD	$\frac{\partial T}{\partial \theta} = 0$
AD	T = 0

Table 2.2: Boundary conditions applied to figure 2.2 for energy equation

2.6 Calculation of Nusselt number

2.6.1 Constant surface temperature condion

At the surface of the solid cylinder (r = 1) equating the rate of heat transfer

$$q_{surface} = -\kappa \left[\frac{\partial T^1}{\partial r'} \right]_{r'=r_0} = h(T_i - T_0) \tag{2.36}$$

Introducing dimensionless variables,

$$-\kappa\frac{(T_i - T_0)}{r_0}\left[\frac{\partial T}{\partial r}\right]_{r=1} = h(T_i - T_0) \qquad (2.37)$$

$$Nu_\theta = \frac{h(2r_0)}{\kappa} = -2\left[\frac{\partial T}{\partial r}\right]_{r=1} \qquad (2.38)$$

2.6.2 Constant heat flux condition

Again, one can equate the rate of heat transfer at the surface of the solid cylinder (r =1),as :

$$q_w = -\kappa\left[\frac{\partial T'}{\partial r'}\right]_{r'=r_0} = h(T'|_{r=r_0} - T_0) \quad \text{(by defination)} \qquad (2.39)$$

Now introducing dimentionless variables,

$$-\kappa\frac{\frac{q_w r_0}{\kappa}}{r_0}\frac{\partial T}{\partial r}\Big|_{r=1} = q_w = hT\big|_{r=1}\frac{q_w r_0}{\kappa} \qquad (2.40)$$

above eq.(2.39) gives

$$\frac{\partial T}{\partial r}\Big|_{r=1} = -1 \qquad (2.41)$$

equating the first and third term of eq.(2.39) gives

$$-\frac{\kappa}{r_0}\frac{\partial T}{\partial r}\Big|_{r=1} = hT\big|_{r=1} \qquad (2.42)$$

Putting the dimensionless temperature gradient from eq.(2.40),(2.41) gives,

$$\frac{\kappa}{r_0} = hT\big|_{r=1} \qquad (2.43)$$

or $$Nu_\theta = \frac{h(2r_0)}{\kappa} = \frac{2}{T}\bigg|_{r=1} \tag{2.44}$$

The Nusselt number so evaluated relate to a fixed value of θ ,and it is useful to Define an average Nusselt number Nu defined as follows:

$$Nu_\theta = \frac{1}{\pi}\int_0^\pi Nu_\theta d\theta \tag{2.45}$$

Thus,equations (2.14),(2.15) and (2.31) provide the theoretical framework for calculating the complete flow and temperature fields. These equations subjected to the boundary conditions have been solved numerically using the finite difference method.These results can be post processed to infer the values of the Nusselt number as a function of the Reynolds number and Prandtl number as well as porosity for the two types of thermal boundary conditions used here in.

Chapter 3

NUMERICAL FORMULATION AND SOLUTION PROCEDURE

The energy equation is solved using the finite difference technique.The equations governing fluid flow are solved using the finite difference method used in a previous work by Shibu (2000) and Shibu *et al.* (2001) and these solutions are used as input to the energy equation. The major difficulty encountered in the solving the Navier-Stokes equation, is due to the non-availability of any obvious equation which can be directly solved for the pressure. Therefore, the pressure field is found indirectly by finding a velocity field that satisfies continuity, along with the Navier-Stokes equations. This involves iterations of the pressure and velocity fields. Such iterations have a very poor convergence on a normal grid. As a remedy, usually a so-called "staggered grid" is used for solving the equations. Therefore the energy equation is also solved using a staggered grid in this work.

In the previous work, the SMAC-Implicit scheme was employed for solving the Navier-Stokes equations. This method is a pressure corrector method, which then uses a Poisson equation for the pressure corrections to obtain correction of the velocity fields, and the "pseudo-pressure" field which enforces the continuity equation. The pseudo-pressure, however, does not satisfy the correct pressure equation which has to be obtained by solving another Poisson equation with the correct boundary conditions. In this work, the implicit scheme with Gauss-Seidel iterations and under-relaxation is used for the solution of energy equation to obtain the temperature field. Although only the steady state solutions are required, we use transient equations to time-step from arbitrary initial conditions to the steady state.

3.1 Staggered grid

In a staggered grid arrangement the computational domain is divided into number of cells as shown in Fig 3.1. The locations of scalars (pressure, viscosity and temperature) are at the centre of the cells, while those of vectors(velocities in r- and θ -directions) are at the centre of cell faces to which they are normal. In such an arrangement, pressure difference between two adjacent cells directly affect the FD equations for the velocity components located at the interface of these cells. Thus the pressure and velocity corrections are directly related to each other, and the pressure-velocity iterations converge quickly.

Cells are labeled with index (i,j) which denote the cell number as counted in θ -and r-directions, respectively; thus T_{ij} is the temperature at the centre of cell (i,j), while $v_r(i,j+1/2)$ is the radial velocity at the centre of the face between cell (i,j) and cell (i,j+1), and so on. Similarly $v_\theta(i+1/2,j)$ is the θ - component of velocity at the centre of face between cell (i,j) and cell (i+1,j), and so on. Because of the staggered grid arrangements, the velocities are not defined at the cell centers, but whenever required, they are found by simple interpolations. Boundary conditions are imposed by setting appropriate velocities in the fictitious cells surrounding the physical domain (see Figure 3.2). In other words, the fictitious cell velocities are expressed in terms of boundary cell velocities for the implementation of boundary conditions.

In Fig 3.2 B'C'F'G' shows the actual physical domain. The domain ADEH is the computational domain. Fictitious cells are shown by dotted lines. Cells CDC'D', EFE'F', ABA'B' and GHG'H' are numbered as (1,1), (m,1), (1,n) and (m,n) respectively, where m and n are the number of cells in θ -and r- directions respectively including the fictitious cells.

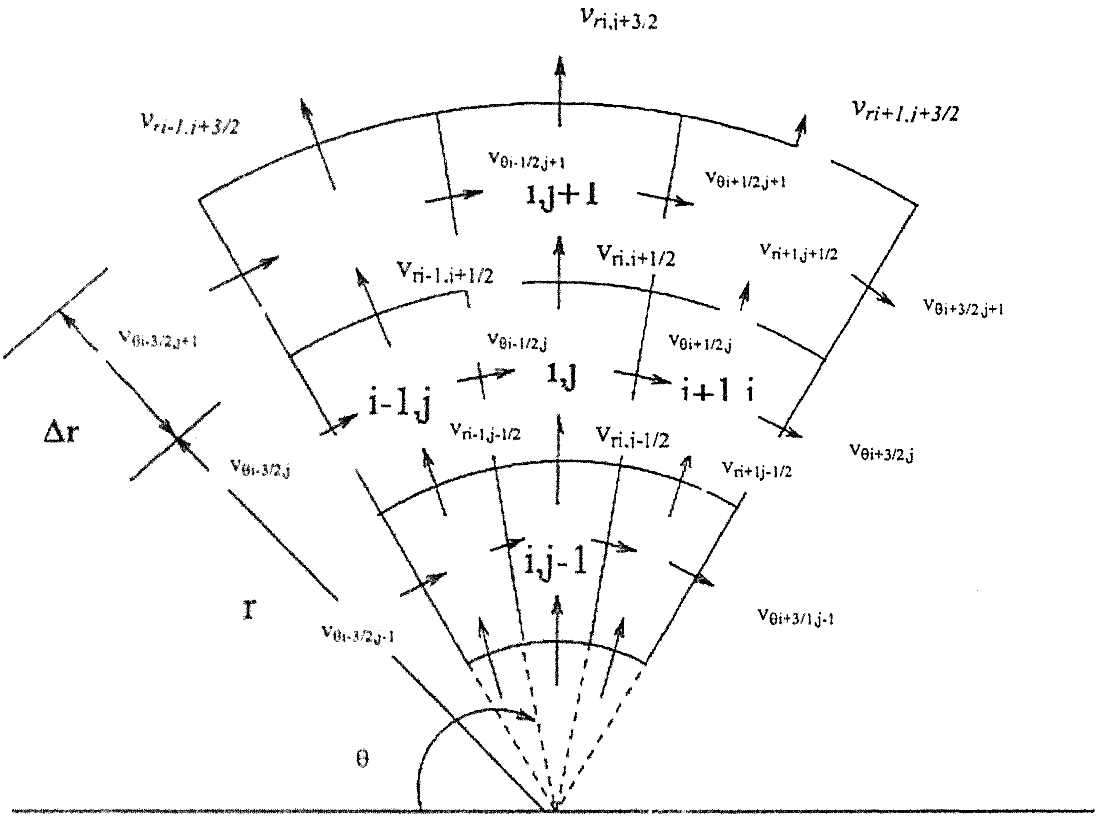

Fig 3.1 Two Dimensional Staggered Grid showing the locations of descretised variables.

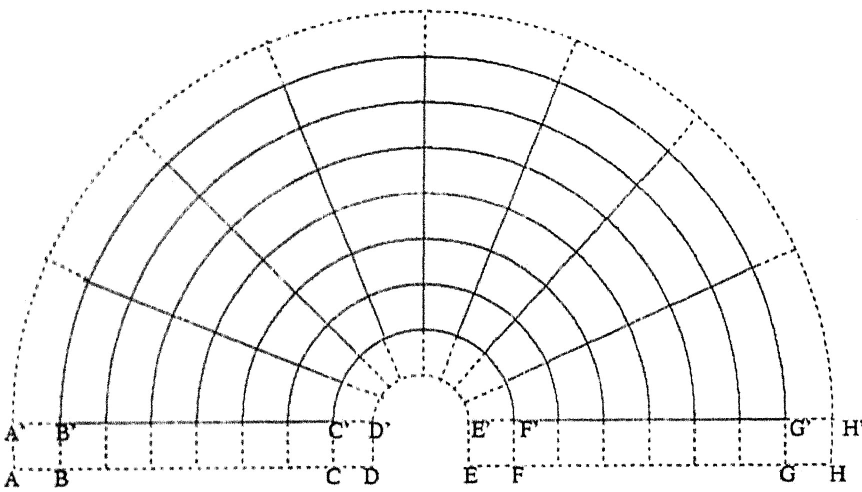

Fig 3.2 Grid Arrangement

3.2 The Energy equation

Consider the equation (2.31) governing the flow of heat for a power-law fluid Formulated in chapter 2, rewritten here

$$\left(\frac{\partial T}{\partial t}+\frac{1}{r}\frac{\partial(rv_rT)}{\partial r}+\frac{1}{r}\frac{\partial(v_\theta T)}{\partial \theta}\right)=\frac{2}{\mathrm{Re}\,\mathrm{Pr}}\left(\frac{1}{r}\frac{\partial}{\partial r}\left(r\frac{\partial T}{\partial r}\right)+\frac{1}{r^2}\frac{\partial^2 T}{\partial \theta^2}\right) \tag{3.1}$$

where Re, Pr are the Reynolds number and Prandtl number, respectively, and v_r, v_θ ,T stand for the non – dimensional velocities in r – and θ - directions, and temperature, respectively.

Eq. (3.1) can be slightly rearranged as :

$$\left(\frac{\partial T}{\partial t}+\frac{1}{r}\frac{\partial(rv_rT)}{\partial r}+\frac{1}{r}\frac{\partial(v_\theta T)}{\partial \theta}\right)=\frac{2}{\mathrm{Re}\,\mathrm{Pr}}\left(\left(\frac{\partial^2 T}{\partial r^2}+\frac{1}{r}\frac{\partial T}{\partial r}\right)+\frac{1}{r^2}\frac{\partial^2 T}{\partial \theta^2}\right) \tag{3.2}$$

The above equation represents the equation of energy, in cylindrical co-ordinates. This equation consists of a transient term, convection terms and diffusion terms, whose discretisations are described in the ensuing sections.

3.3 Discretisation of derivatives

The center of discretisation for energy equation is (i, j). The discretisation of the derivatives of eq. (3.2) is carried out as follows,

- ***Discretisation of the transient term***

$$\left.\frac{\partial T}{\partial t}\right|_{i,j}=\left[\frac{T_{i,j}^{n+1}-T_{i,j}^{n}}{\Delta t}\right]$$

- ***Discretisation of convection term containing*** v_r

$$\left.\frac{1}{r}\frac{\partial(rv_rT)}{\partial r}\right|_{i,j}=\frac{1}{r_j}\left[\frac{\left\{r_{j+\frac{1}{2}}v_{ri,j+\frac{1}{2}}\left(\frac{T_{i,j+1}^{n+1}+T_{i,j}^{n+1}}{2}\right)-r_{j-\frac{1}{2}}v_{ri,j-\frac{1}{2}}\left(\frac{T_{i,j}^{n+1}+T_{i,j-1}^{n+1}}{2}\right)\right\}}{\Delta r}\right]$$

- ***Discretisation of convection term containing*** v_θ

$$\left.\frac{1}{r}\frac{\partial(v_\theta T)}{\partial\theta}\right|_{i,j}=\frac{1}{r_j}\left[\frac{\left\{v_{\theta i+\frac{1}{2},j}\left(\frac{T_{i+1,j}^{n+1}+T_{i,j}^{n+1}}{2}\right)-v_{\theta i-\frac{1}{2},j}\left(\frac{T_{i,j}^{n+1}+T_{i-1,j}^{n+1}}{2}\right)\right\}}{\Delta\theta}\right]$$

- ***Discretisation of second order derivative of temperature with respect to radius in diffusion term***

$$\left.\frac{\partial^2 T}{\partial r^2}\right|_{i,j}=\left[\frac{T_{i,j+1}^{n+1}-2T_{i,j}^{n+1}+T_{i,j-1}^{n+1}}{\Delta r^2}\right]$$

- ***Discretisation of first order derivative of temperature with respect to radius in diffusion term***

$$\left.\frac{1}{r}\frac{\partial T}{\partial r}\right|_{i,j}=\frac{1}{r_j}\left[\frac{T_{i,j+1}^{n+1}-T_{i,j-1}^{n+1}}{2\Delta r}\right]$$

- ***Discretisation of second order derivative of temperature with respect to*** θ ***in diffusion term***

$$\left.\frac{1}{r^2}\frac{\partial^2 T}{\partial\theta^2}\right|_{i,j}=\frac{1}{r_j^2}\left[\frac{T_{i+1,j}^{n+1}-2T_{i,j}^{n+1}+T_{i-1,j}^{n+1}}{\Delta\theta^2}\right]$$

3.3.1 Discretisation of Boundary conditions

The fictitious cells shown in Figure (3.2) facilitate the discretisation of boundary conditions.

(a) For the constant cylinder surface temperature case

Consider cells ... (i −1,2), (i,2), (i+1,2)... as cells on the inner boundary C'F'. So cells ...(i-1,1), (i,1), (i+1,1)... are fictitious cells along D'E'. So when we apply boundary condition for T at inner surface of the cylinder it is implemented as follows :

$$T_{i,1} = 2(T_{surface}) - T_{i,2} \qquad \text{(for } i = 2 \text{ to m-1)}$$

Similarly, consider cells ... (i - 1, n - 1), (i, n-1), (i+1 ,n-1) ... as cells on the outer boundary B'G'. So cells ... (i-1,n), (i, n), (i+1,n) ... are fictitious cells along A'H'. So when we apply the zero-derivative boundary condition for T at the outer boundary, it is as follows :

$$T_{i,n} = -T_{i,n-1} \qquad \text{(for } i=2 \text{ to m-1)}$$

Along B'C' we have the discretisation of boundary condition as follows,

$$T_{1,j} = T_{2,j}$$

similarly along F'G' we have the discretisation of boundary condition as follows,

$$T_{m,j} = T_{m-1,j}$$

(b) For the constant heat flux surface (r = 1)

Here only the boundary condition at r = 1 is different from the previous case.

Consider cells ... (i-1, 2), (i, 2), (i-1, 2)... as cells on the inner boundary C'F'. So cells ...(i-1, 1), (i, 1), (i+1, 1) ... are fictitious cells along D'E'. So when we apply boundary condition, $\frac{\partial T}{\partial r} = -1$, for T at the surface of the solid cylinder as :

$$T_{i,1} = (\Delta r) + T_{i,2} \qquad \text{(for } i=2 \text{ to m-1)}$$

The boundary conditions elsewhere remain the same as in the case of the constant surface temperature.

3.4 Calculation of Nusselt number

(a) For constant cylinder surface temperature

The defining equation for Nusselt number for this case is given by Eq. (2.38) formulated in chapter 2. The local Nusselt number (for a fixed value of θ) is calculated for each surface cell using the following grid point temperature,

$$Nu(i) = -2\frac{(T_{i,2} - T_{i,1})}{\Delta r}$$

(b) For constant heat flux at the surface (r = 1)

The defining equation for Nusselt number for this case is given by Eq. (2.44) formulated in chapter 2. Here the Nusselt number is twice the inverse of the non-dimensionalised temperature at the surface.

$$Nu(i) = \frac{4}{(T_{i,1} + T_{i,2})}$$

The surface averaged values of the Nusselt number are obtained by simple Simpson's one third rule. The values of Nusselt number are important output quantities which are plotted in the next chapter.

3.5 Choice of Numerical Parameters

The grid size used was typically 50x20 for systems with porosity ~0.4, 50x20 for porosity ~0.5, 60x40 for porosity ~0.6 and 60x100 for higher porosities (ε >0.6).

All results reported herein have been checked for mesh independence by using at least two different meshes. In broad terms, as the value of the power-law index decreased below the value of the unity, it became progressively more difficult to achieve the required level of convergence, especially for the values of n $\leq$ 0.5. However in each case, the convergence criterion applied for the temperature field by Gauss-Siedel method was ΔT < 0.00001. And sometimes an under-relaxation factor of 0.7 was used in the Gauss-Siedel iterations to obtain the desired level of convergence.

The CPU times were up to 100 hours on a pentinum II processor for the Navier-Stokes momentum equation solver, but just 1 hour for both constant temperature and constant heat flux cases for the energy equations solver.The time step used are in range of 0.01 – 0.0001 for the Prandtl number range of 1-500.

Chapter 4

RESULTS AND DISCUSSION

In this work, the numerical results of heat transfer for non-Newtonian fluids to tube bank systems have been obtained for the parameter ranges $0.40 \leq \in \leq 0.6$, $1 \geq n \geq 0.5$, $1 \leq Re \leq 500$ and $1 \leq Pr \leq 500$ for both boundary conditions, i.e., the constant wall temperature and constant heat flux at the surface of the solid cylinder. The computer system used to perform these calculations are Linux systems of non-Newtonian fluid mechanics laboratory, Chemical Engineering Department, IIT Kanpur and servers in the Computer Centre working on Linux as their platform. This work mainly concentrated on high Reynolds number ($Re \geq 1.0$) and at high Prandtl number ($Pr \geq 1.0$), and the heat transfer rate in shear thinning fluids is seen to be always higher than that in Newtonian fluids. The results obtained in this work are new and as far as known to us have not been reported previously.

4.1 Validation Of Newtonian Case Results

Initially the solution procedures were validated by comparing the present results with the analytical results available in the literature for a Newtonian fluid. Thus the accuracy of the present results for Newtonian case can be established by comparing the present results with the published work of Mandhani *et al.* (2002). Mandhani *et al.* (2002) have obtained the results of heat transfer, namely Nusselt number, for the flow of a Newtonian fluid for Pr=0.7 & Pr=7.7 over an array of cylinders. A comparison between these two sets of results is in Table 4.1. This table shows that the two values are close and the maximum divergence is less than 3.5%.

Table 4.1: Comparison of present work with the Mandhani et al. (2002) for constant surface temperature condition.

ε	Re	Pr	Nu(Present value)	Nu (Mandhani et al. (2002)
0.99	50.0	0.7	3.300502	3.191410
		7.7	8.060382	7.634112
0.4	500.0	0.7	22.468962	22.601339
		7.7	57.060432	56.718174
0.4	10.0	7.7	11.037856	11.025297

Next, the present solution procedure was validated by comparing the results for the case of single cylinder with the published work of Lange *et al.* (1998). Lange (1998) have obtained the results of heat transfer, namely Nusselt number, for the flow of air (Pr= 0.7148) over a single cylinder case. In the present case, the approximation to a single cylinder case was achieved by using a rather high value of porosity, namely 0.99, which makes the outer boundary ten radii away from the cylinder. The present and the published results are shown in the Table 4.2. The two values are seen to differ by about 10 % atmost.

Table 4.2: Comparison of published work with present work for air (Pr=0.7148) for constant surface temperature condition

Re	Nu (Present value)	Nu (Lange *et al.* (1998)
1	0.913917	0.816
10	1.665181	1.8101
20	2.195308	2.408678
50	3.296901	3.642350
100	4.444632	5.127775
200	6.416176	7.420205
500	11.036654	12.675766

Lange *et al.*(1998) correlated their numerical results by the following expression for the constant temperature boundary condition:

$$Nu = 0.082Re^{0.5} + 0.734\,Re^{x} \qquad (4.1)$$

where $$x = 0.05 + 0.226\,Re^{0.085} \qquad (4.2)$$

These results apply for air in the range of $10^{-4} \leq Re \leq 200$ and entail an uncertainty of approximately 1.5 percent. The values presented by Lange *et al.*(1998) in their graphs and those calculated using Eq. (4.1) and (4.2) seem to be somewhat inconsistent. Limited results were also obtained for a single cylinder case by setting the porosity ϵ=0.999 which makes the outer boundary about 30 cylinder radii large. For Re=100 and Pr=0.7, the present and literature values (Lange *et al.*(1998)) are 4.42 and 4.5 respectively which differ by less than 2 % from each other. In this study, a much more fine grid was used than in the study of Lange *et al.* (1998).

Furthermore, the present solution procedure was validated by comparing with an expression due to Leclair and Hamielee (1968). It was done by comparing the j_H factor for porosity 0.99. The expression for j_H factor is given in eq.(4.3) and eq.(4.4) respectively. The corresponding comparisons is shown in table 4.3.

$$j_H \varepsilon^{0.833} = 1.05\,\mathrm{Re}^{-0.582} \qquad (4.3)$$

$$j_H = \frac{Nu_{av}}{\mathrm{Re}\,\mathrm{Pr}^{1/3}} \qquad (4.4)$$

Table 4.3: Comparisons of j_H for porosity 0.99 for air Pr=0.7

Re	j_H (Using eq.(4.3)	j_H (Using eq.(4.4) for present results)
1	1.0588	1.0206
10	0.2772	0.1850
20	0.1851	0.1218
50	0.1086	0.0731
100	0.0725	0.0493
200	0.0484	0.0355
500	0.0284	0.0244

The comparisons presented in Tables 4.2 and 4.3 illustrate the applicability of the present approach to an otherwise extremely difficult flow problem involving incompressible Newtonian fluids which represent a special case of power law fluid model (n=1).

4.2 RESULTS FOR NON-NEWTONIAN LIQUIDS

The new results for non-Newtonian fluids for porosities 0.4, 0.5 and 0.6 are given in Tables 4.6 to 4.20. In general, it became increasingly difficult to obtain fully converged results at high values of voidage, lower values of n and / or higher values of the Reynolds number.

4.2.1.(a) Results for Constant Surface Temperature

The values of the mean Nusselt member for the constant temperature condition on the cylinder surface are presented in Tables 4.6 to 4.20 for a range of values of the Reynolds Number and voidage for $1 \leq Pr \leq 500$ range and $0.5 \leq n \leq 1$ range. For a constant value of power law index, as the value of porosity increases, the value of the

Nusselt number decreases for the same value of Reynolds number and Prandtl number.

It is seen that the value of the Nusselt number increases as the power law index decreased, i.e., shear thinning lowers the resistance to heat flow and this facilitates heat transfer. This effect increases with the increasing values of the Reynolds number. Also, as expected the value of the Nusselt number is always larger for the case of constant heat flux condition than that for the constant temperature condition. The values of the local Nusselt number are also plotted as a function of Reynolds number and Prandtl number for different values of power law index in the fig. 4.1 to 4.52. Similarly the values of the local Nusselt number are plotted as a function of Reynolds number and Prandtl number with porosity as a parameter in the Fig. 4.103 to 4.136.

An examination of these results suggest the following overall trends:

(i) For a given porosity and values of n, the influence of Prandtl number increases with increasing values of the Reynolds number. This is presumably due to the growing thermal boundary layers at high Reynolds numbers.

(ii) At low values of Reynolds number, the results are influenced much more by the porosity than that by the Prandtl number. However, as the values of the Reynolds number progressively rises, Prandtl number and shear thinning exert greater and greater influence in determining the value of Nusselt number.

(iii) And also the results, at low values of Reynolds number, are not much influenced by power law index. However, as the value of the Reynolds number progressively rises, shearing action influences the heat transfer rate.

The inspection of Fig. 4.1 to 4.52 and 4.103 to 4.136 suggests that at low Peclet number (= RePr), the Nusselt number almost has a constant value over the entire surface (Fig. 4.1). This is purely a conduction result. As the value of the Prandtl

number and/or Peclet number rises, the value of the Nusselt number is seen to be maximum at the front stagnation point, it decreases along the cylinder surface, attains a minimum near the rear stagnation point and finally shows an upturn in some cases (Fig. 4.2-4.50 and 4.103 to 4.136). As the value of the Reynolds number increases, the minima in the Nu-θ plots become more pronounced which is also seen to depend strongly on the value of the porosity. In dense systems (low values of porosity), the Nusselt number shows larger variation over the surface. When the Reynolds number is greater than 100, the value of the Nusselt number seems to peak again after the minimum value. This is presumably due to the interference of the wakes in concentrated systems. Finally, the value of θ at which the Nusselt number goes through a minimum value keeps moving forward which is in the line with the flow field. Once again we can observe that the Nusselt number increases with shear thinning action along the cylinder surface. The behavior of the Nusselt number variation along the cylinder surface for non-Newtonian fluids is qualitatively similar to that for a Newtonian fluid over an array of circular cylinders.

4.2.1.(b) Temperature Field

Some further insights into the nature of heat transfer to/from non-Newtonian fluids can be gained by examining the isotherm plots. These are presented in figures 4.158-4.397, for constant temperature condition and the flow is from left to right in these figures. The inner circle shows the surface of the solid cylinder ($r = 1$). These curves are plotted for temperature values of 0.01 to 1.0 in step of 0.01, the temperature being unity at $r=1$ and zero at $r = r_{\infty}$.

It can be seen from fig 4.158-4.240., that for low values of Reynolds number and Prandtl number isotherms show front and rear symmetry for a given value of porosity and power-law index. This is due to the fact that heat transfer occurs mainly by conduction with negligible convection. As the value of Reynolds number and/or Prandtl number (i.e., Peclet number) keeps on increasing, this symmetry gradually disappears indicating the increasing contribution of convection as shown in figures 4.158-4.240 Same phenomenon is repeated with different values of porosity as shown in figures 4.241-4.397. In general, higher is the porosity, lower is the value of the Reynolds number up to which the temperature field displays front and rear symmetry.

4.2.2.(a) Results for constant heat flux condition

The values of the mean Nusselt number for constant flux boundary condition are presented in Tables 4.6 to 4.20 for a range of values of the system parameters. As expected, the values of the mean Nusselt number are always higher under this condition than those for constant surface temperature condition, though the difference between the two values increases with decreasing porosity and/or increasing Reynolds number. It is seen that the Nusselt number increase as the power law index decreased, i.e., shear thinning lowers the resistance to heat flow. As the value of porosity becomes higher the value of the Nusselt number decreases for the same value of Reynolds number and Prandtl number, while for a given porosity the value of the Nusselt number increased both with Reynolds number and Prandtl number. In this case the local as well as mean Nusselt number are consistently higher than for constant surface temperature condition. The values of the local Nusselt number are also plotted as a function of Reynolds number and Prandtl number with porosity as a parameter in the figures 4.52-4.102 and 4.132-4.155.

The trend in the value of Nusselt number is same as that discussed for constant surface temperature condition. Here the value of the Nusselt number is higher at the front and rear stagnation point as are the mean values. Once again we can observe that the Nusselt number increases with shear thinning action along the cylinder surface. The behavior of the Nusselt number variation along the cylinder surface for non-Newtonian fluids is qualitatively similar to that for a Newtonian fluid over an array of circular cylinders.

4.2.2.(b) TEMPERATURE FIELD

Isotherm plots

Some further insights into the nature of heat transfer of non-Newtonian fluids can be gained by examining the isotherm plots. These are presented in figures 4.398-4.473 for constant heat flux condition and the flow is from left to right in these figures. The inner circle shows the surface of the solid cylinder. These curves are plotted for temperature values of 0.01 to 1.0 in step of 0.05, the temperature being unity at $r=1$ and zero at $r= r_{\infty}$.

It can be seen from fig 4.398-4.473 that for low values of Reynolds number and Prandtl number isotherms show front and rear symmetry for a given value of porosity. This is due to the fact that heat transfer occurs mainly by conduction with negligible convection. As the value of the Reynolds number and/or Prandtl number (i.e., Peclet number) keeps on increasing, this symmetry gradually disappears indicating the increasing contribution of convection as shown in figures 4.398-4.631 As Peclet number (RePr) keeps on increasing it results in less number of isotherms for a definite value of porosity. The outer most isotherm is having a value of 0.05. Inspection of Figures 4.473-4.631 reveals that as porosity increases, Peclet number being the same, more and more isotherms are present as the system goes towards the sparse systems. Same phenomena can be seen for a different

value of porosity as shown in figures 4.473-4.631. In general, higher is the porosity, lower is the value of the Reynolds up to which the temperature field displays front and rear symmetry.

4.3 Validation of non-Newtonian fluids results

Initially, the present solution procedure was validated by comparing j_H factor for the special case of porosities of 0.75 (n=0.748) and 0.714 (n=0.83) with the experimental results of Adams and Bell (1968). The values presented by Adams and Bell (1968) in graphs and those calculated using the equation:

$$j_H = 0.599\,\mathrm{Re}^{-0.667} + 0.003 \tag{4.5}$$

for ε=0.714, n=0.83 and Pr=740.56 (0.5%CMC solution). From the geometric details of tube bundles used by Adams and Bell (1968), their results have been recalculated in the form required here (as shown in Appendix A). A comparison of these results with the present numerical results is shown in the Table 4.4.

Table 4.4. Comparison of the j_H factors

Re	Nu	Re_{A-B}	$j_{H\,numerical}$	$j_{H\,\exp tl}$	$\dfrac{j_{H_{numerical}}}{j_{H_{\exp tl}}}$
5.0	24.887276	16.724	0.122426	0.091807	1.3335
7.5	29.345327	25.086	0.096240	0.070124	1.37243
10.0	33.284916	33.448	0.081868	0.057933	1.42567
20.0	52.959656	66.896	0.0651305	0.036598	1.779619

Furthermore, ε=0.75, n=0.748 and Pr=921.36 (1%CMC solution). From the geometric details of tube bundles used by Adams and Bell (1968), their results have been recalculated in the form required here (as shown in Appendix B). A comparison of these results with the present numerical results is as follows;

Table 4.5. Comparison of the j_H factors

Re	Nu	Re_{A-B}	$j_{H\ numerical}$	$j_{H\ exptl}$	$\frac{j_{H_{numerical}}}{j_{H_{exptl}}}$
1.0	13.823075	3.7860	0.4518098	0.306785	1.47272
2.5	19.361176	9.4654	0.2531237	0.162835	1.55448
5.0	25.442535	18.9308	0.1663151	0.099594	1.66793
7.5	30.383961	28.3962	0.1324111	0.073498	1.80156
10.0	44.131569	37.8616	0.104240	0.059164	1.76186

An examination of this Tables 4.4 & 4.5 shows that the two results differ by a maximum of 78%. While this may seem like a rather large discrepancy, but it must be borne in mind that finite wall effects and maldistribution of flow are always present in experimental study which are altogether neglected in the numerical simulations. Also, while the numerical simulations are based on constant thermo-physical properties, significant temperature intervals are present in the study of Adams and Bell (1968). Bearing in mind these factors, the correspondence seen in Tables 4.4 & 4.5 are acceptable and satisfactory.

Table No.4.6; Reynolds number =1.0, porosity = 0.4

n	Pr	Nu(t)	Nu(f)
1.0	1	7.934439	7.936596
	10	8.036373	8.171126
	50	9.545625	10.459119
	100	12.021615	13.234608
	500	21.006881	21.82945
0.8	1	7.934540	7.935972
	10	8.036493	8.166099
	50	9.633212	10.522439
	100	12.093627	13.262397
	500	21.021563	22.465096
0.6	1	7.960410	7.961659
	10	8.055016	8.170110
	50	9.780549	10.614179
	100	12.106388	13.308061
	500	21.147916	23.050785
0.5	1	7.960517	7.961791
	10	8.055350	8.174158
	50	9.784709	10.620215
	100	12.166709	13.461456
	500	21.342908	23.923456

Table No.4.7; Reynolds number =10.0, porosity = 0.4

n	Pr	Nu(t)	Nu(f)
1.0	1	8.0163260	8.070533
	10	12.143661	13.316152
	50	21.131322	22.901655
	100	27.0191656	29.1559647
	500	48.896416	53.531244
0.8	1	8.0307695	8.155944
	10	12.161279	13.423942
	50	21.244217	23.234256
	100	27.152752	29.737281
	500	49.281631	53.725784
0.6	1	8.035966	8.162755
	10	12.186206	13.444005
	50	21.340579	23.3405218
	100	27.2421238	29.821318
	500	49.760937	53.827808
0.5	1	8.059018	8.186030
	10	12.189671	13.447103
	50	21.396200	23.396727
	100	27.405266	29.825638
	500	49.84706	53.959251

Table No.4.8; Reynolds number =100.0, porosity = 0.4

n	Pr	Nu(t)	Nu(f)
1.0	1	12.900322	14.420811
	10	31.127928	33.938839
	50	59.168449	63.912827
	100	122.544151	128.039513
	500	213.221893	218.962402
0.8	1	13.324706	14.942348
	10	33.801826	37.022709
	50	68.053444	67.731087
	100	124.526047	132.804657
	500	218.111557	227.731079
0.6	1	14.115411	15.958244
	10	38.623264	42.873165
	50	66.444885	78.850395
	100	135.347931	157.943436
	500	246.147354	249.481934
0.5	1	14.754089	16.772413
	10	42.743153	47.799911
	50	89.462036	101.665321
	100	145.083099	168.832169
	500	257.806702	268.358063

Table No.4.9; Reynolds number =200.0, porosity = 0.4

n	Pr	Nu(t)	Nu(f)
1.0	1	17.715052	19.712749
	10	45.128601	49.185493
	50	113.196922	122.697411
	100	155.446106	173.965134
	500	253.412811	259.700409
0.8	1	19.072891	21.266714
	10	50.811386	55.656525
	50	126.156776	147.413635
	100	175.413345	192.377274
	500	267.338562	276.814148
0.6	1	20.898769	23.610092
	10	62.935993	75.452873
	50	153.894180	171.878906
	100	207.5146	221.171646
	500	278.584595	304.141876
0.5	1	22.320176	25.352266
	10	68.229858	77.775620
	50	169.132690	187.320923
	100	223.761124	238.929703
	500	-	-

Table No.4.10; Reynolds number =500.0, porosity = 0.4

n	Pr	Nu(t)	Nu(f)
1.0	1	29.364960	32.431778
	10	71.549950	80.174782
	50	199.541245	211.599335
	100	242.640045	254.563065
	500		
0.8	1	32.872173	37.430359
	10	95.310158	114.532
	50	227.004105	239.641418
	100	238.460571	278.567413
	500		
0.6	1	37.485847	39.1304206
	10	432.6194154	162.072034
	50	235.441217	247.321041
	100	266.582794	279.334762
	500		
0.5	1	38.006926	41.832642
	10	176.515778	187.385422
	50	256.983276	268.021271
	100	272.207733	279.483551
	500		

Table No.4.11; Reynolds number =1.0, porosity = 0.5

n	Pr	Nu(t)	Nu(f)
1.0	1	5.847853	5.8487290
	10	6.001798	6.013905
	50	7.985848	8.6935014
	100	10.201760	10.991025
	500	17.851946	18.912055
0.8	1	5.847913	5.849944
	10	5.993634	6.054933
	50	7.9951415	8.719989
	100	10.018479	10.981187
	500	17.417665	18.892799
0.6	1	5.848024	5.850346
	10	5.994559	6.150870
	50	7.96923488	8.780470
	100	10.1963233	10.998605
	500	17.457107	18.693872
0.5	1	5.8488031	5.8610275
	10	6.010251	6.1725814
	50	7.9964302	8.783092
	100	10.2039752	10.99879102
	500		

Table No.4.12; Reynolds number =100.0, porosity = 0.5

n	Pr	Nu(t)	Nu(f)
1.0	1	10.877949	12.233936
	10	26.076292	28.817455
	50	48.445957	53.074196
	100	64.332642	69.672241
	500	171.454330	196.622559
0.8	1	11.641509	13.158134
	10	29.342411	32.247120
	50	57.242017	62.4138501
	100	71.549431	78.942345
	500	190.817993	208.283539
0.6	1	11.909425	13.428152
	10	31.567934	34.684757
	50	60.582745	66.015411
	100	82.640030	90.591469
	500	207.671860	221.878677
0.5	1	12.507766	14.140772
	10	34.966072	38.579731
	50	67.909447	74.646080
	100	109.641670	133.203979
	500	229.028152	242.216324

Table No.4.13; Reynolds number =10.0, porosity = 0.5

n	Pr	Nu(t)	Nu(f)
1.0	1	5.9967028	6.16780162
	10	10.00723109	11.00173266
	50	17.01846023	18.97831062
	100	21.89105602	24.0965238
	500	39.3967098	42.4890116
0.8	1	5.998009	6.168808
	10	10.013325	11.089046
	50	17.353355	19.082125
	100	22.091156	24.174515
	500	39.424084	42.592155
0.6	1	5.999010	6.168867
	10	10.023359	11.099346
	50	17.391918	19.117094
	100	22.143450	24.218283
	500	39.481960	42.625042
0.5	1	5.999635	6.169416
	10	10.0694650	11.154601
	50	17.545757	19.293976
	100	22.366032	24.473021
	500	39.895378	42.993656

Table No.4.14; Reynolds number =200.0, porosity = 0.5

n	Pr	Nu(t)	Nu(f)
1.0	1	14.86104452	16.98707740
	10	40.09704638	43.44088601
	50	73.8826041	78.9202765
	100	122.72681053	137.8510472
	500	231.9778825	242.9820344
0.8	1	16.154152	18.023235
	10	42.264950	46.192909
	50	77.139107	85.602890
	100	139.725281	171.480865
	500	256.684753	265.087982
0.6	1	17.766781	19.927652
	10	50.340824	55.811890
	50	91.730209	105.045273
	100	175.410706	191.164352
	500	291.873291	293.46003
0.5	1	18.866871	21.247288
	10	56.668926	63.287262
	50	138.407745	159.342453
	100	192.104858	208.570724
	500	293.558350	304.239502

Table No.4.15; Reynolds number =500.0, porosity = 0.5

n	Pr	Nu(t)	Nu(f)
1.0	1	24.671692	27.197191
	10	61.873554	67.928024
	50	164.440140	187.232742
	100	234.197708	248.330505
	500		
0.8	1	27.427446	30.486328
	10	78.516046	132.779495
	50	204.495255	213.182373
	100	248.166275	259.812378
	500		
0.6	1	30.782507	34.594124
	10	99.882957	117.319771
	50	227.452621	242.090790
	100	283.049622	293.547577
	500		
0.5	1	32.213848	36.280319
	10	103.448807	145.886871
	50	237.430145	250.633865
	100	291.745544	298.755615
	500		

Table No.4.16; Reynolds number =1.0, porosity = 0.6

n	Pr	Nu(t)	Nu(f)
1.0	1	4.414944	4.417809
	10	4.623365	4.809139
	50	6.647354	7.25817
	100	8.348444	9.108577
	500	14.361089	15.454818
0.8	1	4.414996	4.417840
	10	4.626966	4.819084
	50	6.651194	7.295737
	100	8.342834	9.123822
	500	14.418490	15.669935
0.6	1	4.424533	4.427312
	10	4.633632	4.823524
	50	6.639102	7.275495
	100	8.376125	9.1339940
	500	14.431066	15.746615
0.5	1	4.424587	4.427317
	10	4.634986	4.829026
	50	6.641713	7.277069
	100	8.388171	9.208723
	500	14.536267	15.941373

Table No.4.17; Reynolds number =10.0,porosity = 0.6

n	Pr	Nu(t)	Nu(f)
1.0	1	4.633389	4.839238
	10	8.448704	9.380105
	50	14.611475	16.155329
	100	18.572514	20.453854
	500	32.872940	35.723591
0.8	1	4.637657	4.846606
	10	8.451797	9.388928
	50	14.593246	16.134794
	100	18.540773	20.415014
	500	32.828190	35.750427
0.6	1	4.638368	4.847233
	10	8.484939	9.399450
	50	14.490101	15.896059
	100	18.585667	20.478066
	500	32.838493	35.816815
0.5	1	4.638368	4.8510602
	10	8.5010790	9.41087662
	50	14.6125062	15.9055468
	100	18.610002317	20.50011567
	500	32.8409201	35.8904272

Table No.4.18; Reynolds number =100.0, porosity = 0.6

n	Pr	Nu(t)	Nu(f)
1.0	1	9.383591	10.586508
	10	22.463772	24.735071
	50	41.510197	45.189659
	100	54.223763	58.949402
	500	138.227753	158.977188
0.8	1	9.714847	10.736677
	10	24.108482	26.395256
	50	45.231358	48.956703
	100	59.765381	64.620941
	500	159.776733	169.460297
0.6	1	9.919545	11.222487
	10	26.787050	29.408550
	50	51.976742	56.860264
	100	71.358162	79.854462
	500	174.877899	189.156952
0.5	1	10.099916	11.416263
	10	26.788191	29.482941
	50	52.206837	57.288868
	100	72.434319	82.889786
	500	176.594315	192.441620

Table No.4.19; Reynolds number =200.0, porosity = 0.6

n	Pr	Nu(t)	Nu(f)
1.0	1	13.108223	14.641165
	10	32.736610	35.696430
	50	61.060459	66.398125
	100	101.986938	126.515434
	500	208.733551	223.521561
0.8	1	14.027789	15.648171
	10	36.270531	39.614288
	50	70.541786	77.570686
	100	129.566742	137.270782
	500	236.029968	249.409546
0.6	1	15.921167	17.148172
	10	42.826439	45.091190
	50	85.816048	91.924561
	100	119.369812	134.720230
	500	253.720093	265.709259
0.5	1	16.435616	18.387285
	10	47.680515	52.78582
	50	87.990746	94.542900
	100	162.498703	179.779251
	500	278.983856	286.505707

Table No.4.20; Reynolds number =500.0, porosity = 0.6

n	Pr	Nu(t)	Nu(f)
1.0	1	22.080944	23.800337
	10	56.175209	60.045734
	50	137.498016	172.751877
	100	188.836365	219.978104
	500	278.377197	287.058685
0.8	1	24.010752	26.607241
	10	66.757576	75.825409
	50	166.523087	182.637512
	100	221.351349	233.809479
	500	278.377319	312.638275
0.6	1	26.816025	29.964300
	10	80.452332	96.514900
	50	199.987335	211.520767
	100	257.210480	260.914978
	500	278.377441	334.940674
0.5	1	27.913700	31.291368
	10	81.723160	91.012787
	50	208.022507	220.703491
	100	268.975189	271.482666

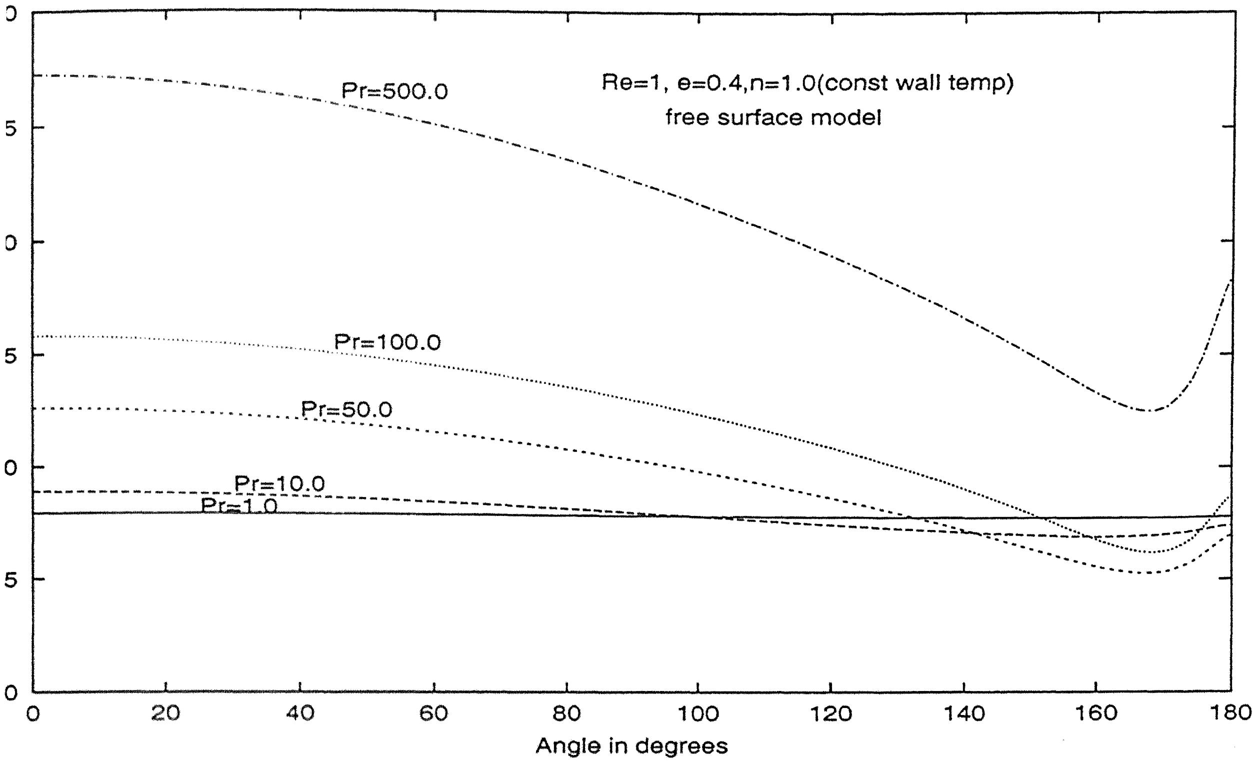

Figure 4.1: Variation of Nusselt number with angle for Re=1.0,e=0.4 and n=1.0 for constant surface temperature condition

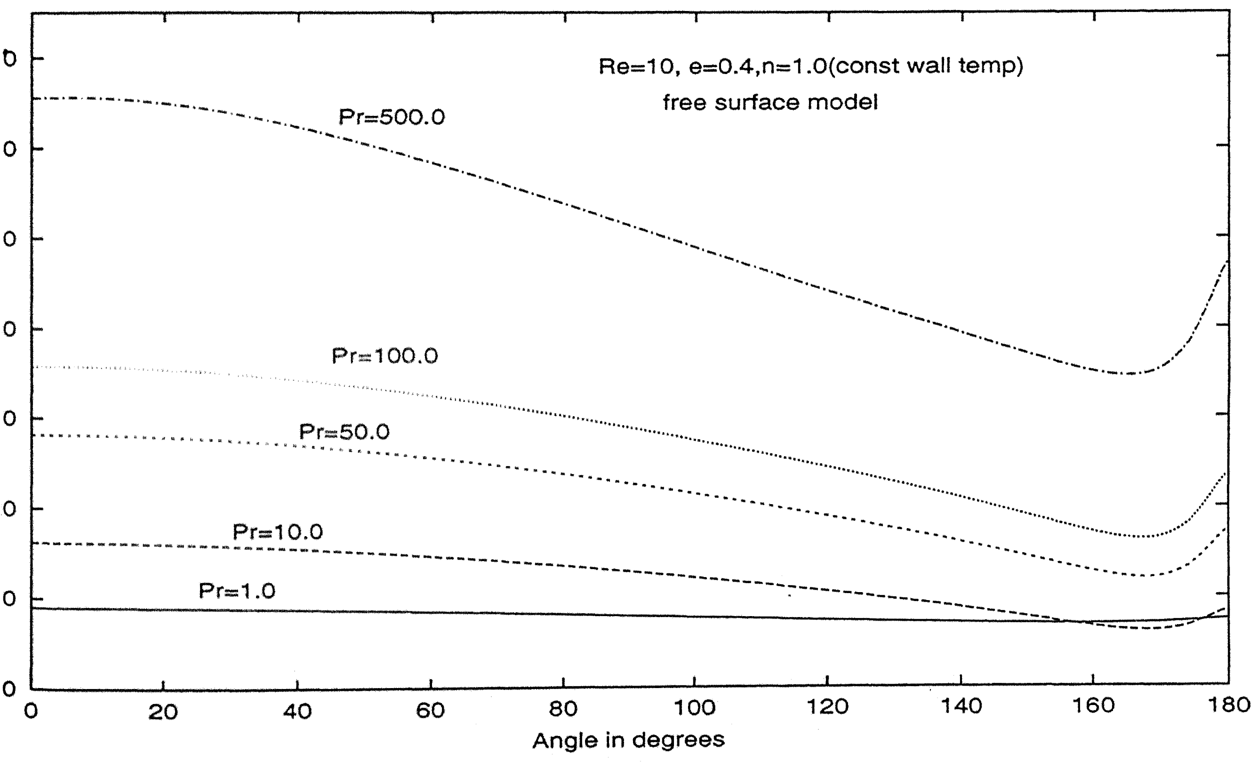

Figure 4.2: Variation of Nusselt number with angle for Re=10.0,e=0.4 and n=1.0 for constant surface temperature condition

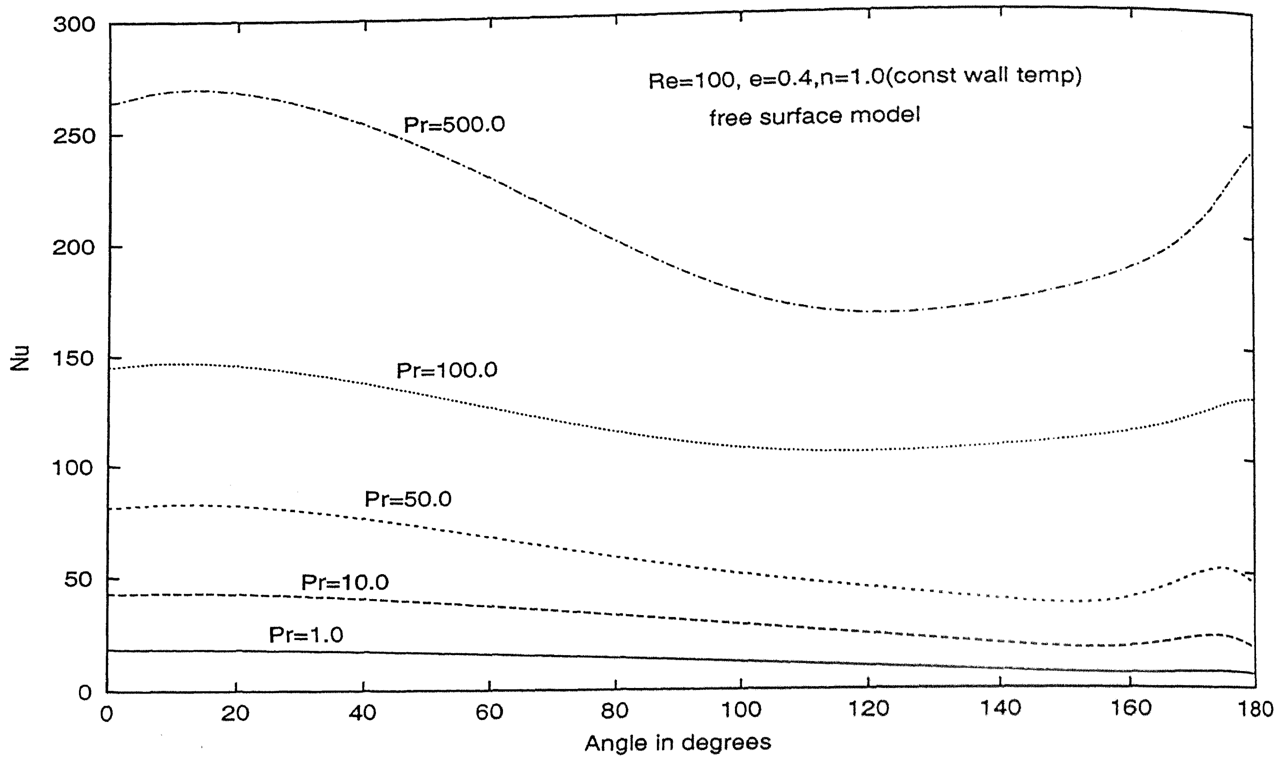

Figure 4.3: Variation of Nusselt number with angle for Re=100.0,e=0.4 and n=1.0 for constant surface temperature condition

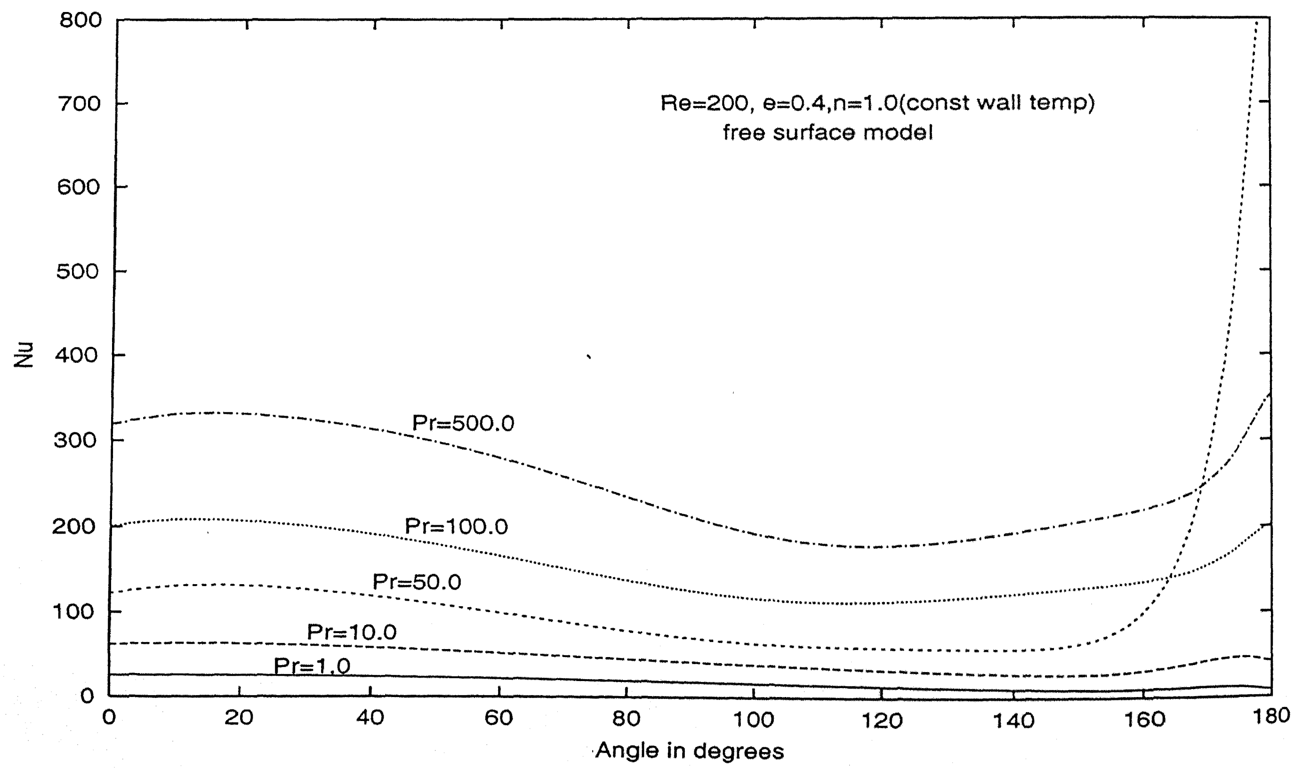

Figure 4.4: Variation of Nusselt number with angle for Re=200.0,e=0.4 and n=1.0 for constant surface temperature condition

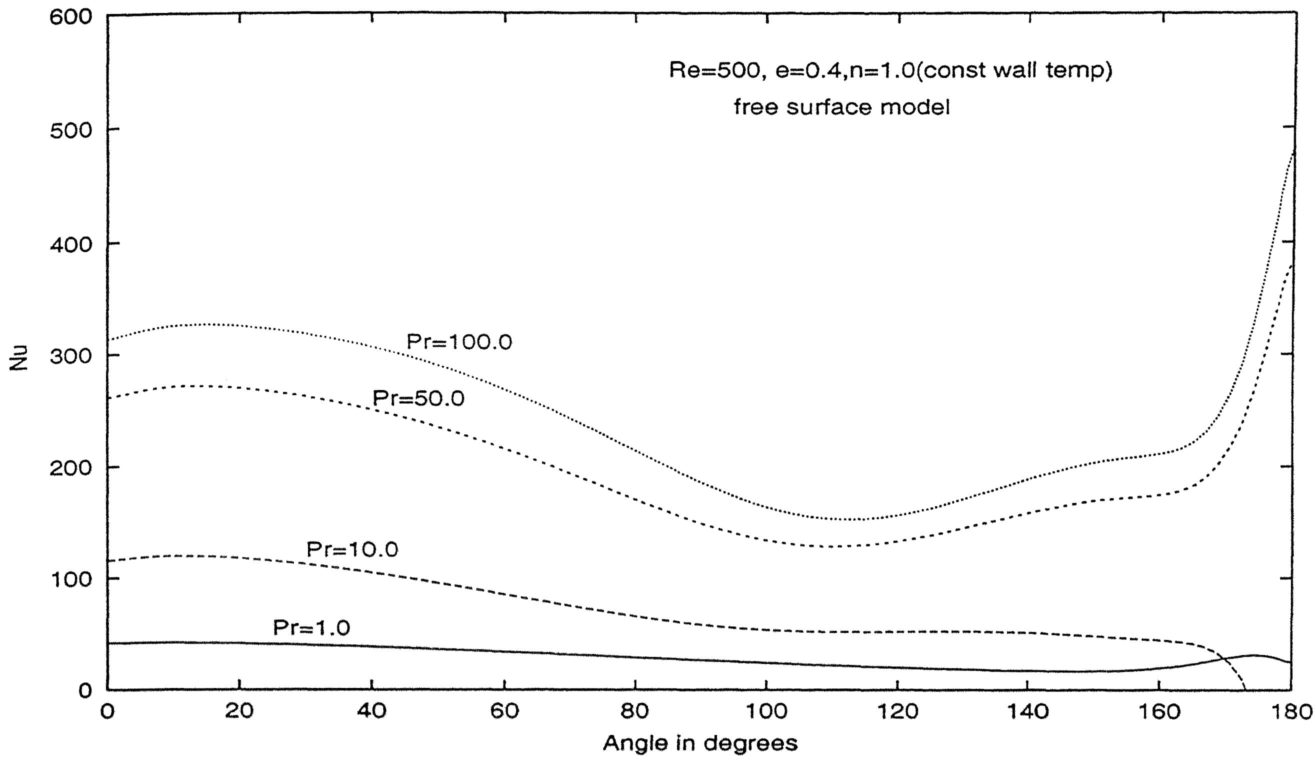

Figure 4.5: Variation of Nusselt number with angle for Re=500.0,e=0.4 and n=1.0 for constant surface temperature condition

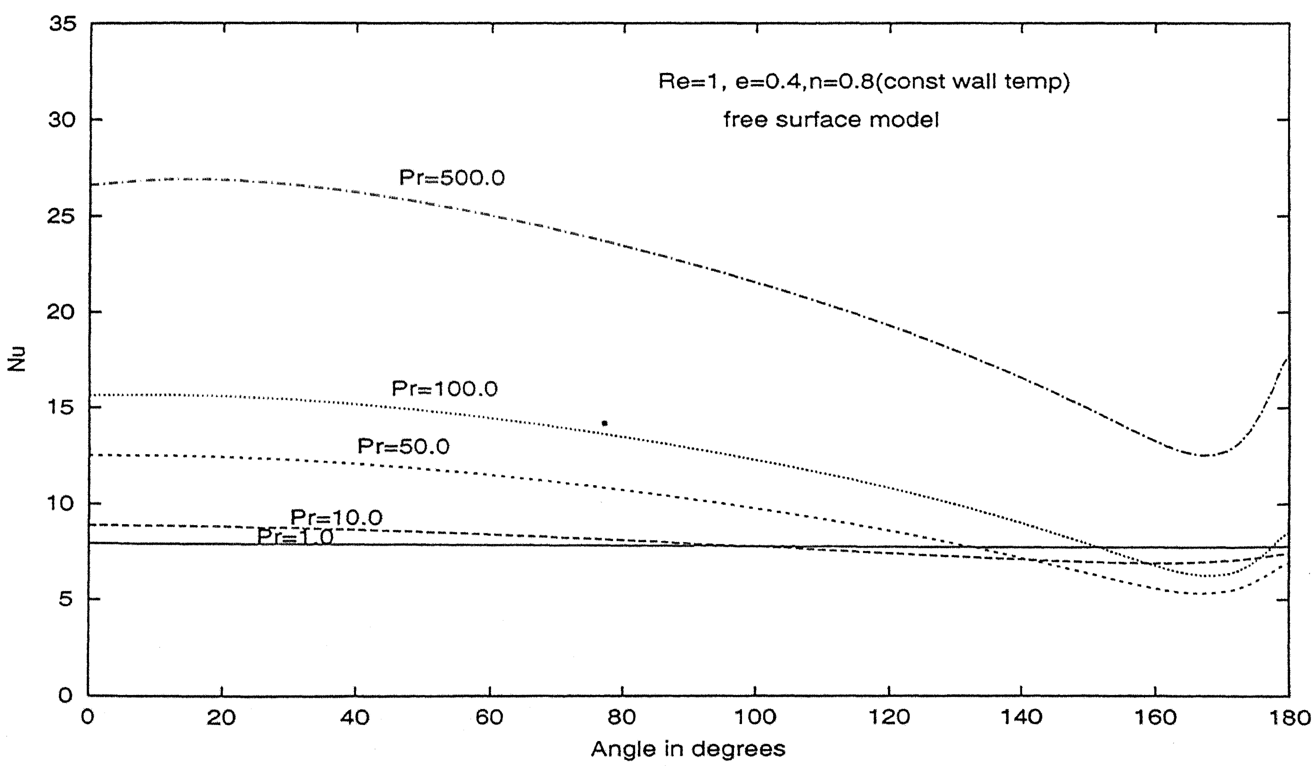

Figure 4.6: Variation of Nusselt number with angle for Re=1.0,e=0.4 and n=0.8 for constant surface temperature condition

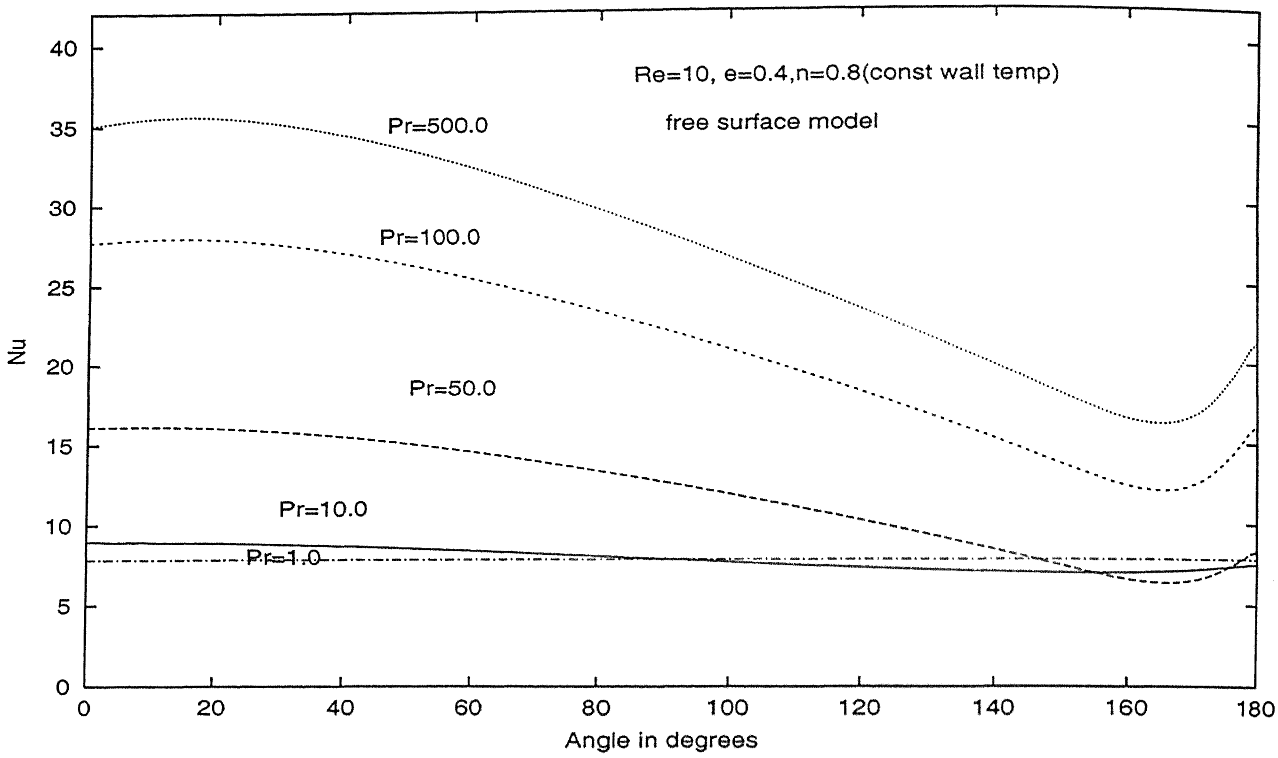

Figure 4.7: Variation of Nusselt number with angle for Re=10.0,e=0.4 and n=0.8 for constant surface temperature condition

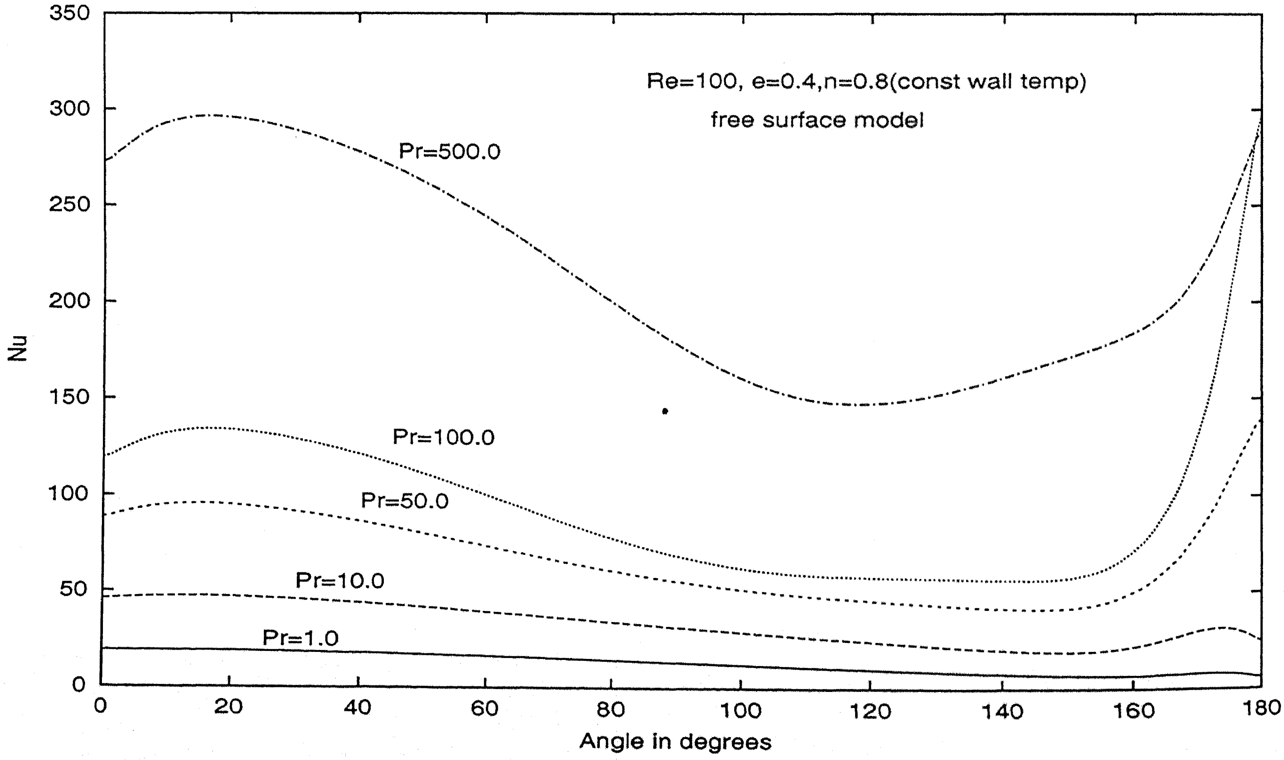

Figure 4.8: Variation of Nusselt number with angle for Re=100.0,e=0.4 and n=0.8 for constant surface temperature condition

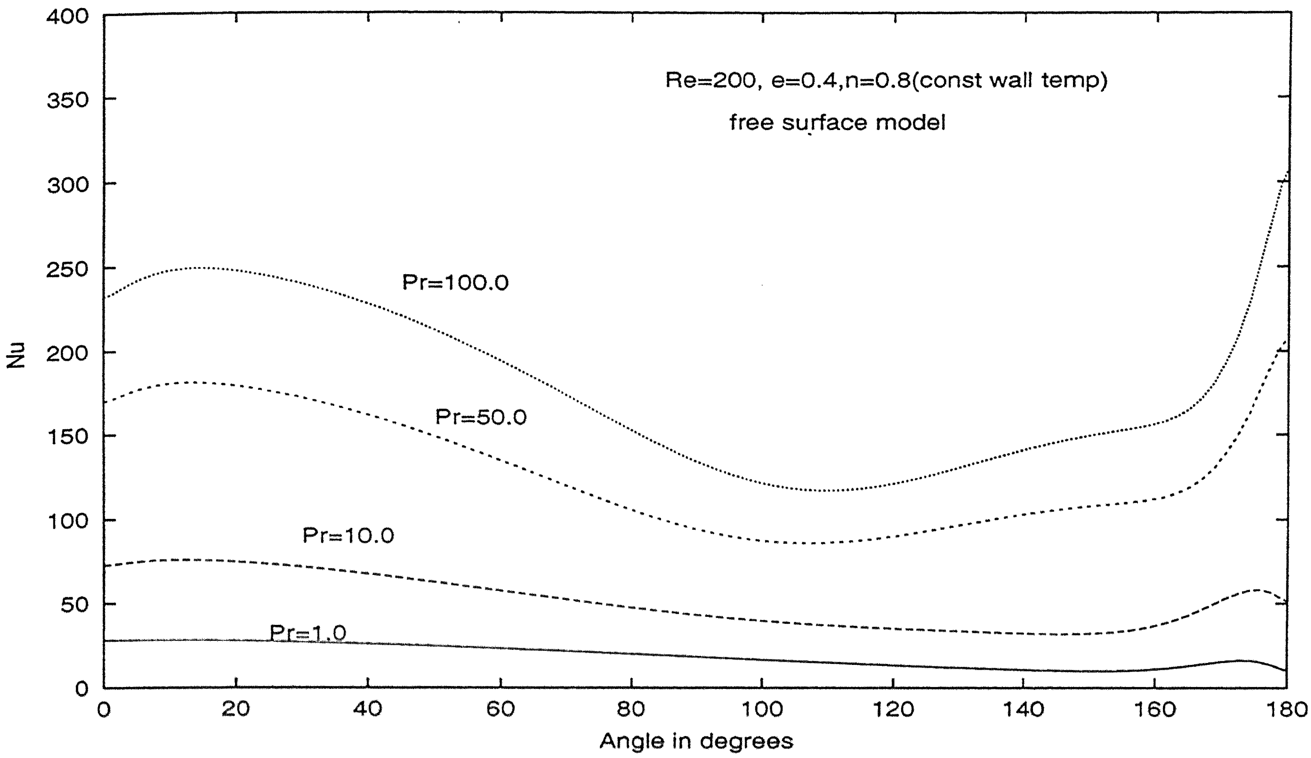

Figure 4.9: Variation of Nusselt number with angle for Re=200.0,e=0.4 and n=0.8 for constant surface temperature condition

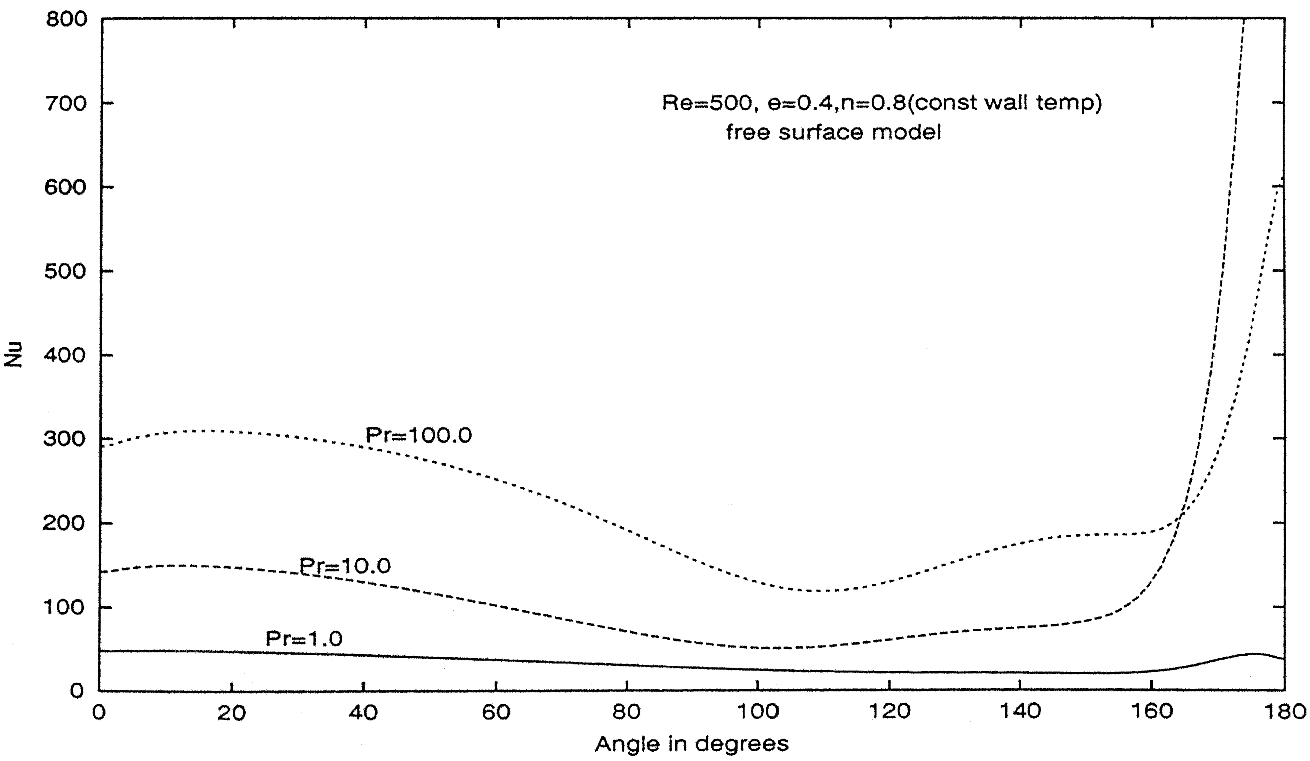

Figure 4.10: Variation of Nusselt number with angle for Re=500.0,e=0.4 and n=0.8 for constant surface temperature condition

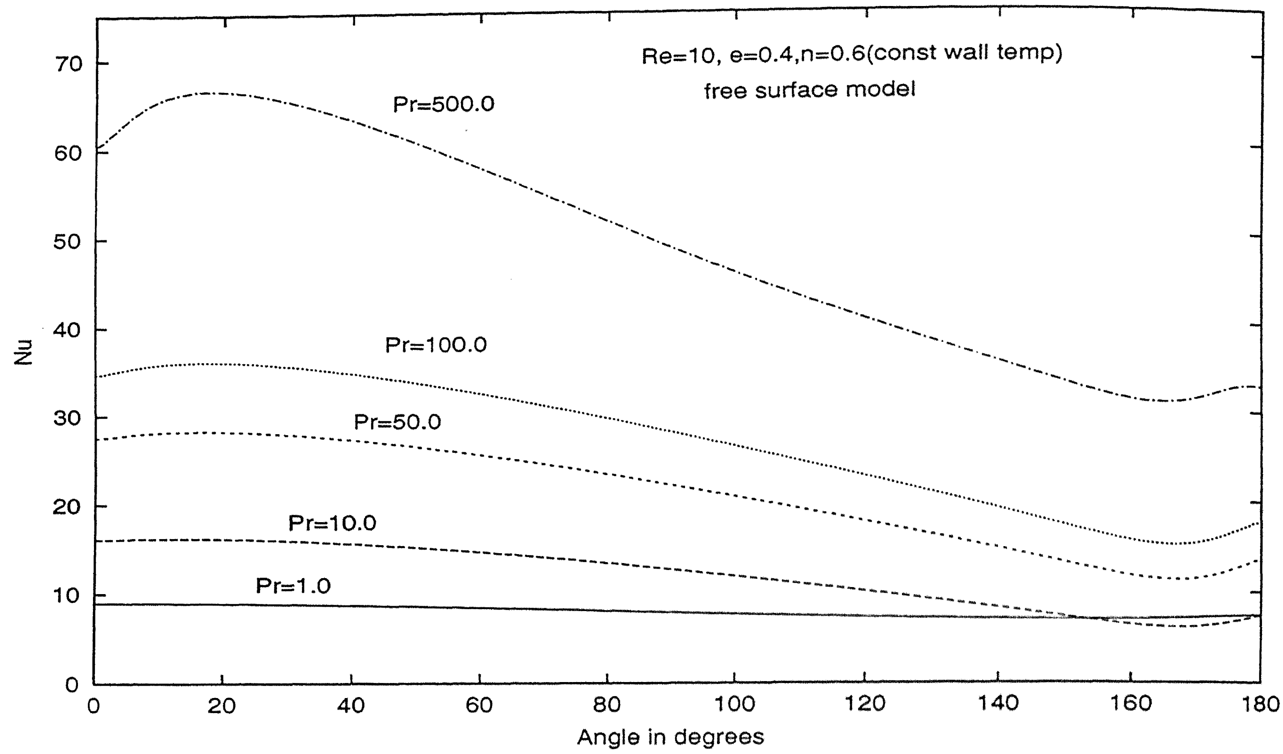

Figure 4.11: Variation of Nusselt number with angle for Re=10.0,e=0.4 and n=0.6 for constant surface temperature condition

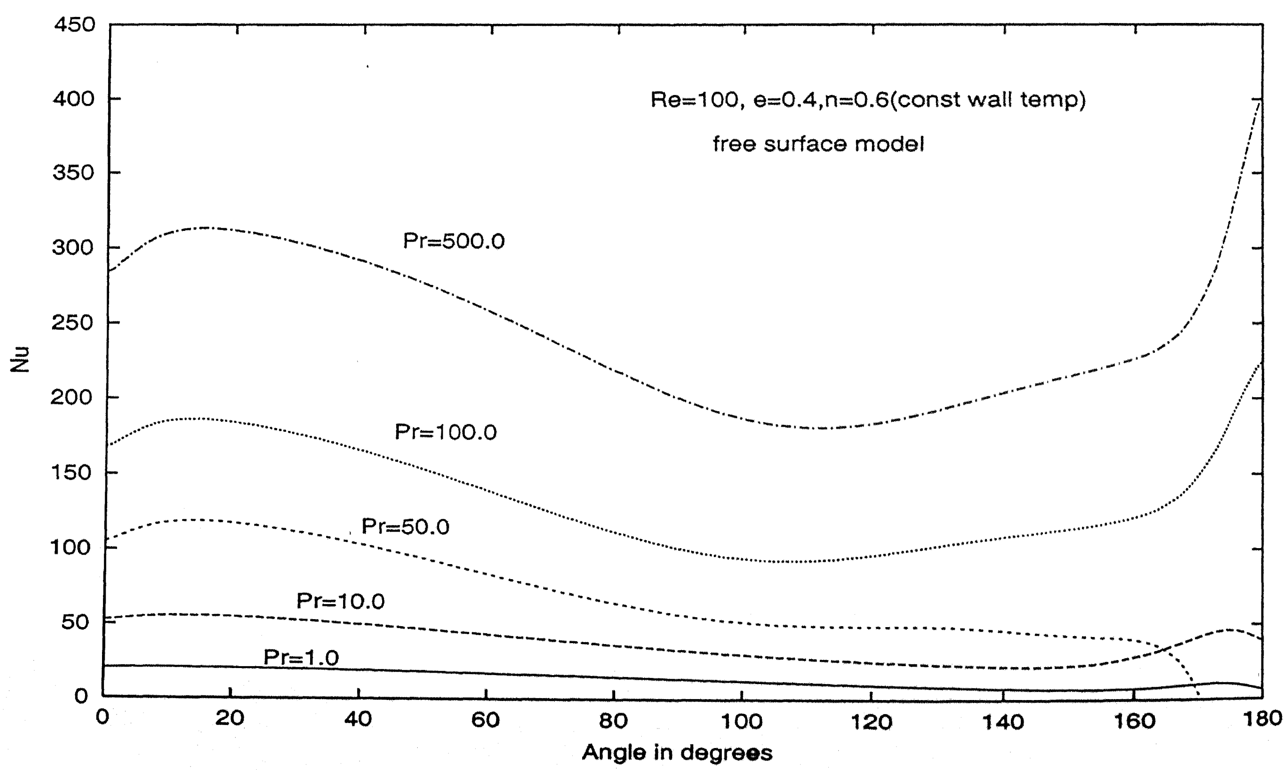

Figure 4.12: Variation of Nusselt number with angle for Re=100.0,e=0.4 and n=0.6 for constant surface temperature condition

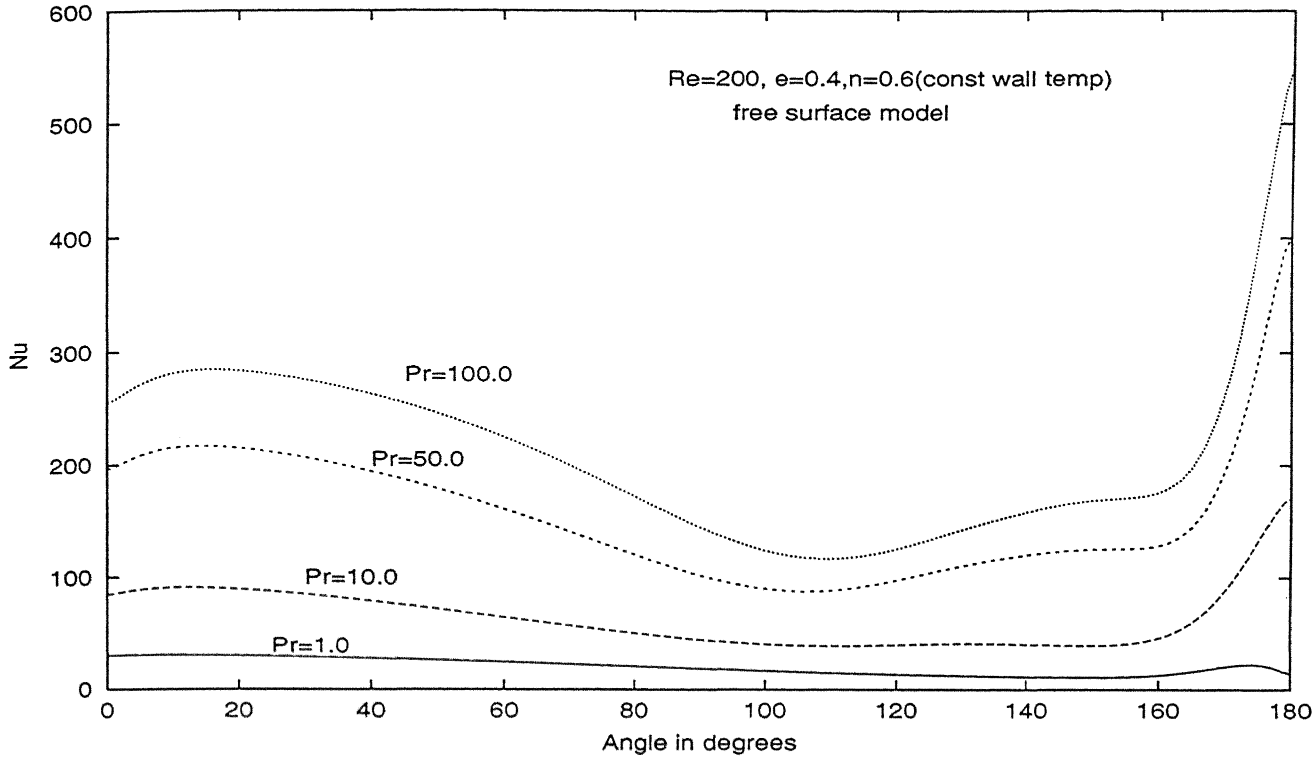

Figure 4.13: Variation of Nusselt number with angle for Re=200.0,e=0.4 and n=0.6 for constant surface temperature condition

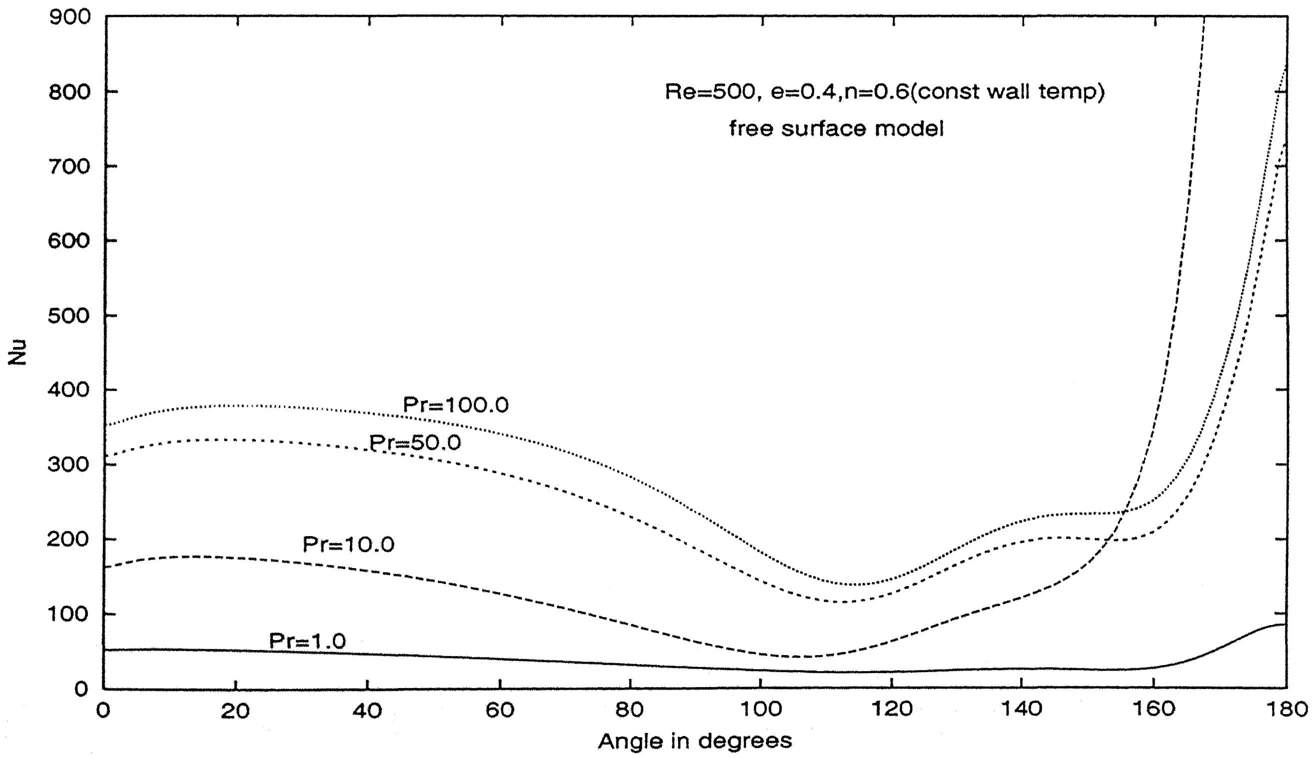

Figure 4.14: Variation of Nusselt number with angle for Re=500.0,e=0.4 and n=0.6 for constant surface temperature condition

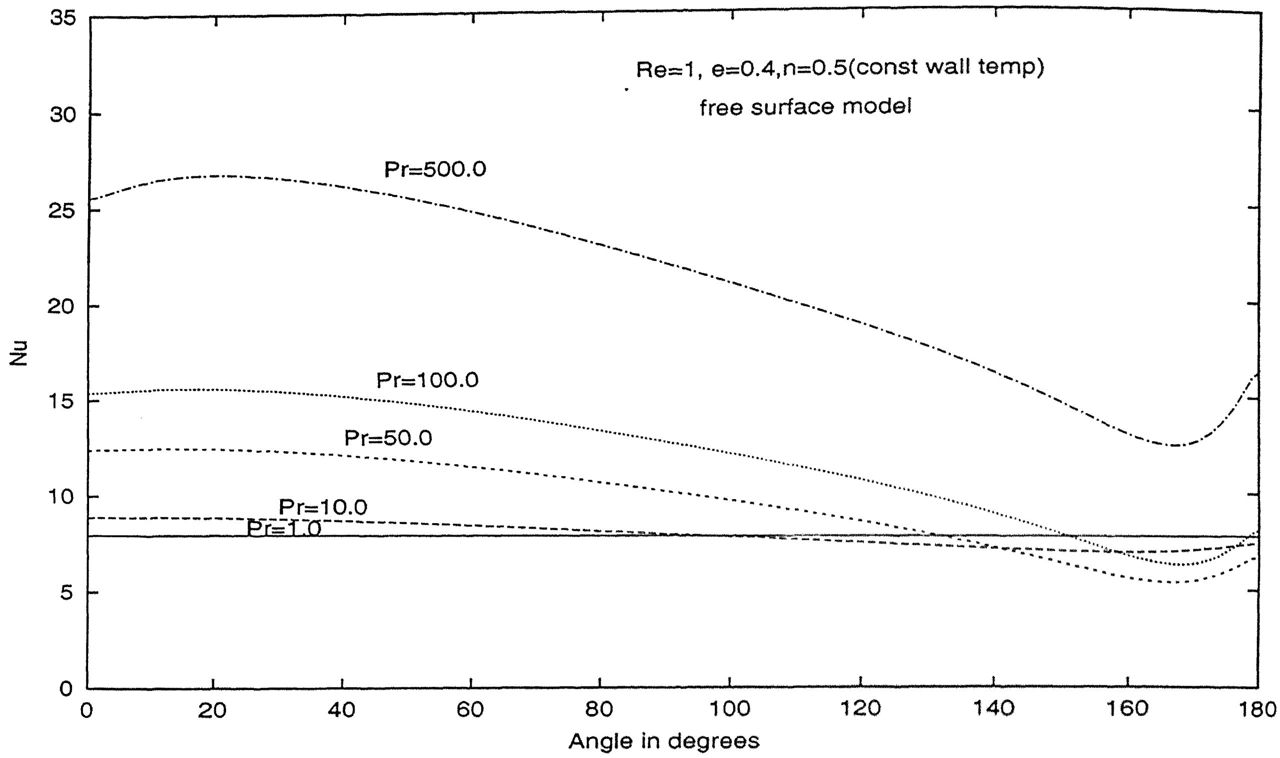

Figure 4.15: Variation of Nusselt number with angle for Re=1.0,e=0.4 and n=0.5 for constant surface temperature condition

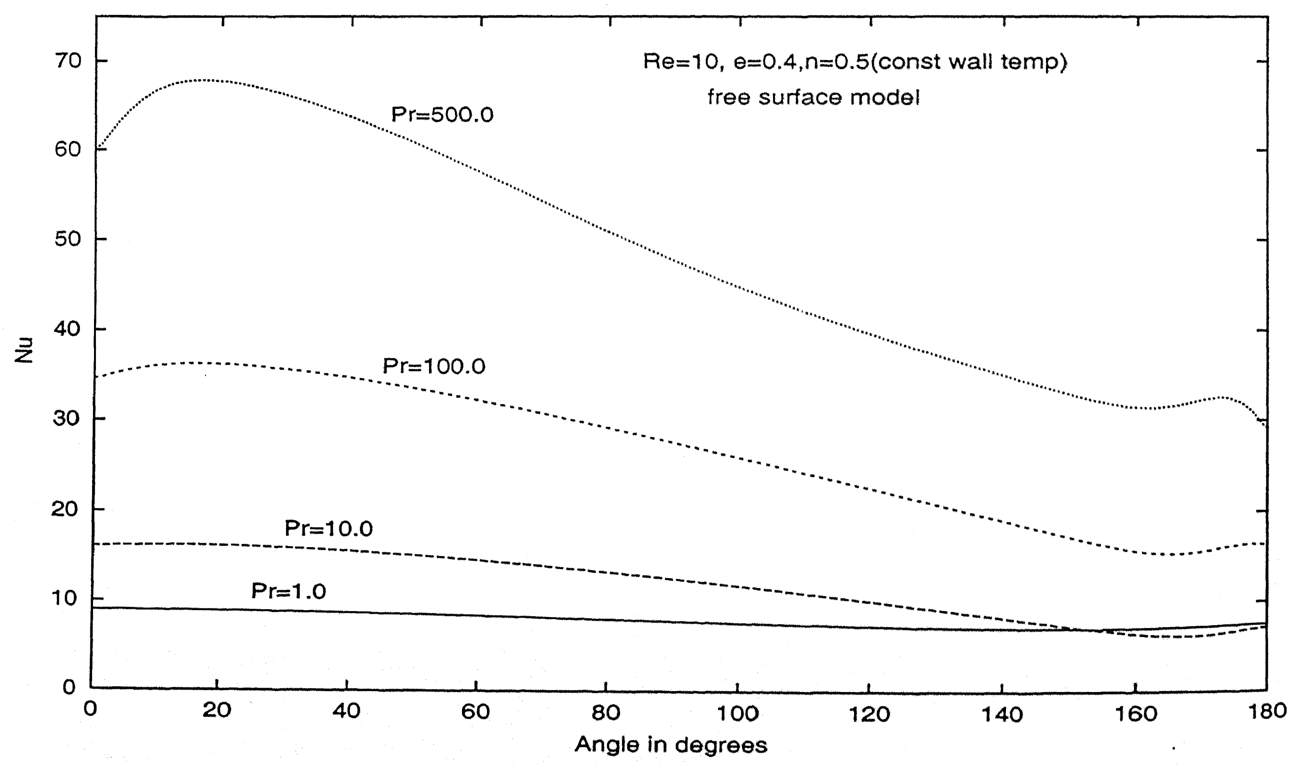

Figure 4.16: Variation of Nusselt number with angle for Re=10.0,e=0.4 and n=0.5 for constant surface temperature condition

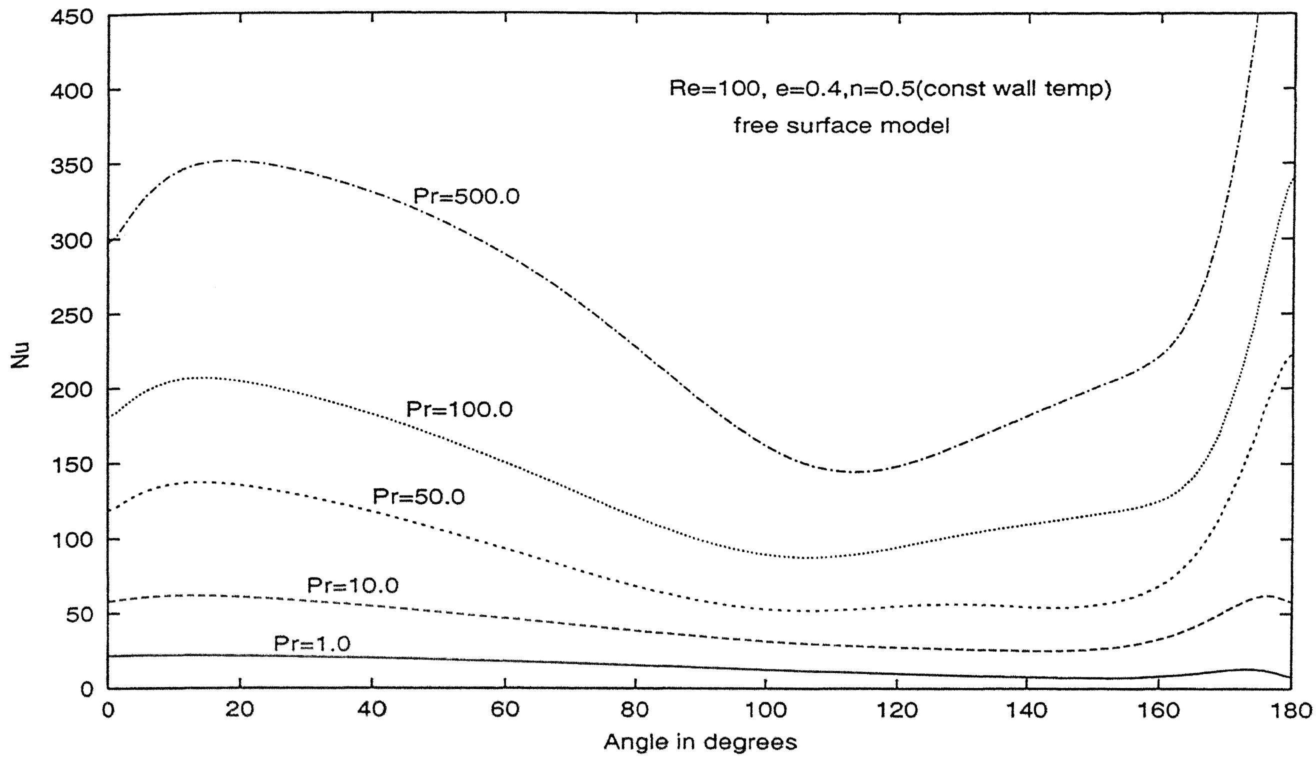

Figure 4.17: Variation of Nusselt number with angle for Re=100.0,e=0.4 and n=0.5 for constant surface temperature condition

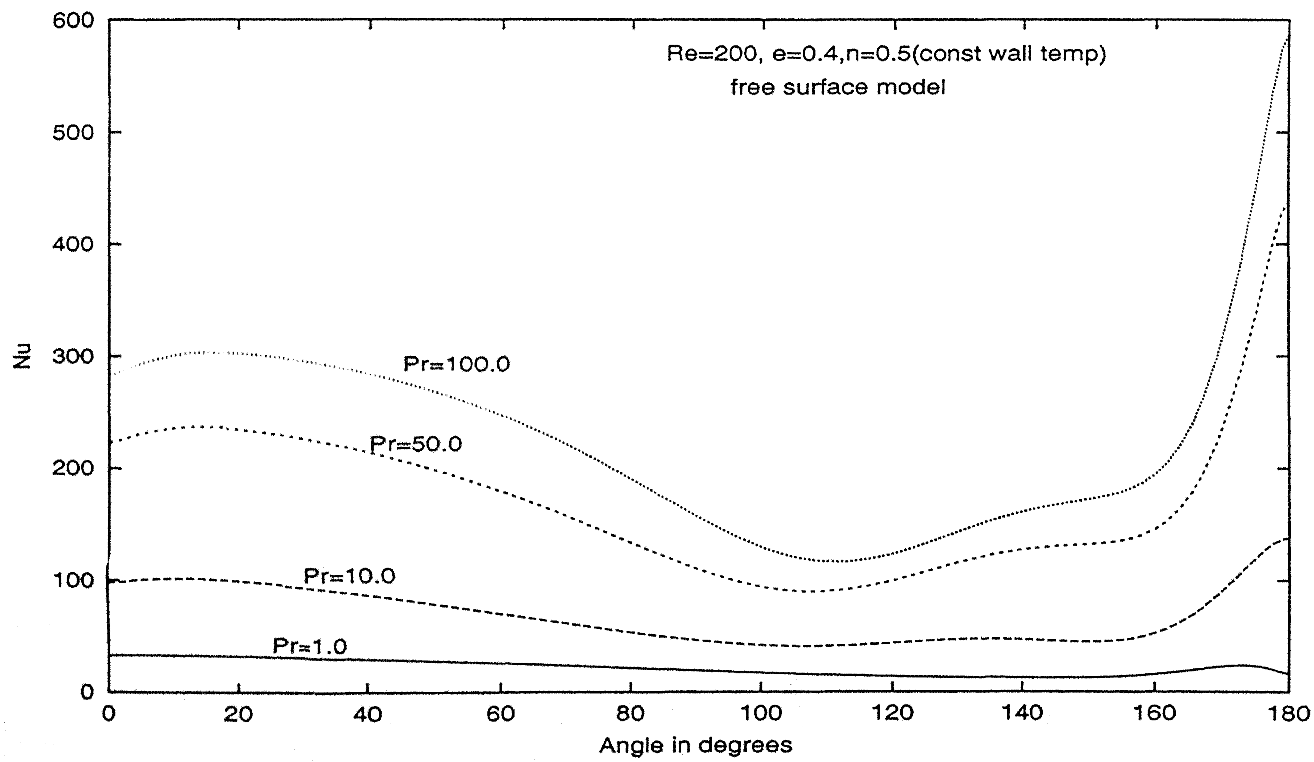

Figure 4.18: Variation of Nusselt number with angle for Re=200.0,e=0.4 and n=0.5 for constant surface temperature condition

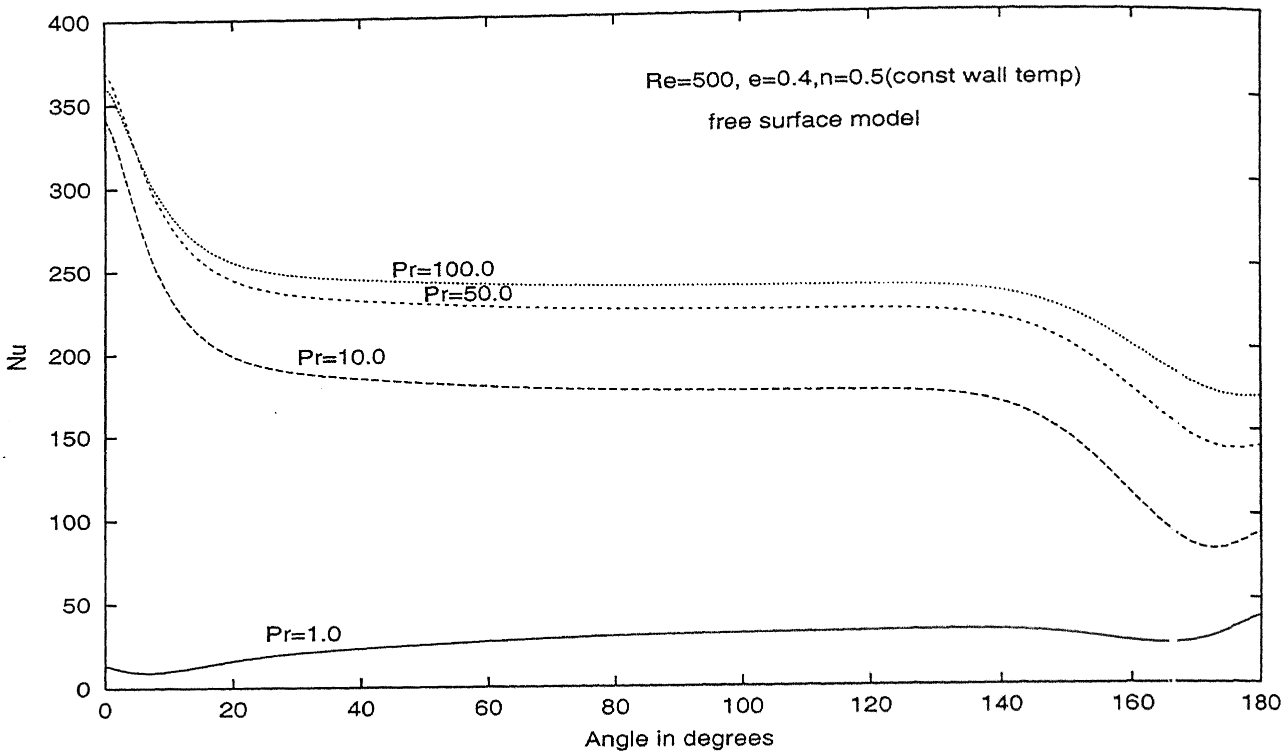

Figure 4.19: Variation of Nusselt number with angle for Re=1.0,e=0.4 and n=0.5 for constant surface temperature condition

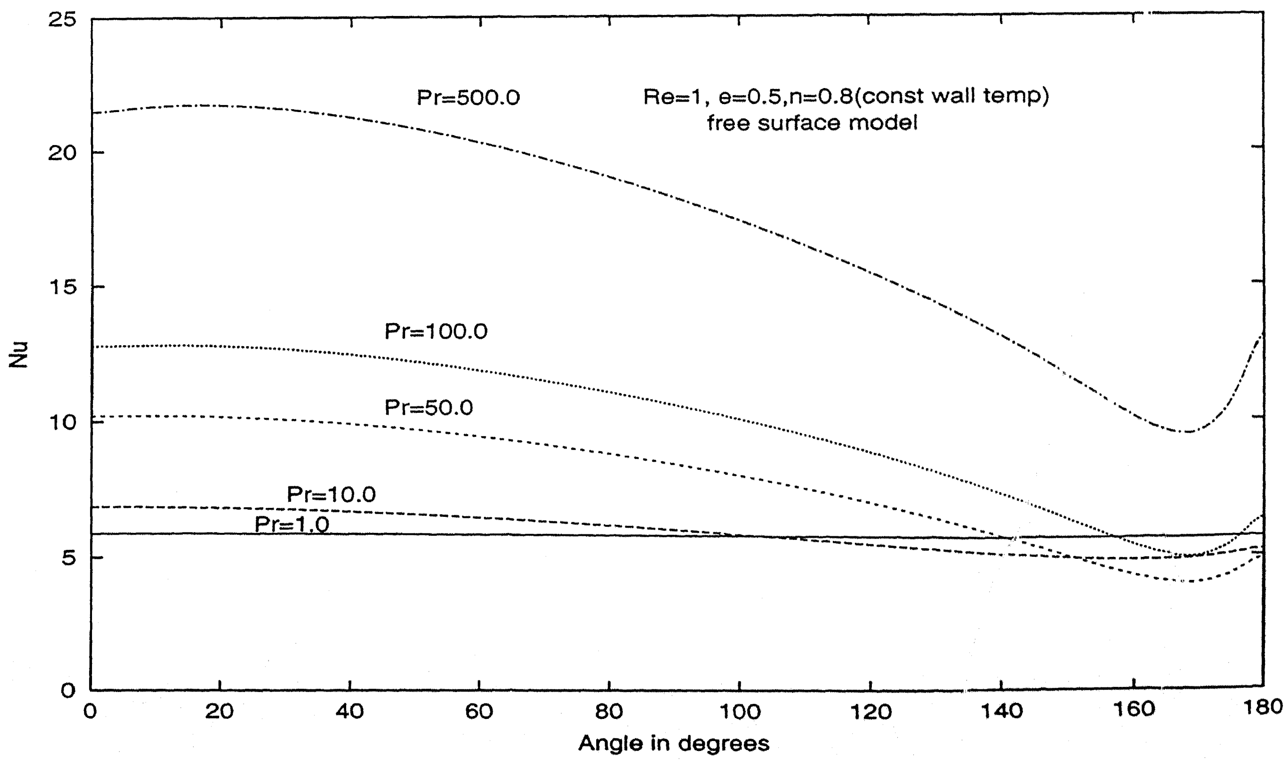

Figure 4.20: Variation of Nusselt number with angle for Re=1.0,e=0.5 and n=0.8 for constant surface temperature condition

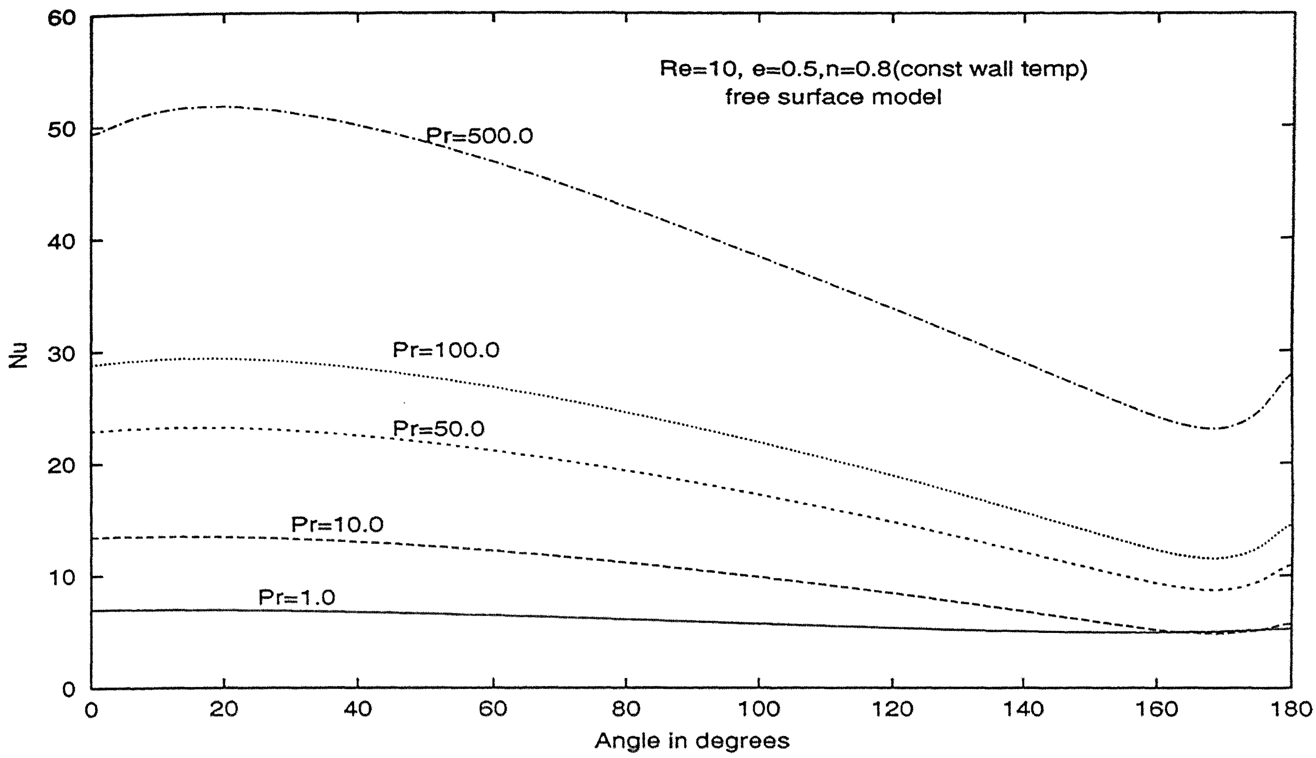

Figure 4.21: Variation of Nusselt number with angle for Re=10.0,e=0.5 and n=0.8 for constant surface temperature condition

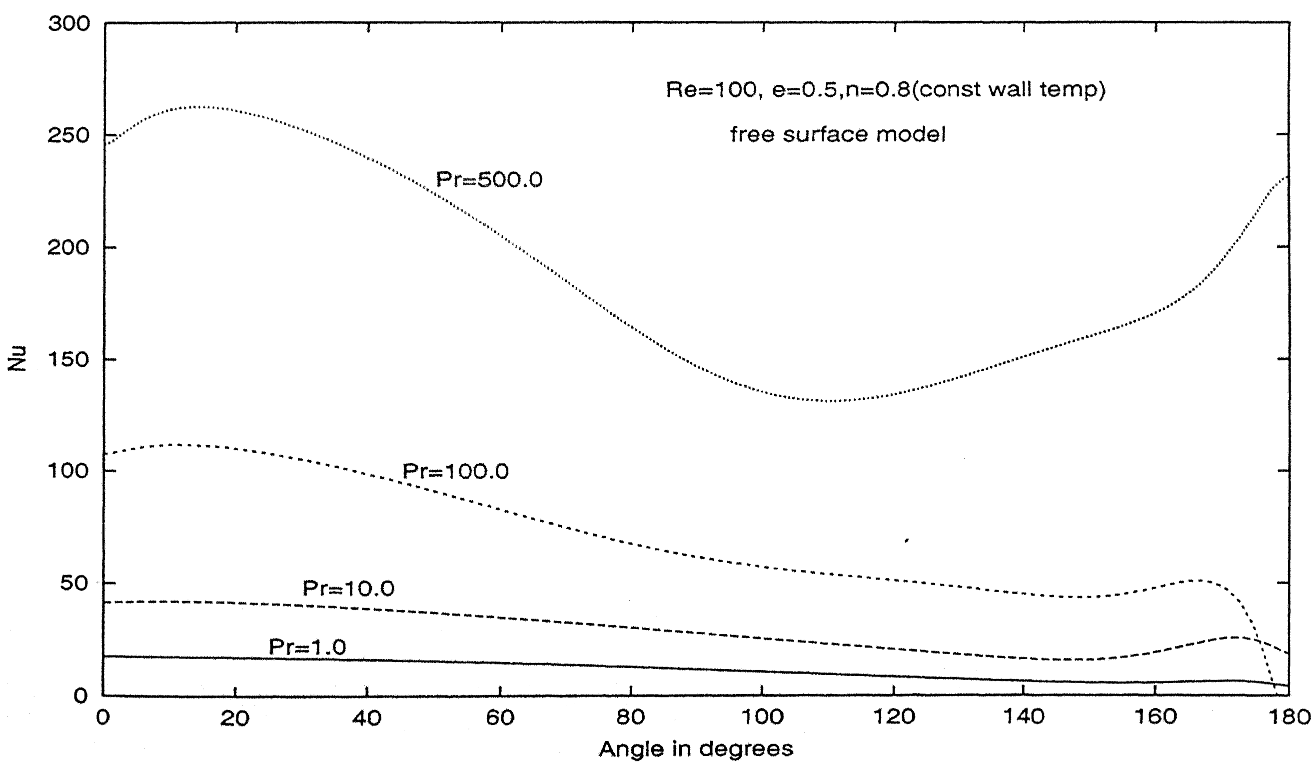

Figure 4.22: Variation of Nusselt number with angle for Re=100.0,e=0.5 and n=0.8 for constant surface temperature condition

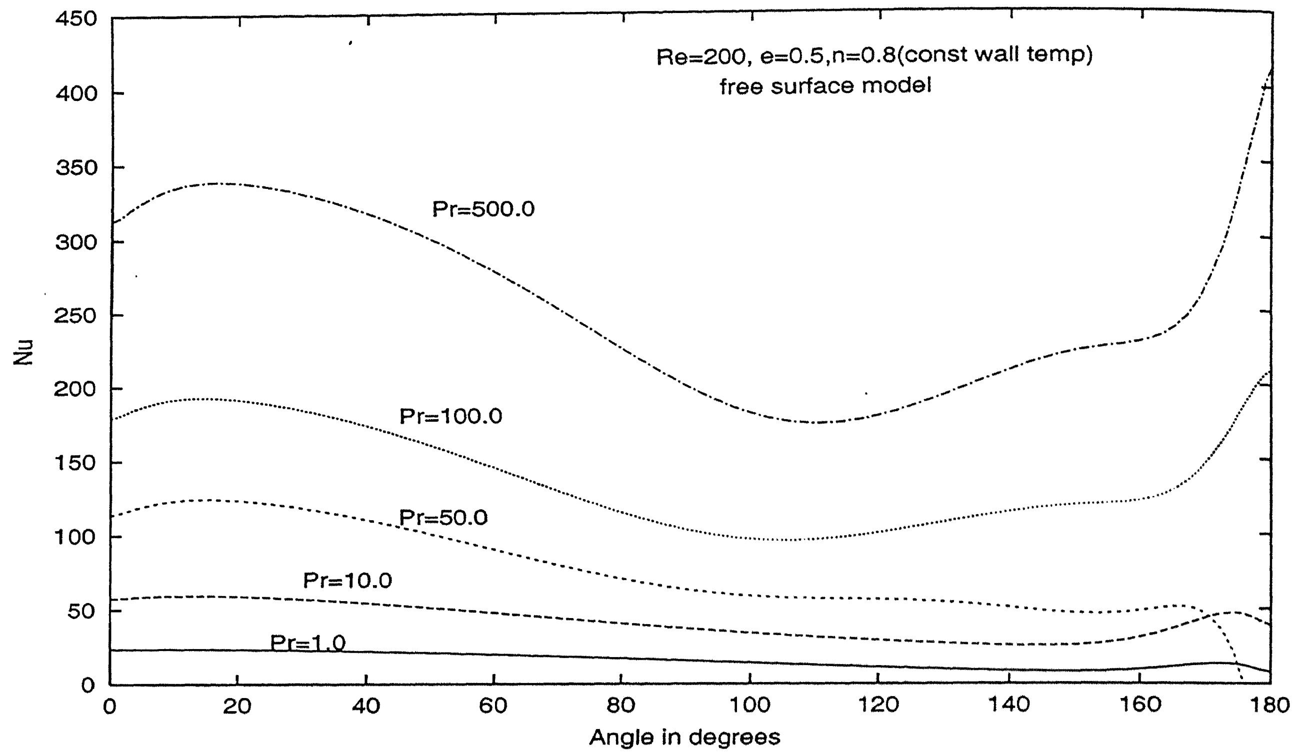

Figure 4.23: Variation of Nusselt number with angle for Re=200.0,e=0.5 and n=0.8 for constant surface temperature condition

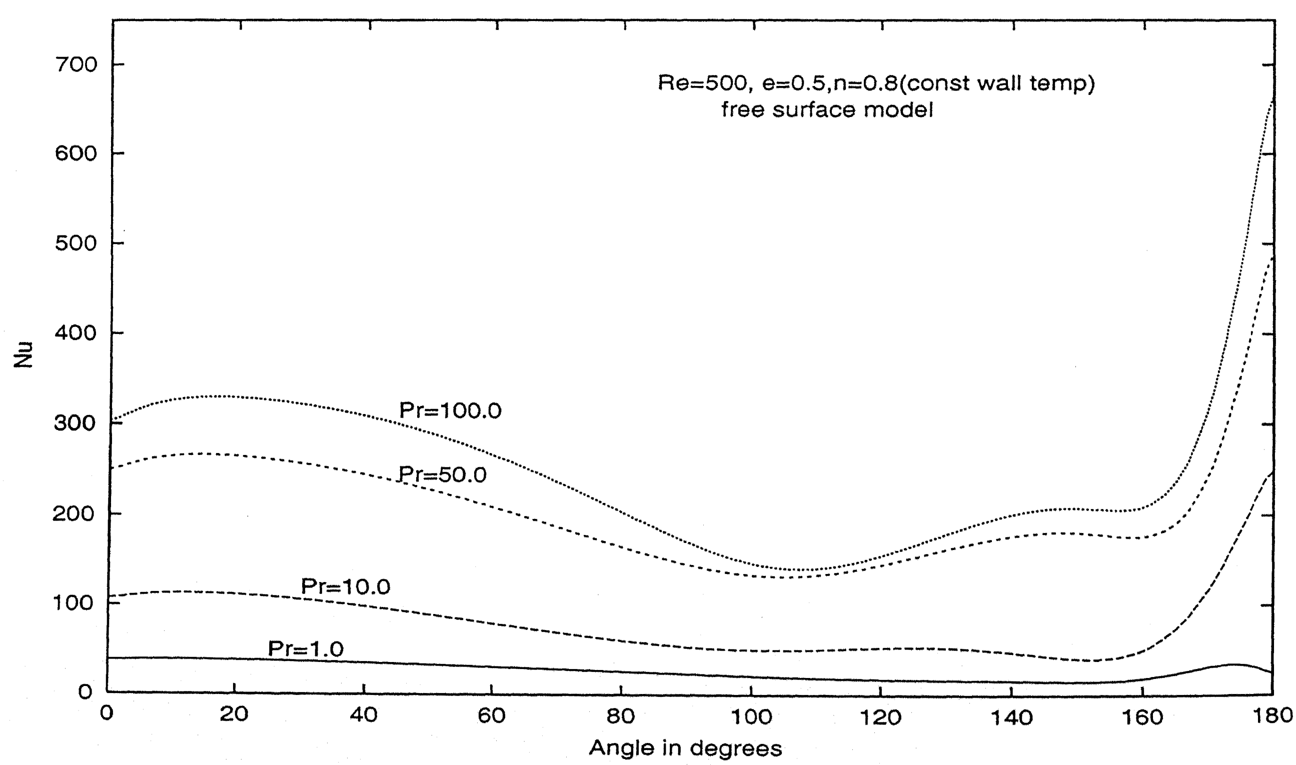

Figure 4.24: Variation of Nusselt number with angle for Re=500.0,e=0.5 and n=0.8 for constant surface temperature condition

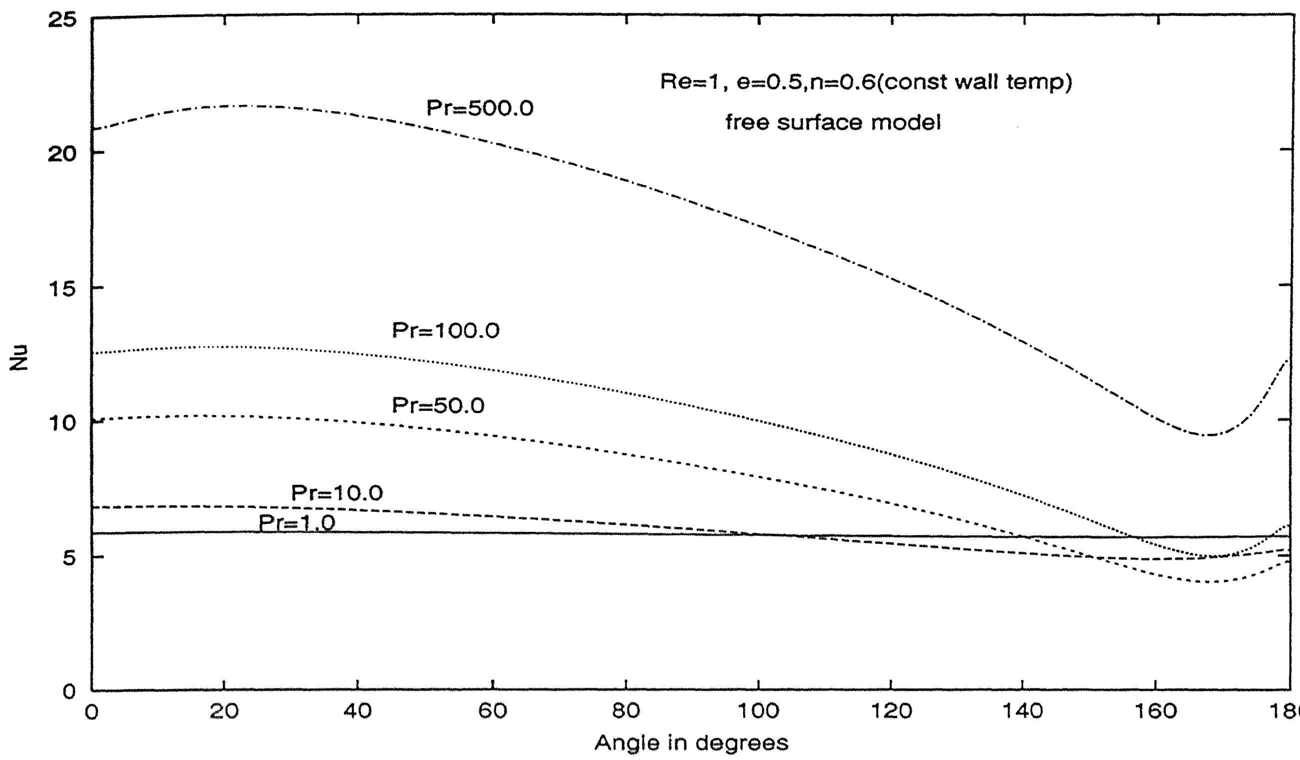

Figure 4.25: Variation of Nusselt number with angle for Re=1.0,e=0.5 and n=0.6 for constant surface temperature condition

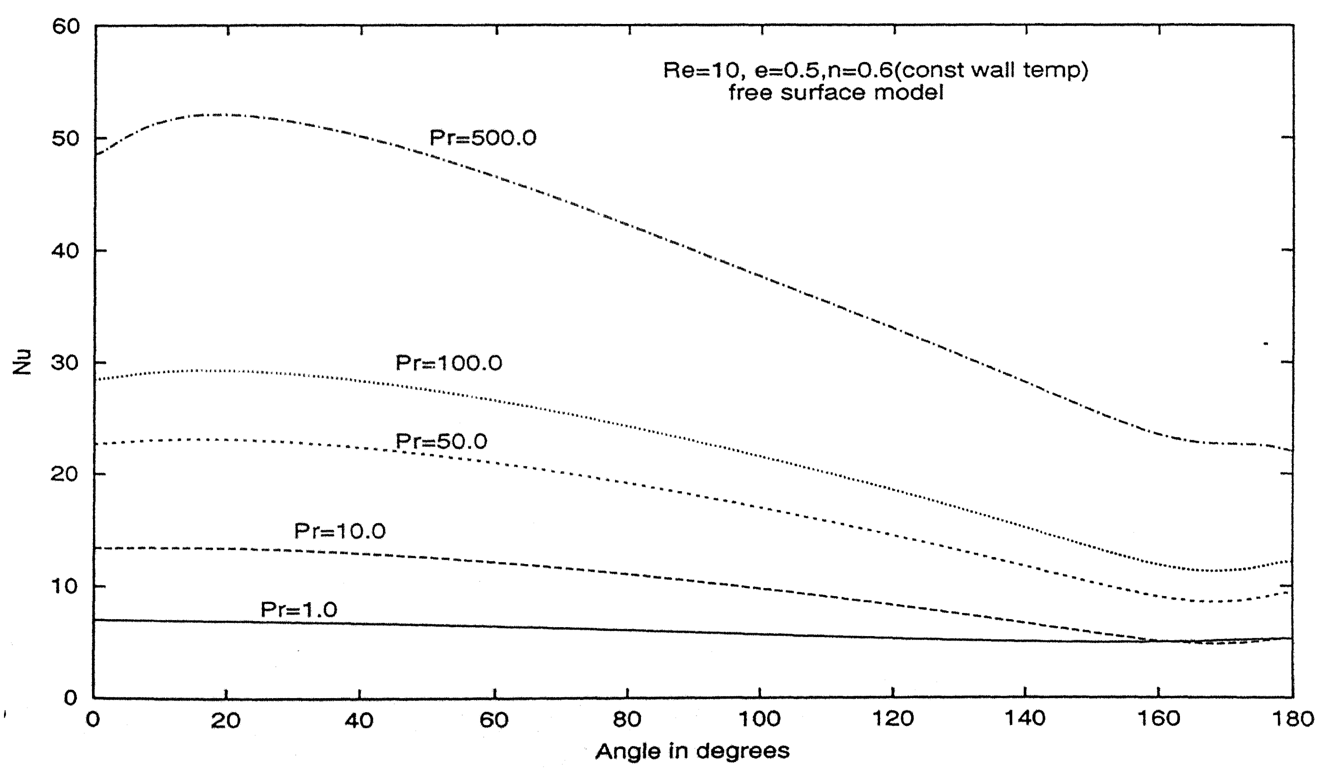

Figure 4.26: Variation of Nusselt number with angle for Re=10.0,e=0.5 and n=0.6 for constant surface temperature condition

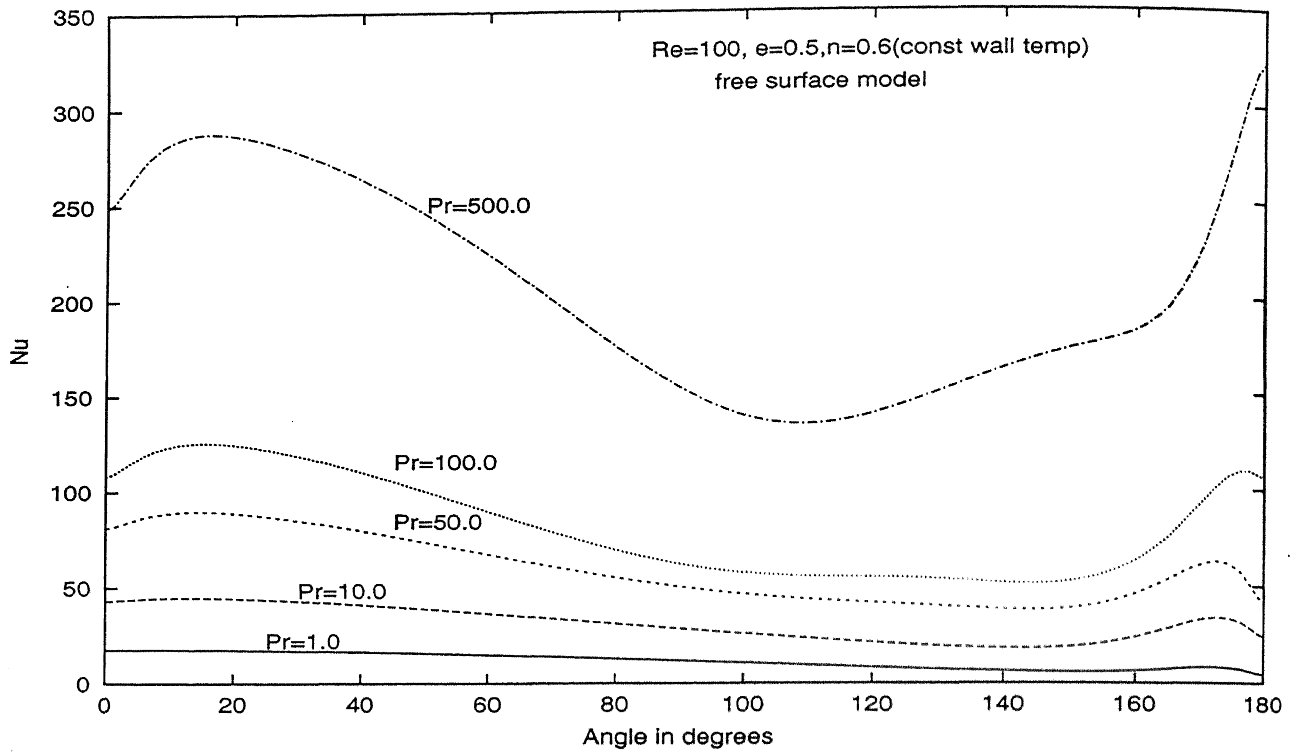

Figure 4.27: Variation of Nusselt number with angle for Re=100.0,e=0.5 and n=0.6 for constant surface temperature condition

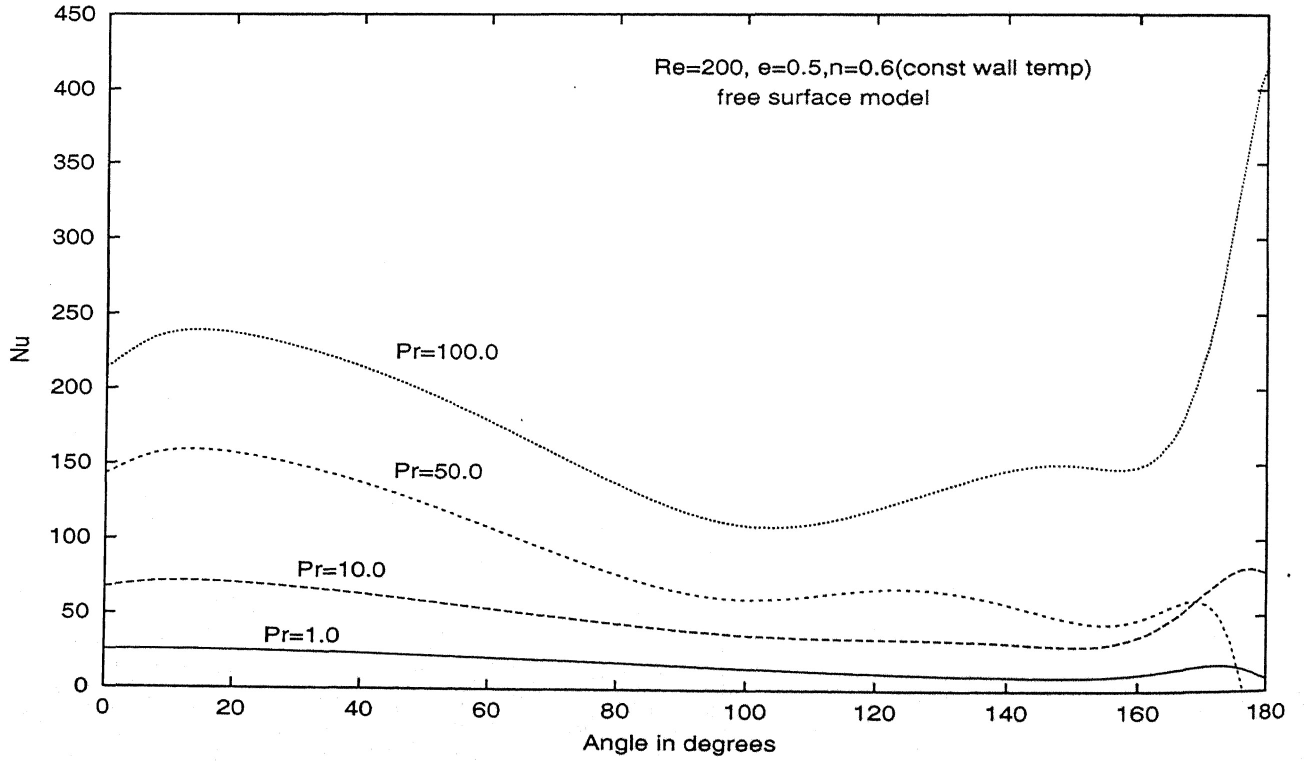

Figure 4.28: Variation of Nusselt number with angle for Re=200.0,e=0.5 and n=0.6 for constant surface temperature condition

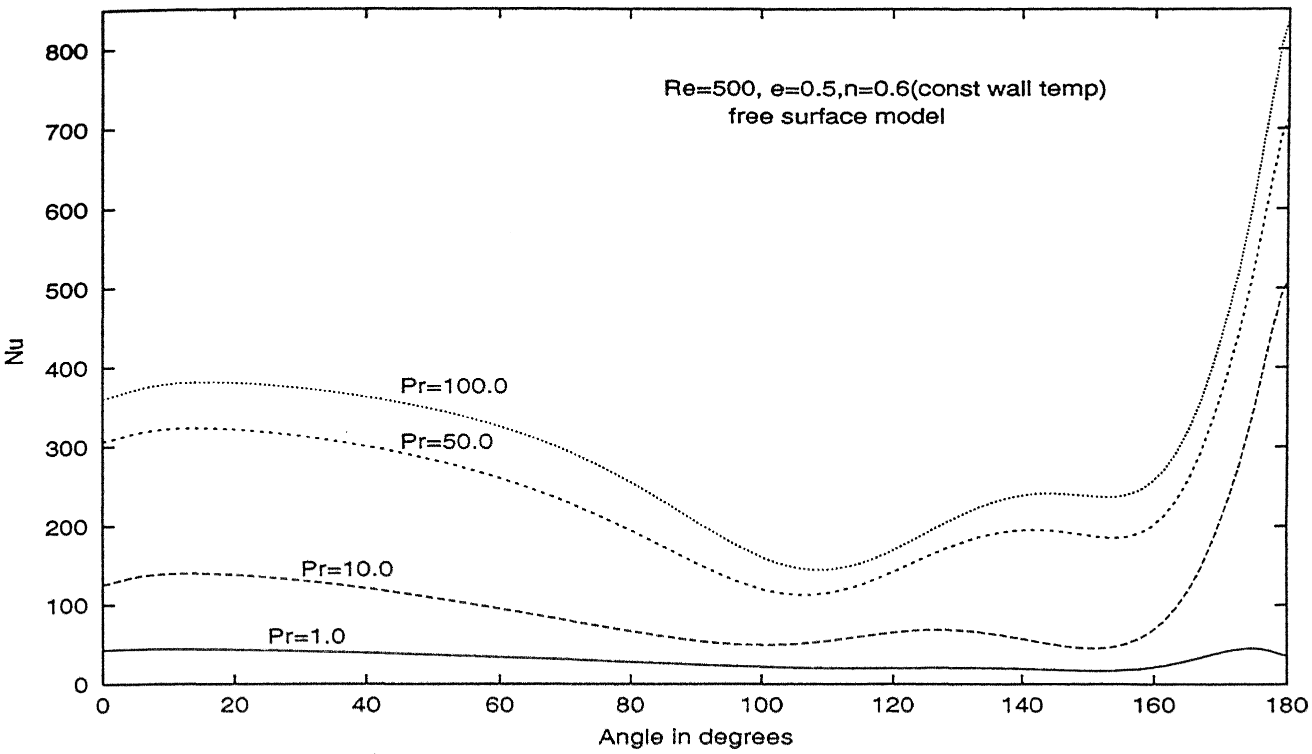

Figure 4.29: Variation of Nusselt number with angle for Re=500.0,e=0.5 and n=0.6 for constant surface temperature condition

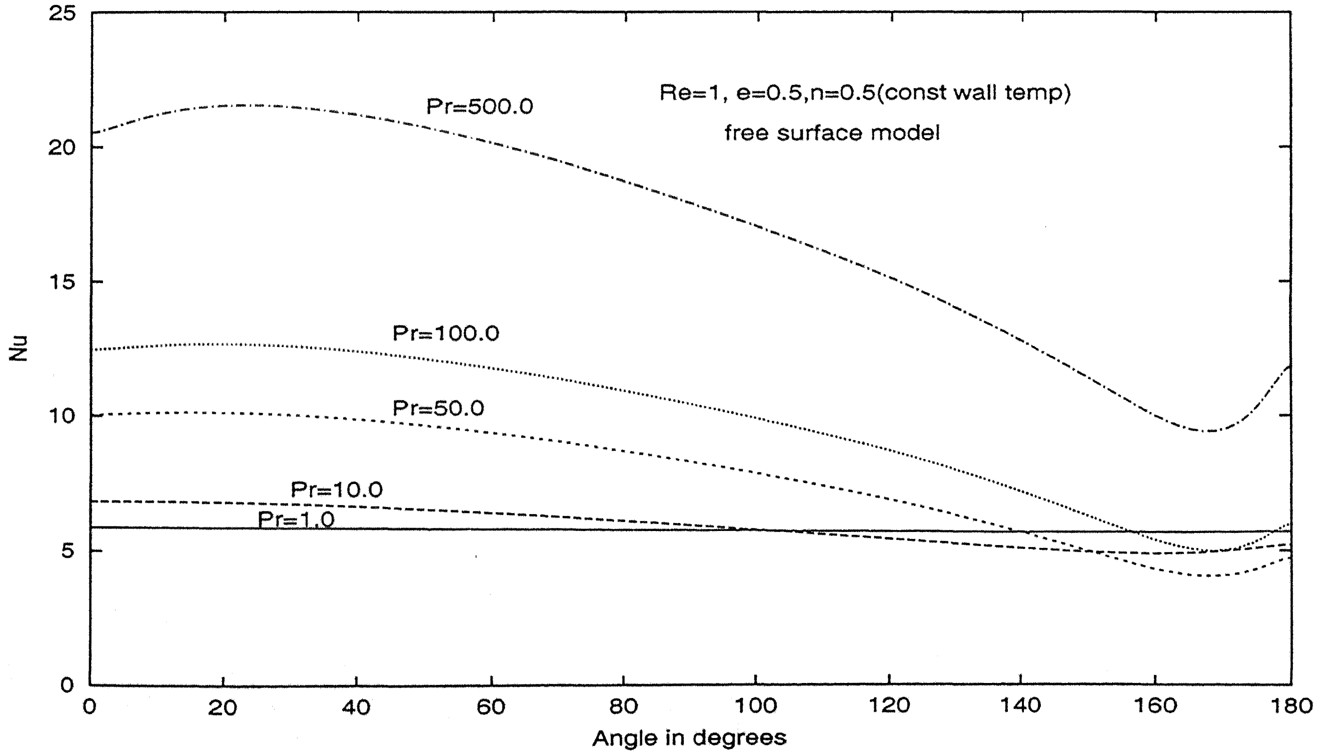

Figure 4.30: Variation of Nusselt number with angle for Re=1.0,e=0.5 and n=0.5 for constant surface temperature condition

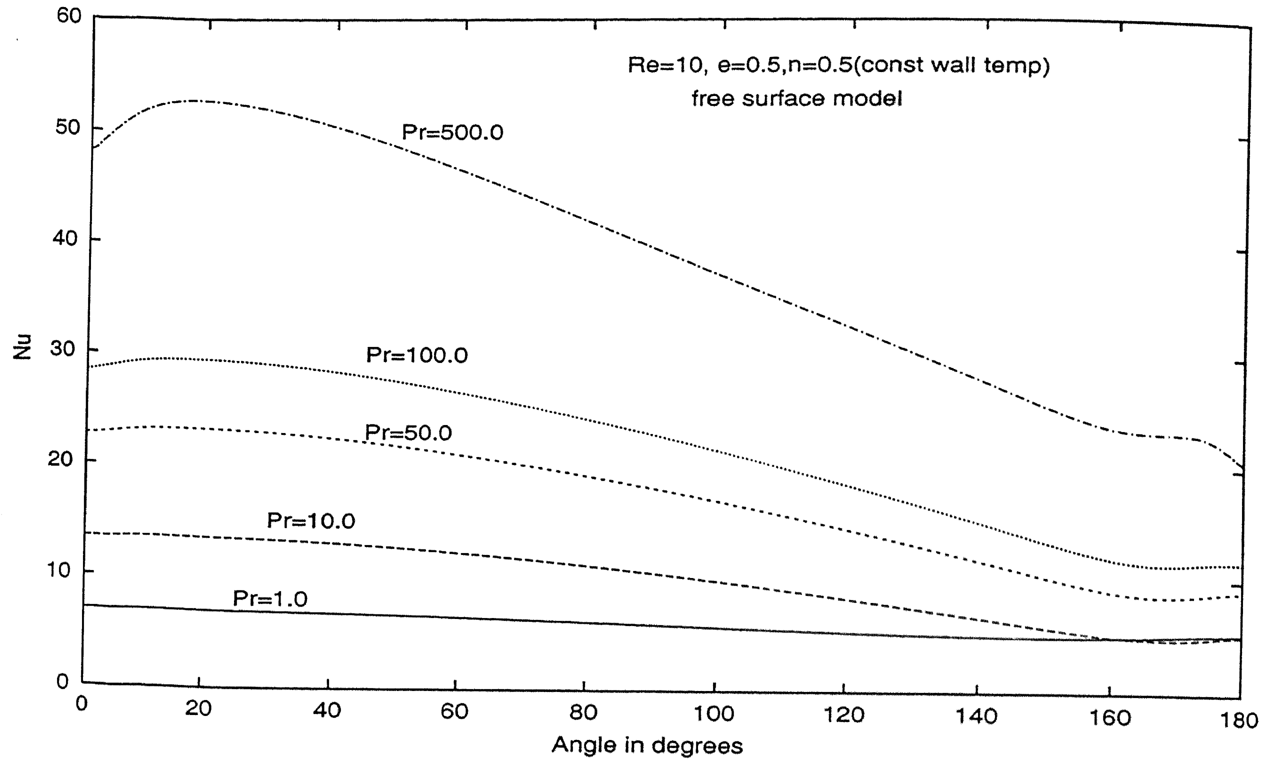

.: Variation of Nusselt number with angle for Re=10.0,e=0.5 and n=0.5 for constant surface tempera

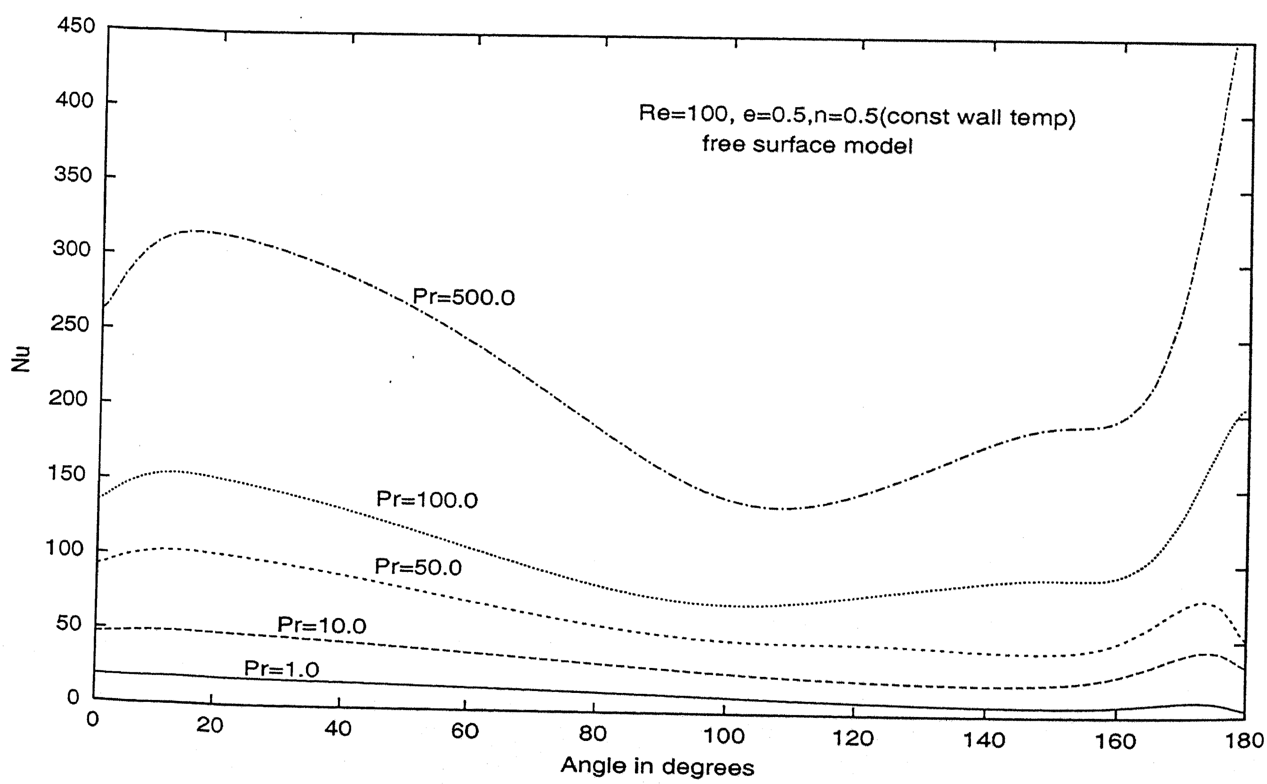

Figure 4.32: Variation of Nusselt number with angle for Re=100.0,e=0.5 and n=0.5 for constant surface temperature condition

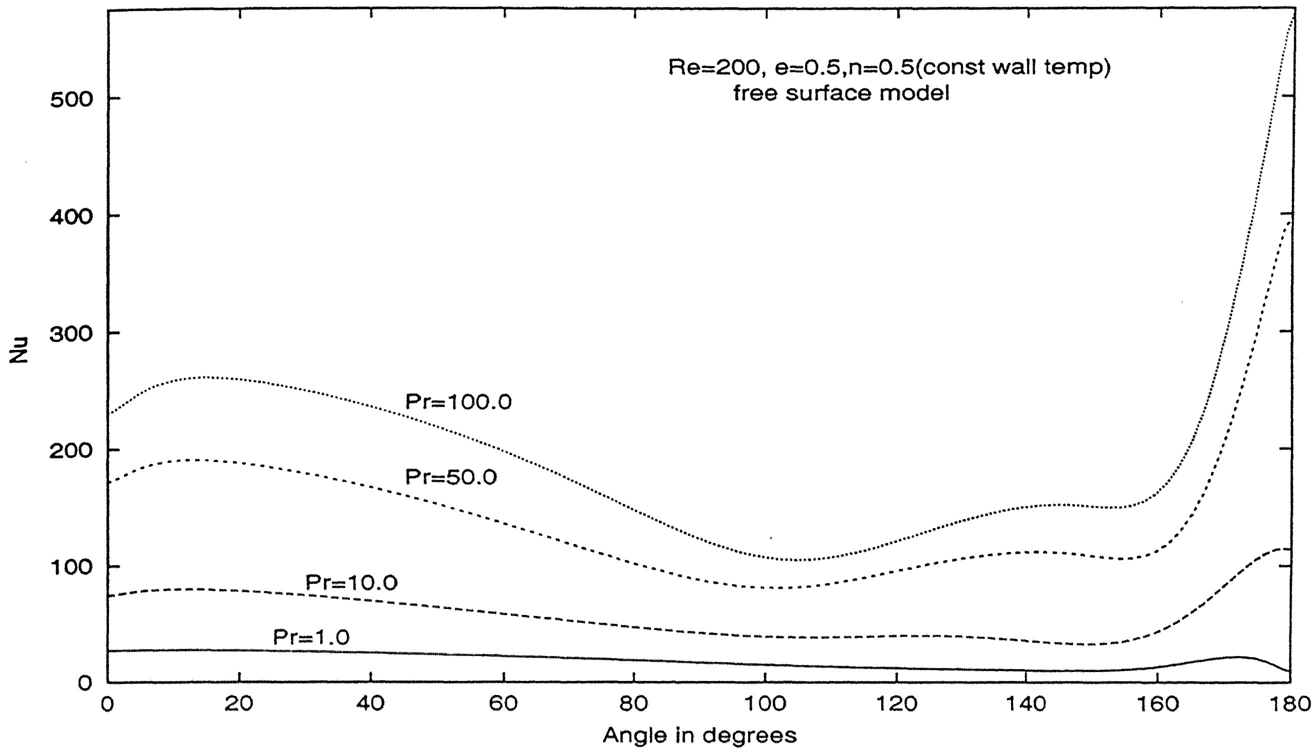

Figure 4.33: Variation of Nusselt number with angle for Re=200.0,e=0.5 and n=0.5 for constant surface temperature condition

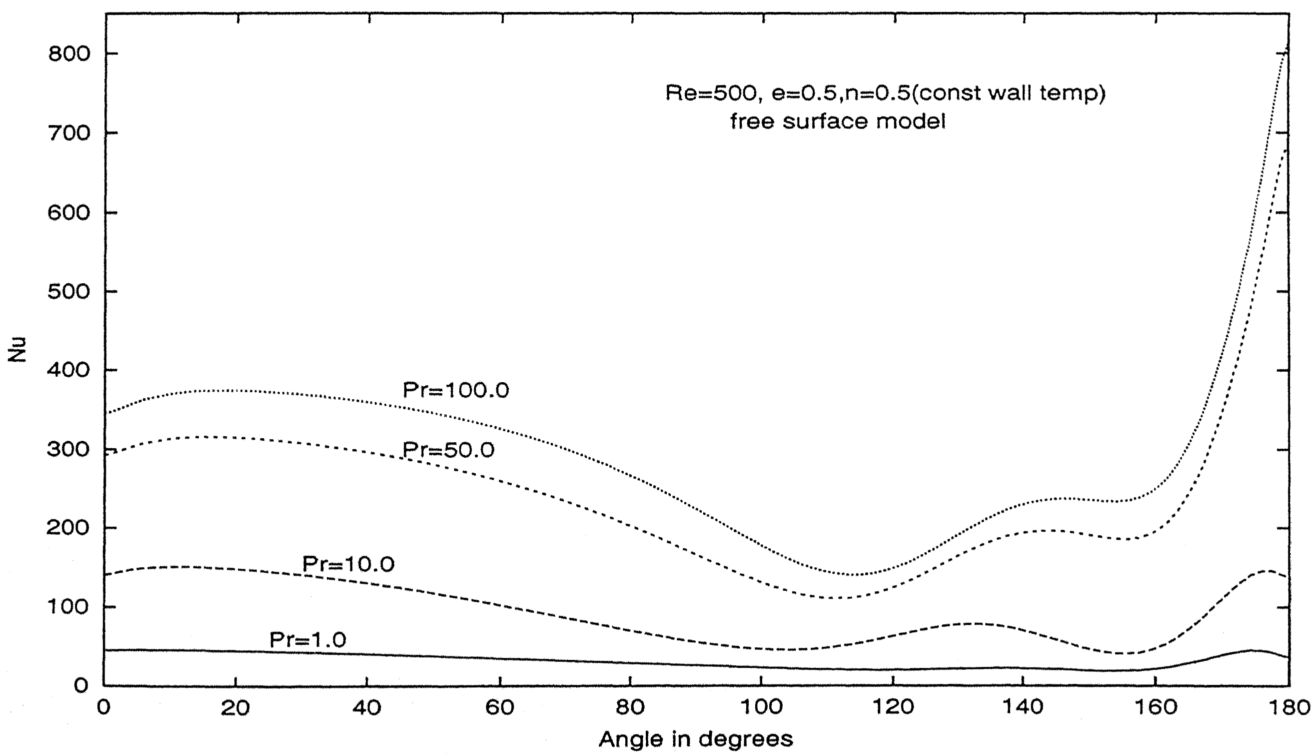

Figure 4.34: Variation of Nusselt number with angle for Re=500.0,e=0.5 and n=0.5 for constant surface temperature condition

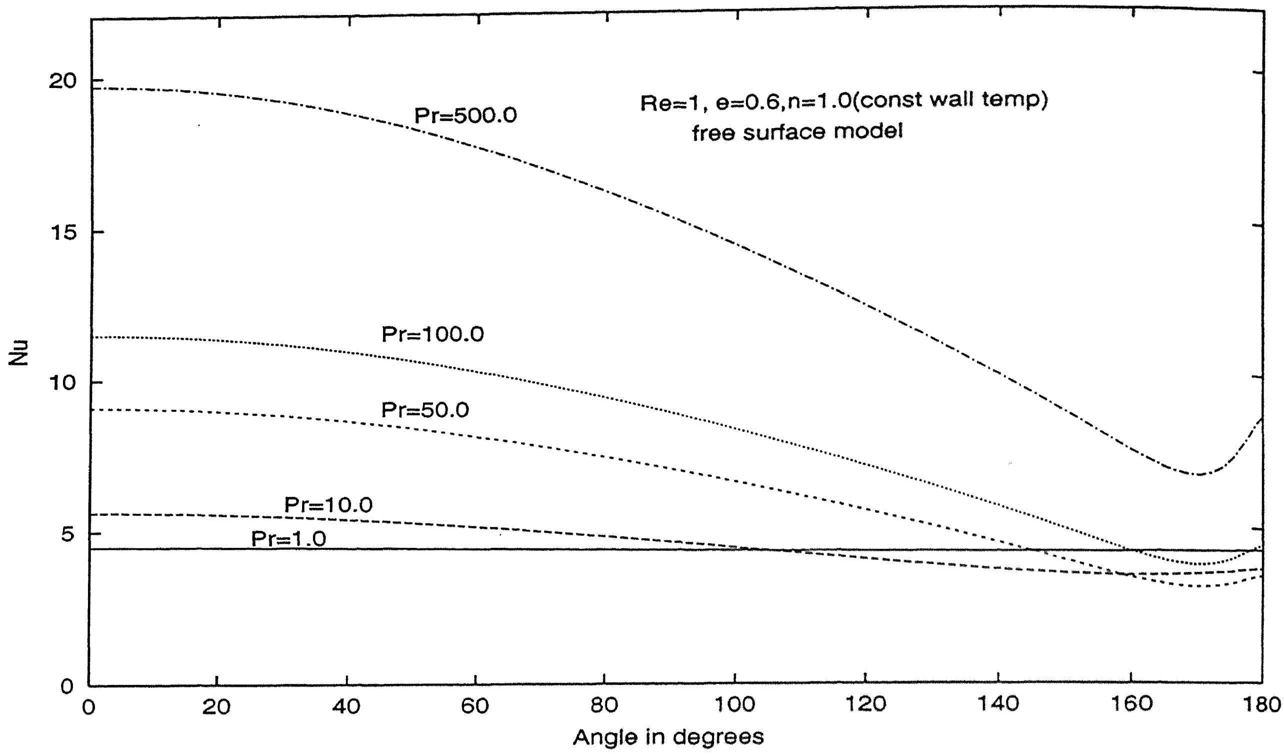

Figure 4.35: Variation of Nusselt number with angle for Re=1.0,e=0.6 and n=1.0 for constant surface temperature condition

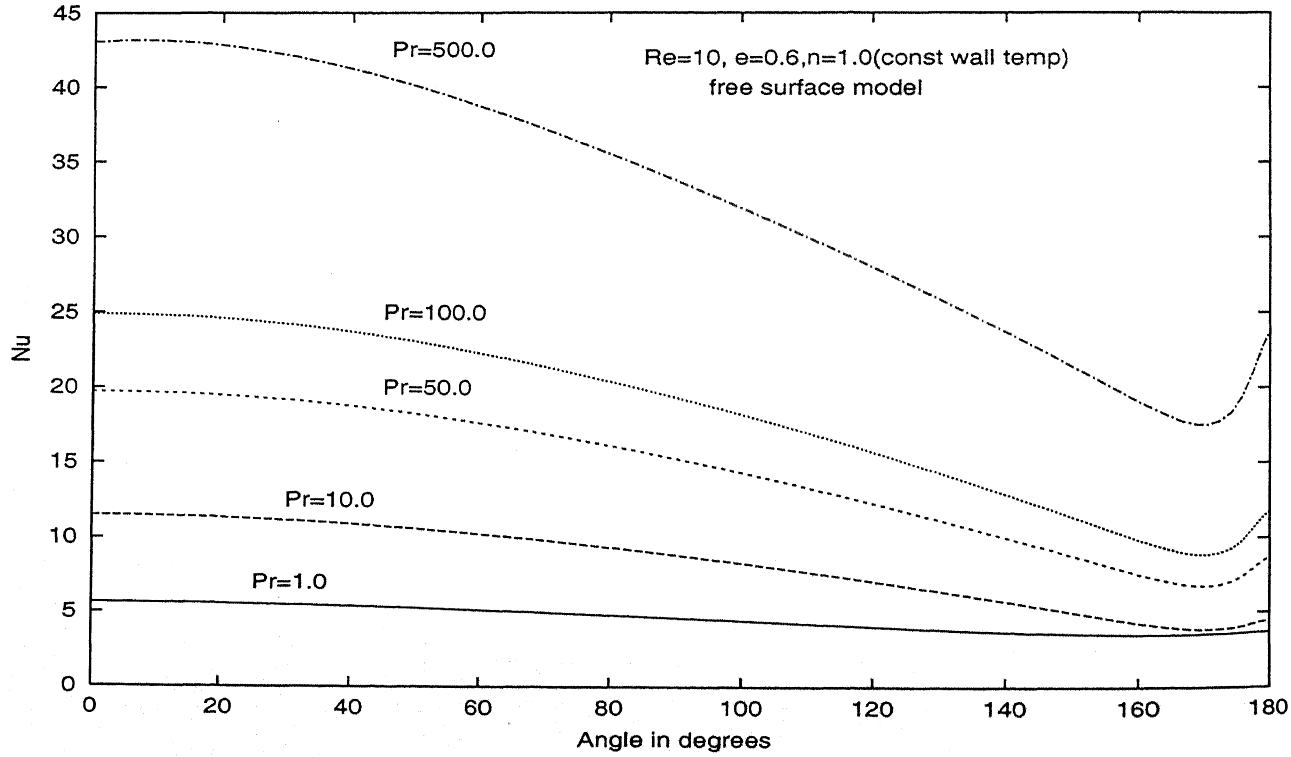

Figure 4.36: Variation of Nusselt number with angle for Re=10.0,e=0.6 and n=1.0 for constant surface temperature condition

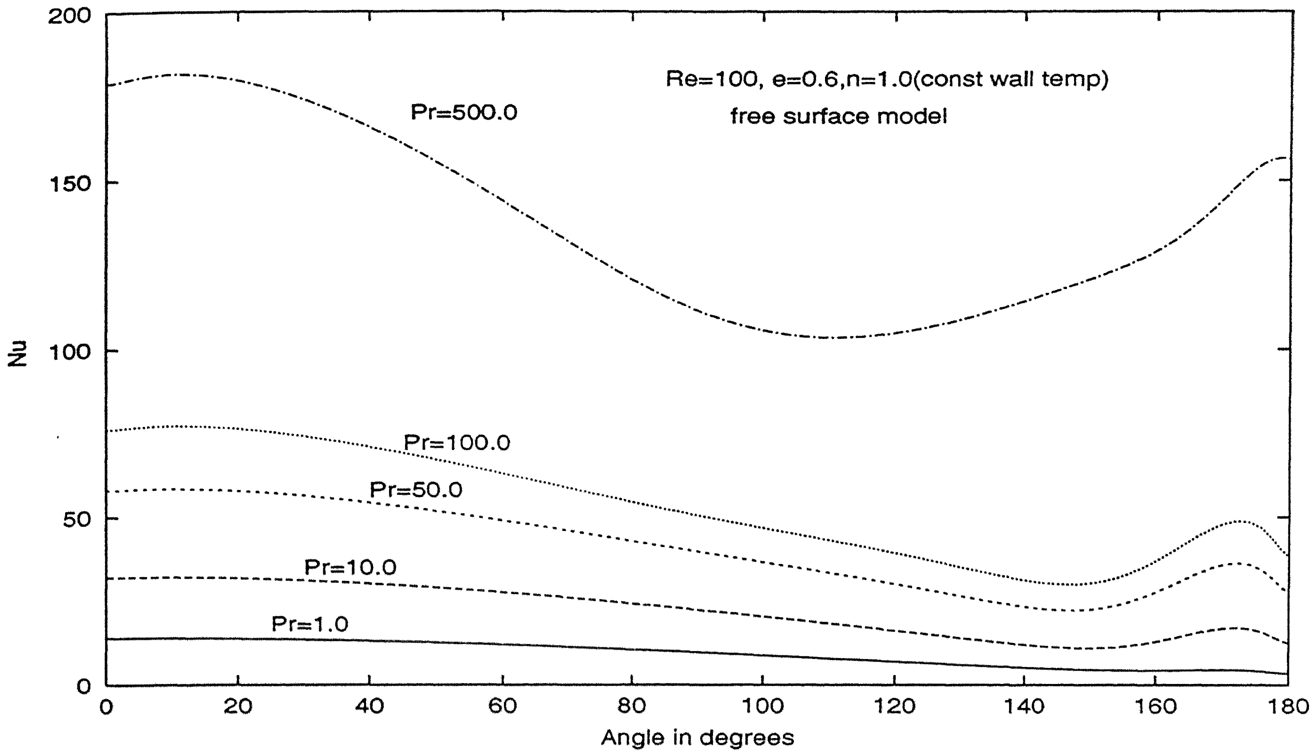

Figure 4.37: Variation of Nusselt number with angle for Re=100.0,e=0.6 and n=1.0 for constant surface temperature condition

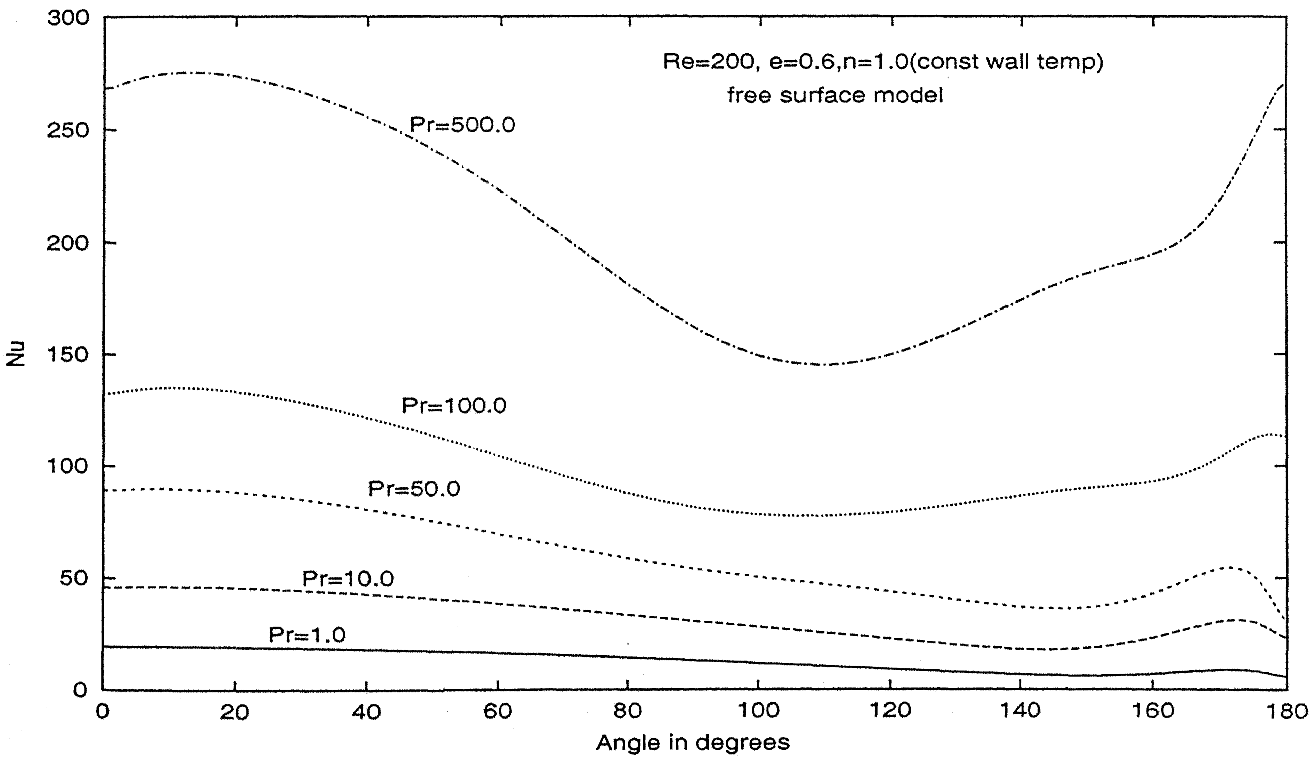

Figure 4.38: Variation of Nusselt number with angle for Re=200.0,e=0.6 and n=1.0 for constant surface temperature condition

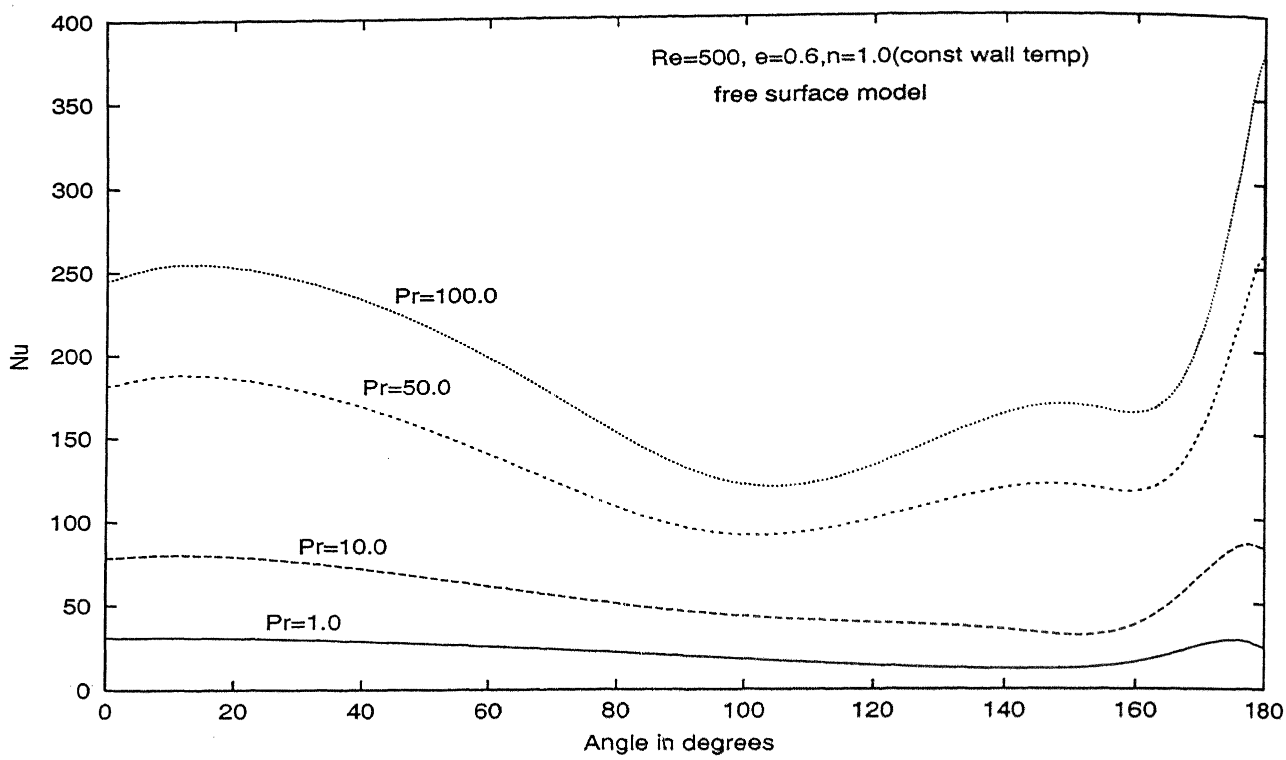

Figure 4.39: Variation of Nusselt number with angle for Re=500.0,e=0.6 and n=1.0 for constant surface temperature condition

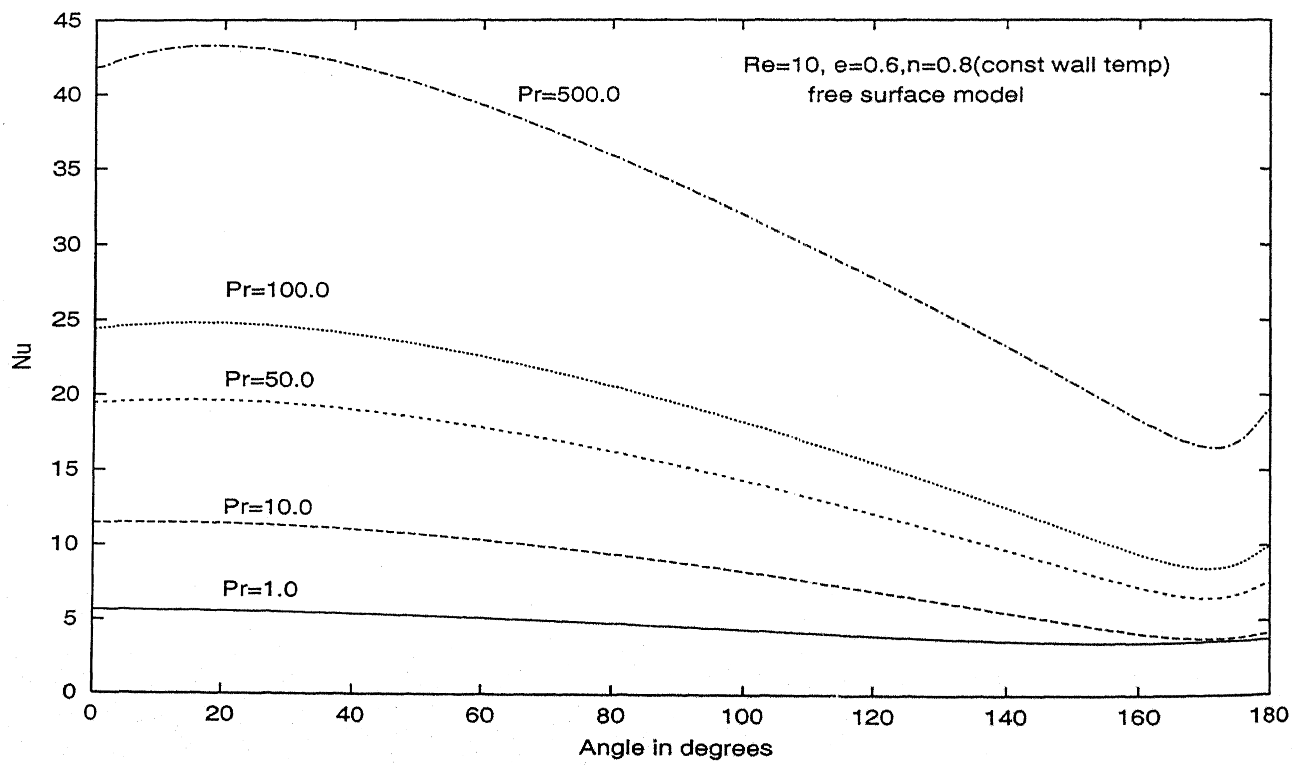

Figure 4.40: Variation of Nusselt number with angle for Re=10.0,e=0.6 and n=0.8 for constant surface temperature condition

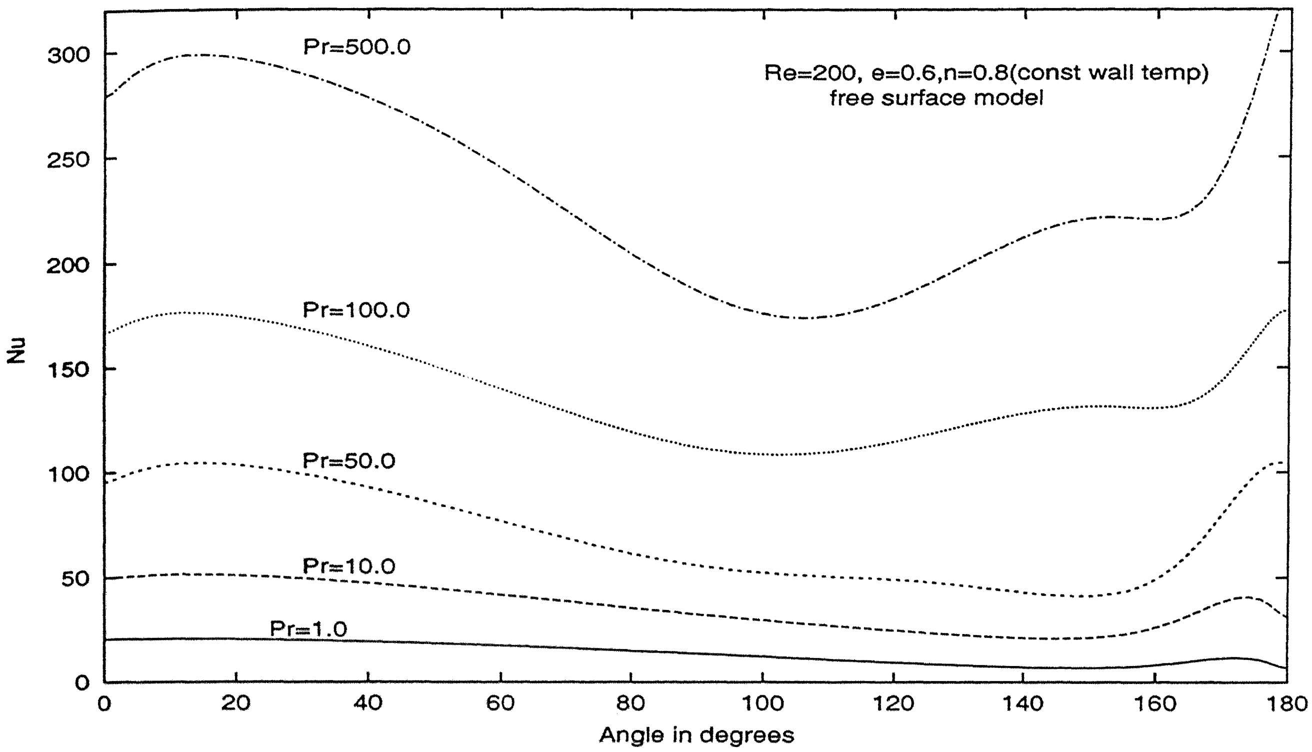

Figure 4.41: Variation of Nusselt number with angle for Re=200.0,e=0.6 and n=0.8 for constant surface temperature condition

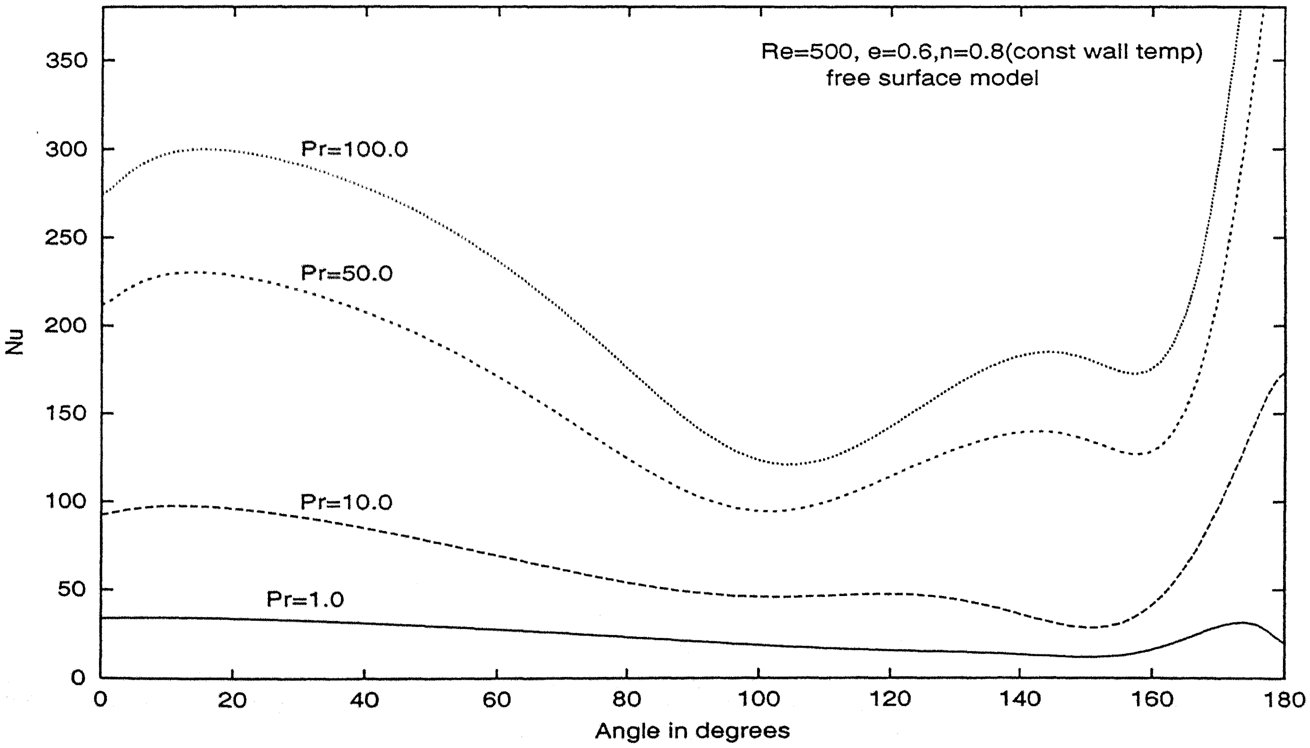

Figure 4.42: Variation of Nusselt number with angle for Re=500.0,e=0.6 and n=0.8 for constant surface temperature condition

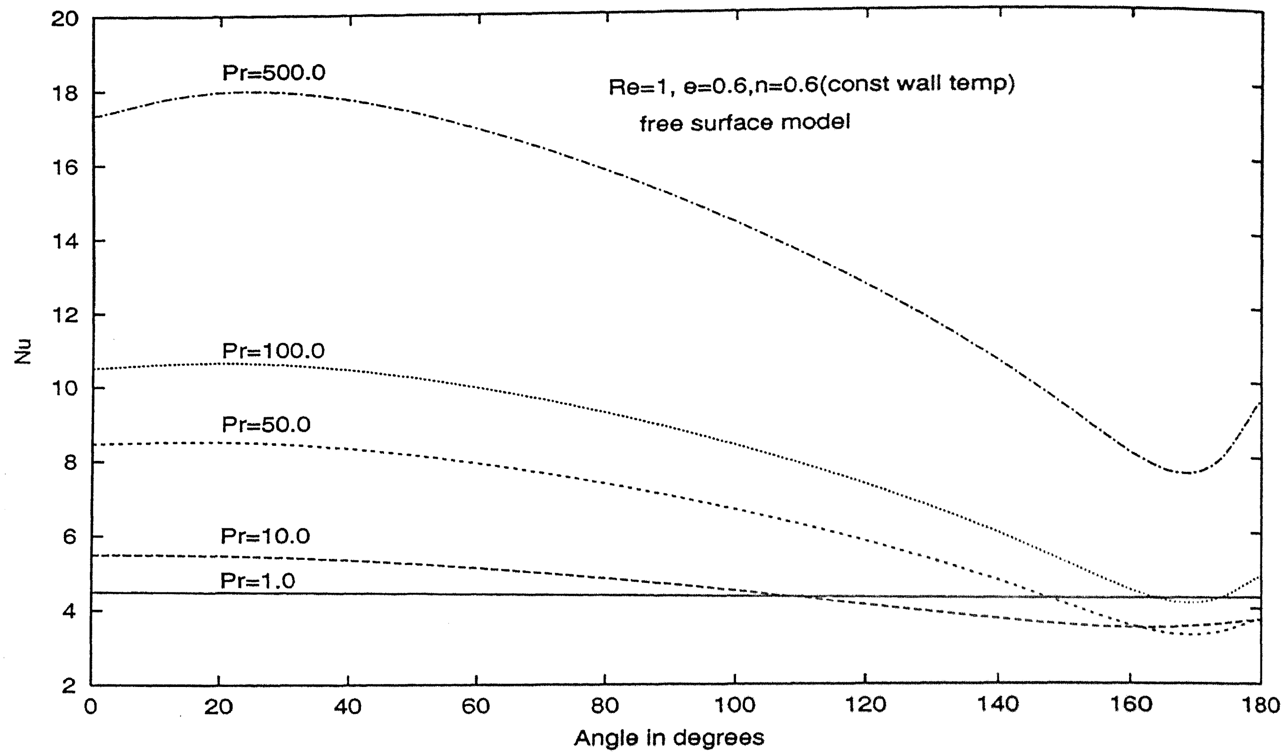

Figure 4.43: Variation of Nusselt number with angle for Re=1.0,e=0.6 and n=0.6 for constant surface temperature condition

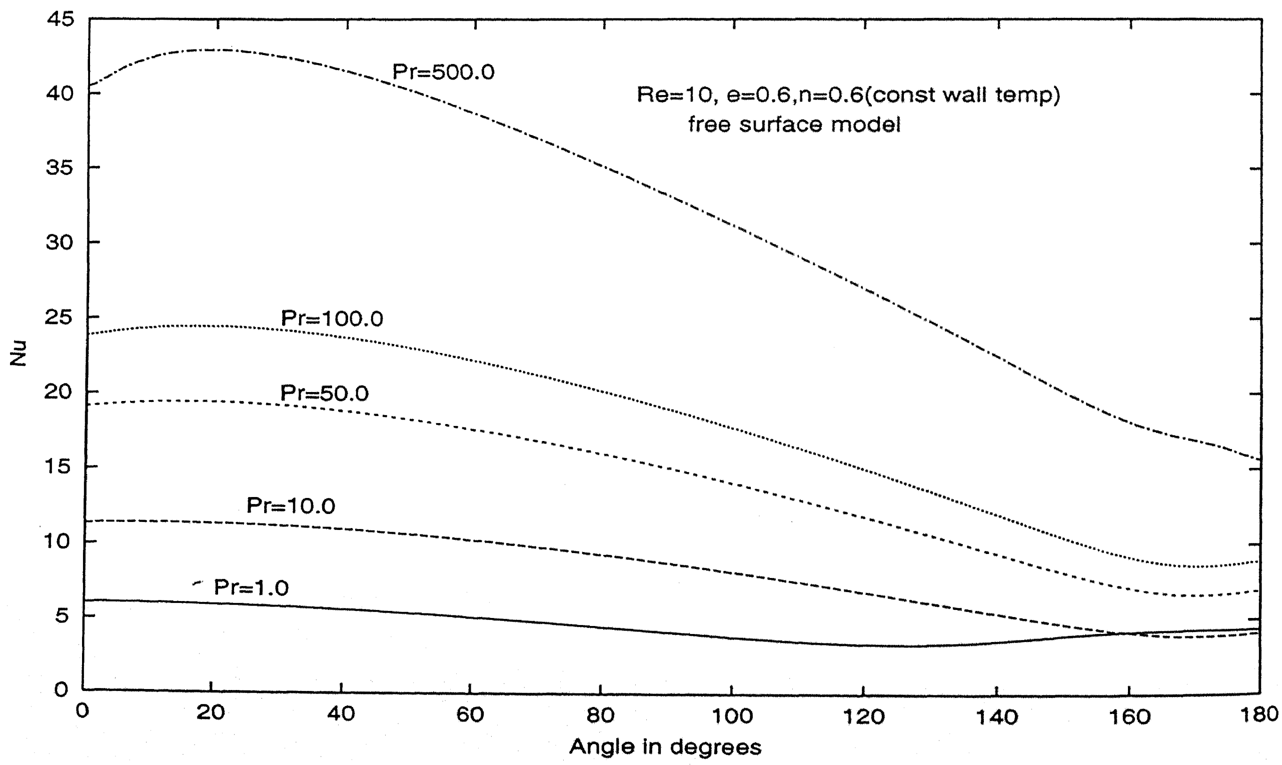

Figure 4.44: Variation of Nusselt number with angle for Re=10.0,e=0.6 and n=0.6 for constant surface temperature condition

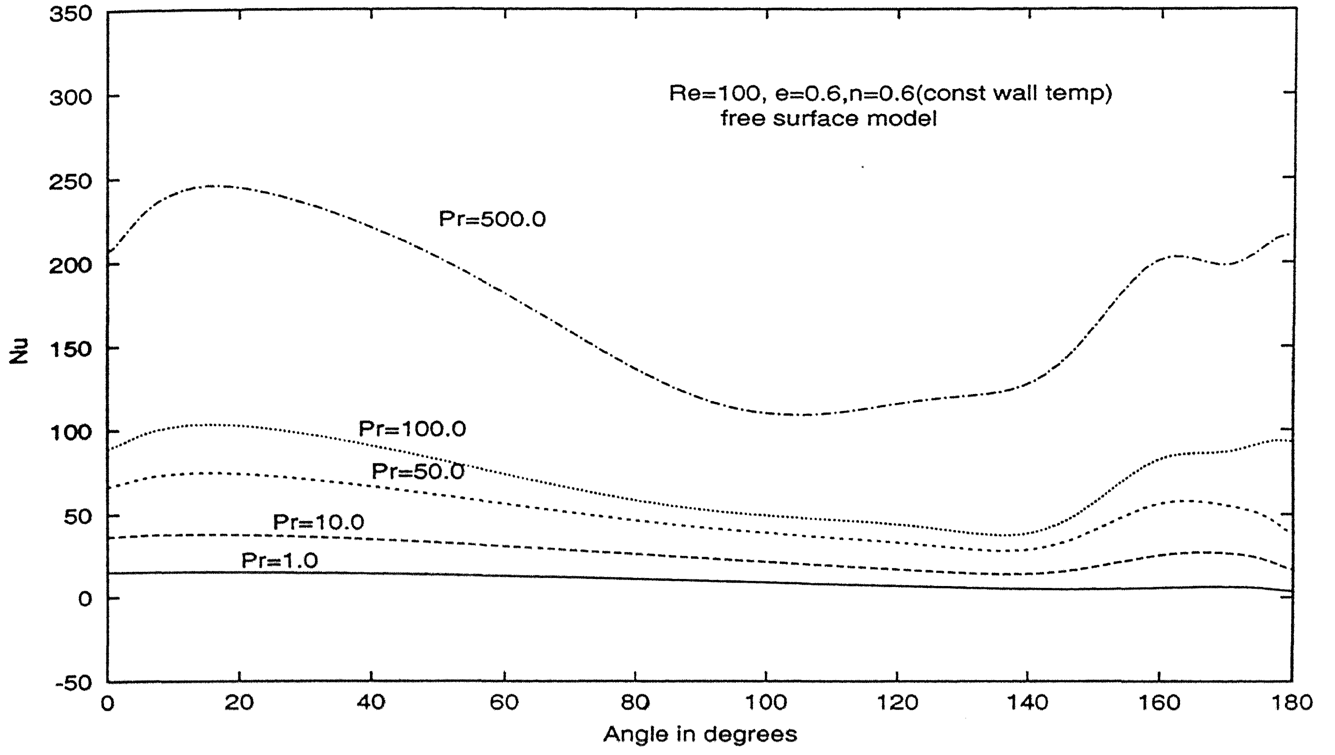

Figure 4.45: Variation of Nusselt number with angle for Re=100.0,e=0.6 and n=0.6 for constant surface temperature condition

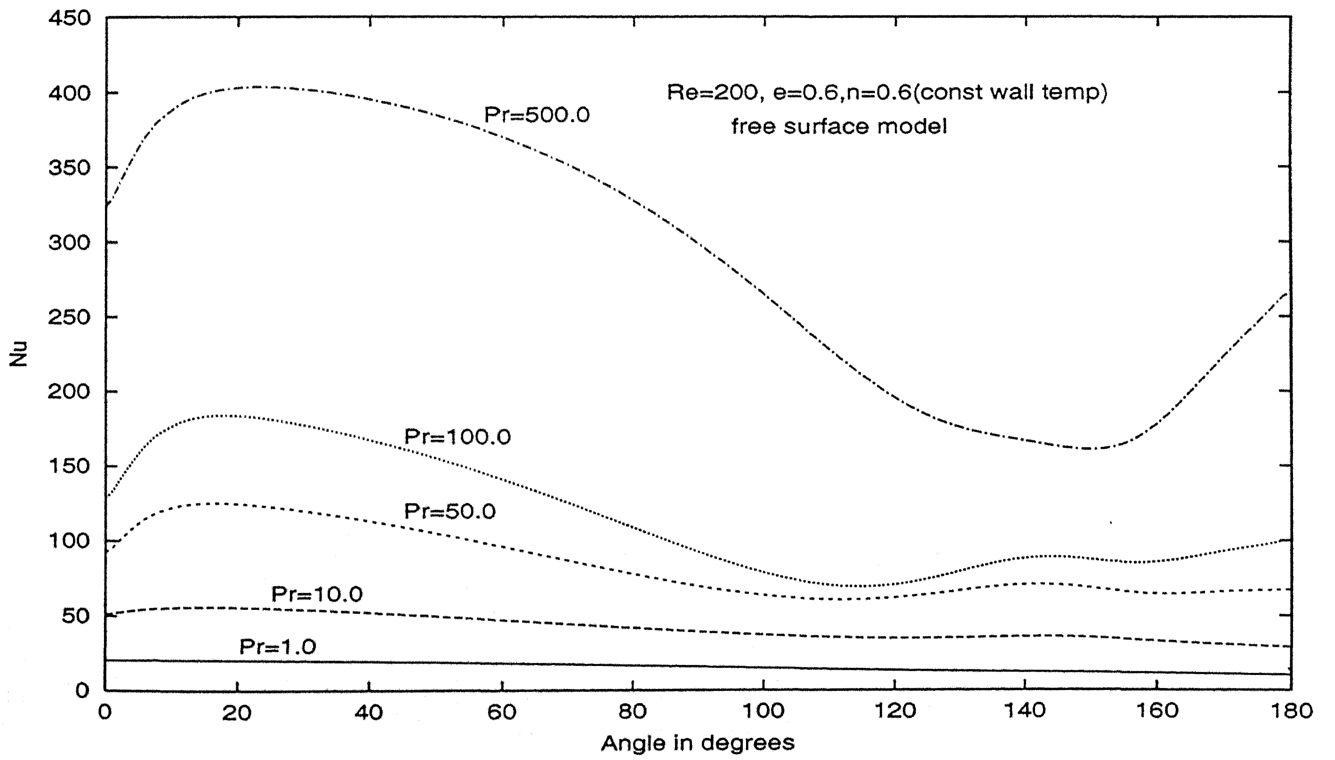

Figure 4.46: Variation of Nusselt number with angle for Re=200.0,e=0.6 and n=0.6 for constant surface temperature condition

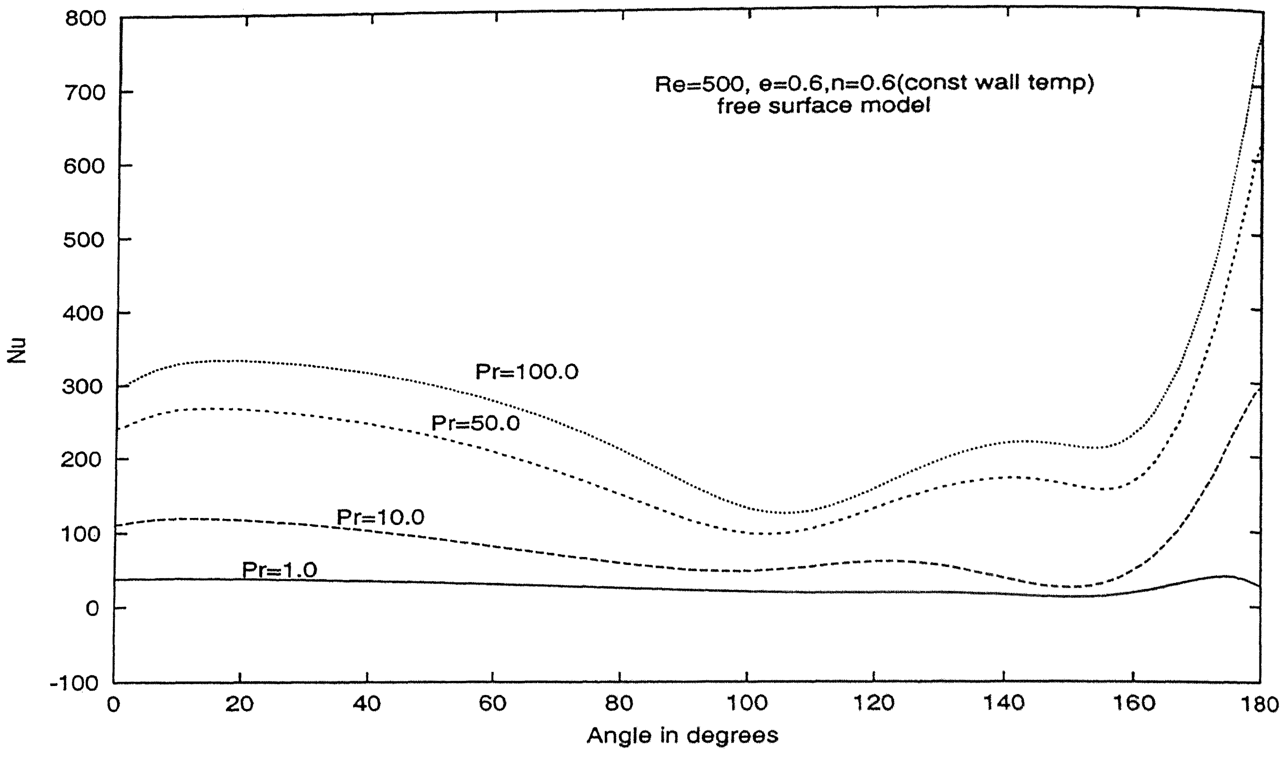

Figure 4.47: Variation of Nusselt number with angle for Re=500.0,e=0.6 and n=0.6 for constant surface temperature condition

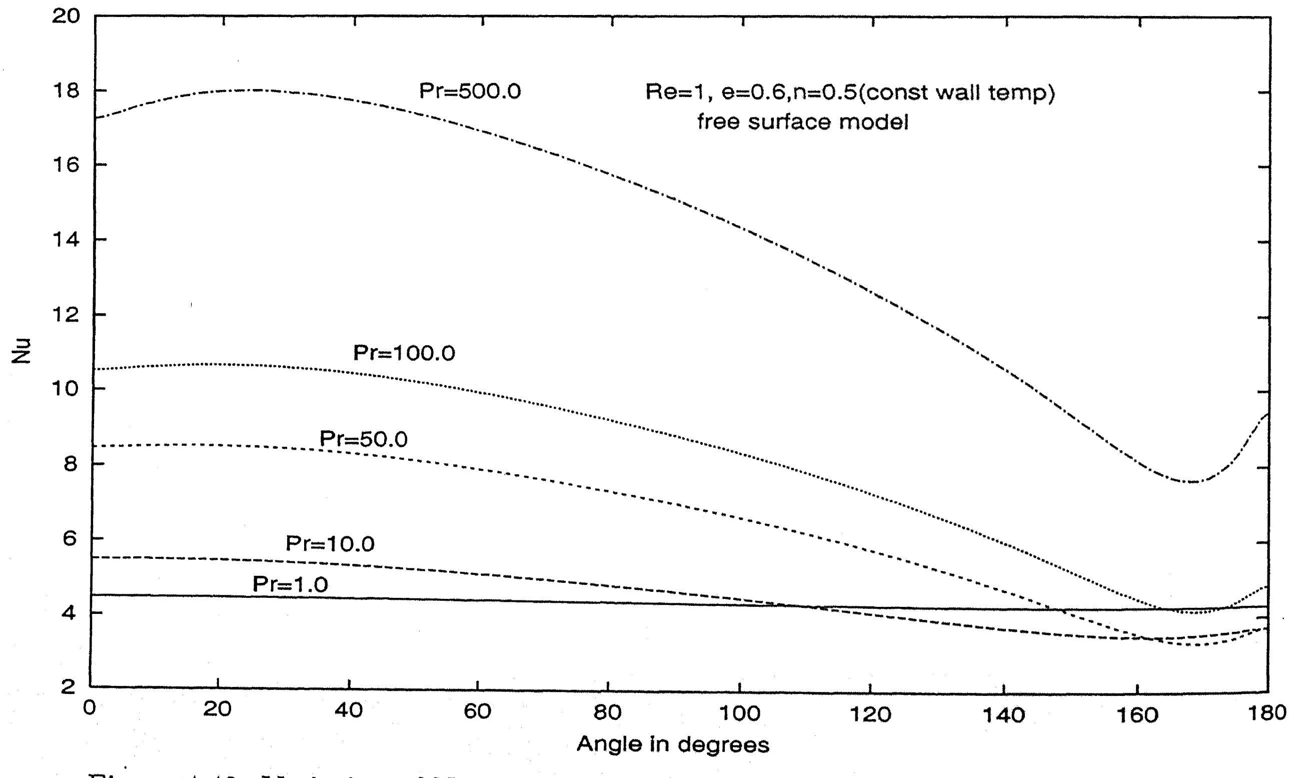

Figure 4.48: Variation of Nusselt number with angle for Re=1.0,e=0.6 and n=0.5 for constant surface temperature condition

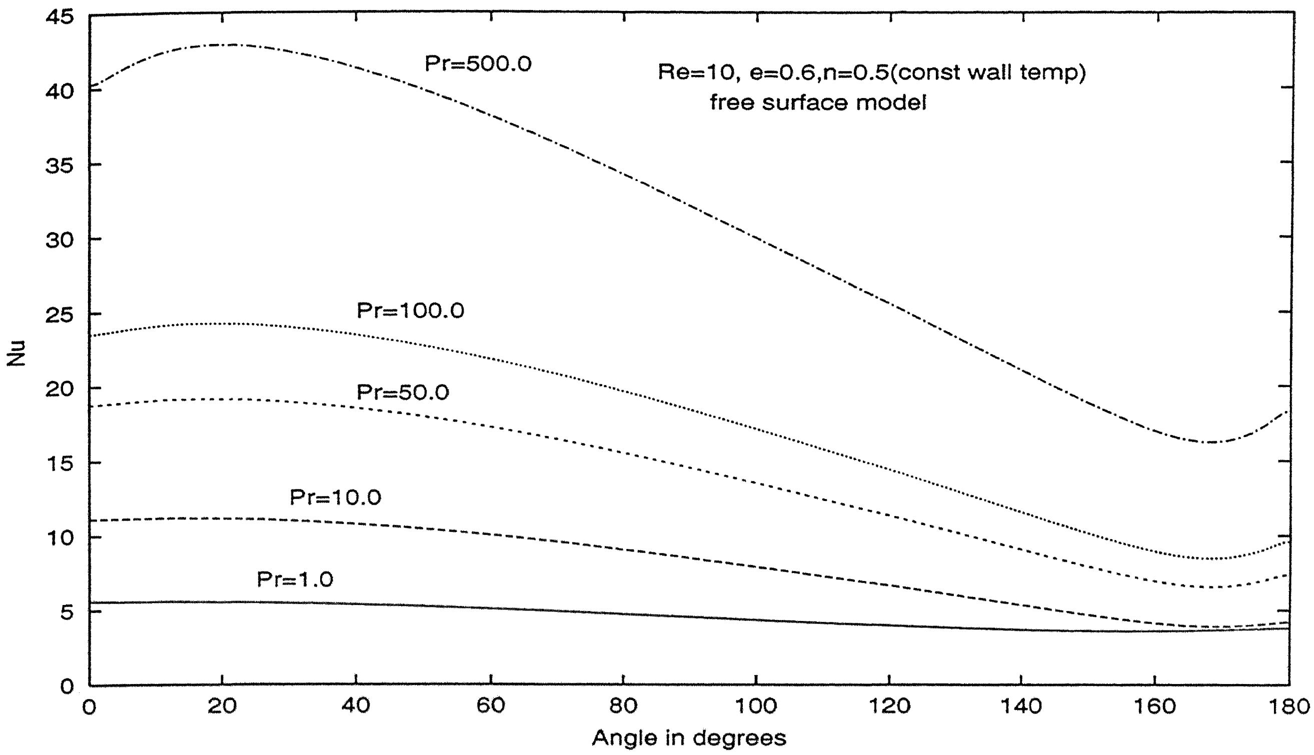

Figure 4.49: Variation of Nusselt number with angle for Re=10.0,e=0.5 and n=0.5 for constant surface temperature condition

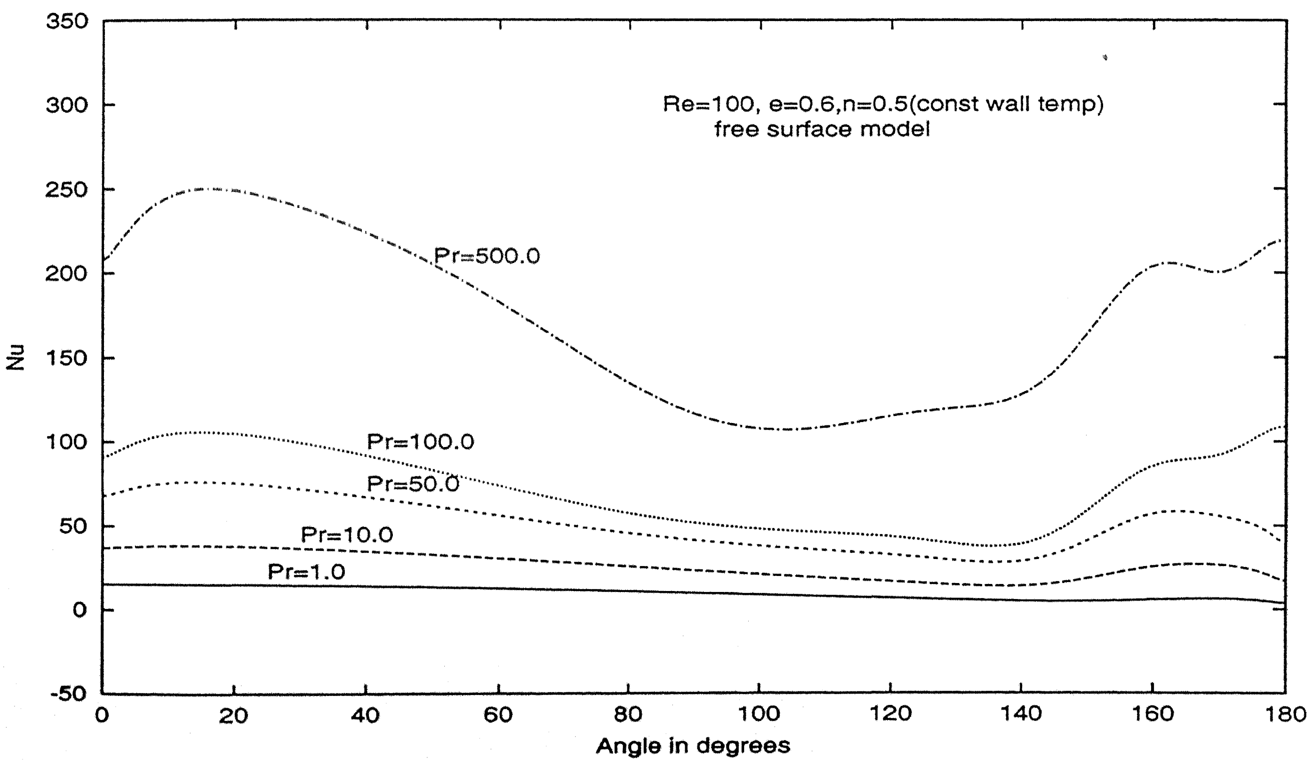

Figure 4.50: Variation of Nusselt number with angle for Re=100.0,e=0.6 and n=0.5 for constant surface temperature condition

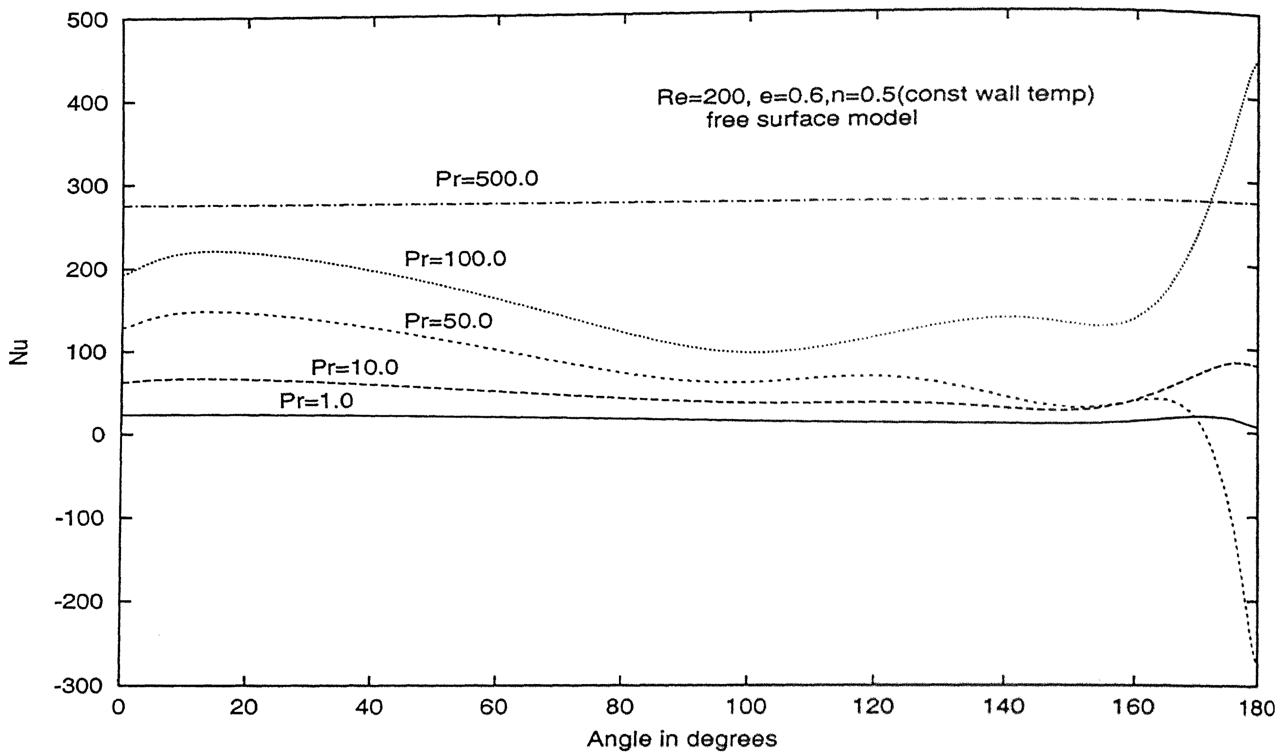

Figure 4.51: Variation of Nusselt number with angle for Re=200.0,e=0.6 and n=0.5 for constant surface temperature condition

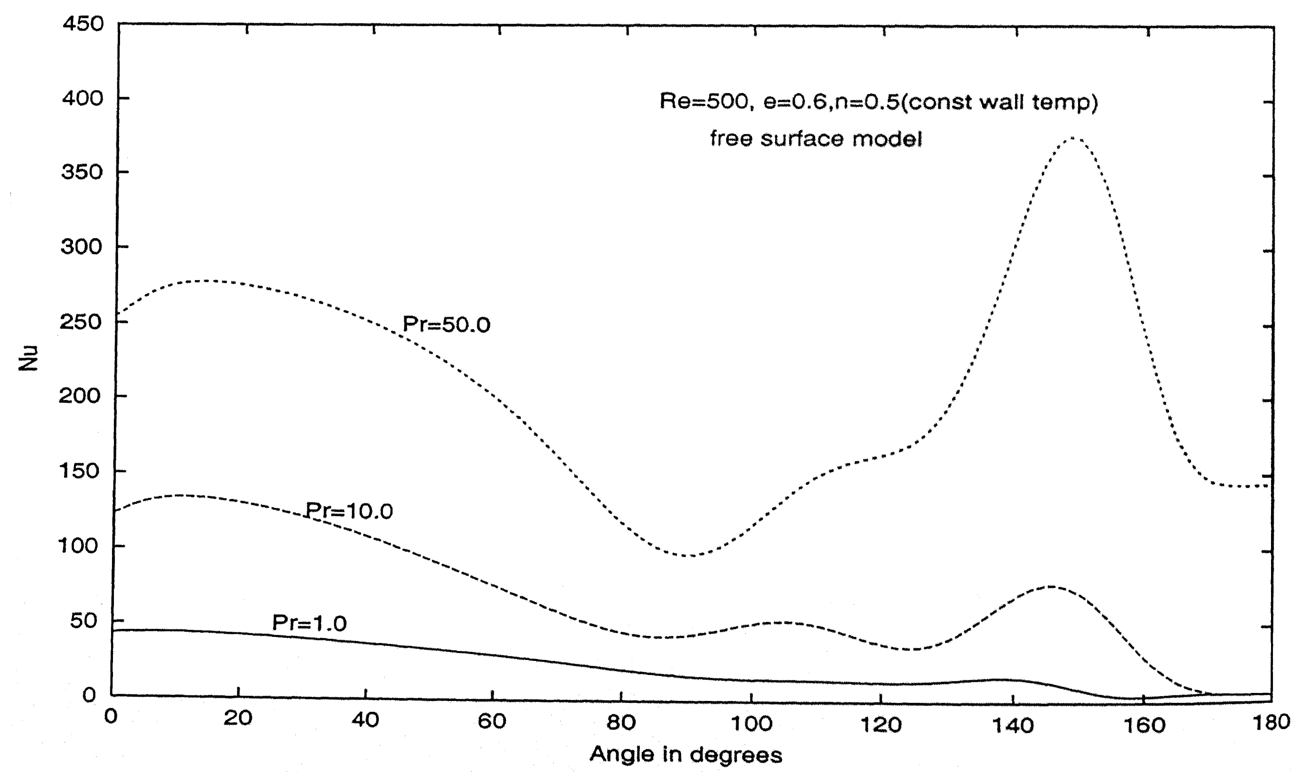

Figure 4.52: Variation of Nusselt number with angle for Re=500.0,e=0.6 and n=0.5 for constant surface temperature condition

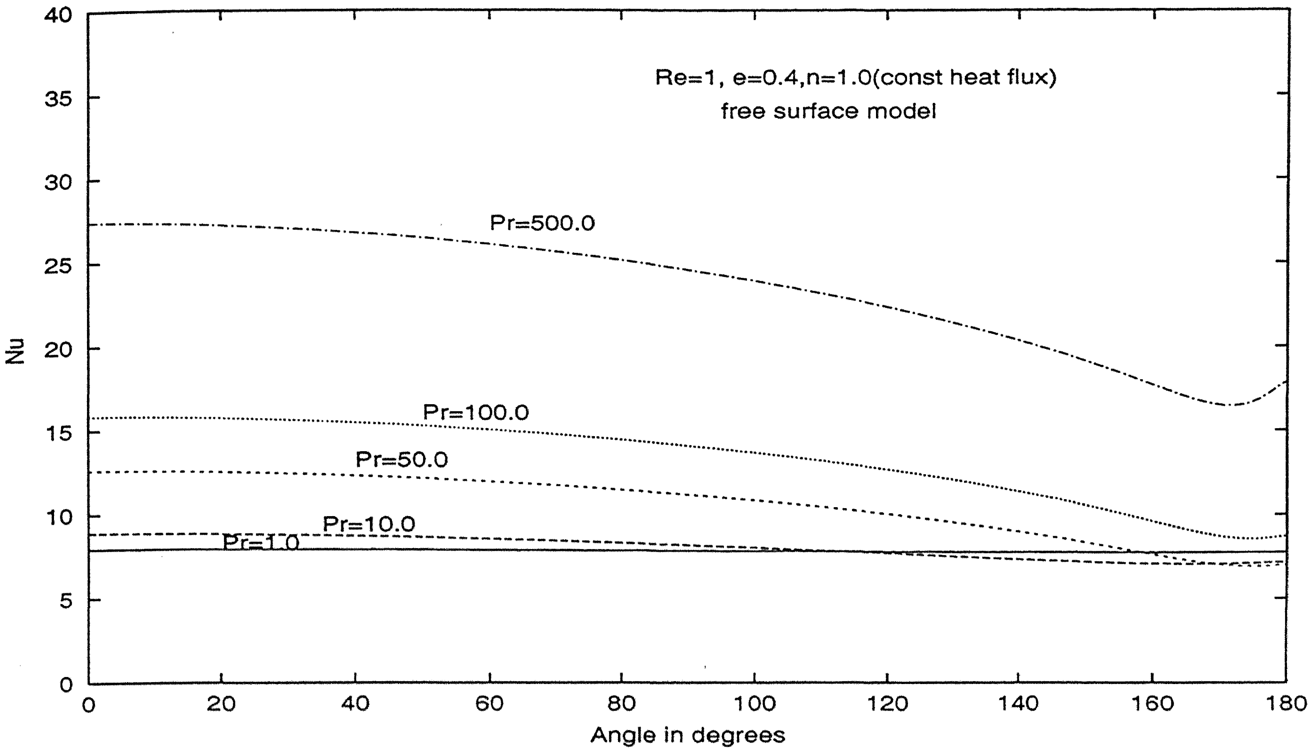

Figure 4.53: Variation of Nusselt number with angle for Re=1.0,e=0.4 and n=1.0 for constant heat flux condition

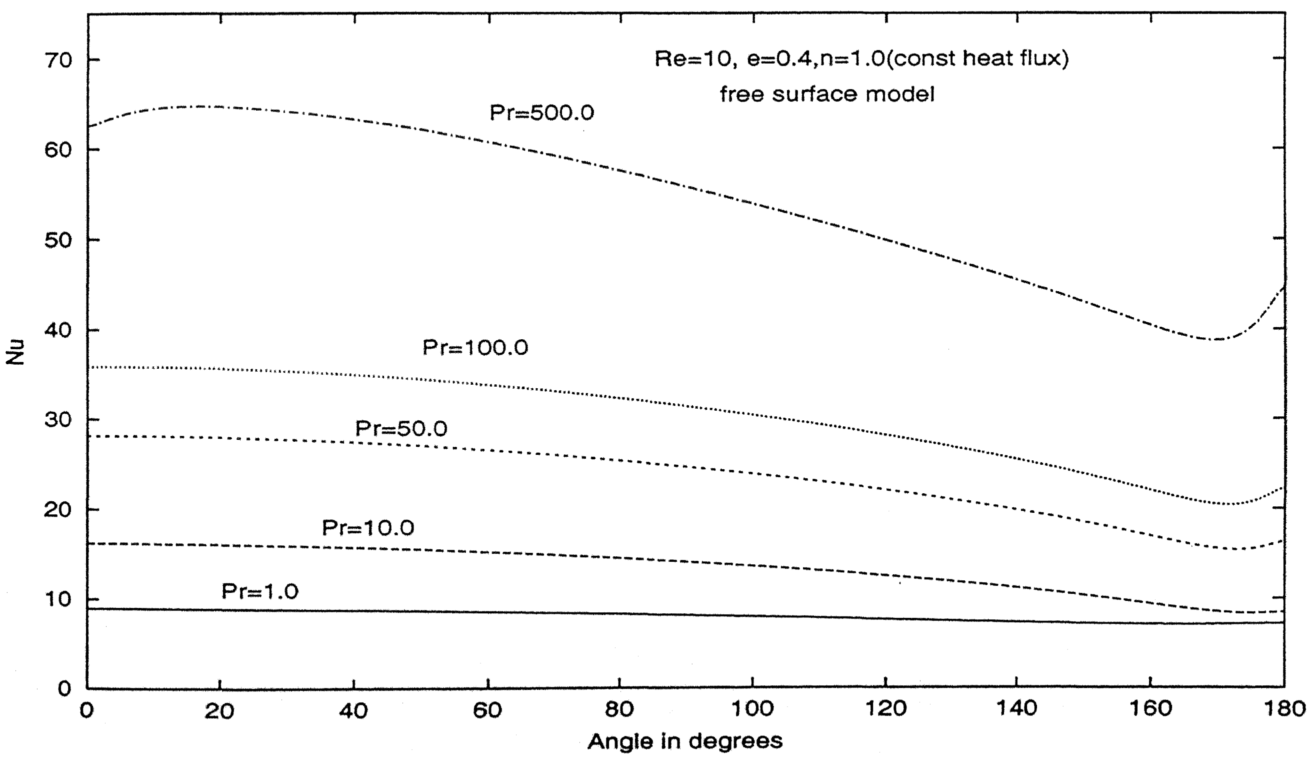

Figure 4.54: Variation of Nusselt number with angle for Re=10.0,e=0.4 and n=1.0 for constant surface temperature condition

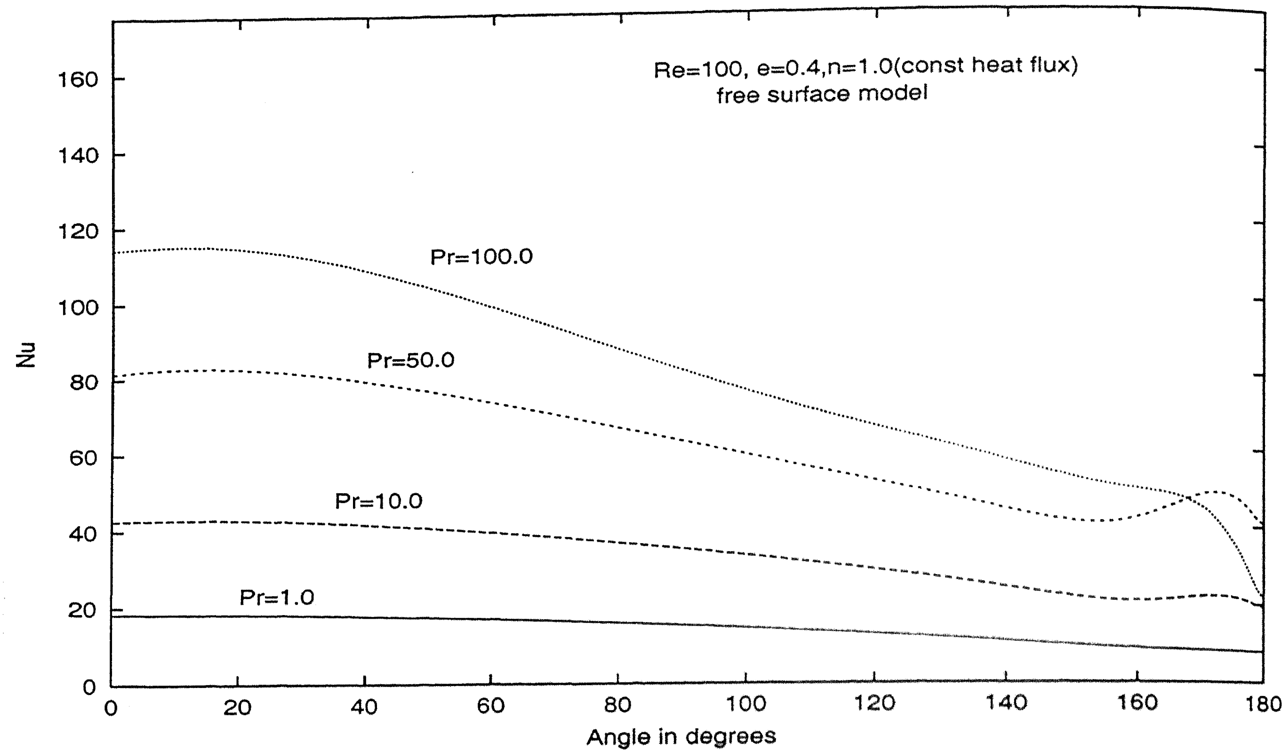

Figure 4.55: Variation of Nusselt number with angle for Re=100.0,e=0.4 and n=1.0 for constant heat flux condition

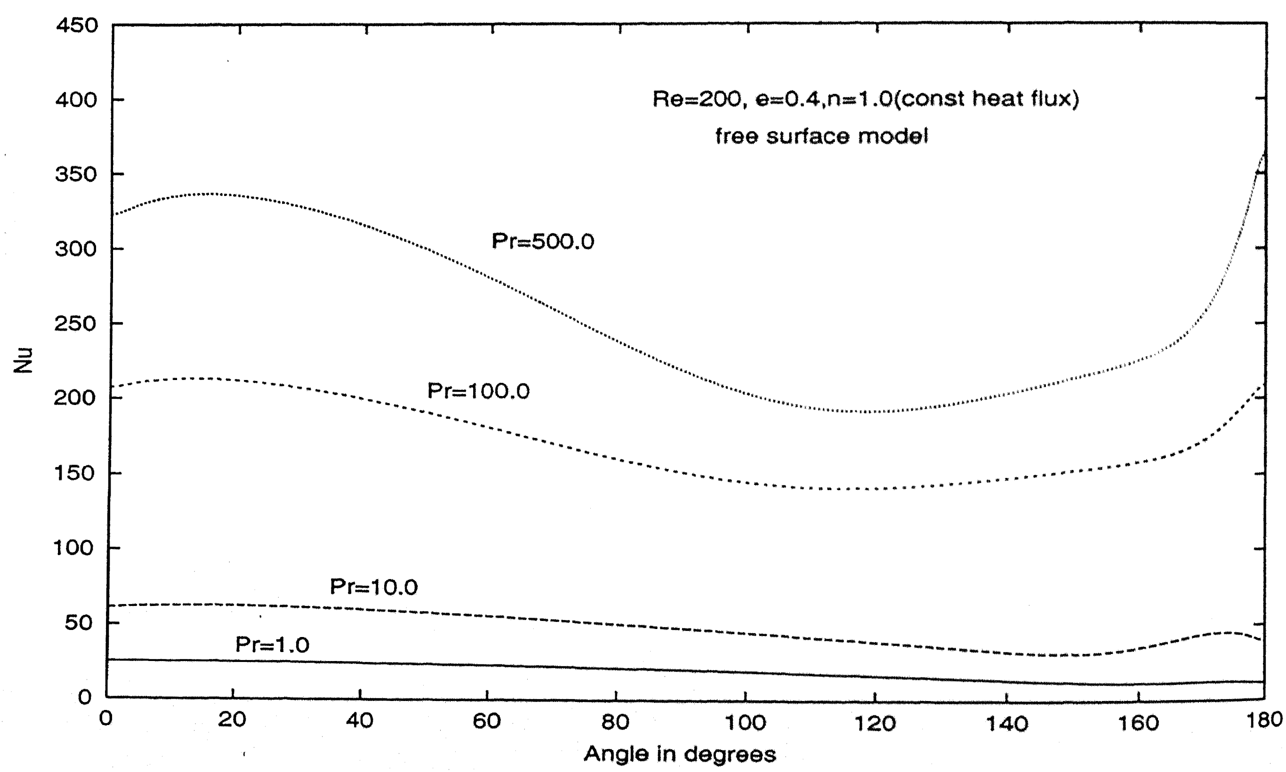

Figure 4.56: Variation of Nusselt number with angle for Re=200.0,e=0.4 and n=1.0 for constant heat flux condition

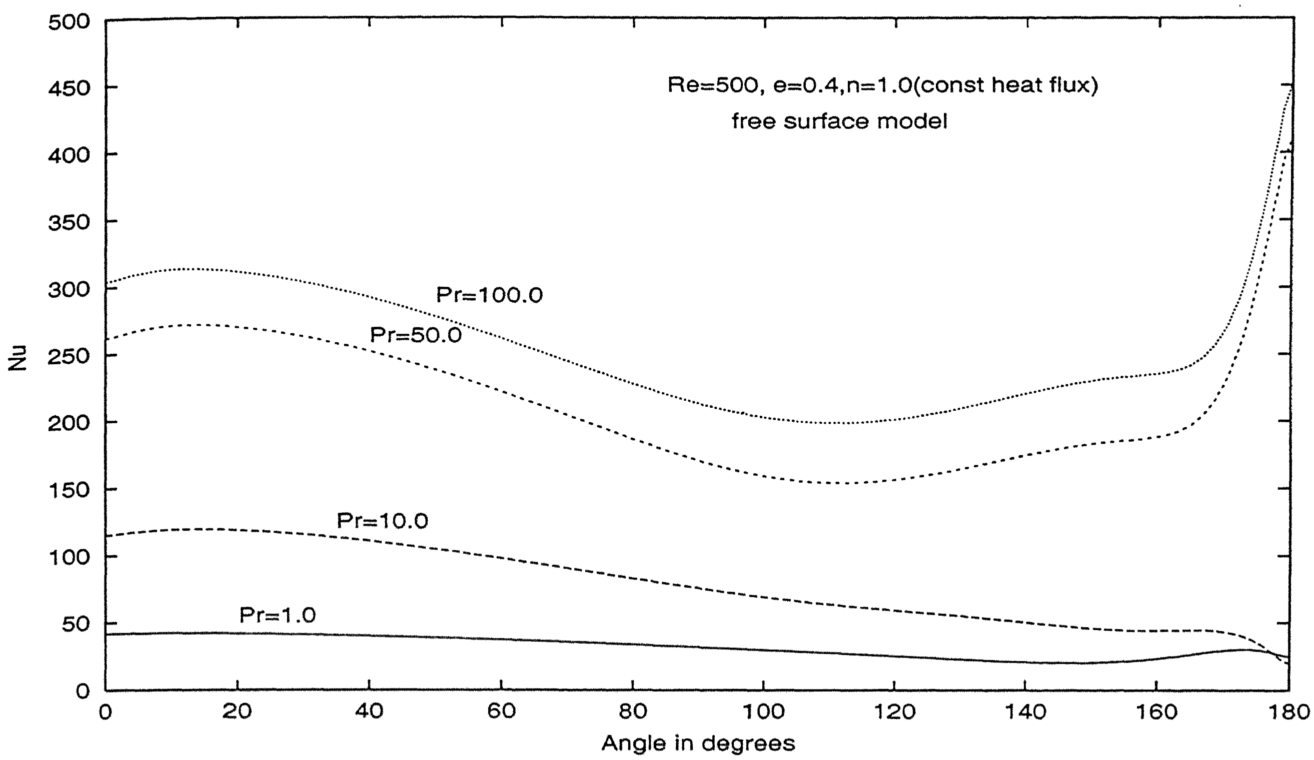

Figure 4.57: Variation of Nusselt number with angle for Re=500.0,e=0.4 and n=1.0 for constant heat flux condition

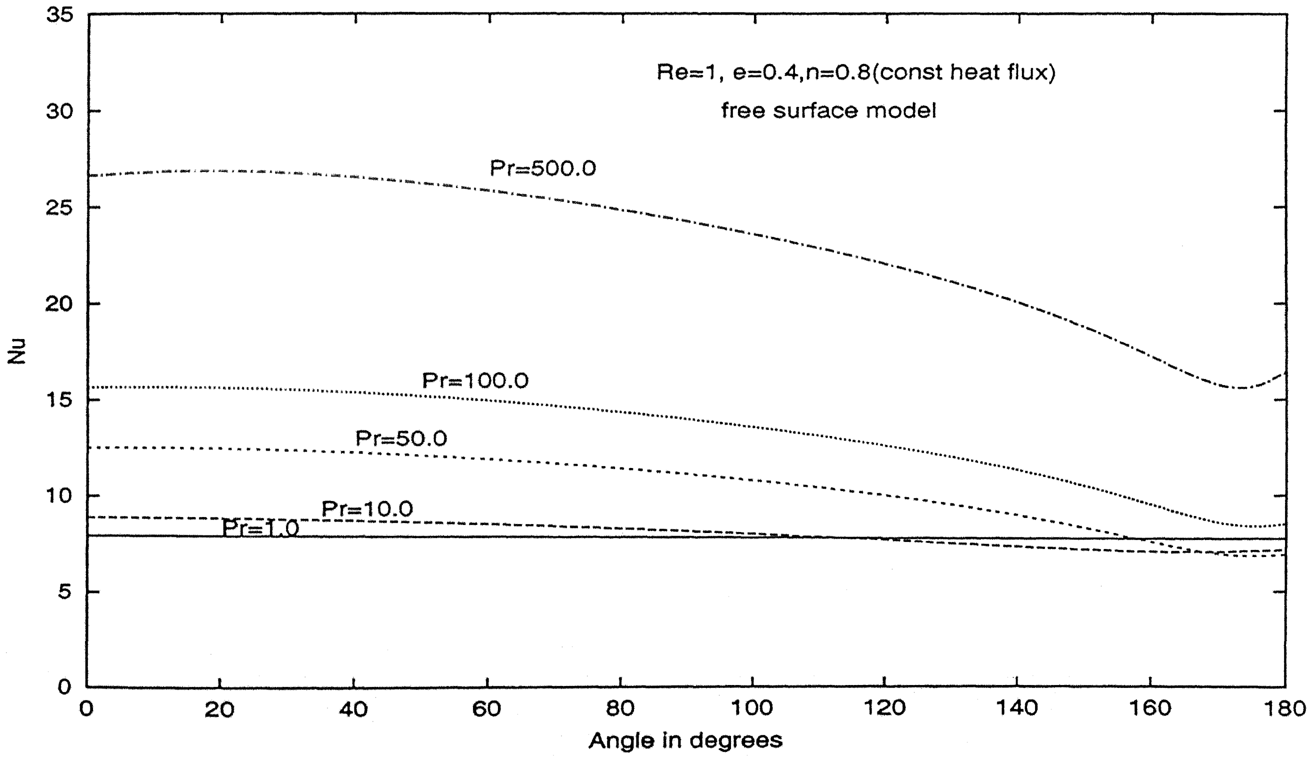

Figure 4.58: Variation of Nusselt number with angle for Re=1.0,e=0.4 and n=0.8 for constant heat flux condition

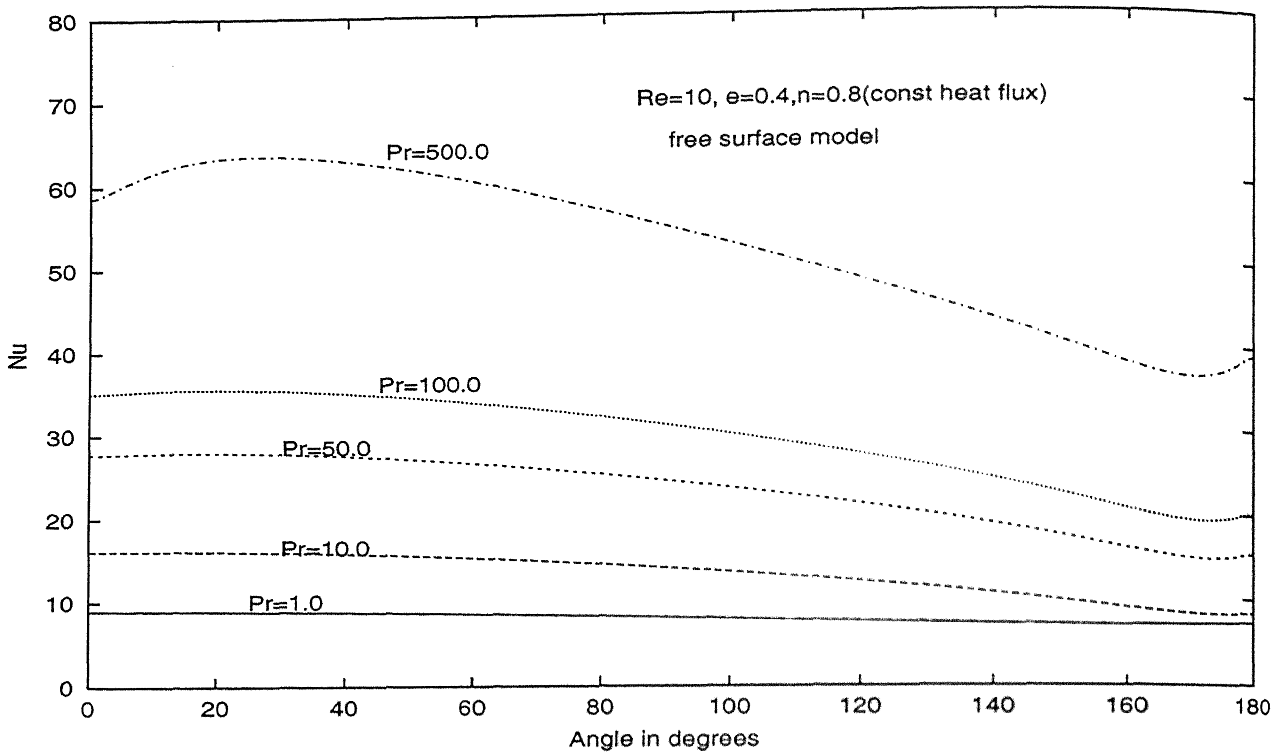

Figure 4.59: Variation of Nusselt number with angle for Re=10.0,e=0.4 and n=0.8 for constant heat flux condition

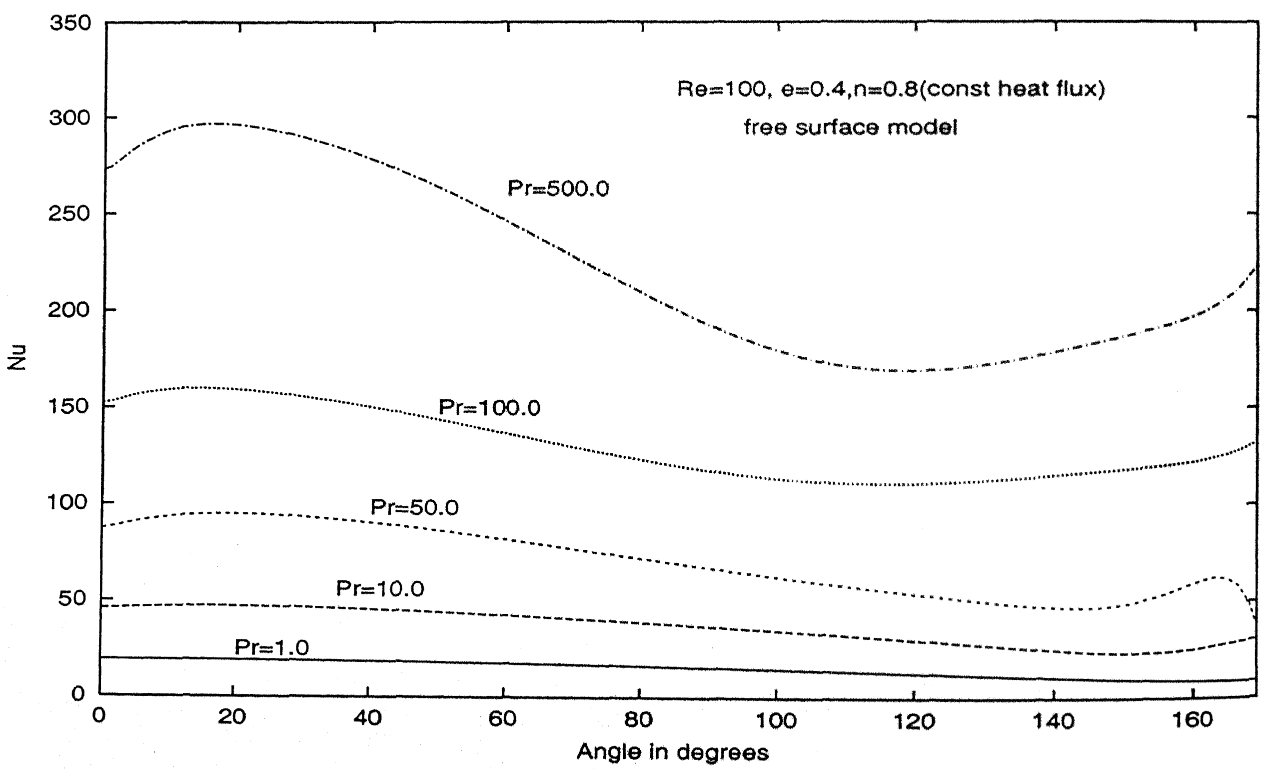

Figure 4.60: Variation of Nusselt number with angle for Re=100.0,e=0.4 and n=0.8 for constant heat flux condition

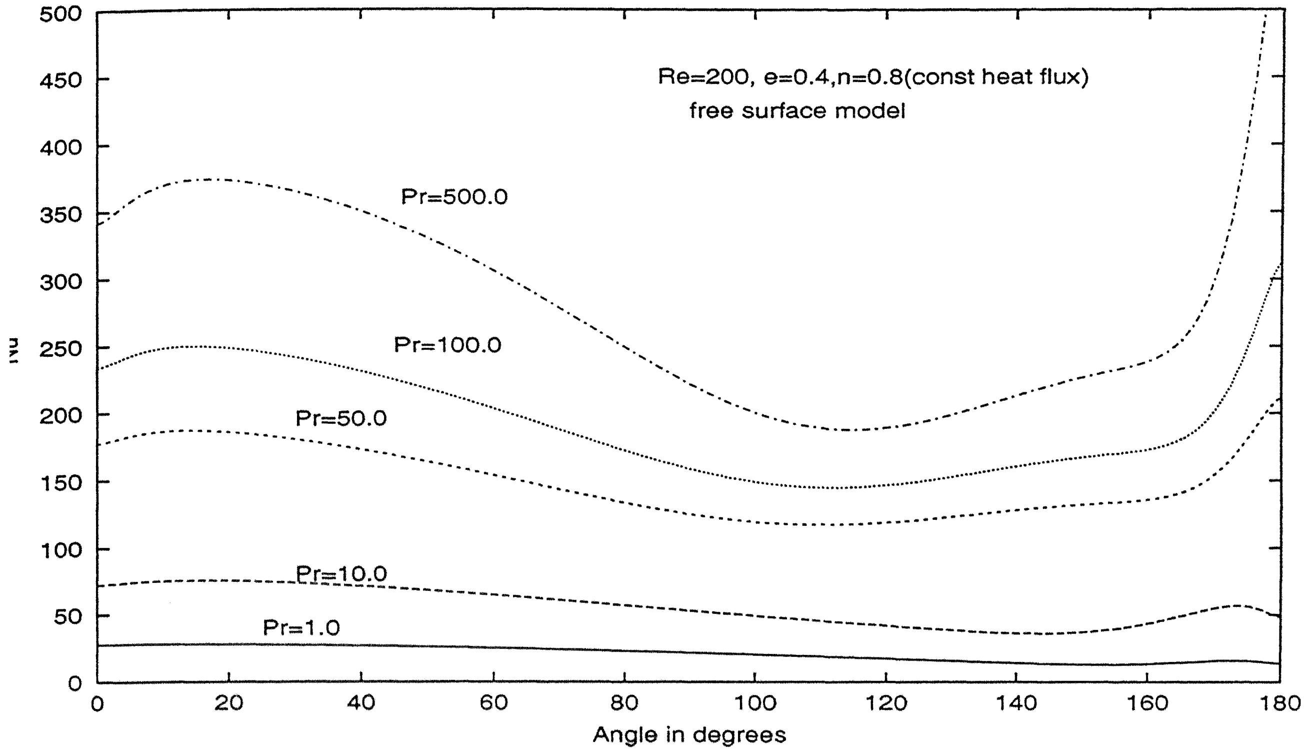

Figure 4.61: Variation of Nusselt number with angle for Re=200.0,e=0.4 and n=0.8 for constant heat flux condition

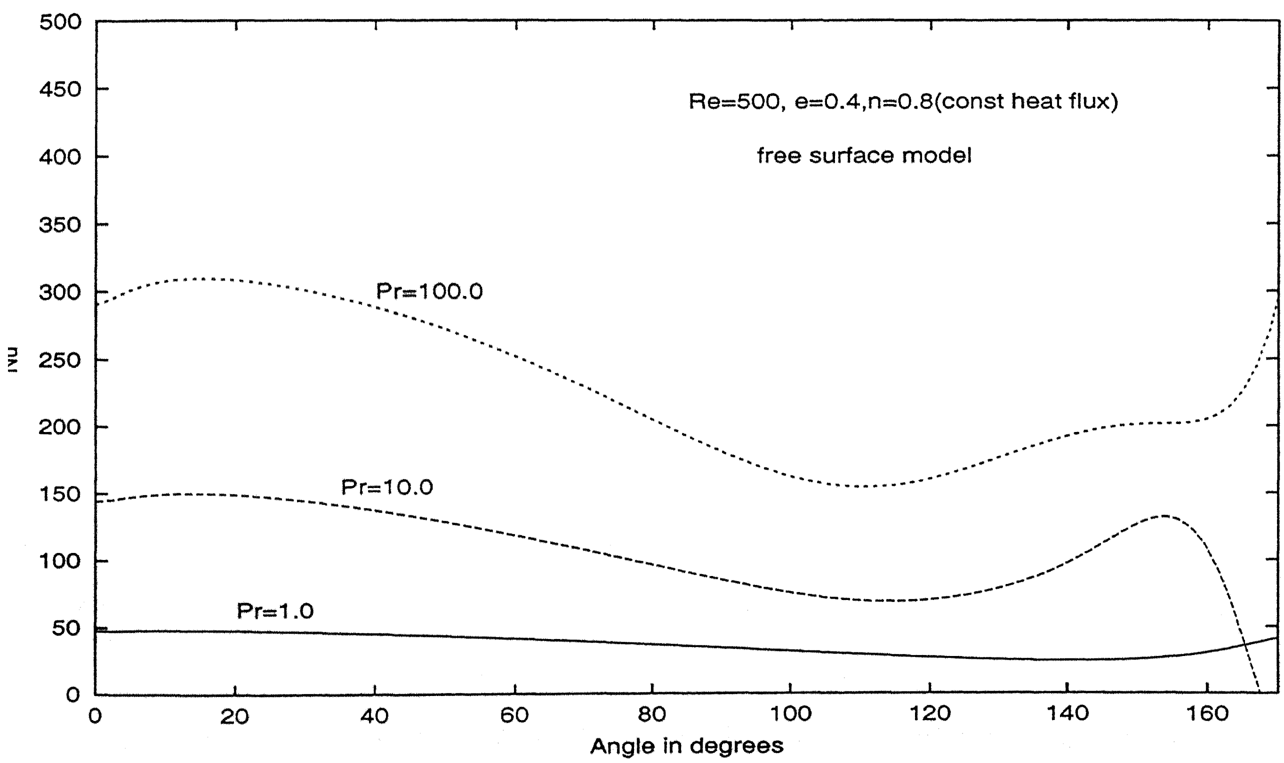

Figure 4.62: Variation of Nusselt number with angle for Re=500.0,e=0.4 and n=0.8 for constant heat flux condition

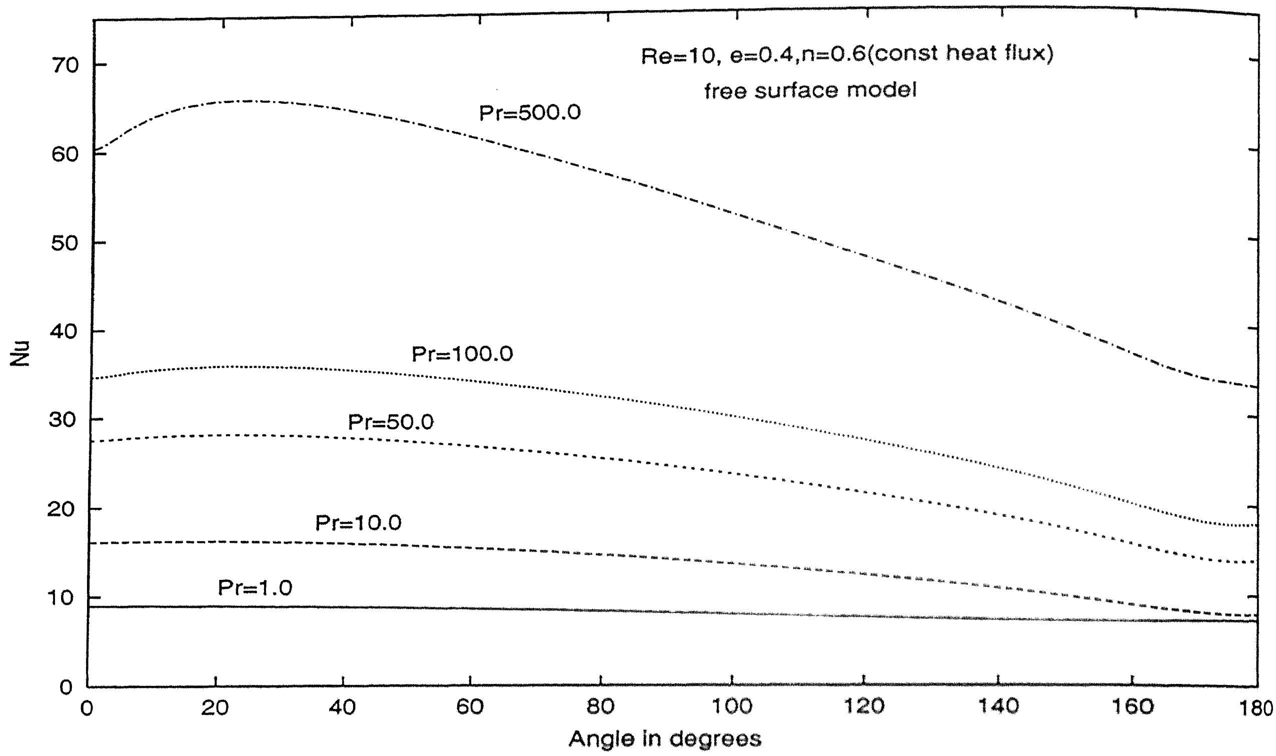

Figure 4.63: Variation of Nusselt number with angle for Re=10.0,e=0.4 and n=0.6 for constant heat flux condition

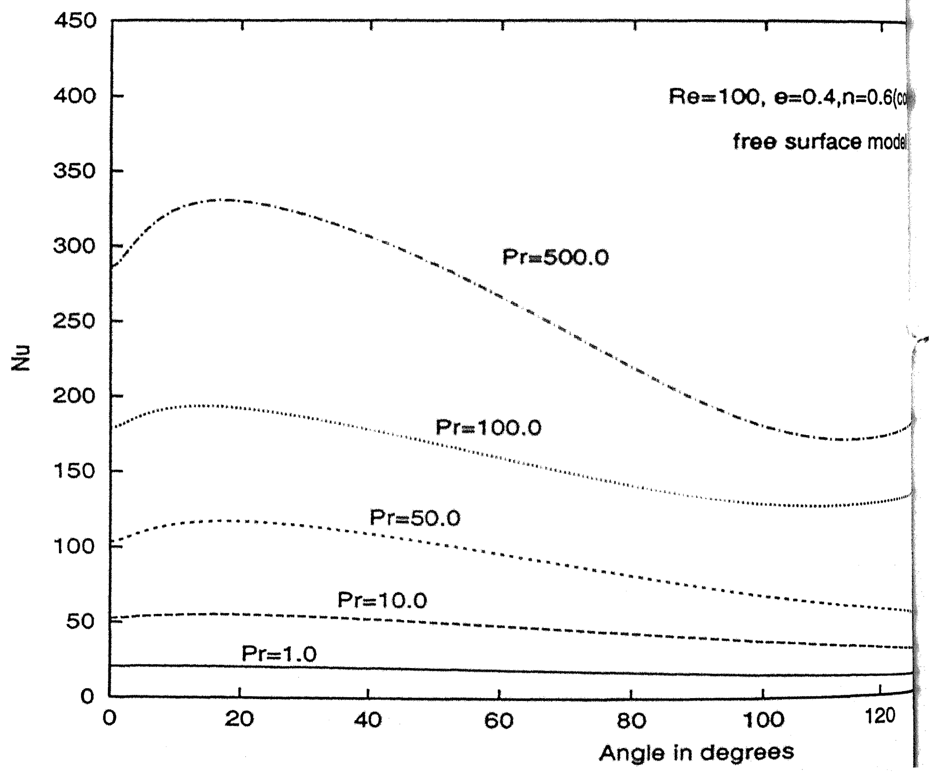

Figure 4.64: Variation of Nusselt number with angle for Re=100.0,e=0.4 and n=0.6 for constant heat flux condition

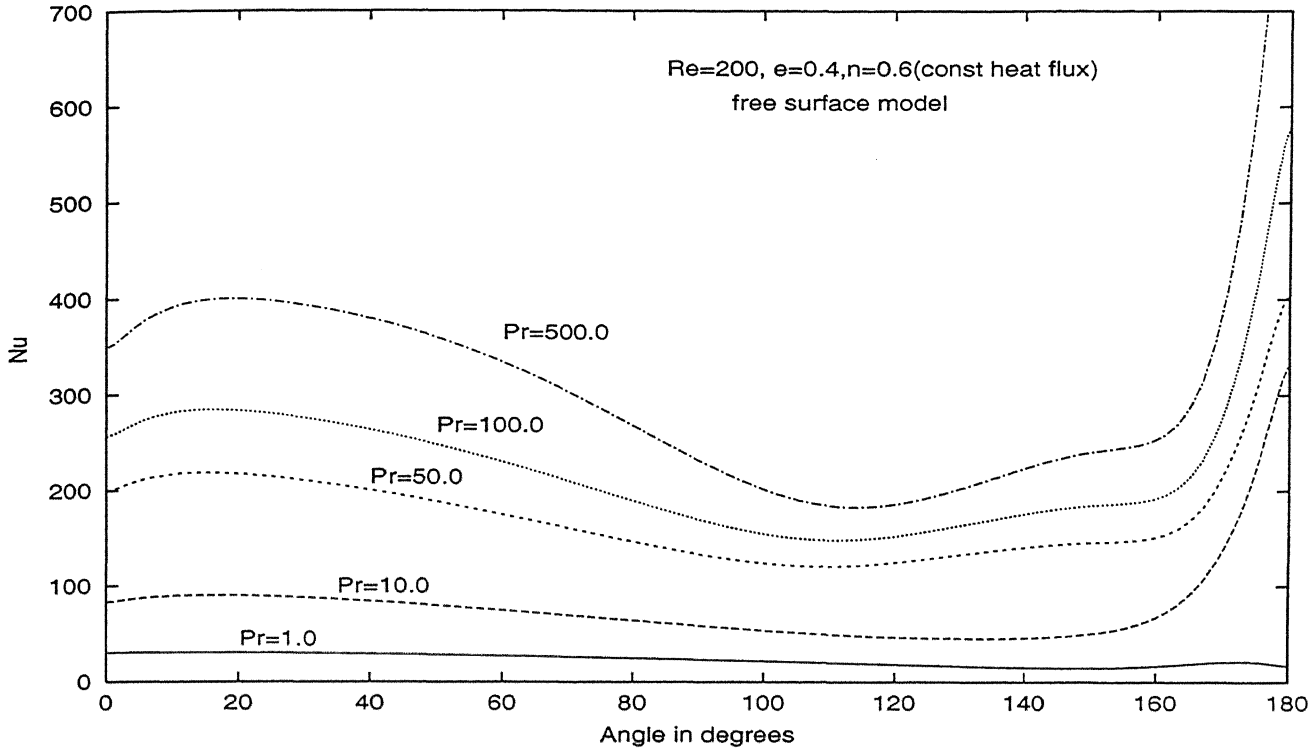

Figure 4.65: Variation of Nusselt number with angle for Re=200.0,e=0.4 and n=0.6 for constant heat flux condition

Figure 4.66: Variation of Nusselt number with angle for Re=500.0,e=0.4 and n=0.6 for constant heat flux condition

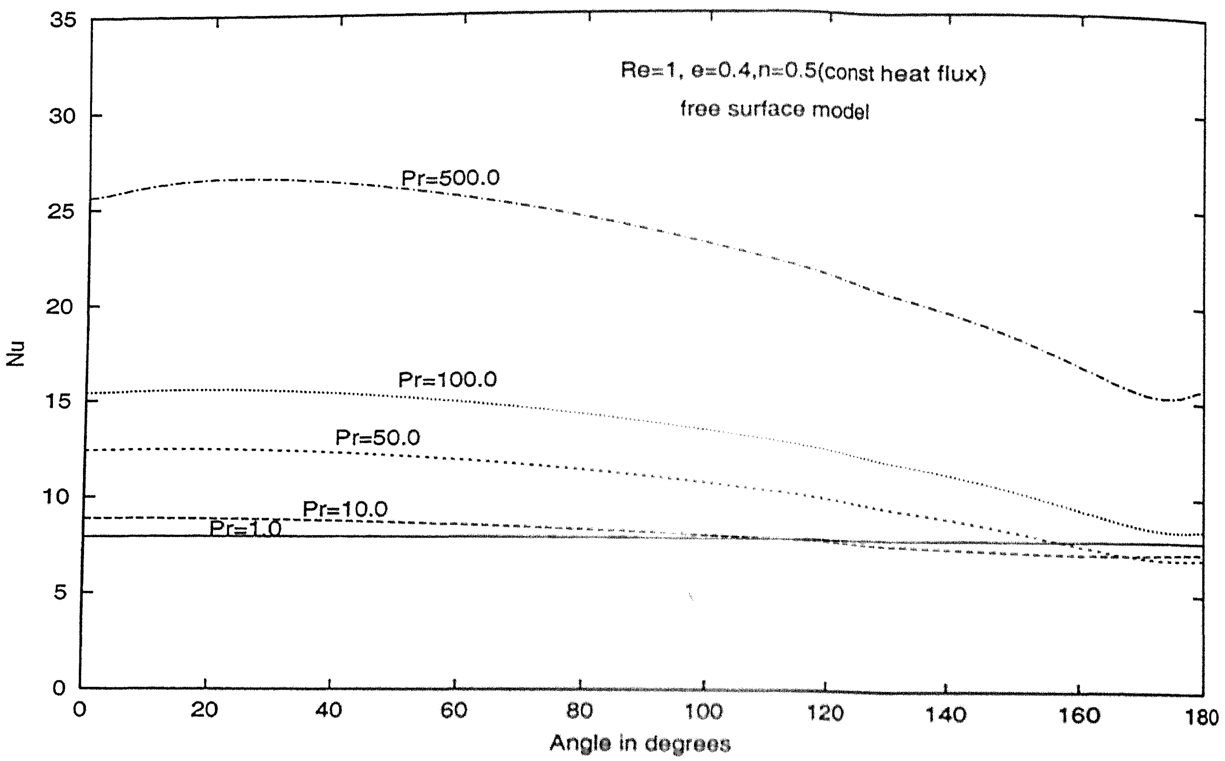

Figure 4.67: Variation of Nusselt number with angle for Re=1.0,e=0.4 and n=0.5 for constant heat flux condition

Figure 4.68: Variation of Nusselt number with angle for Re=10.0,e=0.4 and n=0.5 for constant heat flux condition

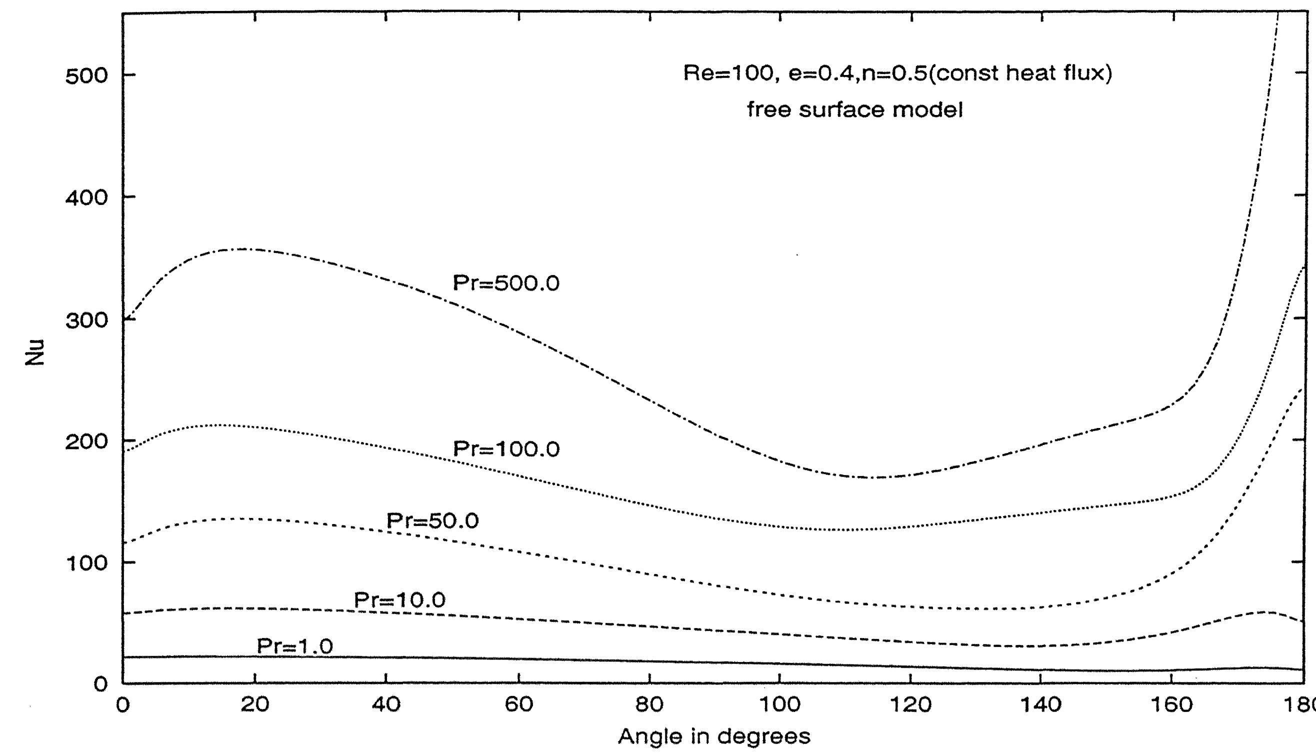

gure 4.69: Variation of Nusselt number with angle for Re=100.0,e=0.4 and n=0.5 for constant heat flux condi

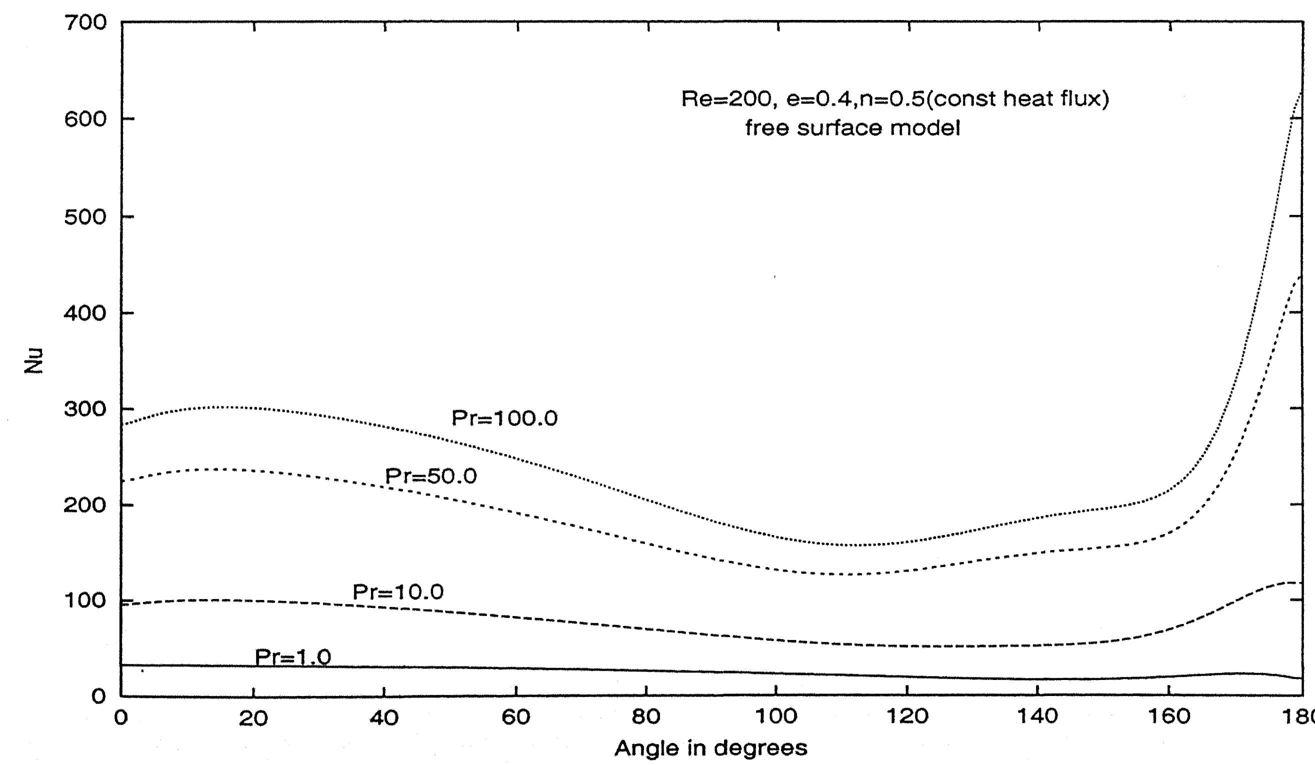

gure 4.70: Variation of Nusselt number with angle for Re=200.0,e=0.4 and n=0.5 for constant heat flux condi

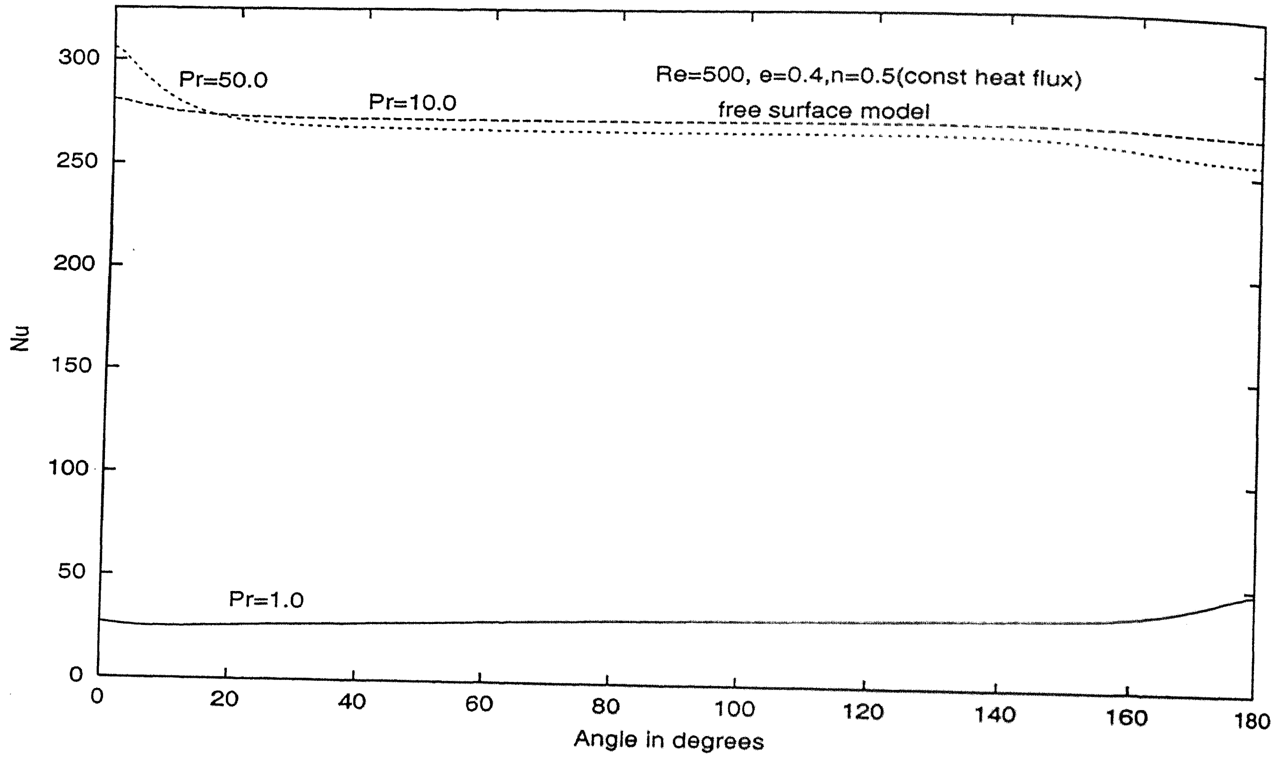

Figure 4.71: Variation of Nusselt number with angle for Re=1.0,e=0.4 and n=0.5 for constant heat flux condition

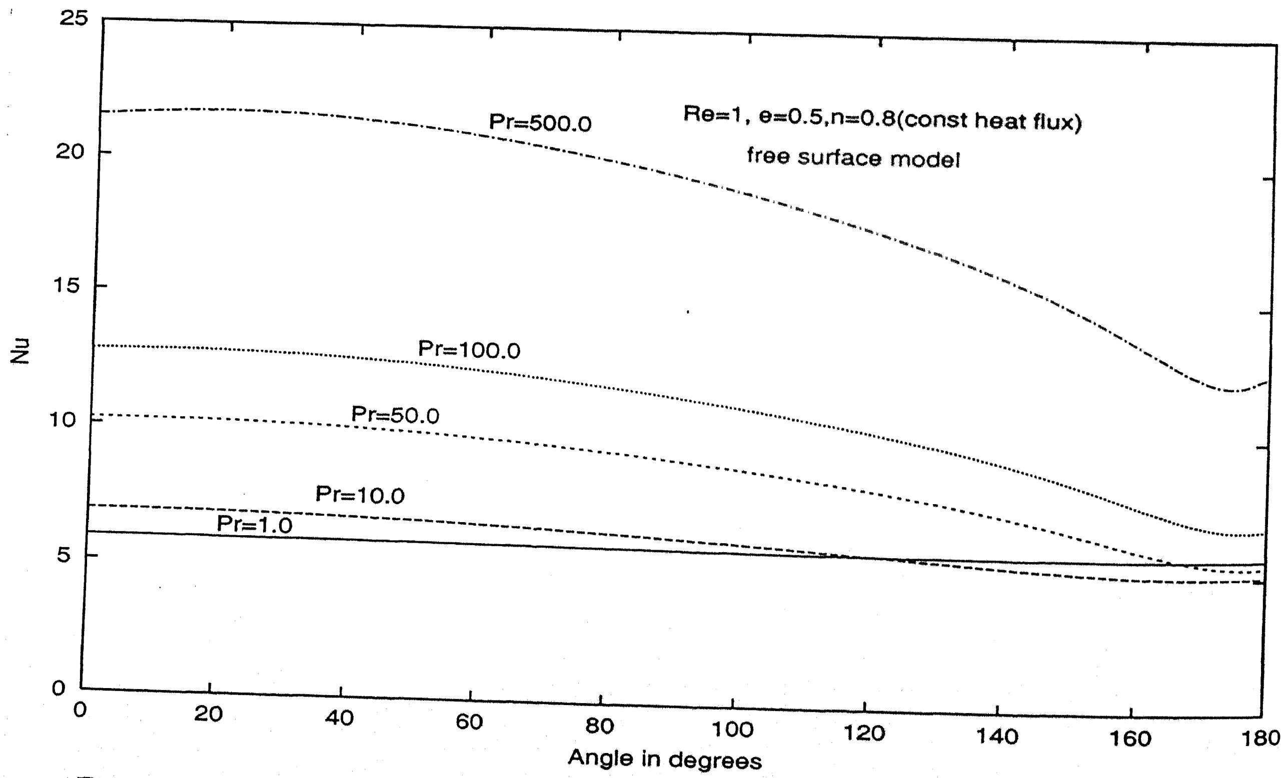

Figure 4.72: Variation of Nusselt number with angle for Re=1.0,e=0.5 and n=0.8 for constant heat flux condition

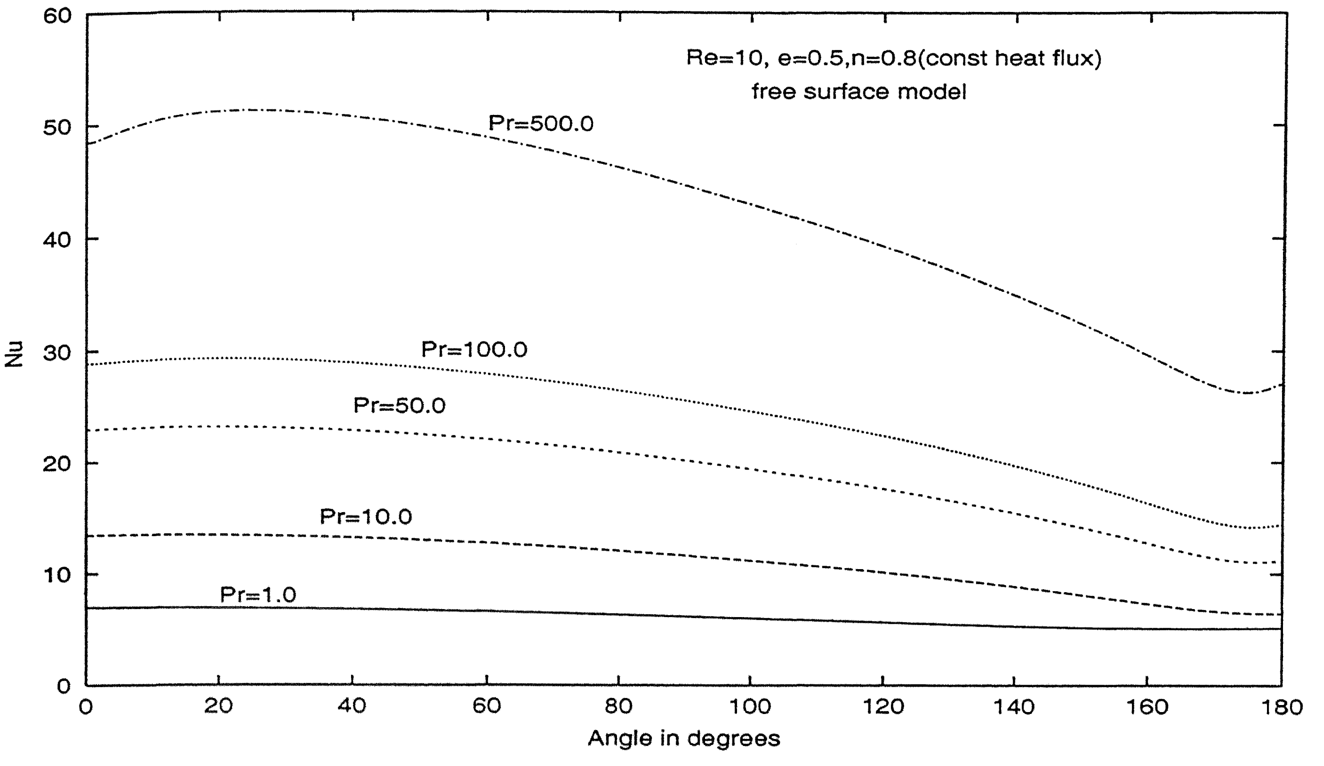

Figure 4.73: Variation of Nusselt number with angle for Re=10.0,e=0.5 and n=0.8 for constant heat flux condition

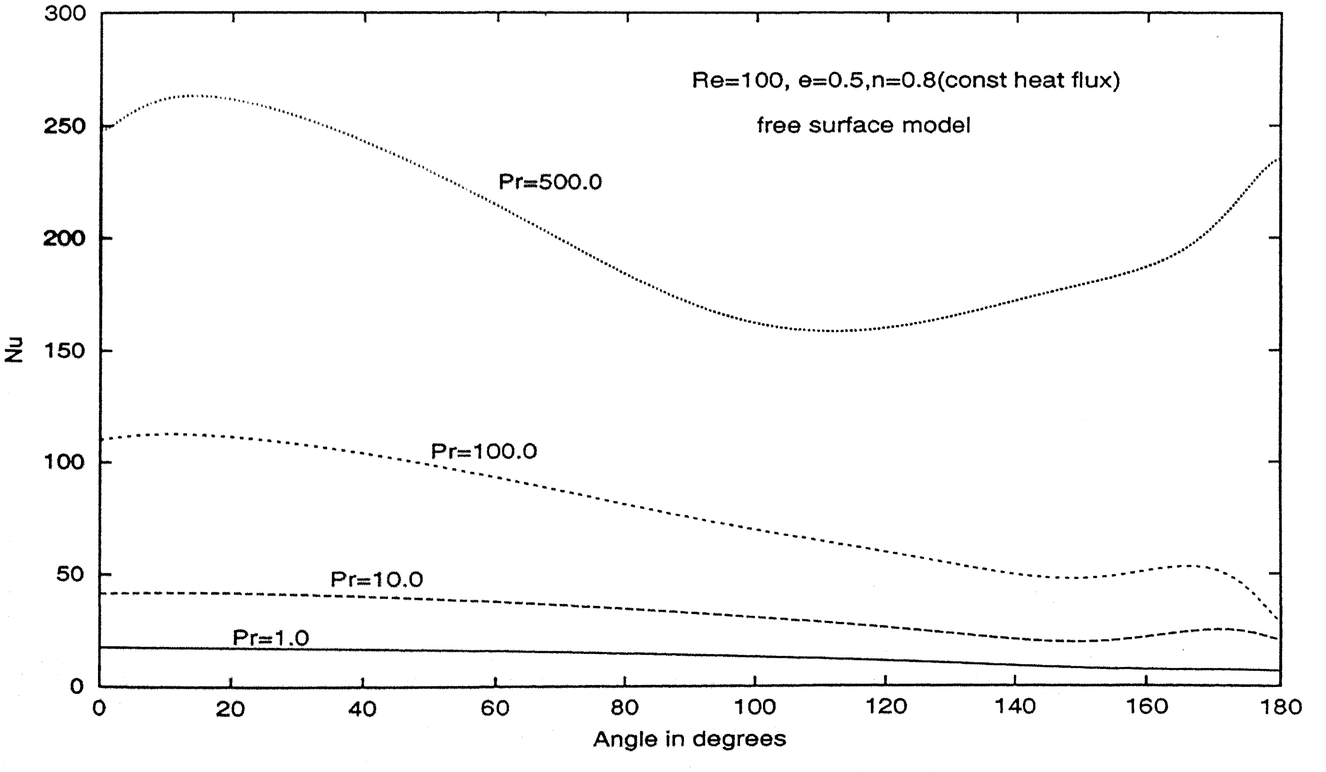

Figure 4.74: Variation of Nusselt number with angle for Re=100.0,e=0.5 and n=0.8 for constant heat flux condition

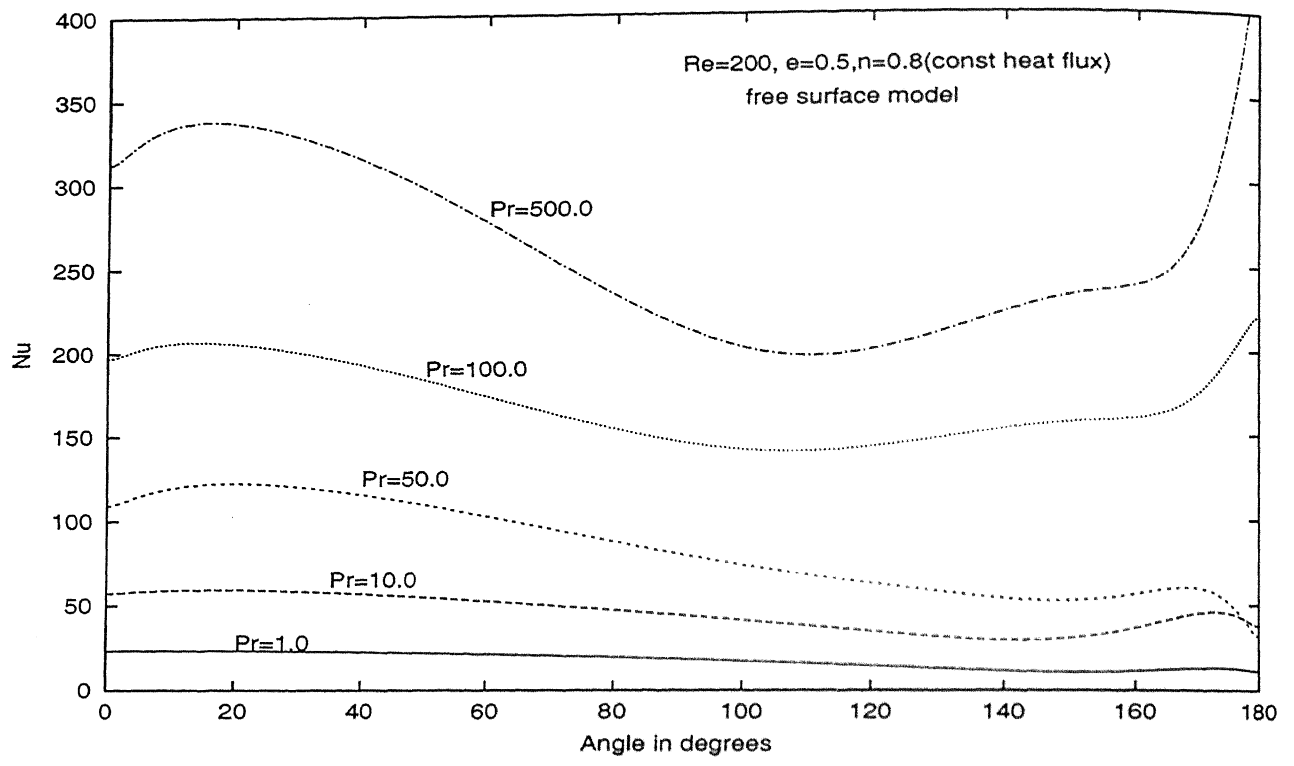

Figure 4.75: Variation of Nusselt number with angle for Re=200.0,e=0.5 and n=0.8 for constant heat flux condition

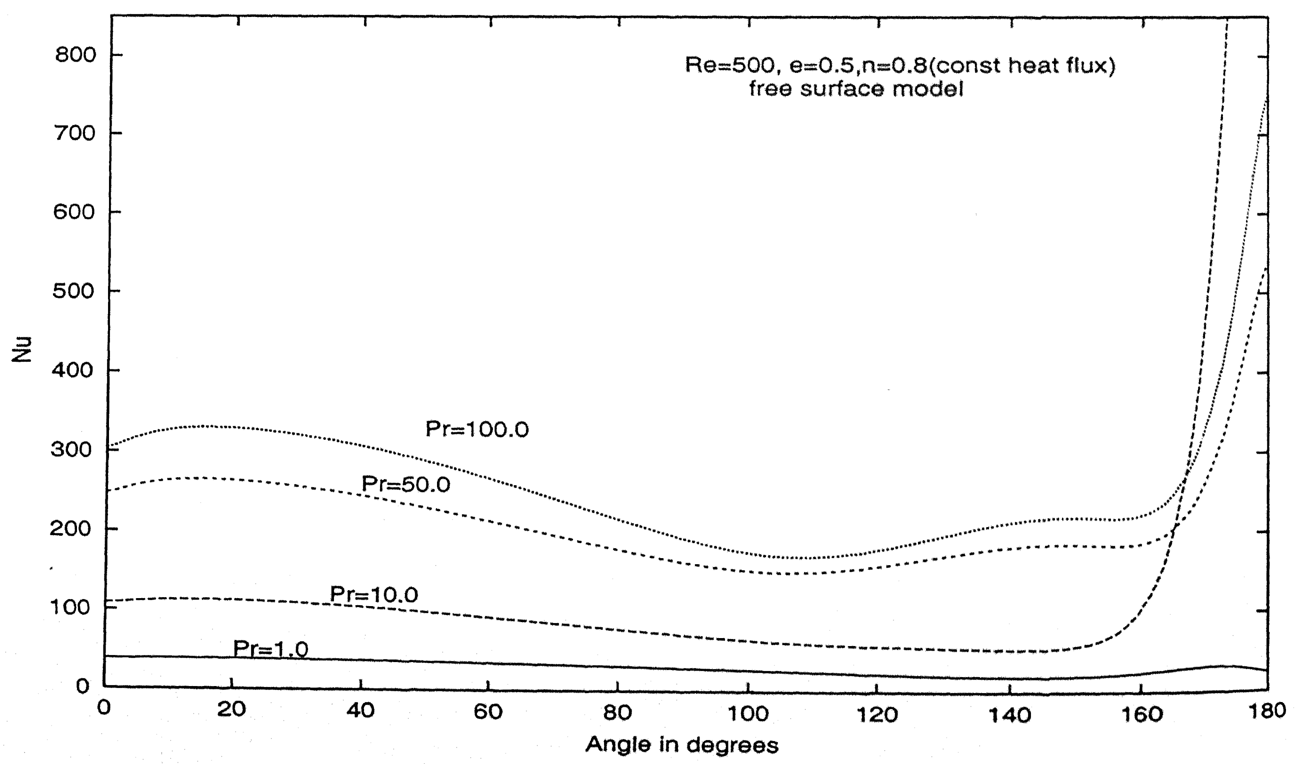

Figure 4.76: Variation of Nusselt number with angle for Re=500.0,e=0.5 and n=0.8 for constant heat flux condition

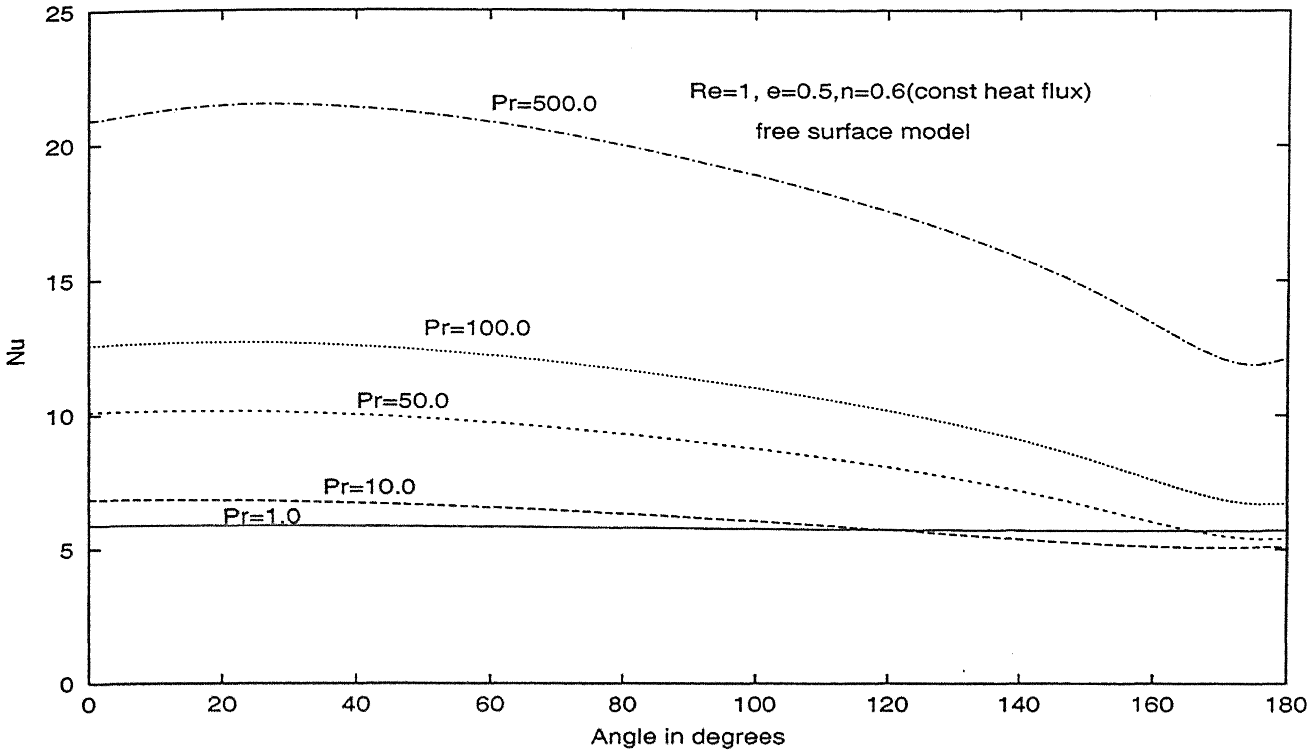

Figure 4.77: Variation of Nusselt number with angle for Re=1.0,e=0.5 and n=0.6 for constant heat flux condition

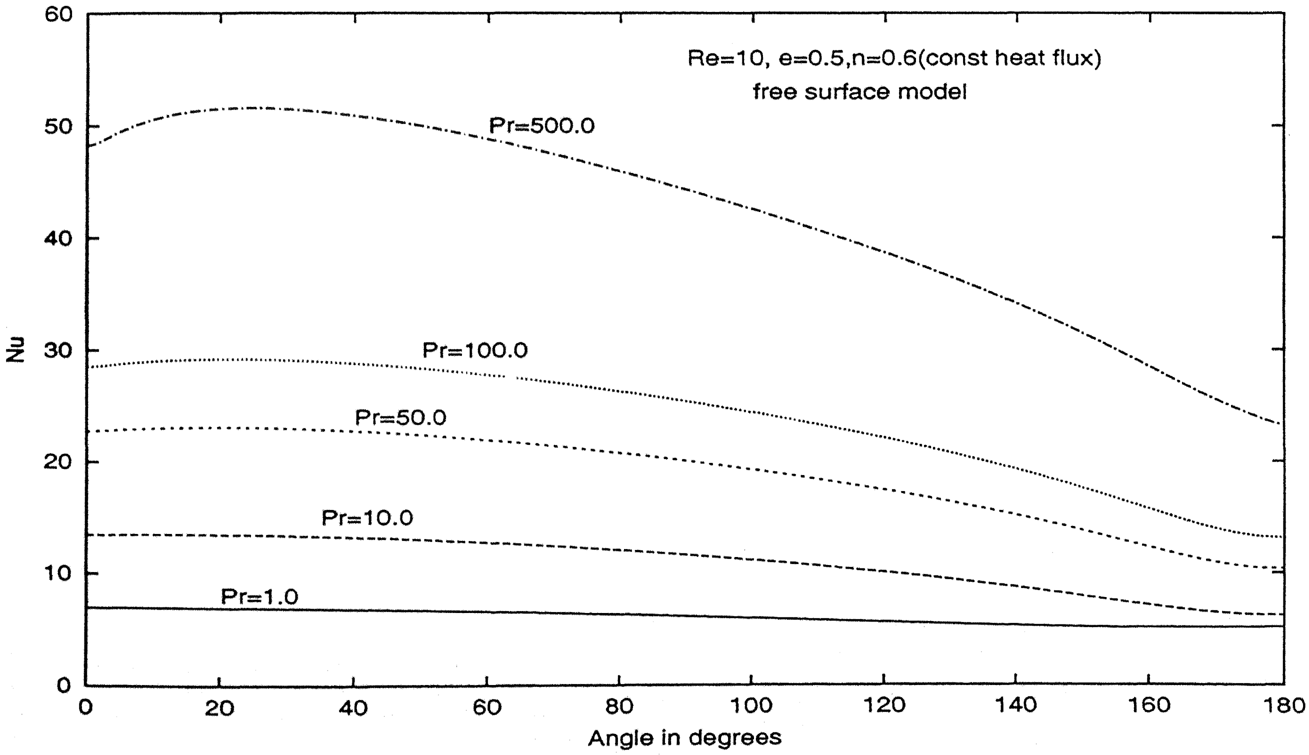

Figure 4.78: Variation of Nusselt number with angle for Re=10.0,e=0.5 and n=0.6 for constant heat flux condition

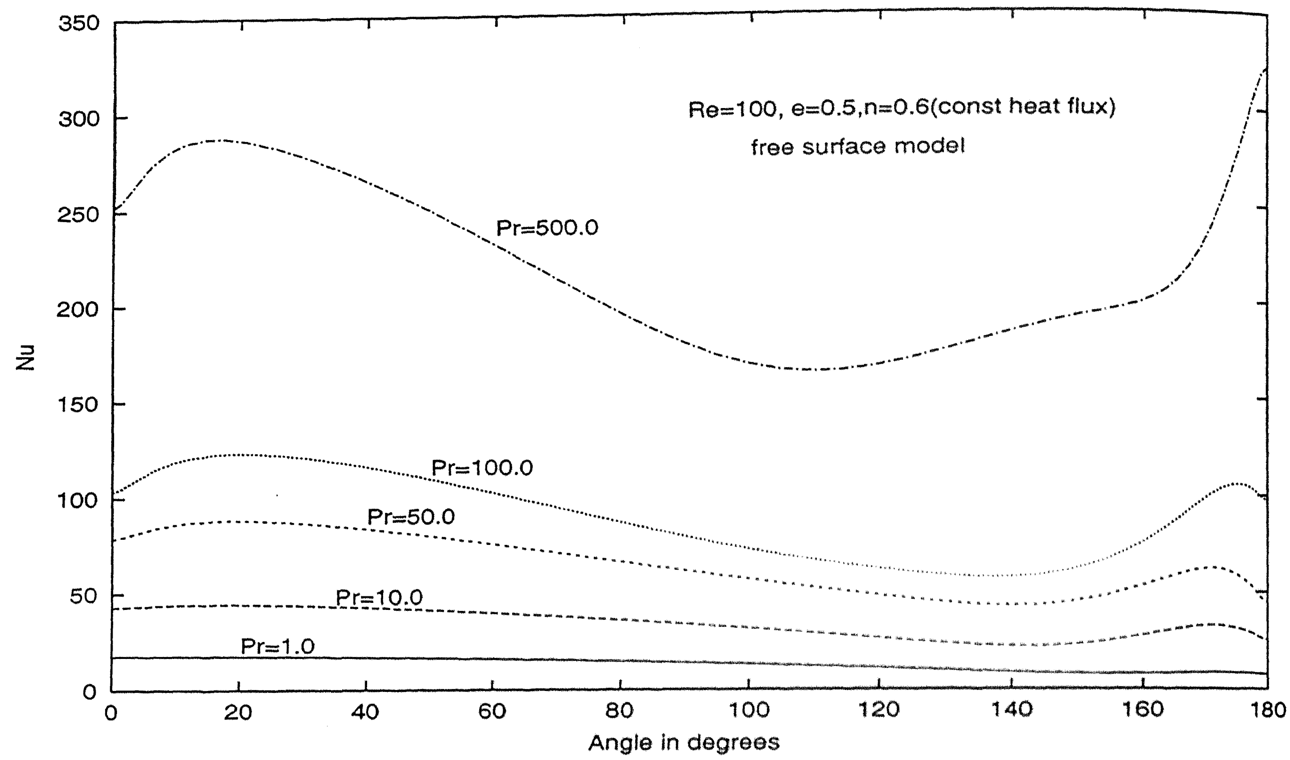

Figure 4.79: Variation of Nusselt number with angle for Re=100.0,e=0.5 and n=0.6 for constant heat flux condition

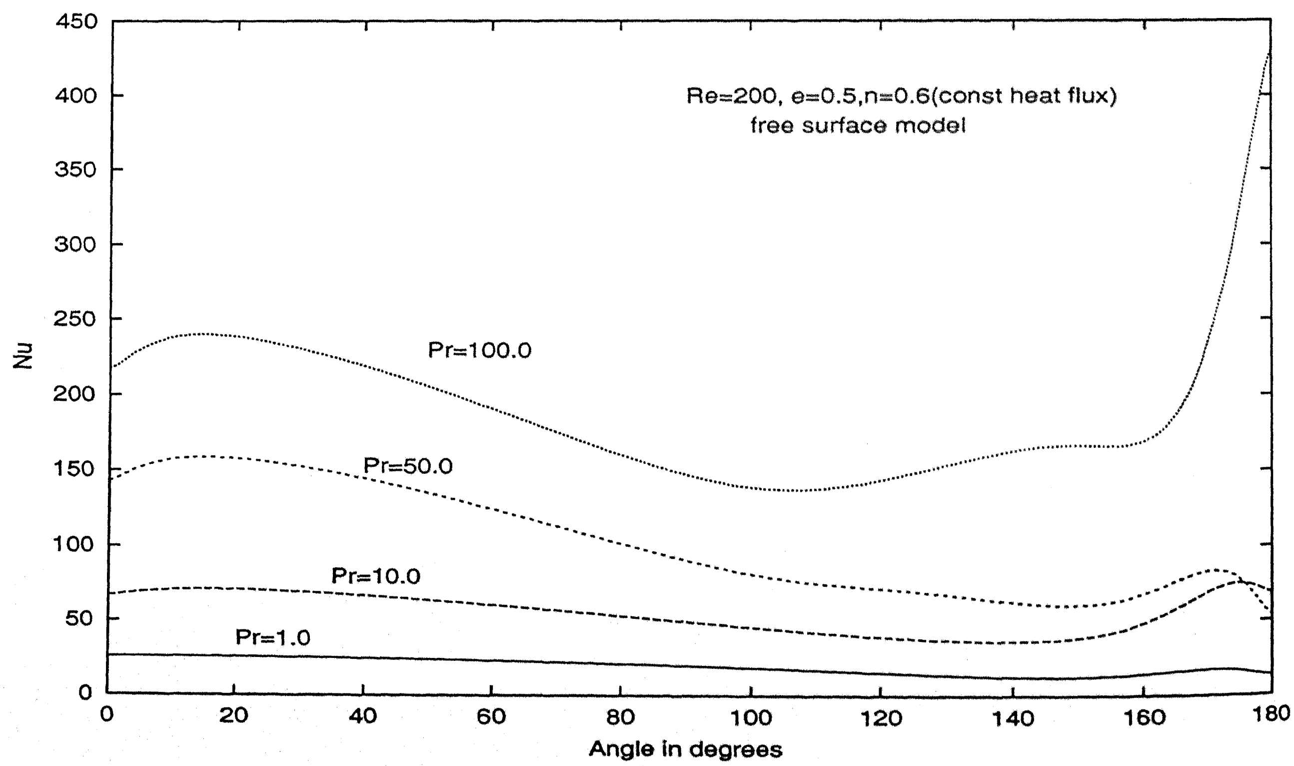

Figure 4.80: Variation of Nusselt number with angle for Re=200.0,e=0.5 and n=0.6 for constant heat flux condition

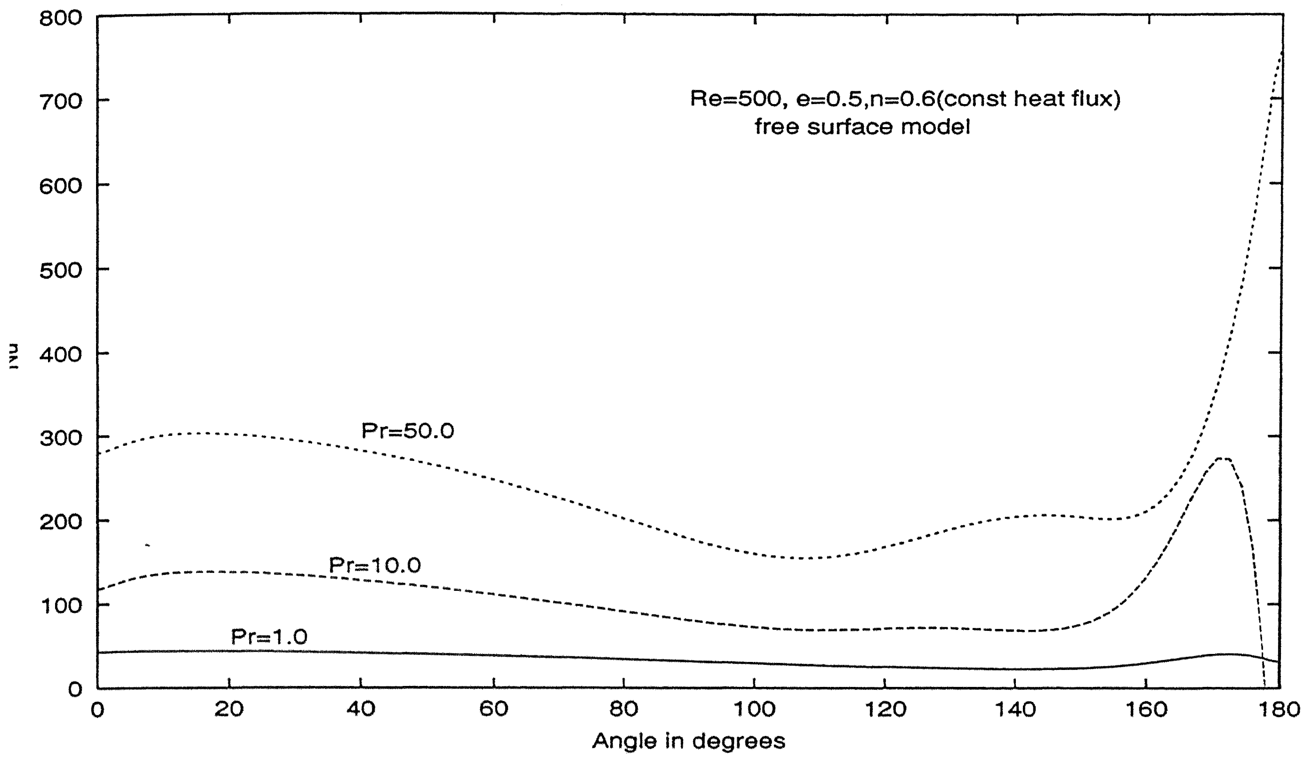

Figure 4.81: Variation of Nusselt number with angle for Re=500.0,e=0.5 and n=0.6 for constant heat flux condition

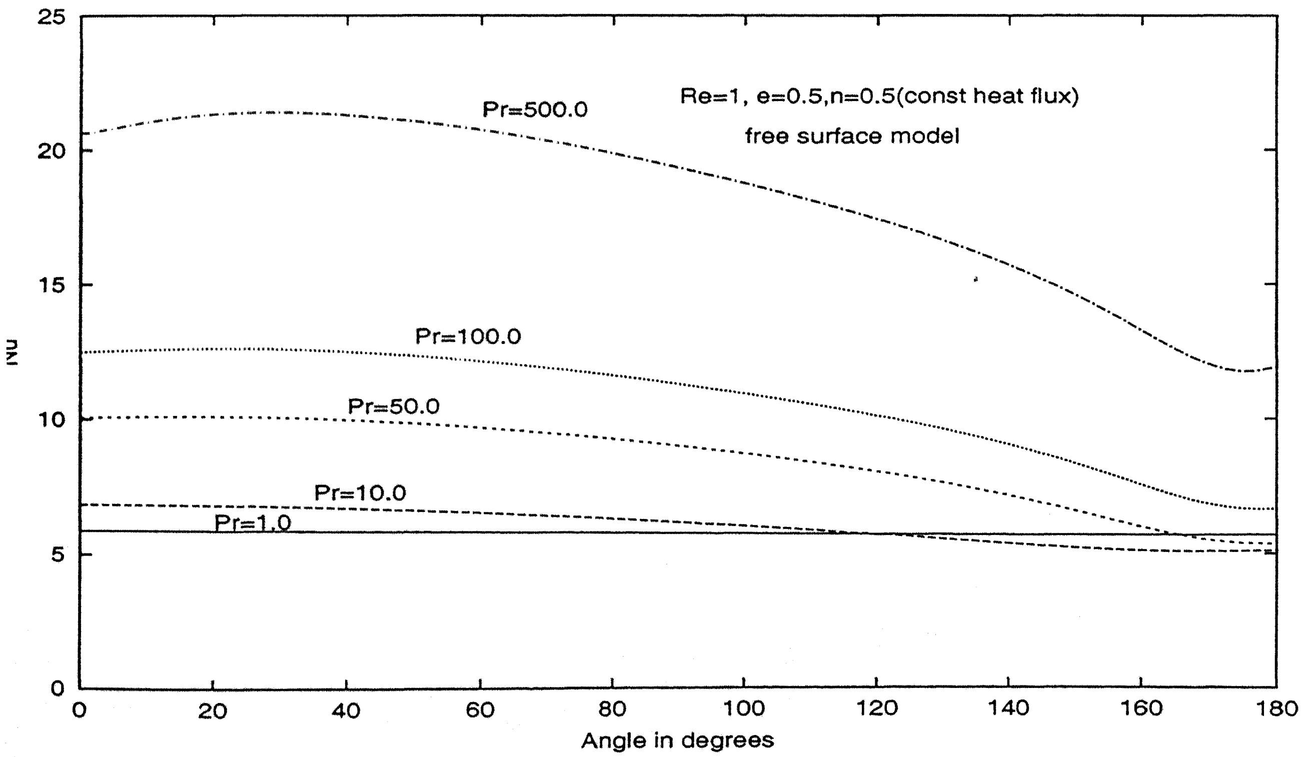

Figure 4.82: Variation of Nusselt number with angle for Re=1.0,e=0.5 and n=0.5 for constant heat flux condition

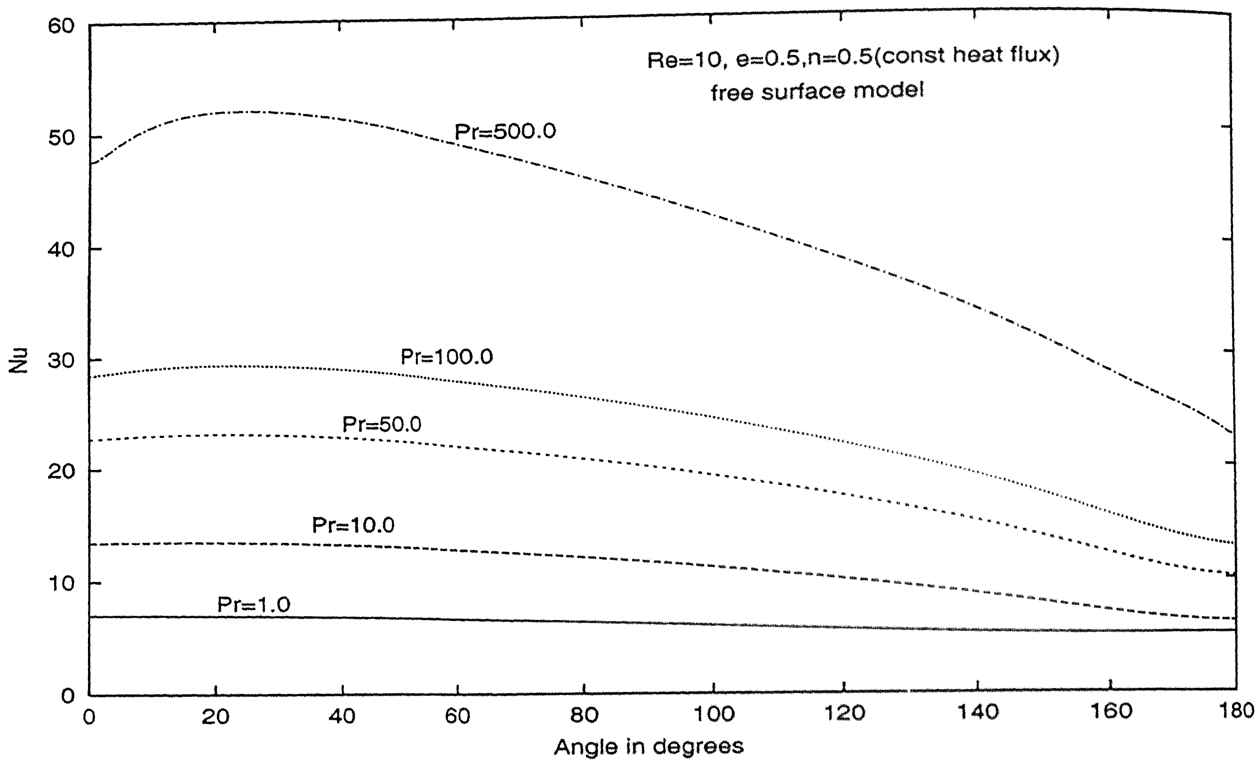

Figure 4.83: Variation of Nusselt number with angle for Re=10.0,e=0.5 and n=0.5 for constant heat flux condition

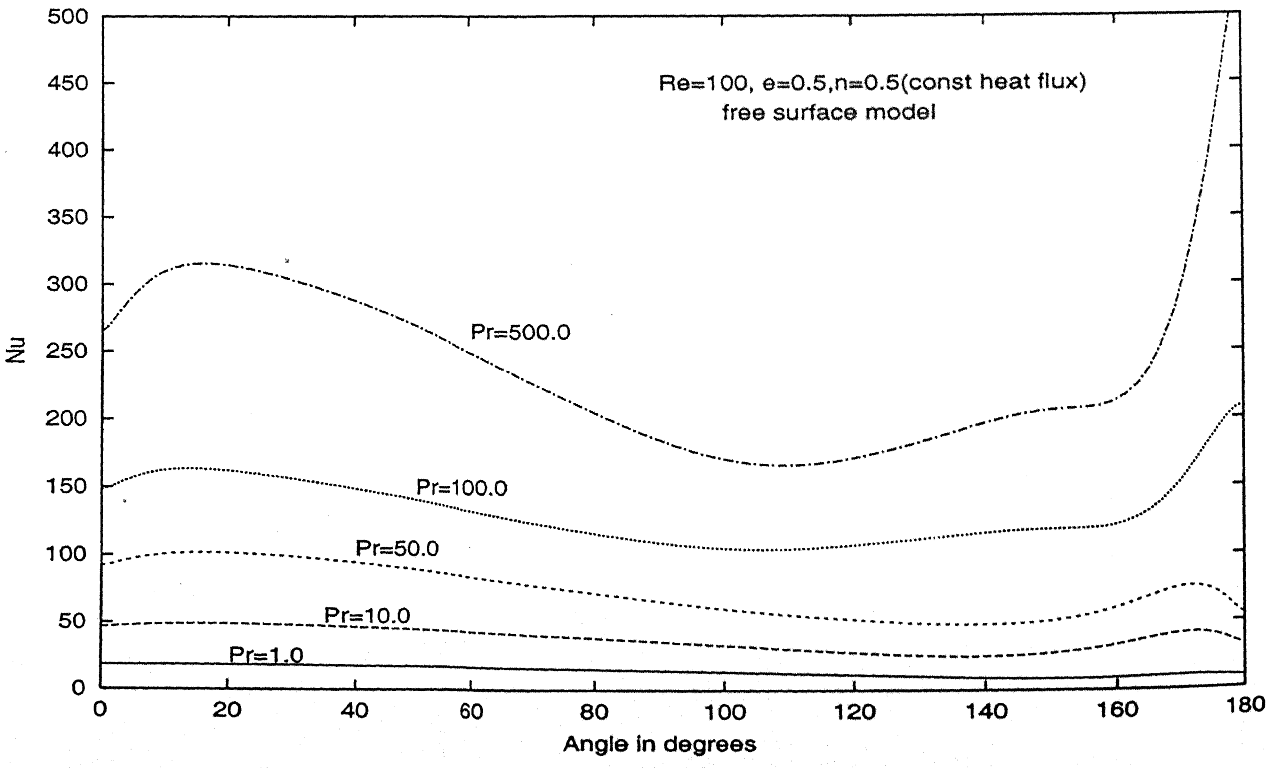

Figure 4.84: Variation of Nusselt number with angle for Re=100.0,e=0.5 and n=0.5 for constant heat flux condition

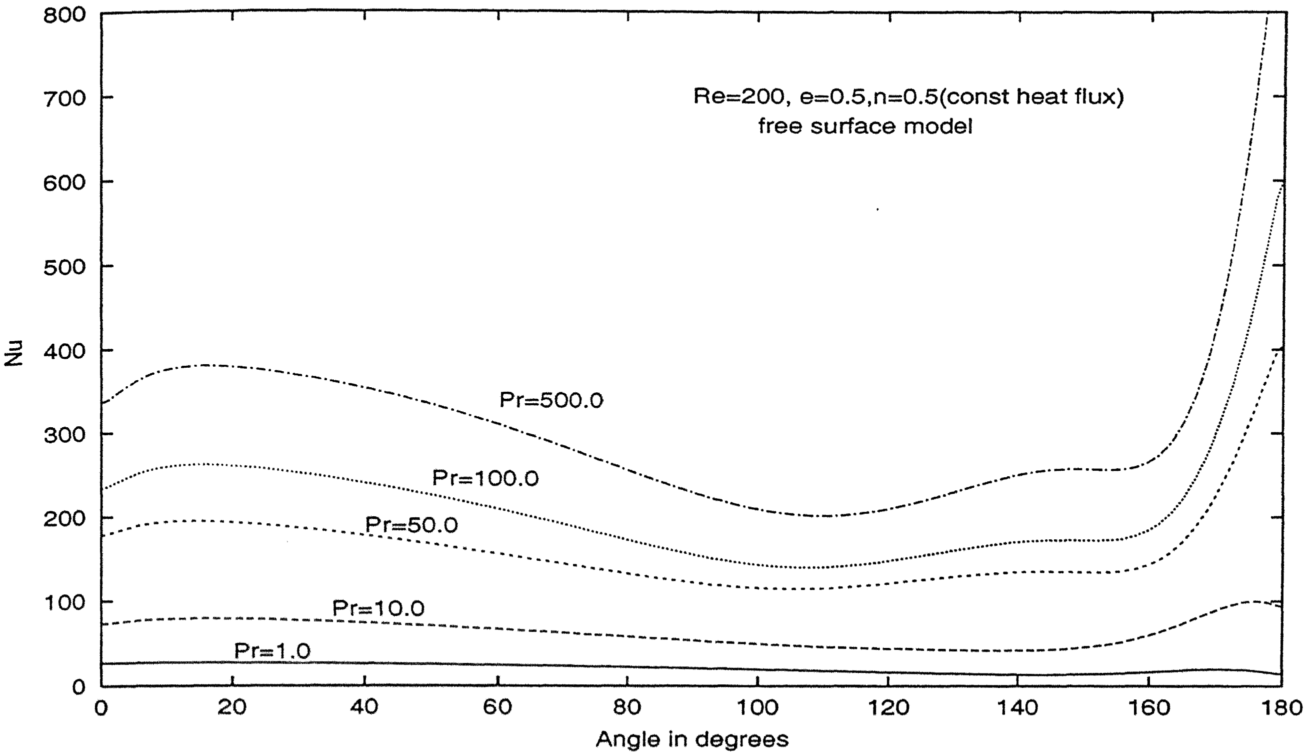

Figure 4.85: Variation of Nusselt number with angle for Re=200.0,e=0.5 and n=0.5 for constant heat flux condition

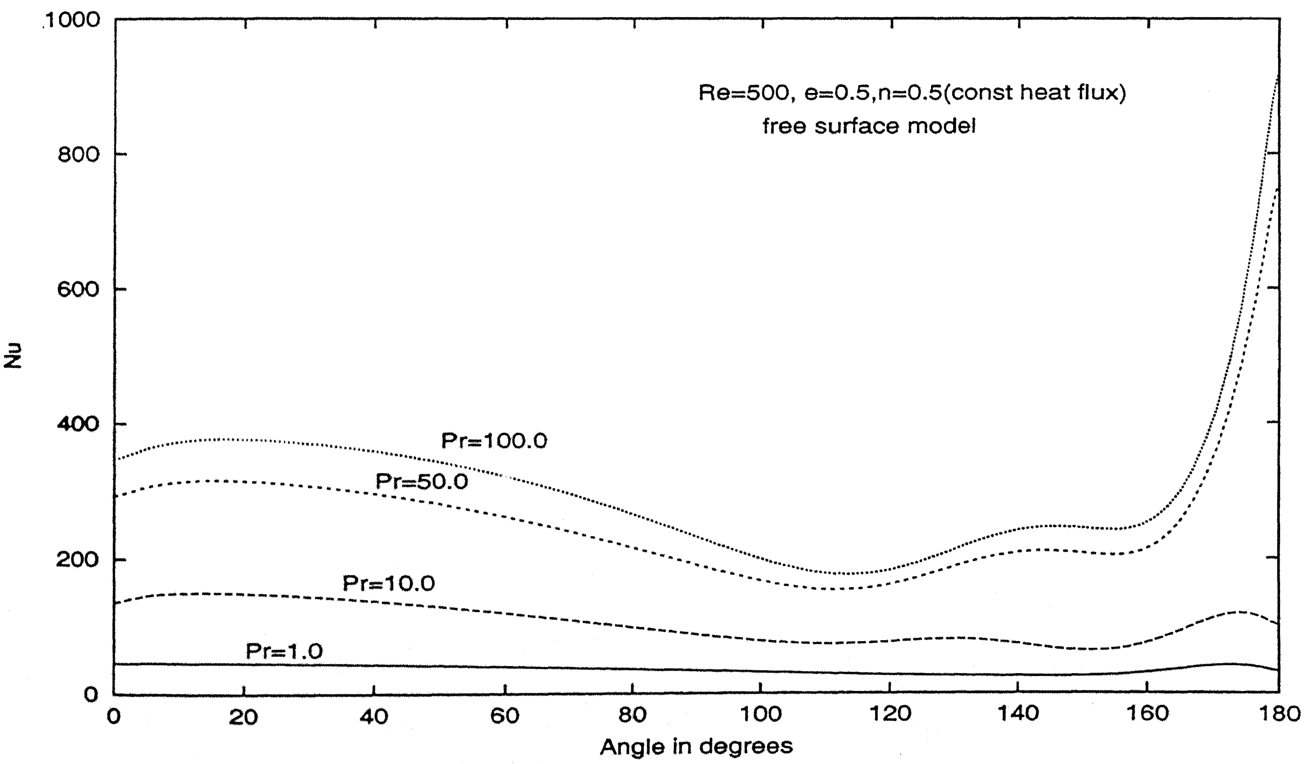

Figure 4.86: Variation of Nusselt number with angle for Re=500.0,e=0.5 and n=0.5 for constant heat flux condition

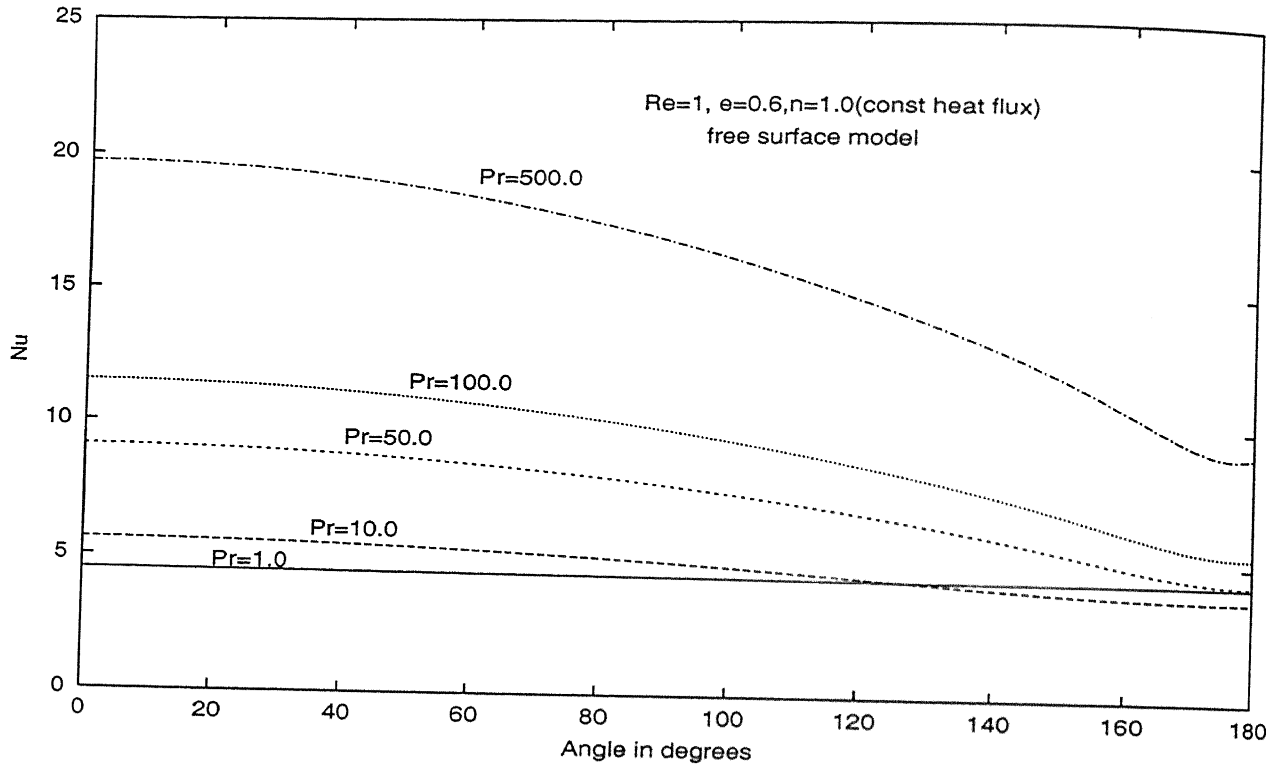

Figure 4.87: Variation of Nusselt number with angle for Re=1.0,e=0.6 and n=1.0 for constant heat flux condition

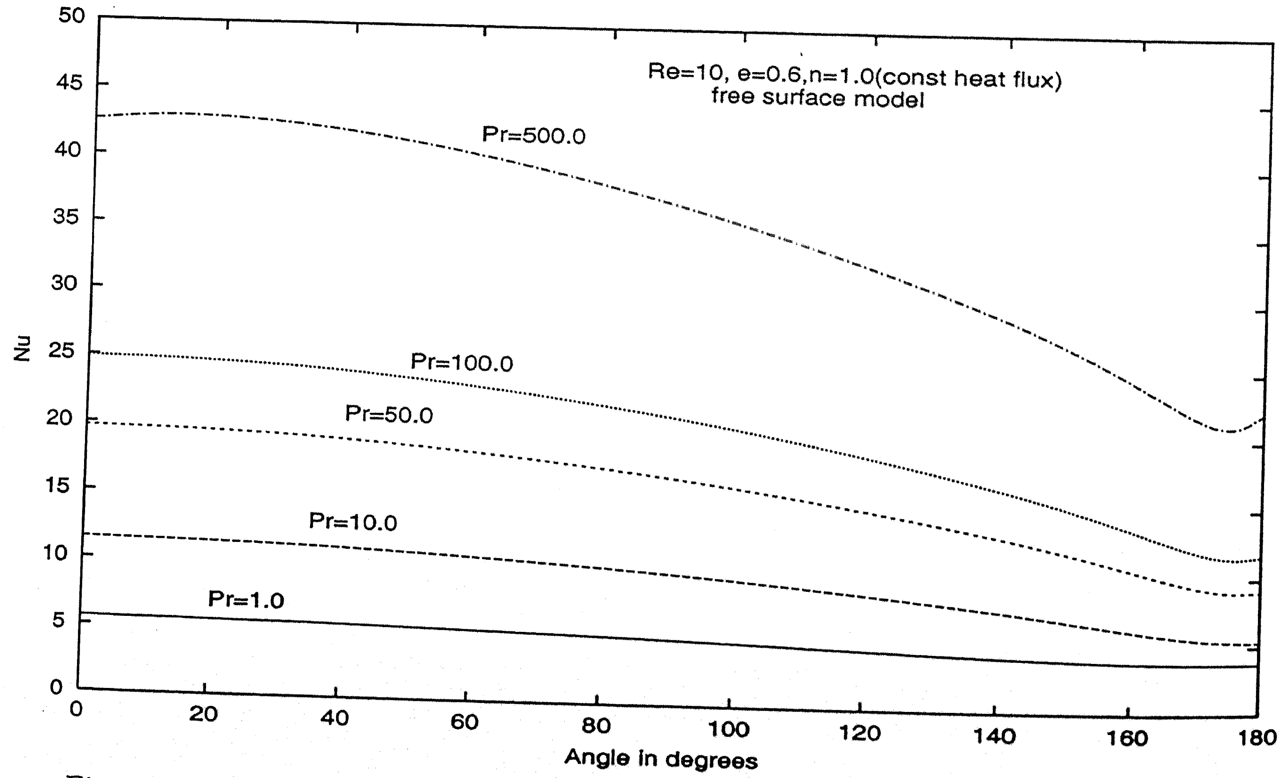

Figure 4.88: Variation of Nusselt number with angle for Re=10.0,e=0.6 and n=1.0 for constant heat flux condition

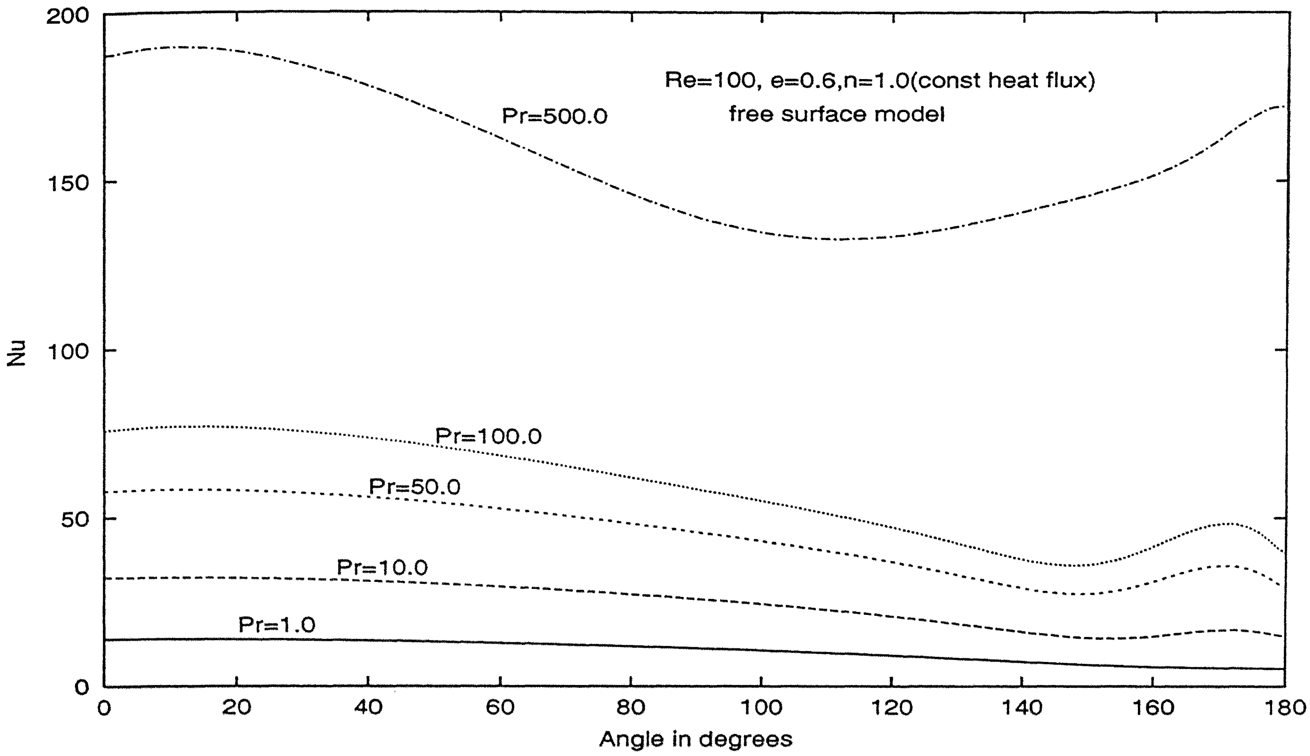

Figure 4.89: Variation of Nusselt number with angle for Re=100.0,e=0.6 and n=1.0 for constant heat flux condition

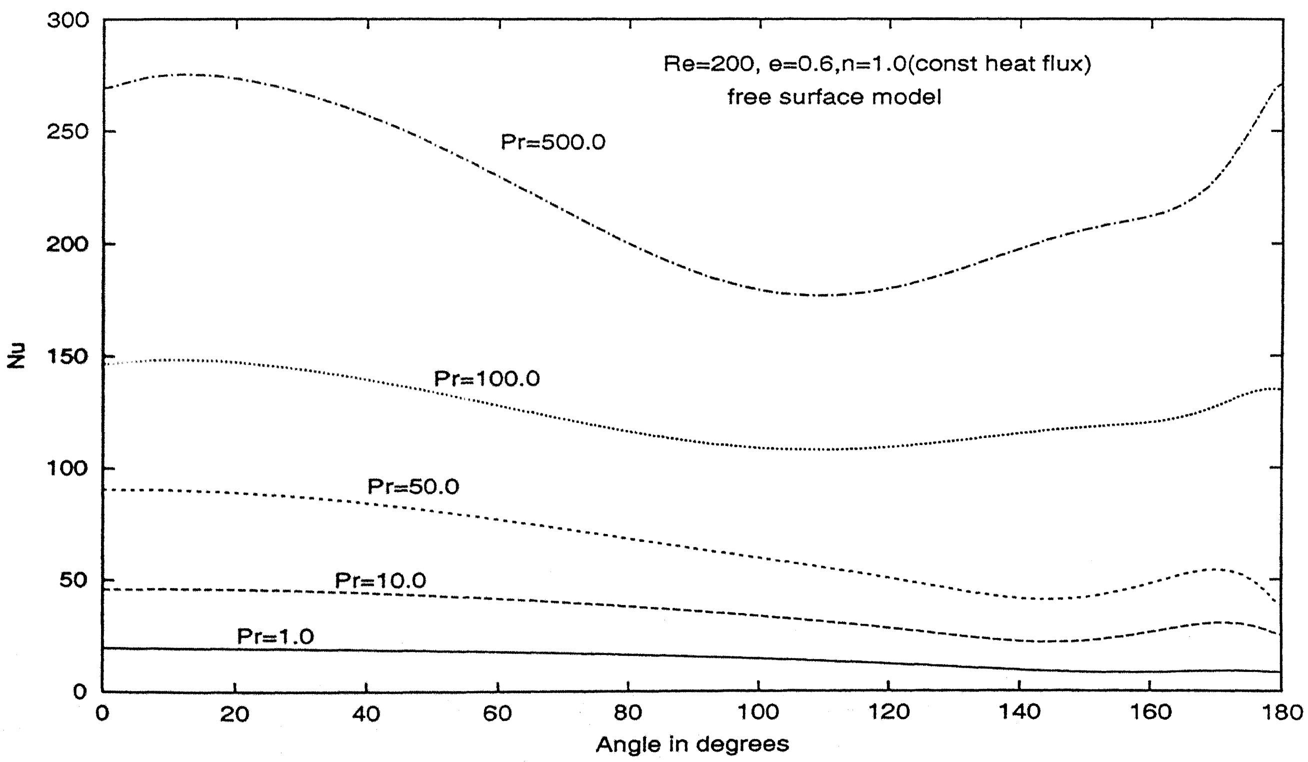

Figure 4.90: Variation of Nusselt number with angle for Re=200.0,e=0.6 and n=1.0 for constant heat flux condition

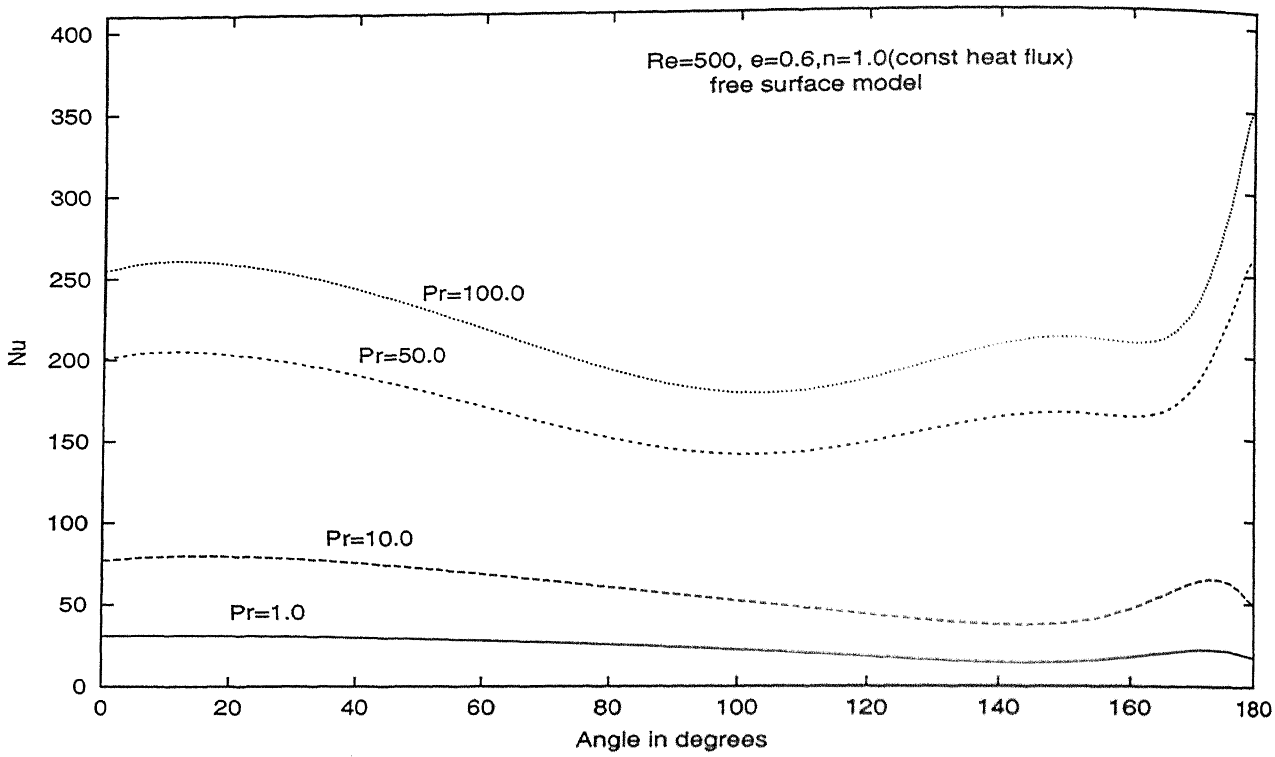

Figure 4.91: Variation of Nusselt number with angle for Re=500.0,e=0.6 and n=1.0 for constant heat flux condition

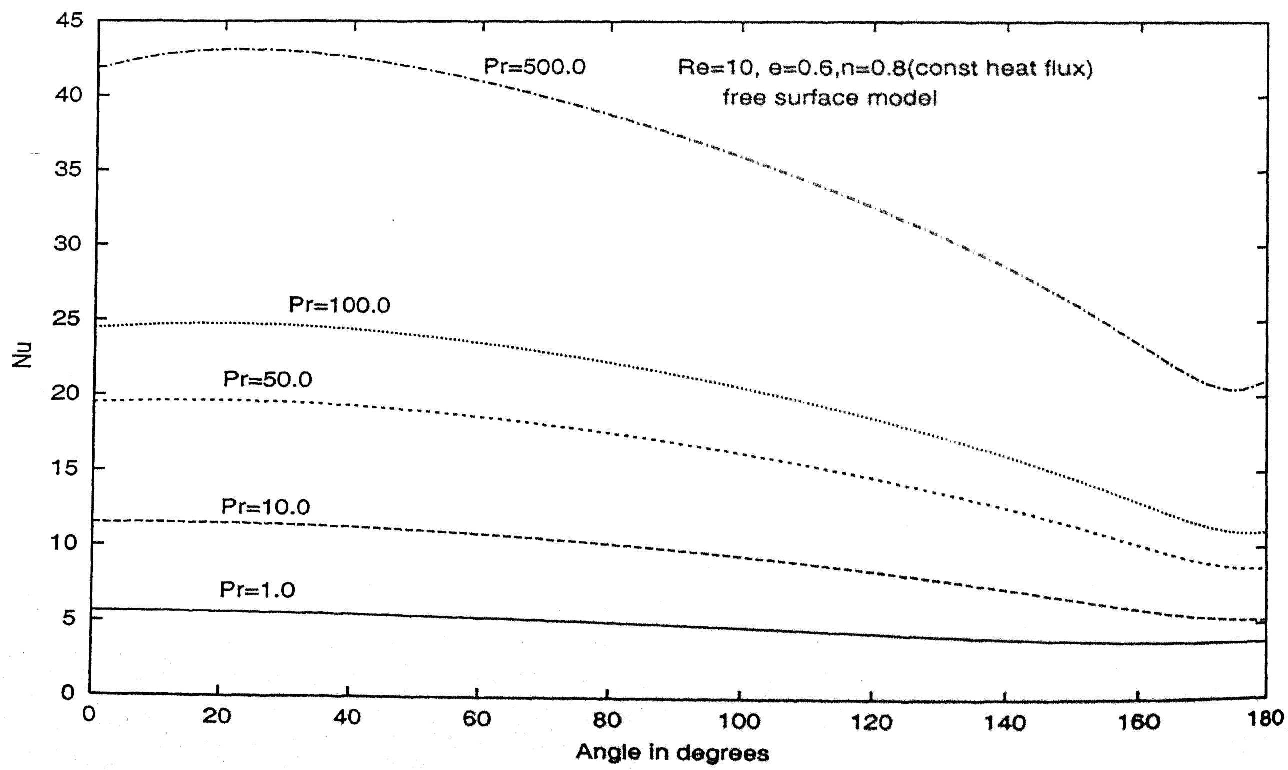

Figure 4.92: Variation of Nusselt number with angle for Re=10.0,e=0.6 and n=0.8 for constant heat flux condition

Re=500, e=0.6,n=0.8(const heat flux)

free surface model

Figure 4.93: Variation of Nusselt number with angle for Re=200.0,e=0.6 and n=0.8 for constant heat flux condition

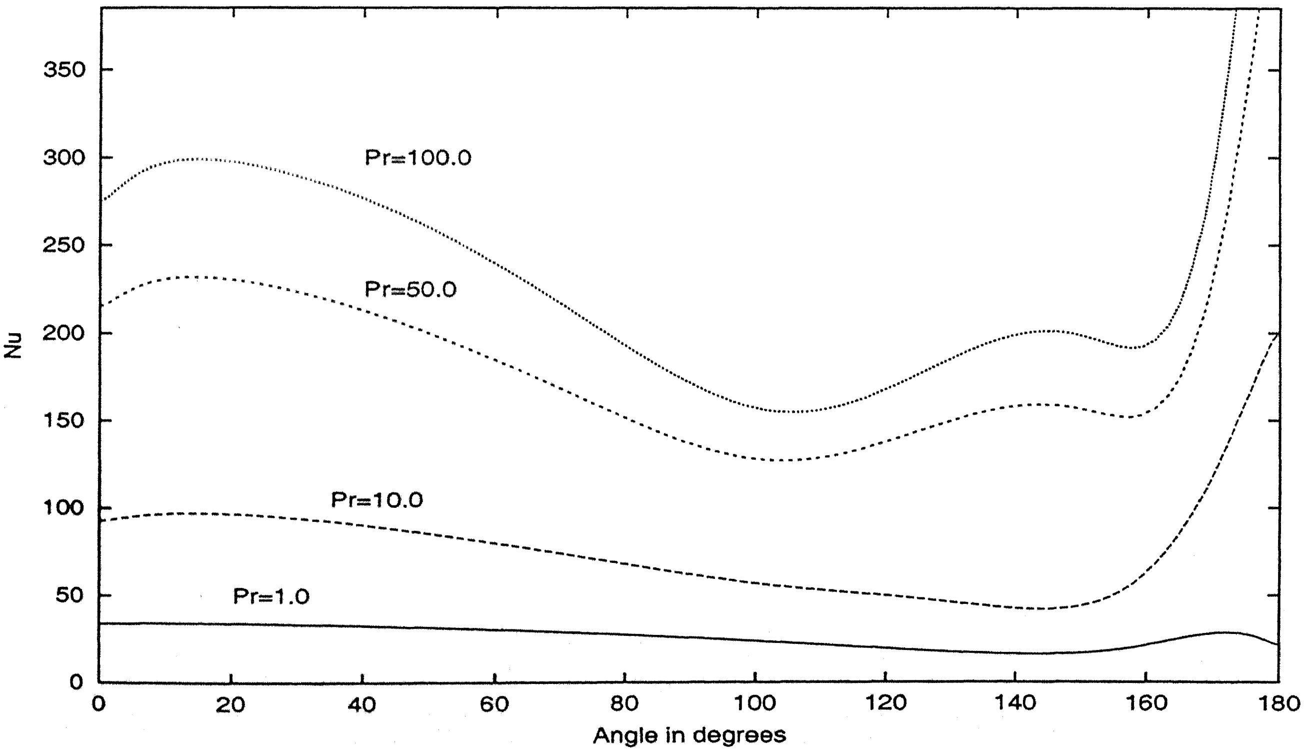

Figure 4.94: Variation of Nusselt number with angle for Re=500.0,e=0.6 and n=0.8 for constant heat flux condition

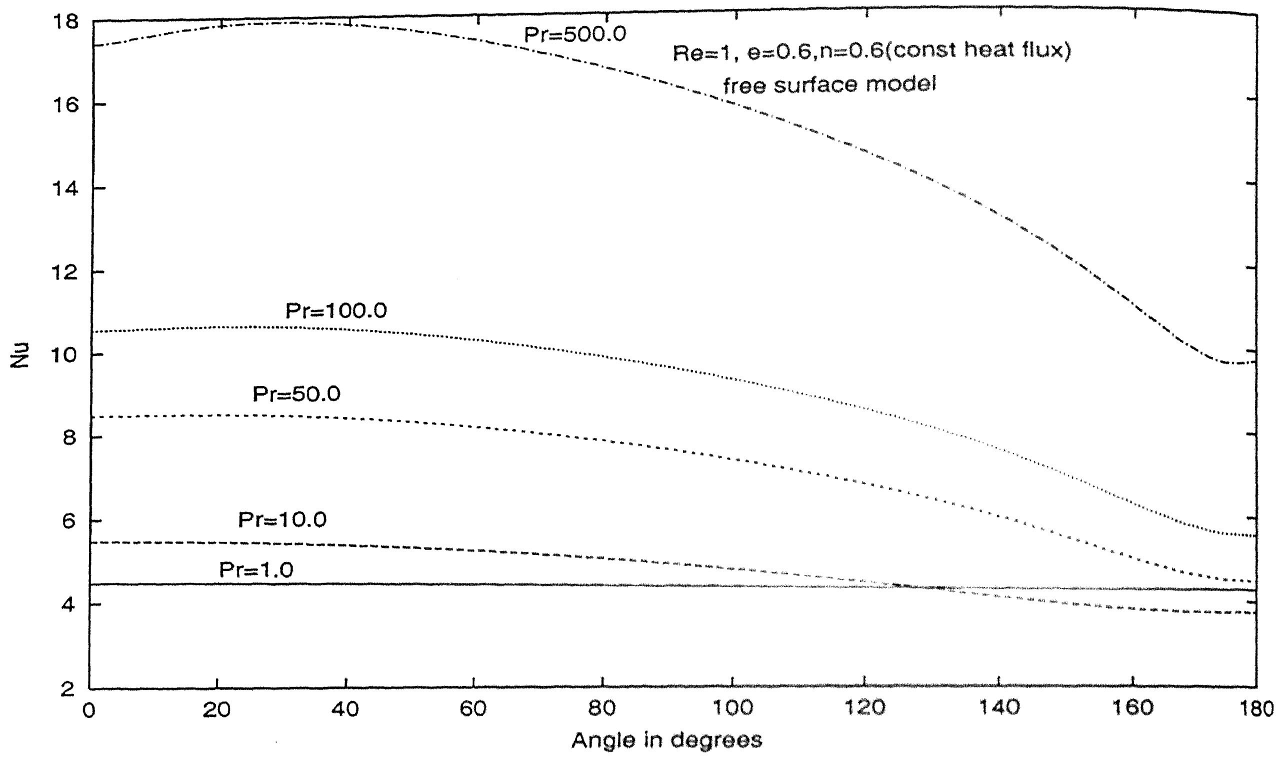

Figure 4.95: Variation of Nusselt number with angle for Re=1.0,e=0.6 and n=0.6 for constant heat flux condition

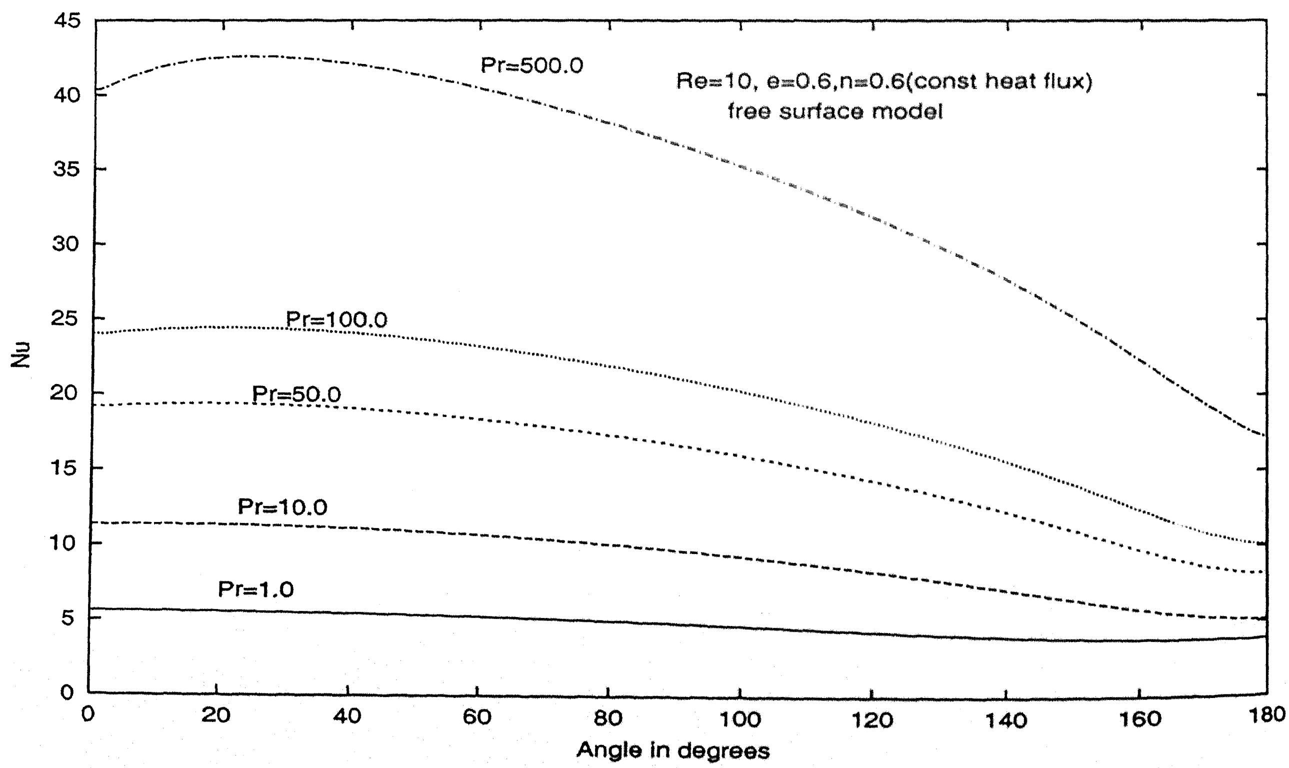

Figure 4.96: Variation of Nusselt number with angle for Re=10.0,e=0.6 and n=0.6 for constant heat flux condition

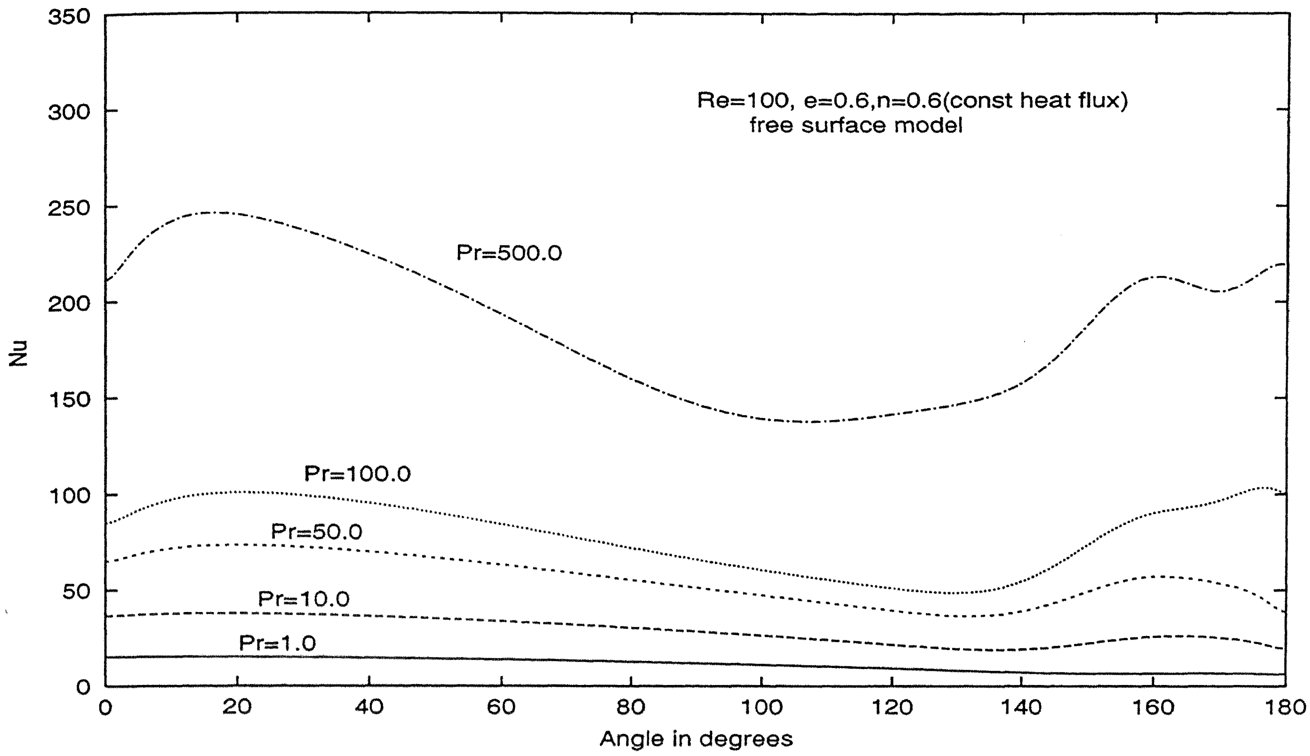

Figure 4.97: Variation of Nusselt number with angle for Re=100.0,e=0.6 and n=0.6 for constant heat flux condition

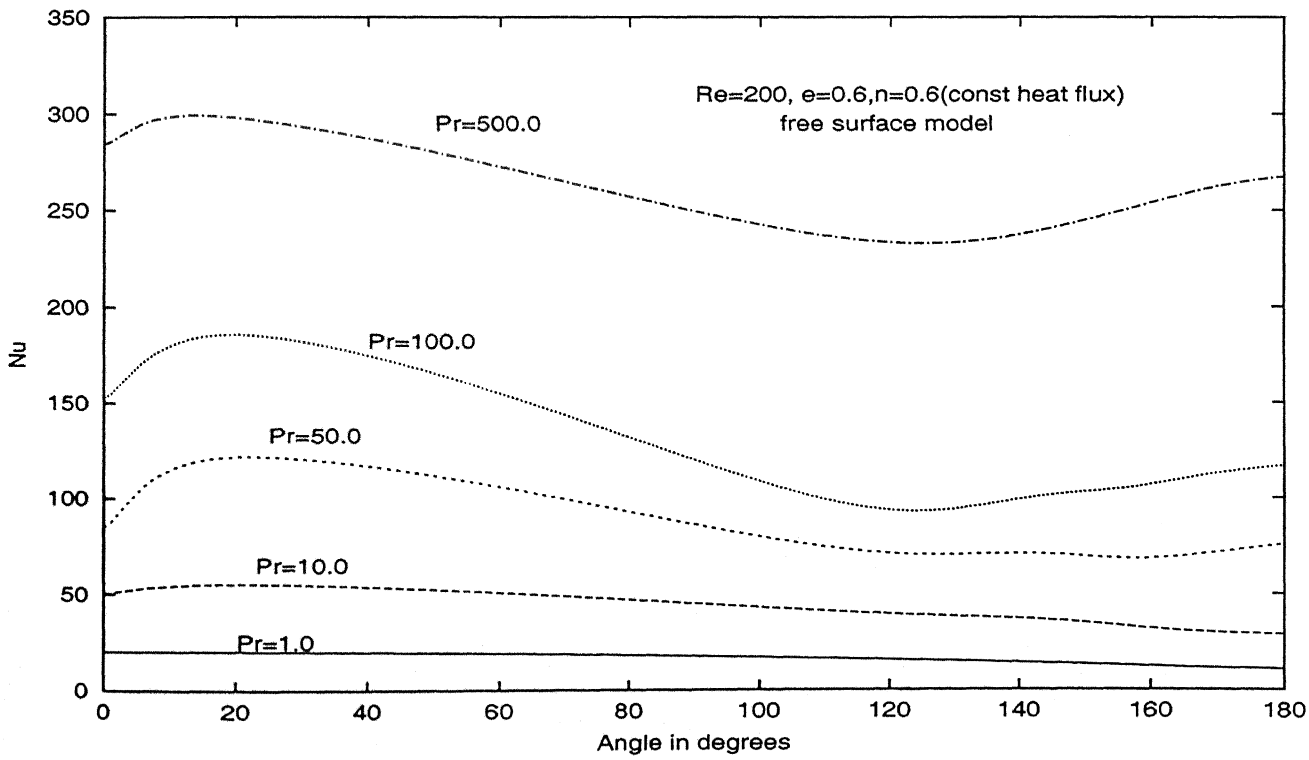

Figure 4.98: Variation of Nusselt number with angle for Re=200.0,e=0.6 and n=0.6 for constant heat flux condition

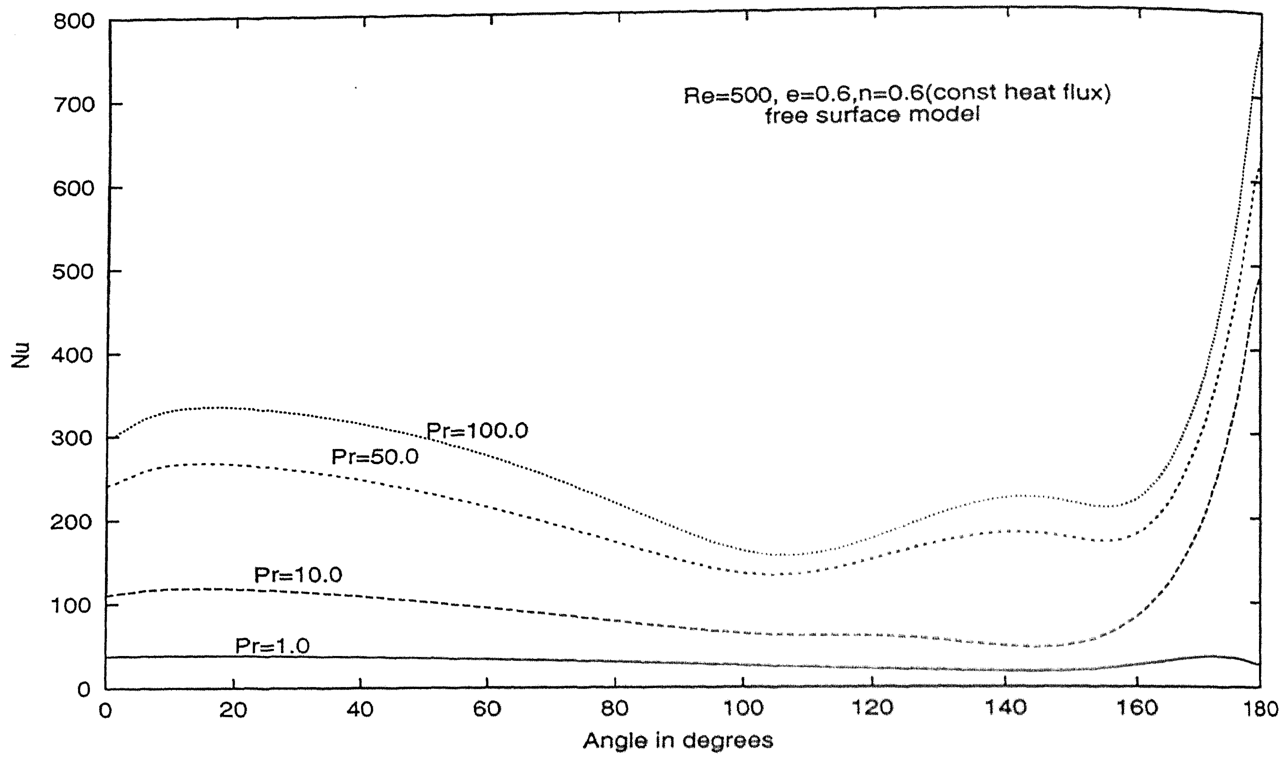

Figure 4.99: Variation of Nusselt number with angle for Re=500.0,e=0.6 and n=0.6 for constant heat flux condition

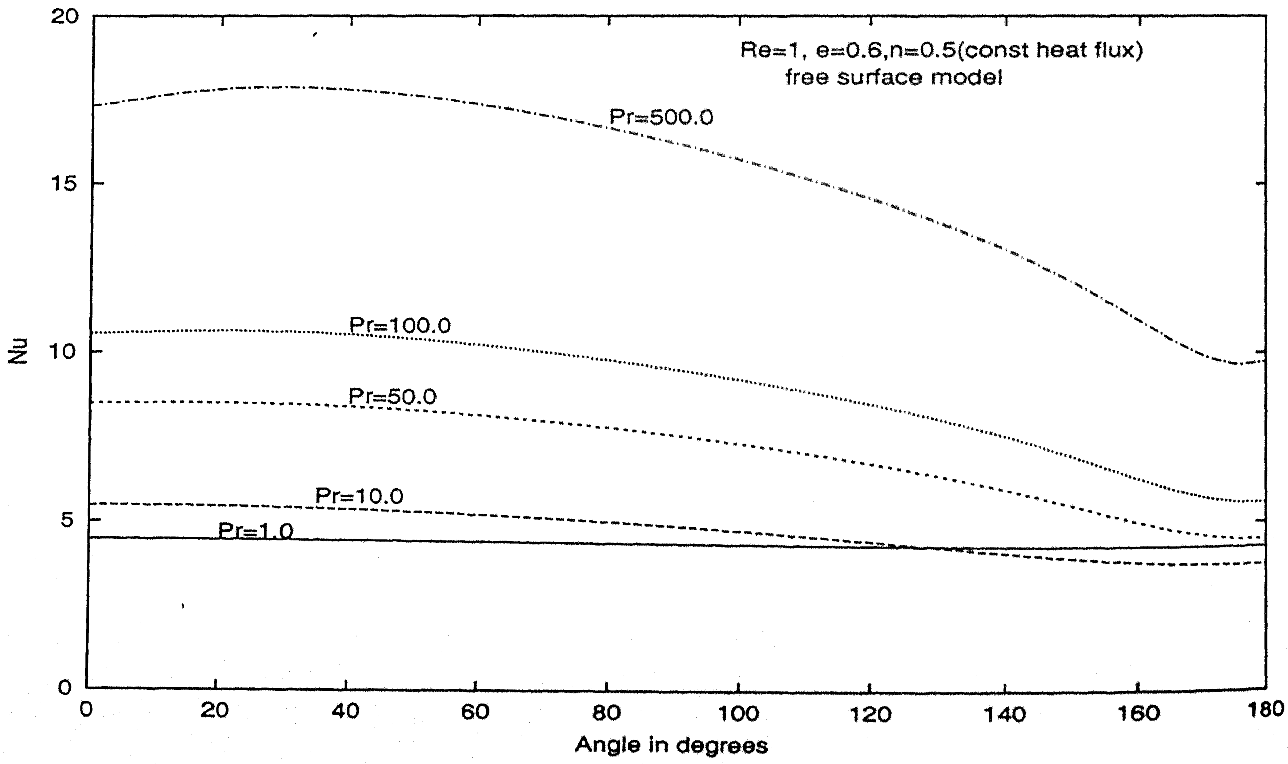

Figure 4.100: Variation of Nusselt number with angle for Re=1.0,e=0.6 and n=0.5 for constant heat flux condition

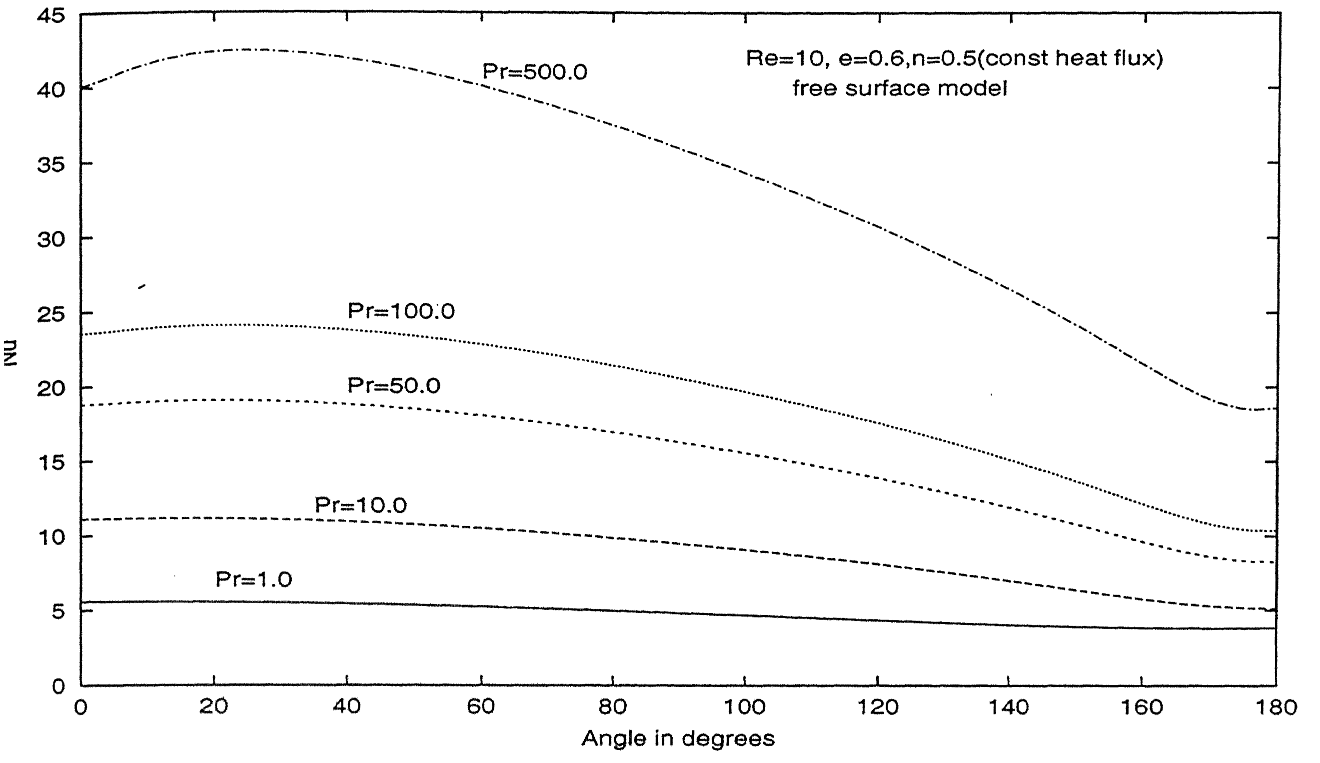

Figure 4.101: Variation of Nusselt number with angle for Re=10.0,e=0.5 and n=0.5 for constant heat flux condition

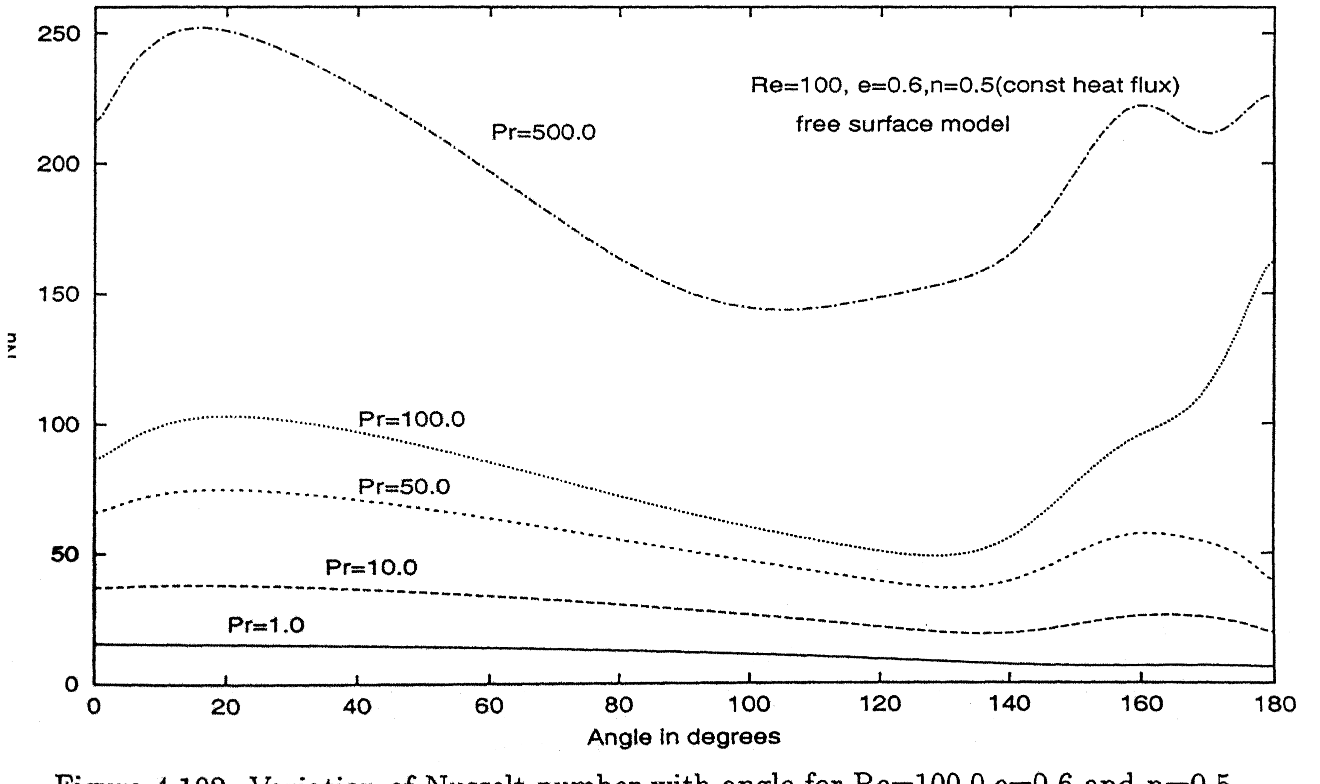

Figure 4.102: Variation of Nusselt number with angle for Re=100.0,e=0.6 and n=0.5 for constant heat flux condition

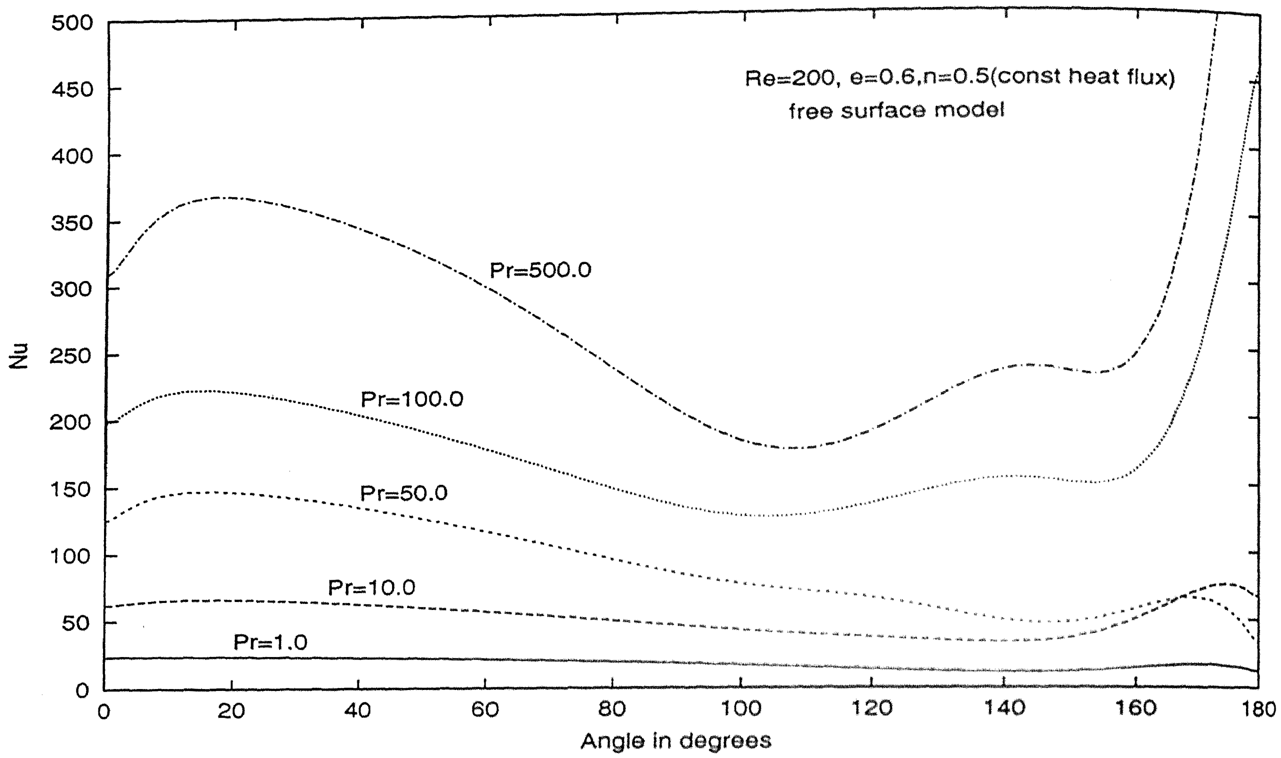

Figure 4.103: Variation of Nusselt number with angle for Re=200.0,e=0.6 and n=0.5 for constant heat flux condition

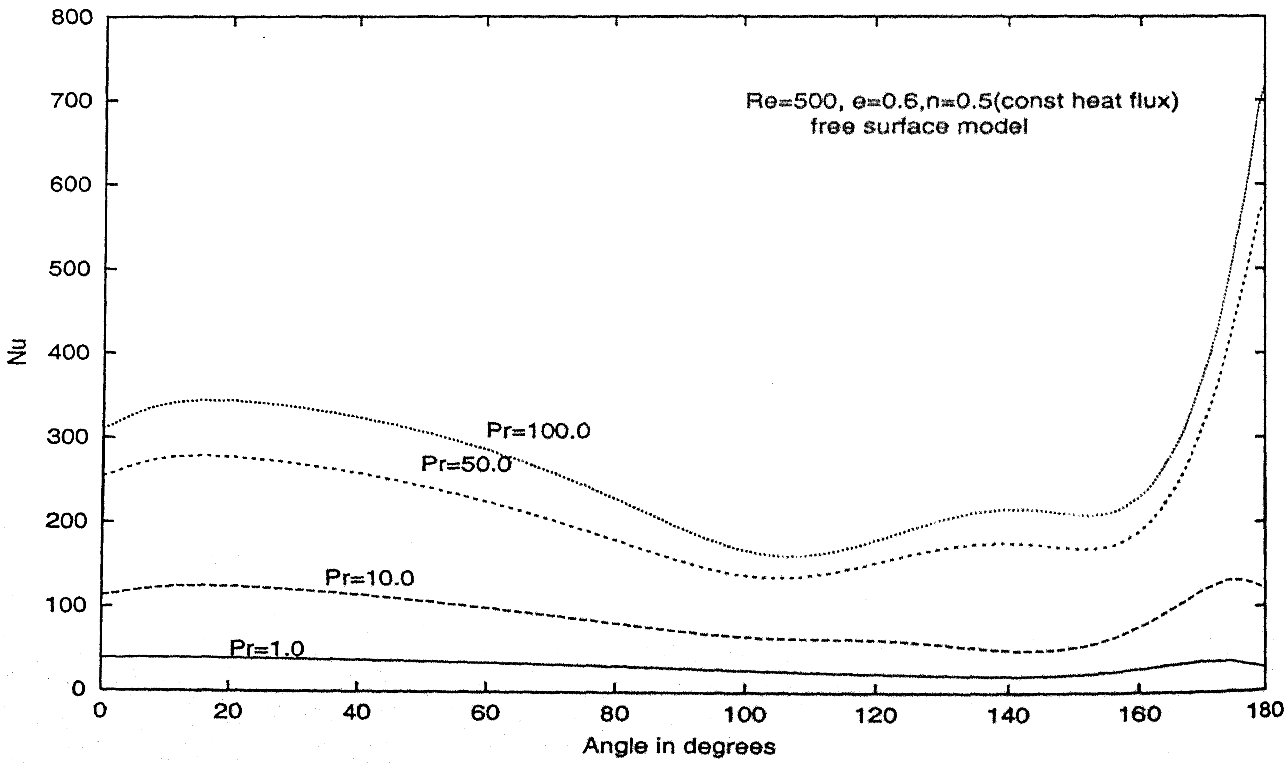

Figure 4.104: Variation of Nusselt number with angle for Re=500.0,e=0.6 and n=0.5 for constant heat flux condition

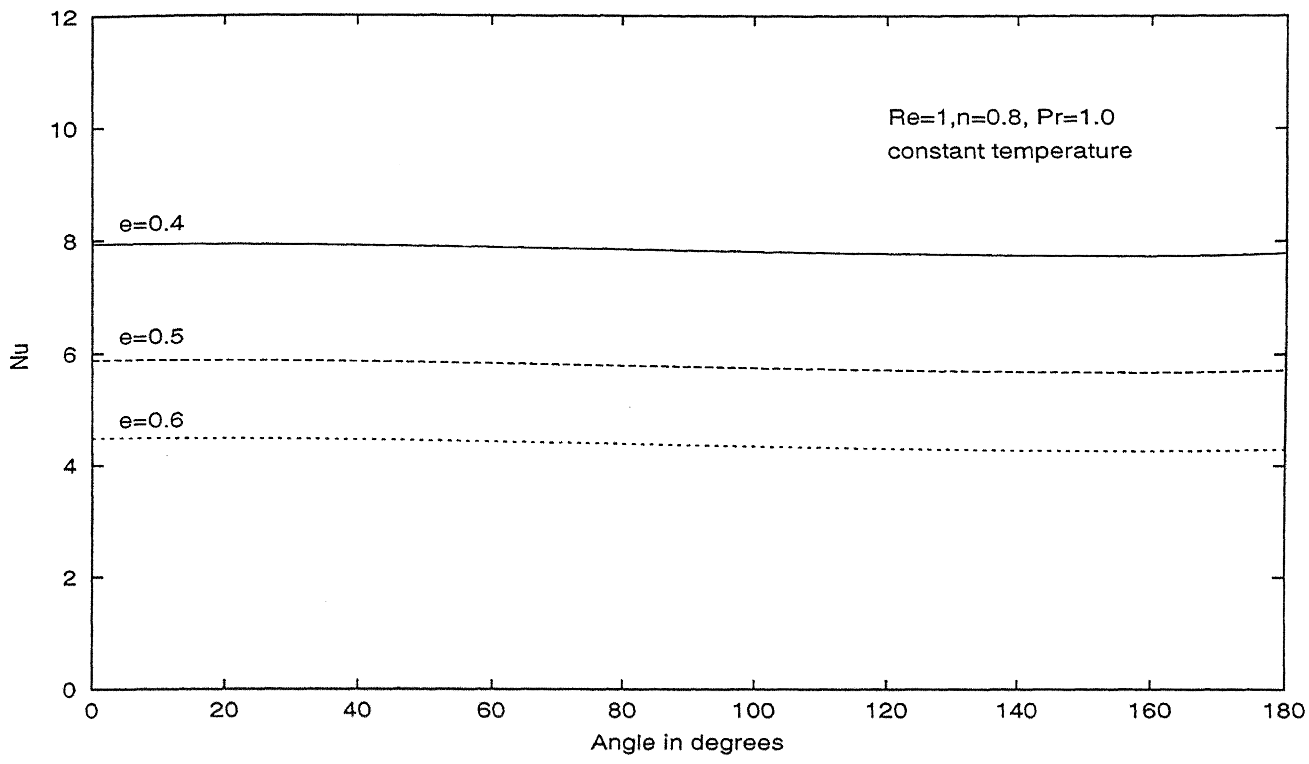

Figure 4.103:Variation of Nusselt number with angle for Re=1,n=0.8 and Pr=1 for constant wall teperature

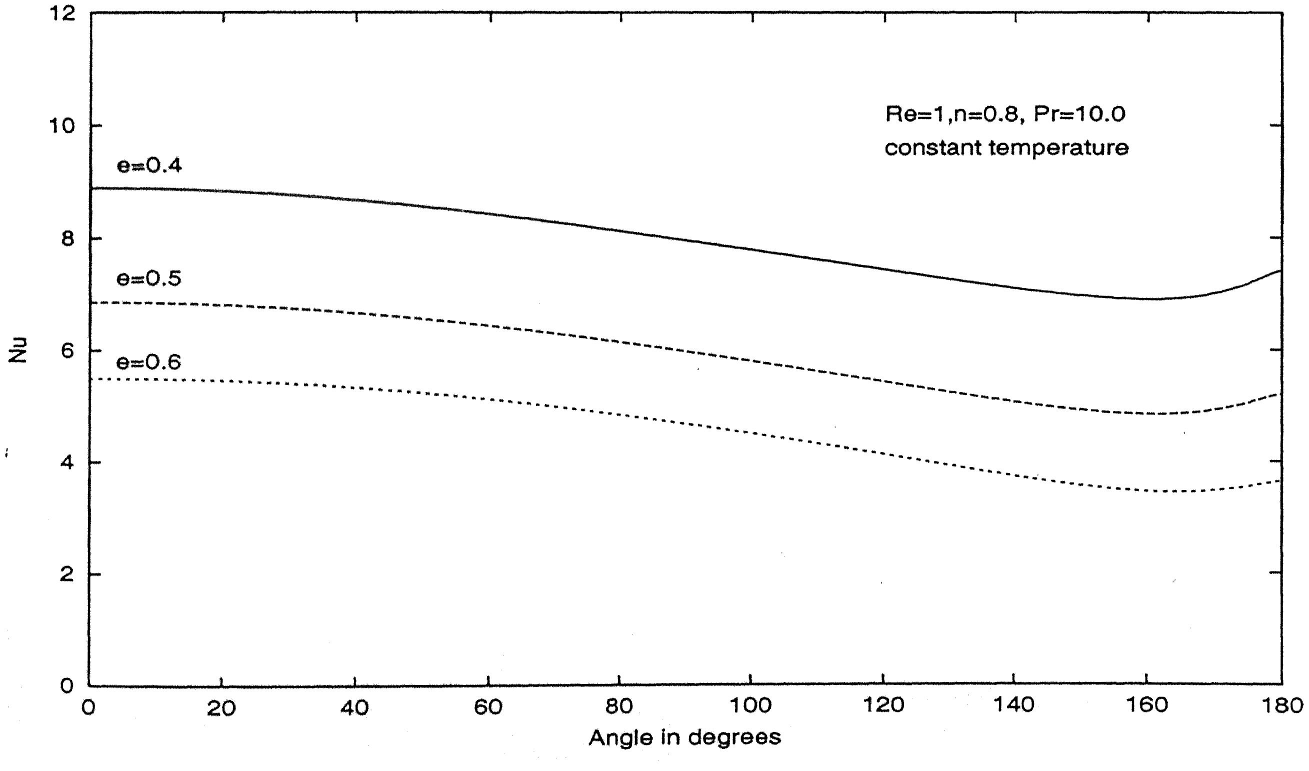

Figure 4.104:Variation of Nusselt number with angle for Re=1,n=0.8 and Pr=10 for constant wall teperature

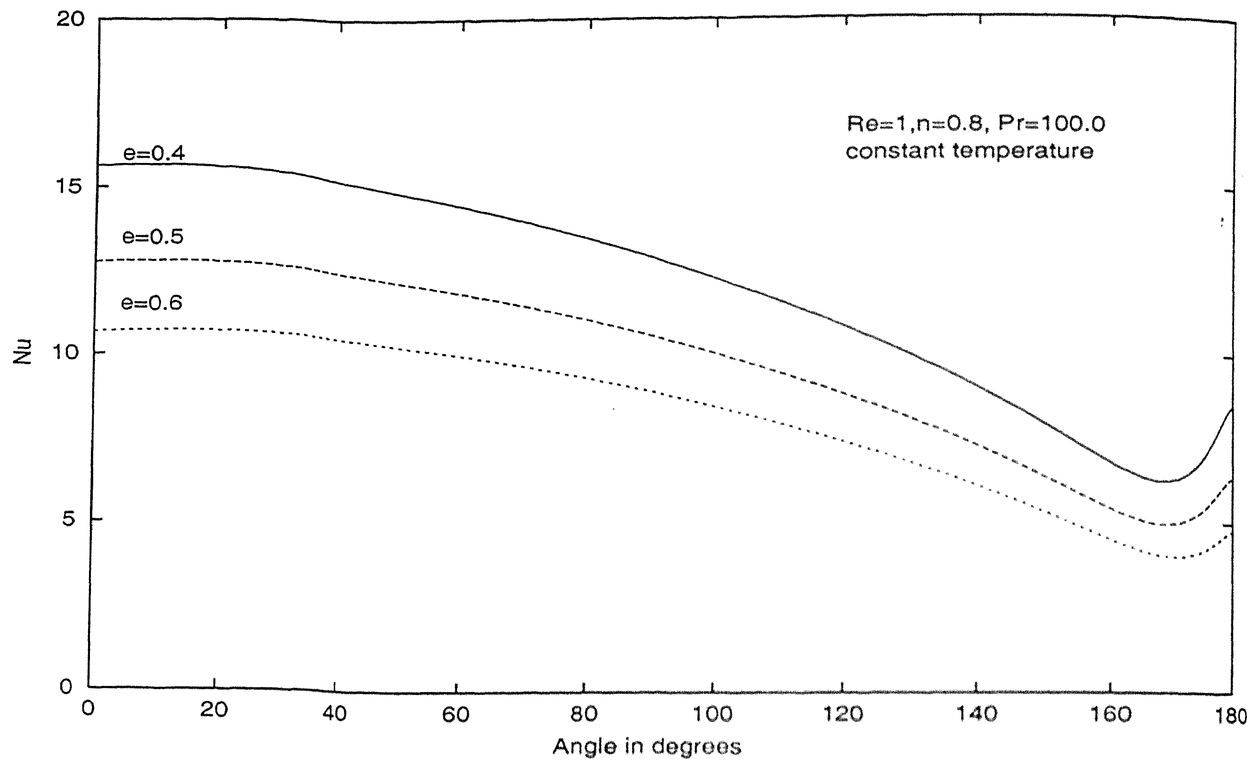

Figure 4.105:Variation of Nusselt number with angle for Re=1,n=0.8 and Pr=100 for constant wall teperature

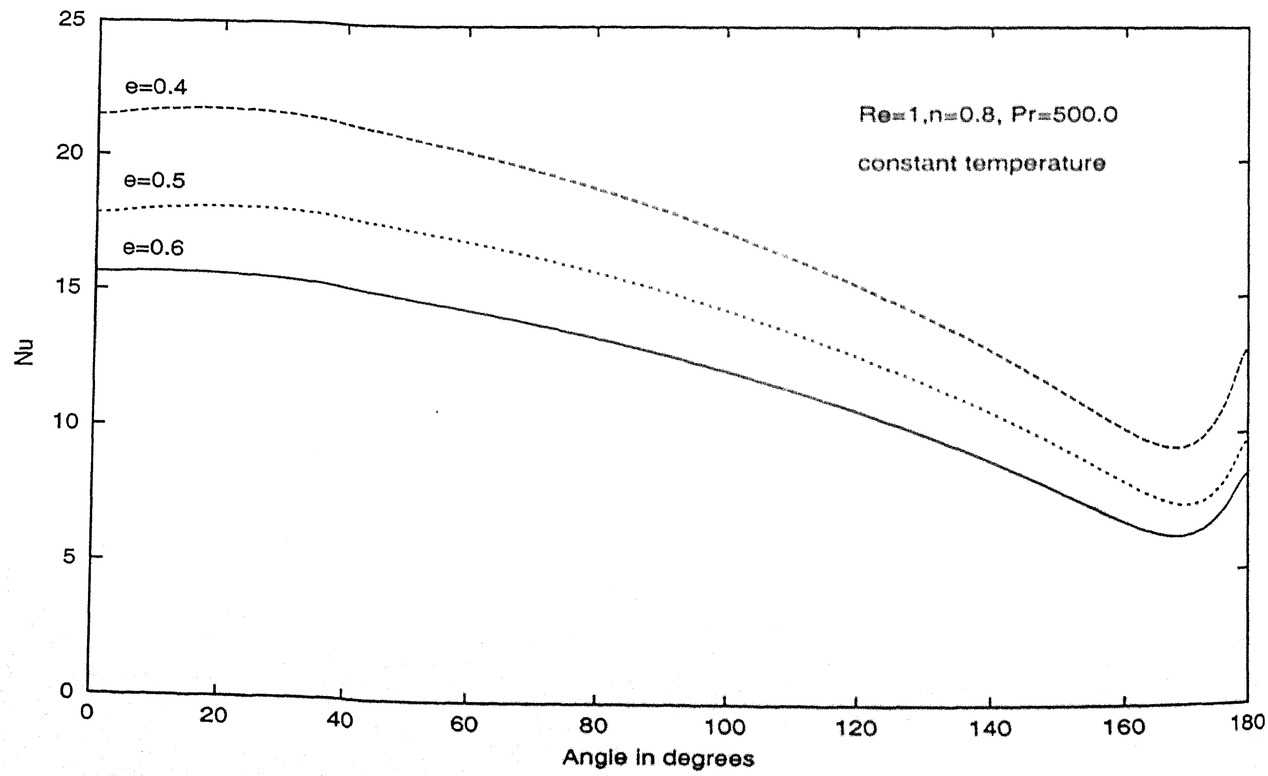

Figure 4.106:Variation of Nusselt number with angle for Re=1,n=0.8 and Pr=500 for constant wall teperature

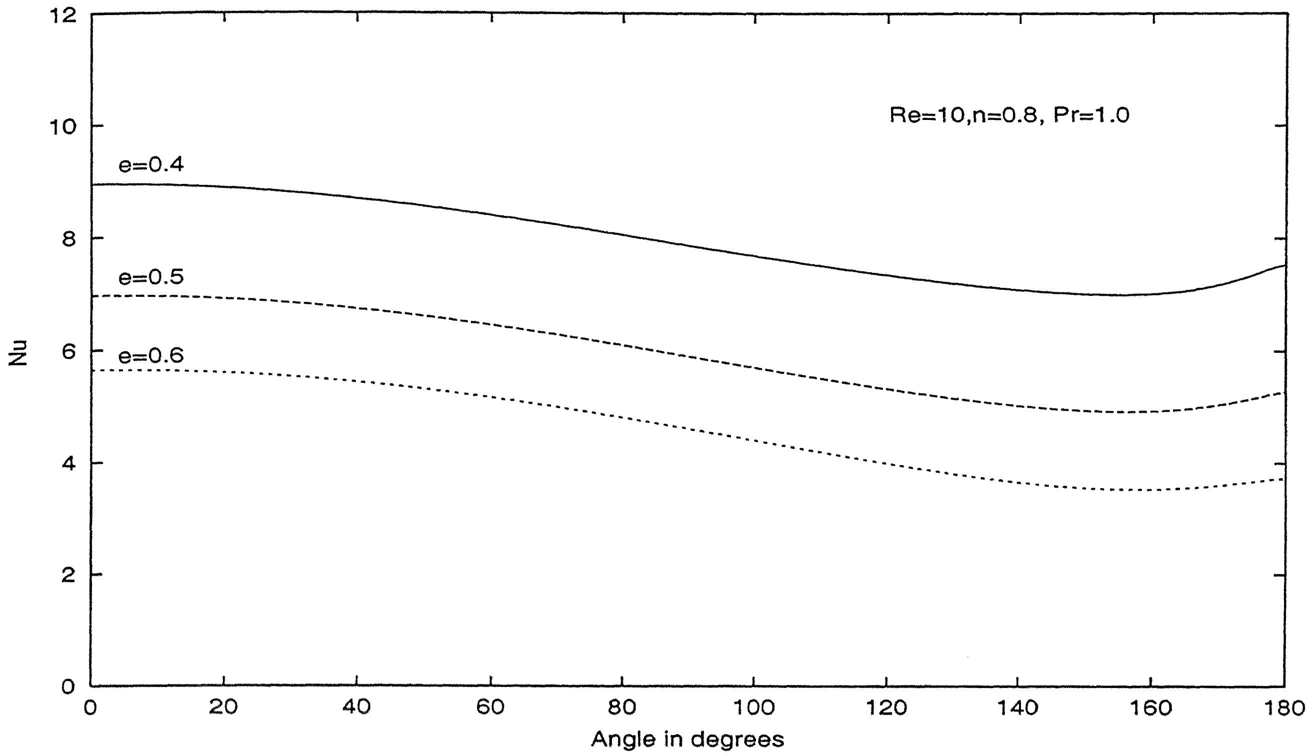

Figure 4.107:Variation of Nusselt number with angle for Re=10,n=0.8 and Pr=1 for constant wall teperature

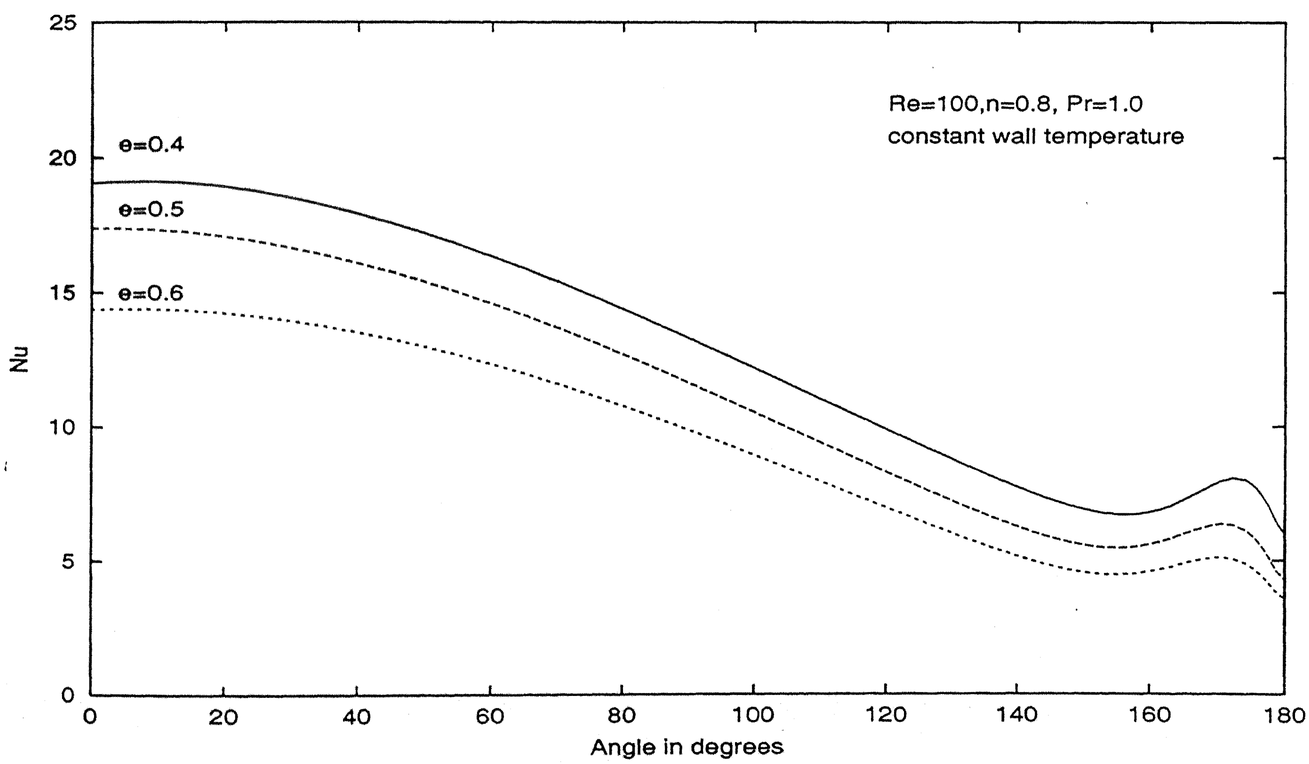

Figure 4.108:Variation of Nusselt number with angle for Re=100,n=0.8 and Pr=1 for constant wall teperature

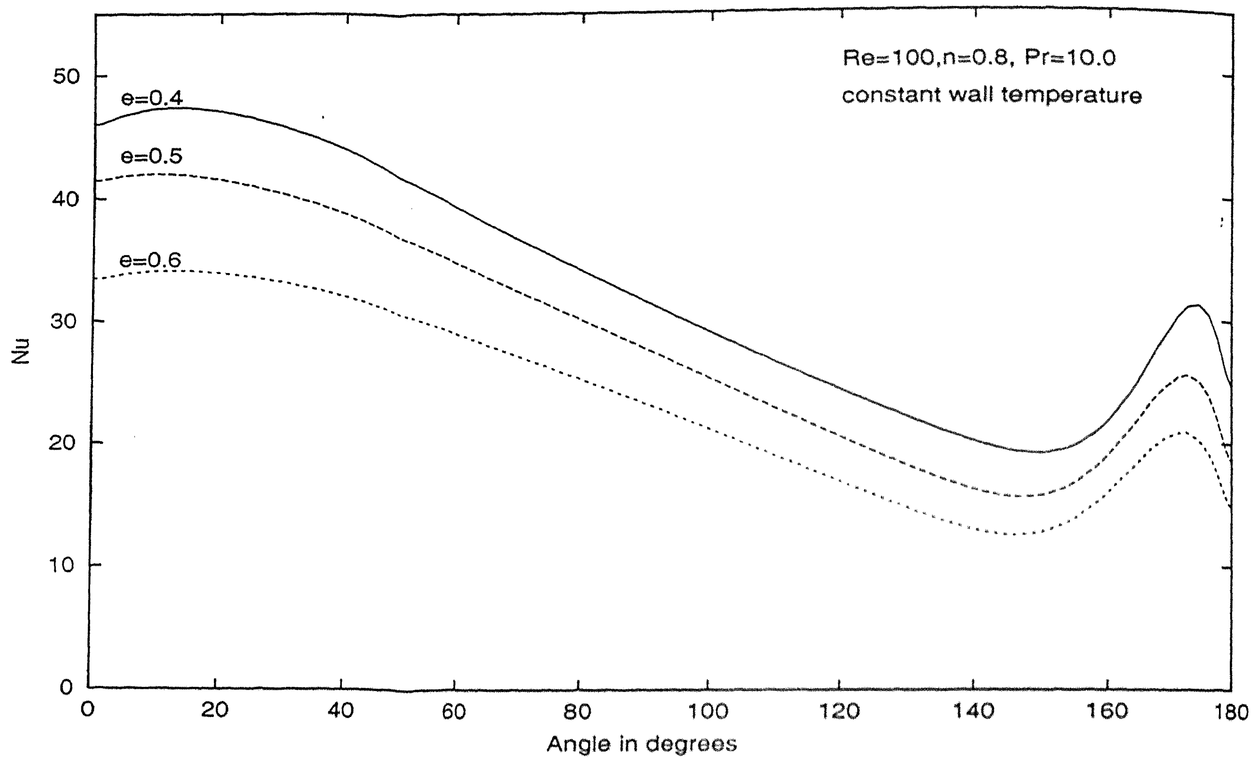

Figure 4.109:Variation of Nusselt number with angle for Re=100,n=0.8 and Pr=10 for constant wall teperature

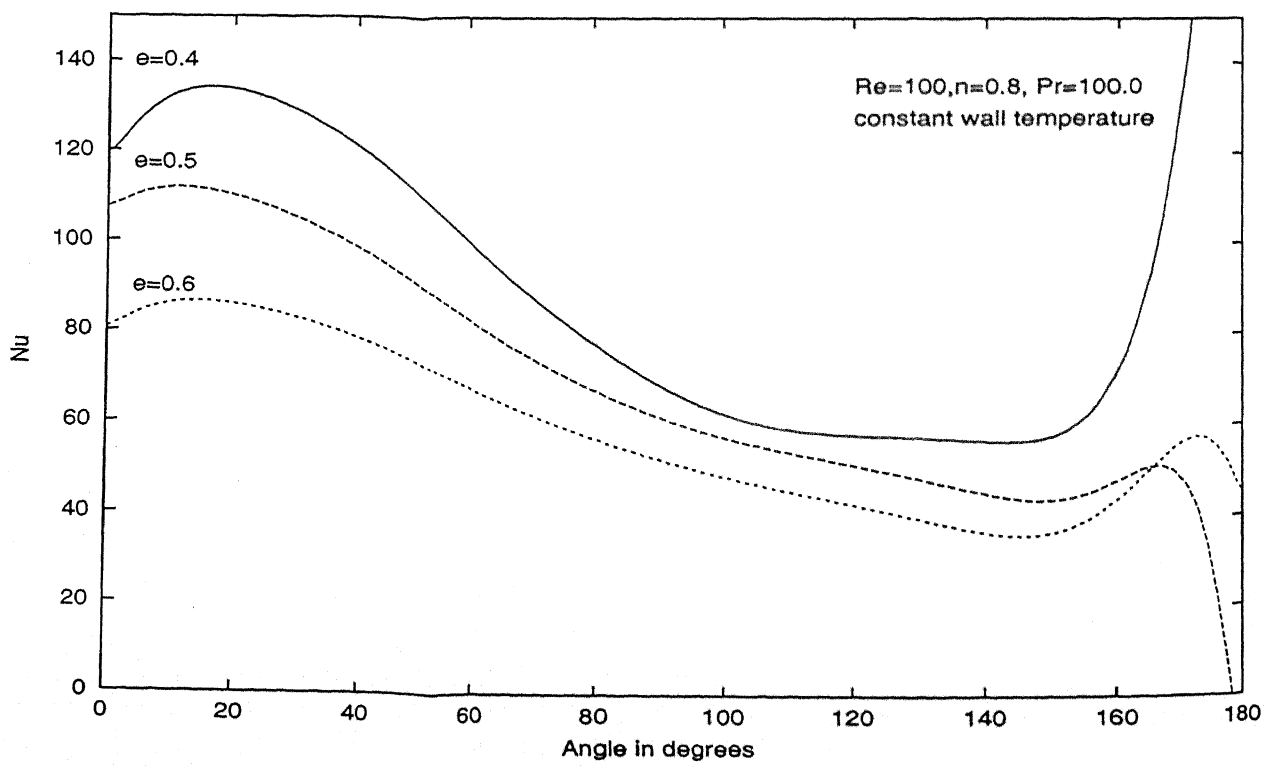

Figure 4.110:Variation of Nusselt number with angle for Re=100,n=0.8 and Pr=100 for constant wall teperature

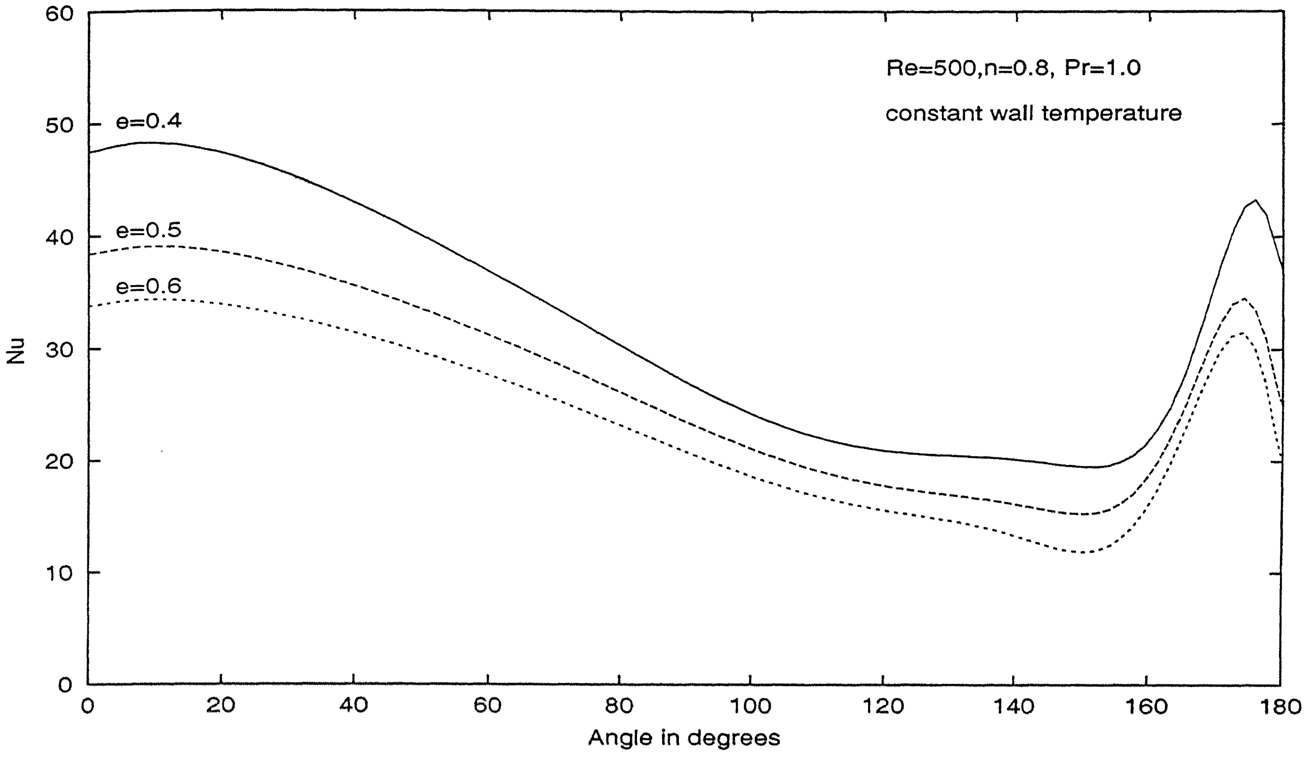

Figure 4.111:Variation of Nusselt number with angle for Re=500,n=0.8 and Pr=1 for constant wall teperature

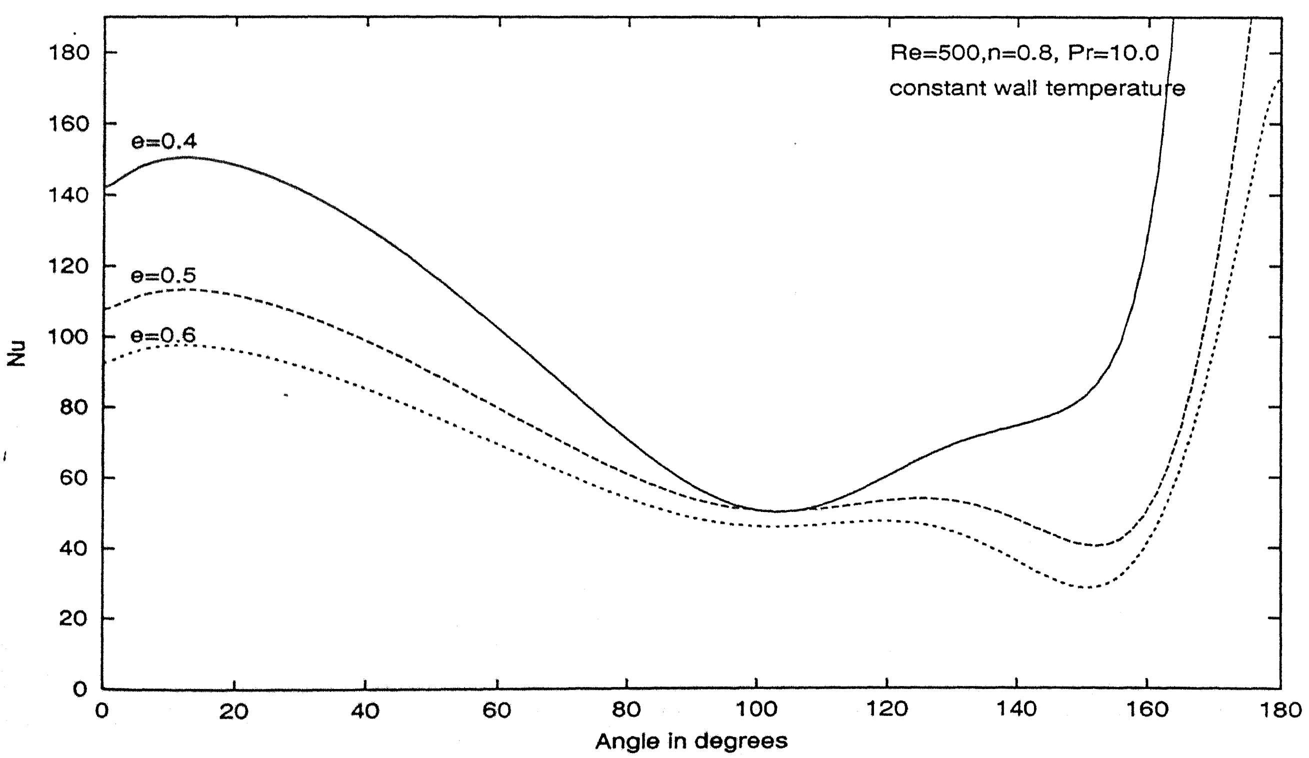

Figure 4.112:Variation of Nusselt number with angle for Re=500,n=0.8 and Pr=10 for constant wall teperature

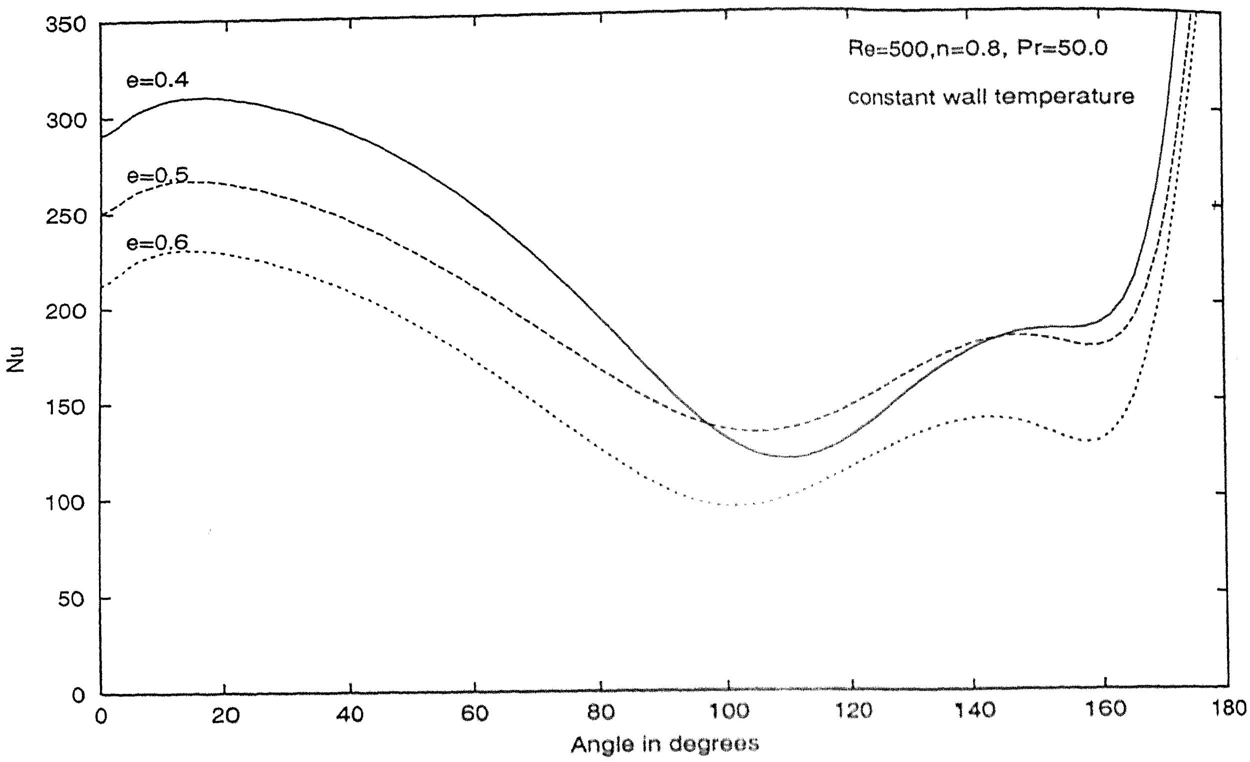

Figure 4.113:Variation of Nusselt number with angle for Re=500,n=0.8 and Pr=50 for constant wall teperature

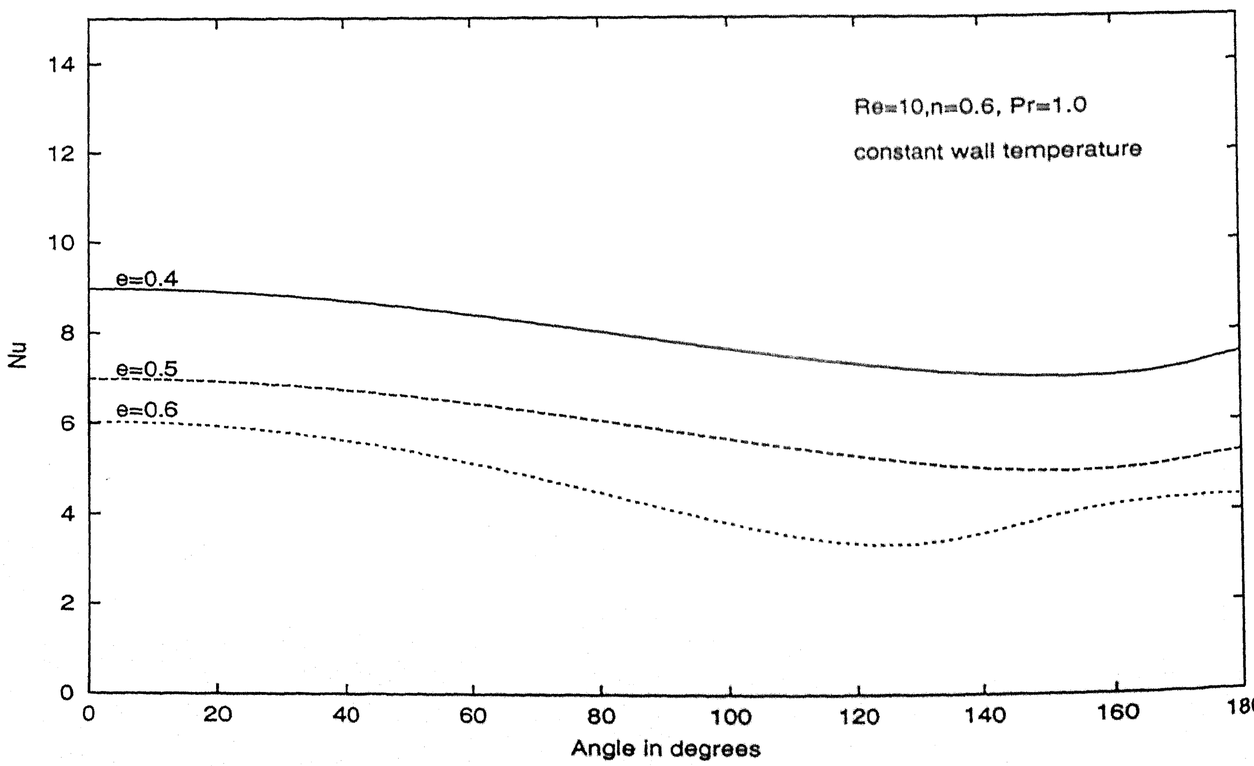

Figure 4.114:Variation of Nusselt number with angle for Re=10,n=0.6 and Pr=1 for constant wall tep ature

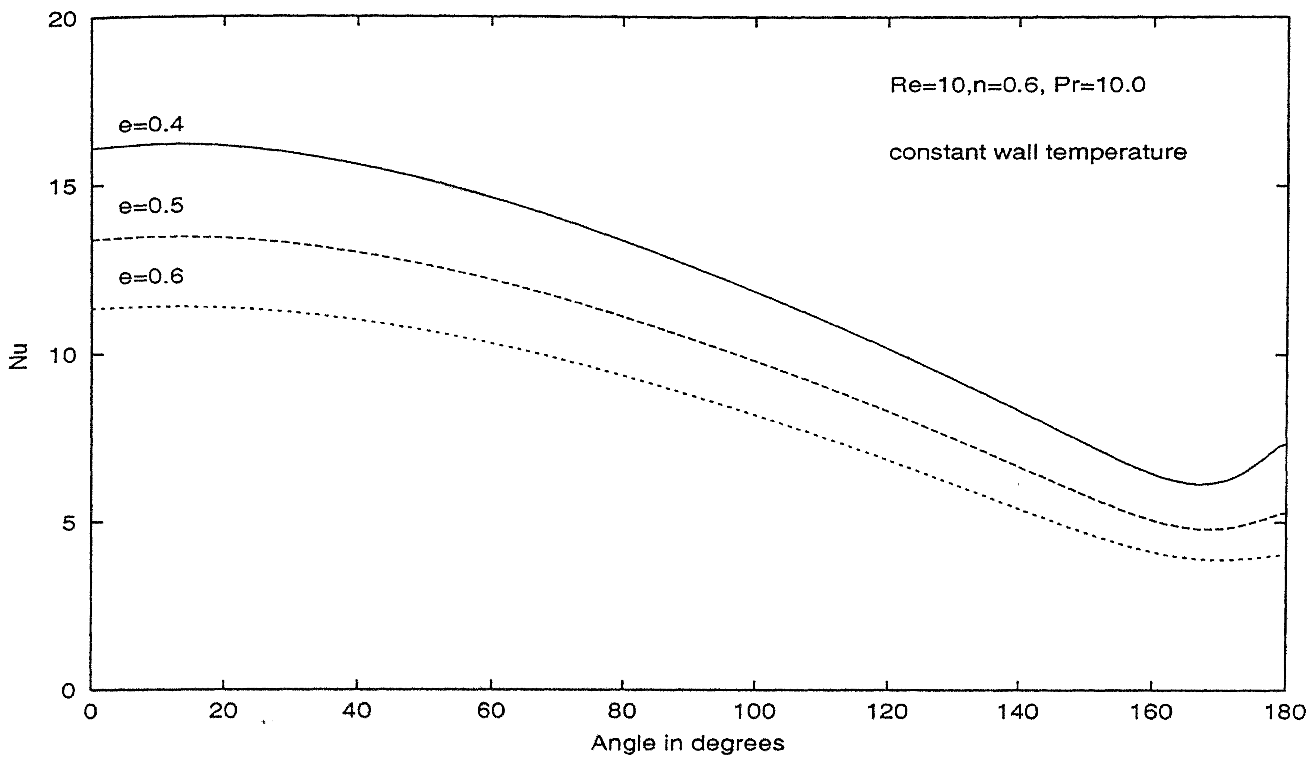

Figure 4.115:Variation of Nusselt number with angle for Re=10,n=0.6 and Pr=10 for constant wall teperature

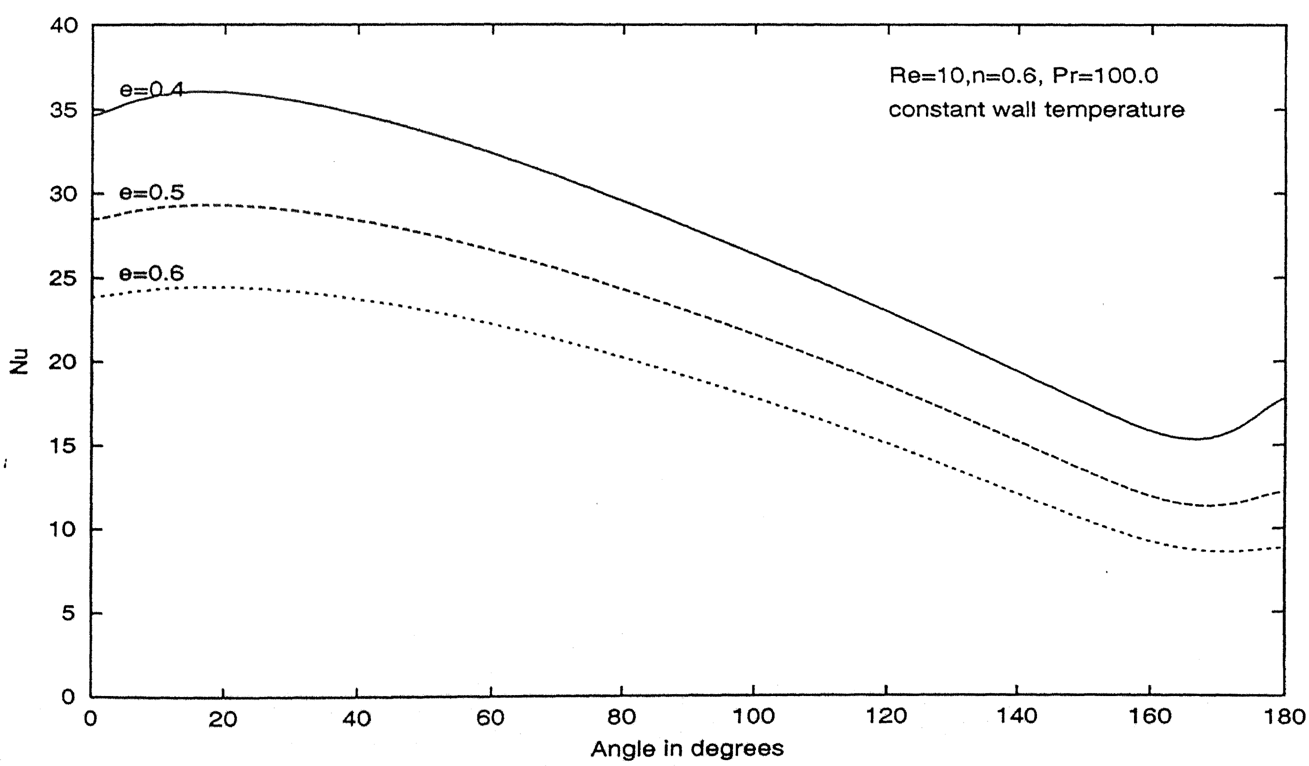

Figure 4.116:Variation of Nusselt number with angle for Re=10,n=0.6 and Pr=100 for constant wall teperature

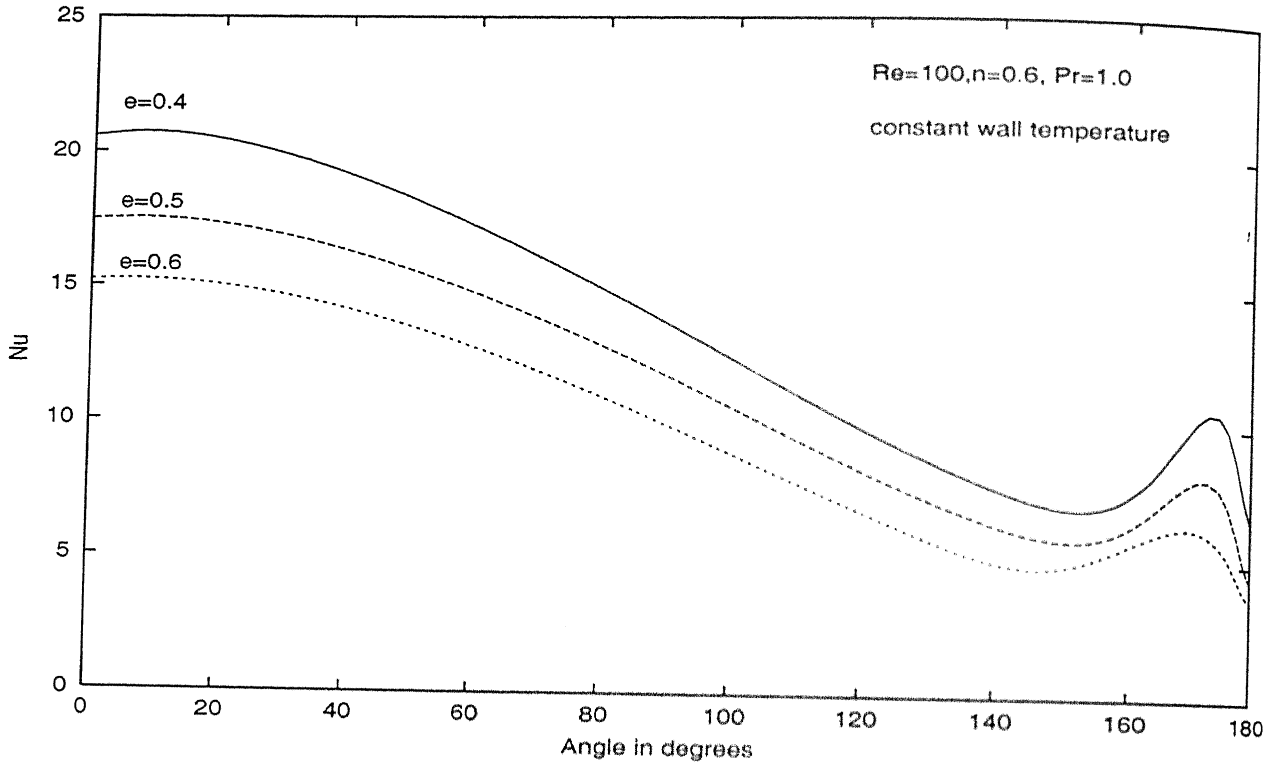

Figure 4.117:Variation of Nusselt number with angle for Re=100,n=0.6 and Pr=1 for constant wall teperature

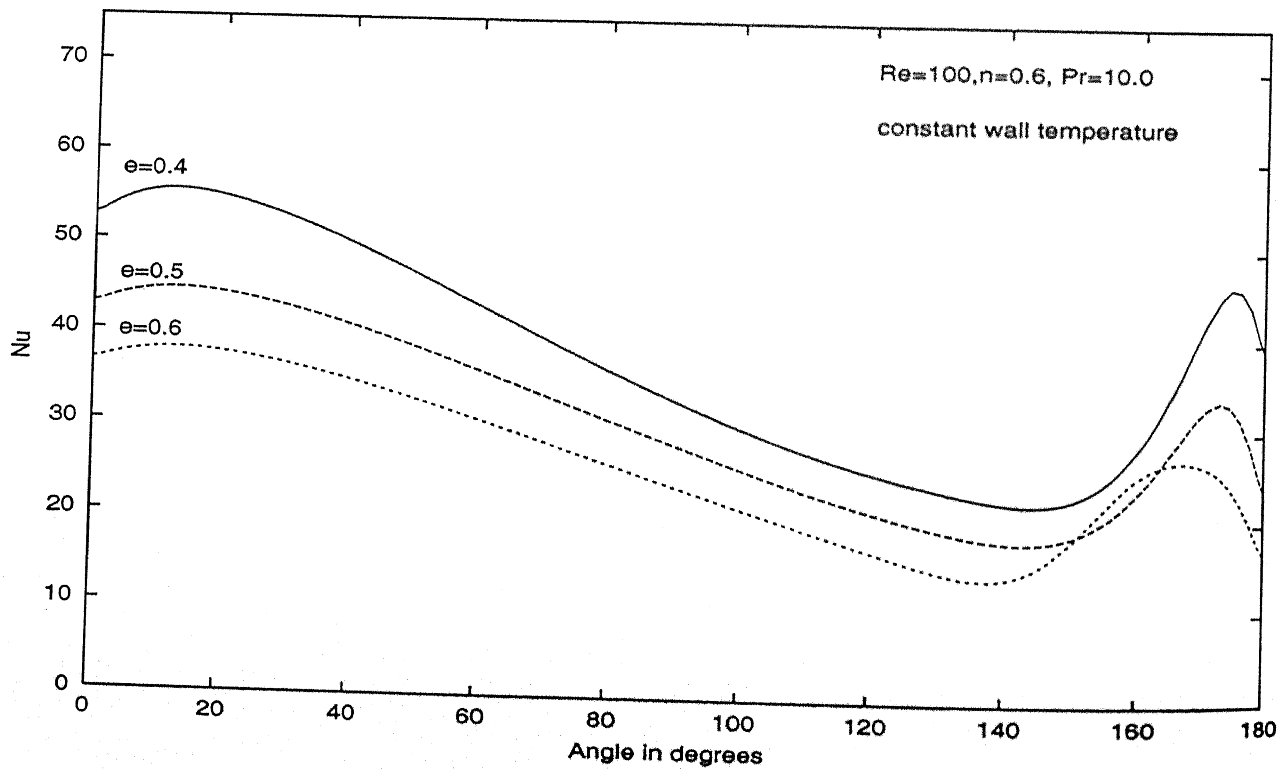

Figure 4.118:Variation of Nusselt number with angle for Re=100,n=0.6 and Pr=10 for constant wall teperature

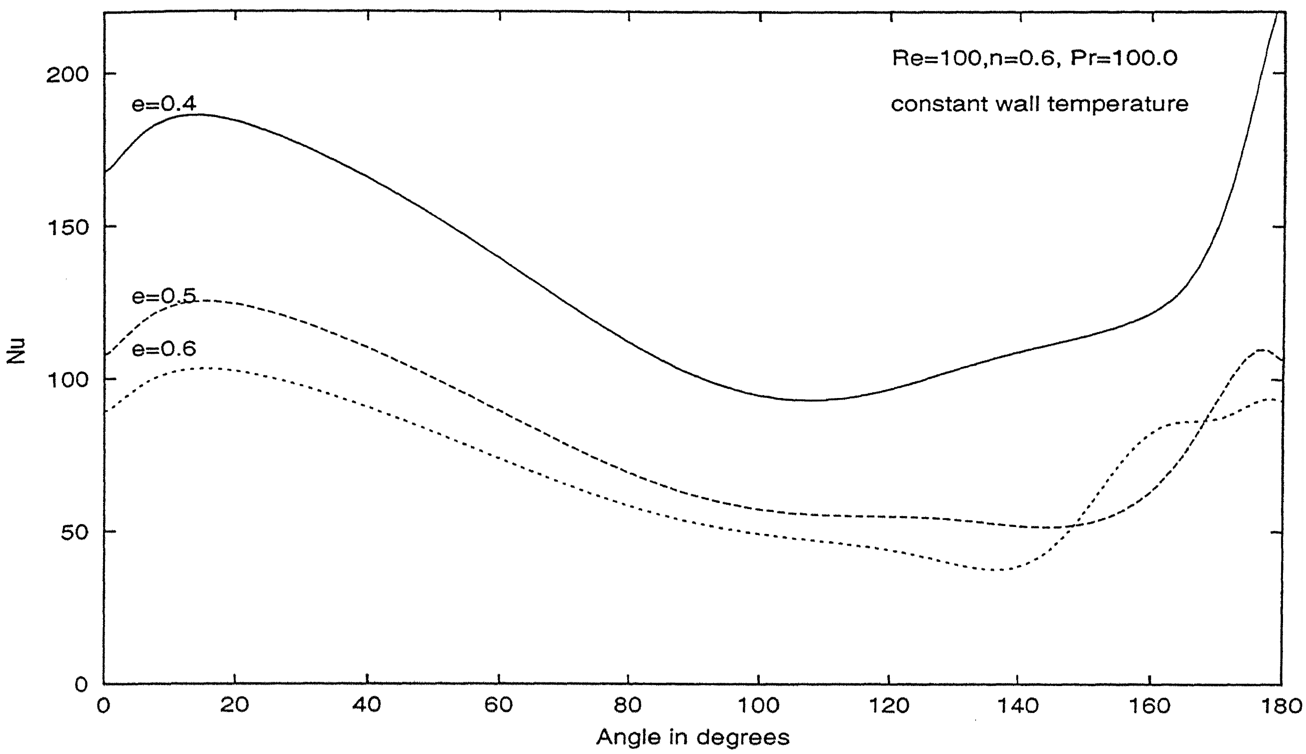

Figure 4.119:Variation of Nusselt number with angle for Re=100,n=0.6 and Pr=100 for constant wall teperature

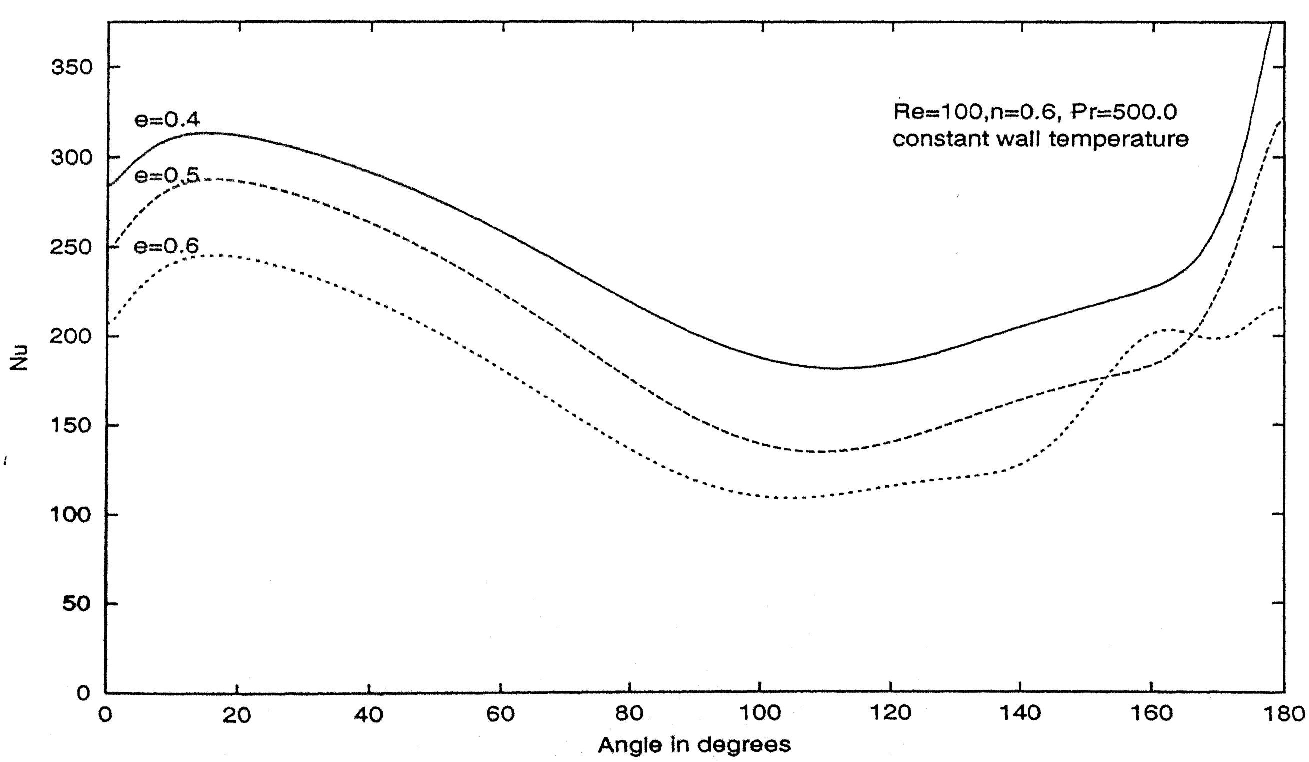

Figure 4.120:Variation of Nusselt number with angle for Re=100,n=0.6 and Pr=500 for constant wall teperature

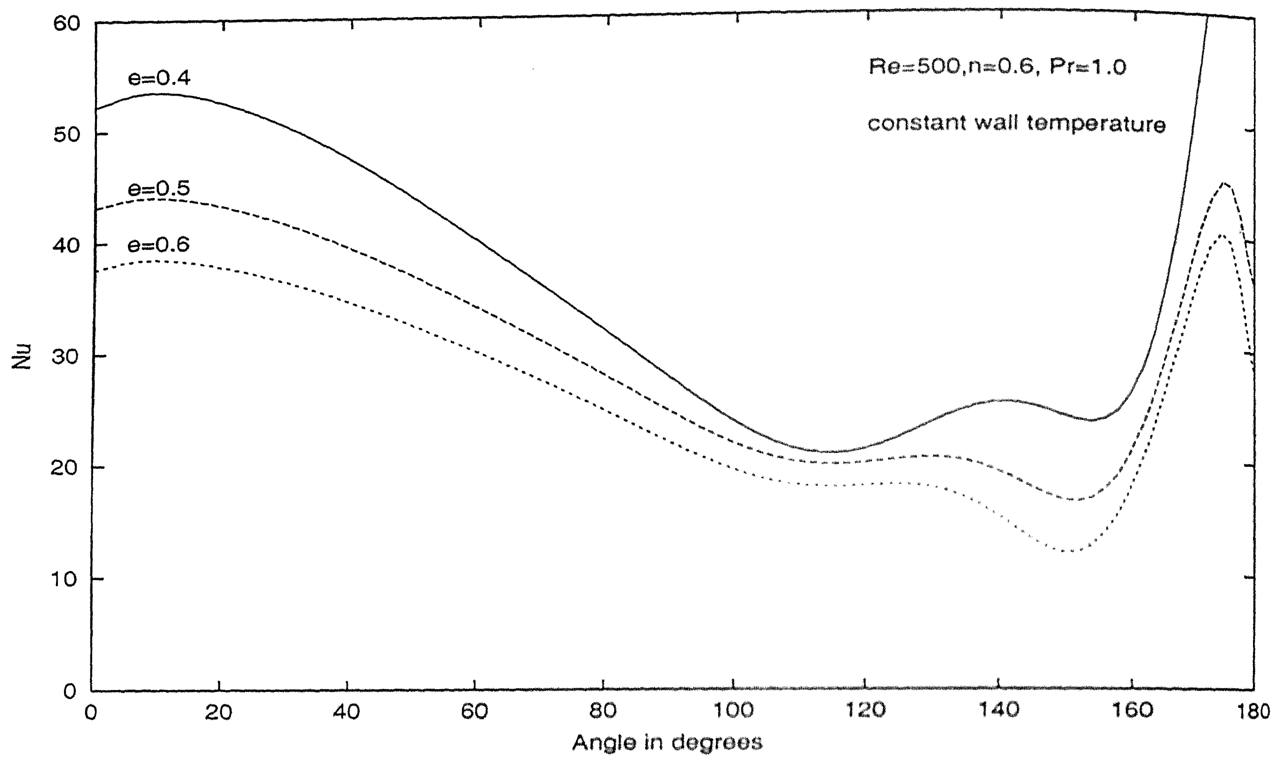

Figure 4.121:Variation of Nusselt number with angle for Re=500,n=0.6 and Pr=1 for constant wall teperature

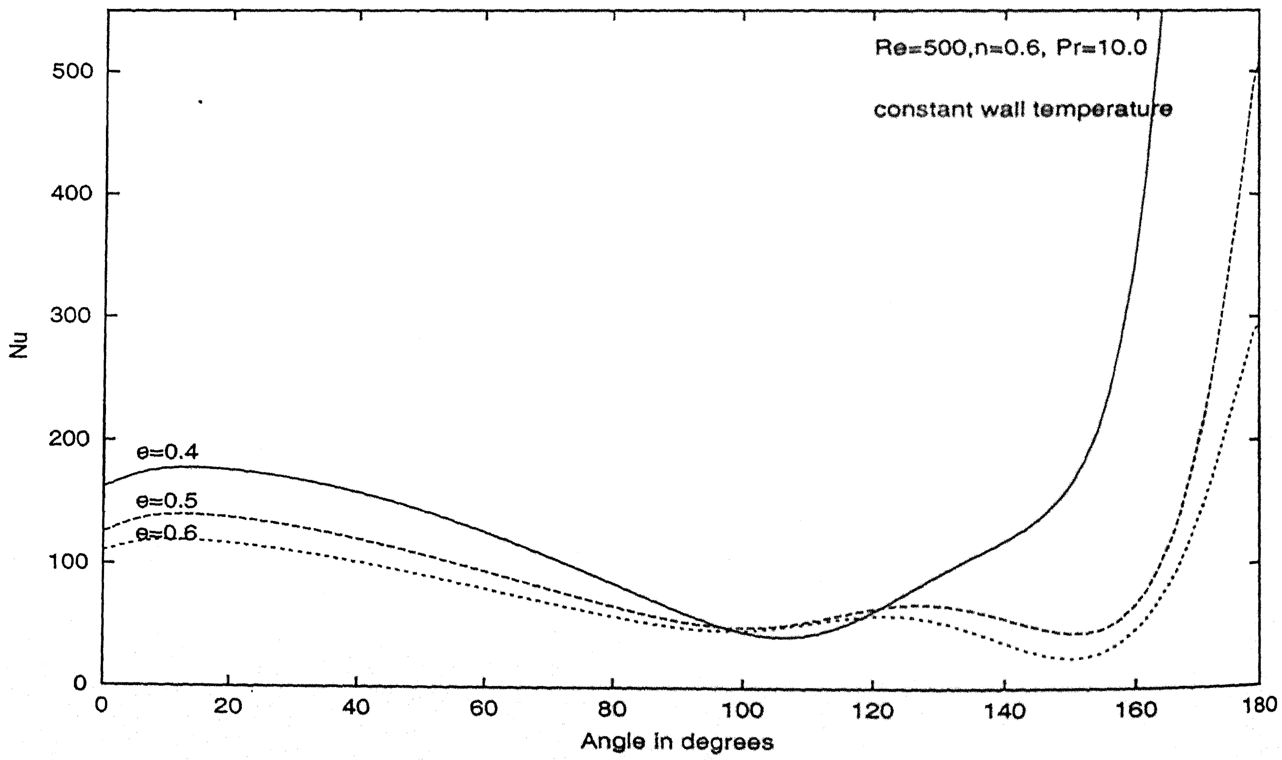

Figure 4.122:Variation of Nusselt number with angle for Re=500,n=0.6 and Pr=10 for constant surface temperature condition

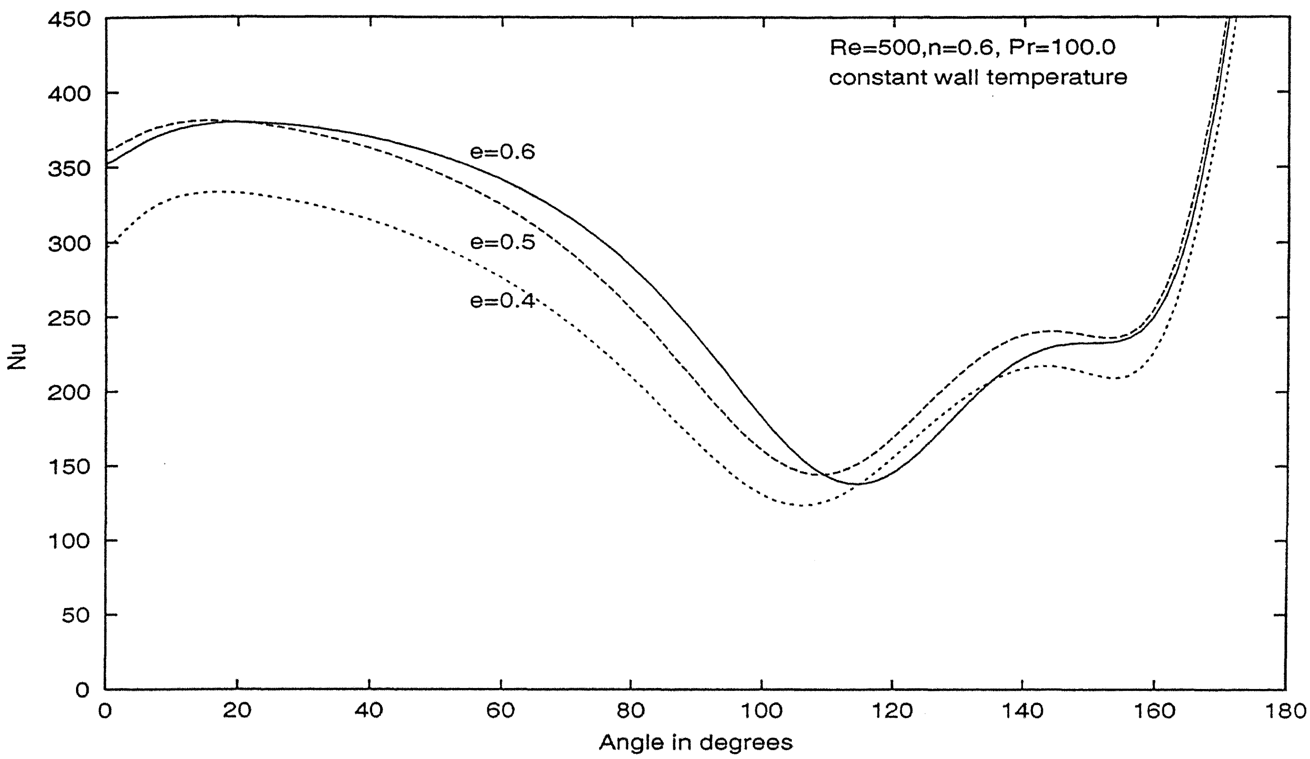

Figure 4.123:Variation of Nusselt number with angle for Re=500,n=0.6 and Pr=100 for constant wall teperature

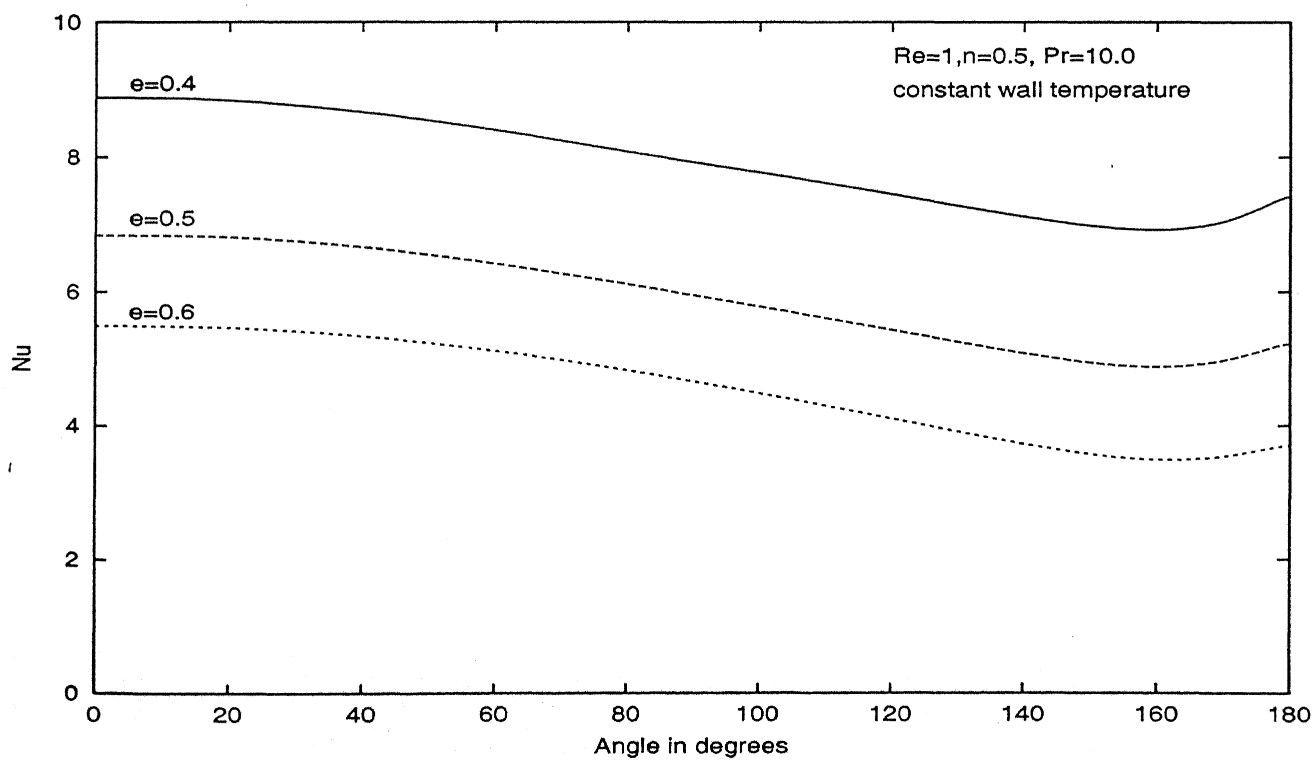

Figure 4.124:Variation of Nusselt number with angle for Re=1,n=0.5 and Pr=10 for constant wall teperature

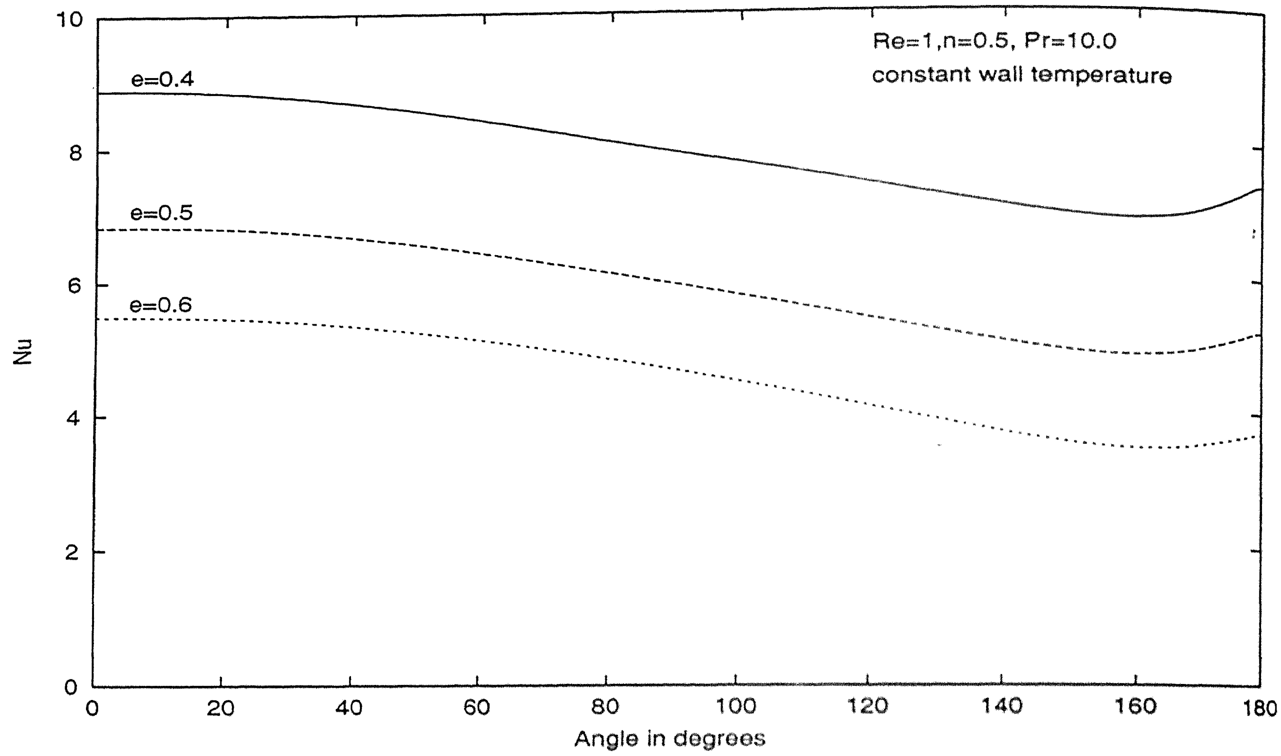

Figure 4.125:Variation of Nusselt number with angle for Re=1,n=0.5 and Pr=50 for constant wall teperature

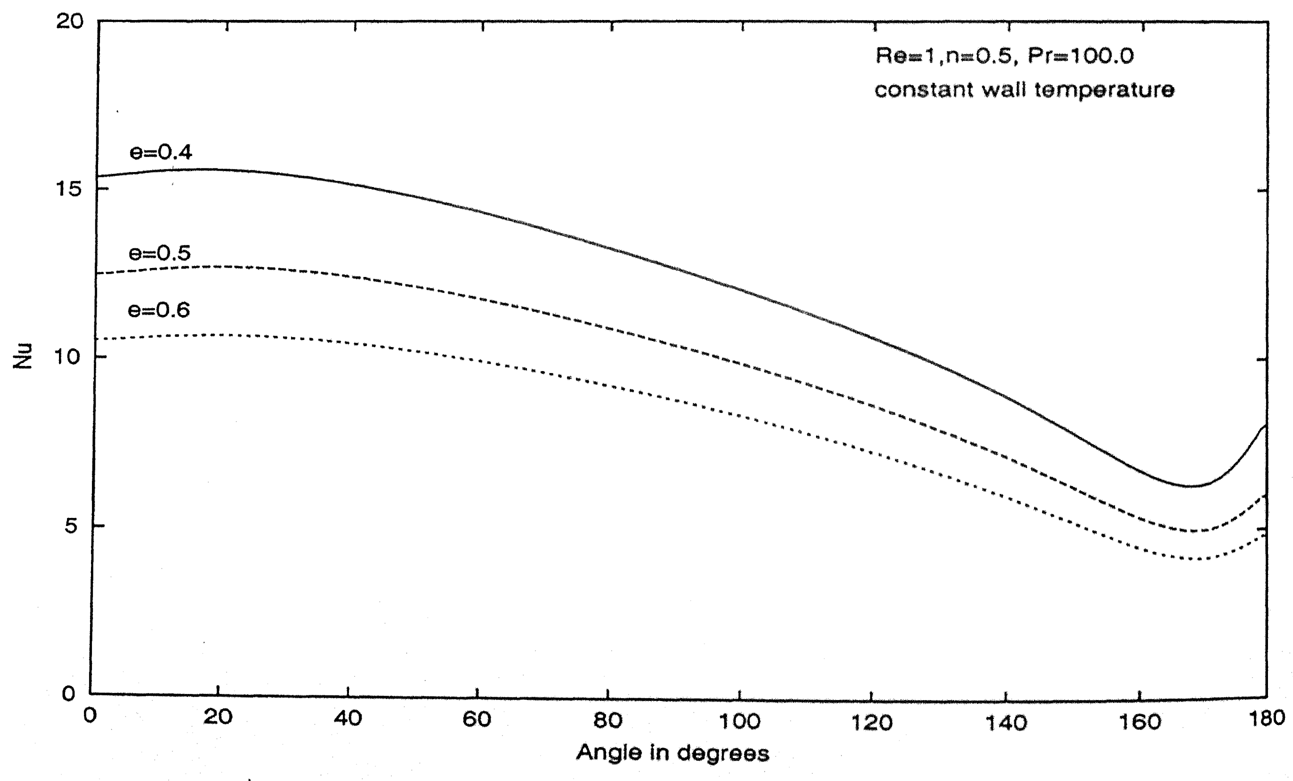

Figure 4.126:Variation of Nusselt number with angle for Re=1,n=0.5 and Pr=100 for constant wall teperature

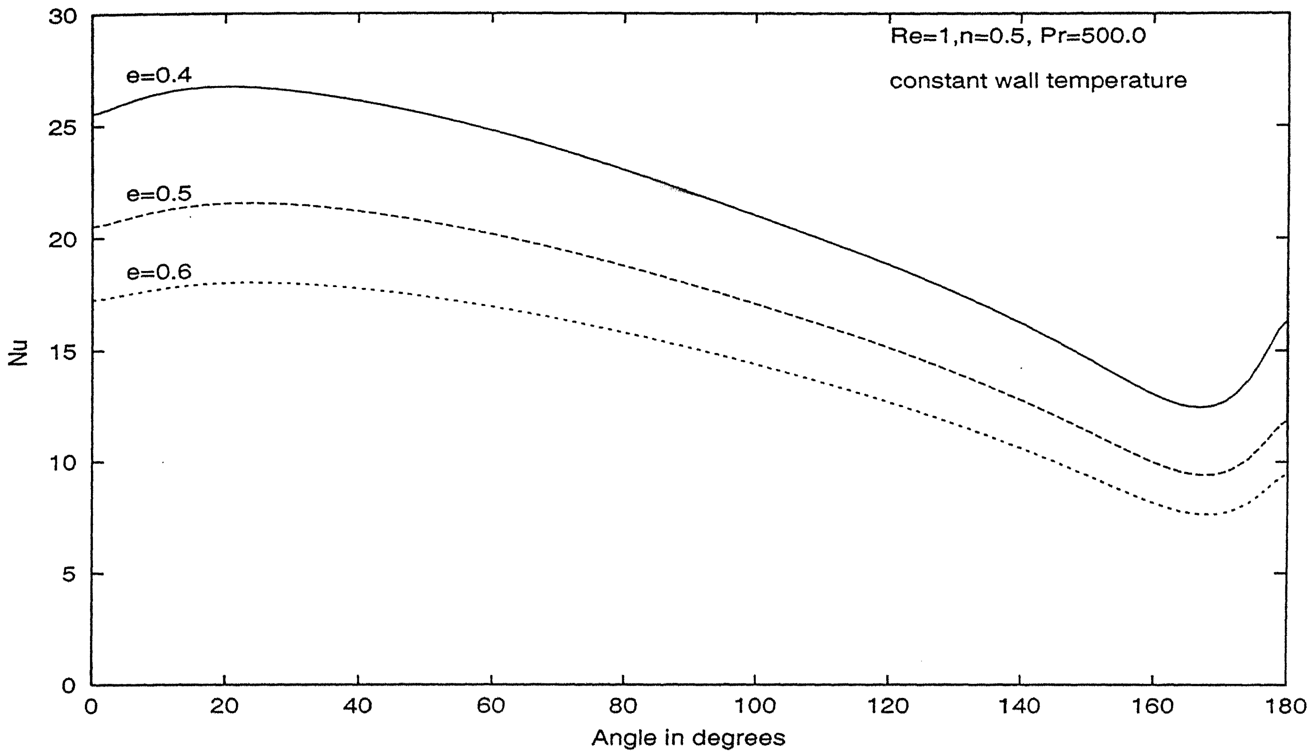

Figure 4.127:Variation of Nusselt number with angle for Re=1,n=0.5 and Pr=500 for constant wall teperature

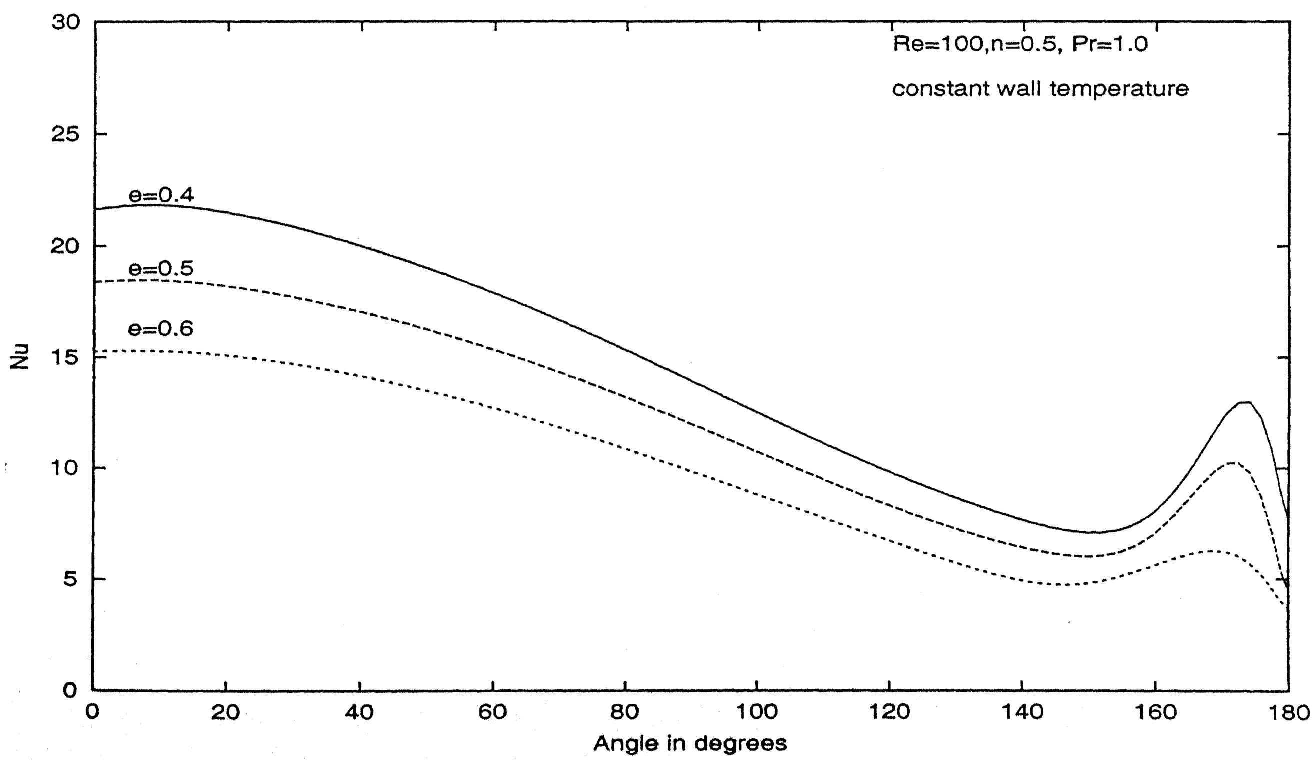

Figure 4.128:Variation of Nusselt number with angle for Re=100,n=0.5 and Pr=1 for constant wall teperature

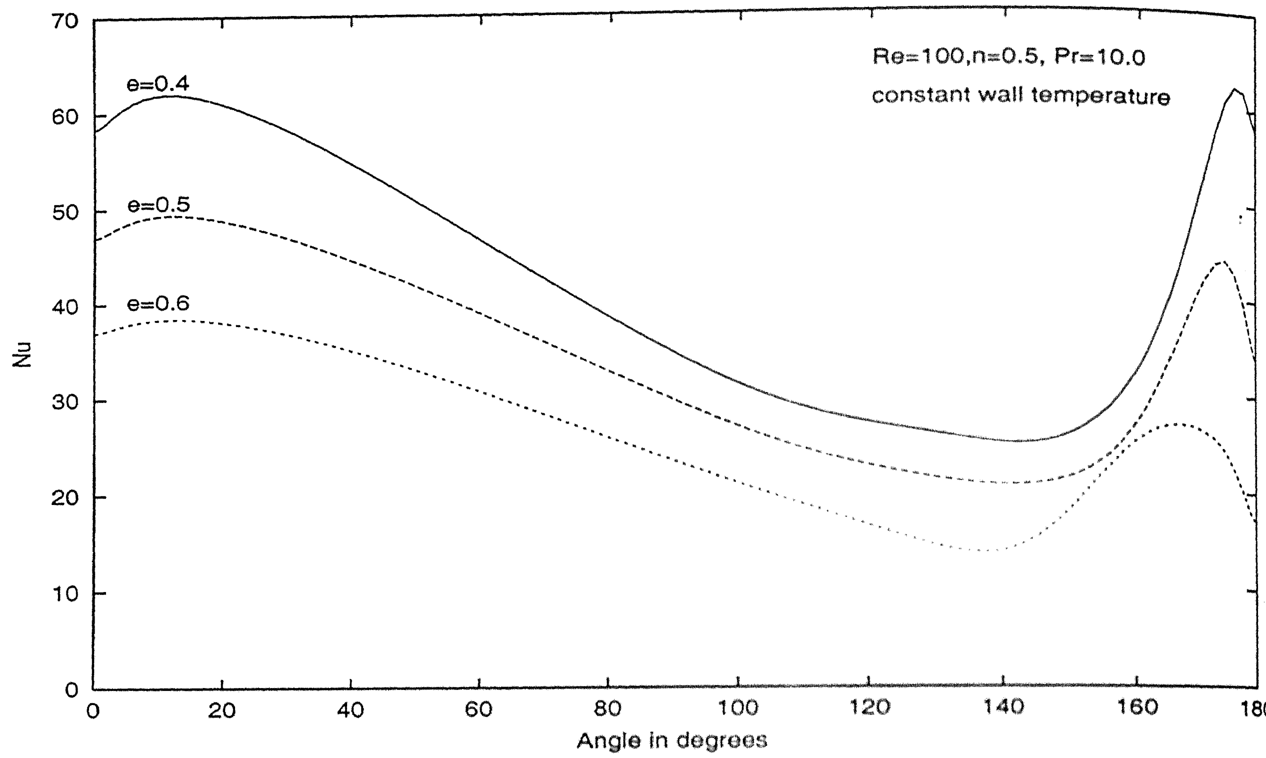

Figure 4.129:Variation of Nusselt number with angle for Re=100,n=0.5 and Pr=10 for constant wall teperature

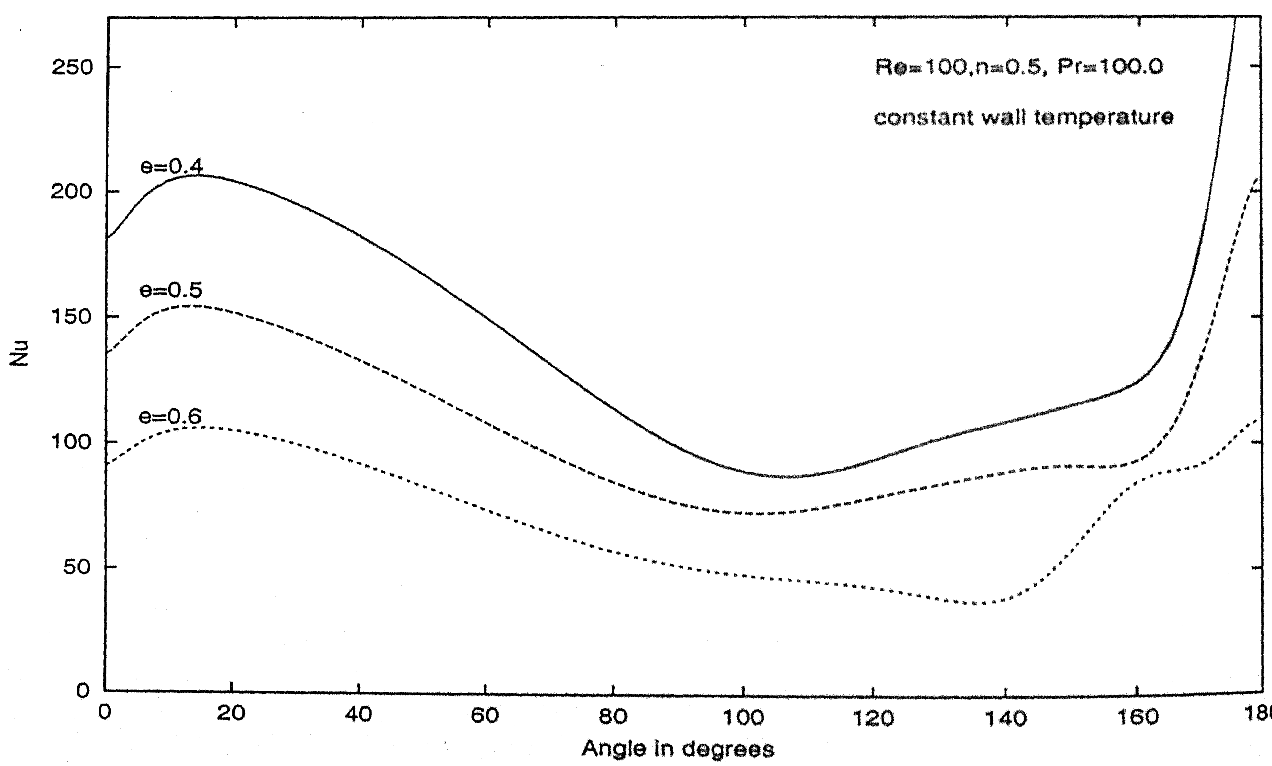

Figure 4.130:Variation of Nusselt number with angle for Re=100,n=0.5 and Pr=100 for constant wall teperature

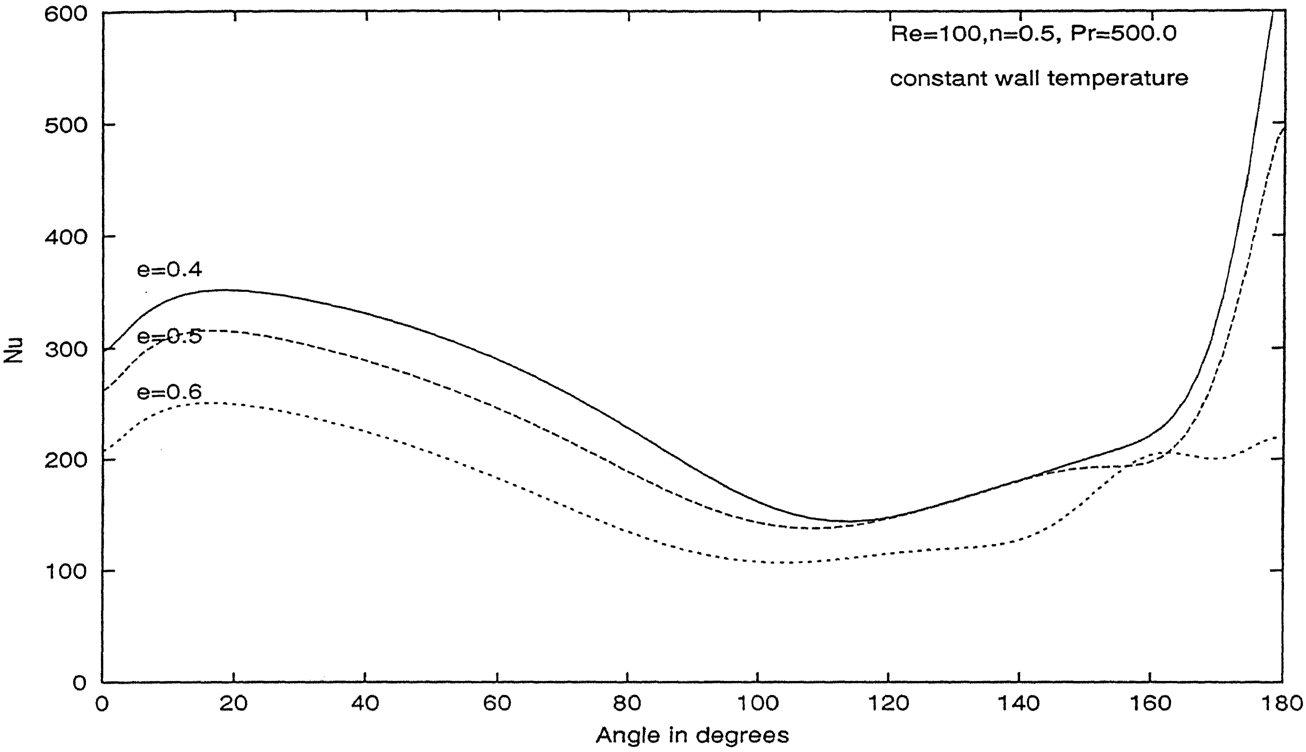

Figure 4.131:Variation of Nusselt number with angle for Re=100,n=0.5 and Pr=500 for constant wall teperature

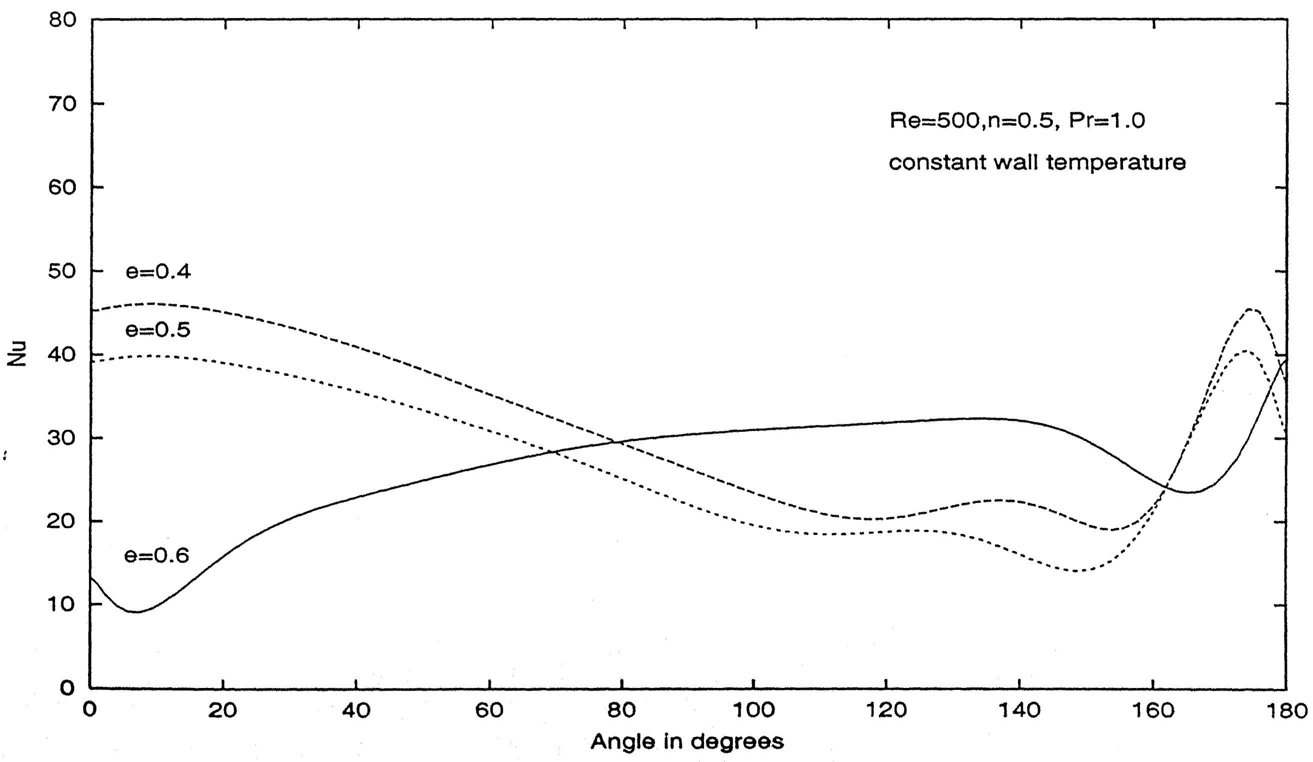

Figure 4.132:Variation of Nusselt number with angle for Re=500,n=0.5 and Pr=1 for constant wall teperature

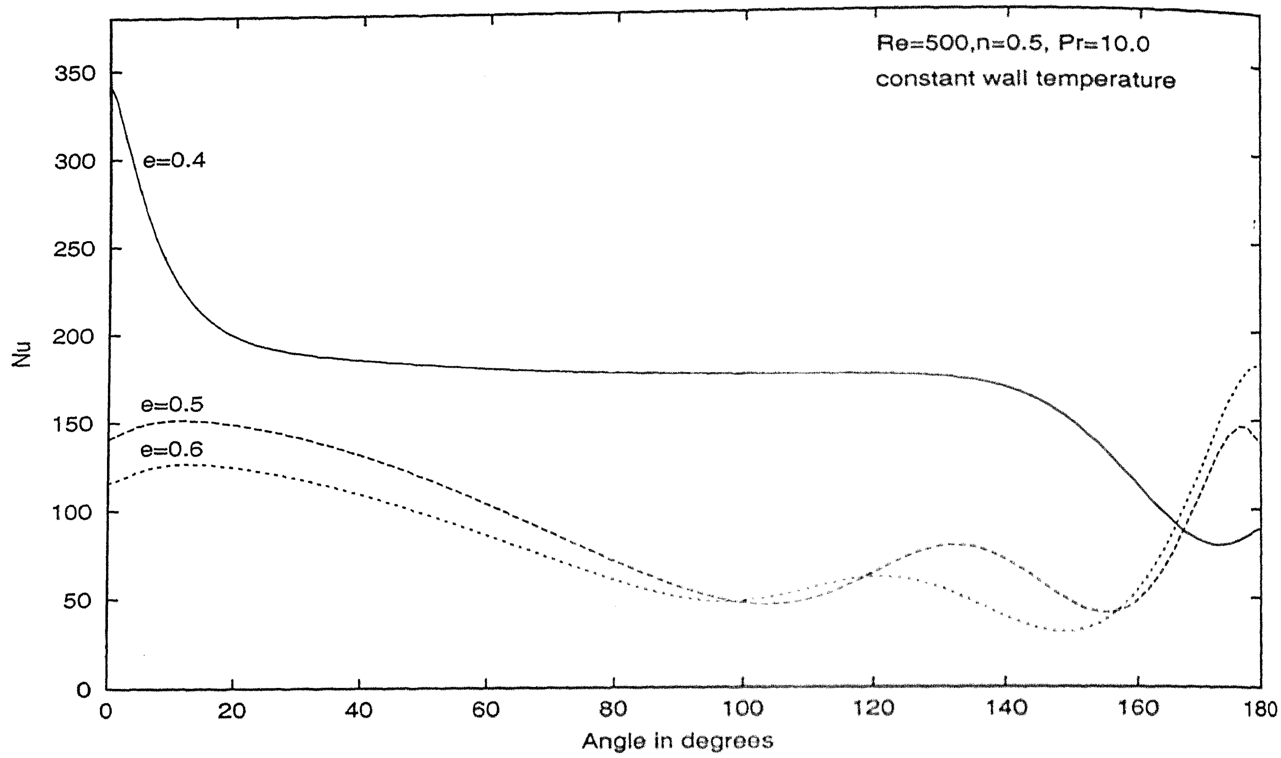

Figure 4.133:Variation of Nusselt number with angle for Re=500,n=0.5 and Pr=10

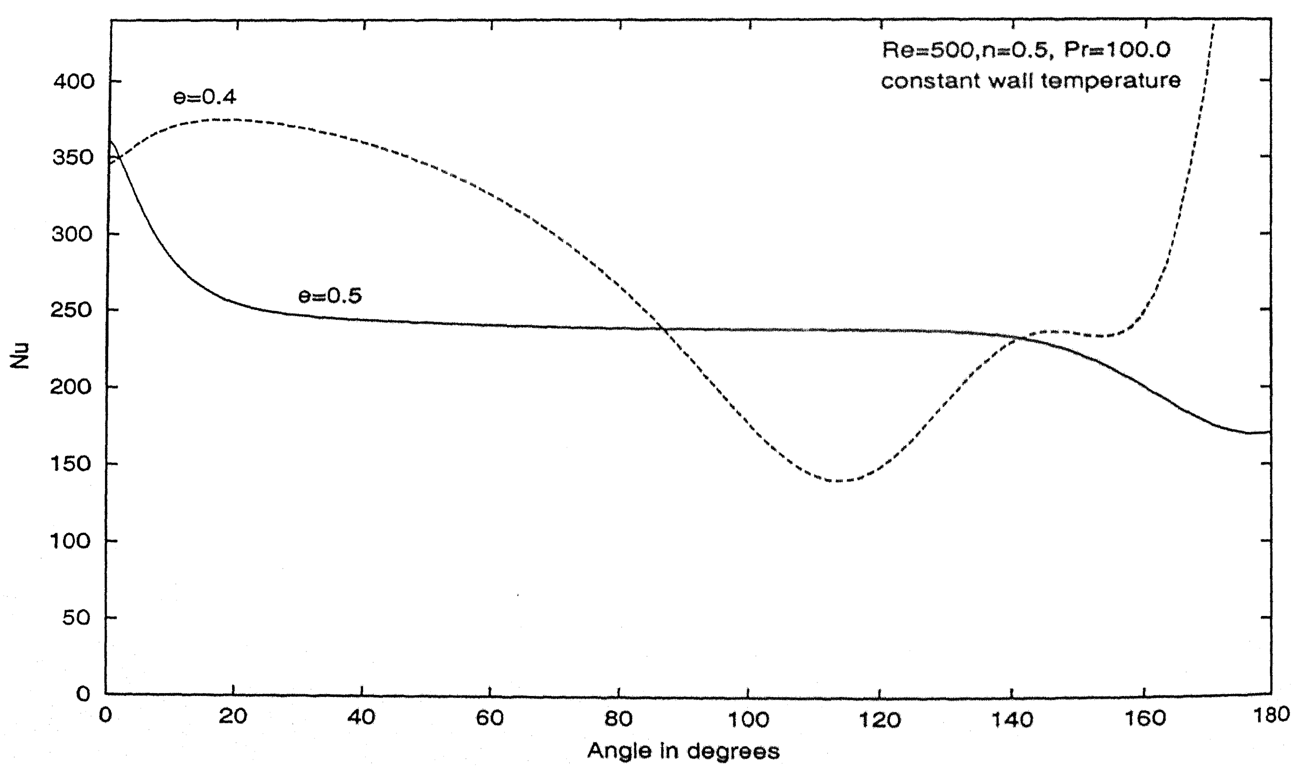

Figure 4.134:Variation of Nusselt number with angle for Re=500,n=0.5 and Pr=100

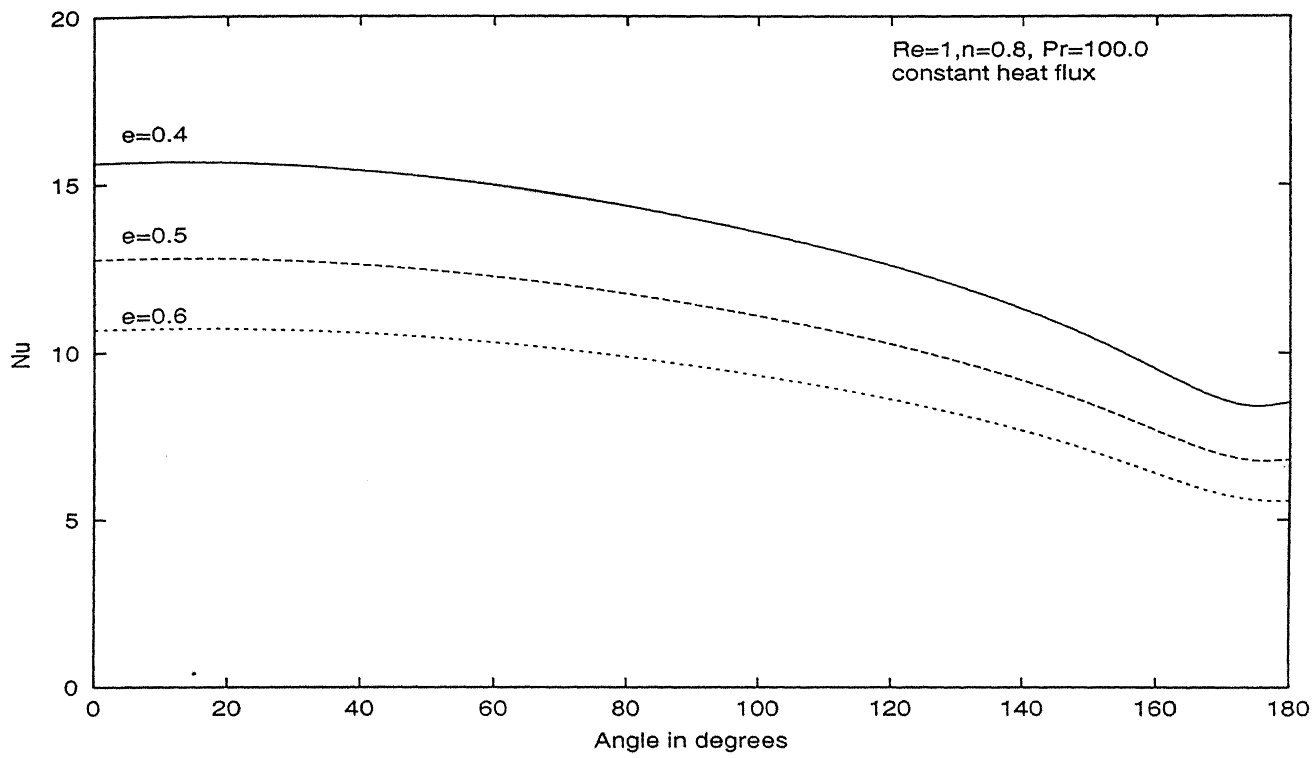

Figure 4.135:Variation of Nusselt number with angle for Re=1,n=0.8 and Pr=100 for constant heat flux

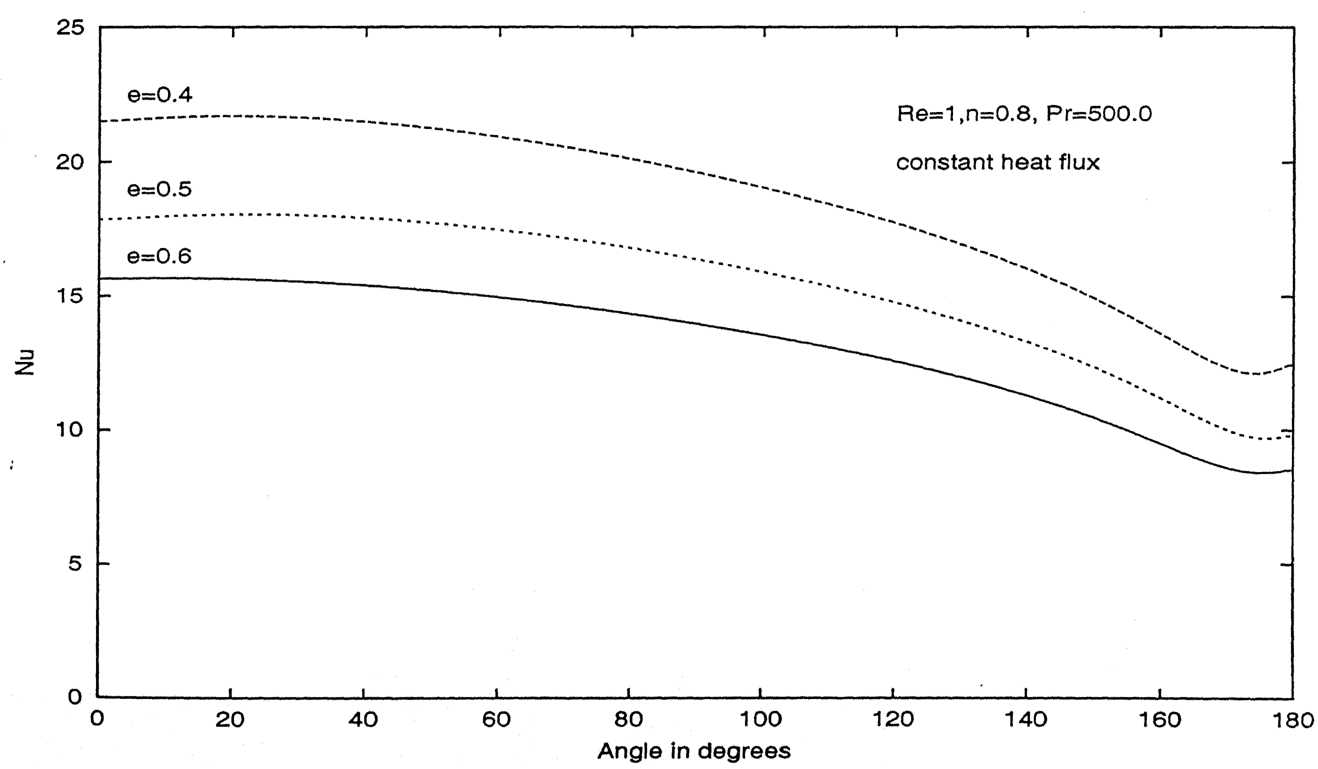

Figure 4.136:Variation of Nusselt number with angle for Re=1,n=0.8 and Pr=500 for constant heat flux

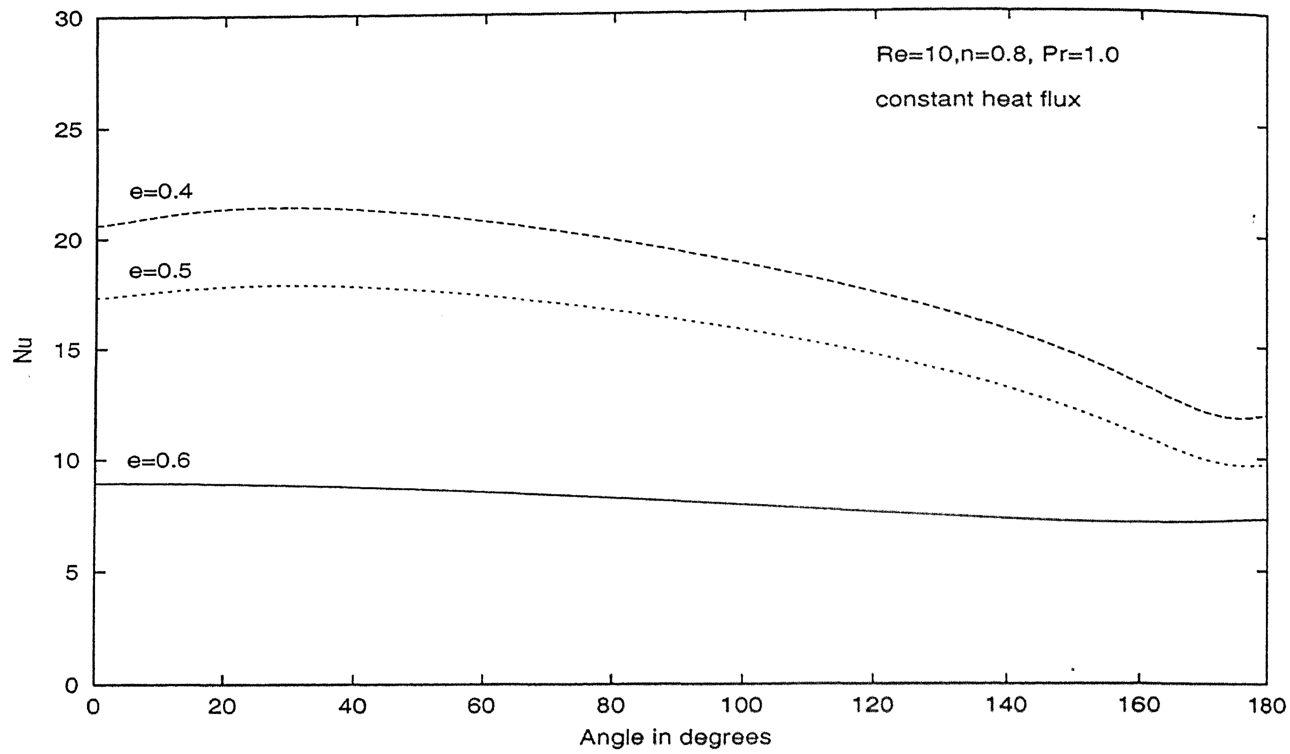

Figure 4.137:Variation of Nusselt number with angle for Re=10,n=0.8 and Pr=1 for constant heat flux

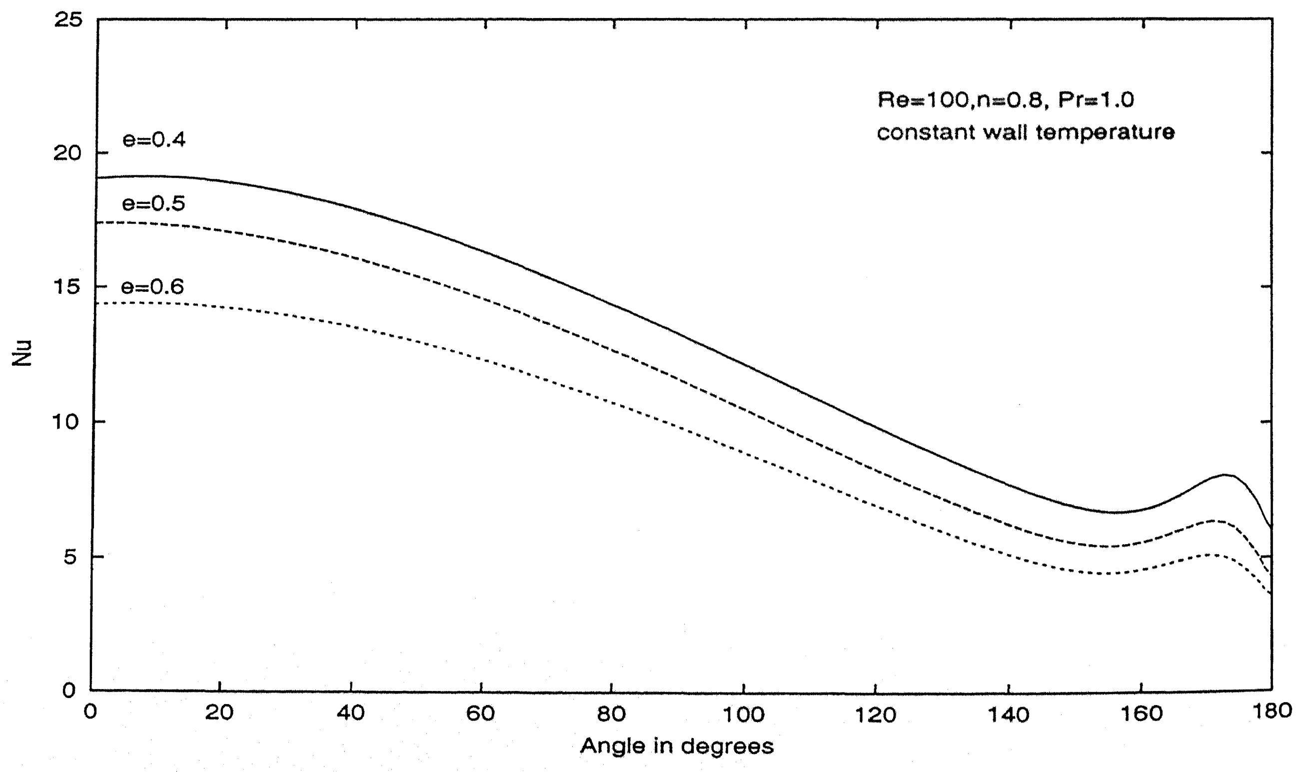

Figure 4.138:Variation of Nusselt number with angle for Re=100,n=0.8 and Pr=1 for constant heat flux

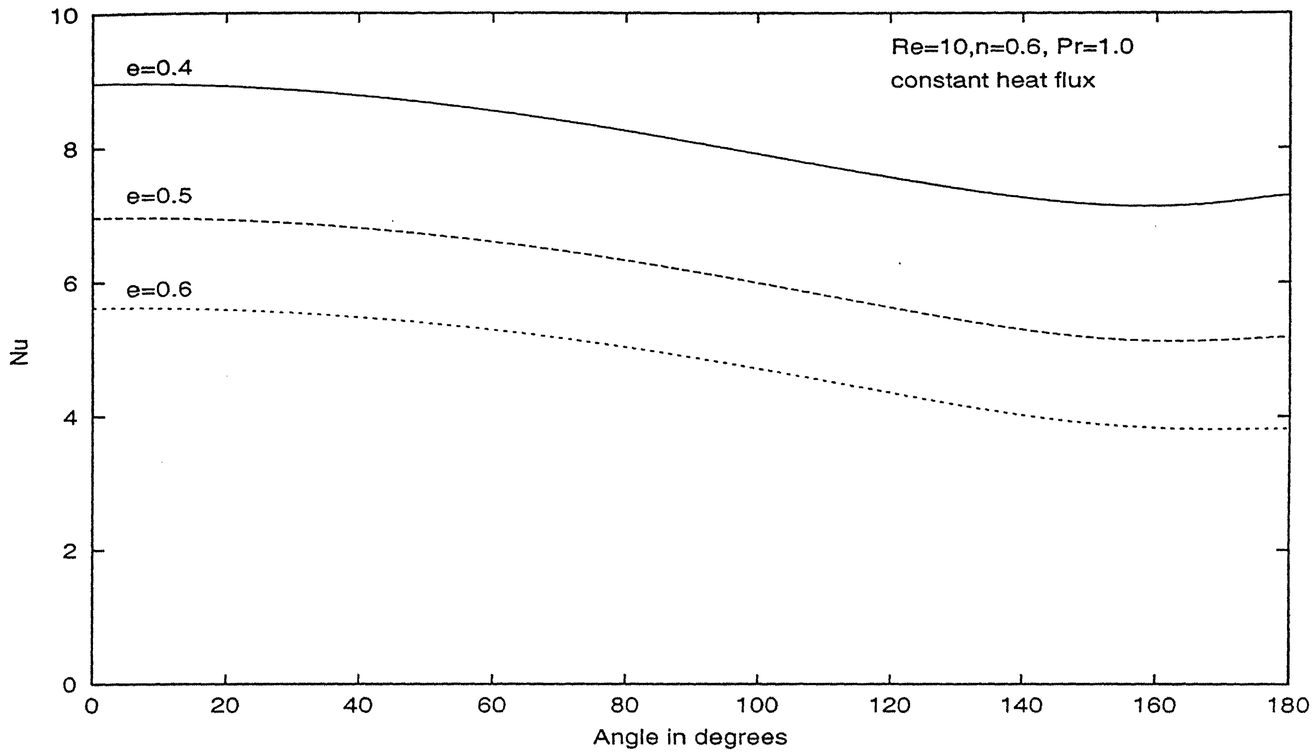

Figure 4.139:Variation of Nusselt number with angle for Re=10,n=0.6 and Pr=1 for constant heat flux

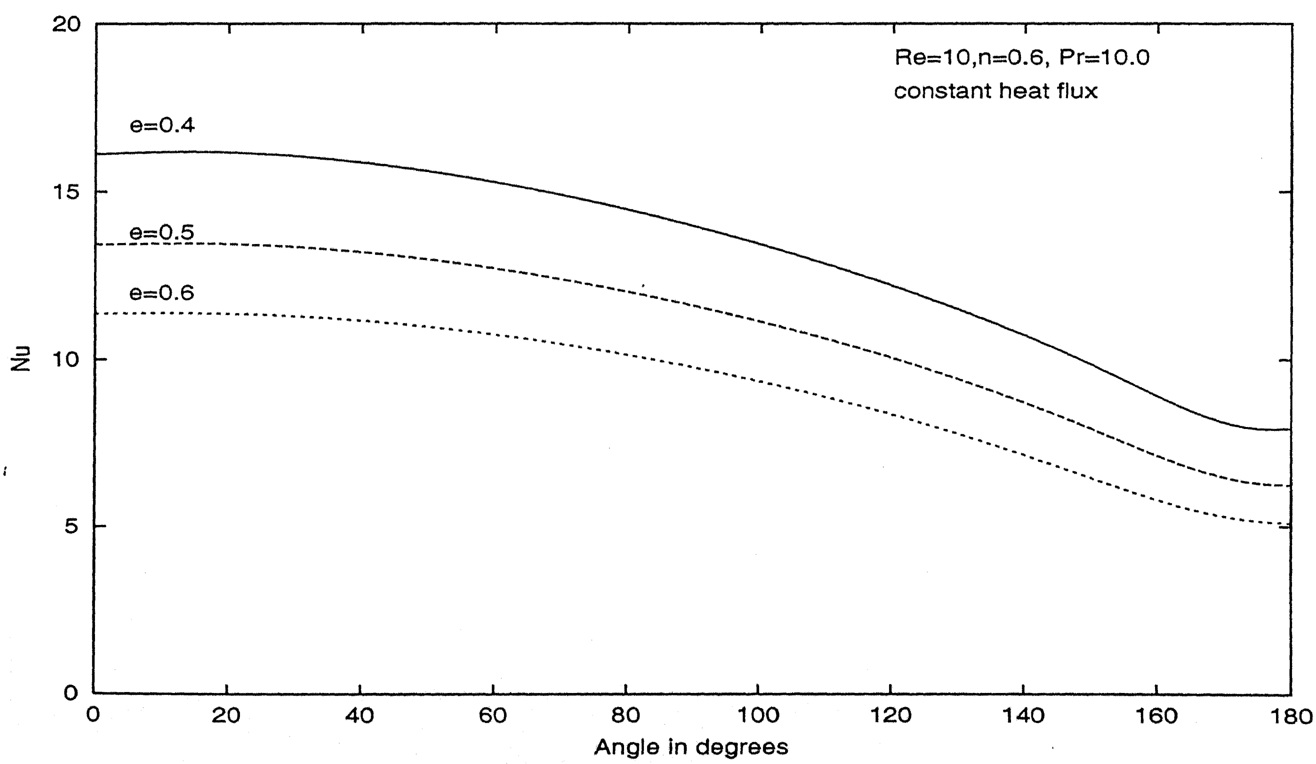

Figure 4.140:Variation of Nusselt number with angle for Re=10,n=0.6 and Pr=10 for constant heat flux

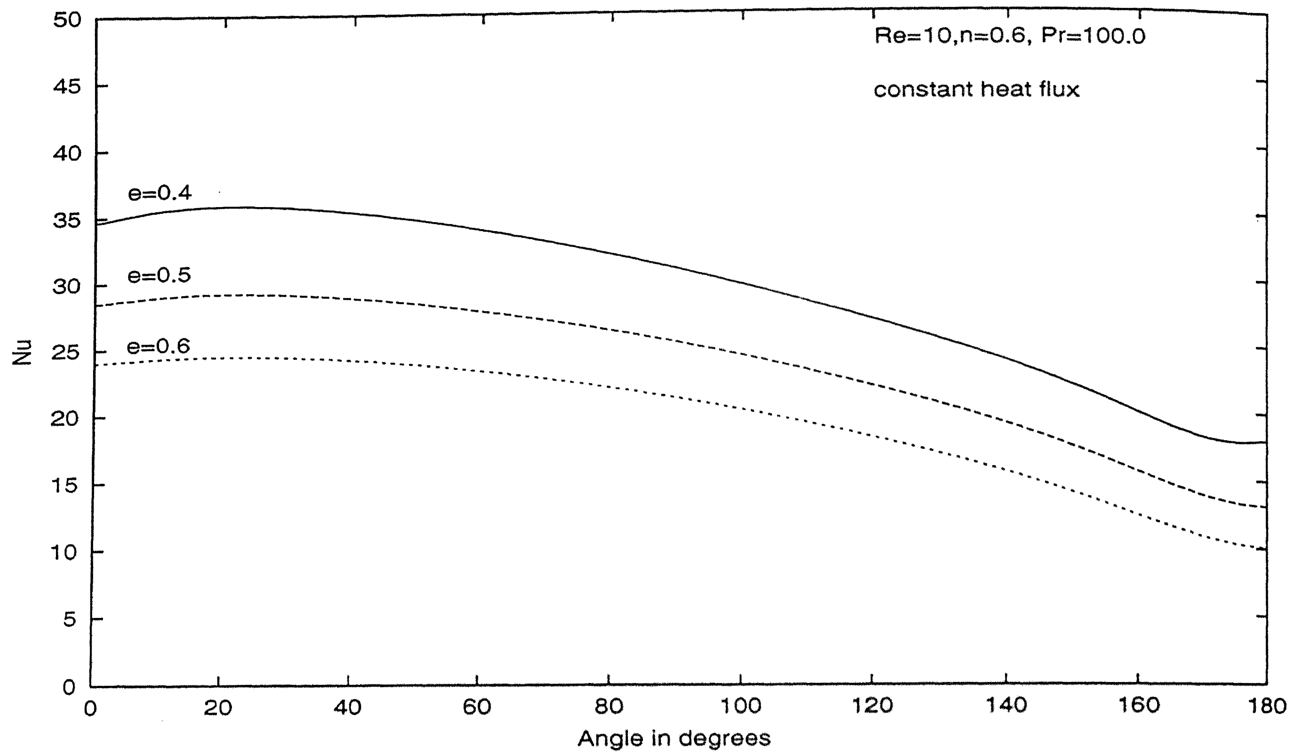

Figure 4.141:Variation of Nusselt number with angle for Re=10,n=0.6 and Pr=100 for constant heat flux

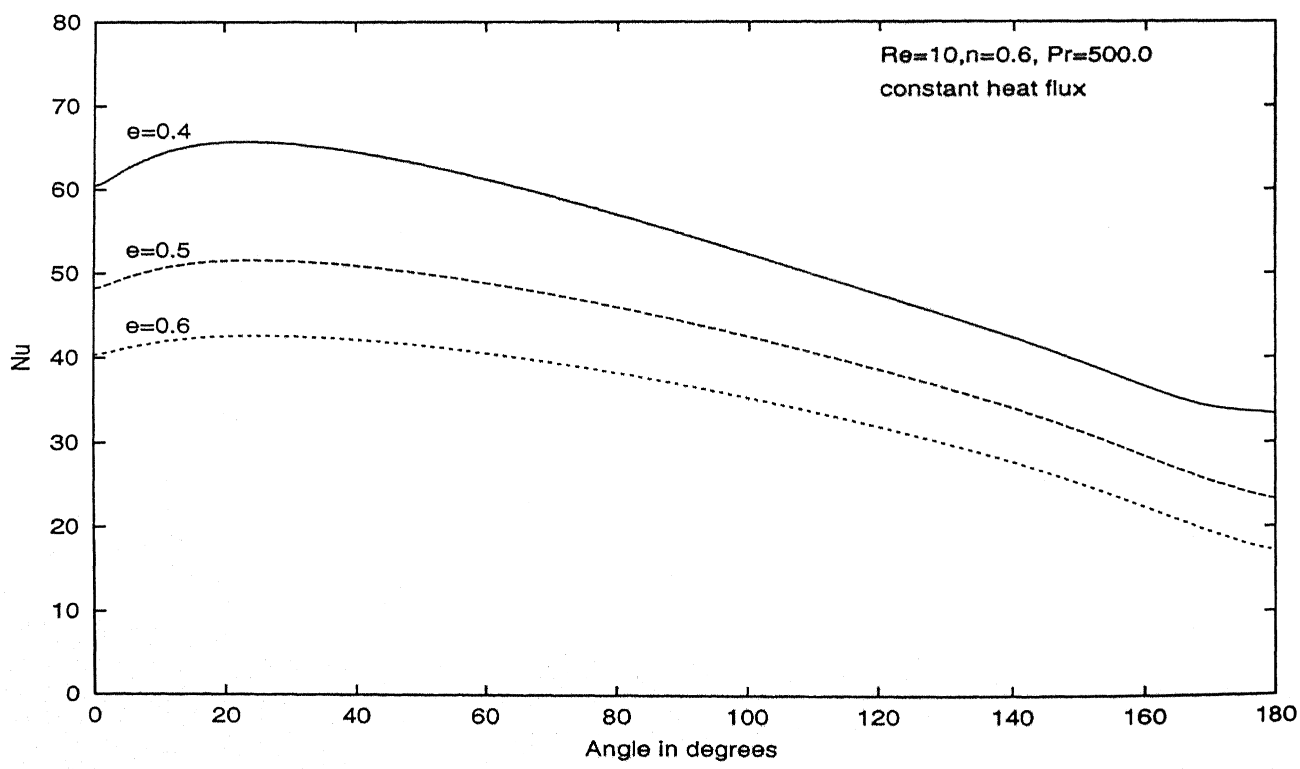

Figure 4.142:Variation of Nusselt number with angle for Re=10,n=0.6 and Pr=500 for constant heat flux

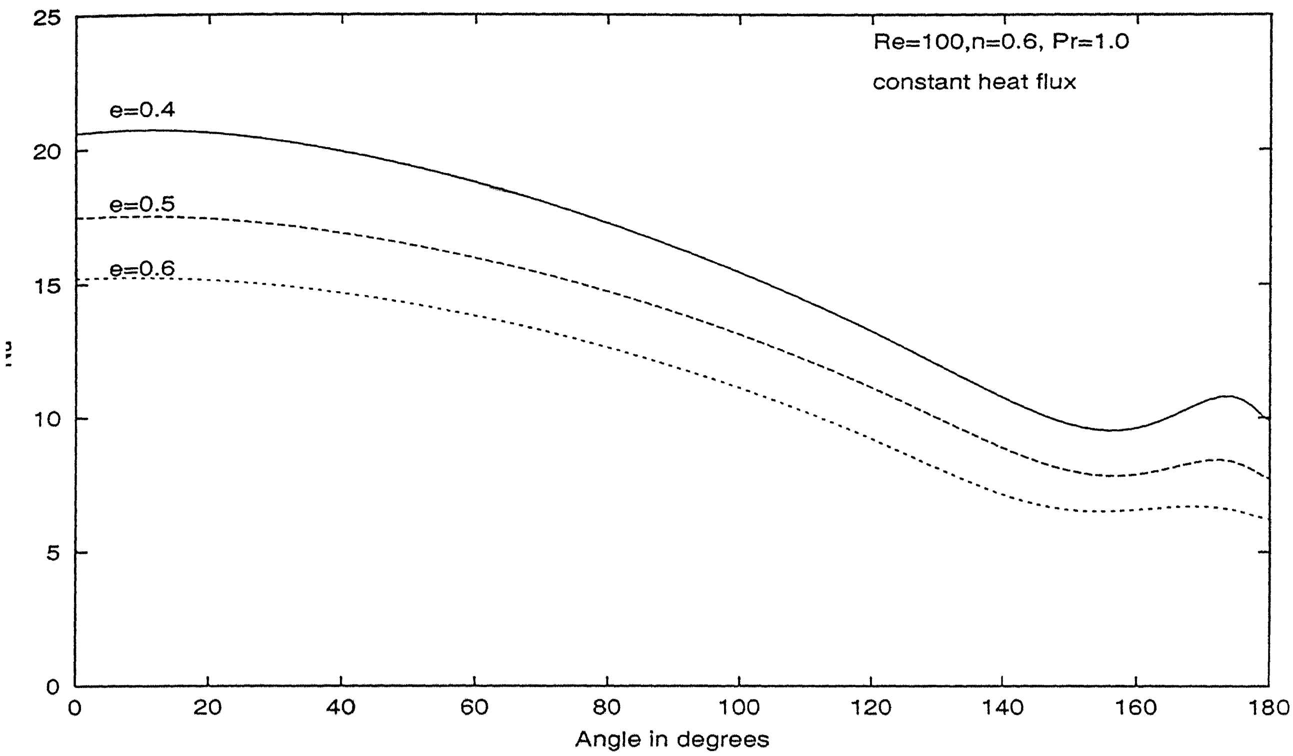

Figure 4.143:Variation of Nusselt number with angle for Re=100,n=0.6 and Pr=1 for constant heat flux

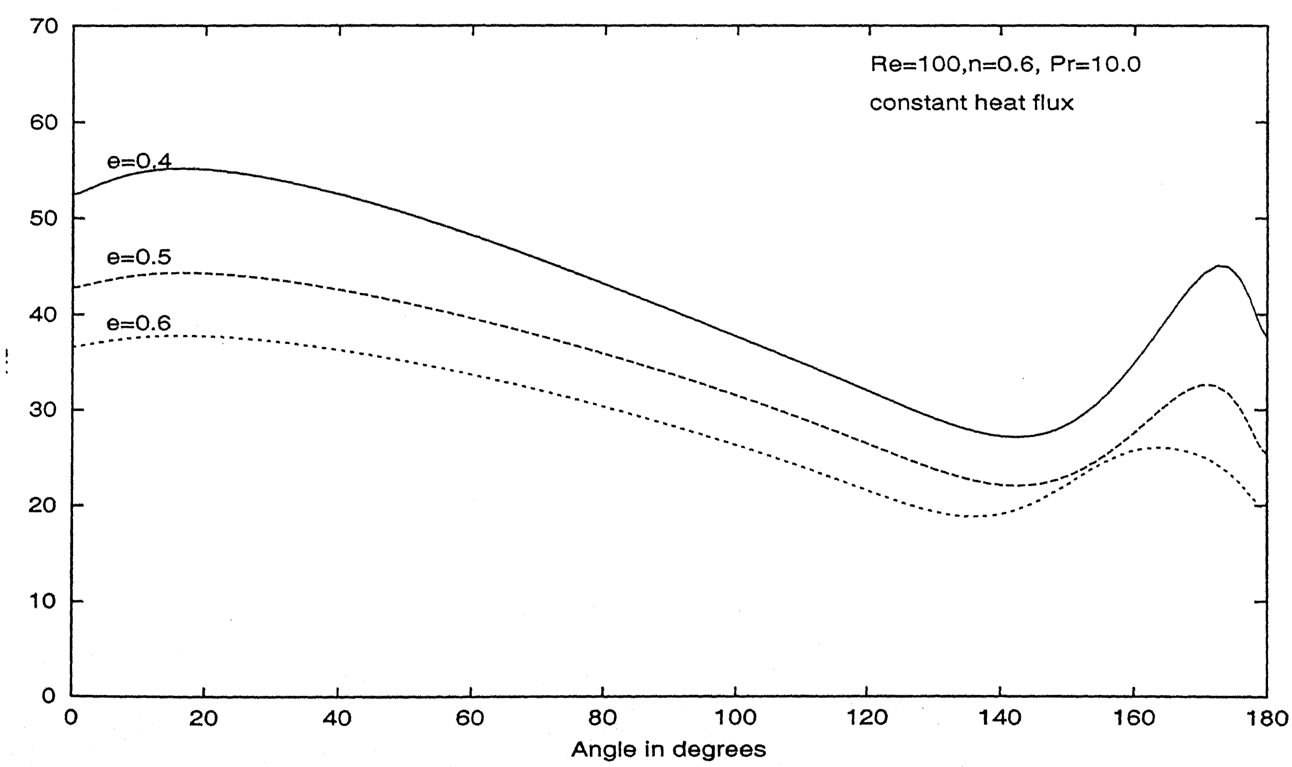

Figure 4.144:Variation of Nusselt number with angle for Re=100,n=0.6 and Pr=10 for constant heat flux

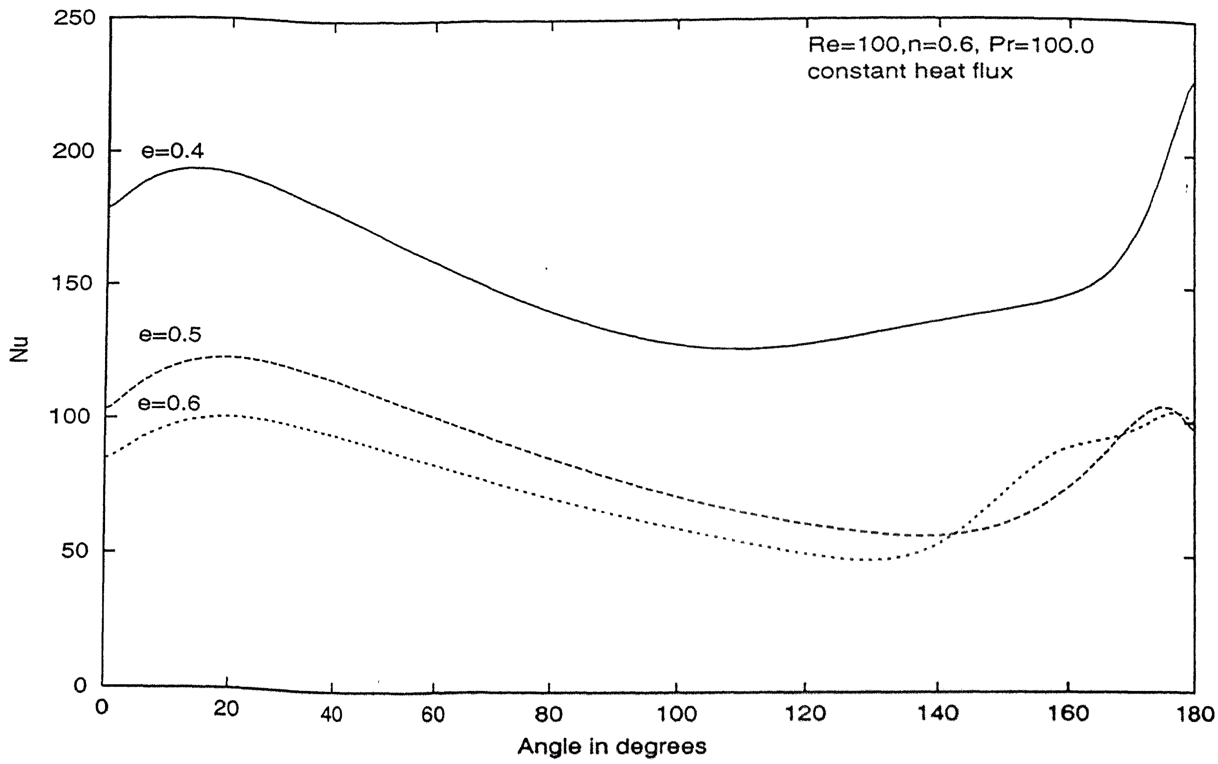

Figure 4.145:Variation of Nusselt number with angle for Re=100,n=0.6 and Pr=100 for constant heat flux

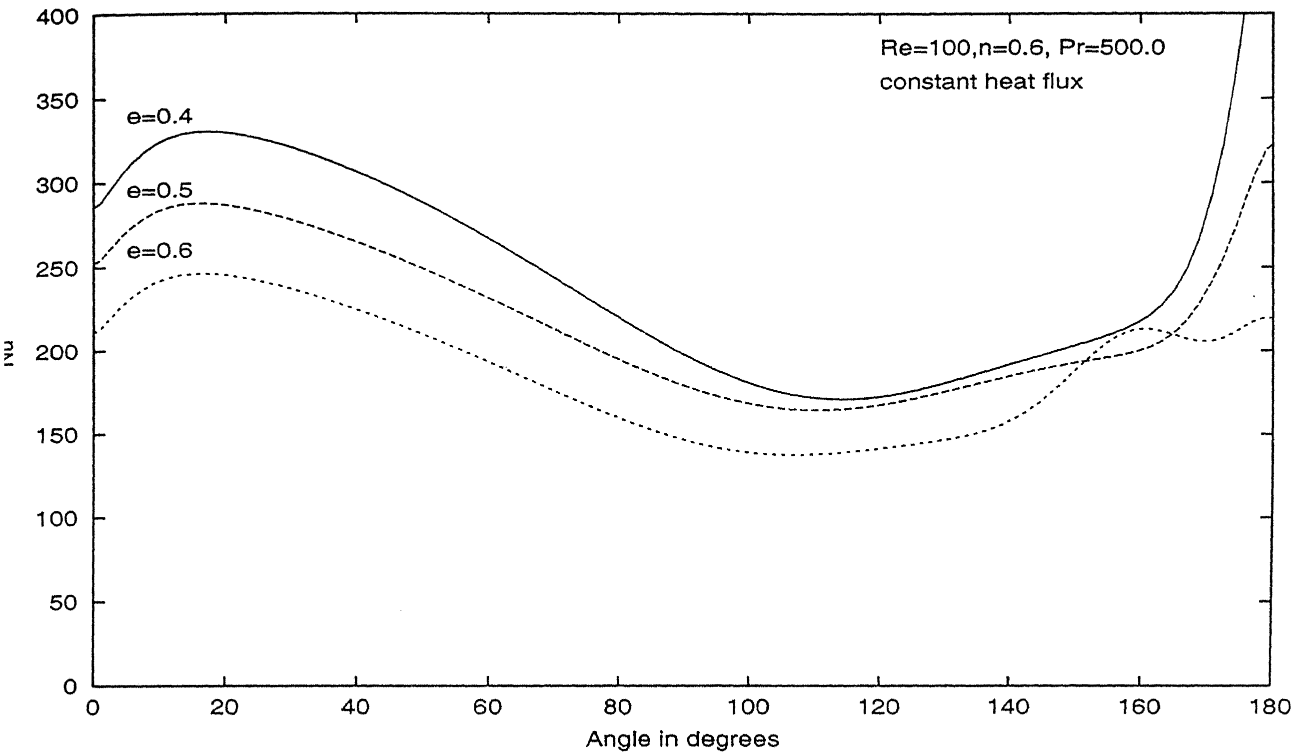

Figure 4.146:Variation of Nusselt number with angle for Re=100,n=0.6 and Pr=500 for constant heat flux

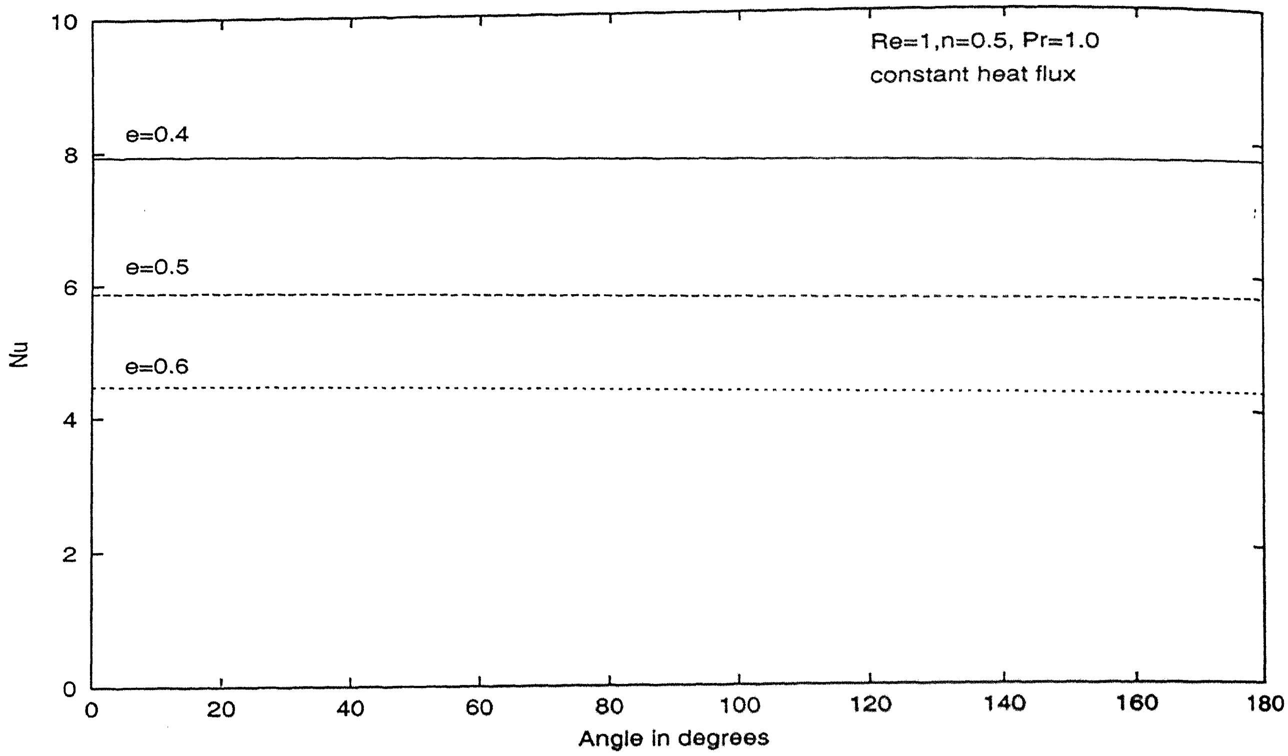

Figure 4.147:Variation of Nusselt number with angle for Re=1,n=0.5 and Pr=1 for constant heat flux

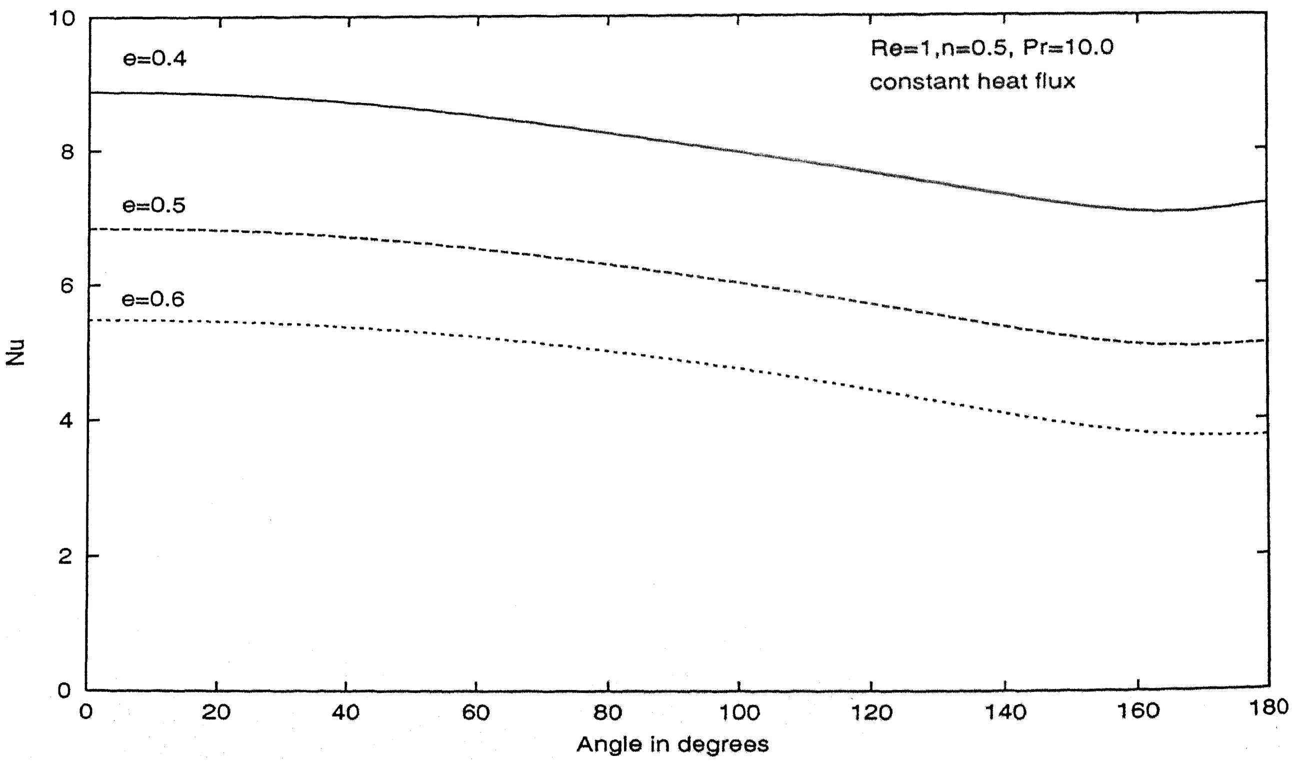

Figure 4.148:Variation of Nusselt number with angle for Re=1,n=0.5 and Pr=10 for constant heat flux

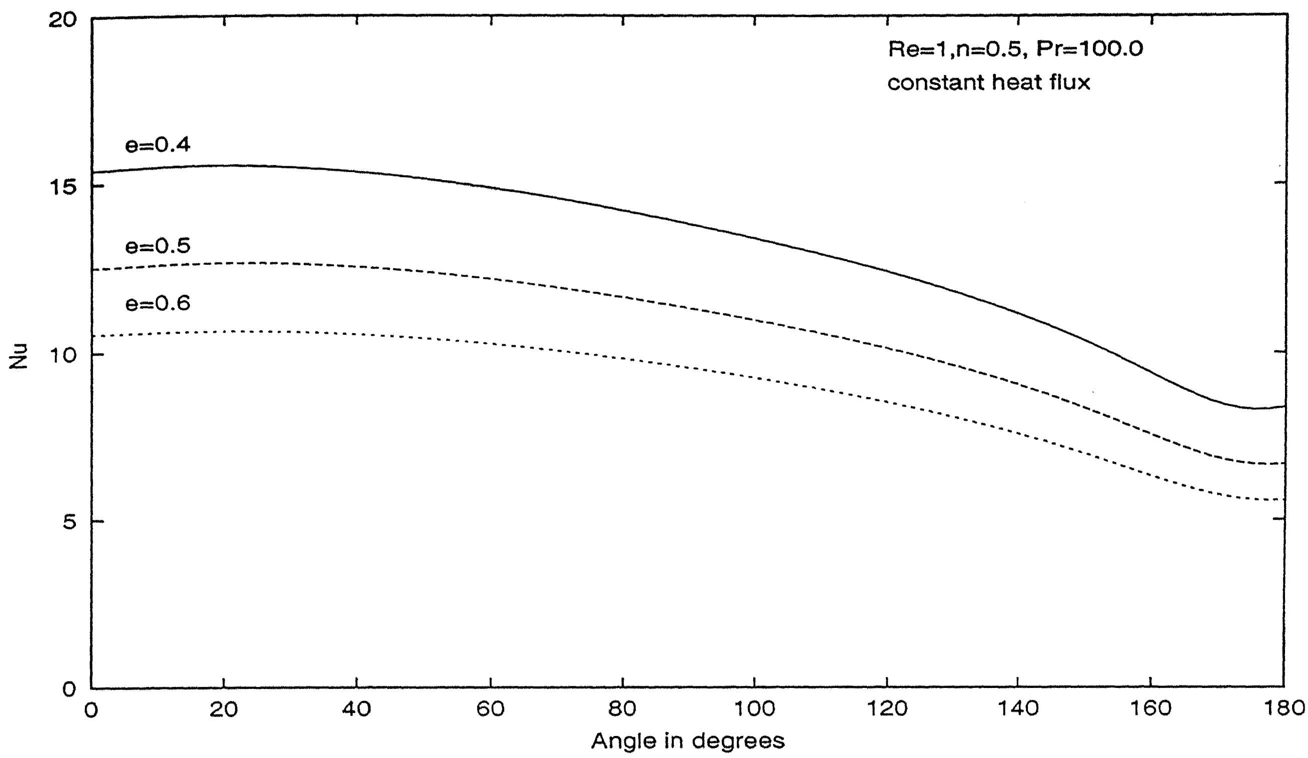

Figure 4.149:Variation of Nusselt number with angle for Re=1,n=0.5 and Pr=100 for constant heat flux

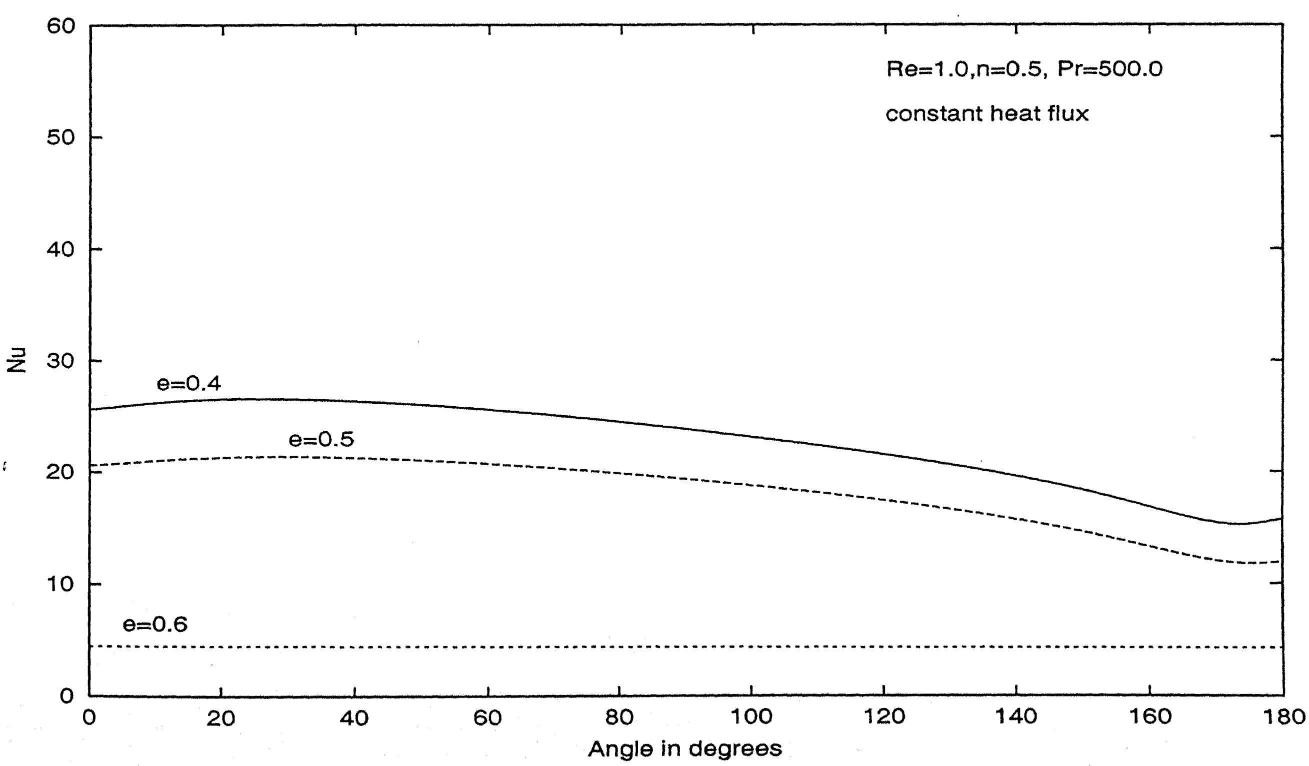

Figure 4.150:Variation of Nusselt number with angle for Re=1,n=0.5 and Pr=500 for constant heat flux

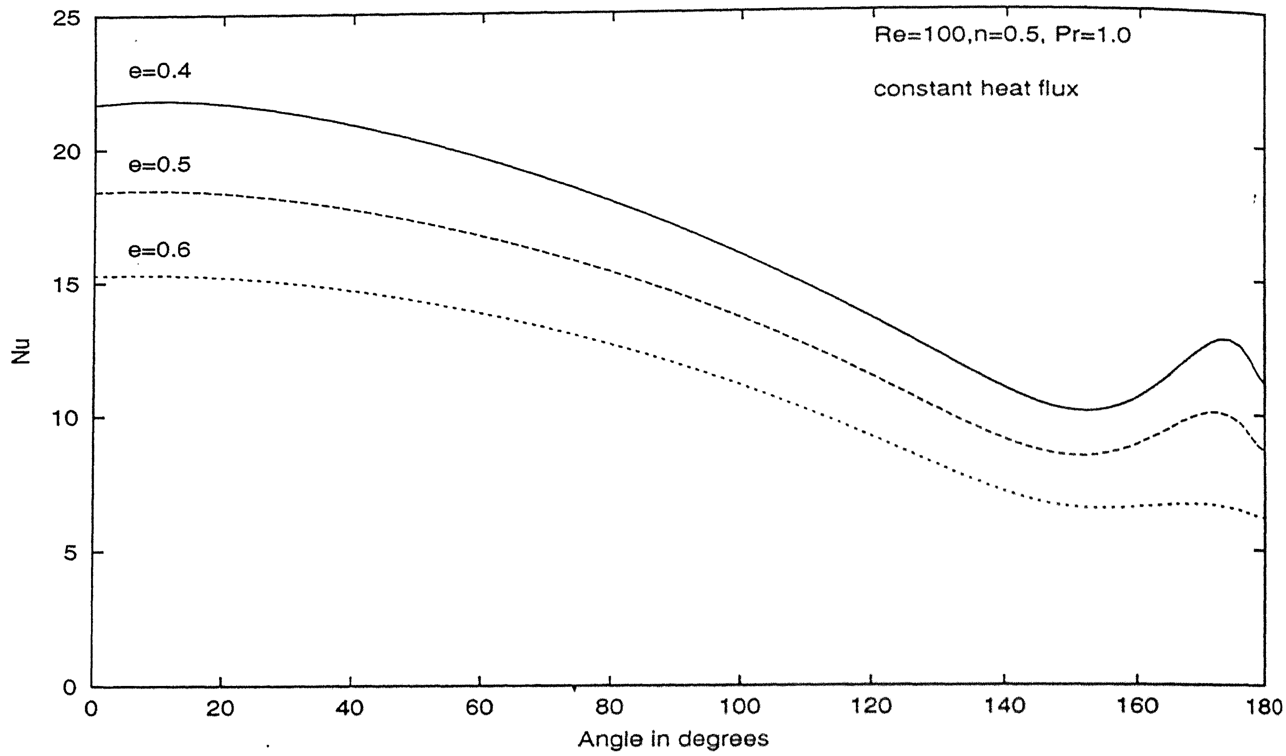

Figure 4.151:Variation of Nusselt number with angle for Re=100,n=0.5 and Pr=1 for constant heat flux

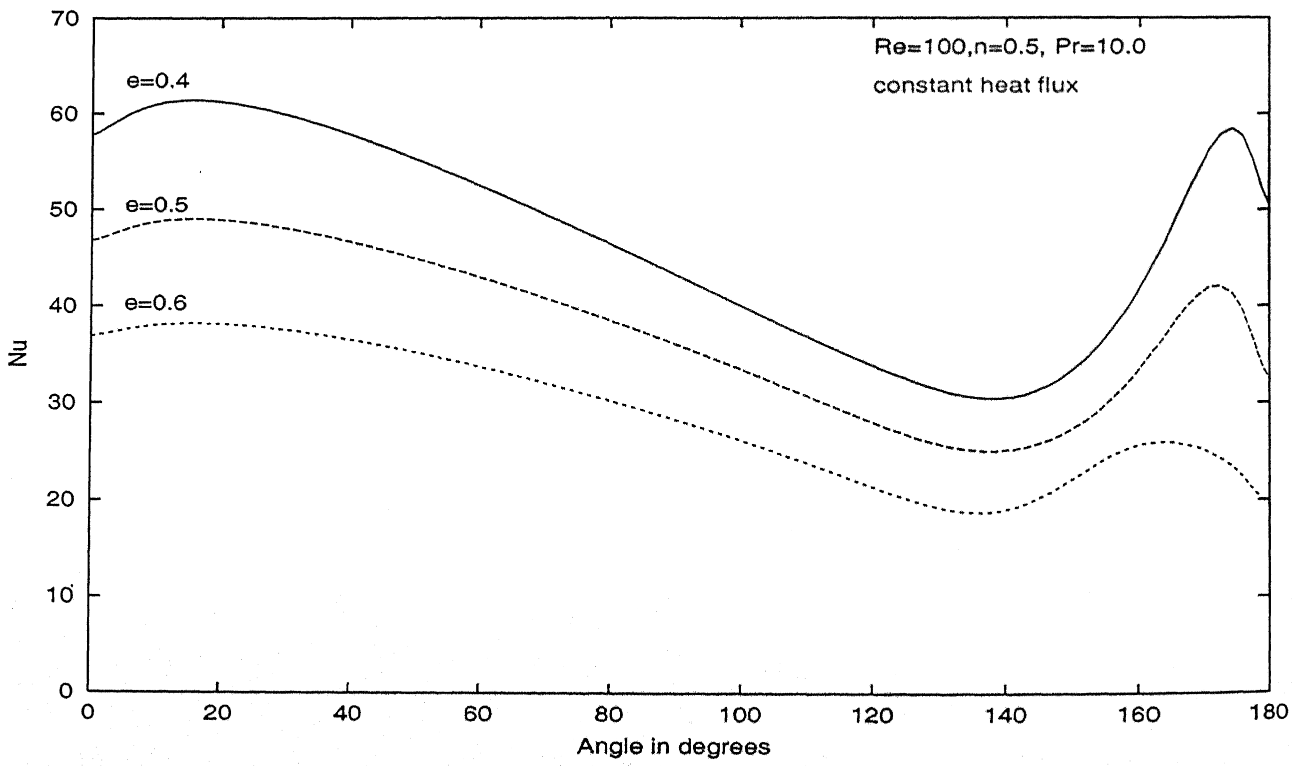

Figure 4.152:Variation of Nusselt number with angle for Re=100,n=0.5 and Pr=10 for constant heat flux

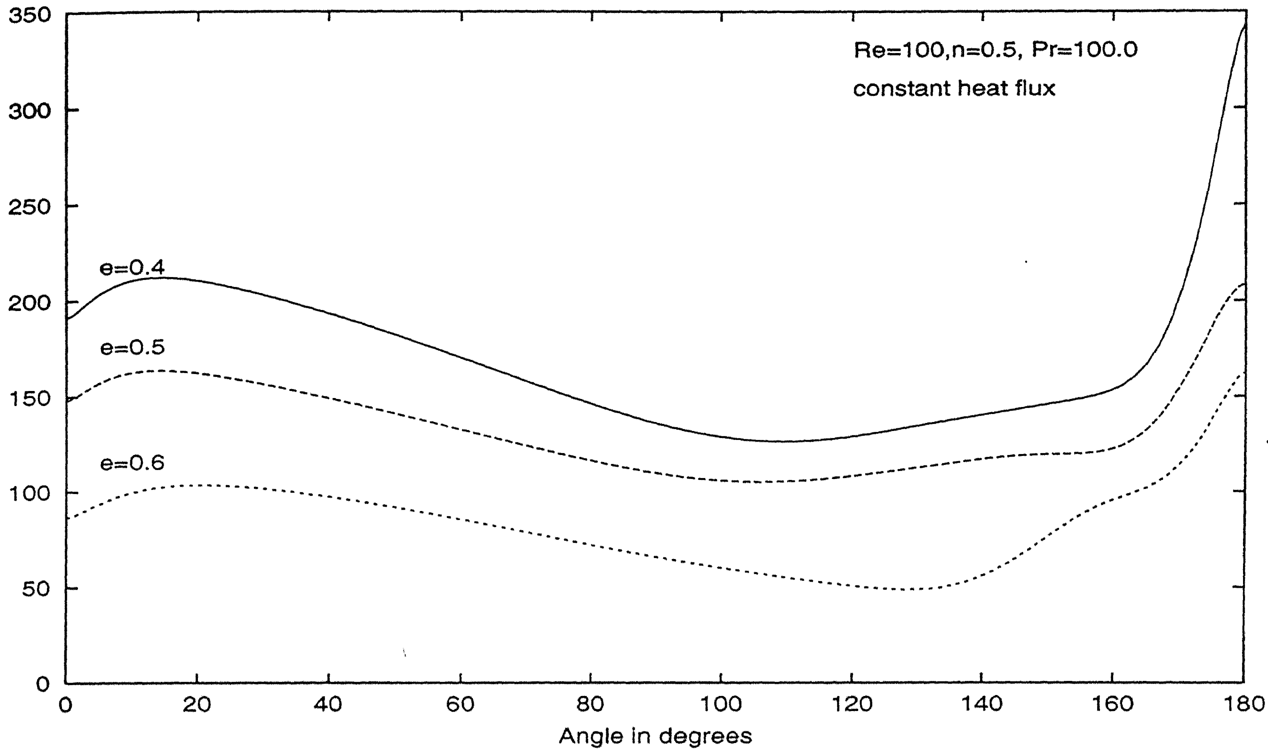

Figure 4.153:Variation of Nusselt number with angle for Re=100,n=0.5 and Pr=100 for constant heat flux

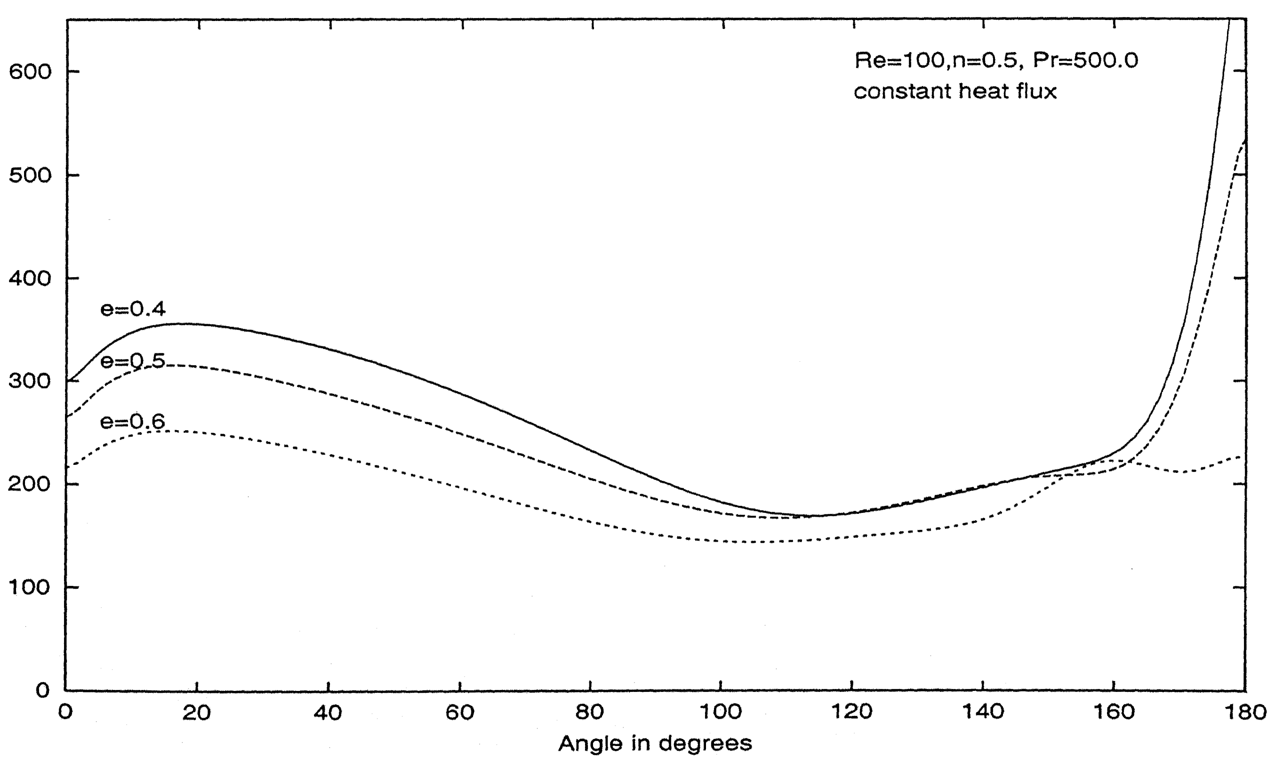

Figure 4.154:Variation of Nusselt number with angle for Re=100,n=0.5 and Pr=500 for constant heat flux

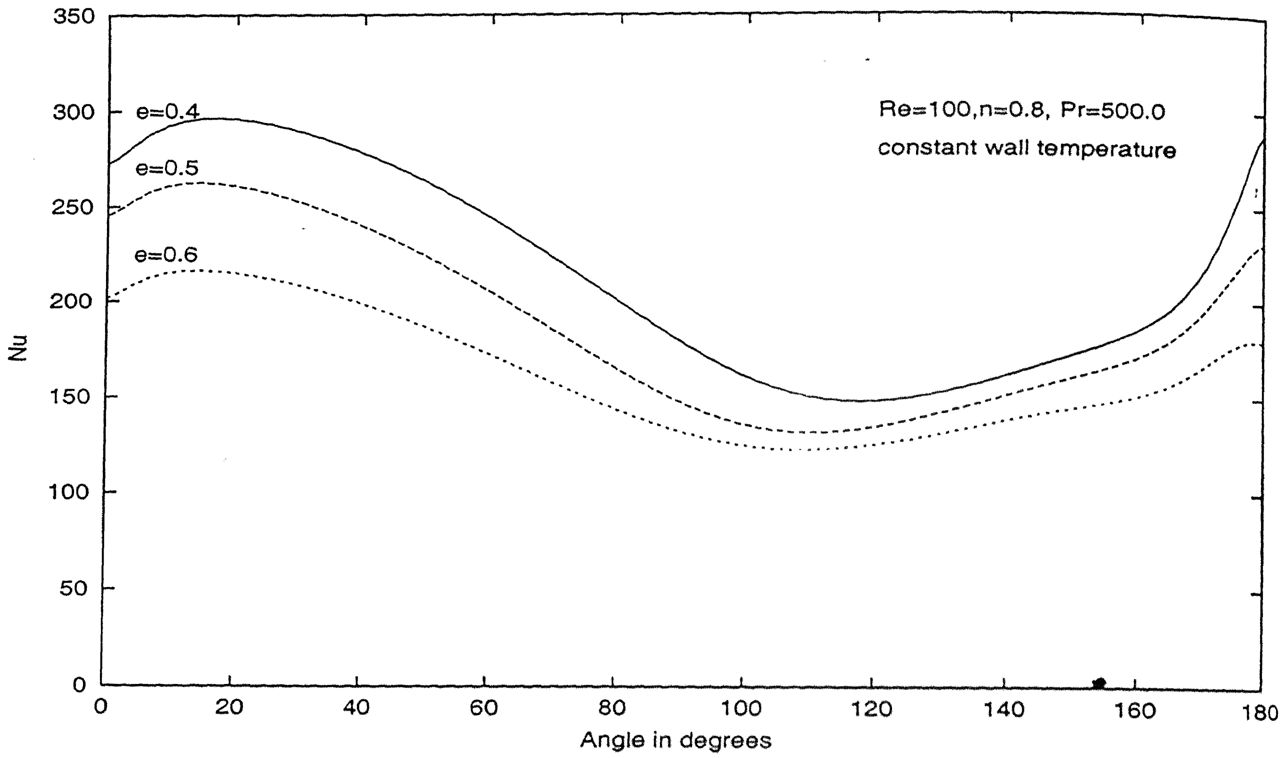

Figure 4.155:Variation of Nusselt number with angle for Re=100,n=0.8 and Pr=500 for constant heat flux

Figure 4.158.

Isotherms for Re=1.0,n=1.0,and porosity 0.4 Pr=1.0(const wall temperature)

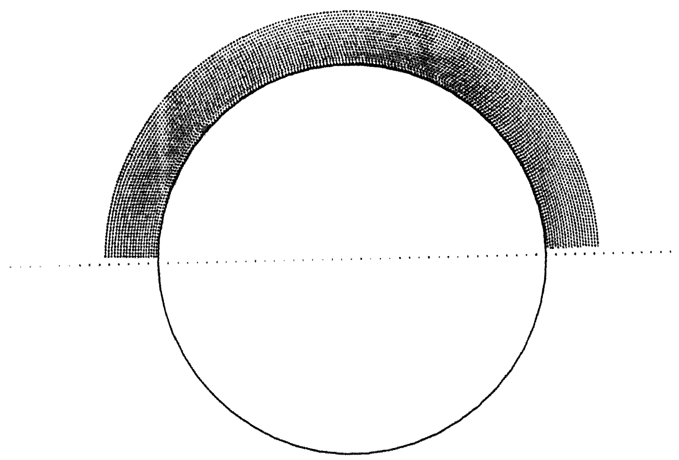

Figure 4.159.

Isotherms for Re=1.0,n=1.0,and porosity 0.4 Pr=10.0(const wall temperature)

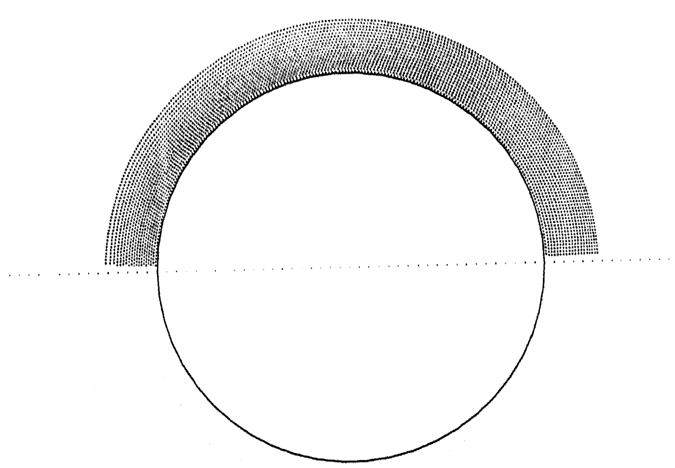

Figure 4.160

Isotherms for Re=1.0,n=1.0,and porosity 0.4 Pr=50.0(const wall temperature)

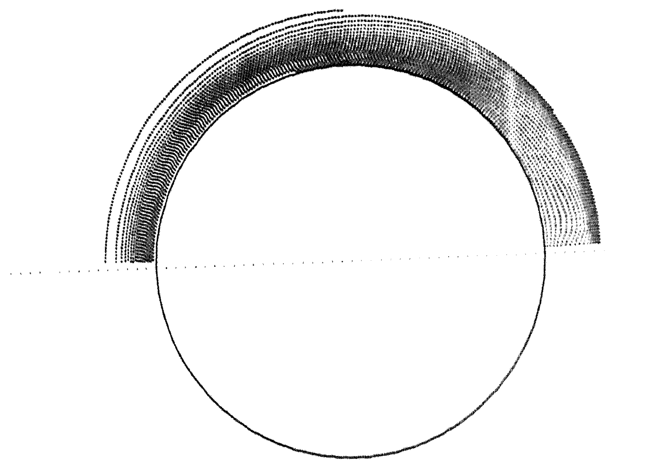

Figure 4.161

Isotherms for Re=1.0,n=1.0,and porosity 0.4 Pr=100.0(const wall temperature)

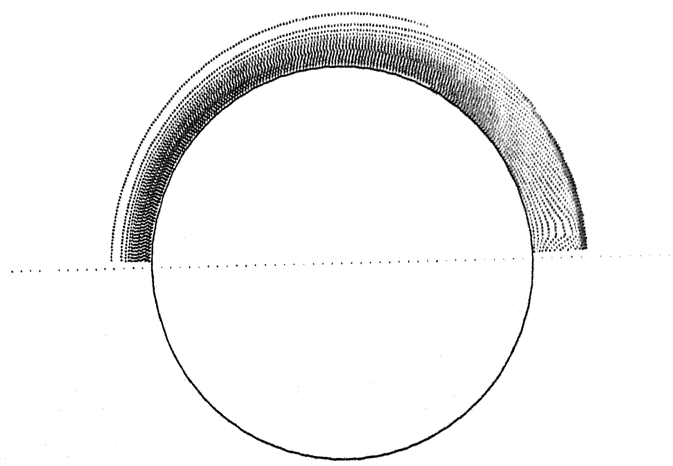

Figure 4.162

Isotherms for Re=1.0,n=1.0,and porosity 0.4 Pr=500.0(const wall temperature)

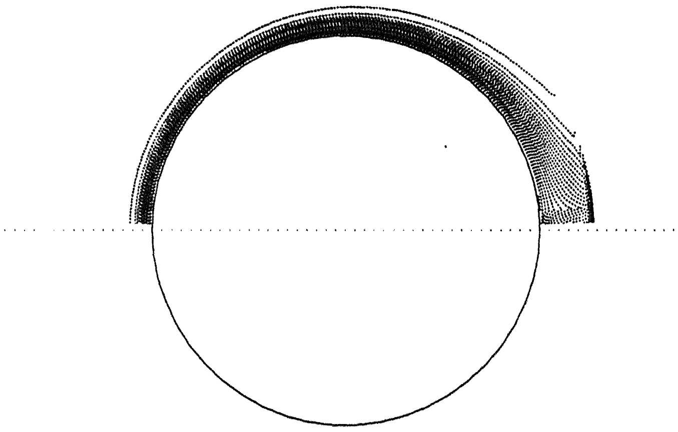

Figure 4.163

Isotherms for Re=10.0,n=1.0,and porosity 0.4 Pr=1.0(const wall temperature)

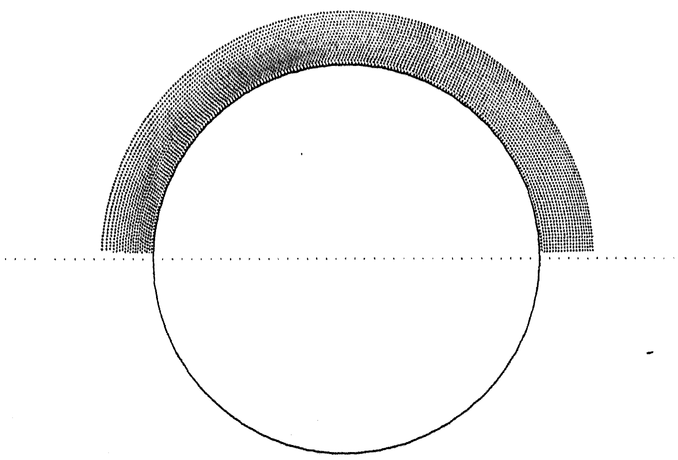

Figure 4.164

Isotherms for Re=10.0,n=1.0,and porosity 0.4 Pr=10.0(const wall temperature)

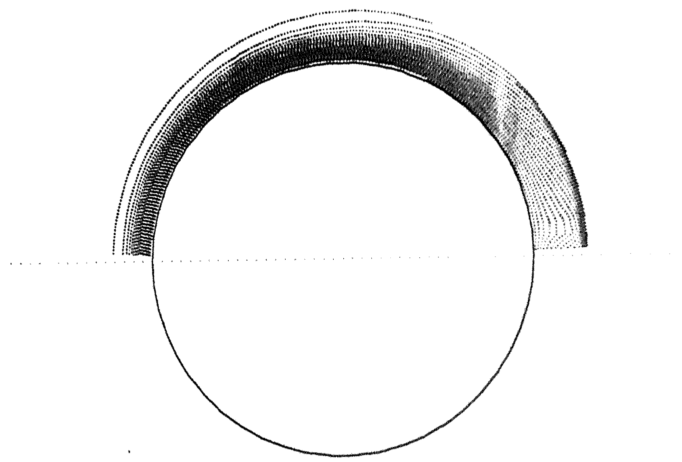

Figure 4.165

Isotherms for Re=10.0,n=1.0,and porosity 0.4 Pr=50.0(const wall temperature)

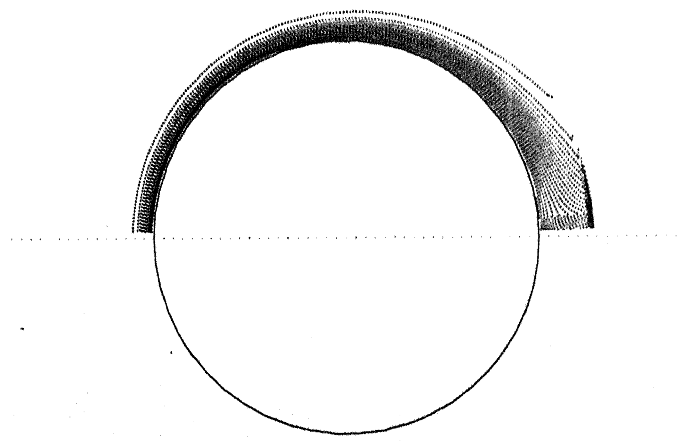

Figure 4.166

Isotherms for Re=10.0,n=1.0,and porosity 0.4 Pr=100.0(const wall temperature)

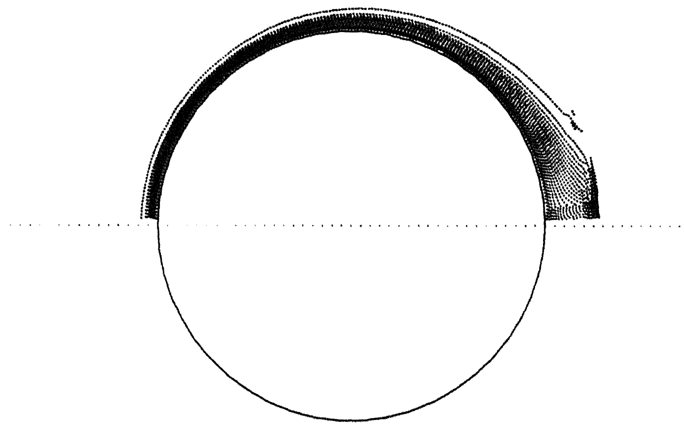

Figure 4.167

Isotherms for Re=10.0,n=1.0,and porosity 0.4 Pr=500.0(const wall temperature)

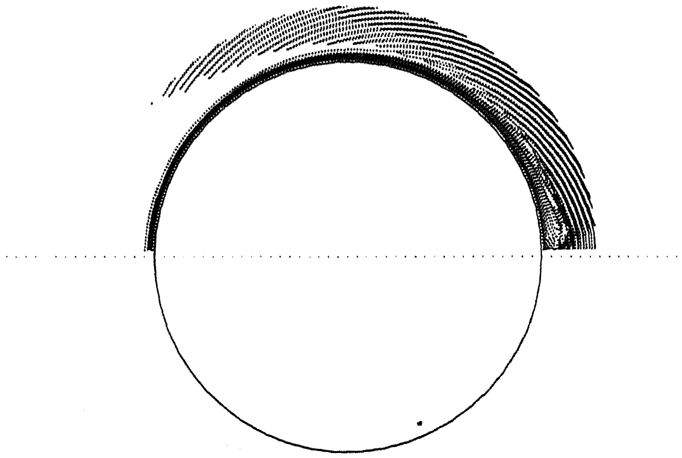

Figure 4.168

Isotherms for Re=100.0,n=1.0,and porosity 0.4 Pr=1.0(const wall temperature)

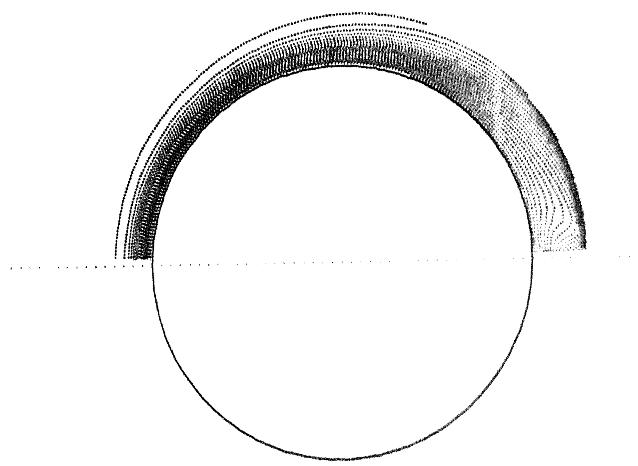

Figure 4.169

Isotherms for Re=100.0,n=1.0,and porosity 0.4 Pr=10.0(const wall temperature)

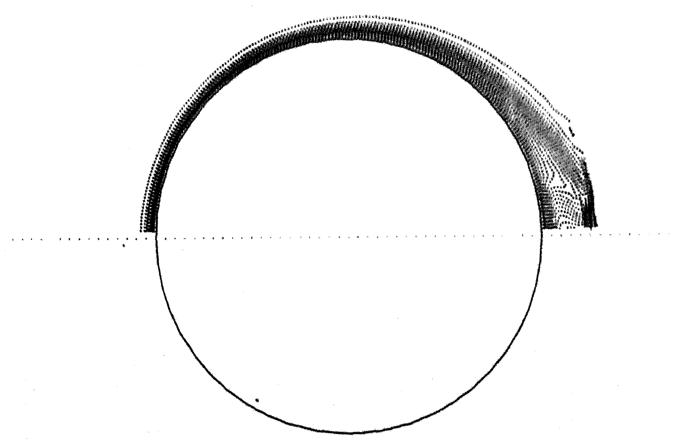

Figure 4.170

Isotherms for Re=100.0,n=1.0,and porosity 0.4 Pr=50.0(const wall temperature)

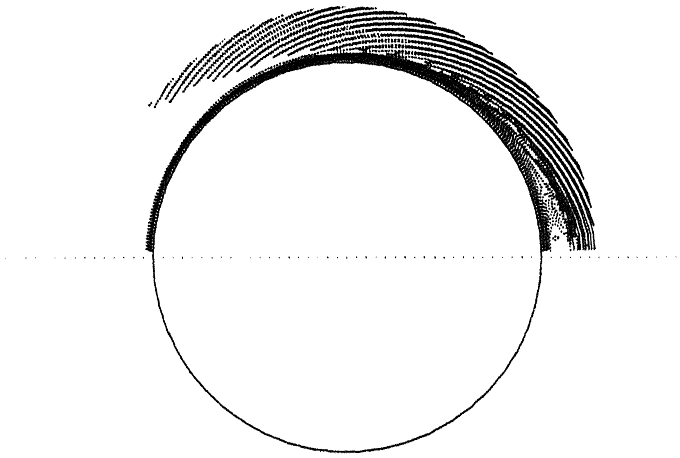

Figure 4.171

Isotherms for Re=100.0,n=1.0,and porosity 0.4 Pr=100.0(const wall temperature)

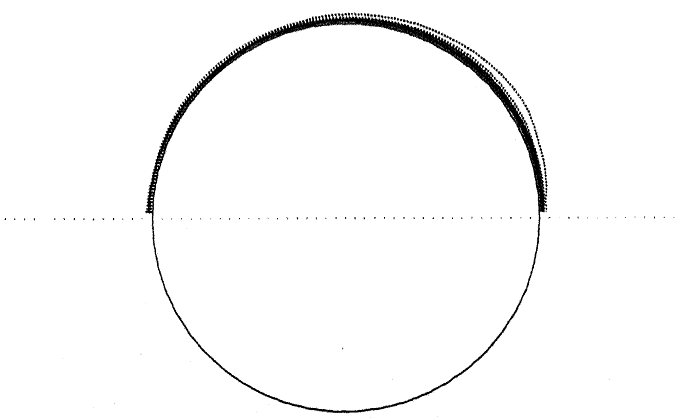

Figure 4.172

Isotherms for Re=100.0,n=1.0,and porosity 0.4 Pr=100.0(const wall temperature)

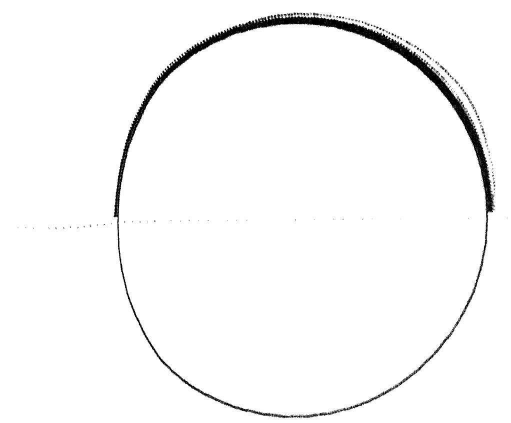

Figure 4.173

Isotherms for Re=200.0,n=1.0,and porosity 0.4 Pr=1.0(cont wall temperature)

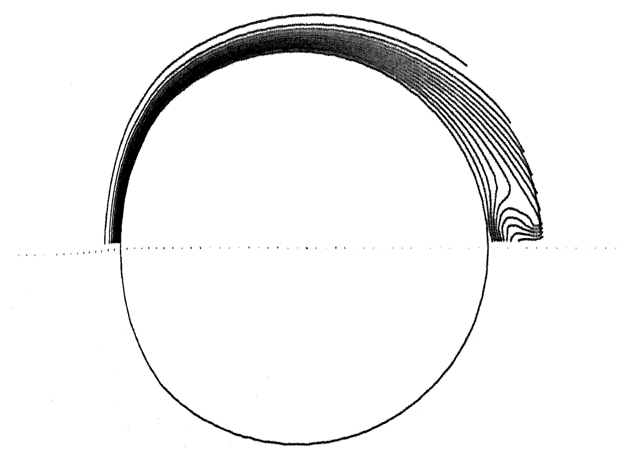

Figure 4.174.

Isotherms for Re=200.0,n=1.0,and porosity 0.4 Pr=10.0(const wall temperature)

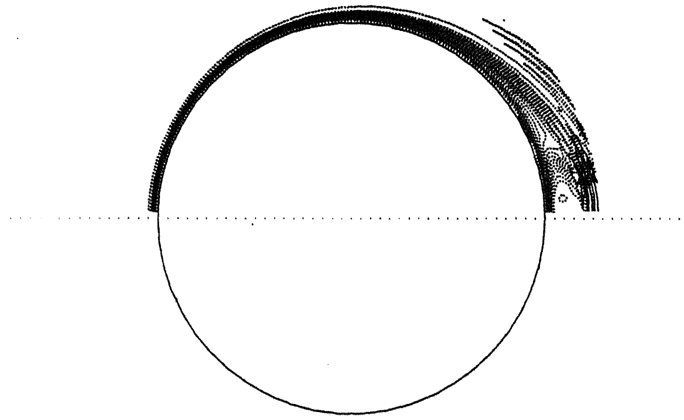

Figure 4.175

Isotherms for Re=200.0,n=1.0,and porosity 0.4 Pr=50.0(const wall temperature)

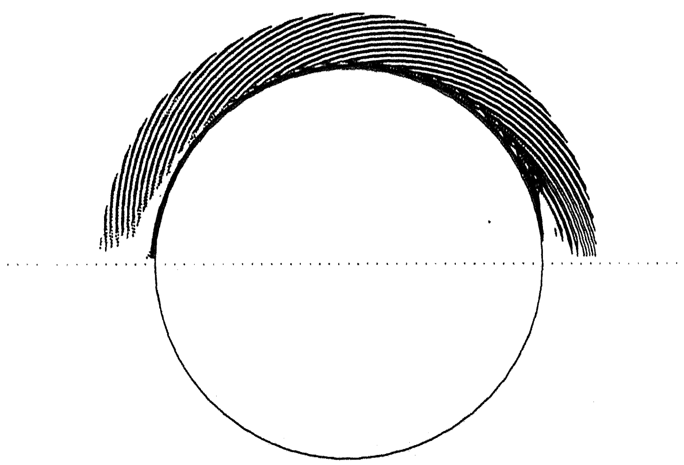

Figure 4.176

Isotherms for Re=200.0,n=1.0,and porosity 0.4 Pr=100.0(const wall temperature)

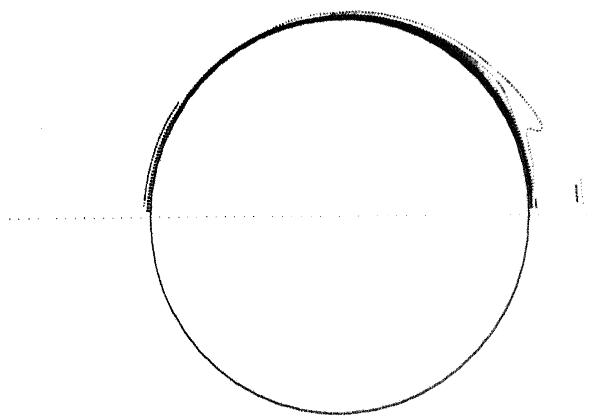

Figure 4.177

Isotherms for Re=200.0,n=1.0,and porosity 0.4 Pr=500.0(const wall temperature)

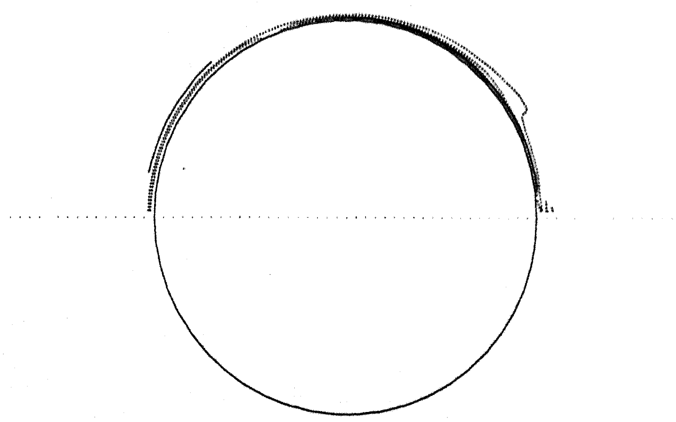

Figure 4.178

Isotherms for Re=500.0,n=1.0,and porosity 0.4 Pr=1.0(const wall temperature)

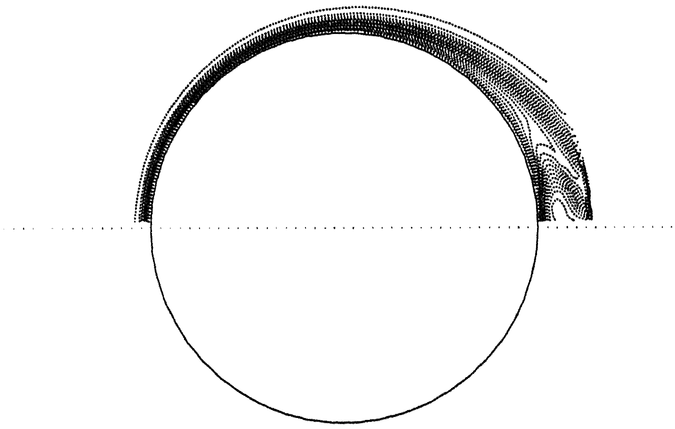

Figure 4.179

Isotherms for Re=500.0,n=1.0,and porosity 0.4 Pr=10.0(const wall temperature)

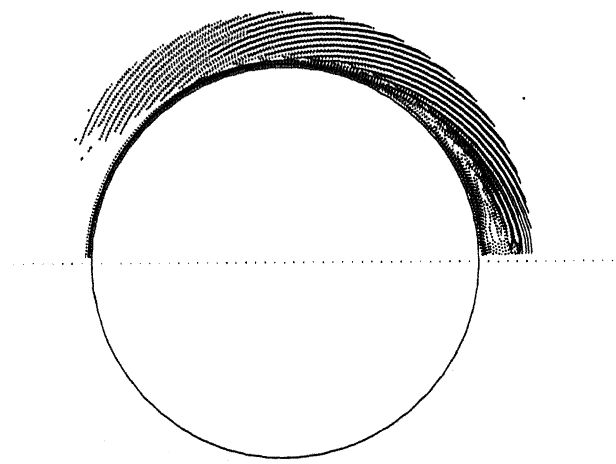

Figure 4.180

Isotherms for Re=500.0,n=1.0,and porosity 0.4 Pr=50.0(const wall temperature)

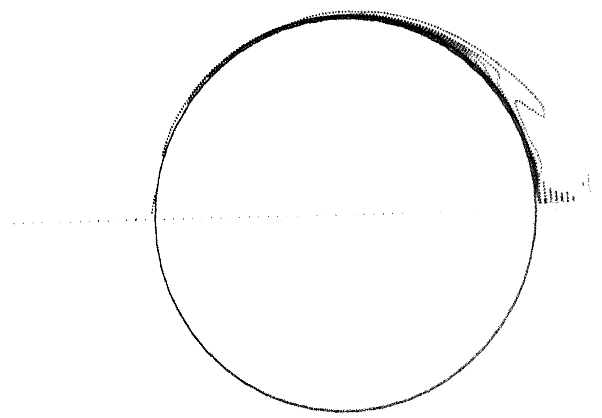

Figure 4.181

Isotherms for Re=500.0,n=1.0,and porosity 0.4 Pr=100.0(const wall temperature)

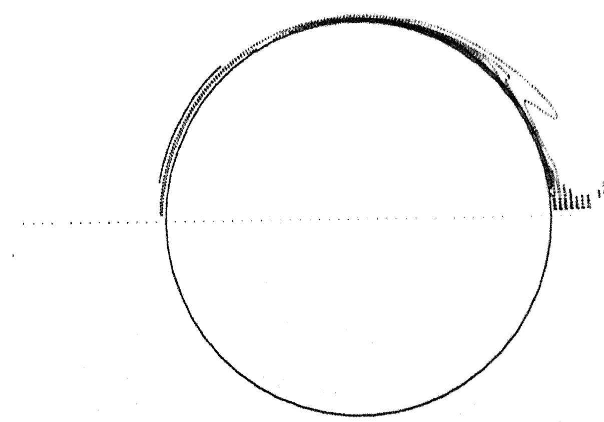

Figure 4.182

Isotherms for Re=1.0,n=0.8,and porosity 0.4 Pr=1.0(const wall temperature)

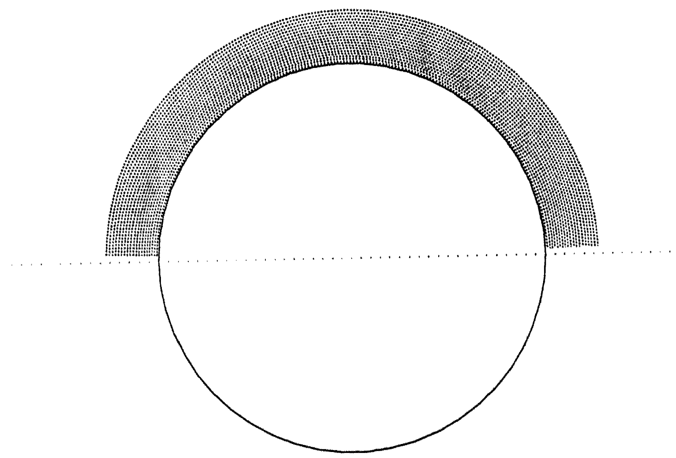

Figure 4.183

Isotherms for Re=1.0,n=0.8,and porosity 0.4 Pr=10.0(const wall temperature)

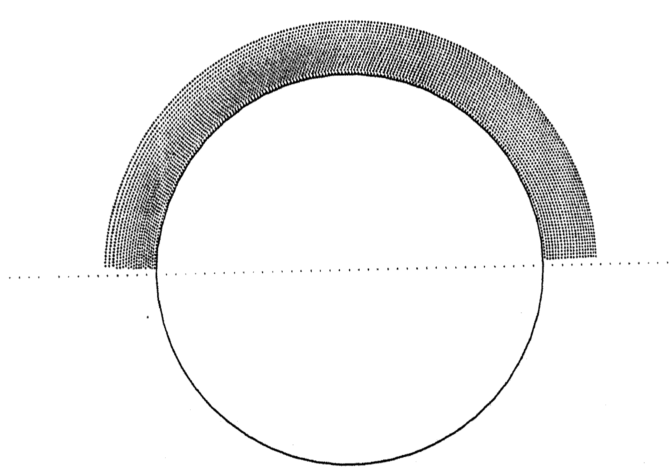

Figure 4.184

Isotherms for Re=1.0,n=0.8,and porosity 0.4 Pr=50.0(const wall temperature)

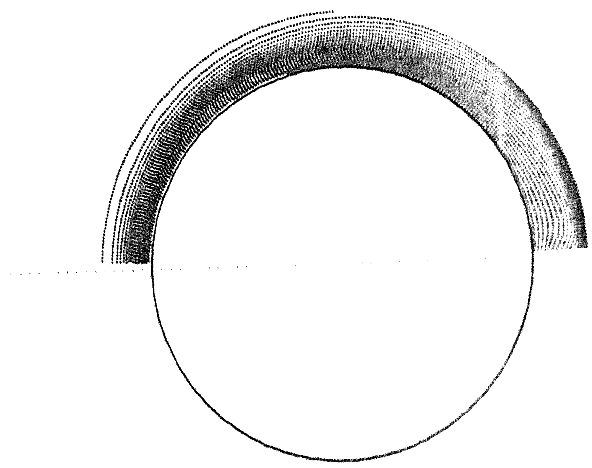

Figure 4.185

Isotherms for Re=1.0,n=0.8,and porosity 0.4 Pr=100.0(const wall temperature)

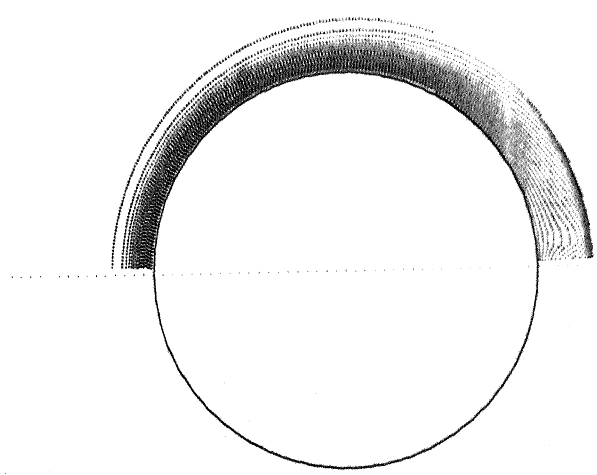

Figure 4.186

Isotherms for Re=1.0,n=0.8,and porosity 0.4 Pr=500.0(const wall temperature)

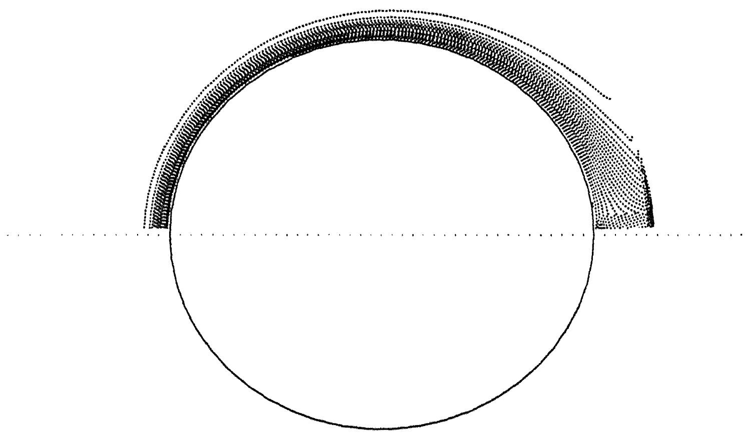

Figure 4.187

Isotherms for Re=10.0,n=0.8,and porosity 0.4 Pr=1.0(cont wall temperature)

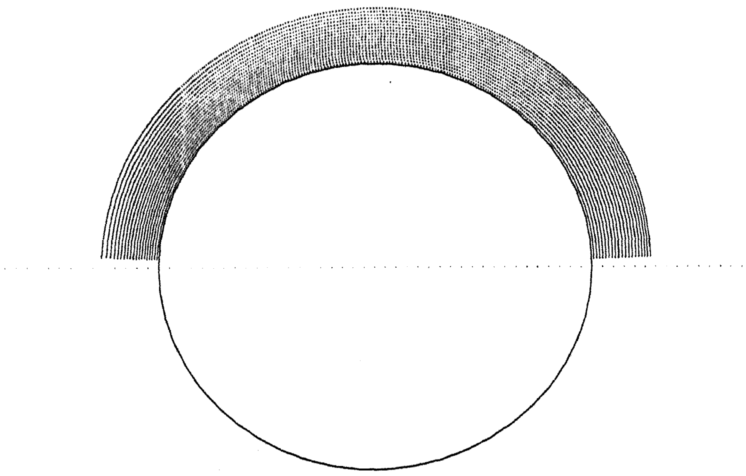

Figure 4.188

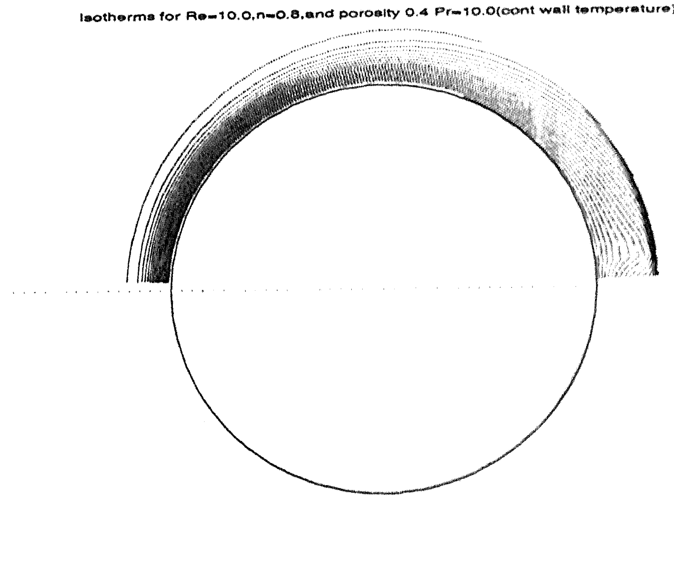

Figure 4.189

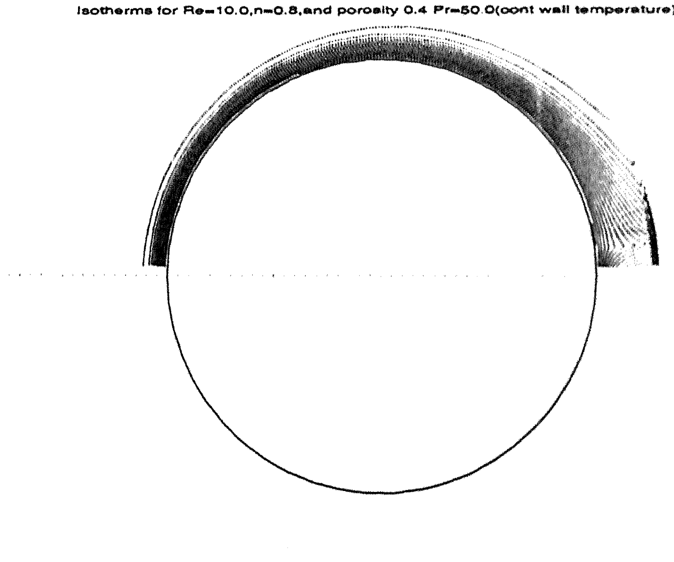

Figure 4.190

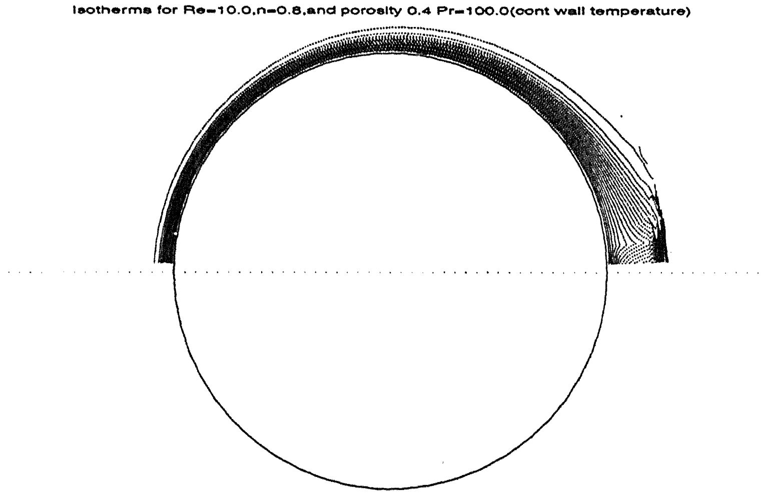

Figure 4.191

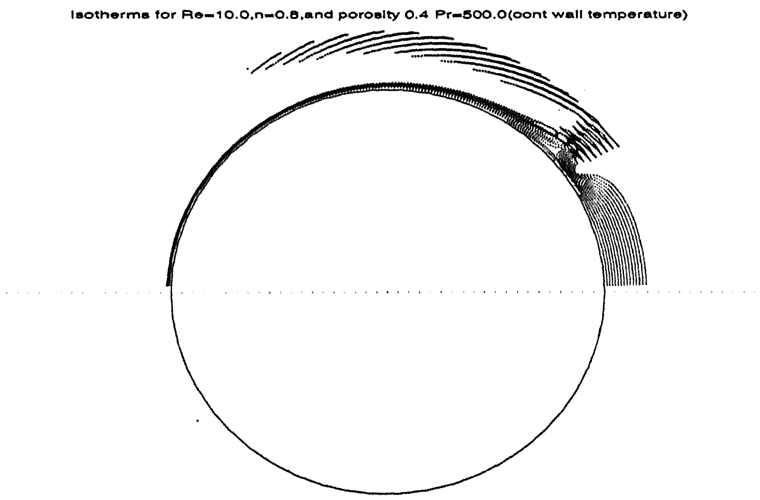

Figure 4.192

Isotherms for Re=100.0,n=0.8,and porosity 0.4 Pr=1.0(const wall temperature)

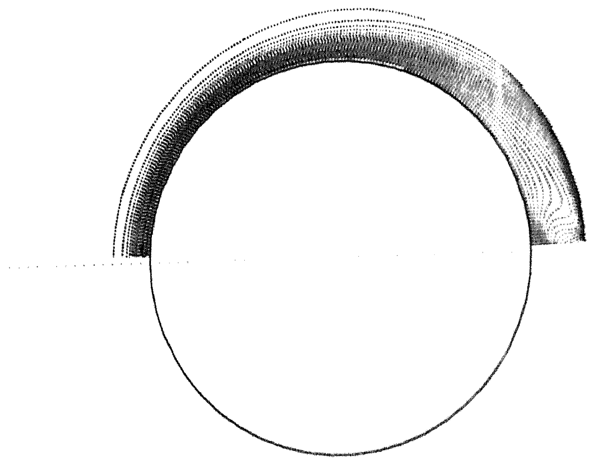

Figure 4.193

Isotherms for Re=100.0,n=0.8,and porosity 0.4 Pr=10.0(const wall temperature)

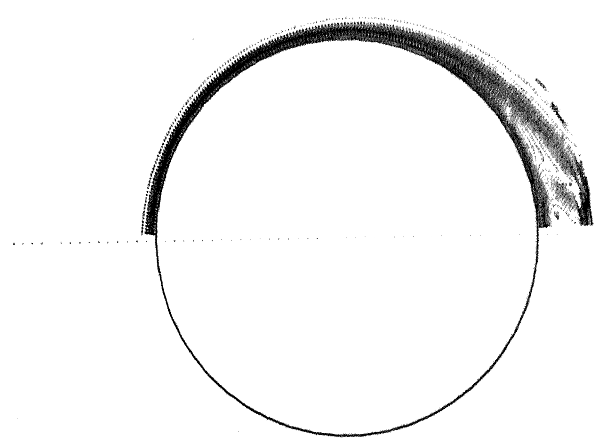

Figure 4.194

Isotherms for Re=100.0,n=0.8,and porosity 0.4 Pr=50.0(const wall temperature)

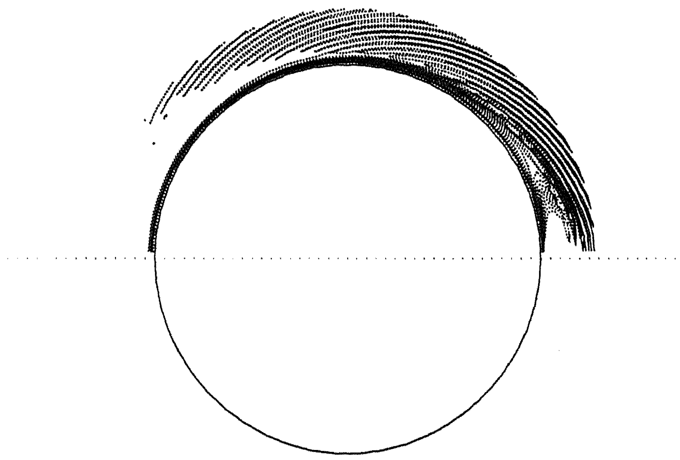

Figure 4.195

Isotherms for Re=100.0,n=0.8,and porosity 0.4 Pr=100.0(const wall temperature)

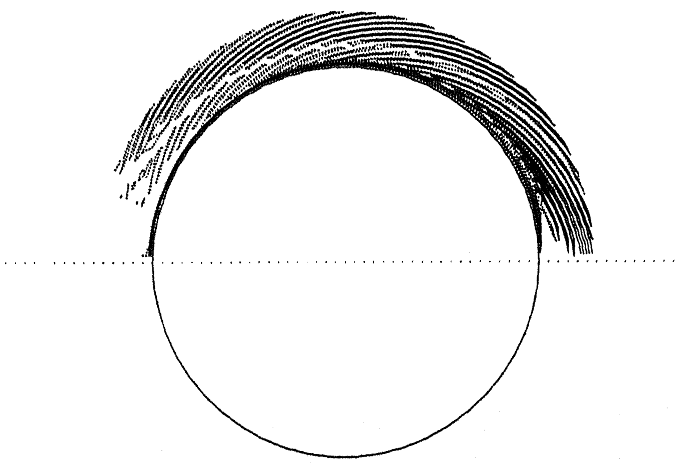

Figure 4.196

Isotherms for Re=100.0,n=0.8,and porosity 0.4 Pr=100.0(const wall temperature)

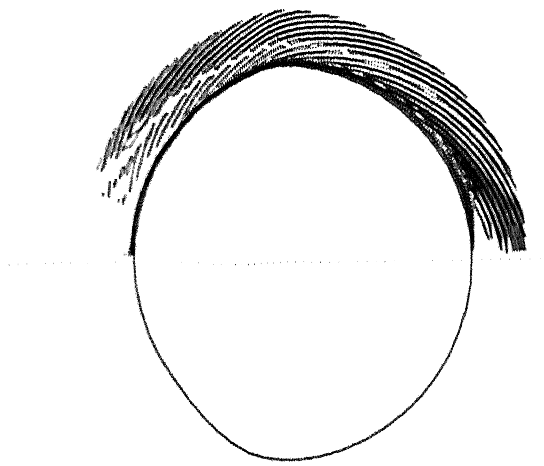

Figure 4.197

Isotherms for Re=200.0,n=0.8,and porosity 0.4 Pr=1.0(const wall temperature)

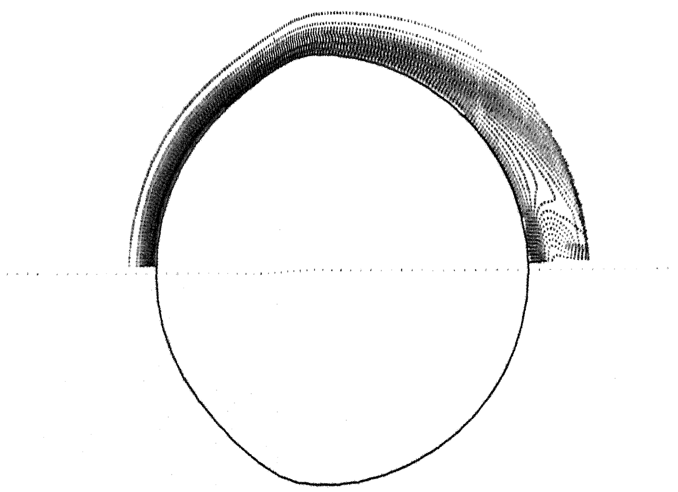

Figure 4.198

Isotherms for Re=200.0,n=0.8,and porosity 0.4 Pr=10.0(const wall temperature)

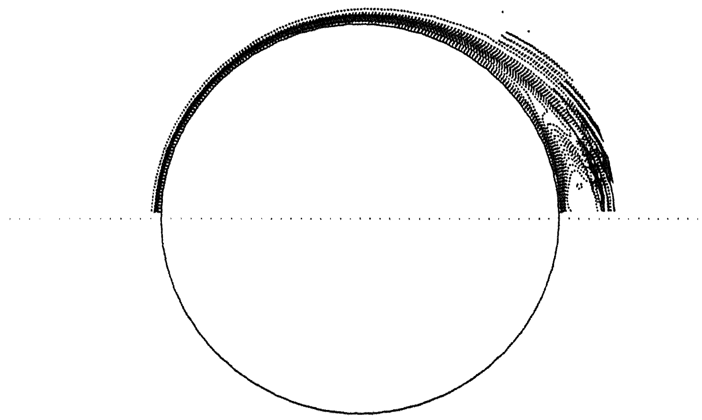

Figure 4.199

Isotherms for Re=200.0,n=0.8,and porosity 0.4 Pr=50.0(const wall temperature)

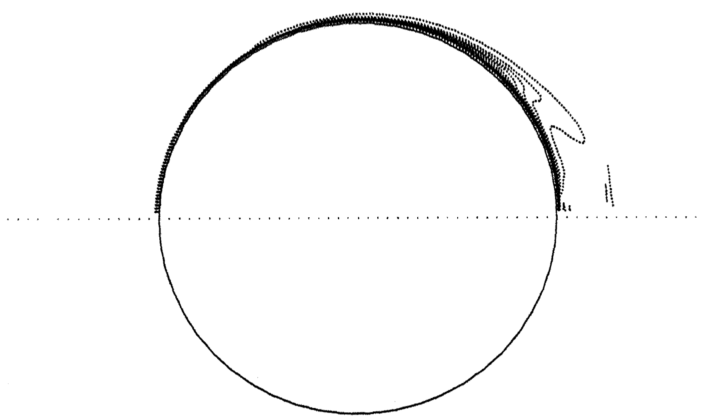

Figure 4.200

Isotherms for Re=200.0,n=0.8,and porosity 0.4 Pr=100.0(const wall temperature)

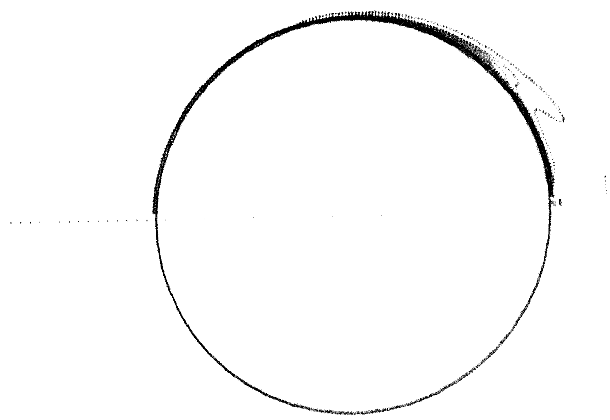

Figure 4.201

Isotherms for Re=200.0,n=0.8,and porosity 0.4 Pr=500.0(const wall temperature)

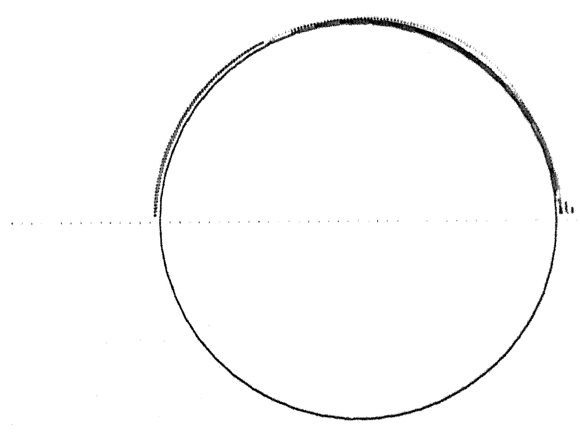

Figure 4.202

Isotherms for Re=500.0,n=0.8,and porosity 0.4 Pr=1.0(const wall temperature)

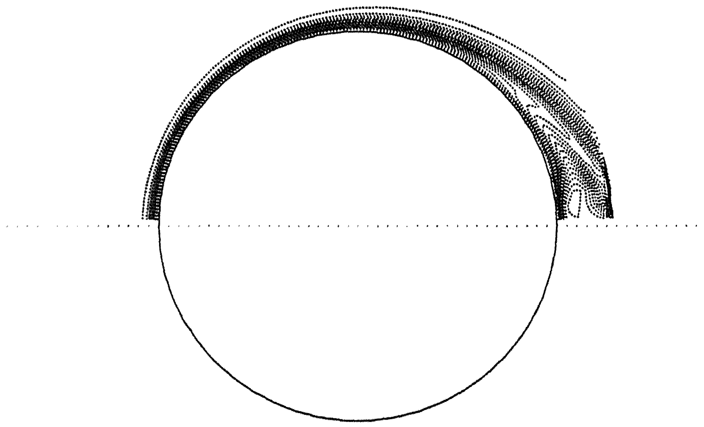

Figure 4.203

Isotherms for Re=500.0,n=0.8,and porosity 0.4 Pr=10.0(const wall temperature)

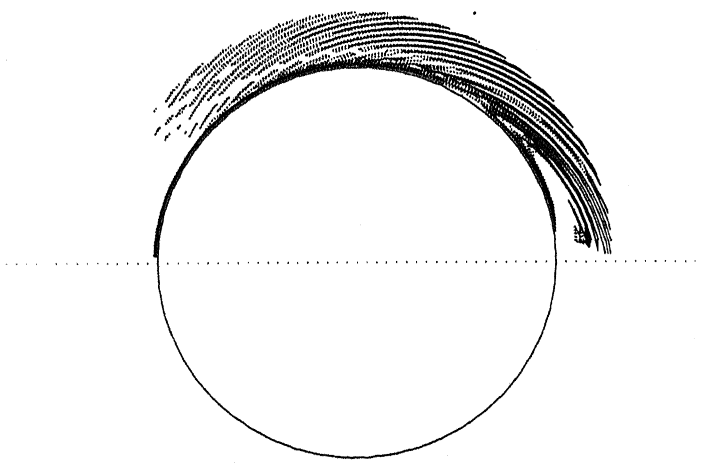

Figure 4.204

Isotherms for Re=500.0,n=0.8,and porosity 0.4 Pr=50.0(const wall temperature)

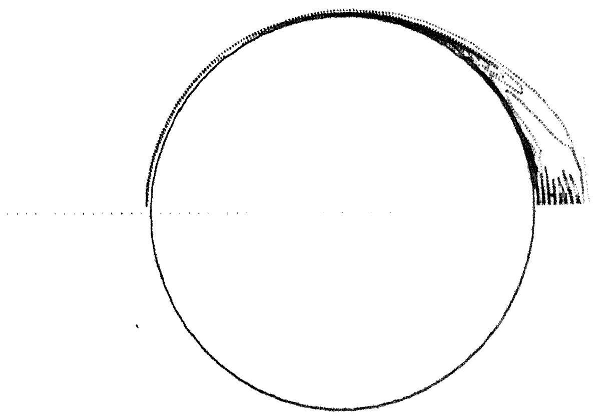

Figure 4.205

Isotherms for Re=500.0,n=0.8,and porosity 0.4 Pr=100.0(const wall temperature)

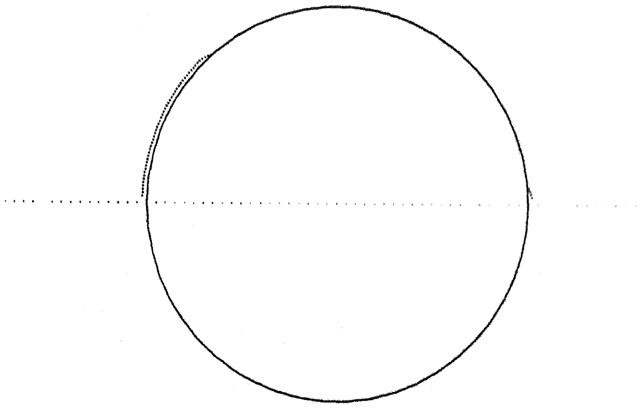

Figure 4.206

Isotherms for Re=10.0,n=0.6,and porosity 0.4 Pr=1.0(cont wall temperature)

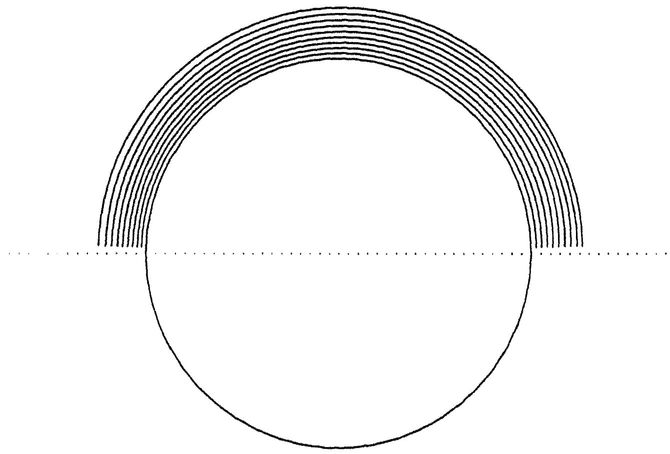

Figure 4.207

Isotherms for Re=10.0,n=0.6,and porosity 0.4 Pr=10.0(cont wall temperature)

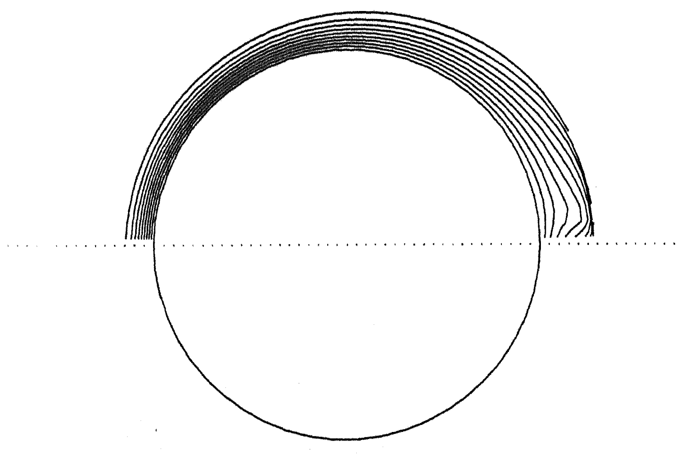

Figure 4.208

Isotherms for Re=10.0,n=0.6,and porosity 0.4 Pr=50.0(cont wall temperature)

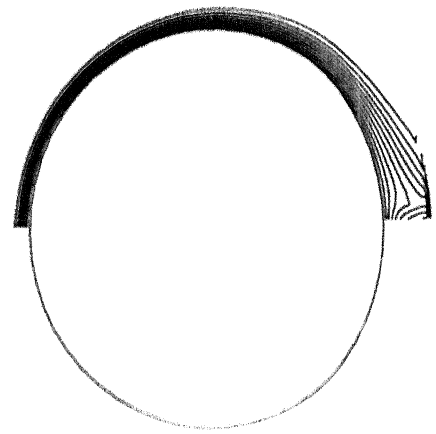

Figure 4.209

Isotherms for Re=10.0,n=0.6,and porosity 0.4 Pr=100.0(cont wall temperature)

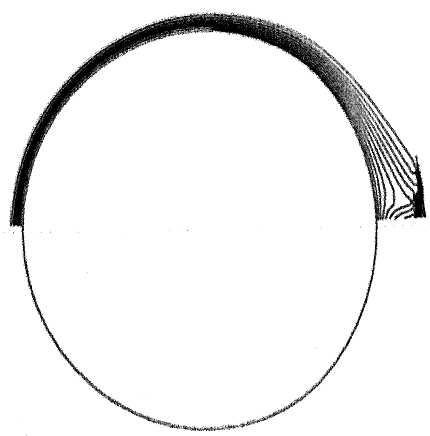

Figure 4.210

Isotherms for Re=10.0,n=0.6,and porosity 0.4 Pr=500.0(cont wall temperature)

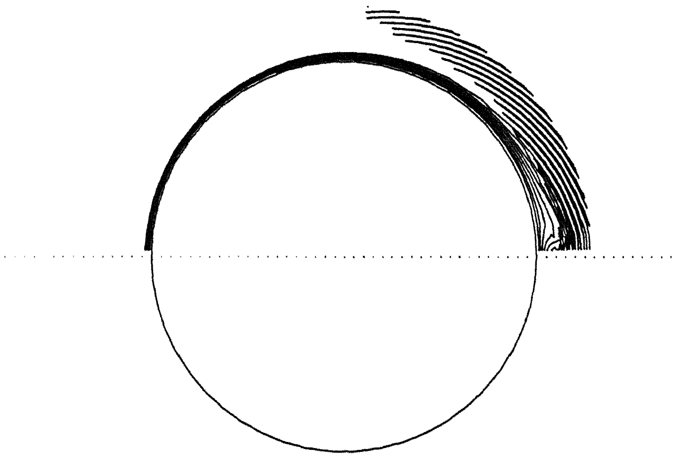

Figure 4.211

Isotherms for Re=100.0,n=0.6,and porosity 0.4 Pr=1.0(cont wall temperature)

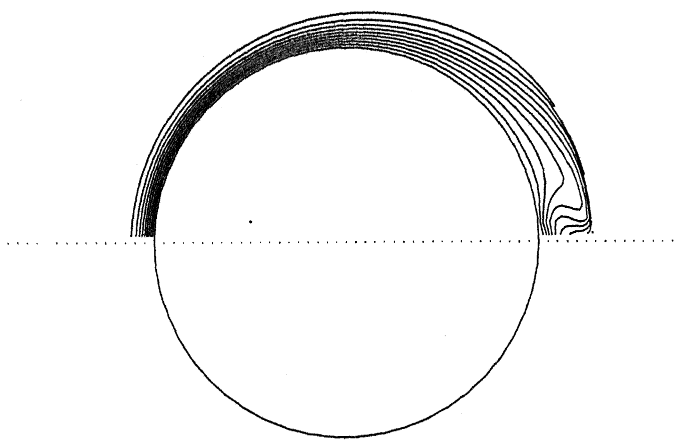

Figure 4.212

Isotherms for Re=100.0,n=0.6,and porosity 0.4 Pr=10.0(cont wall temperature)

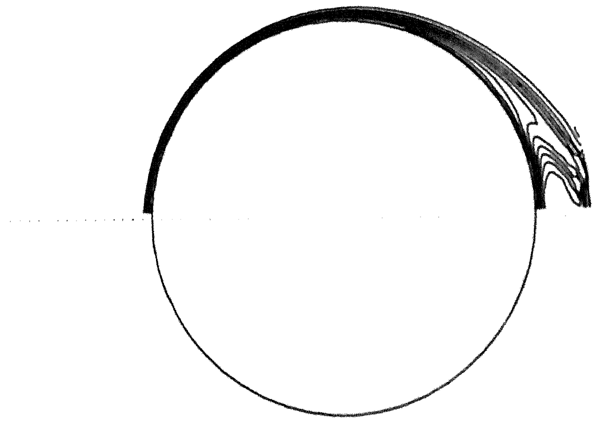

Figure 4.213

Isotherms for Re=100.0,n=0.6,and porosity 0.4 Pr=50.0(cont wall temperature)

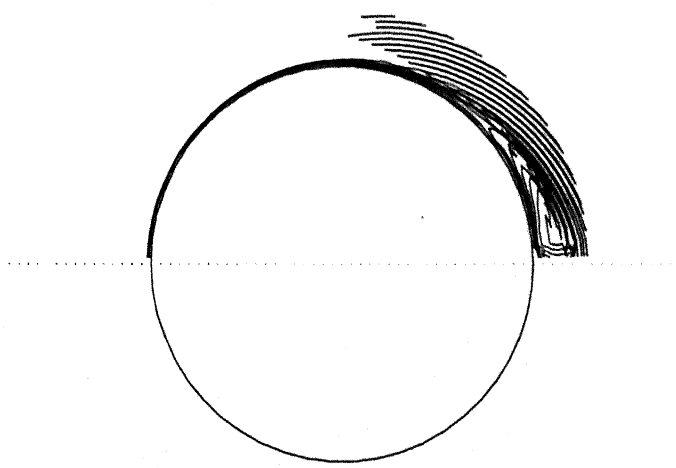

Figure 4.214

Isotherms for Re=100.0,n=0.6,and porosity 0.4 Pr=100.0(cont wall temperature)

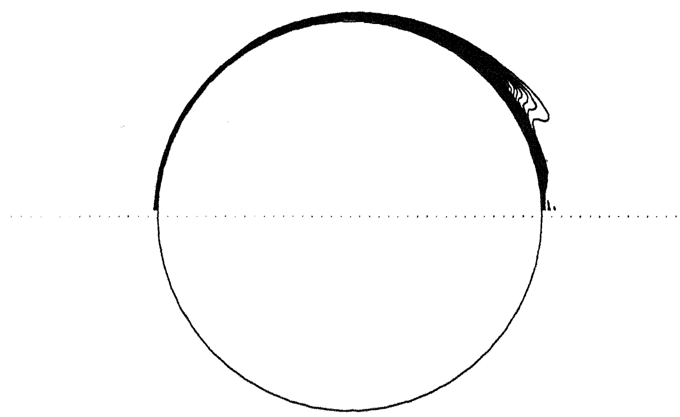

Figure 4.215

Isotherms for Re=100.0,n=0.6,and porosity 0.4 Pr=500.0(cont wall temperature)

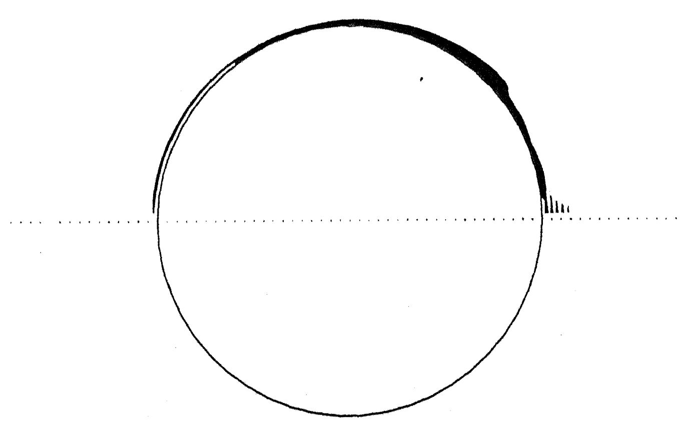

Figure 4.216

Isotherms for Re=200.0,n=0.6,and porosity 0.4 Pr=1.0(cont wall temperature)

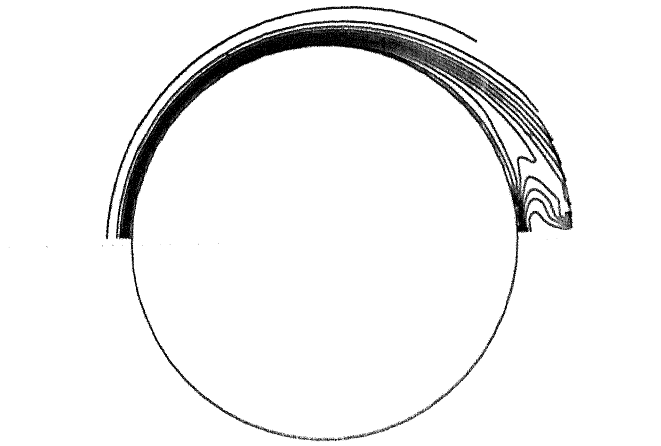

Figure 4.217

Isotherms for Re=200.0,n=0.6,and porosity 0.4 Pr=10.0(cont wall temperature)

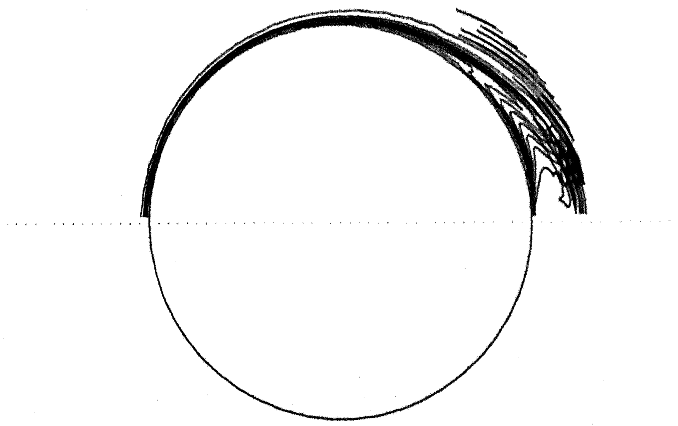

Figure 4.218

Isotherms for Re=200.0,n=0.6,and porosity 0.4 Pr=50.0(cont wall temperature)

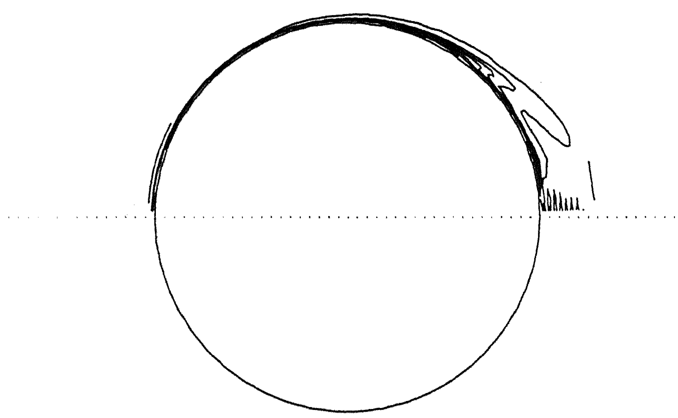

Figure 4.219

Isotherms for Re=200.0,n=0.6,and porosity 0.4 Pr=100.0(cont wall temperature)

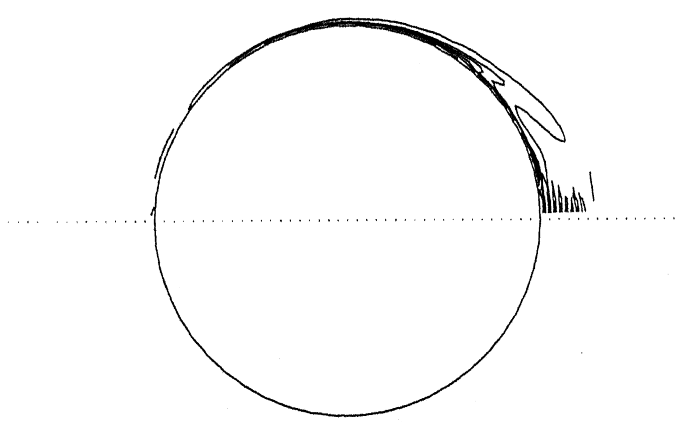

Figure 4.220

Isotherms for Re=200.0,n=0.6,and porosity 0.4 Pr=500.0(cont wall temperature)

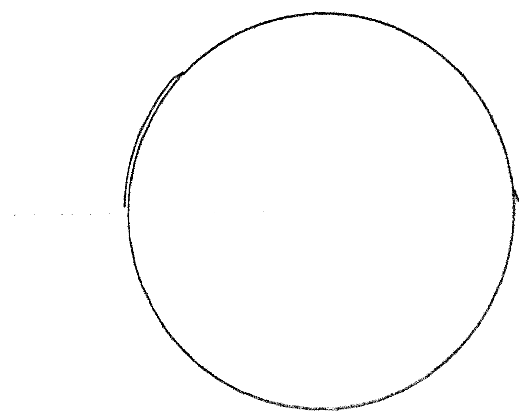

Figure 4.221

Isotherms for Re=500.0,n=0.6,and porosity 0.4 Pr=1.0(cont wall temperature)

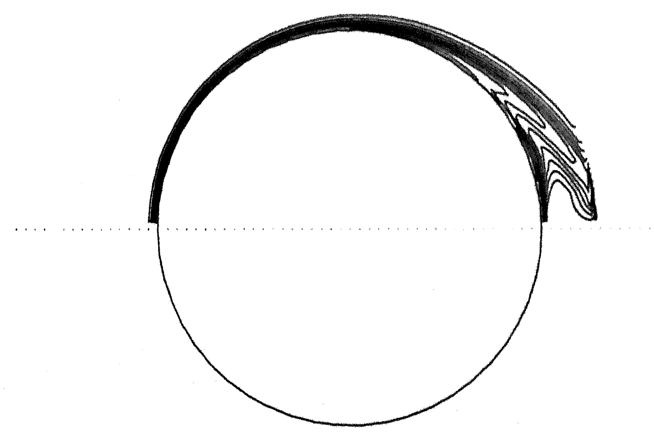

Figure 4.222

Isotherms for Re=500.0,n=0.6,and porosity 0.4 Pr=10.0(cont wall temperature)

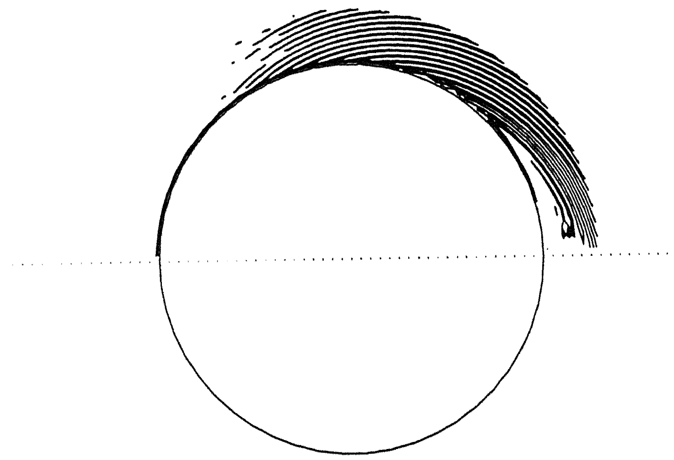

Figure 4.223

Isotherms for Re=500.0,n=0.6,and porosity 0.4 Pr=50.0(cont wall temperature)

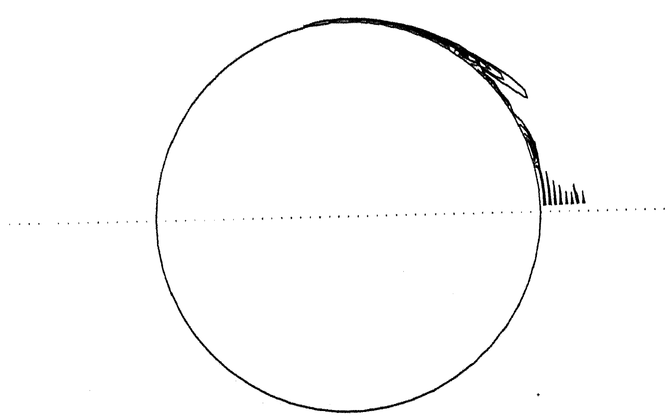

Figure 4.224

Isotherms for Re=500.0,n=0.6,and porosity 0.4 Pr=100.0(cont wall temperature)

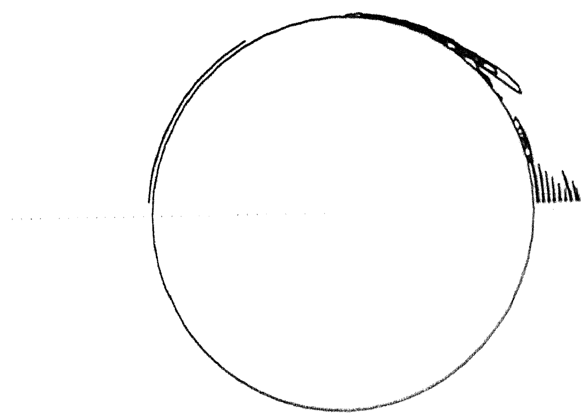

Figure 4.225

Isotherms for Re=500.0,n=0.6,and porosity 0.4 Pr=500.0(cont wall temperature)

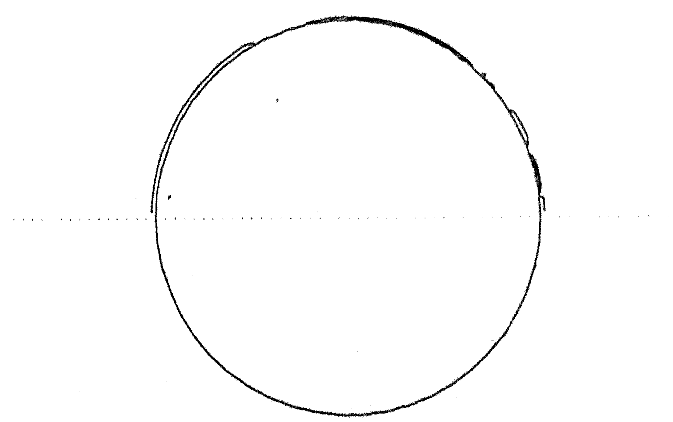

Figure 4.226

Isotherms for Re=1.0,n=0.5,and porosity 0.4 Pr=1.0(const wall temperature)

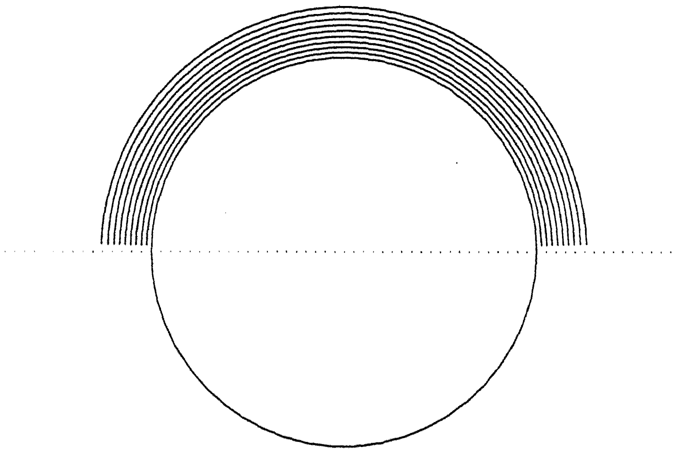

Figure 4.227

Isotherms for Re=1.0,n=0.5,and porosity 0.4 Pr=10.0(const wall temperature)

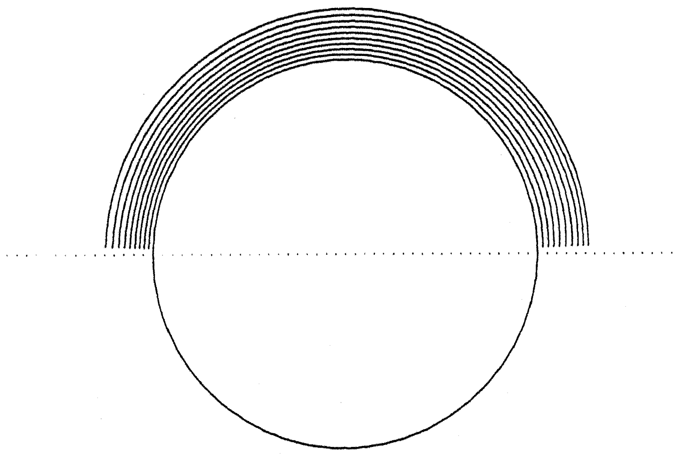

Figure 4.228

Isotherms for Re=1.0,n=0.5,and porosity 0.4 Pr=50.0(const wall temperature)

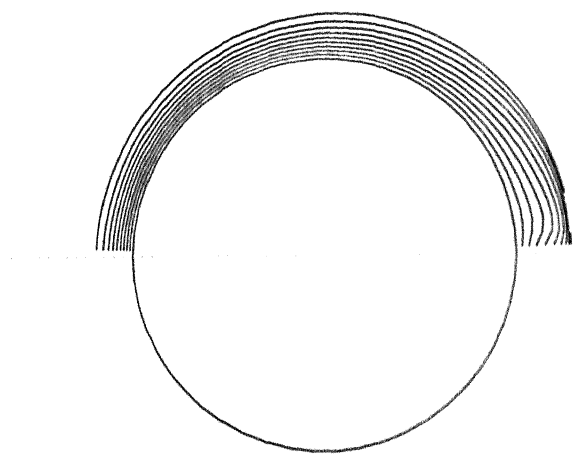

Figure 4.229

Isotherms for Re=1.0,n=0.5,and porosity 0.4 Pr=100.0(const wall temperature)

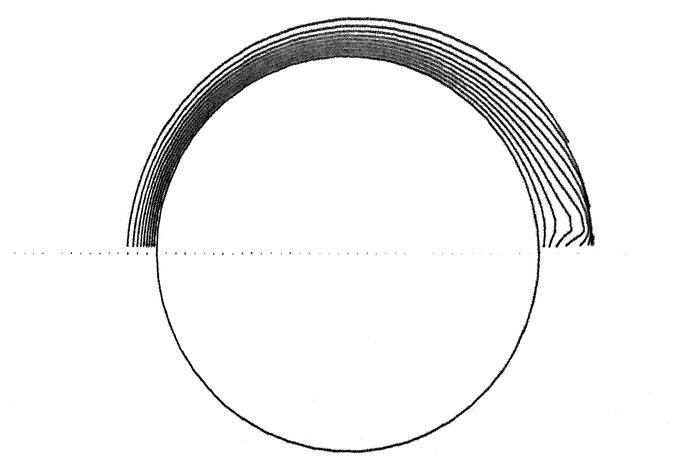

Figure 4.230

Isotherms for Re=1.0,n=0.5,and porosity 0.4 Pr=500.0(const wall temperature)

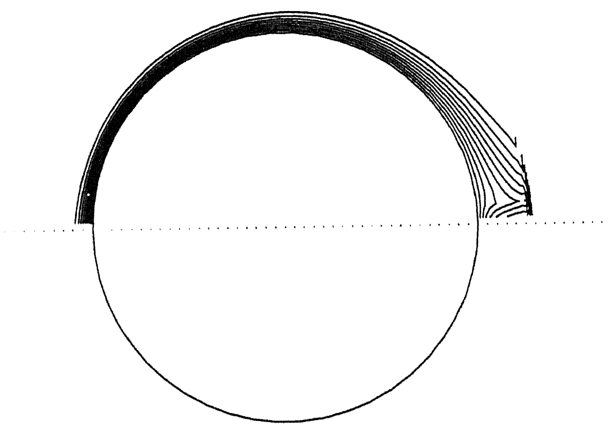

Figure 4.231

Isotherms for Re=10,n=0.5,and porosity 0.4 Pr=1.0(const wall temp)

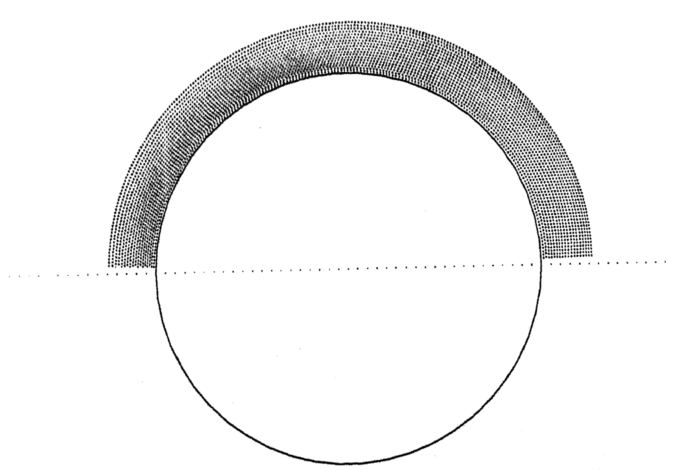

Figure 4.232

Isotherms for Re=10.0,n=0.5,and porosity 0.4 Pr=10.0(const wall temperature)

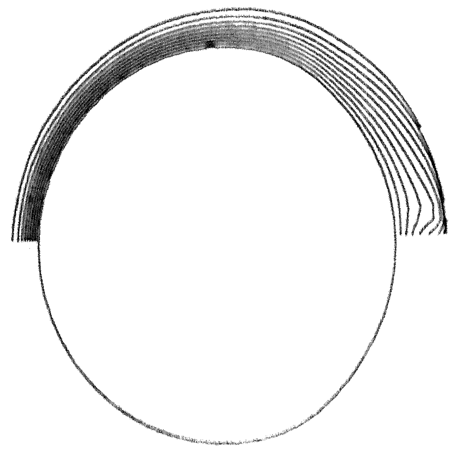

Figure 4.233

Isotherms for Re=10.0,n=0.5,and porosity 0.4 Pr=100.0(const wall temperature)

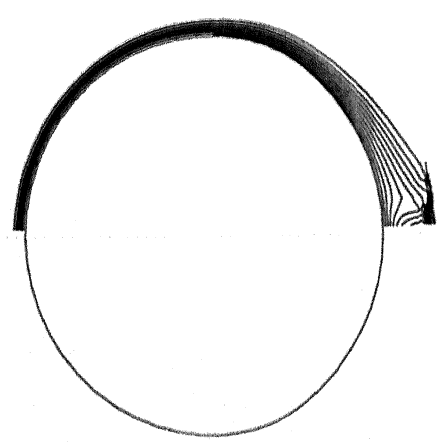

Figure 4.234

Isotherms for Re=10.0,n=0.5,and porosity 0.4 Pr=100.0(const wall temperature)

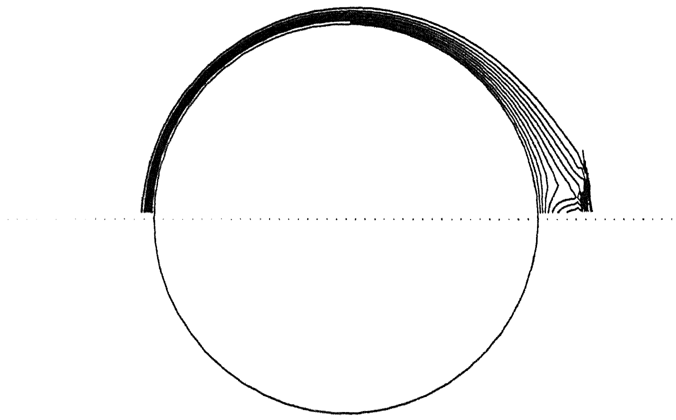

Figure 4.235

Isotherms for Re=10.0,n=0.5,and porosity 0.4 Pr=500.0(const wall temperature)

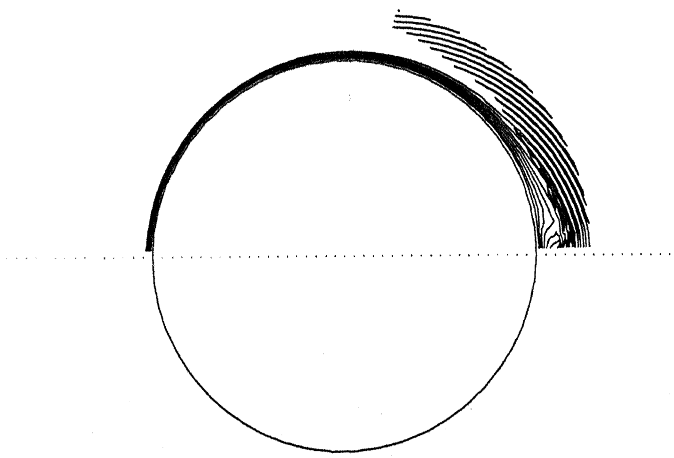

Figure 4.236

Isotherms for Re=100.0,n=0.5,and porosity 0.4 Pr=1.0(const wall temperature)

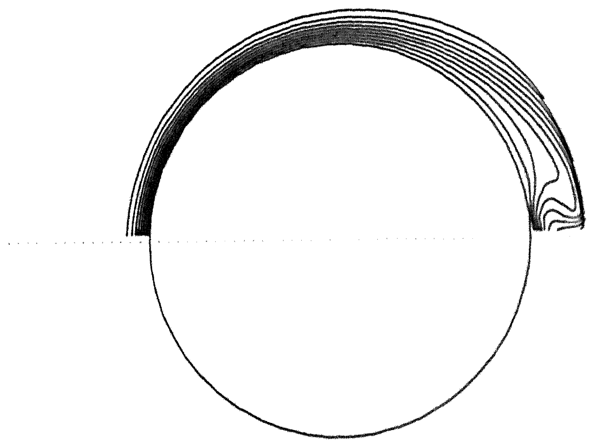

Figure 4.237

Isotherms for Re=100.0,n=0.5,and porosity 0.4 Pr=10.0(const wall temperature)

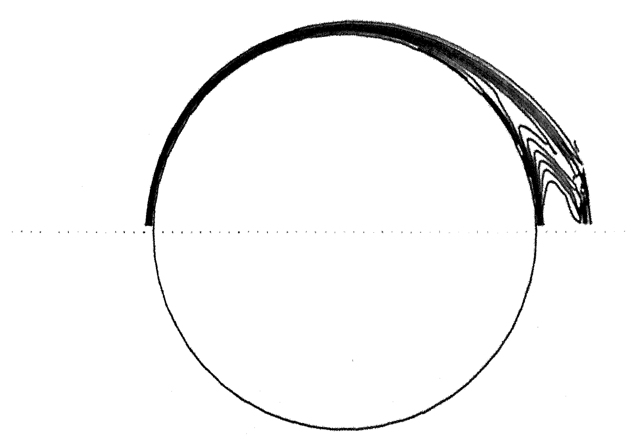

Figure 4.238

Isotherms for Re=100.0,n=0.5,and porosity 0.4 Pr=50.0(const wall temperature)

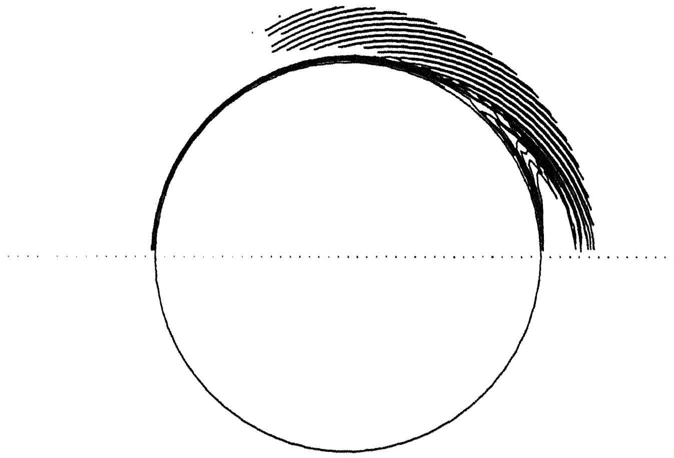

Figure 4.239

Isotherms for Re=100.0,n=0.5,and porosity 0.4 Pr=100.0(const wall temperature)

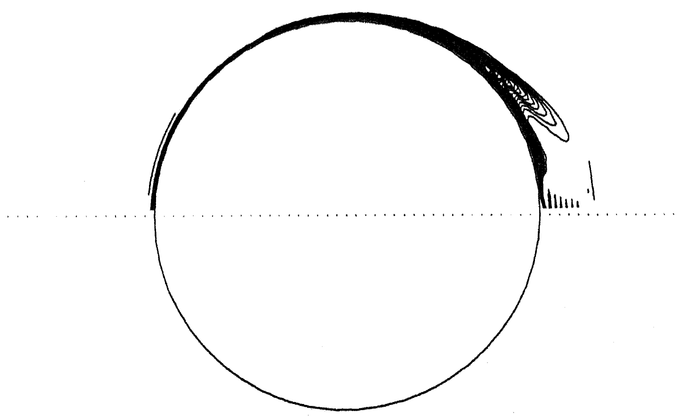

Figure 4.240

Isotherms for Re=100.0,n=0.5,and porosity 0.4 Pr=500.0(const wall temperature)

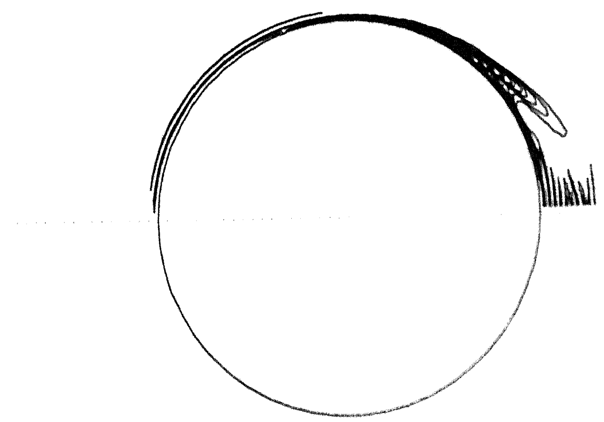

Figure 4.241

Isotherms for Re=1.0,n=0.8,and porosity 0.5 Pr=1.0(const wall temperature)

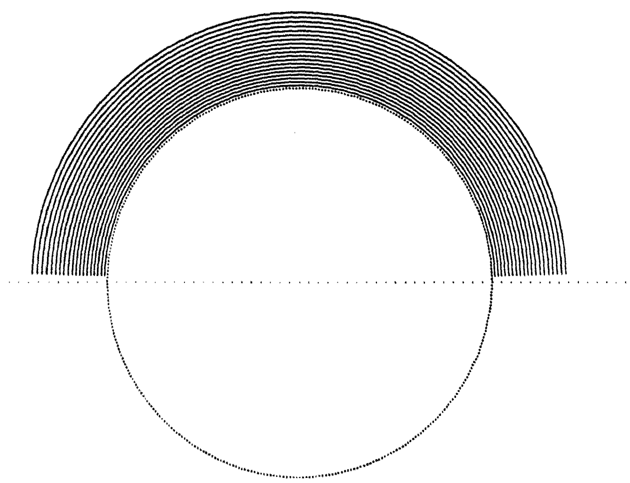

Figure 4.242

Isotherms for Re=1.0,n=0.8,and porosity 0.5 Pr=10.0(const wall temperature)

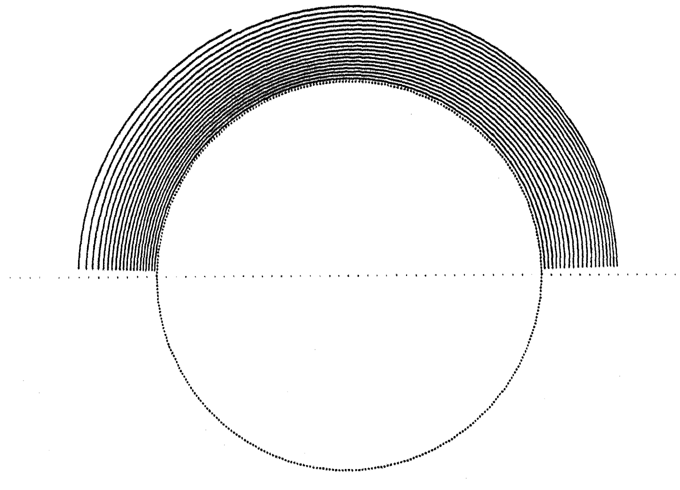

Figure 4.243

Isotherms for Re=1.0,n=0.8,and porosity 0.5 Pr=50.0(const wall temperature)

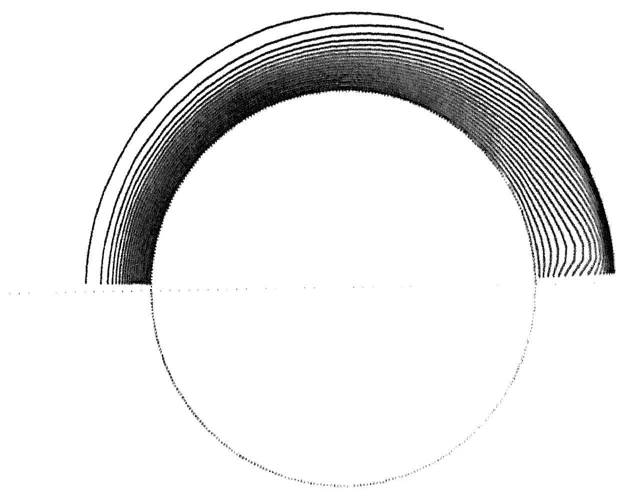

Figure 4.244

Isotherms for Re=1.0,n=0.8,and porosity 0.5 Pr=100.0(const wall temperature)

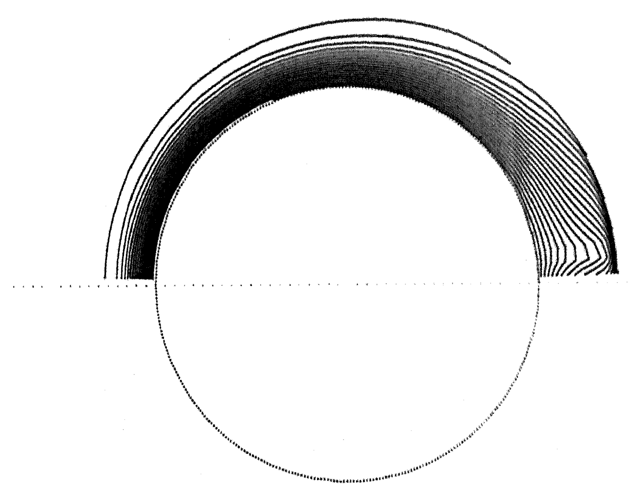

Figure 4.245

Isotherms for Re=1.0,n=0.8,and porosity 0.5 Pr=100.0(const wall temperature)

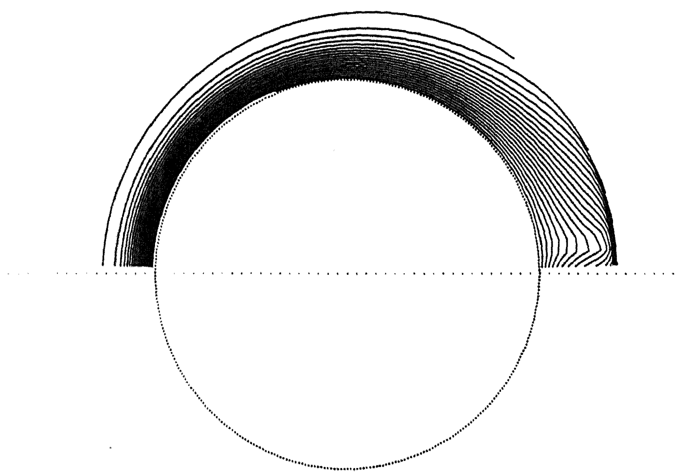

Figure 4.246

Isotherms for Re=1.0,n=0.8,and porosity 0.5 Pr=500.0(const wall temperature)

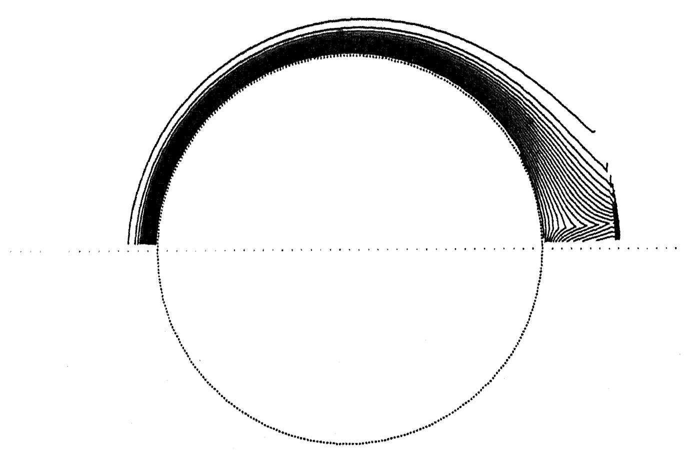

Figure 4.247

Isotherms for Re=10,n=0.8,and porosity 0.5 Pr=1.0(cont wall temp)

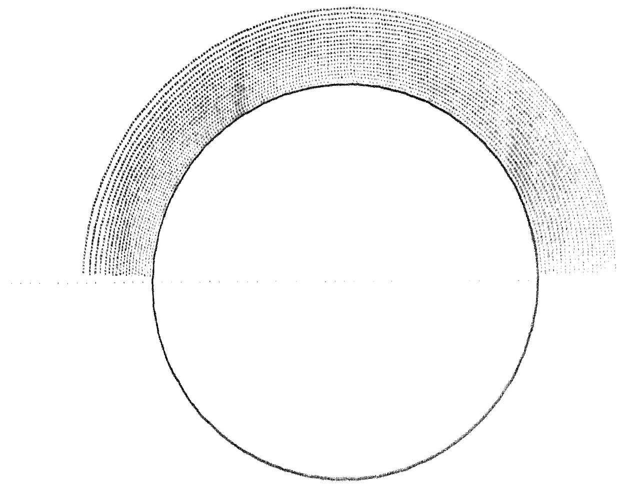

Figure 4.248

Isotherms for Re=10,n=0.8,and porosity 0.5 Pr=10.0(cont wall temp)

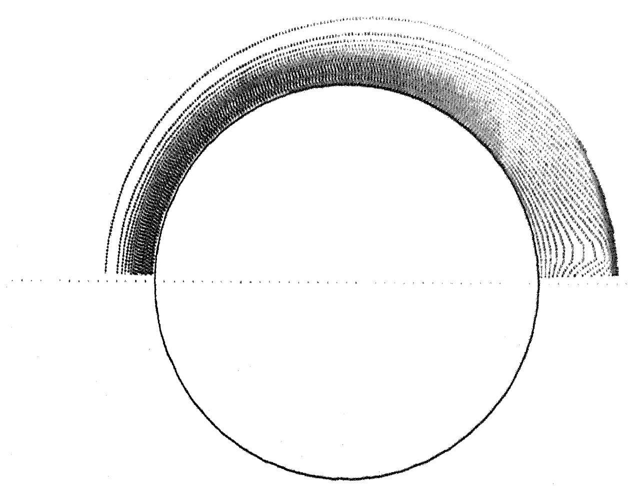

Figure 4.249

Isotherms for Re=10,n=0.8,and porosity 0.5 Pr=50.0(cont wall temp)

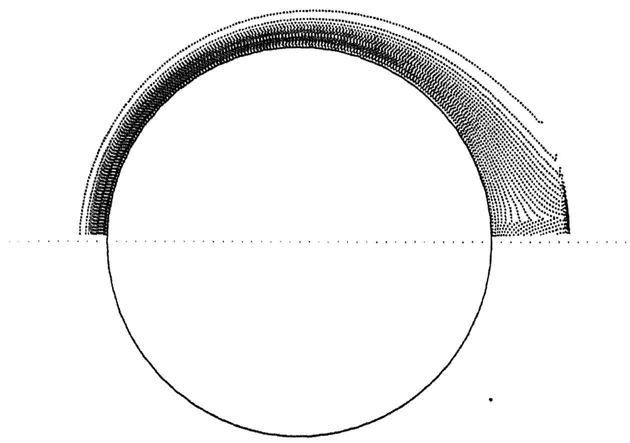

Figure 4.250

Isotherms for Re=10,n=0.8,and porosity 0.5 Pr=100.0(cont wall temp)

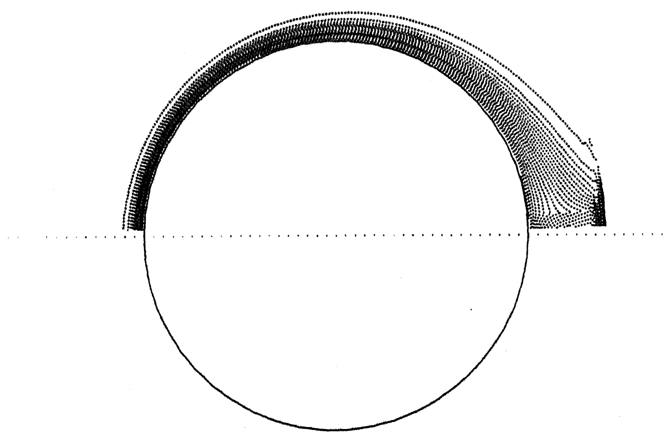

Figure 4.251

Isotherms for Re=10,n=0.8,and porosity 0.5 Pr=500.0(cont wall temp)

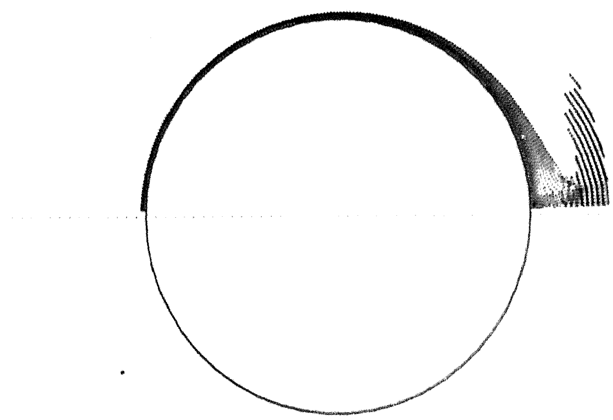

Figure 4.252

Isotherms for Re=100.0,n=0.8,and porosity 0.5 Pr=1.0(const wall temperature)

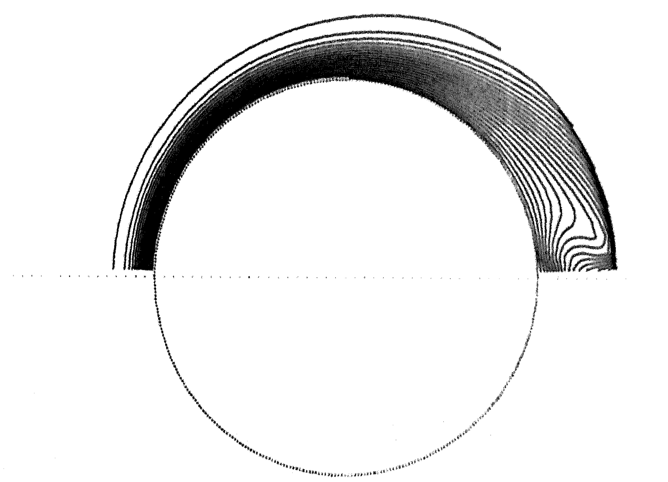

Figure 4.253

Isotherms for Re=100.0,n=0.8,and porosity 0.5 Pr=10.0(const wall temperature)

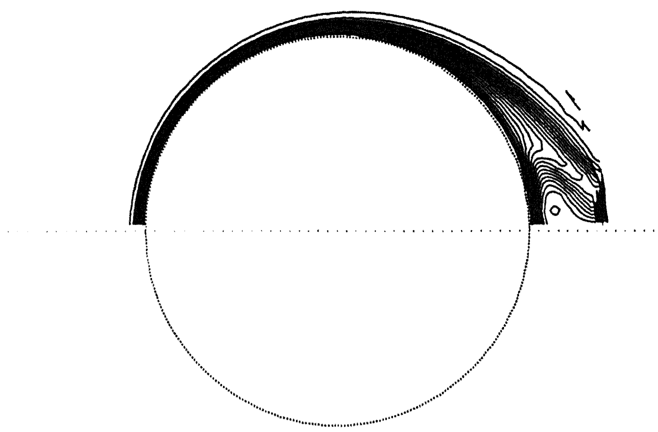

Figure 4.254

Isotherms for Re=100.0,n=0.8,and porosity 0.5 Pr=10.0(const wall temperature)

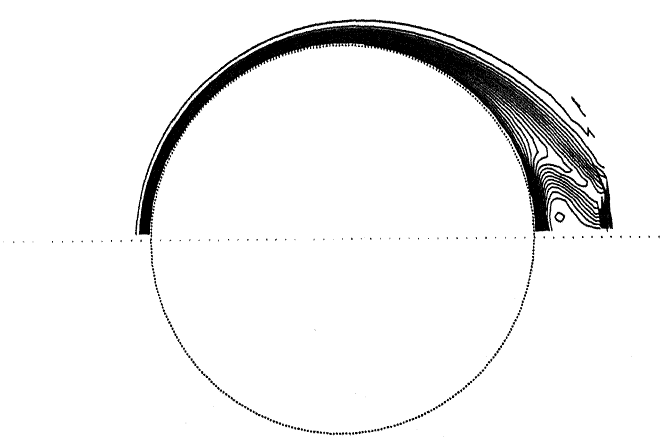

Figure 4.255

Isotherms for Re=100.0,n=0.8,and porosity 0.5 Pr=100.0(const wall temperature)

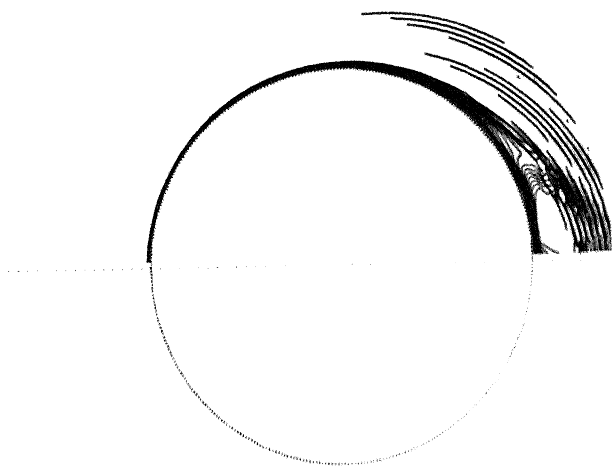

Figure 4.256

Isotherms for Re=100.0,n=0.8,and porosity 0.5 Pr=100.0(const wall temperature)

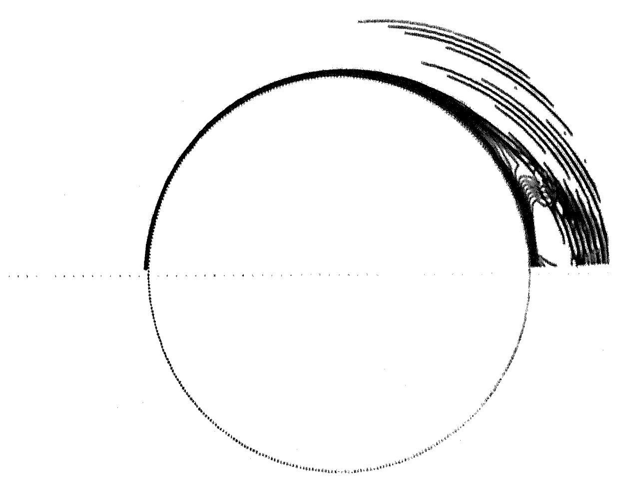

Figure 4.257

Isotherms for Re=200,n=0.8,and porosity 0.5 Pr=1.0(cont wall temp)

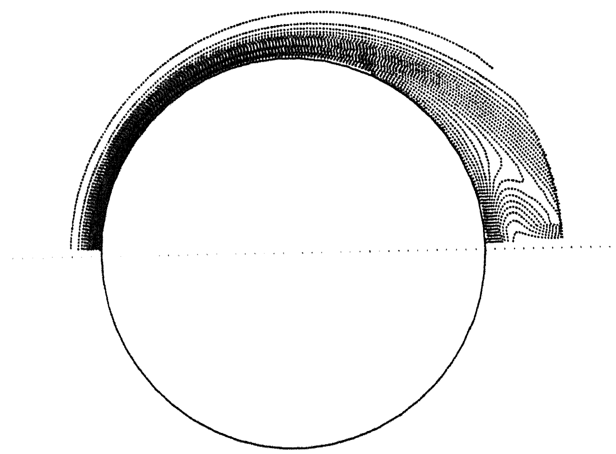

Figure 4.258

Isotherms for Re=200,n=0.8,and porosity 0.5 Pr=10.0(cont wall temp)

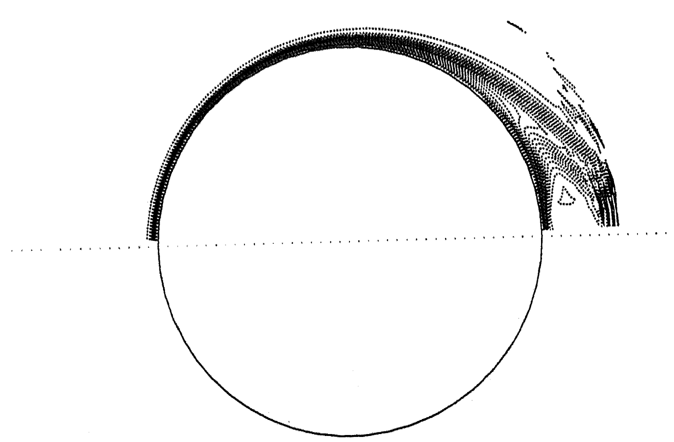

Figure 4.259

Isotherms for Re=200,n=0.8,and porosity 0.5 Pr=50.0(cont wall temp)

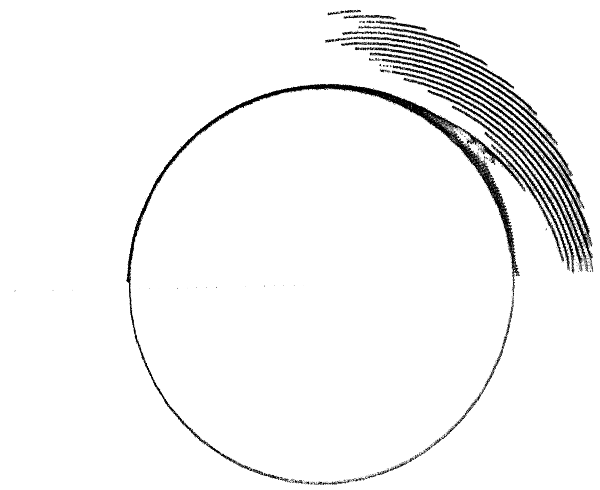

Figure 4.260

Isotherms for Re=200,n=0.8,and porosity 0.5 Pr=100.0(cont wall temp)

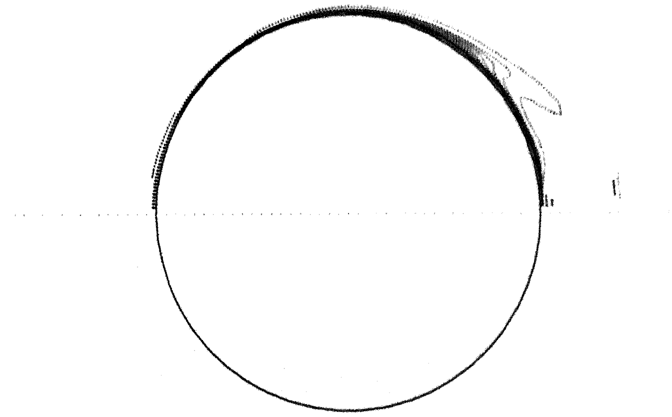

Figure 4.261

Isotherms for Re=200,n=0.8,and porosity 0.5 Pr=500.0(cont wall temp)

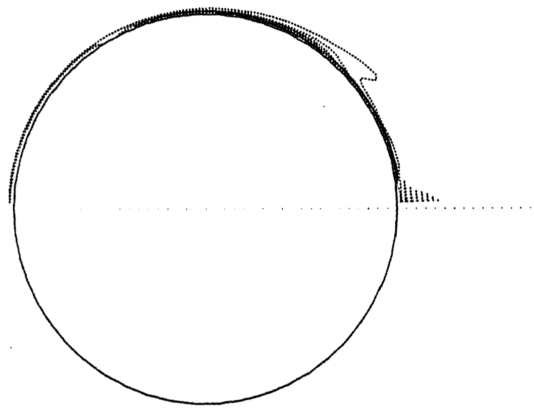

Figure 4.262

Isotherms for Re=500,n=0.8,and porosity 0.5 Pr=1.0(cont wall temp)

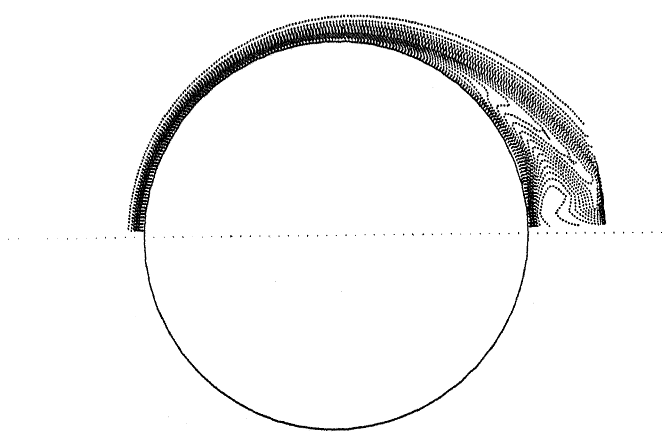

Figure 4.263

Isotherms for Re=500,n=0.8,and porosity 0.5 Pr=10.0(cont wall temp)

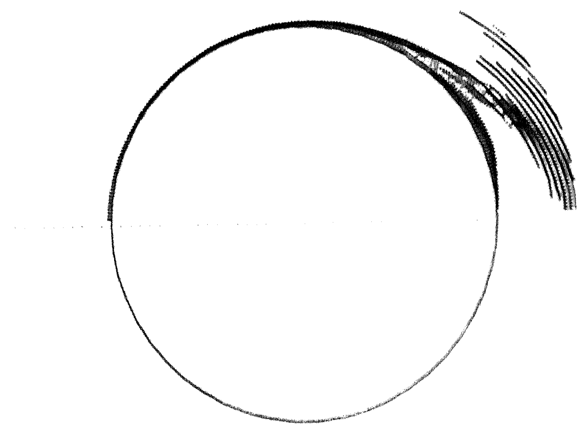

Figure 4.264

Isotherms for Re=500,n=0.8,and porosity 0.5 Pr=50.0(cont wall temp)

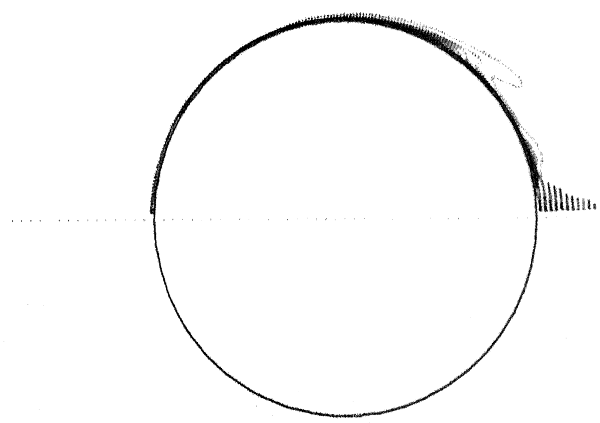

Figure 4.265

Isotherms for Re=500,n=0.8,and porosity 0.5 Pr=100.0(cont wall temp)

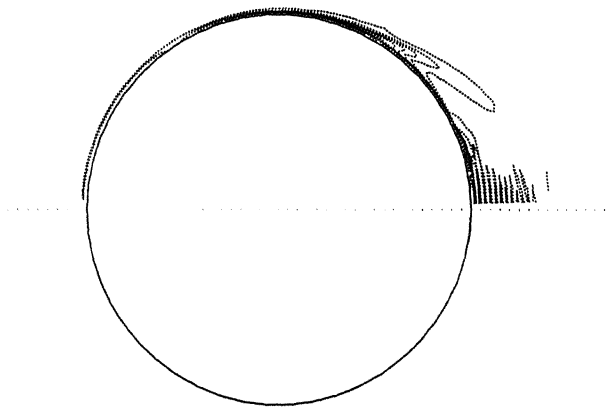

Figure 4.266

Isotherms for Re=1.0,n=0.6,and porosity 0.5 Pr=1.0(const wall temperature)

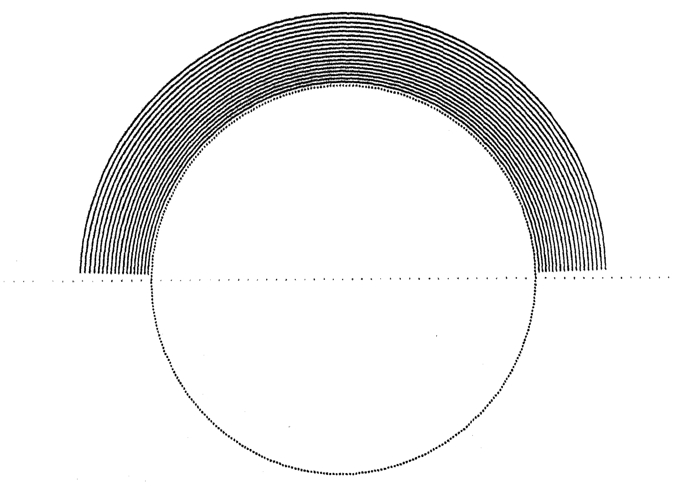

Figure 4.267

Isotherms for Re=1.0,n=0.6,and porosity 0.5 Pr=10.0(const wall temperature)

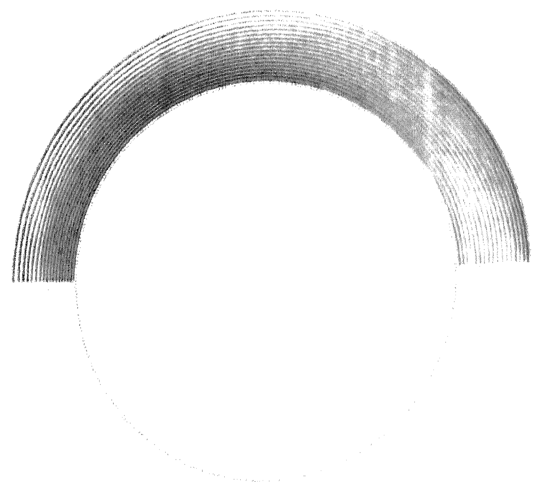

Figure 4.268

Isotherms for Re=1.0,n=0.6,and porosity 0.5 Pr=50.0(const wall temperature)

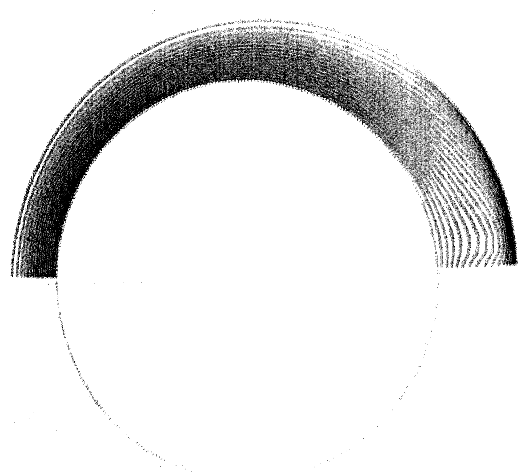

Figure 4.269

Isotherms for Re=1.0,n=0.6,and porosity 0.5 Pr=100.0(const wall temperature)

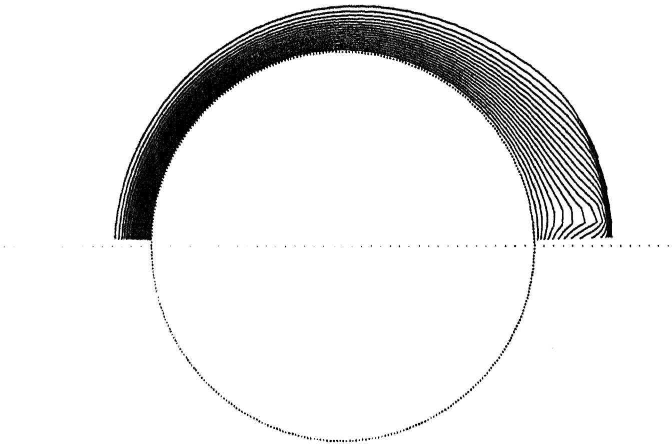

Figure 4.270

Isotherms for Re=1.0,n=0.6,and porosity 0.5 Pr=500.0(const wall temperature)

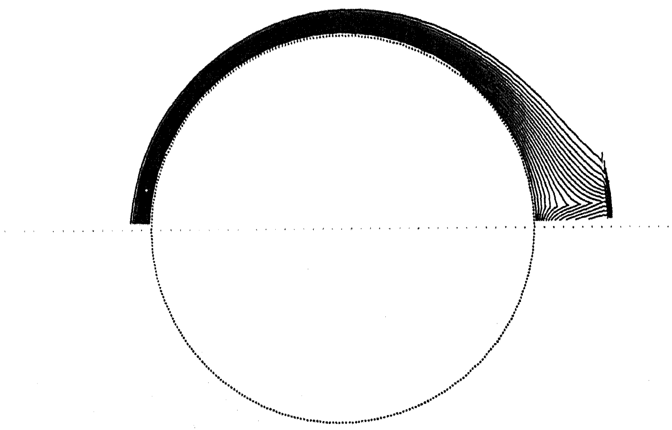

Figure 4.271

Isotherms for Re=10.0,n=0.6,and porosity 0.5 Pr=1.0(const wall temperature)

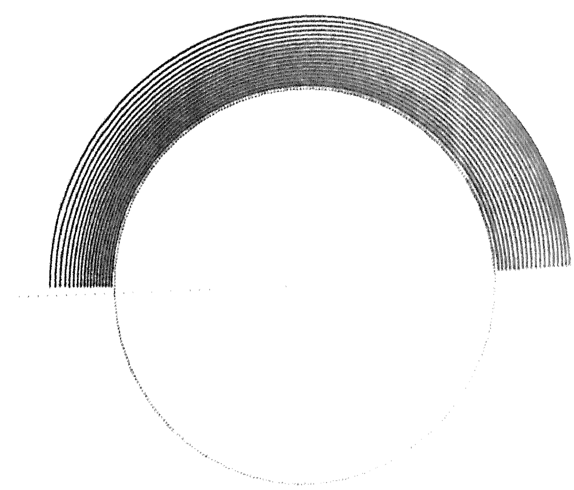

Figure 4.272

Isotherms for Re=10.0,n=0.6,and porosity 0.5 Pr=10.0(const wall temperature)

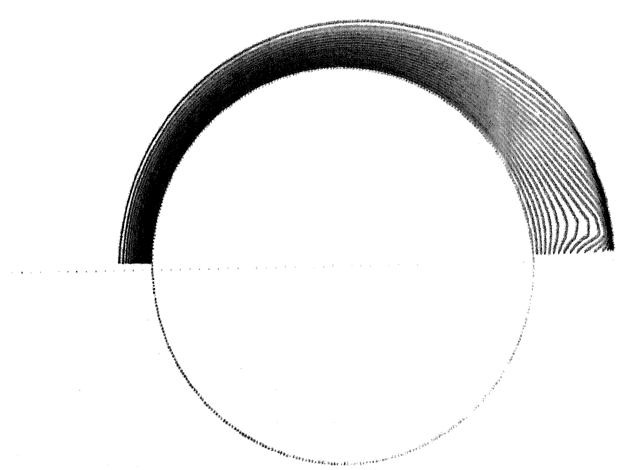

Figure 4.273

Isotherms for Re=10.0,n=0.6,and porosity 0.5 Pr=50.0(const wall temperature)

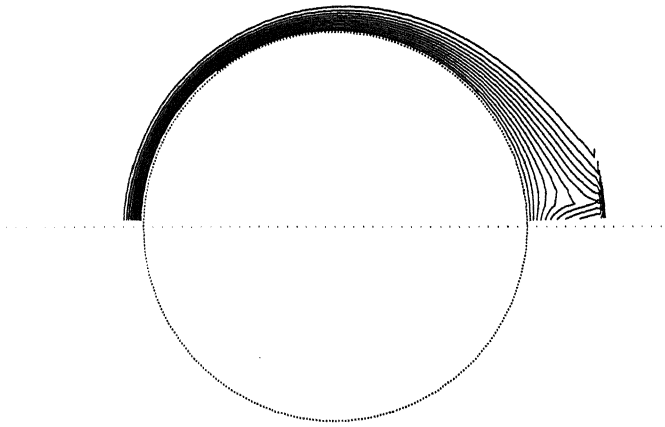

Figure 4.274

Isotherms for Re=10.0,n=0.6,and porosity 0.5 Pr=100.0(const wall temperature)

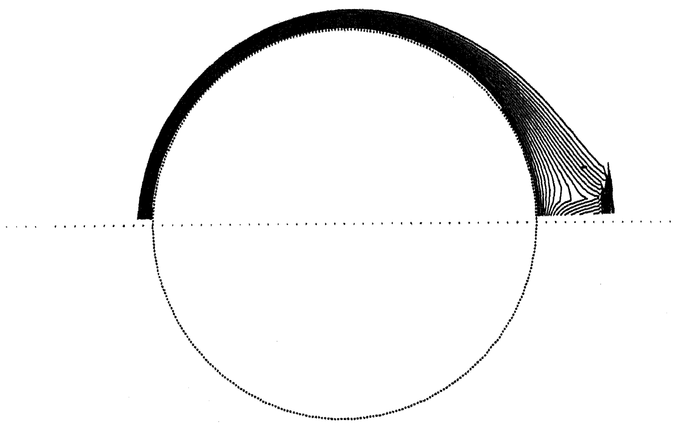

Figure 4.275

Isotherms for Re=10.0,n=0.6,and porosity 0.5 Pr=500.0(const wall temperature)

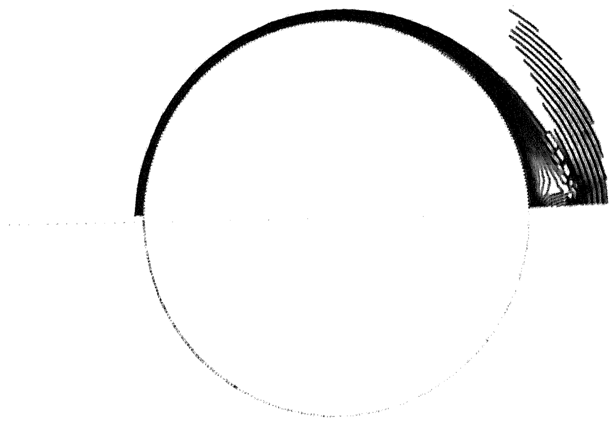

Figure 4.276

Isotherms for Re=100.0,n=0.6,and porosity 0.5 Pr=1.0(const wall temperature)

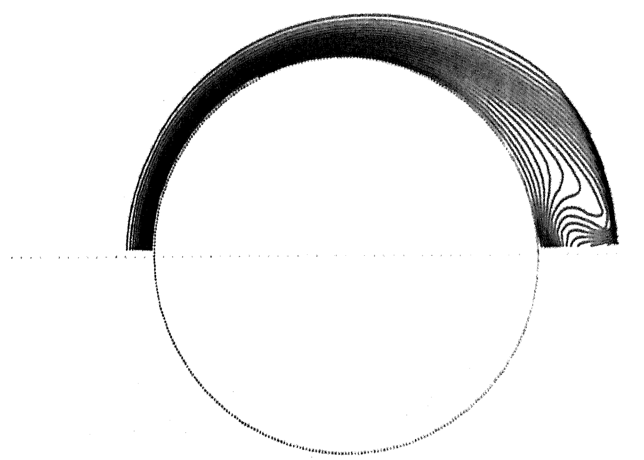

Figure 4.277

Isotherms for Re=100.0,n=0.6,and porosity 0.5 Pr=10.0(const wall temperature)

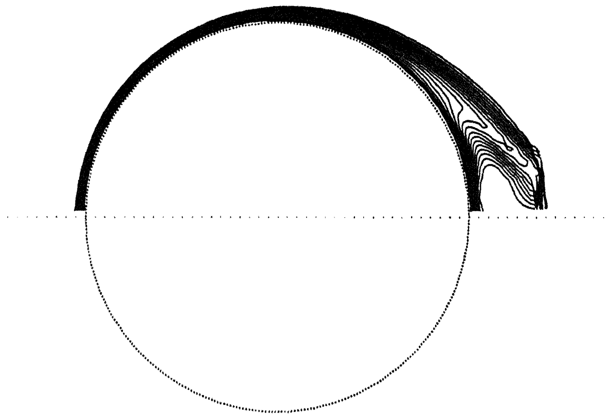

Figure 4.278

Isotherms for Re=100.0,n=0.6,and porosity 0.5 Pr=100.0(const wall temperature)

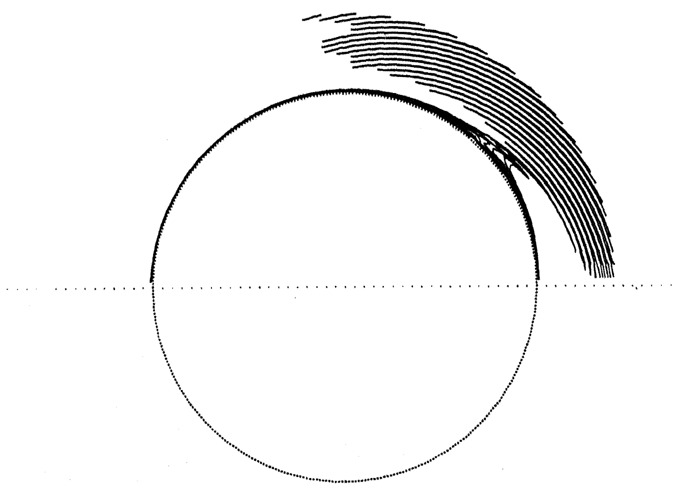

Figure 4.279

Isotherms for Re=100.0,n=0.6,and porosity 0.5 Pr=500.0(const wall temperature)

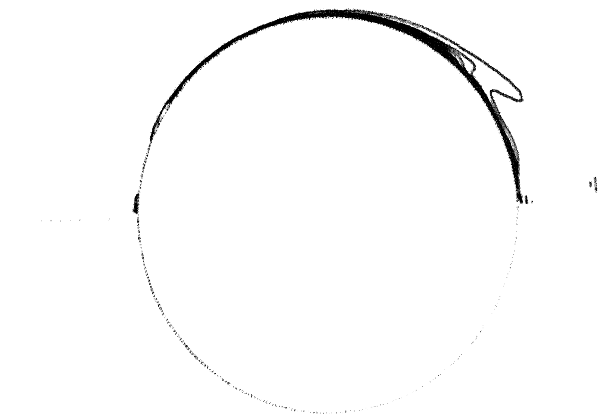

Figure 4.280

Isotherms for Re=200,n=0.6,and porosity 0.5 Pr=1.0(cont wall temp)

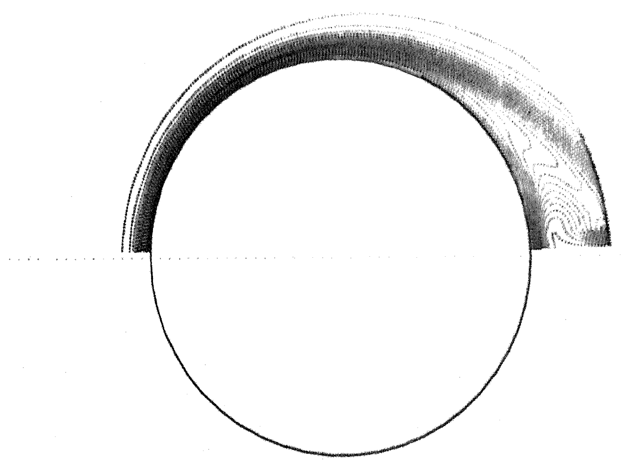

Figure 4.281

Isotherms for Re=200,n=0.6,and porosity 0.5 Pr=10.0(cont wall temp)

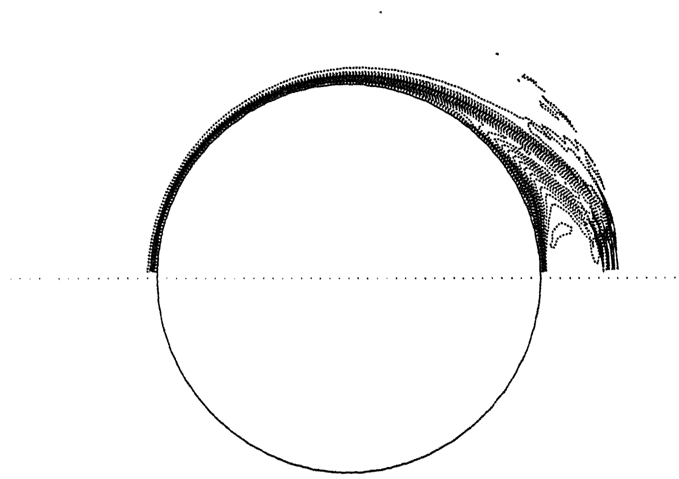

Figure 4.282

Isotherms for Re=200,n=0.6,and porosity 0.5 Pr=50.0(cont wall temp)

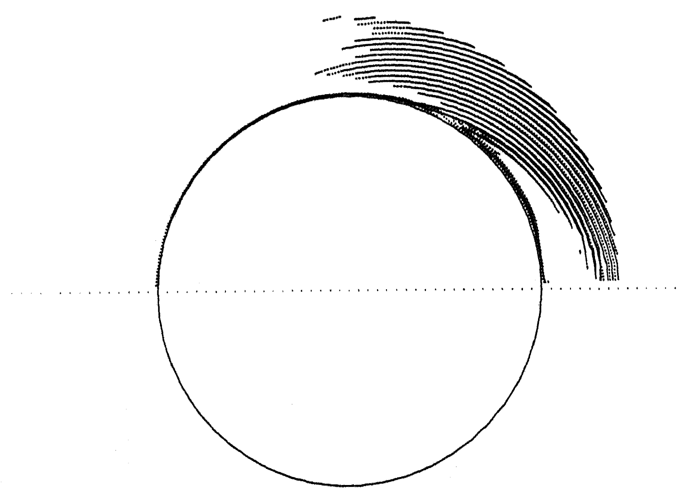

Figure 4.283

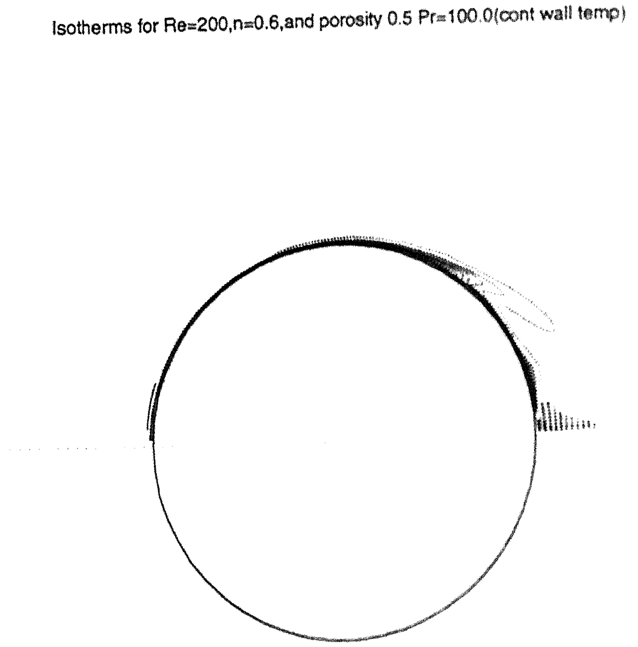

Figure 4.284

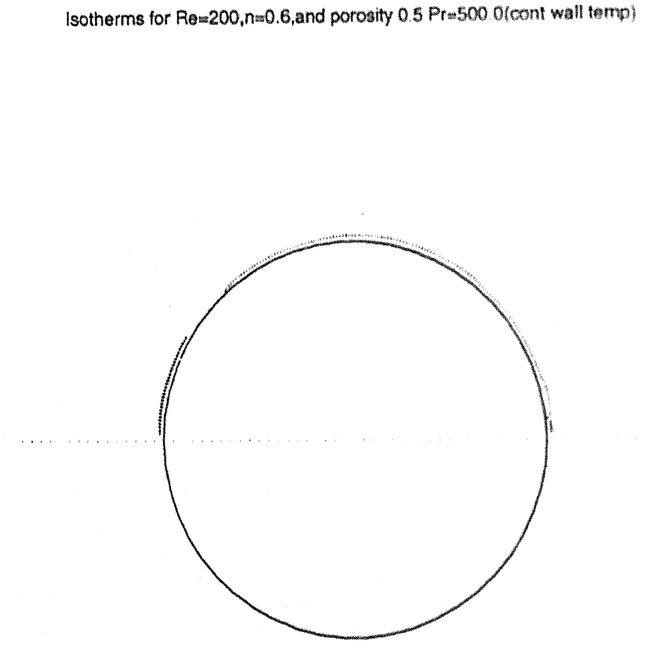

Figure 4.285

Isotherms for Re=500,n=0.6,and porosity 0.5 Pr=1.0(cont wall temp)

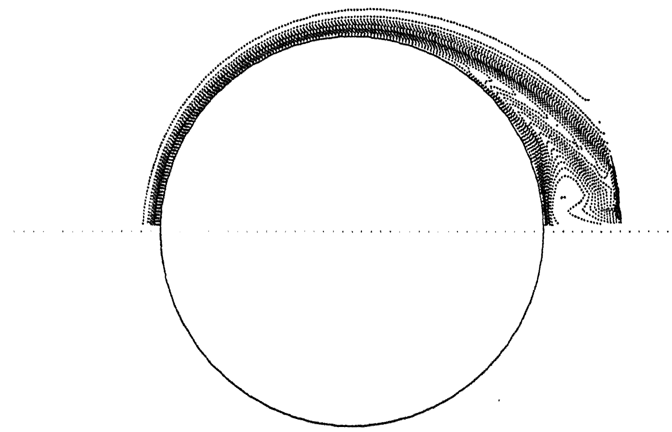

Figure 4.285

Isotherms for Re=500,n=0.6,and porosity 0.5 Pr=10.0(cont wall temp)

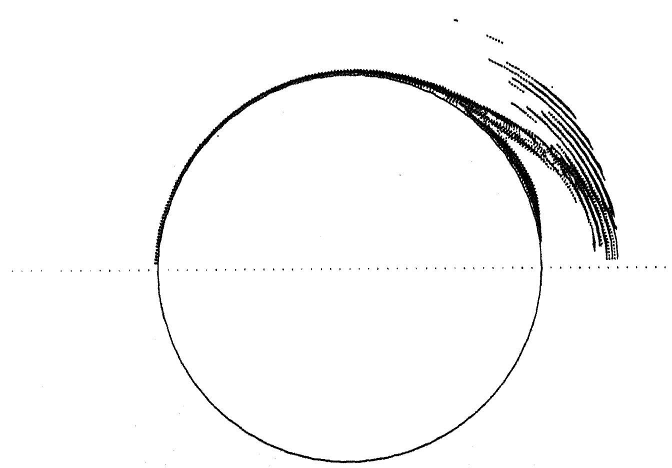

Figure 4.286

Isotherms for Re=500,n=0.6,and porosity 0.5 Pr=50.0(cont wall temp)

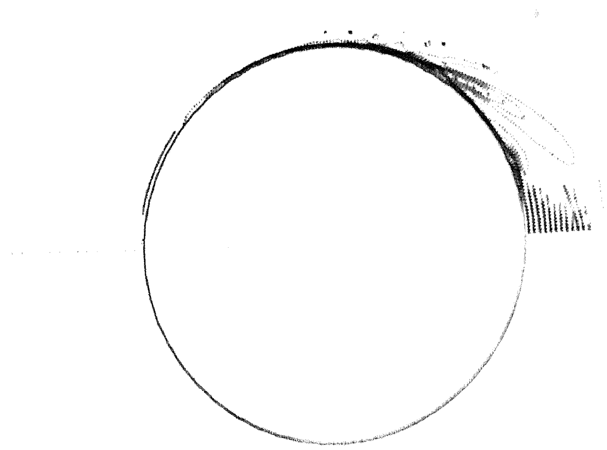

Figure 4.287

Isotherms for Re=500,n=0.6,and porosity 0.5 Pr=100.0(cont wall temp)

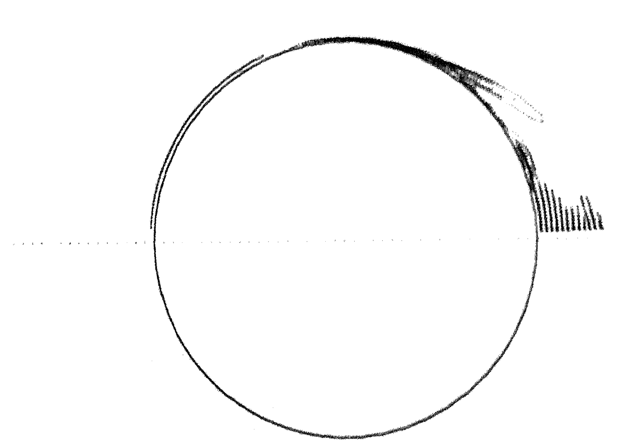

Figure 4.288

Isotherms for Re=1.0,n=0.5,and porosity 0.5 Pr=1.0(const wall temperature)

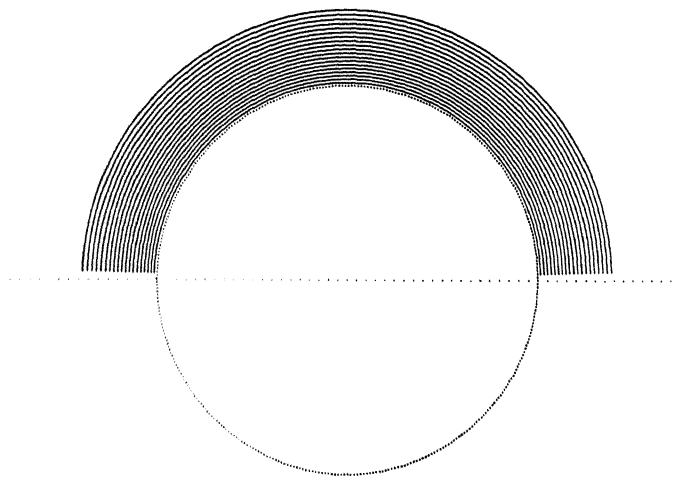

Figure 4.289

Isotherms for Re=1.0,n=0.5,and porosity 0.5 Pr=10.0(const wall temperature)

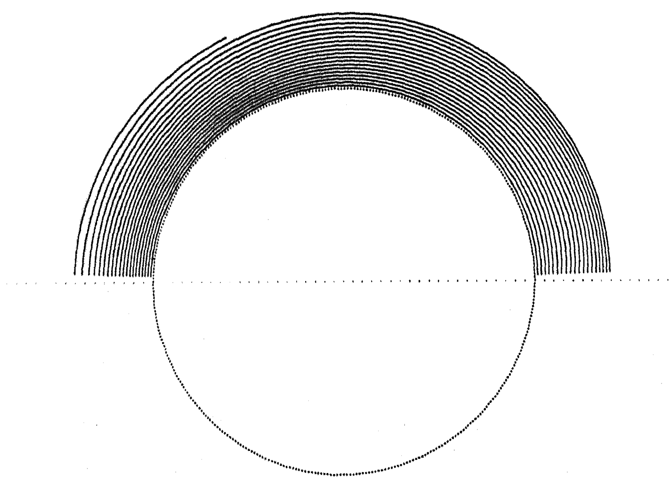

Figure 4.290

Isotherms for Re=1.0,n=0.5,and porosity 0.5 Pr=50.0(const wall temperature)

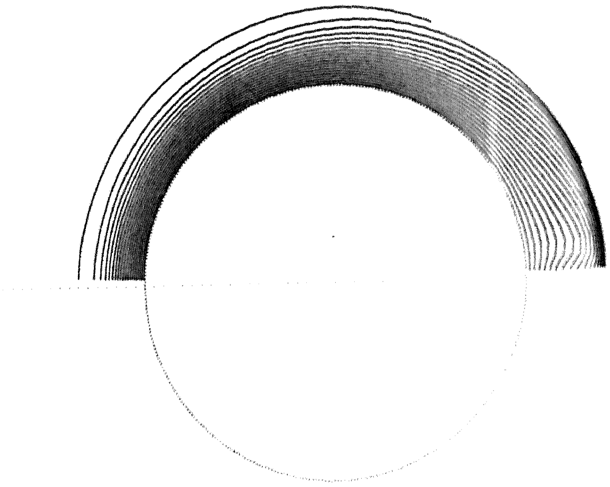

Figure 4.291

Isotherms for Re=1.0,n=0.5,and porosity 0.5 Pr=100.0(const wall temperature)

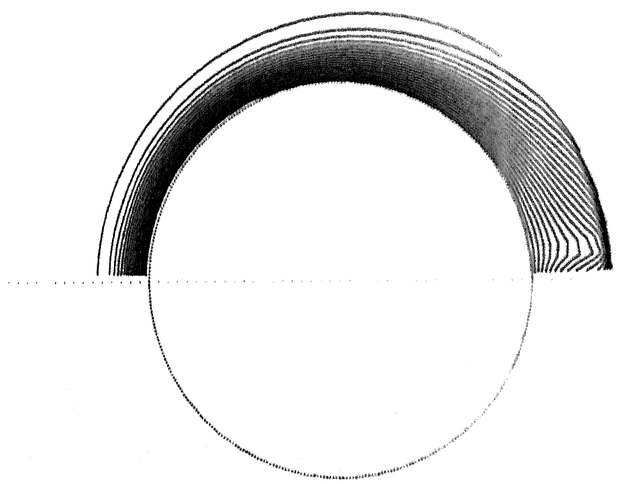

Figure 4.292

Isotherms for Re=1.0,n=0.5,and porosity 0.5 Pr=500.0(const wall temperature)

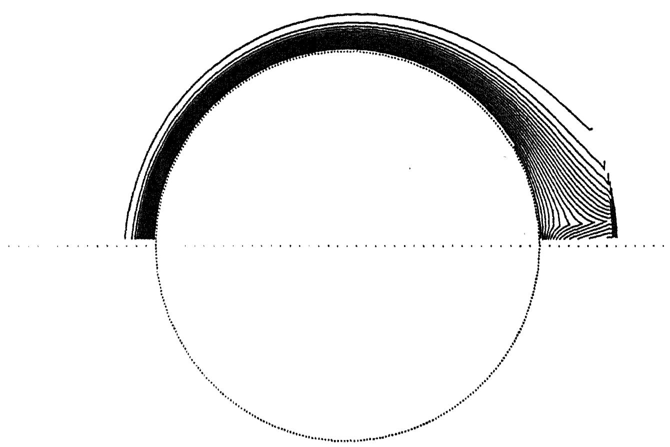

Figure 4.293

Isotherms for Re=10,n=0.5,and porosity 0.5 Pr=1.0(cont wall temp)

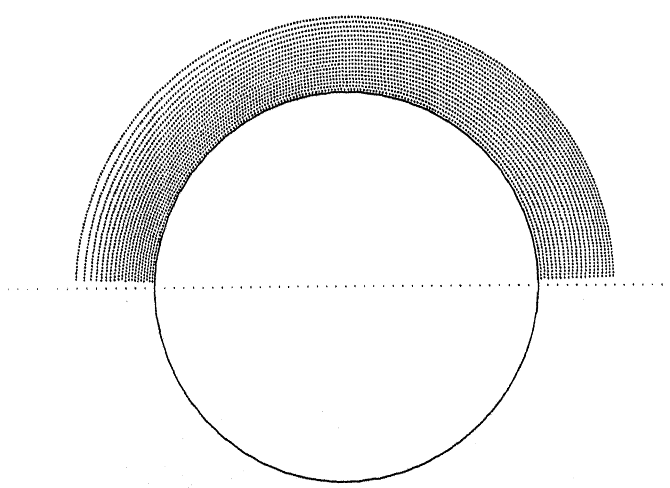

Figure 4.294

Isotherms for Re=10,n=0.5,and porosity 0.5 Pr=10.0(cont wall temp)

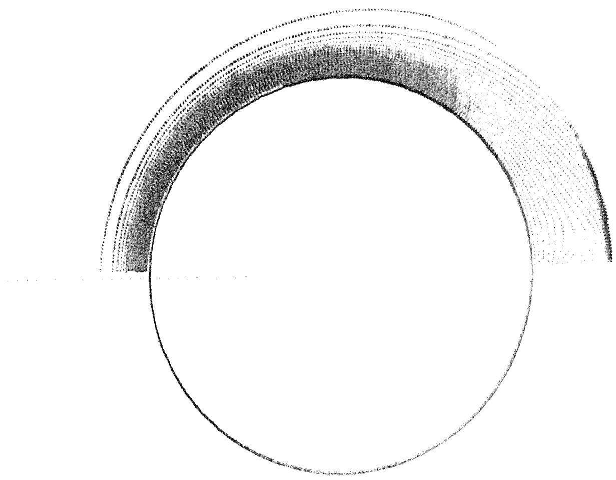

Figure 4.295

Isotherms for Re=10,n=0.5,and porosity 0.5 Pr=50.0(cont wall temp)

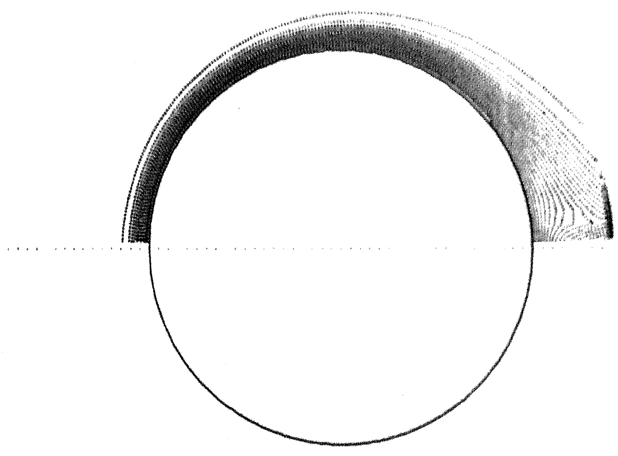

Figure 4.296

Isotherms for Re=10,n=0.5,and porosity 0.5 Pr=100.0(cont wall temp)

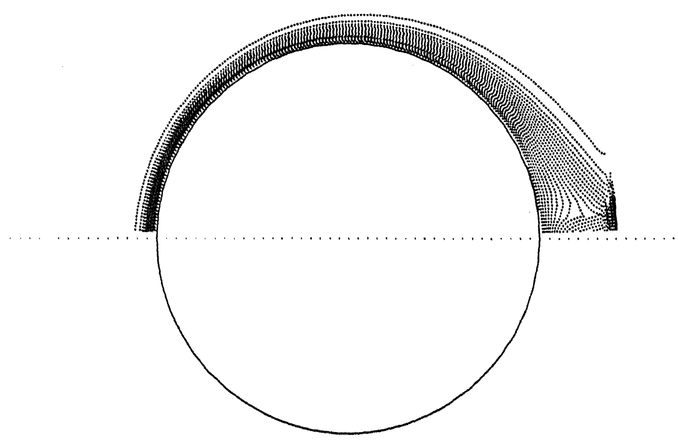

Figure 4.297

Isotherms for Re=10,n=0.5,and porosity 0.5 Pr=500.0(cont wall temp)

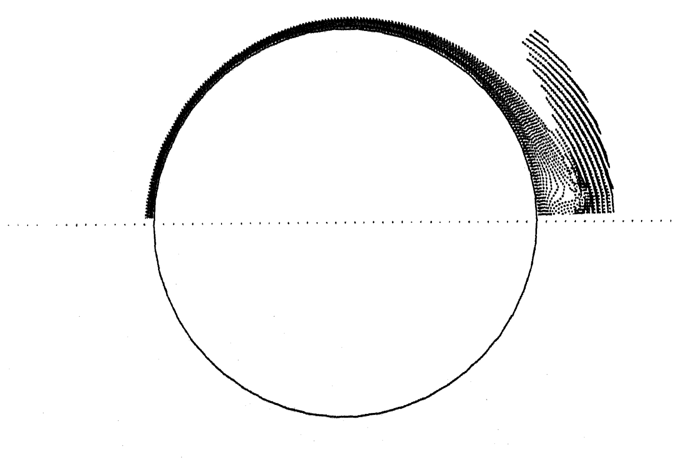

Figure 4.298

Isotherms for Re=100,n=0.5,and porosity 0.5 Pr=1.0(cont wall temp)

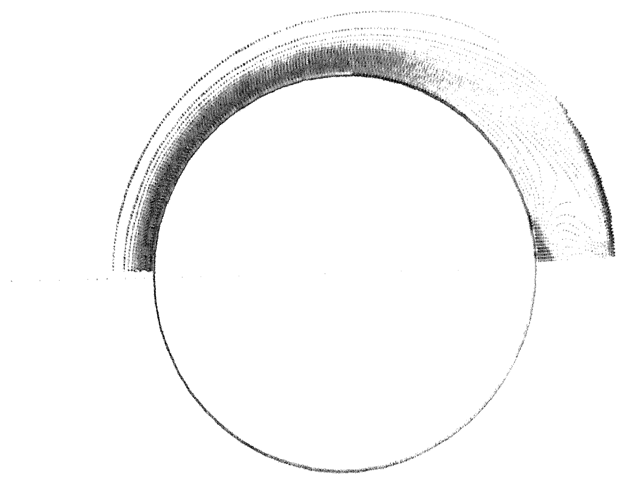

Figure 4.299

Isotherms for Re=100,n=0.5,and porosity 0.5 Pr=10.0(cont wall temp)

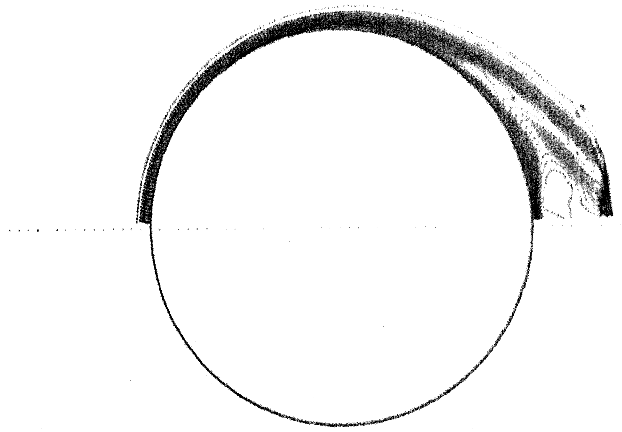

Figure 4.300

Isotherms for Re=100,n=0.5,and porosity 0.5 Pr=50.0(cont wall temp)

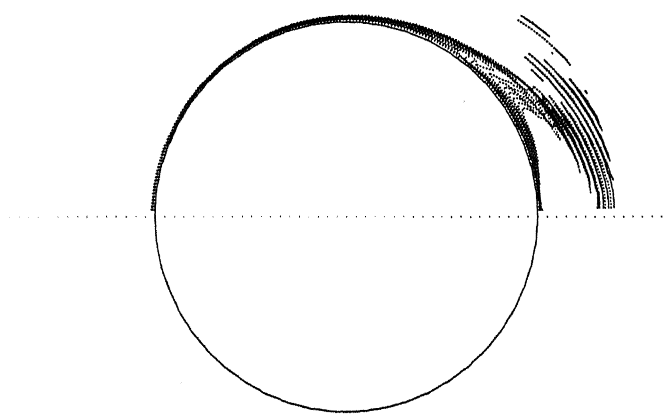

Figure 4.301

Isotherms for Re=100,n=0.5,and porosity 0.5 Pr=100.0(cont wall temp)

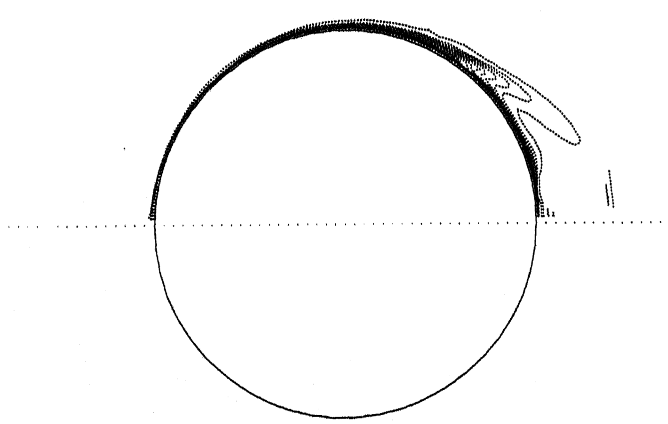

Figure 4.302

Isotherms for Re=100,n=0.5,and porosity 0.5 Pr=500.0(cont wall temp)

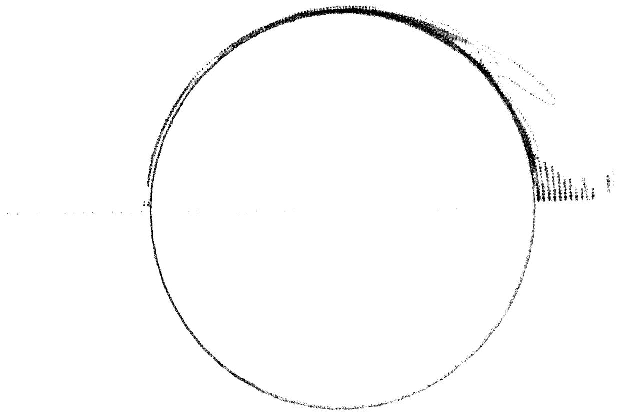

Figure 4.303

Isotherms for Re=200.0,n=0.5,and porosity 0.5 Pr=1.0(const wall temperature)

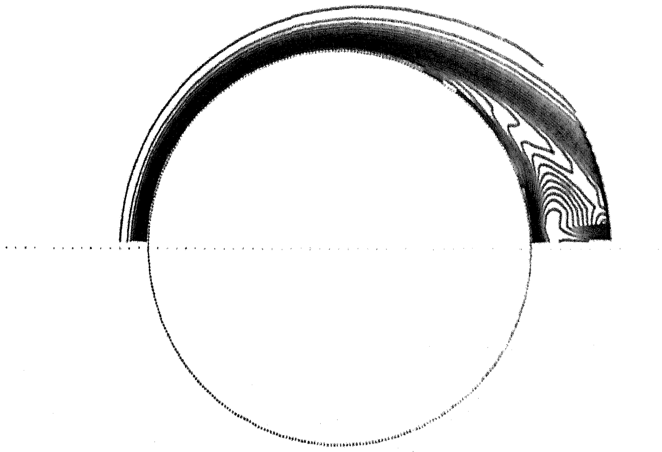

Figure 4.304

Isotherms for Re=200.0,n=0.5,and porosity 0.5 Pr=10.0(const wall temperature)

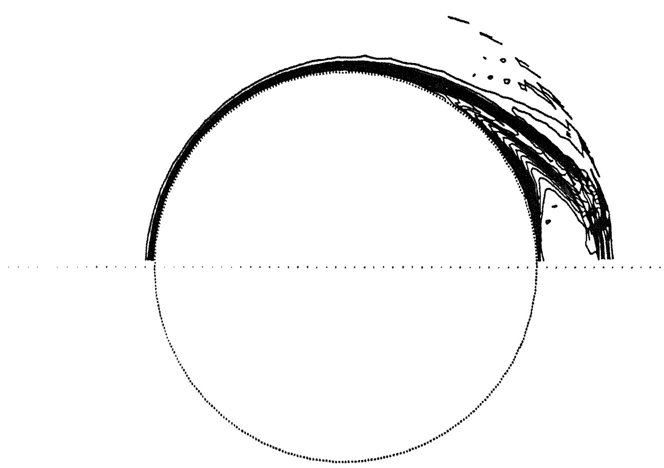

Figure 4.305

Isotherms for Re=200.0,n=0.5,and porosity 0.5 Pr=50.0(const wall temperature)

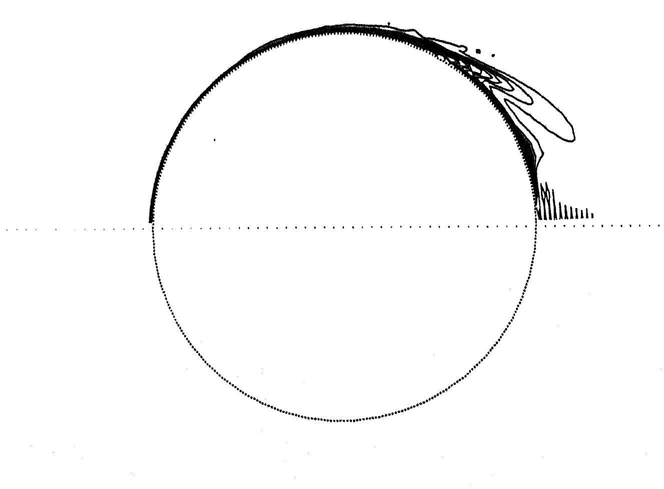

Figure 4.306

Isotherms for Re=200.0,n=0.5,and porosity 0.5 Pr=100.0(const wall temperature)

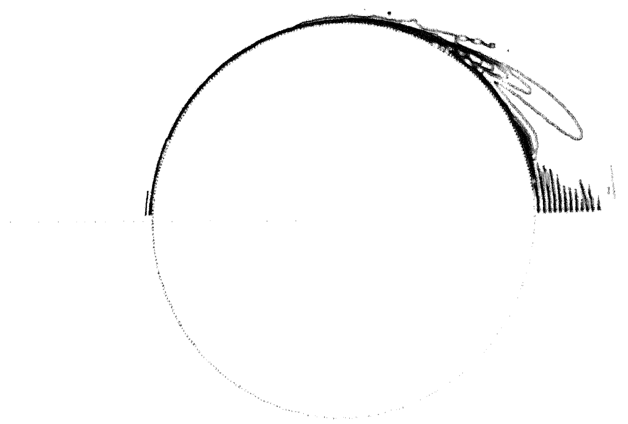

Figure 4.307

Isotherms for Re=200.0,n=0.5,and porosity 0.5 Pr=500.0(const wall temperature)

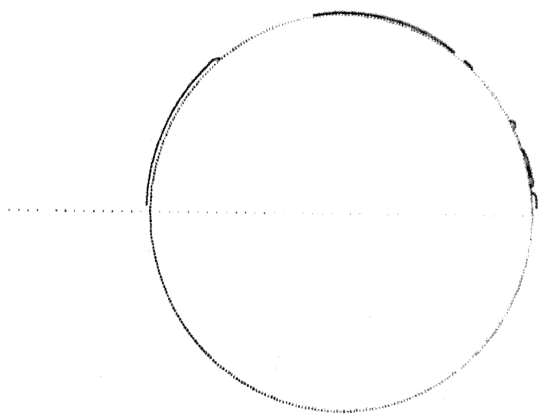

Figure 4.308

Isotherms for Re=500,n=0.5,and porosity 0.5 Pr=1.0(cont wall temp)

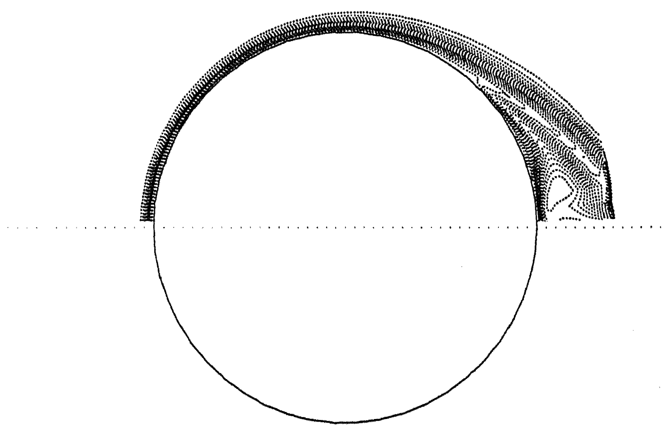

Figure 4.309

Isotherms for Re=500,n=0.5,and porosity 0.5 Pr=10.0(cont wall temp)

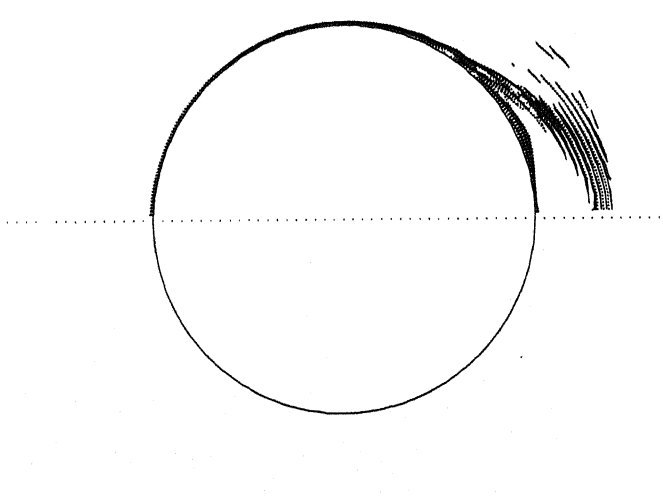

Figure 4.310

Isotherms for Re=500,n=0.5,and porosity 0.5 Pr=50.0(cont wall temp)

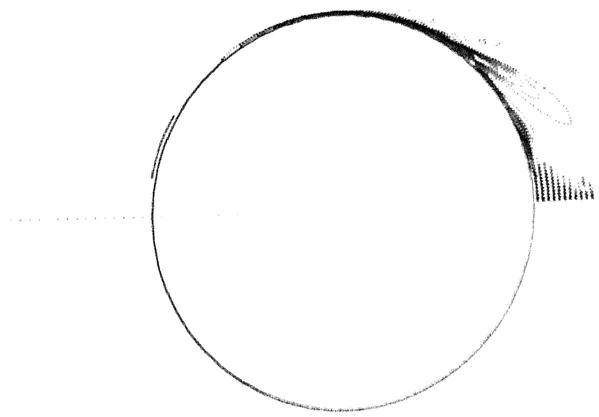

Figure 4.311

Isotherms for Re=500,n=0.5,and porosity 0.5 Pr=100.0(cont wall temp)

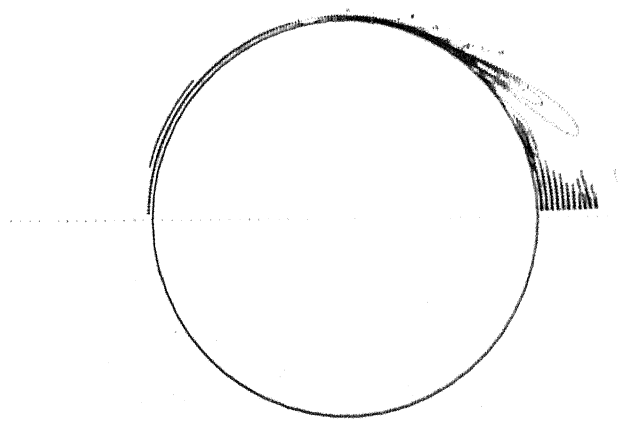

Figure 4.312

Isotherms for Re=1.0,n=1.0,and porosity 0.6 Pr=1.0(const wall temperature)

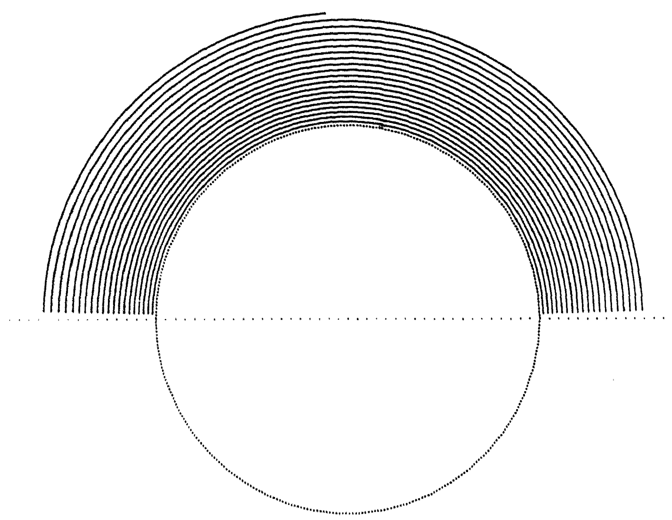

Figure 4.313

Isotherms for Re=1.0,n=1.0,and porosity 0.6 Pr=10.0(const wall temperature)

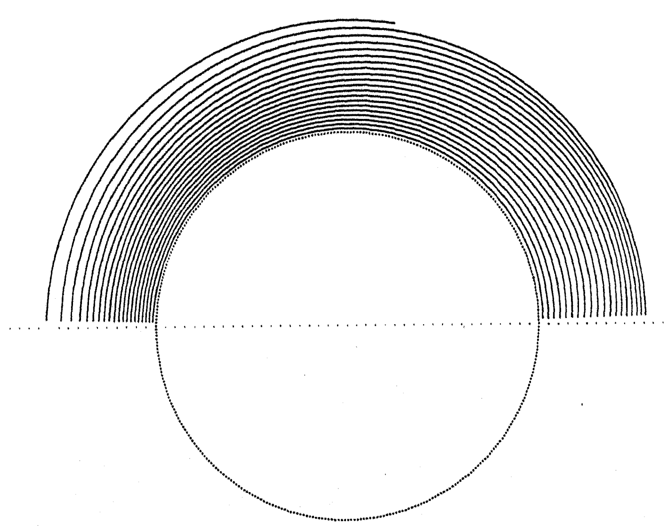

Figure 4.314

Isotherms for Re=1.0,n=1.0,and porosity 0.6 Pr=50.0(const wall temperature)

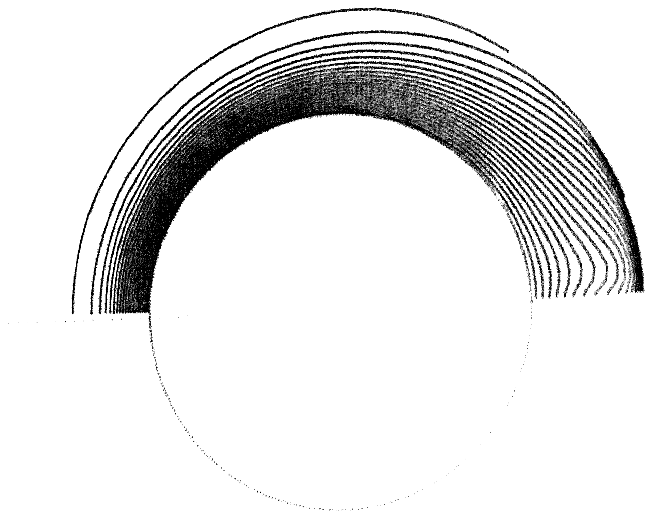

Figure 4.315

Isotherms for Re=1.0,n=1.0,and porosity 0.6 Pr=100.0(const wall temperature)

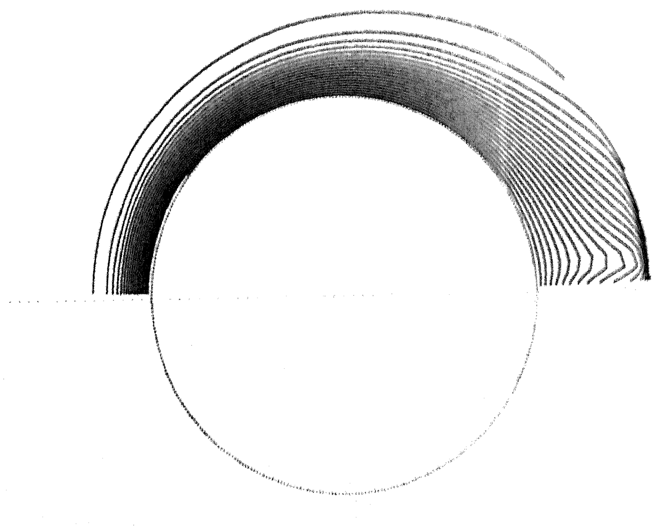

Figure 4.316

Isotherms for Re=1.0,n=1.0,and porosity 0.6 Pr=500.0(const wall temperature)

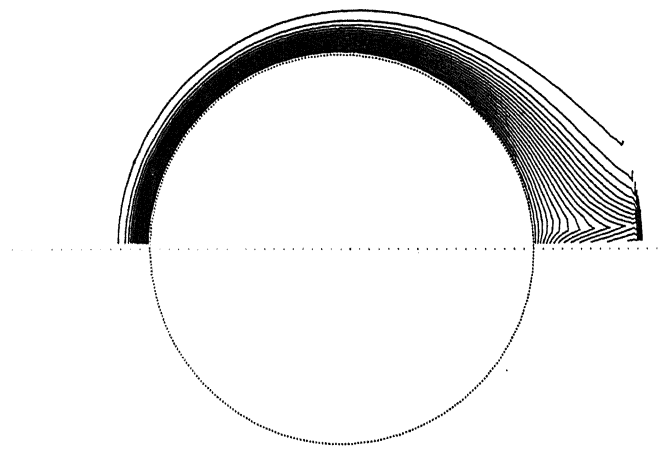

Figure 4.317

Isotherms for Re=10.0,n=1.0,and porosity 0.6 Pr=1.0(const wall temperature)

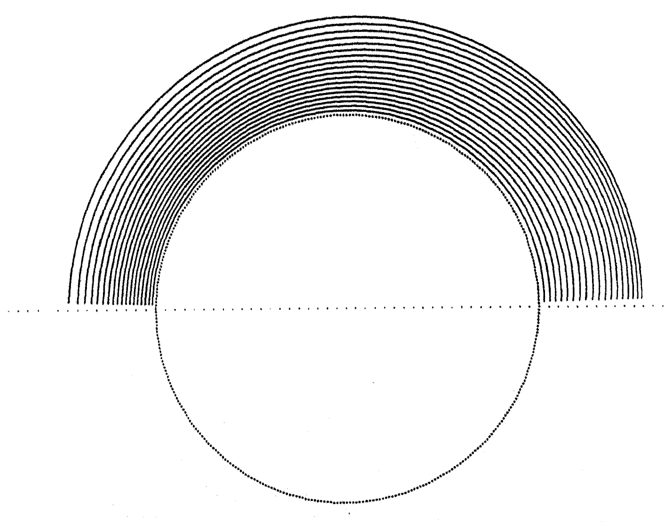

Figure 4.318

Isotherms for Re=10.0,n=1.0,and porosity 0.6 Pr=10.0(const wall temperature)

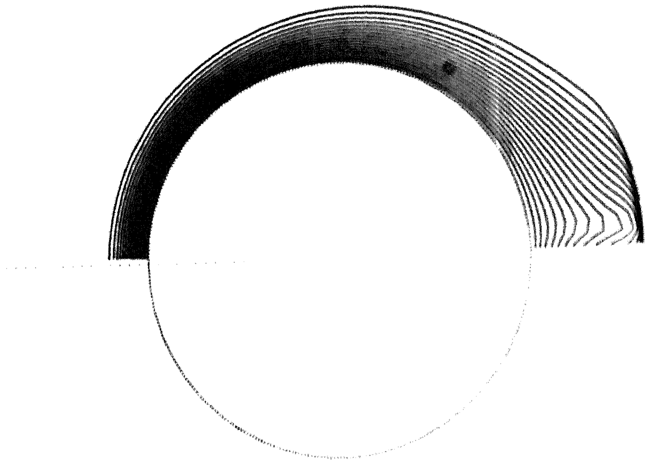

Figure 4.319

Isotherms for Re=10.0,n=1.0,and porosity 0.6 Pr=50.0(const wall temperature)

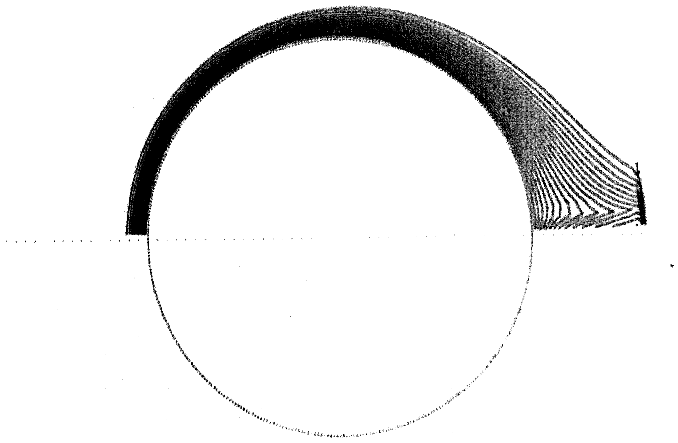

Figure 4.320

Isotherms for Re=10.0,n=1.0,and porosity 0.6 Pr=100.0(const wall temperature)

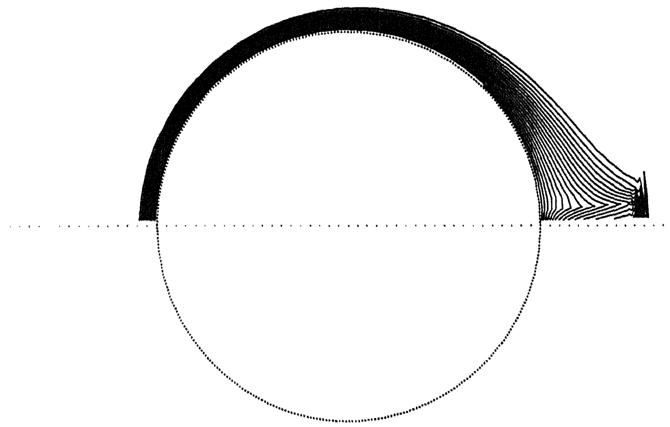

Figure 4.321

Isotherms for Re=10.0,n=1.0,and porosity 0.6 Pr=500.0(const wall temperature)

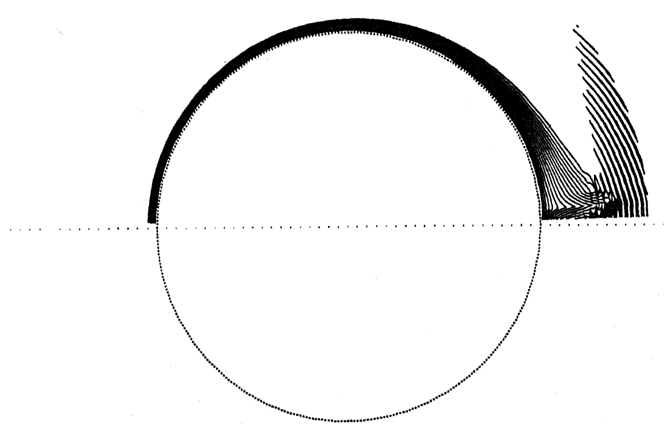

Figure 4.322

Isotherms for Re=100.0,n=1.0,and porosity 0.6 Pr=1.0(const wall temperature)

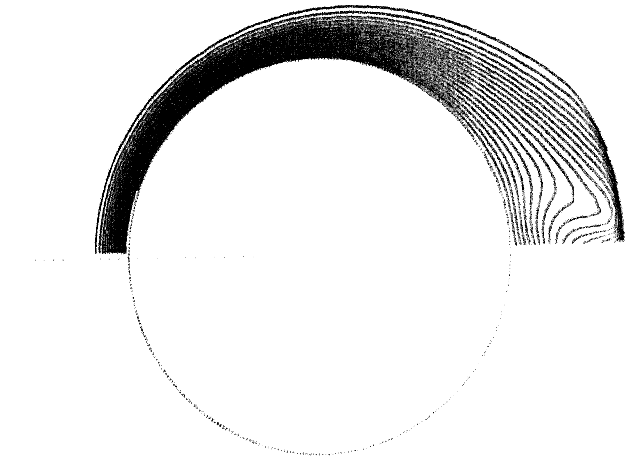

Figure 4.323

Isotherms for Re=100.0,n=1.0,and porosity 0.6 Pr=10.0(const wall temperature)

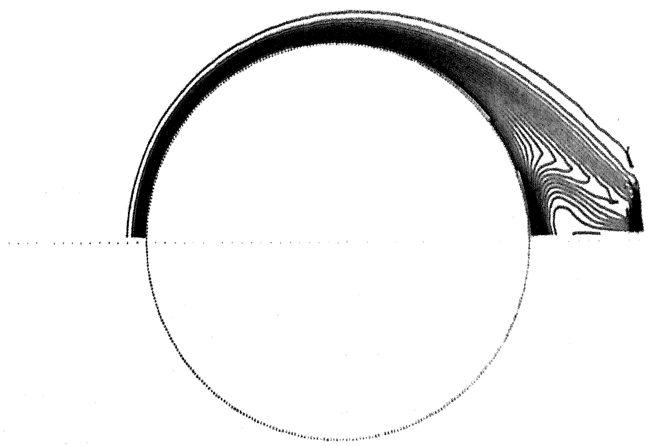

Figure 4.324

Isotherms for Re=100.0,n=1.0,and porosity 0.6 Pr=50.0(const wall temperature)

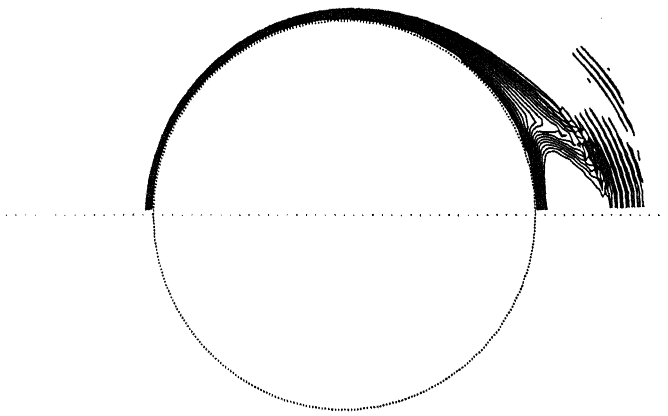

Figure 4.325

Isotherms for Re=100.0,n=1.0,and porosity 0.6 Pr=100.0(const wall temperature)

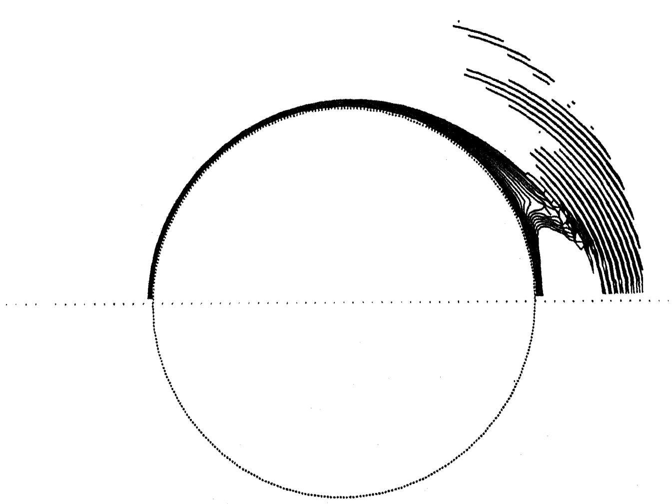

Figure 4.326

Isotherms for Re=100.0,n=1.0,and porosity 0.6 Pr=500.0(const wall temperature)

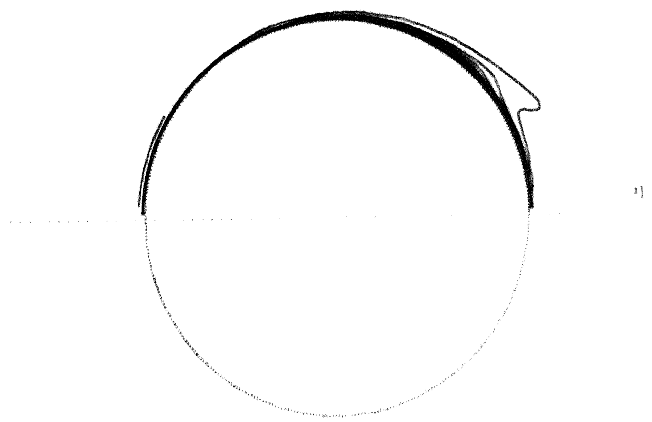

Figure 4.327

Isotherms for Re=200.0,n=1.0,and porosity 0.6 Pr=1.0(const wall temperature)

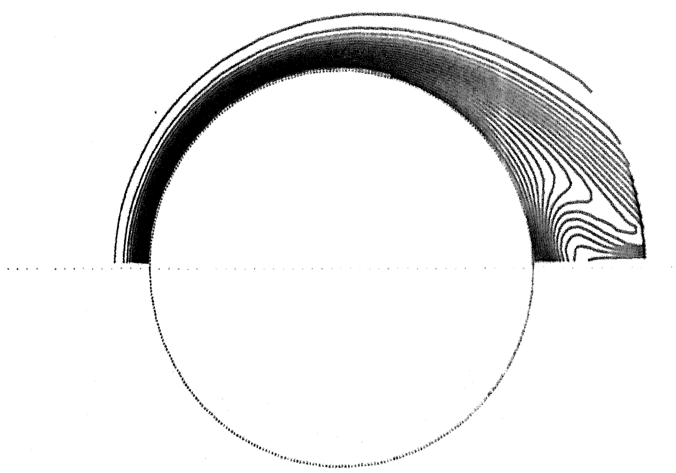

Figure 4.328

Isotherms for Re=200.0,n=1.0,and porosity 0.6 Pr=10.0(const wall temperature)

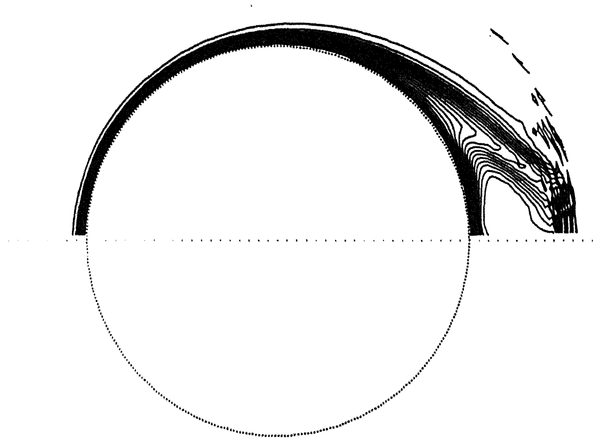

Figure 4.329

Isotherms for Re=200.0,n=1.0,and porosity 0.6 Pr=50.0(const wall temperature)

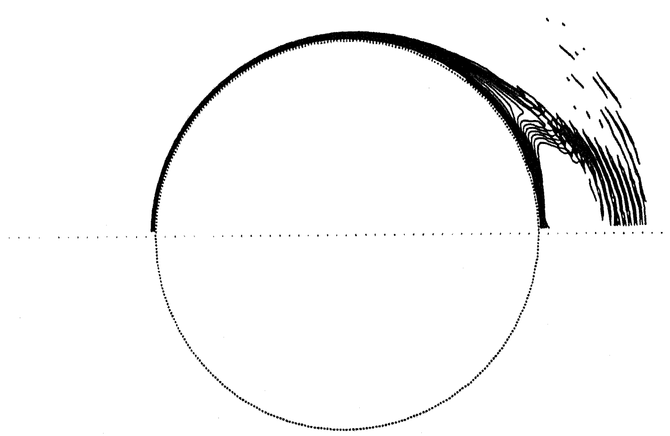

Figure 4.330

Isotherms for Re=200.0,n=1.0,and porosity 0.6 Pr=100.0(const wall temperature)

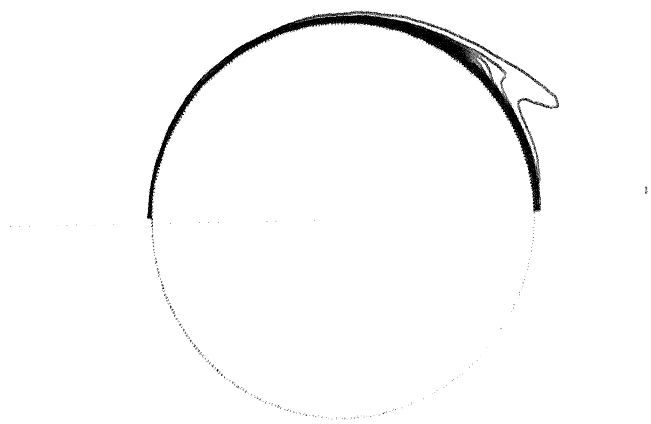

Figure 4.331

Isotherms for Re=200.0,n=1.0,and porosity 0.6 Pr=500.0(const wall temperature)

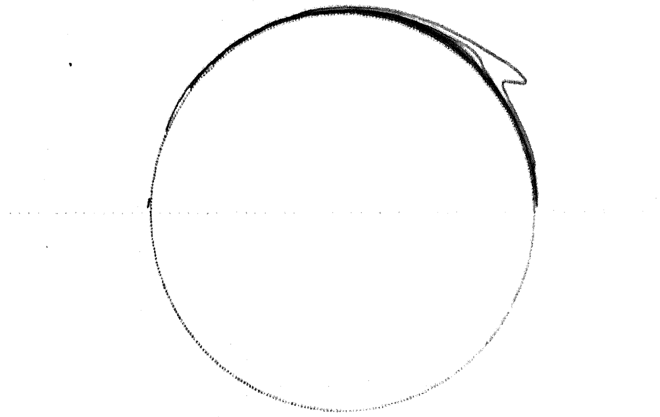

Figure 4.332

Isotherms for Re=500.0,n=1.0,and porosity 0.6 Pr=1.0(const wall temperature)

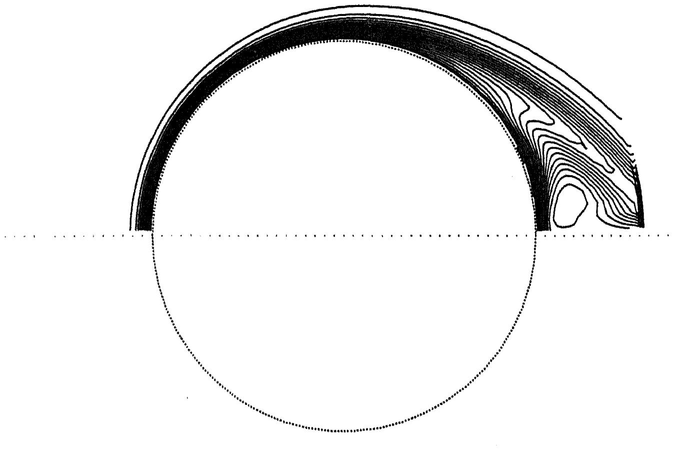

Figure 4.333

Isotherms for Re=500.0,n=1.0,and porosity 0.6 Pr=10.0(const wall temperature)

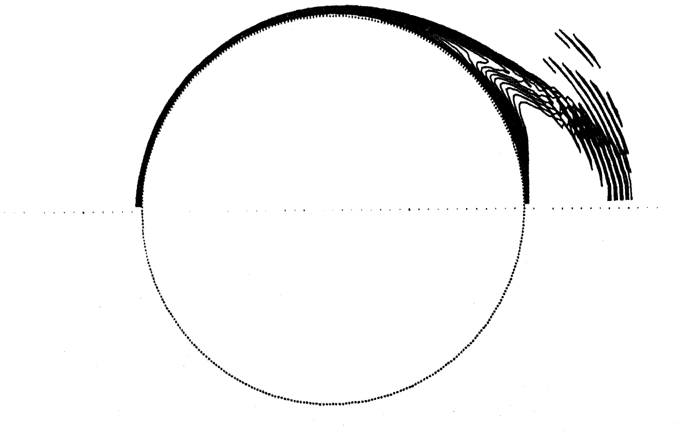

Figure 4.334

Isotherms for Re=500.0,n=1.0,and porosity 0.6 Pr=50.0(const wall temperature)

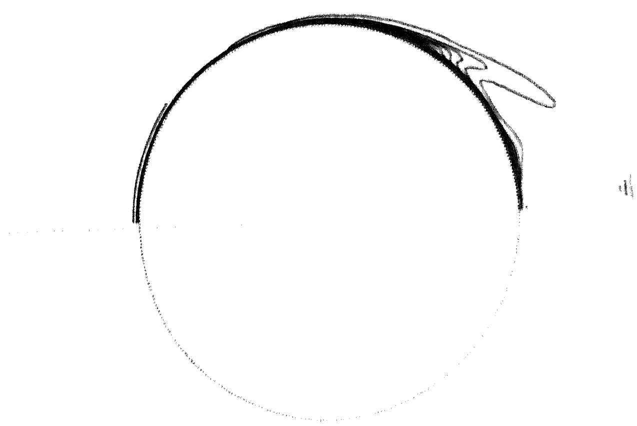

Figure 4.335

Isotherms for Re=500.0,n=1.0,and porosity 0.6 Pr=100.0(const wall temperature)

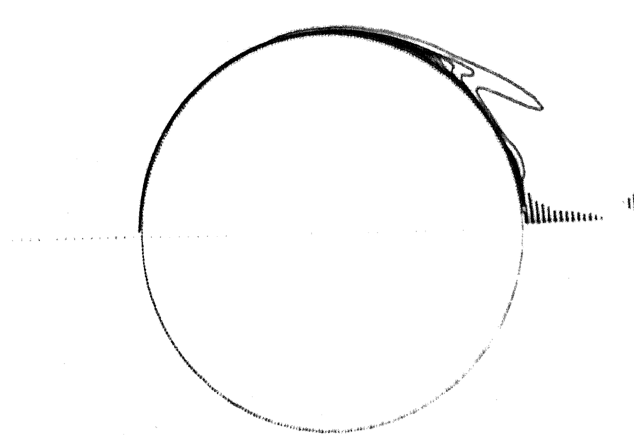

Figure 4.336

Isotherms for Re=1.0,n=0.8,and porosity 0.6,Pr=1.0(const wall temperature)

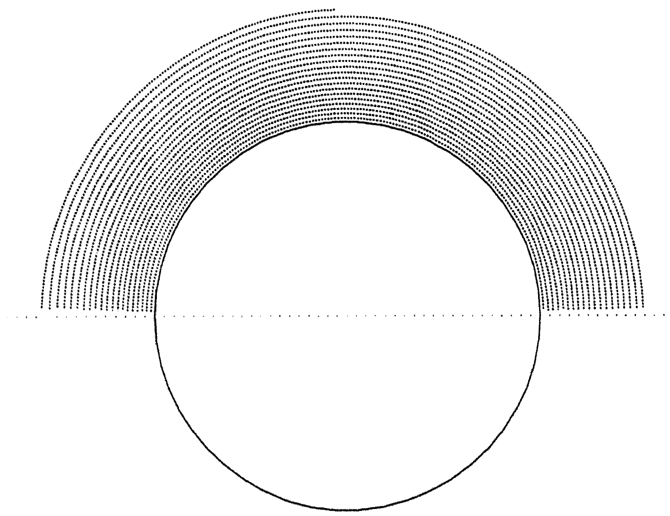

Figure 4.337

Isotherms for Re=1.0,n=0.8,and porosity 0.6,Pr=10.0(const wall temperature)

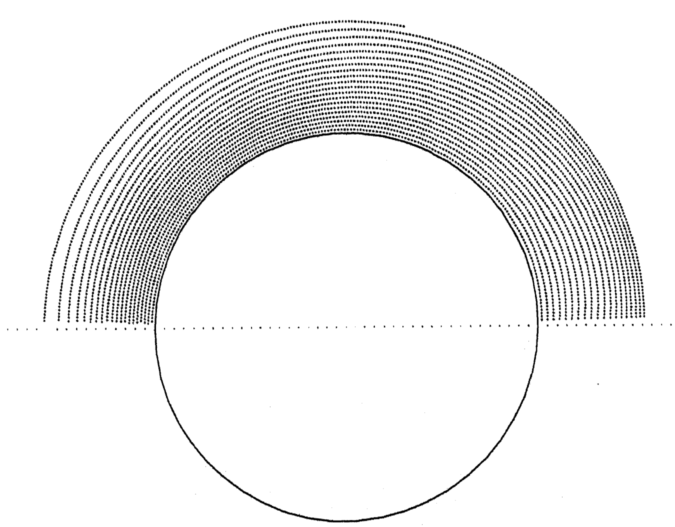

Figure 4.338

Isotherms for Re=1.0,n=0.8,and porosity 0.6,Pr=50.0(const wall temperature)

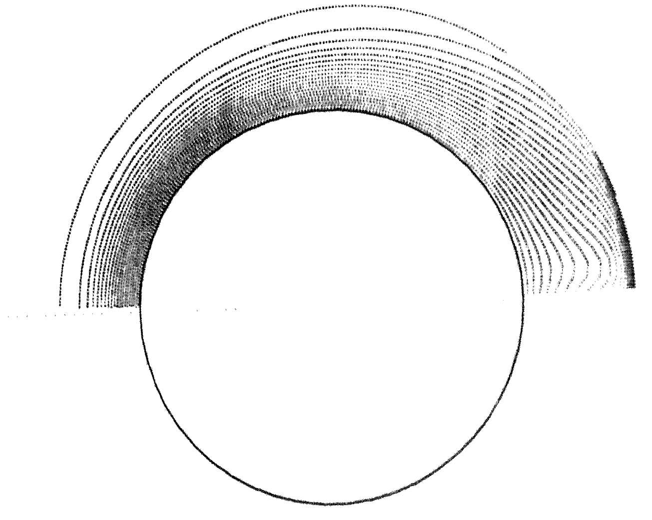

Figure 4.339

Isotherms for Re=10.0,n=0.8,and porosity 0.6 Pr=100.0(const wall temperature)

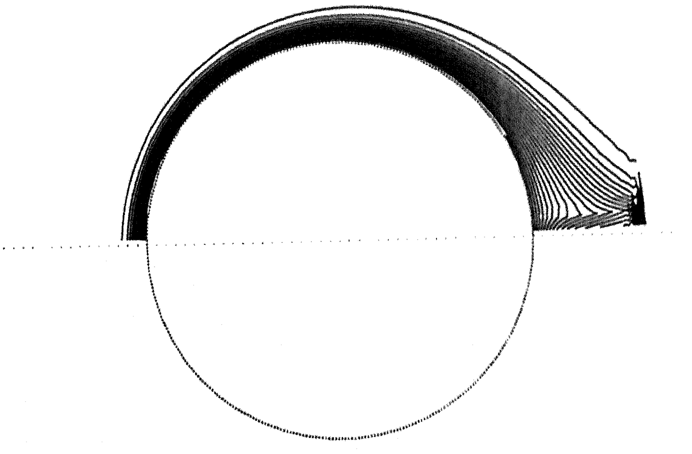

Figure 4.340

Isotherms for Re=10.0,n=0.8,and porosity 0.6 Pr=500.0(const wall temperature)

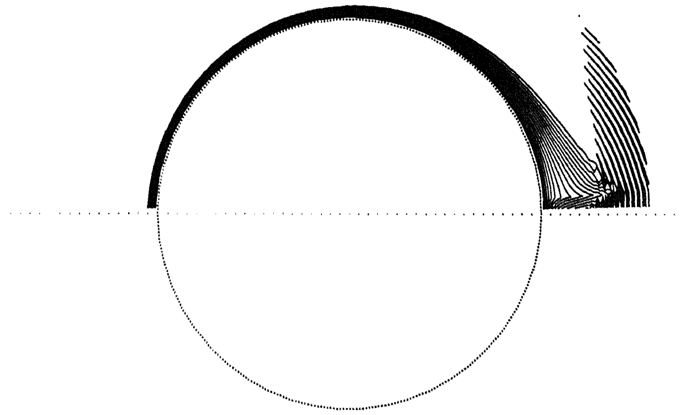

Figure 4.341

Isotherms for Re=10.0,n=0.8,and porosity 0.6 Pr=1.0(const wall temperature)

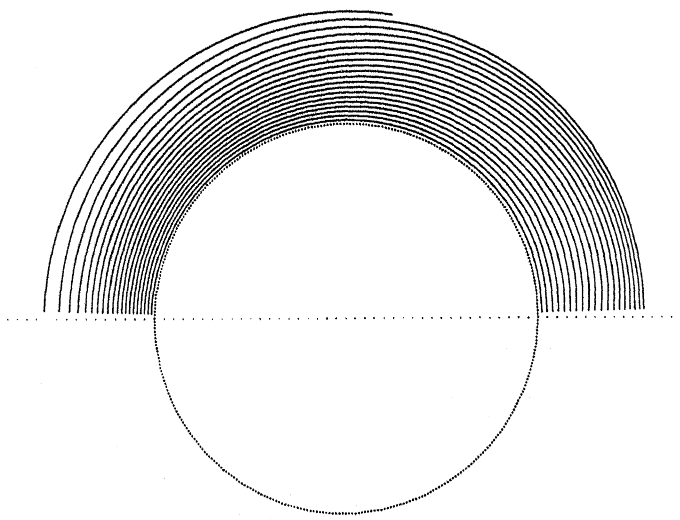

Figure 4.342

Isotherms for Re=10.0,n=0.8,and porosity 0.6 Pr=10.0(const wall temperature)

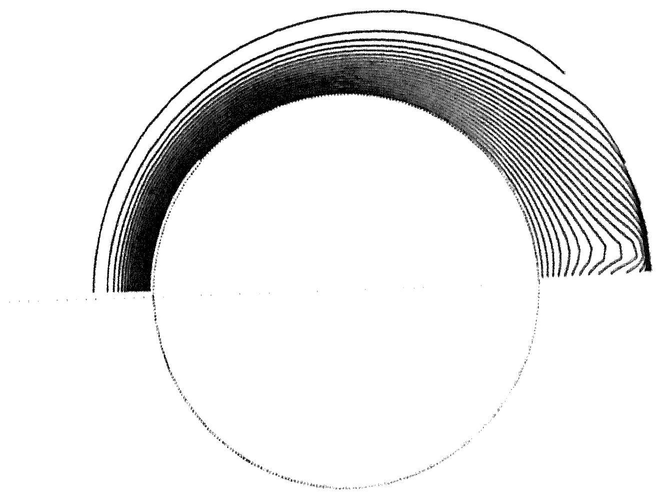

Figure 4.343

Isotherms for Re=10.0,n=0.8,and porosity 0.6 Pr=50.0(const wall temperature)

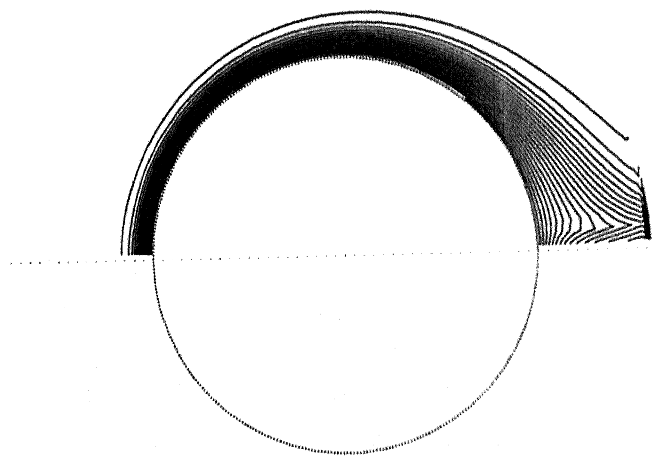

Figure 4.344

Isotherms for Re=10.0,n=0.8,and porosity 0.6 Pr=100.0(const wall temperature)

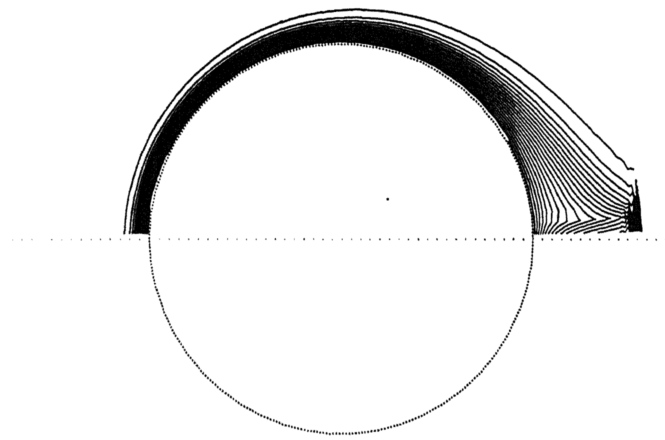

Figure 4.345

Isotherms for Re=10.0,n=0.8,and porosity 0.6 Pr=500.0(const wall temperature)

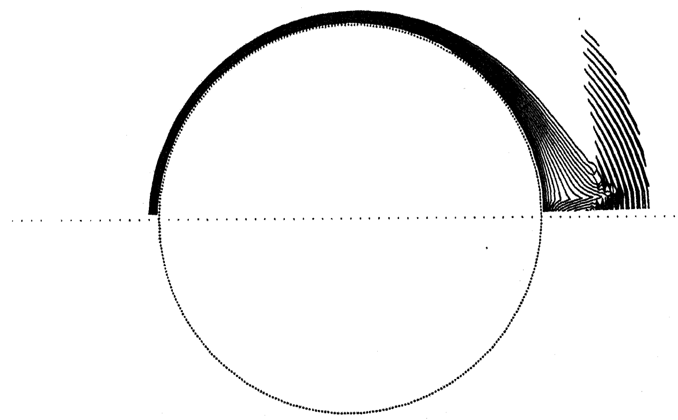

Figure 4.346

Isotherms for Re=200.0,n=0.8,and porosity 0.6 Pr=1.0(const wall temperature)

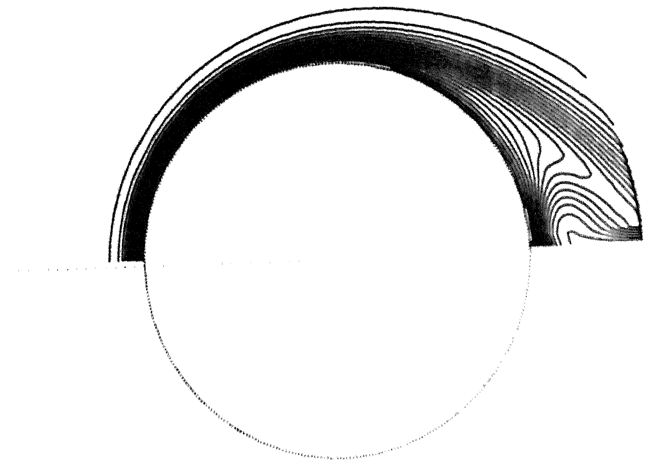

Figure 4.347

Isotherms for Re=100.0,n=0.8,and porosity 0.6,Pr=10.0(const wall temperature)

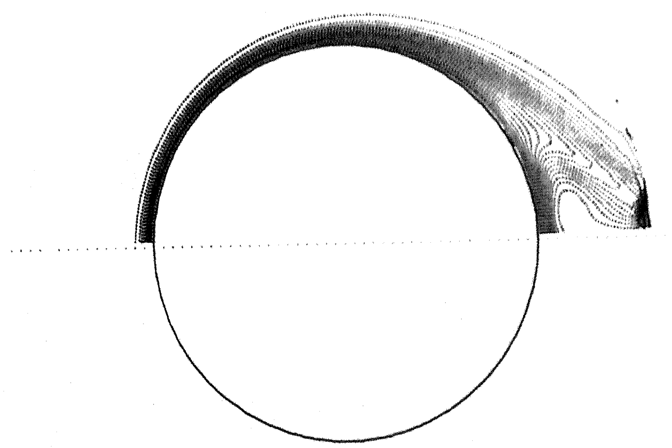

Figure 4.348

Isotherms for Re=100.0,n=0.8,and porosity 0.6,Pr=50.0(const wall temperature)

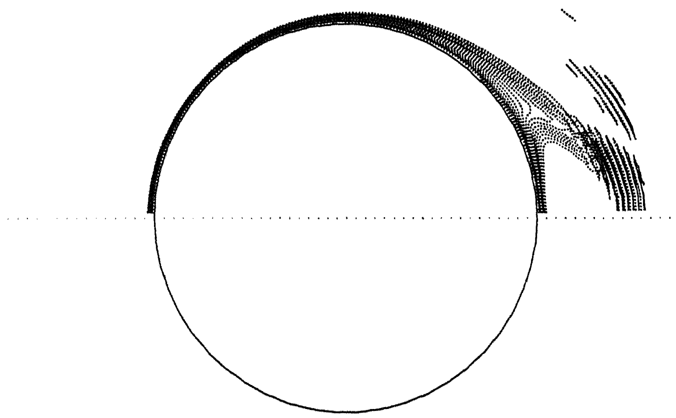

Figure 4.349

Isotherms for Re=100.0,n=0.8,and porosity 0.6,Pr=100.0(const wall temperature)

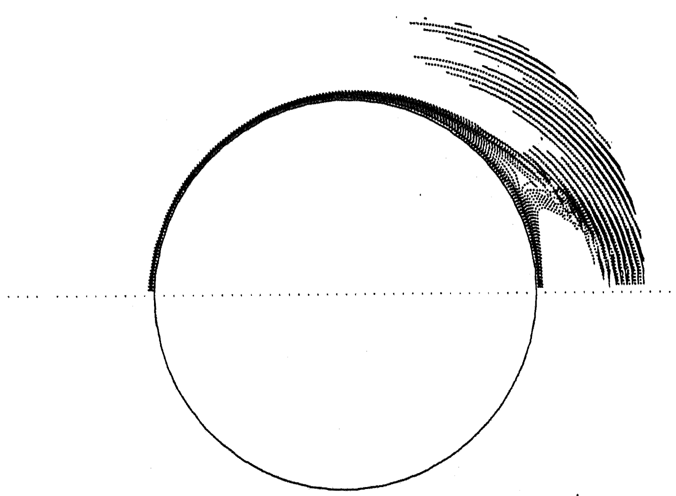

Figure 4.350

Isotherms for Re=100.0,n=0.8,and porosity 0.6,Pr=500.0(const wall temperature)

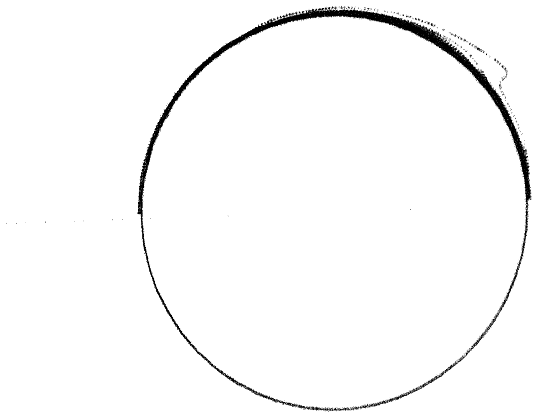

Figure 4.351

Isotherms for Re=200.0,n=0.8,and porosity 0.6 Pr=1.0(const wall temperature)

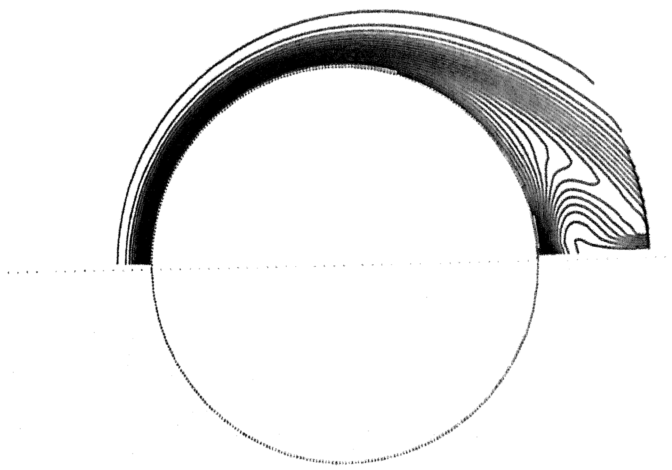

Figure 4.352

Isotherms for Re=200.0,n=0.8,and porosity 0.6 Pr=10.0(const wall temperature)

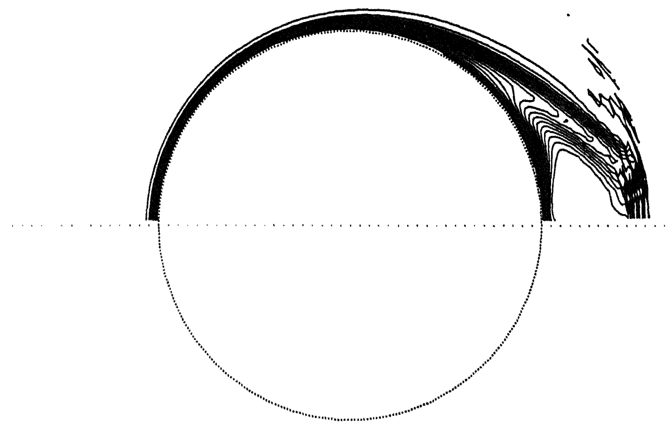

Figure 4.353

Isotherms for Re=200.0,n=0.8,and porosity 0.6 Pr=50.0(const wall temperature)

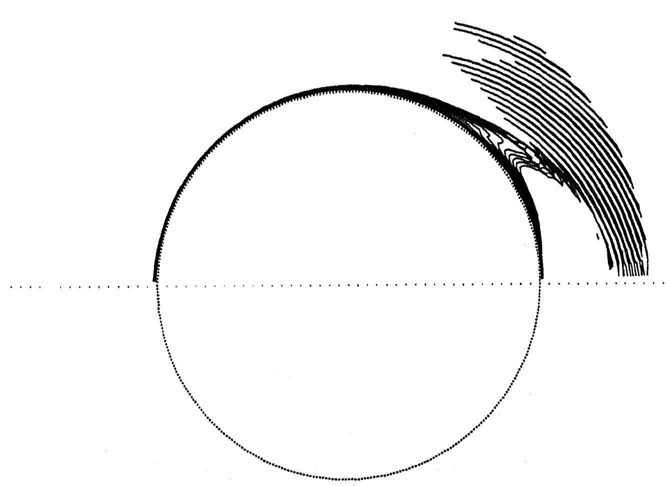

Figure 4.354

Isotherms for Re=200.0,n=0.8,and porosity 0.6 Pr=100.0(const wall temperature)

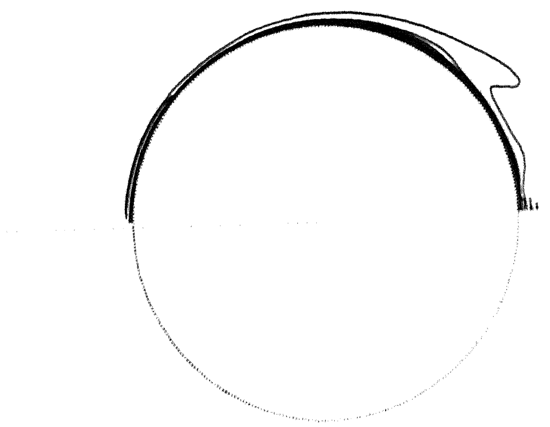

Figure 4.355

Isotherms for Re=200.0,n=0.8,and porosity 0.6 Pr=500.0(const wall temperature)

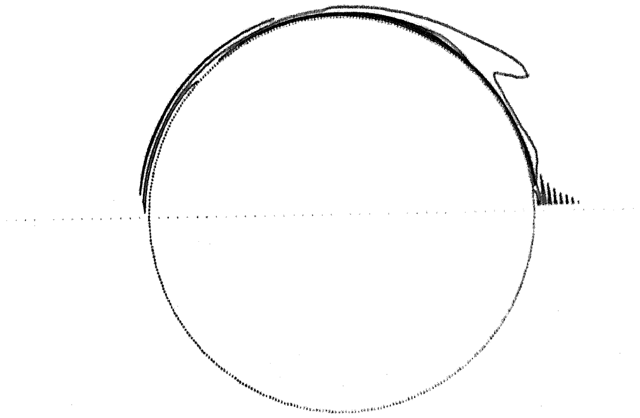

Figure 4.356

Isotherms for Re=500.0,n=0.8,and porosity 0.6 Pr=1.0(const wall temperature)

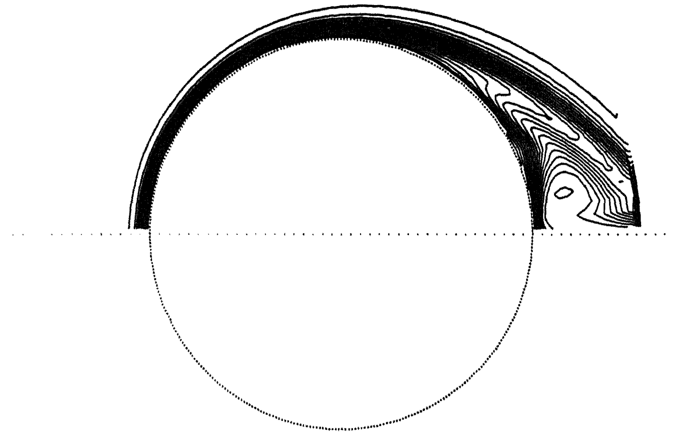

Figure 4.357

Isotherms for Re=500.0,n=0.8,and porosity 0.6 Pr=10.0(const wall temperature)

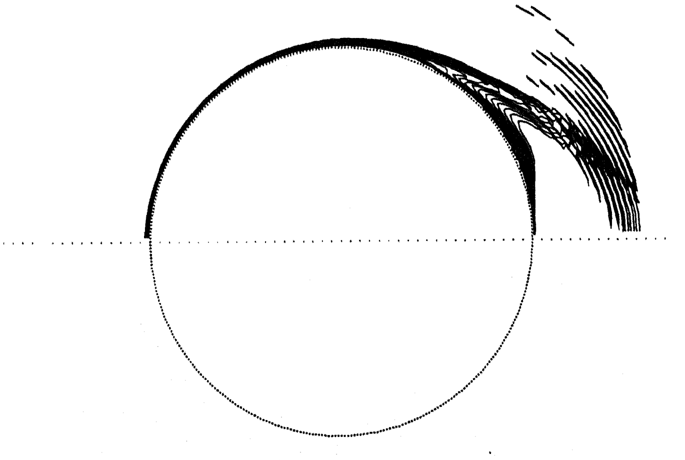

Figure 4.358

Isotherms for Re=500.0,n=0.8,and porosity 0.6 Pr=50.0(const wall temperature)

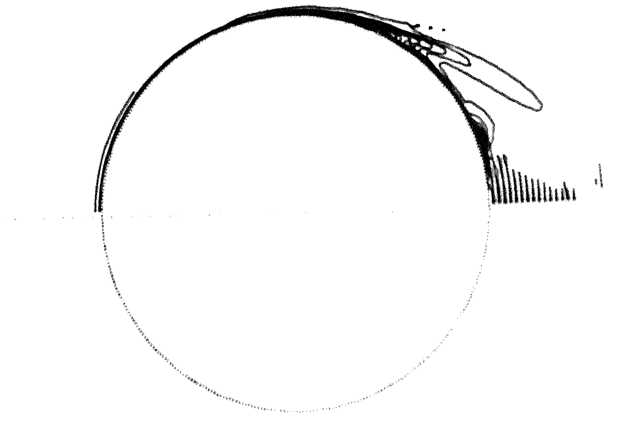

Figure 4.359

Isotherms for Re=500.0,n=0.8,and porosity 0.6 Pr=100.0(const wall temperature)

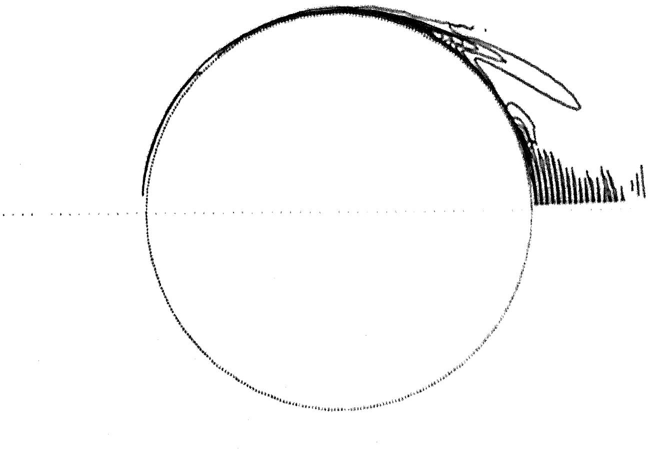

Figure 4.360

Isotherms for Re=1.0,n=0.6,and porosity 0.6 Pr=1.0(const wall temperature)

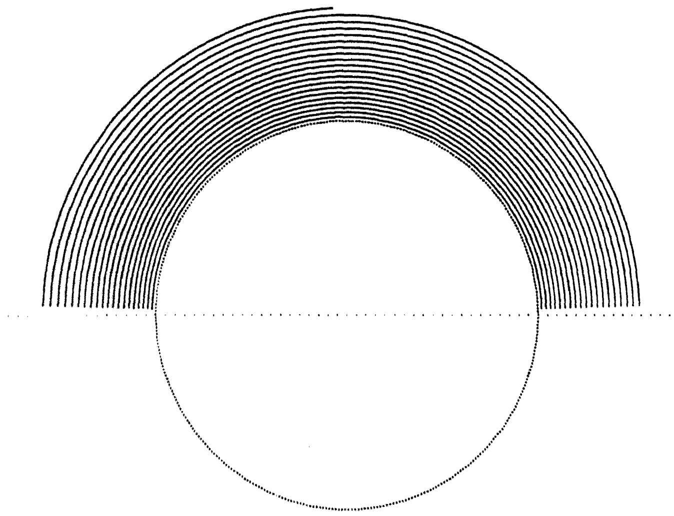

Figure 4.361

Isotherms for Re=1.0,n=0.6,and porosity 0.6 Pr=10.0(const wall temperature)

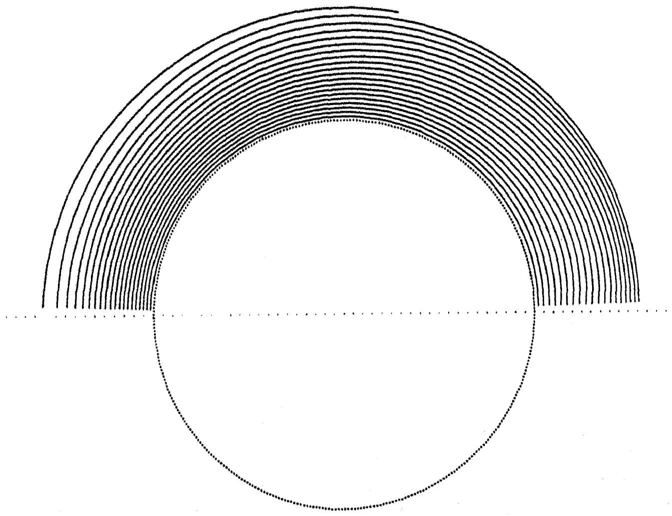

Figure 4.362

Isotherms for Re=1.0,n=0.6,and porosity 0.6 Pr=50.0(const wall temperature)

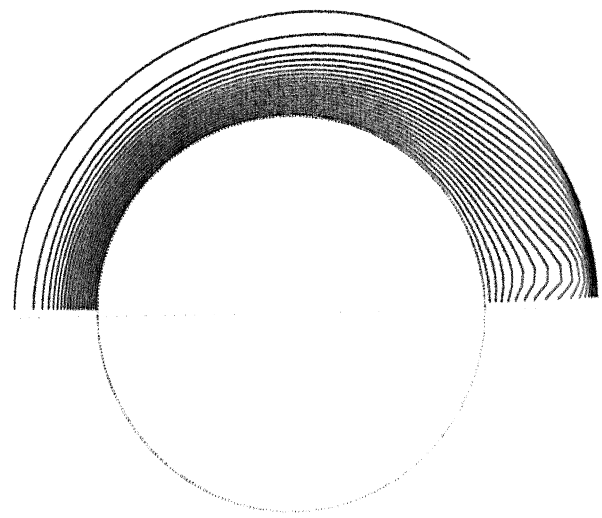

Figure 4.363

Isotherms for Re=1.0,n=0.6,and porosity 0.6 Pr=100.0(const wall temperature)

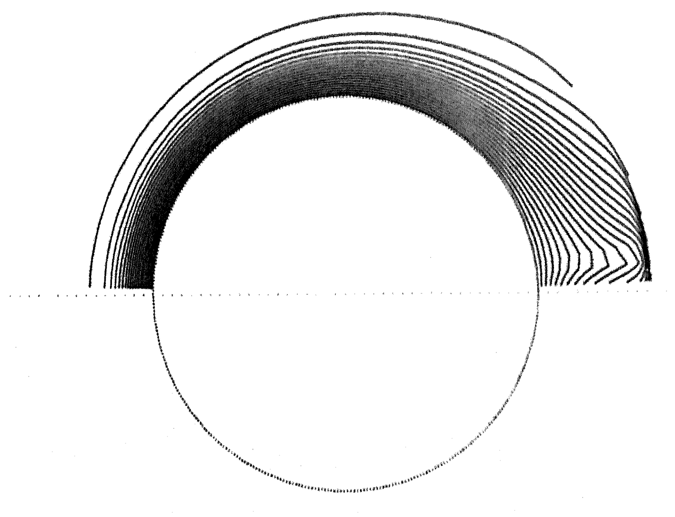

Figure 4.364

Isotherms for Re=1.0,n=0.6,and porosity 0.6 Pr=500.0(const wall temperature)

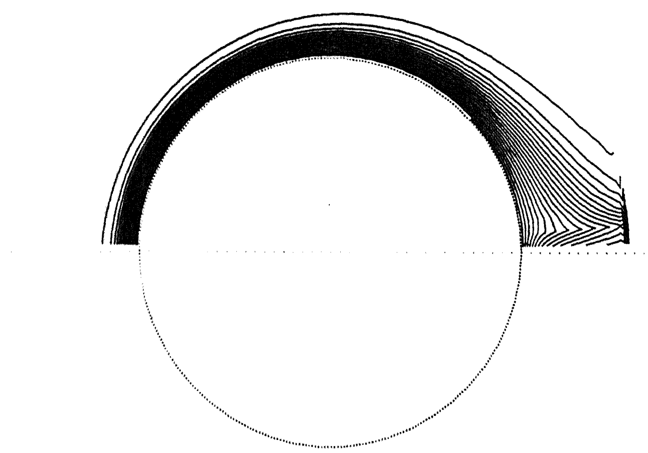

Figure 4.365

Isotherms for Re=10.0,n=0.6,and porosity 0.6 Pr=1.0(const wall temperature)

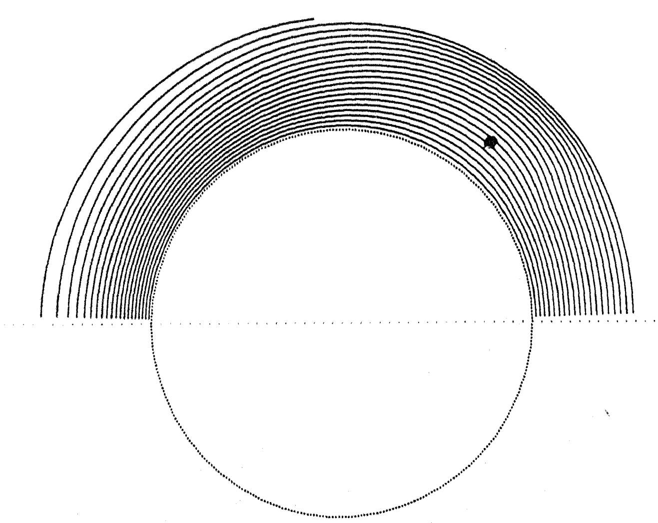

Figure 4.366

Isotherms for Re=10.0,n=0.6,and porosity 0.6 Pr=10.0(const wall temperature)

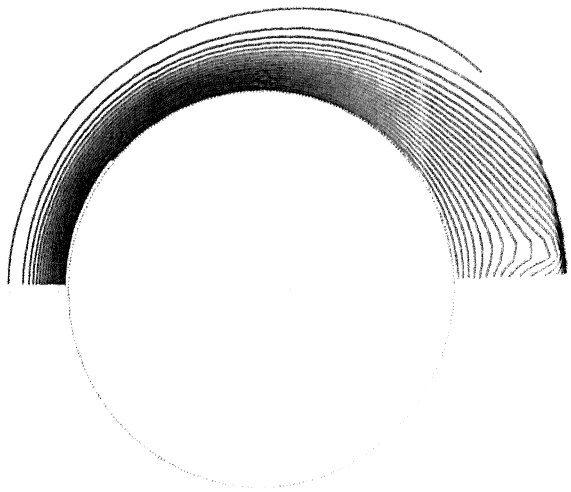

Figure 4.367

Isotherms for Re=10.0,n=0.6,and porosity 0.6 Pr=50.0(const wall temperature)

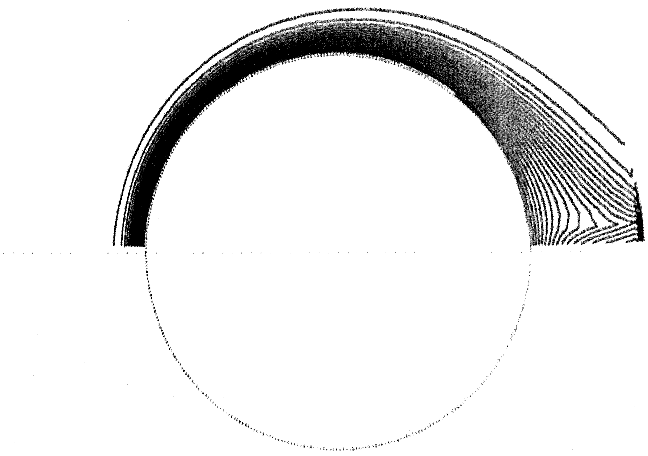

Figure 4.368

Isotherms for Re=10.0,n=0.6,and porosity 0.6 Pr=100.0(const wall temperature)

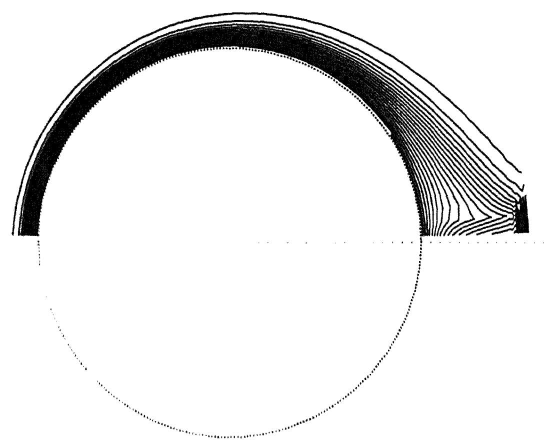

Figure 4.369

Isotherms for Re=10.0,n=0.6,and porosity 0.6 Pr=500.0(const wall temperature)

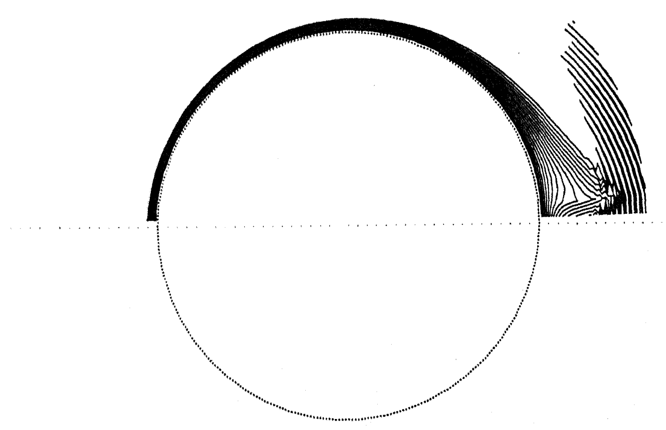

Figure 4.370

Isotherms for Re=100.0,n=0.6,and porosity 0.6 Pr=1.0(const wall temperature)

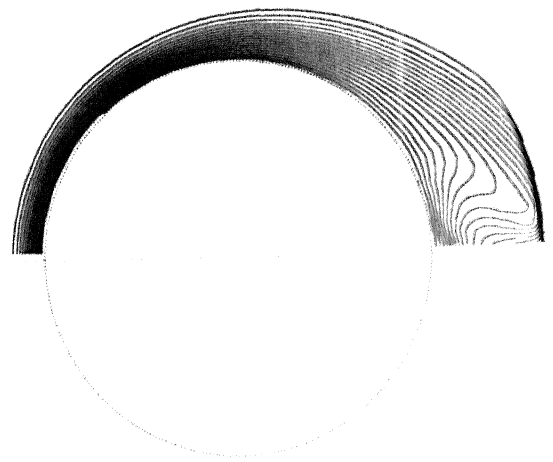

Figure 4.371

Isotherms for Re=100.0,n=0.6,and porosity 0.6 Pr=10.0(const wall temperature)

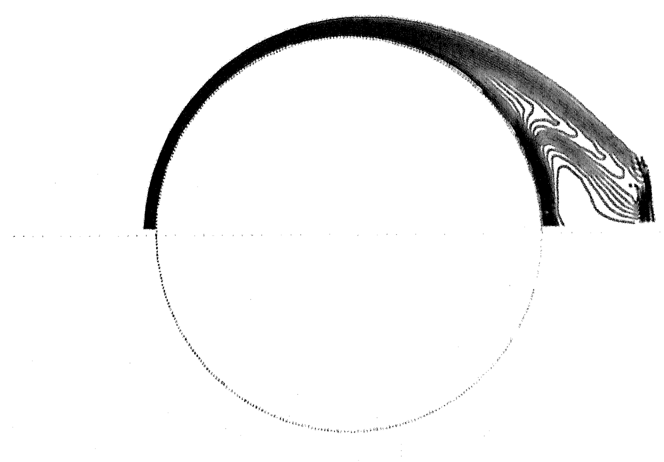

Figure 4.372

Isotherms for Re=100.0,n=0.6,and porosity 0.6 Pr=50.0(const wall temperature)

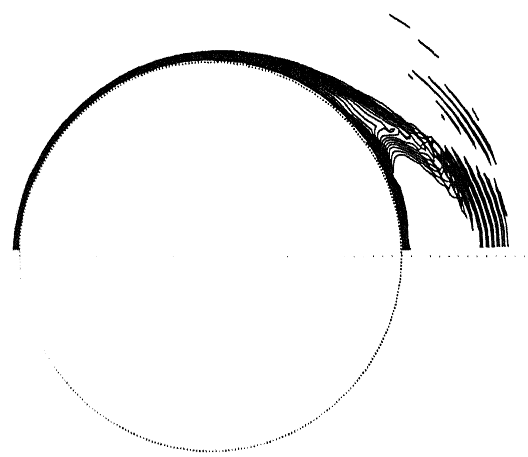

Figure 4.373

Isotherms for Re=100.0,n=0.6,and porosity 0.6 Pr=100.0(const wall temperature)

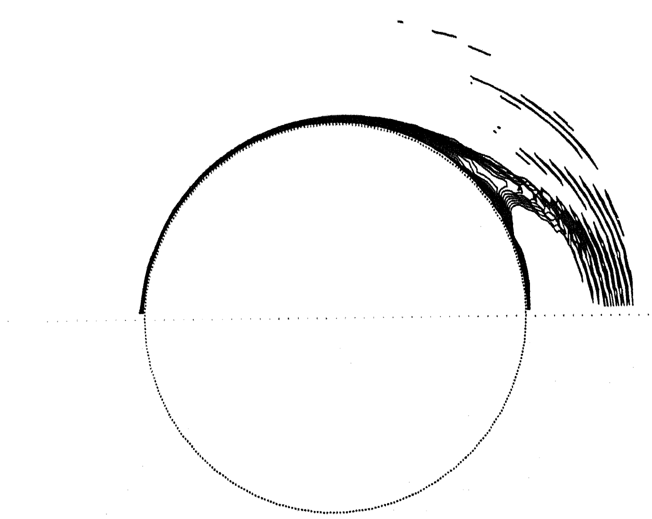

Figure 4.374

Isotherms for Re=100.0,n=0.6,and porosity 0.6 Pr=500.0(const wall temperature)

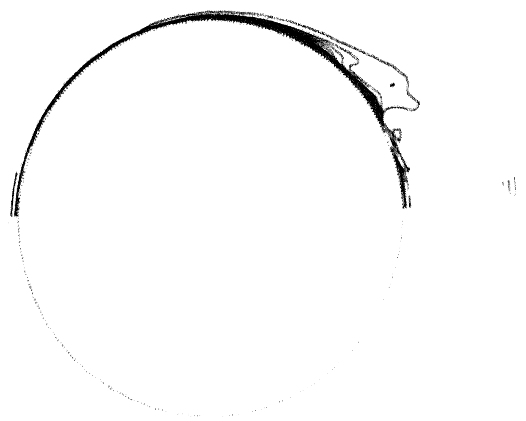

Figure 4.375

Isotherms for Re=200.0,n=0.6,and porosity 0.6 Pr=1.0(const wall temperature)

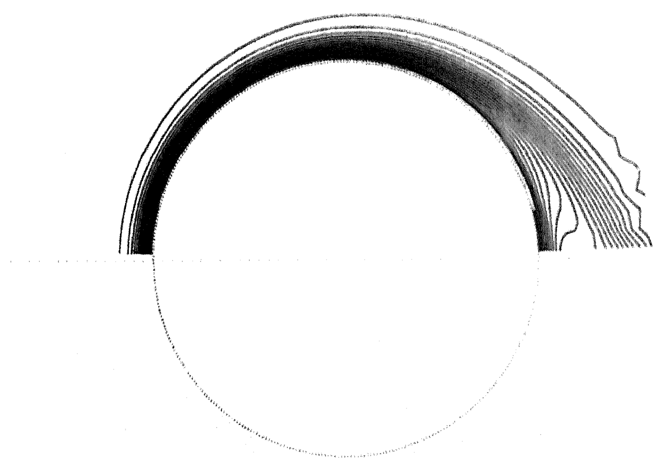

Figure 4.376

Isotherms for Re=200.0,n=0.6,and porosity 0.6 Pr=10.0(const wall temperature)

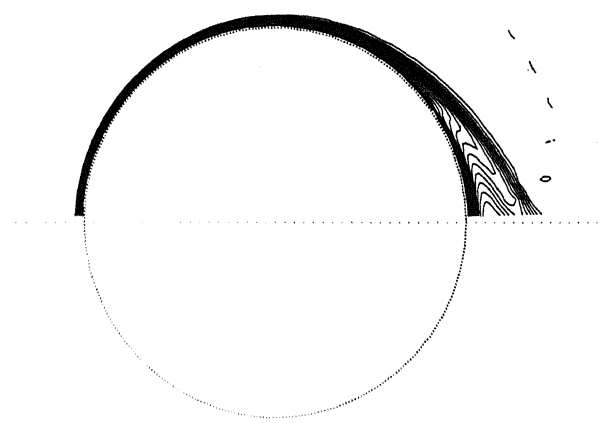

Figure 4.377

Isotherms for Re=200.0,n=0.6,and porosity 0.6 Pr=50.0(const wall temperature)

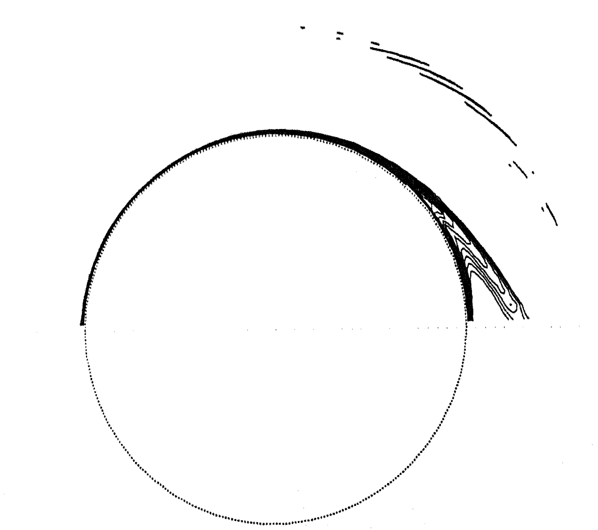

Figure 4.378

Isotherms for Re=200.0,n=0.6,and porosity 0.6 Pr=100.0(const wall temperature)

Figure 4.379

Isotherms for Re=200.0,n=0.6,and porosity 0.6 Pr=500.0(const wall temperature)

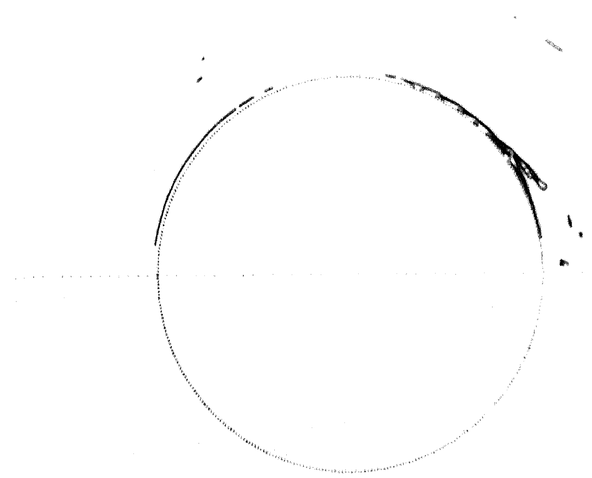

Figure 4.380

Isotherms for Re=500.0,n=0.6,and porosity 0.6 Pr=1.0(const wall temperature)

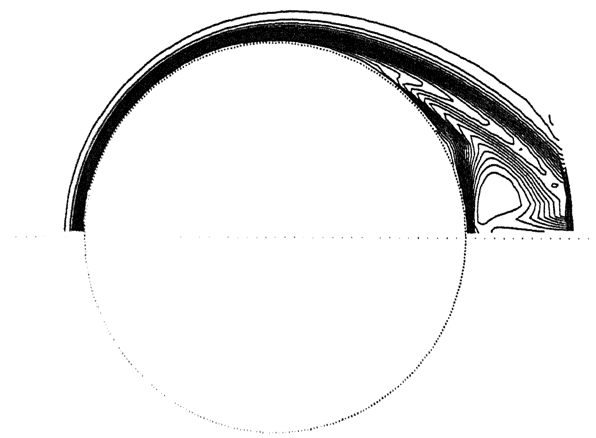

Figure 4.381

Isotherms for Re=500.0,n=0.6,and porosity 0.6 Pr=10.0(const wall temperature)

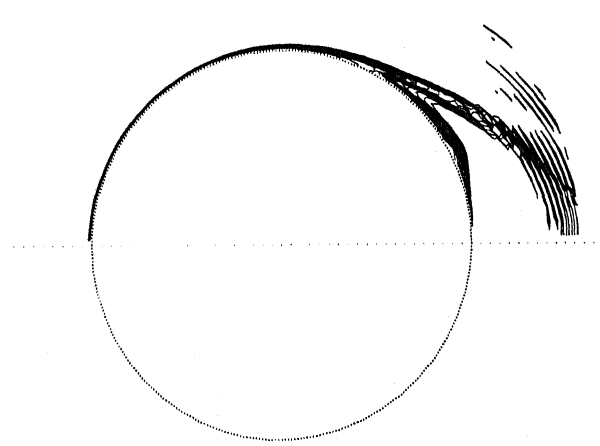

Figure 4.382

Isotherms for Re=500.0,n=0.6,and porosity 0.6 Pr=50.0(const wall temperature)

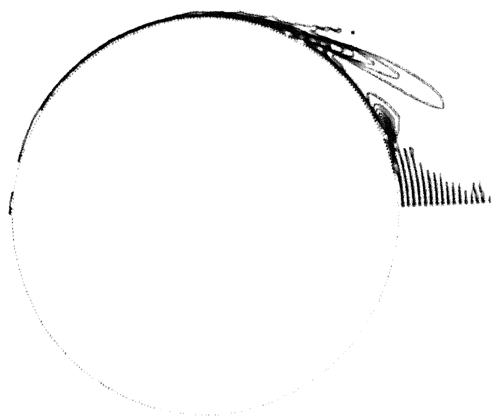

Figure 4.383

Isotherms for Re=500.0,n=0.6,and porosity 0.6 Pr=100.0(const wall temperature)

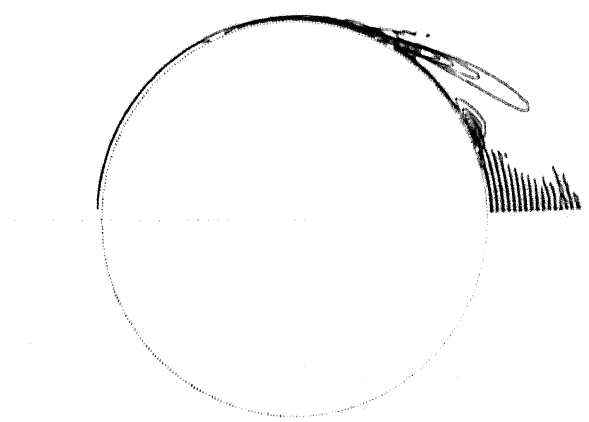

Figure 4.384

Isotherms for Re=1.0,n=0.5,and porosity 0.6 Pr=1.0(const wall temperature)

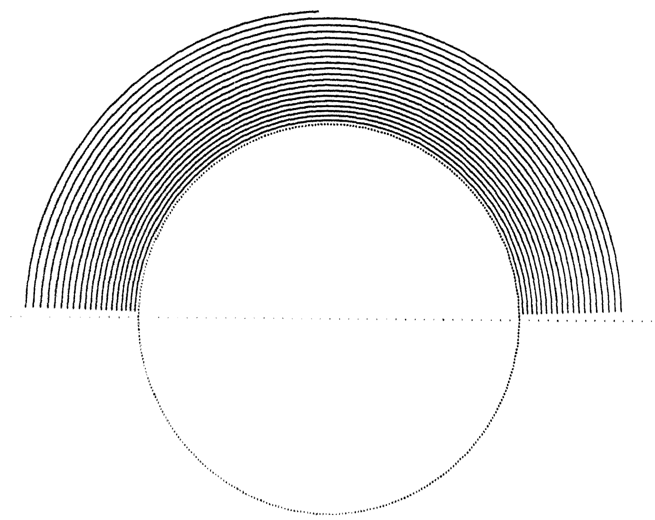

Figure 4.385

Isotherms for Re=1.0,n=0.5,and porosity 0.6 Pr=10.0(const wall temperature)

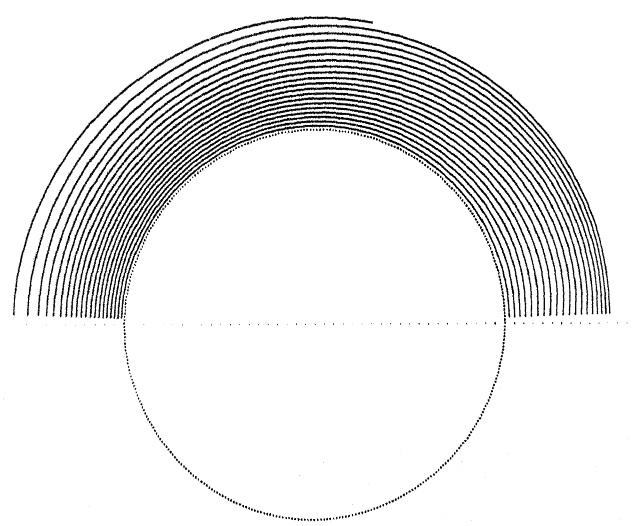

Figure 4.386

Isotherms for Re=1.0,n=0.5,and porosity 0.6 Pr=50.0(const wall temperature)

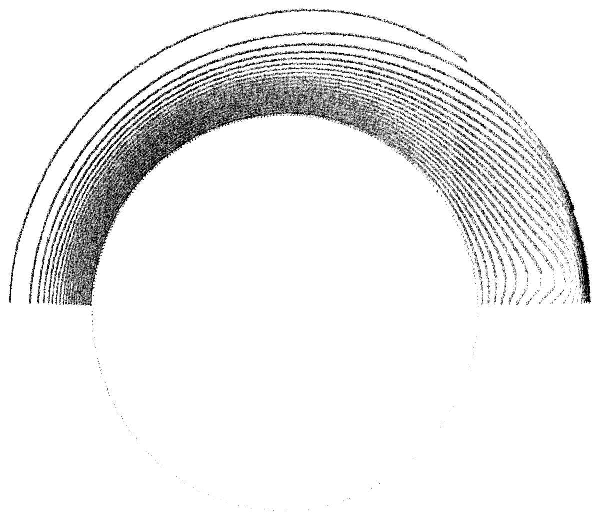

Figure 4.387

Isotherms for Re=1.0,n=0.5,and porosity 0.6 Pr=100.0(const wall temperature)

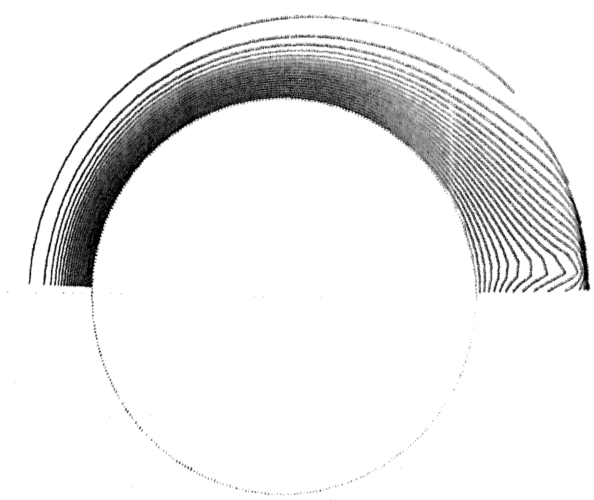

Figure 4.388

Isotherms for Re=1.0,n=0.5,and porosity 0.6 Pr=500.0(const wall temperature)

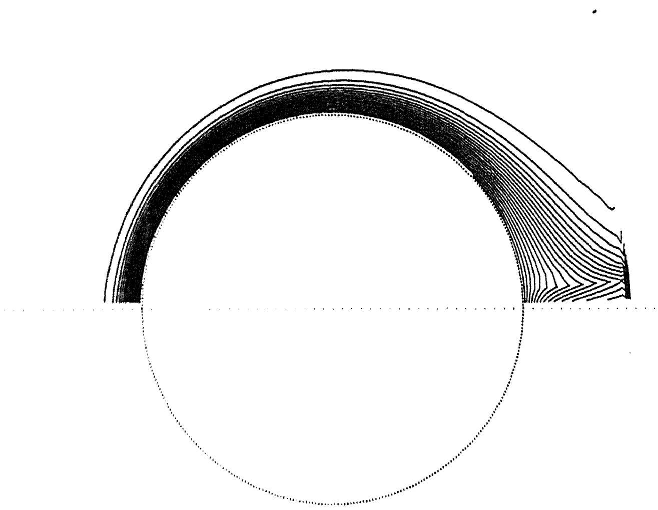

Figure 4.389

Isotherms for Re=10 0,n=0.5,and porosity 0.6 Pr=1.0(const wall temperature)

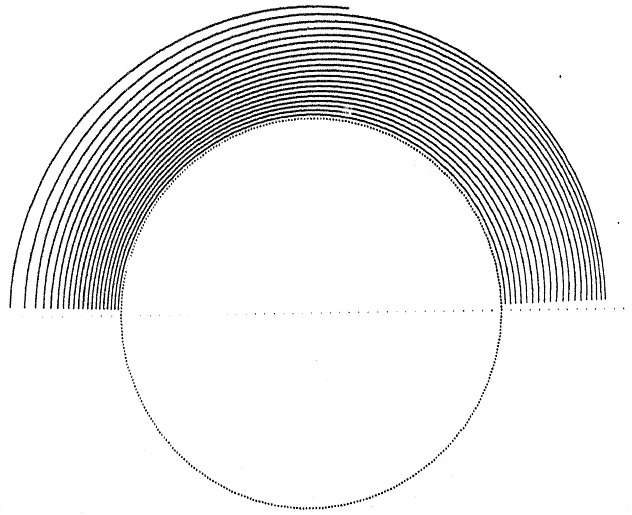

Figure 4.390

Isotherms for Re=10.0,n=0.5,and porosity 0.6 Pr=10.0(const wall temperature)

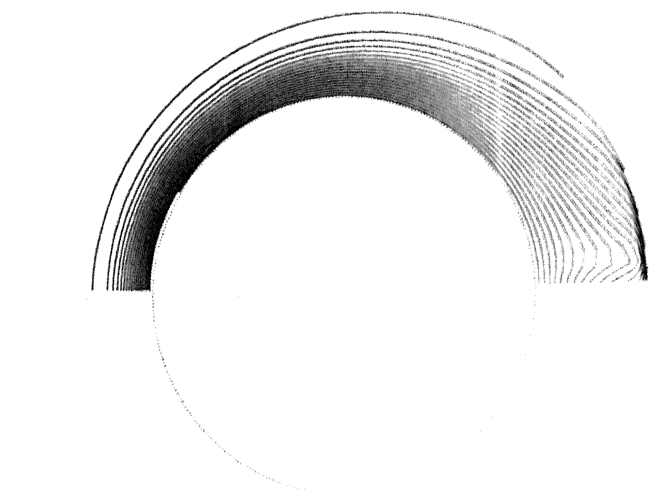

Figure 4.391

Isotherms for Re=10.0,n=0.5,and porosity 0.6 Pr=50.0(const wall temperature)

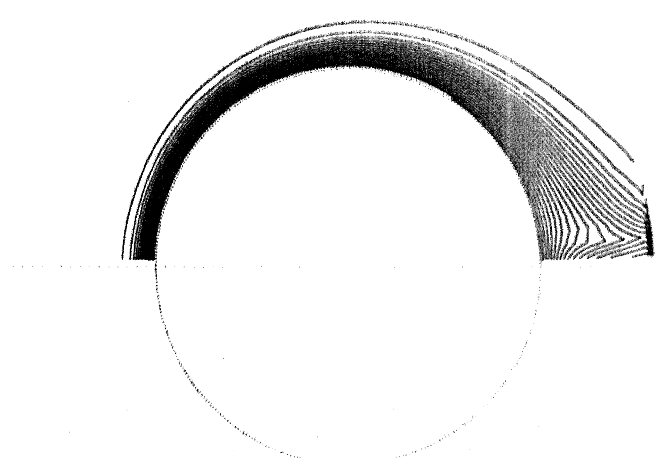

Figure 4.392

Isotherms for Re=10.0,n=0.5,and porosity 0.6 Pr=100.0(const wall temperature)

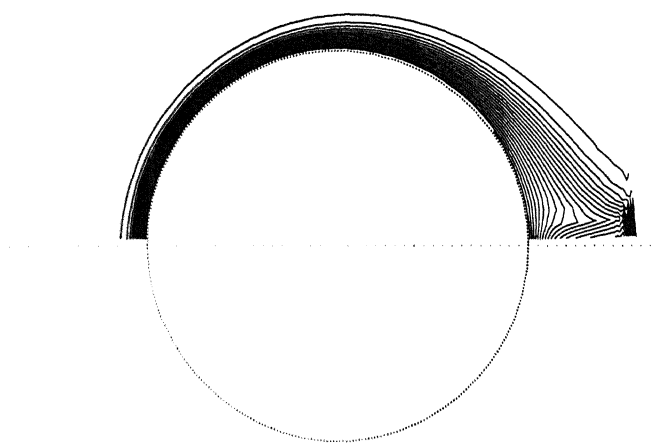

Figure 4.393

Isotherms for Re=10.0,n=0.5,and porosity 0.6 Pr=500.0(const wall temperature)

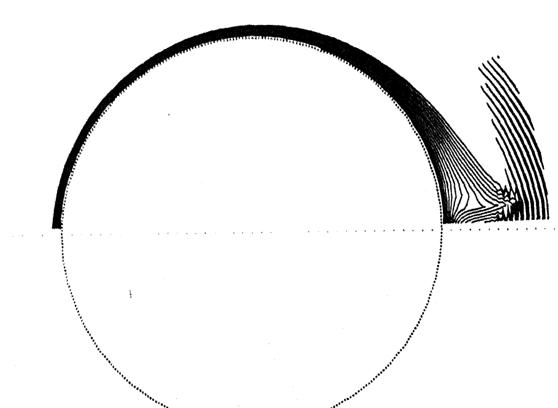

Figure 4.394

Isotherms for Re=100.0,n=0.5,and porosity 0.6 Pr=1.0(const wall temperature)

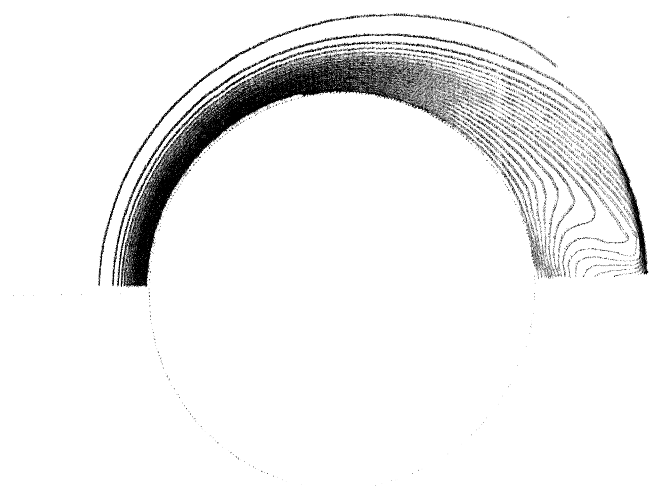

Figure 4.395

Isotherms for Re=100.0,n=0.5,and porosity 0.6 Pr=10.0(const wall temperature)

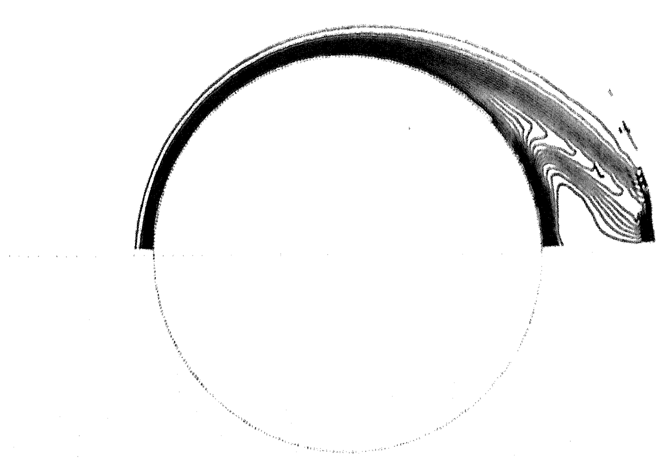

Figure 4.396

Isotherms for Re=100.0,n=0.5,and porosity 0.6 Pr=50.0(const wall temperature)

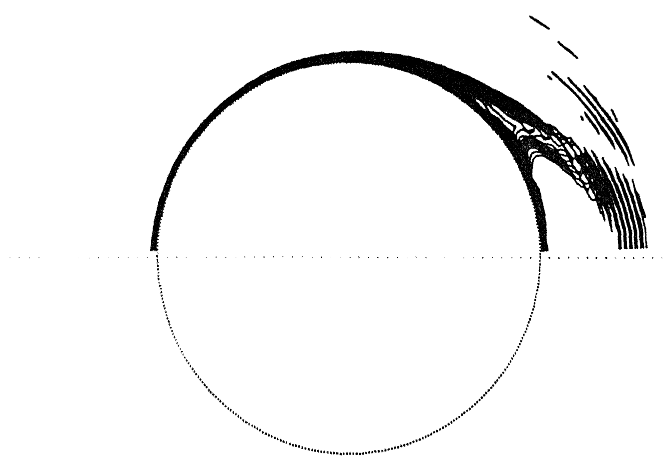

Figure 4.397

Isotherms for Re=100.0,n=0.5,and porosity 0.6 Pr=100.0(const wall temperature)

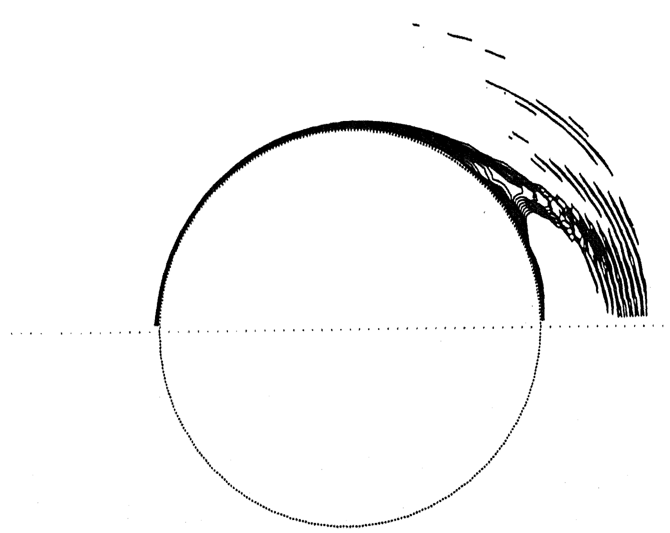

Figure 4.398.

Isotherms for Re=1.0,n=1.0,and porosity 0.4 Pr=1.0(const heat flux)

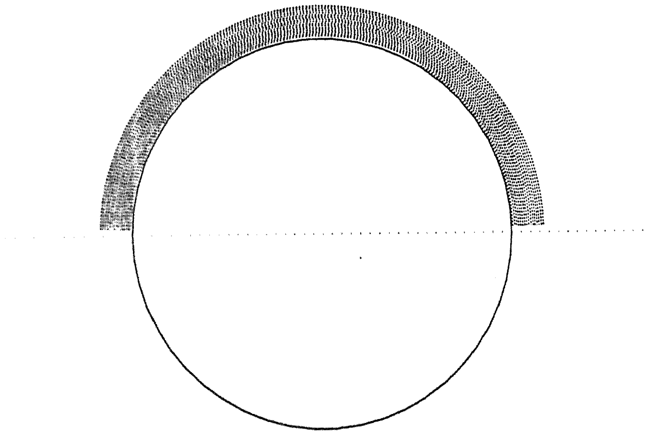

Figure 4.399.

Isotherms for Re=1.0,n=1.0,and porosity 0.4 Pr=10.0(const heat flux)

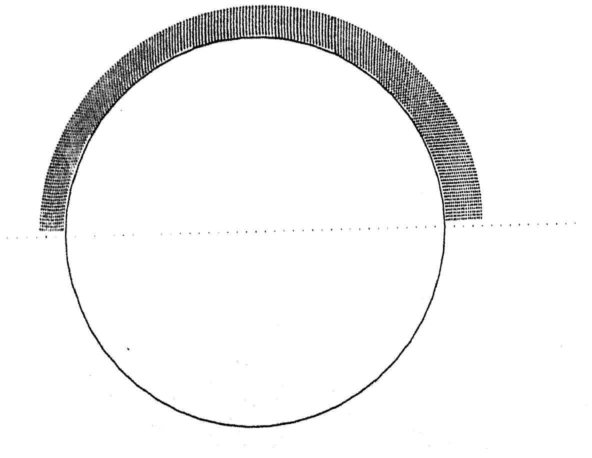

Figure 4.400

Isotherms for Re=1.0,n=1.0,and porosity 0.4 Pr=50.0(const heat flux)

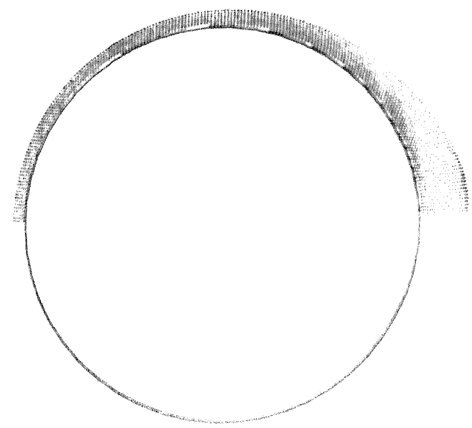

Figure 4.401

Isotherms for Re=1.0,n=1.0,and porosity 0.4 Pr=100.0(const heat flux)

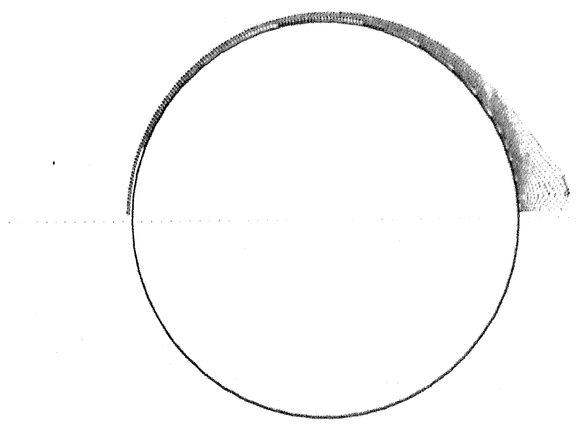

Figure 4.402

Isotherms for Re=1.0,n=1.0,and porosity 0.4 Pr=500.0(const heat flux)

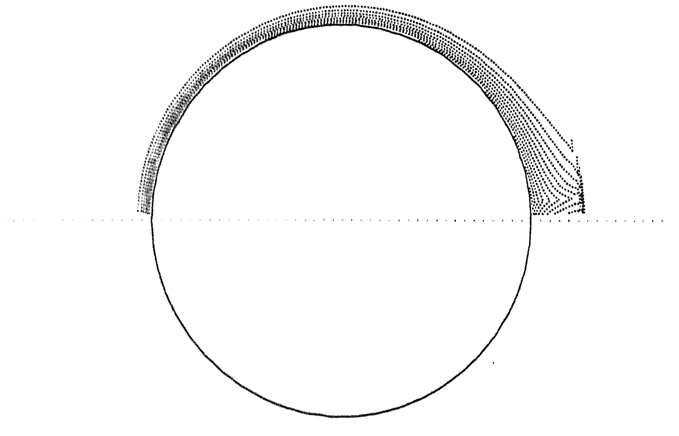

Figure 4.403

Isotherms for Re=10.0,n=1.0,and porosity 0.4 Pr=1.0(const heat flux)

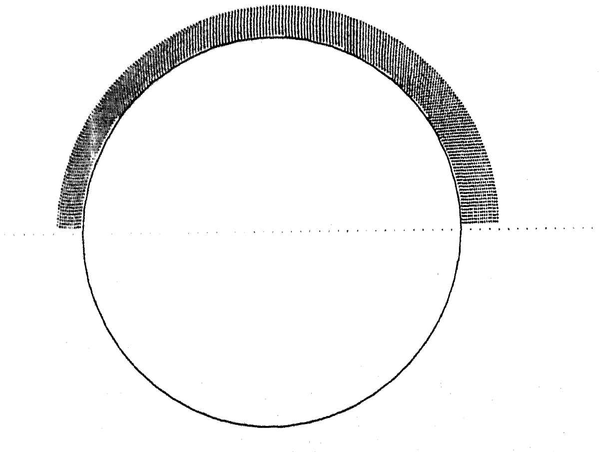

Figure 4.404

Isotherms for Re=10.0,n=1.0,and porosity 0.4 Pr=10.0(const heat flux)

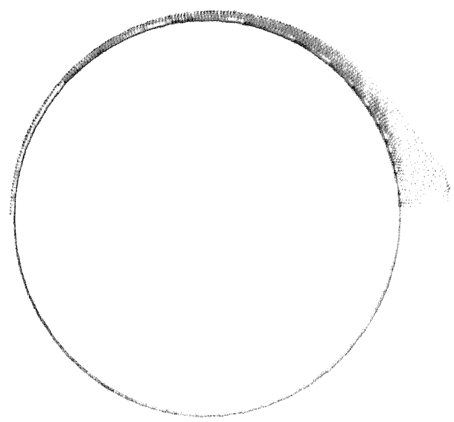

Figure 4.405

Isotherms for Re=10.0,n=1.0,and porosity 0.4 Pr=100.0(const heat flux)

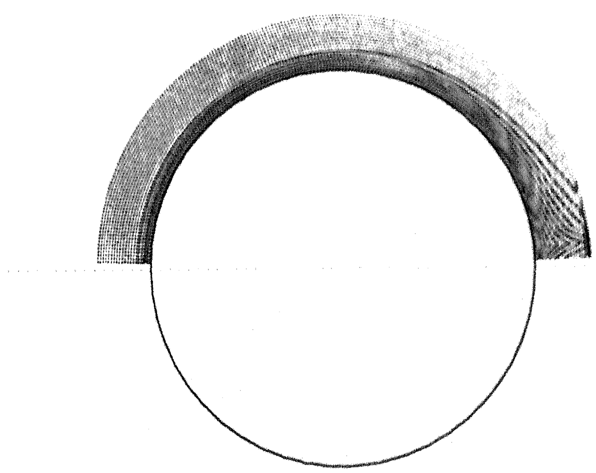

Figure 4.406

Isotherms for Re=10.0,n=1.0,and porosity 0.4 Pr=100.0(const heat flux)

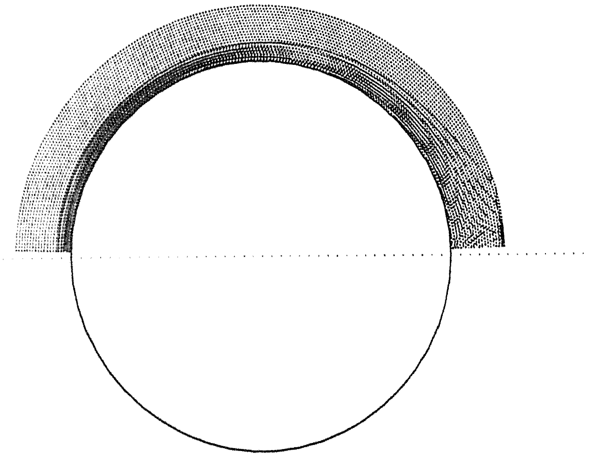

Figure 4.407

Isotherms for Re=10.0,n=1.0,and porosity 0.4 Pr=500.0(const heat flux)

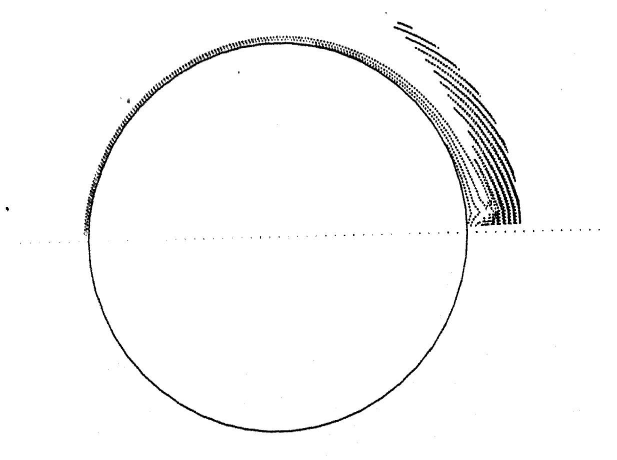

Figure 4.408

Isotherms for Re=100.0,n=1.0,and porosity 0.4 Pr=1.0(const heat flux)

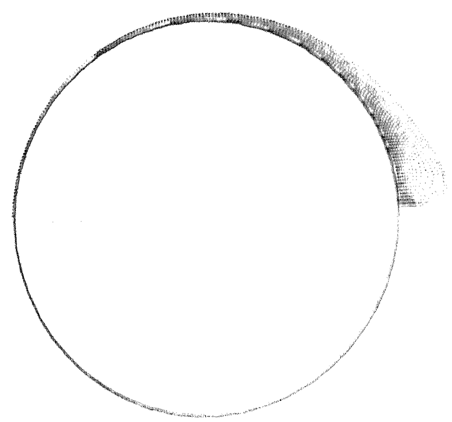

Figure 4.409

Isotherms for Re=100.0,n=1.0,and porosity 0.4 Pr=10.0(const heat flux)

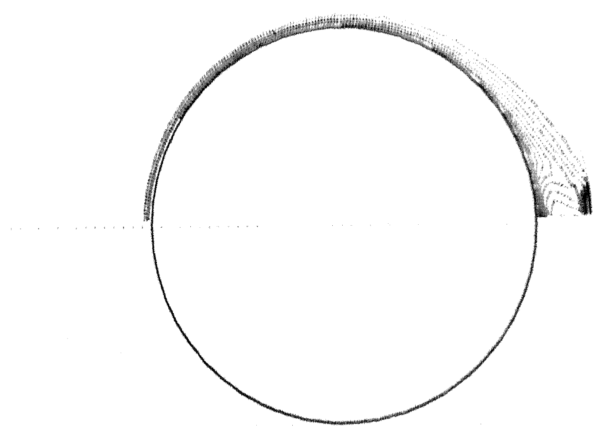

Figure 4.410

Isotherms for Re=100.0,n=1.0,and porosity 0.4 Pr=10.0(const heat flux)

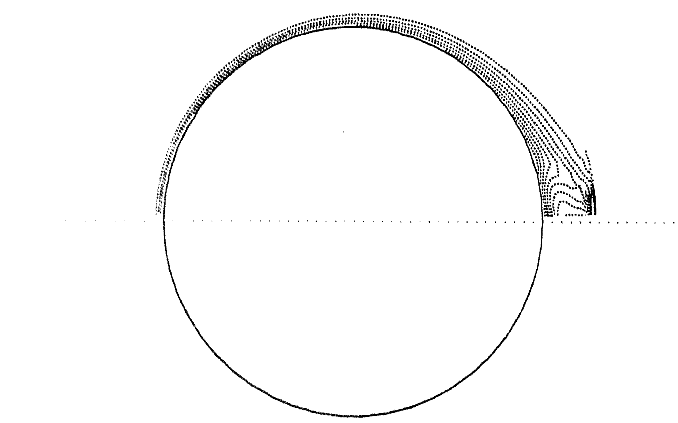

Figure 4.411

Isotherms for Re=100.0,n=1.0,and porosity 0.4 Pr=100.0(const heat flux)

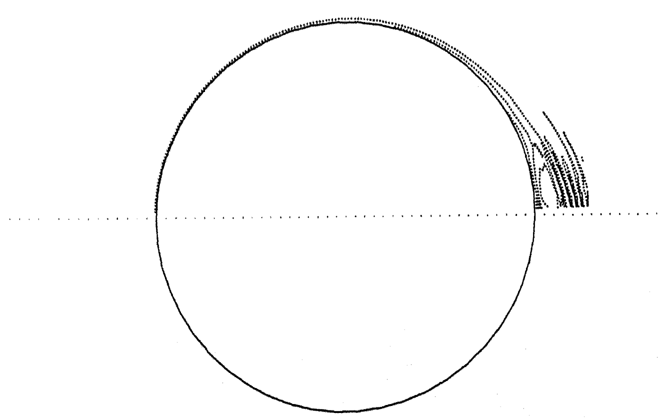

Figure 4.412

Isotherms for Re=100.0,n=1.0,and porosity 0.4 Pr=100.0(const heat flux)

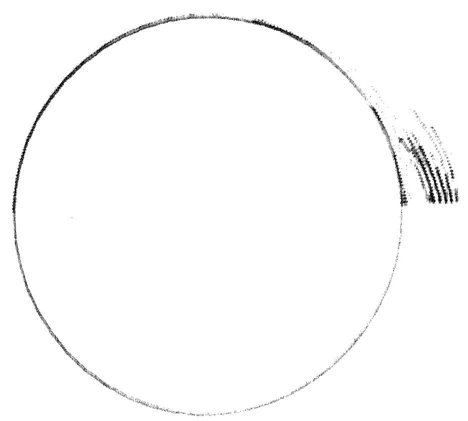

Figure 4.413

Isotherms for Re=200.0,n=1.0,and porosity 0.4 Pr=10.0(const heat flux)

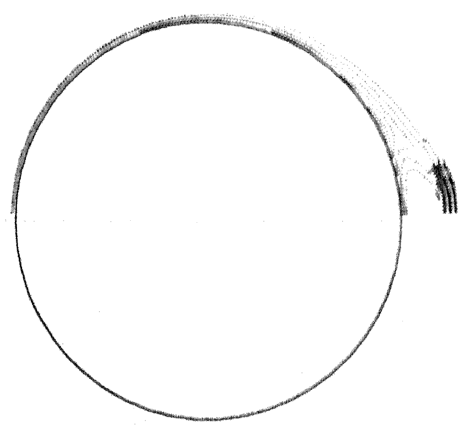

Figure 4.414

Isotherms for Re=200.0,n=1.0,and porosity 0.4 Pr=10.0(const heat flux)

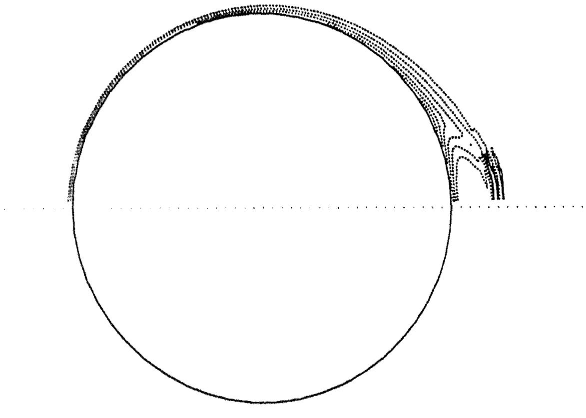

Figure 4.415

Isotherms for Re=200.0,n=1.0,and porosity 0.4 Pr=100.0(const heat flux)

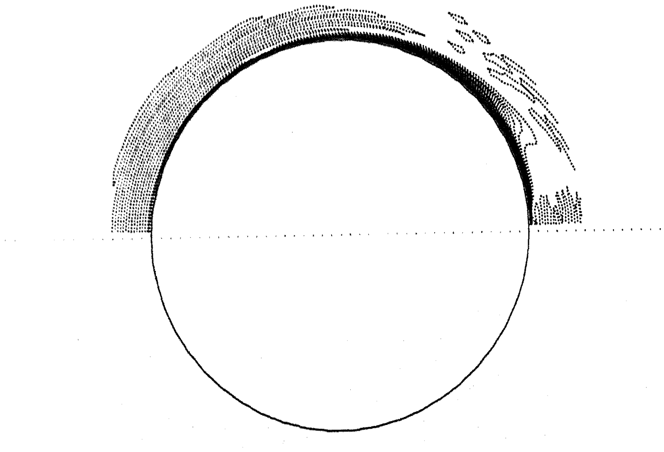

Figure 4.416

Isotherms for Re=200.0,n=1.0,and porosity 0.4 Pr=100.0(const heat flux)

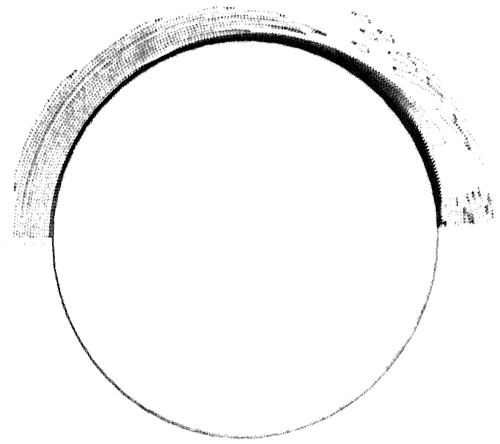

Figure 4.417

Isotherms for Re=200.0,n=1.0,and porosity 0.4 Pr=500.0(const heat flux)

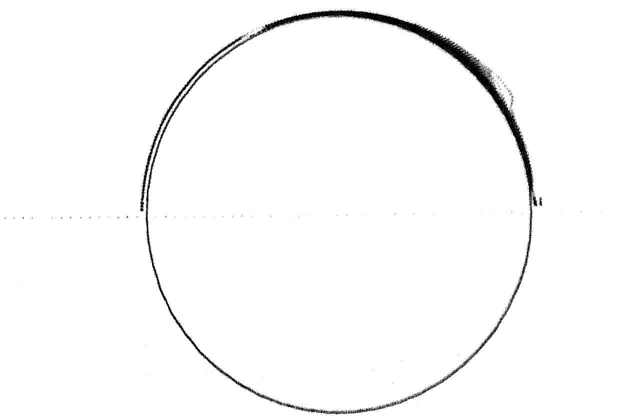

Figure 4.418

Isotherms for Re=500.0,n=1.0,and porosity 0.4 Pr=1.0(const heat flux)

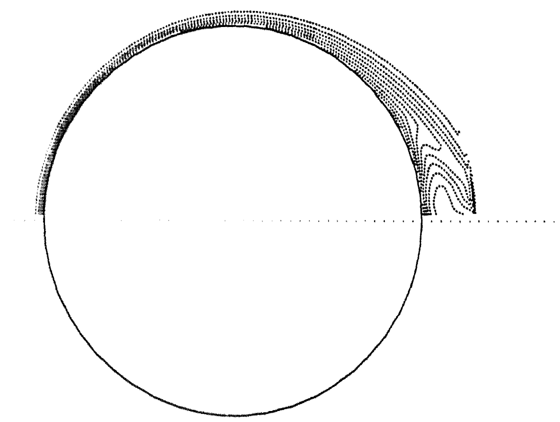

Figure 4.419

Isotherms for Re=500.0,n=1.0,and porosity 0.4 Pr=10.0(const heat flux)

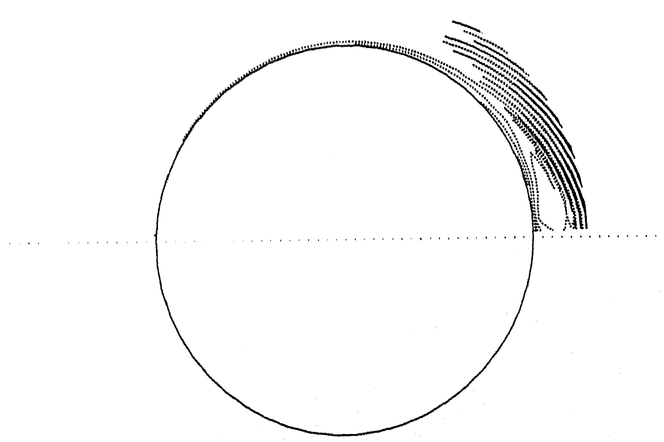

Figure 4.420

Isotherms for Re=500.0,n=1.0,and porosity 0.4 Pr=50.0(const heat flux)

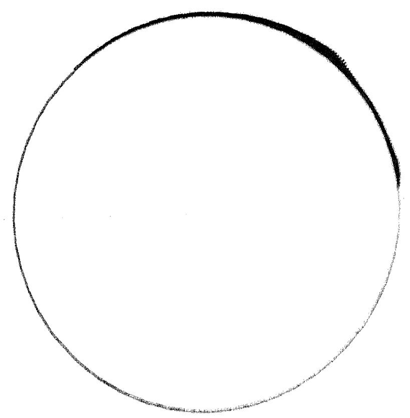

Figure 4.421

Isotherms for Re=500.0,n=1.0,and porosity 0.4 Pr=100.0(const heat flux)

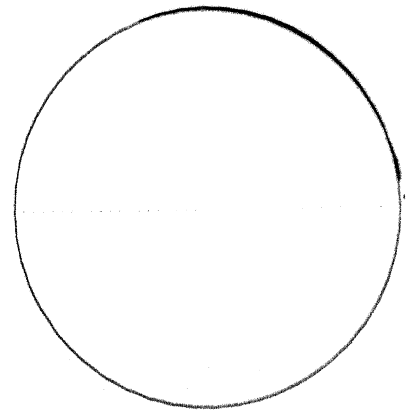

Figure 4.422

Isotherms for Re=1.0,n=0.8,and porosity 0.4 Pr=1.0(const heat flux)

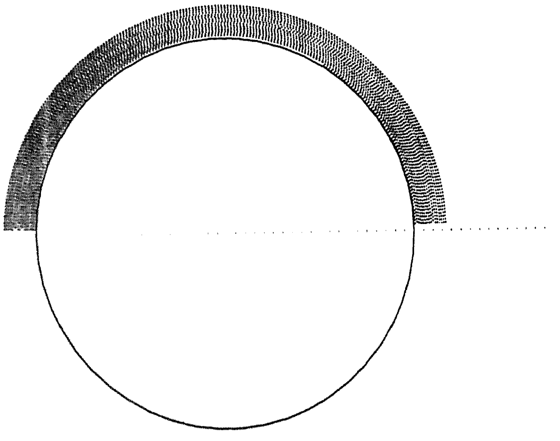

Figure 4.423

Isotherms for Re=1.0,n=0.8,and porosity 0.4 Pr=10.0(const heat flux)

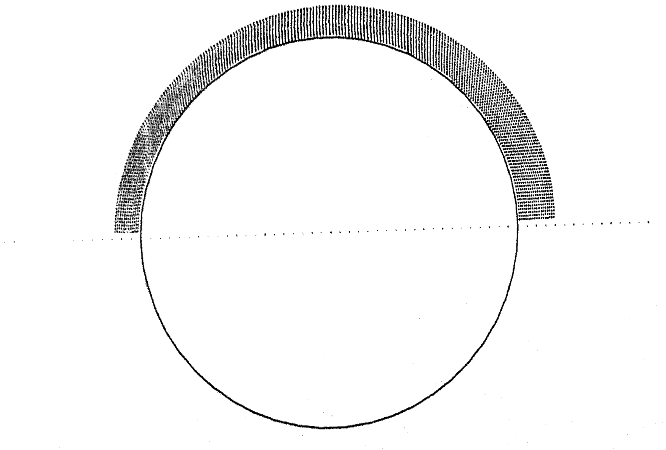

Figure 4.424

Isotherms for Re=1.0,n=0.8,and porosity 0.4 Pr=50.0(const heat flux)

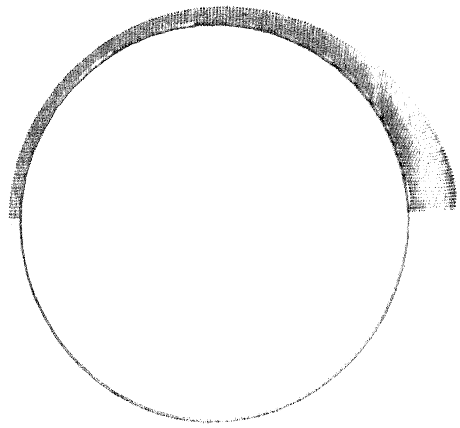

Figure 4.425

Isotherms for Re=1.0,n=0.8,and porosity 0.4 Pr=100.0(const heat flux)

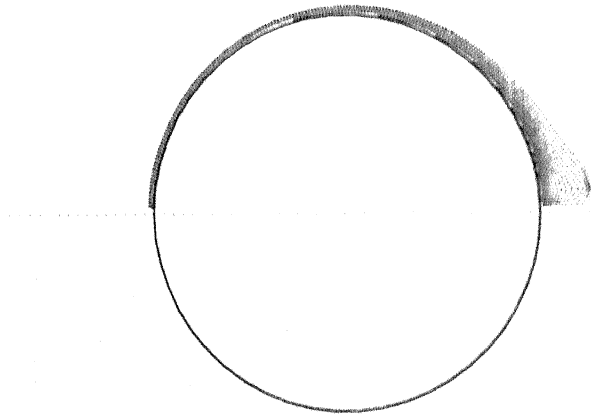

Figure 4.426

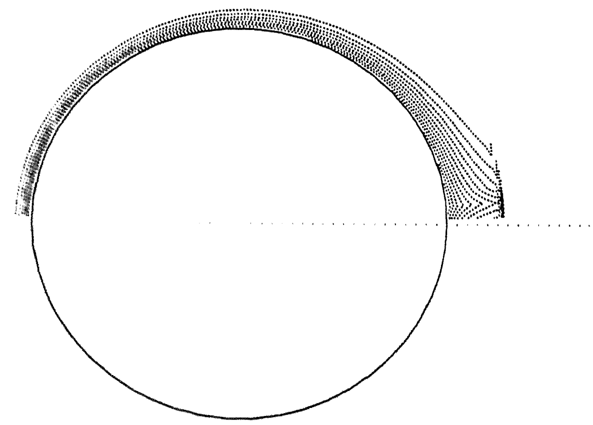

Isotherms for Re=1.0,n=0.8,and porosity 0.4 Pr=500.0(const heat flux)

Figure 4.427

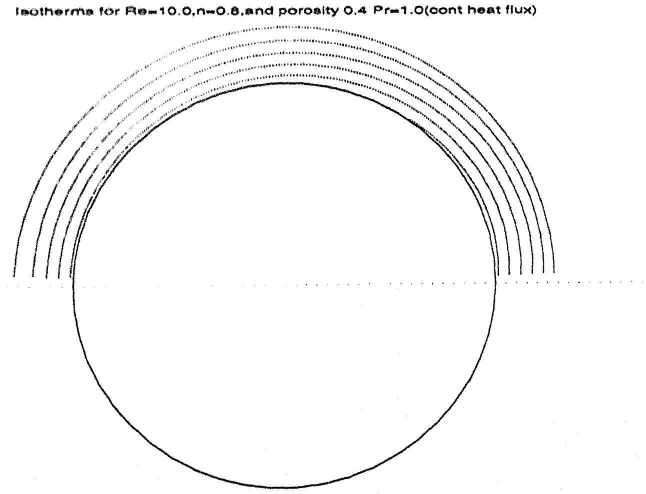

Isotherms for Re=10.0,n=0.8,and porosity 0.4 Pr=1.0(cont heat flux)

Figure 4.428

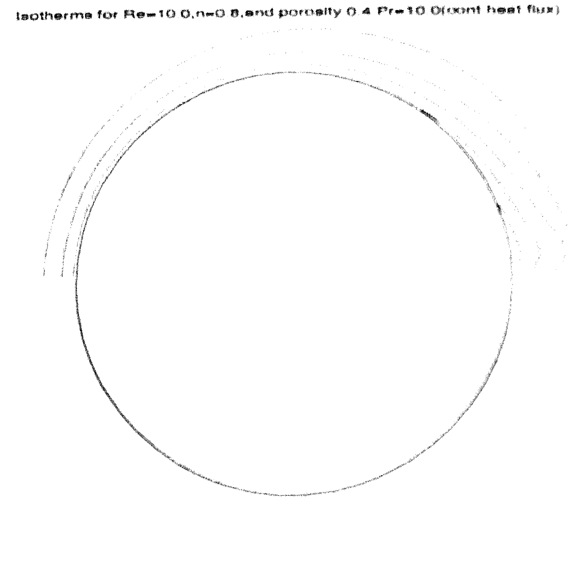

Figure 4.429

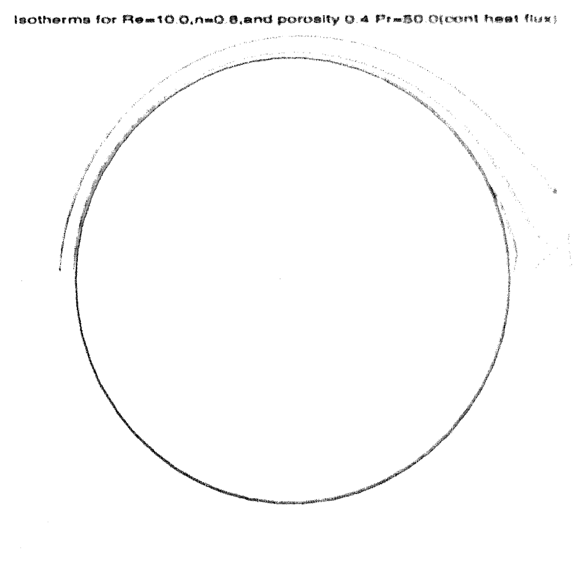

Figure 4.430

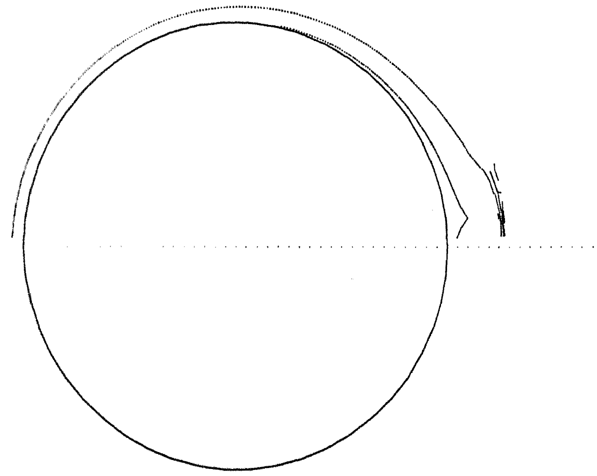

Figure 4.431

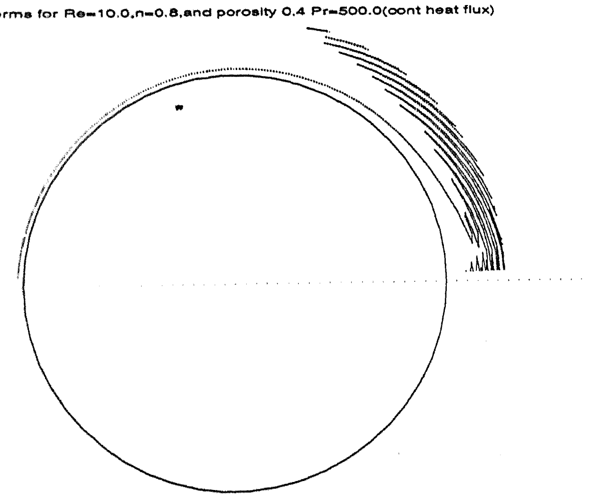

Figure 4.432

Isotherms for Re=100.0,n=0.8,and porosity 0.4 Pr=1.0(const heat flux)

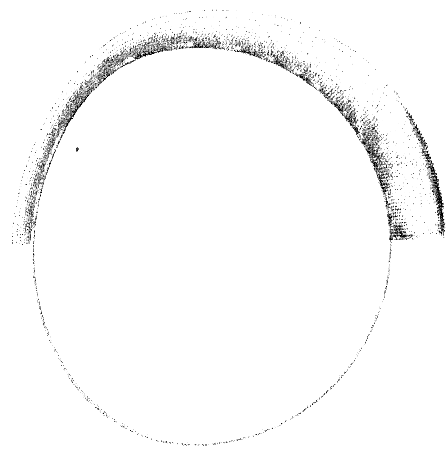

Figure 4.433

Isotherms for Re=100.0,n=0.8,and porosity 0.4 Pr=10.0(const heat flux)

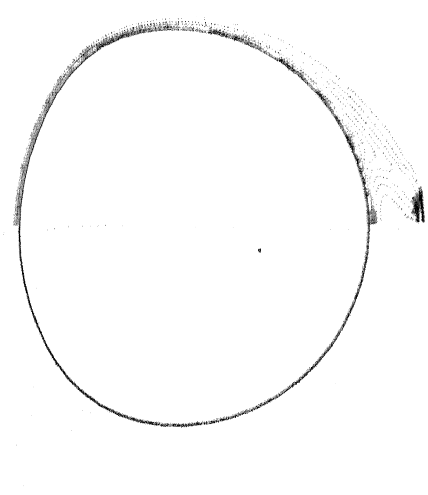

Figure 4.434

Isotherms for Re=100.0,n=0.8,and porosity 0.4 Pr=50.0(const heat flux)

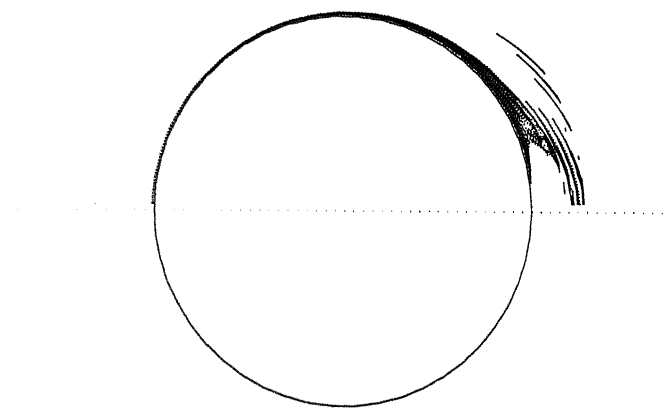

Figure 4.435

Isotherms for Re=100.0,n=0.8,and porosity 0.4 Pr=100.0(const heat flux)

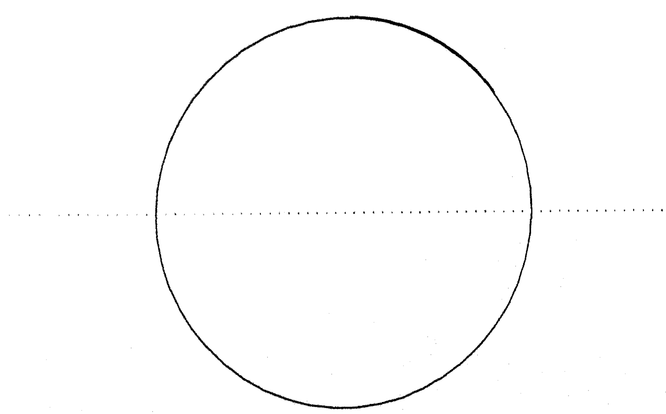

Figure 4.436

Isotherms for Re=100.0,n=0.8,and porosity 0.4 Pr=100.0(const heat flux)

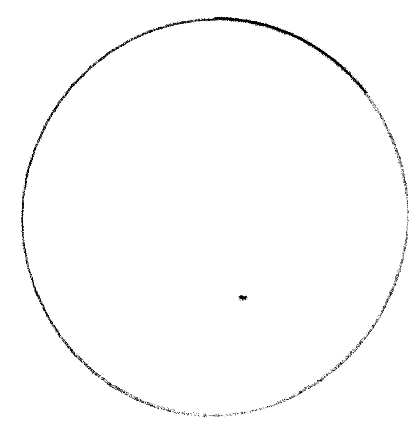

Figure 4.437

Isotherms for Re=200.0,n=0.8,and porosity 0.4 Pr=1.0(const heat flux)

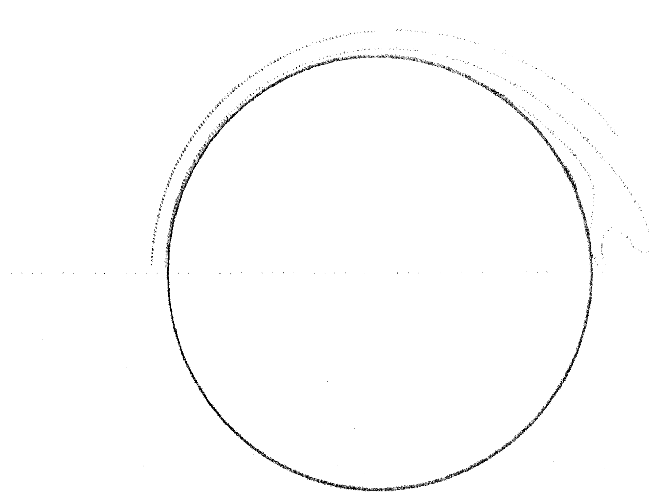

Figure 4.438

Isotherms for Re=200.0,n=0.8,and porosity 0.4 Pr=10.0(const heat flux)

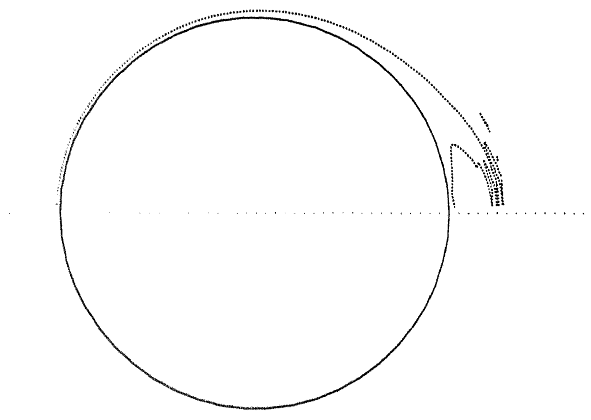

Figure 4.439

Isotherms for Re=200.0,n=0.8,and porosity 0.4 Pr=50.0(const heat flux)

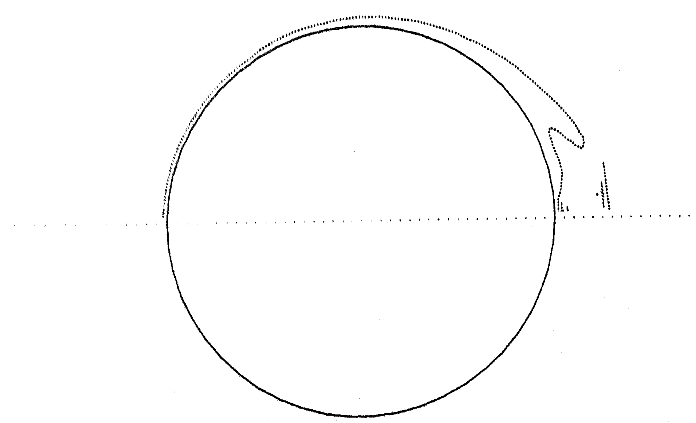

Figure 4.440

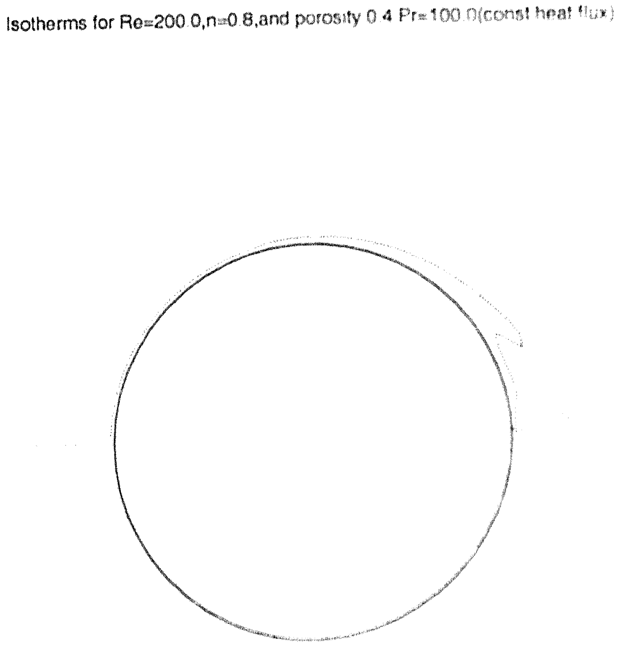

Figure 4.441

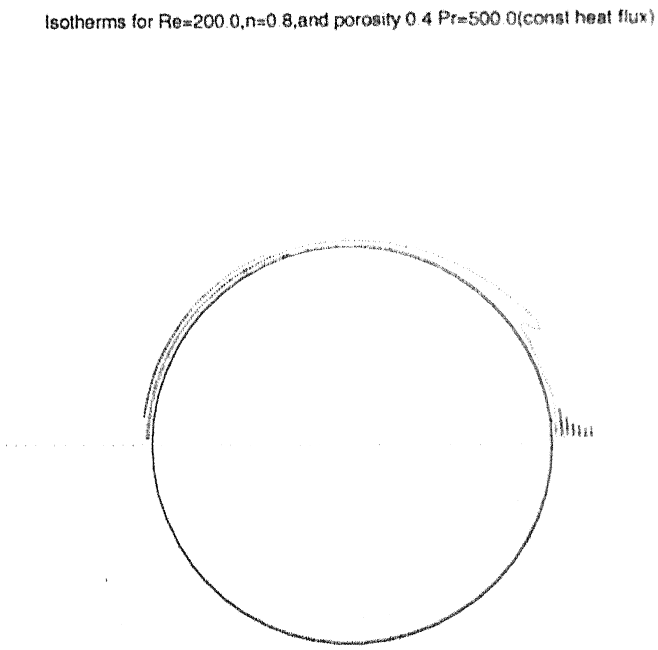

Figure 4.442

Isotherms for Re=500.0,n=0.8,and porosity 0.4 Pr=1.0(const heat flux)

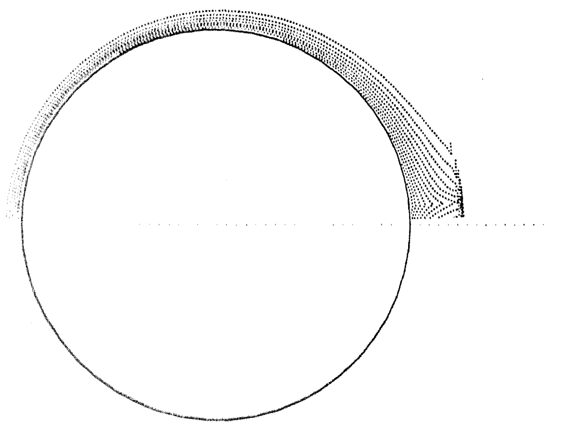

Figure 4.443

Isotherms for Re=500.0,n=0.8,and porosity 0.4 Pr=10.0(const heat flux)

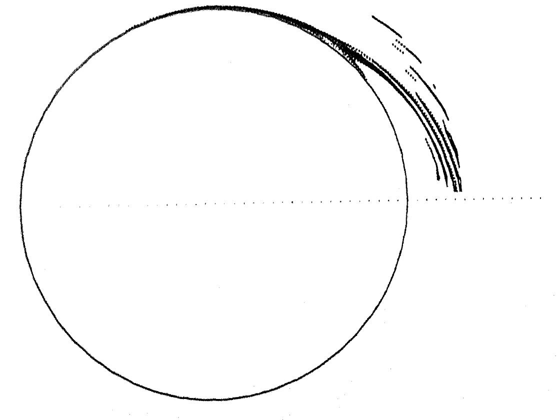

Figure 4.444

Isotherms for Re=500.0,n=0.8,and porosity 0.4 Pr=10.0(const heat flux)

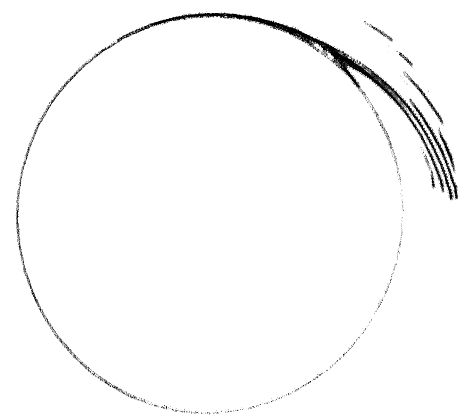

Figure 4.445

Isotherms for Re=500,n=0.8,and porosity 0.4 Pr=100.0(cont wall heat flux)

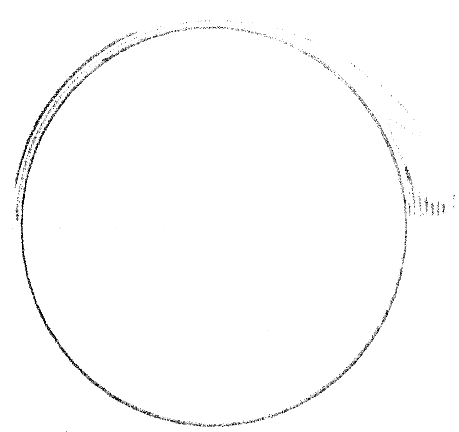

Figure 4.446

Isotherms for Re=10.0,n=0.6,and porosity 0.4 Pr=1.0(const heat flux)

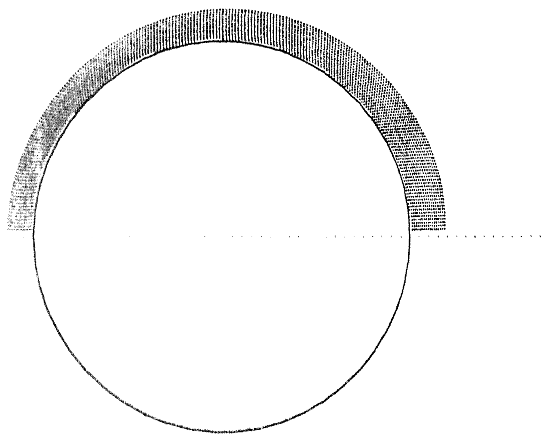

Figure 4.447

Isotherms for Re=10.0,n=0.6,and porosity 0.4 Pr=10.0(const heat flux)

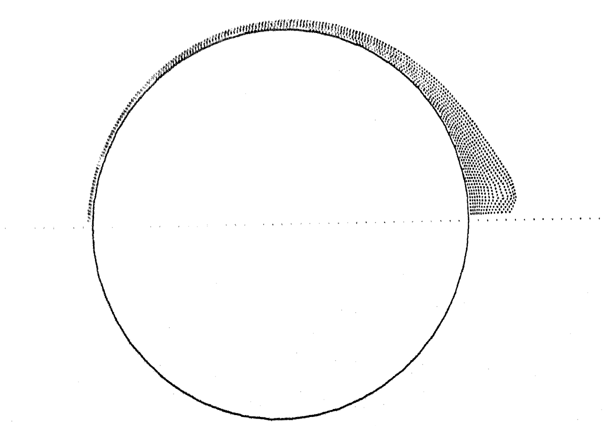

Figure 4.448

Isotherms for Re=10.0,n=0.6,and porosity 0.4 Pr=50.0(const heat flux)

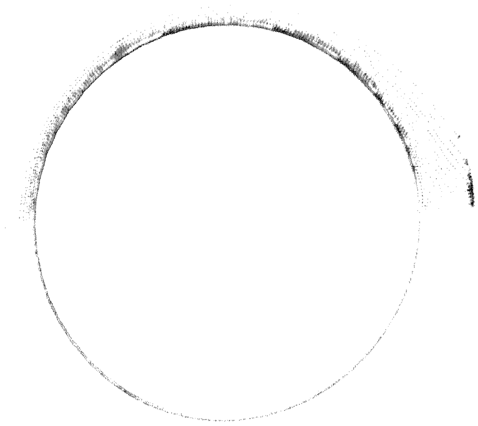

Figure 4.449

Isotherms for Re=10.0,n=0.6,and porosity 0.4 Pr=100.0(const heat flux)

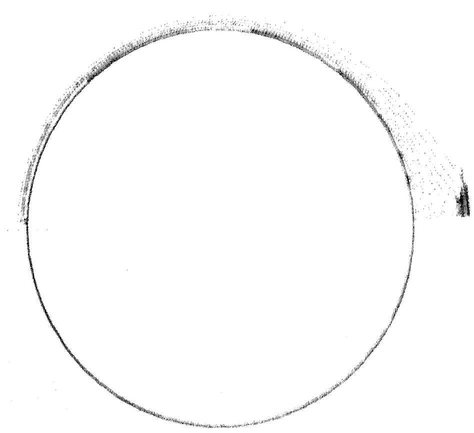

Figure 4.450

Isotherms for Re=10.0,n=0.6,and porosity 0.4 Pr=500.0(const heat flux)

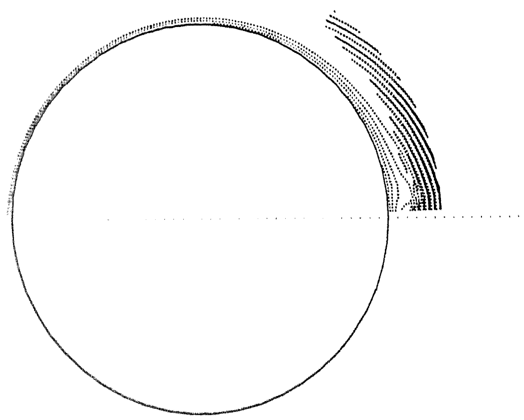

Figure 4.451

Isotherms for Re=100.0,n=0.6,and porosity 0.4 Pr=1.0(const heat flux)

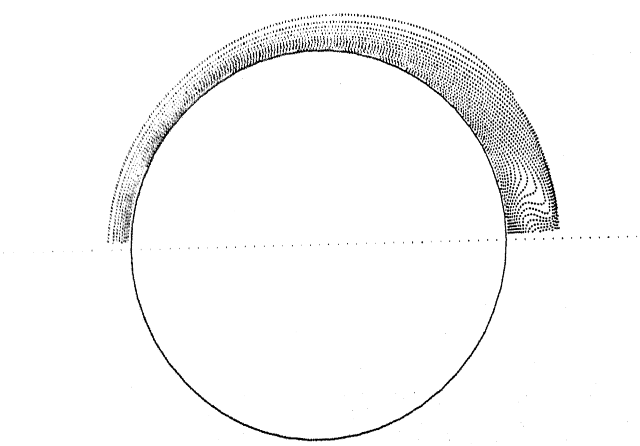

Figure 4.452

Isotherms for Re=100.0,n=0.6,and porosity 0.4 Pr=10.0(const heat flux)

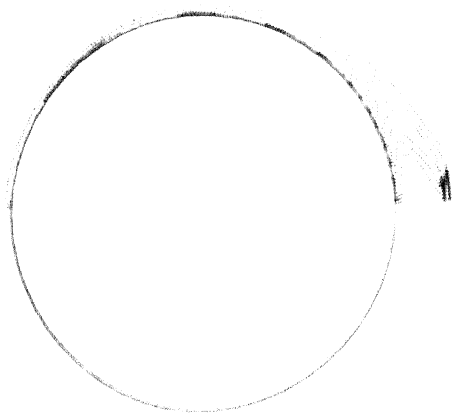

Figure 4.453

Isotherms for Re=100.0,n=0.6,and porosity 0.4 Pr=50.0(const heat flux)

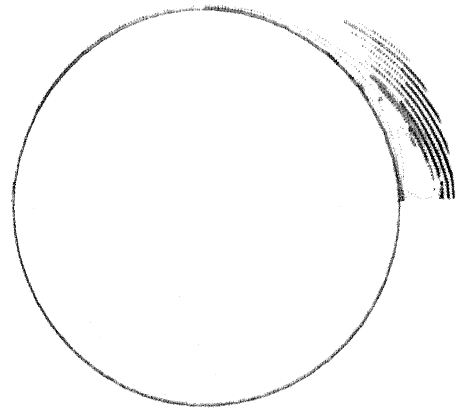

Figure 4.454

Isotherms for Re=100.0,n=0.6,and porosity 0.4 Pr=100.0(const heat flux)

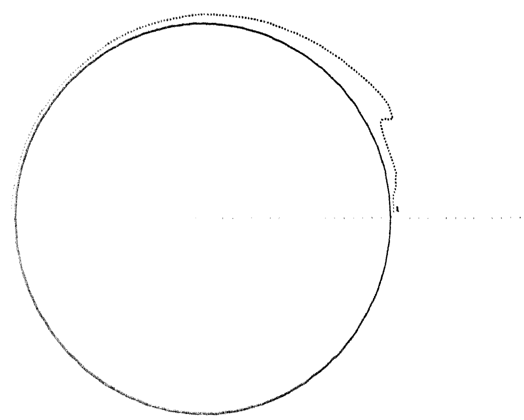

Figure 4.455

Isotherms for Re=100.0,n=0.6,and porosity 0.4 Pr=500.0(const heat flux)

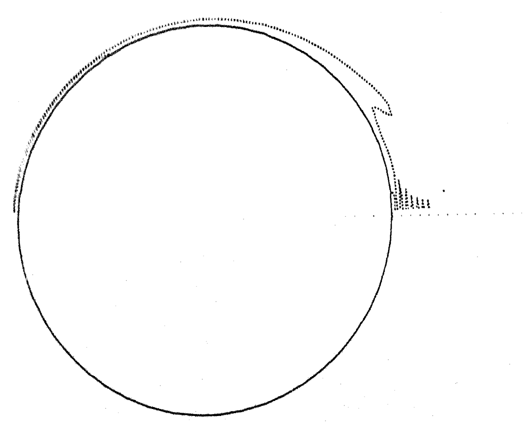

Figure 4.456

Isotherms for Re=200.0,n=0.6,and porosity 0.4 Pr=1.0(const heat flux)

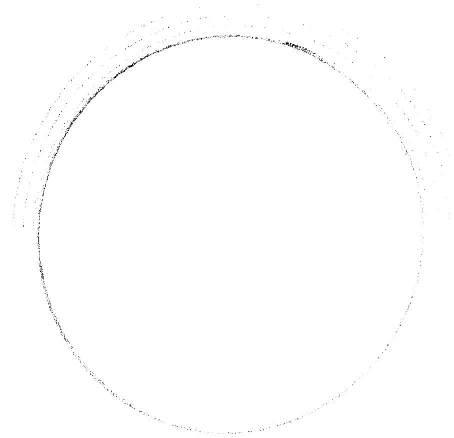

Figure 4.457

Isotherms for Re=200.0,n=0.6,and porosity 0.4 Pr=10.0(const heat flux)

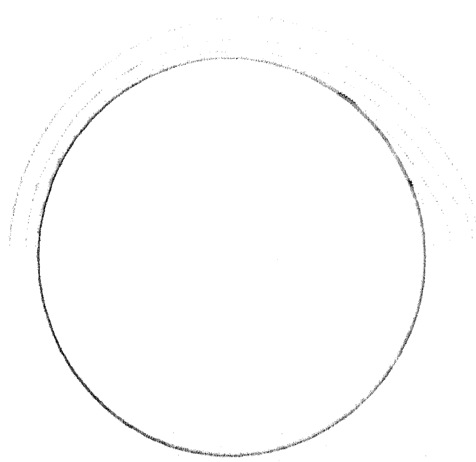

Figure 4.458

Isotherms for Re=200.0,n=0.6,and porosity 0.4 Pr=50.0(const heat flux)

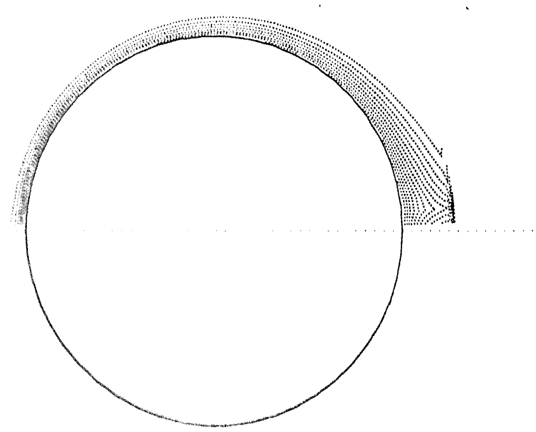

Figure 4.459

Isotherms for Re=200.0,n=0.6,and porosity 0.4 Pr=100.0(const heat flux)

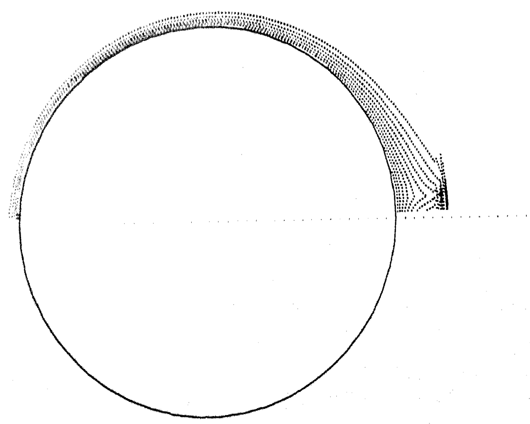

Figure 4.460

Isotherms for Re=200.0,n=0.6,and porosity 0.4 Pr=500.0(const heat flux)

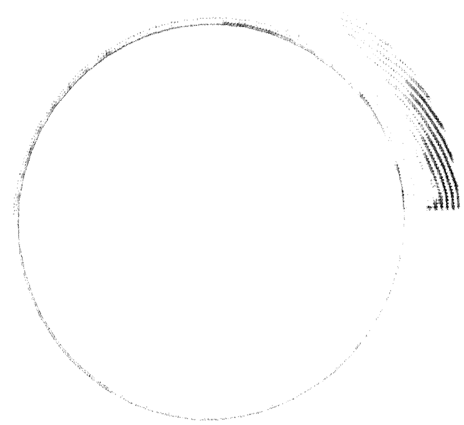

Figure 4.461

Isotherms for Re=1.0,n=0.5,and porosity 0.4 Pr=1.0(const heat flux)

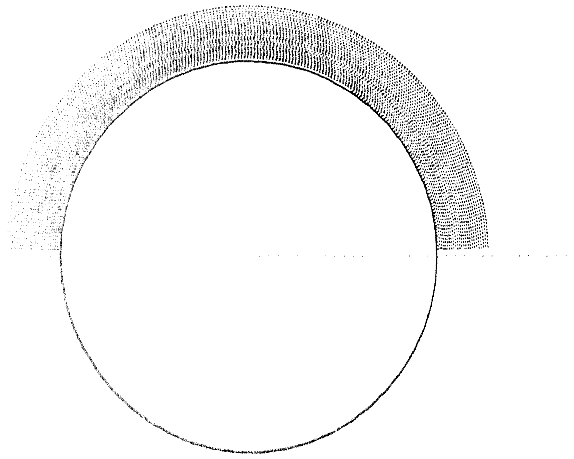

Figure 4.462

Isotherms for Re=1.0,n=0.5,and porosity 0.4 Pr=10.0(const heat flux)

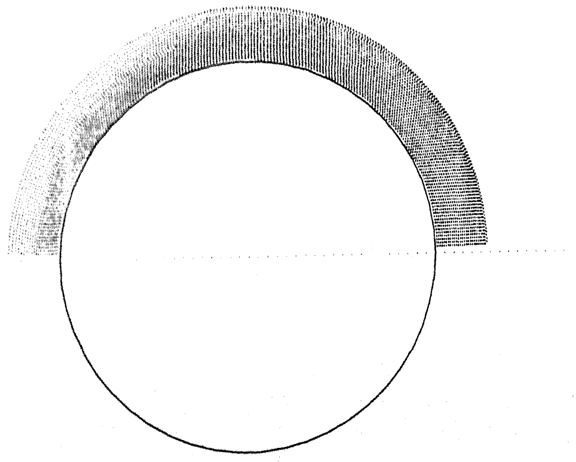

Figure 4.463

Isotherms for Re=1.0,n=0.5,and porosity 0.4 Pr=50.0(const heat flux)

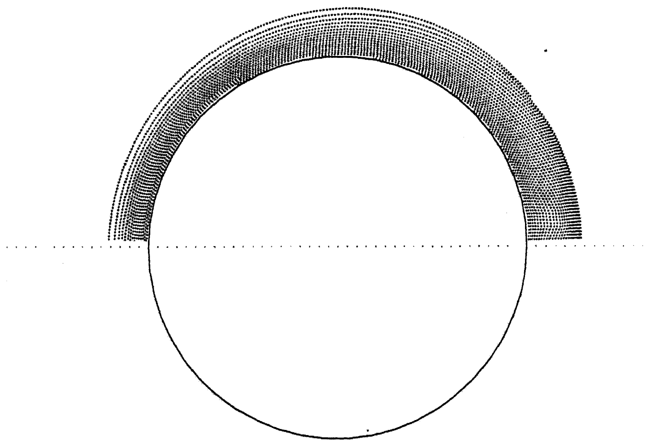

Figure 4.464

Isotherms for Re=1.0,n=0.5,and porosity 0.4 Pr=100.0(const heat flux)

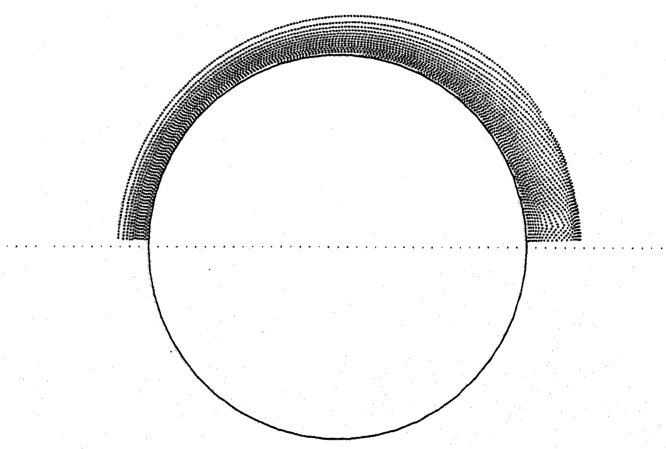

Figure 4.465

Isotherms for Re=1.0,n=0.5,and porosity 0.4 Pr=500.0(const heat flux)

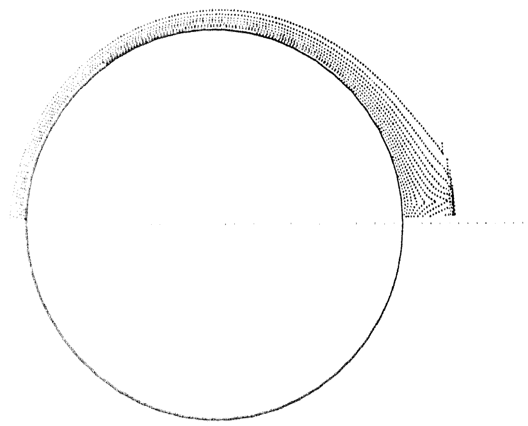

Figure 4.466

Isotherms for Re=10.0,n=0.5,and porosity 0.4 Pr=100.0(const heat flux)

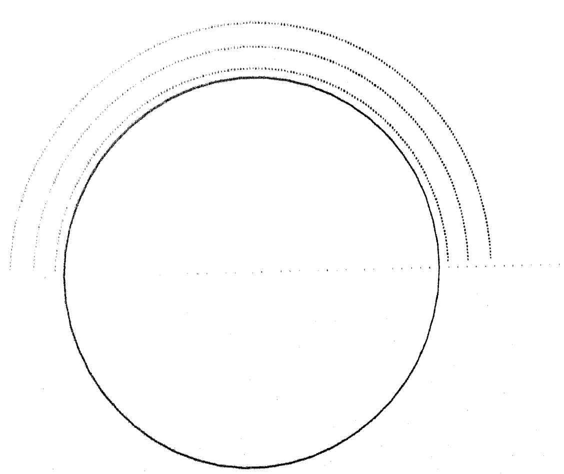

Figure 4.467

Isotherms for Re=10.0,n=0.5,and porosity 0.4 Pr=100.0(const heat flux)

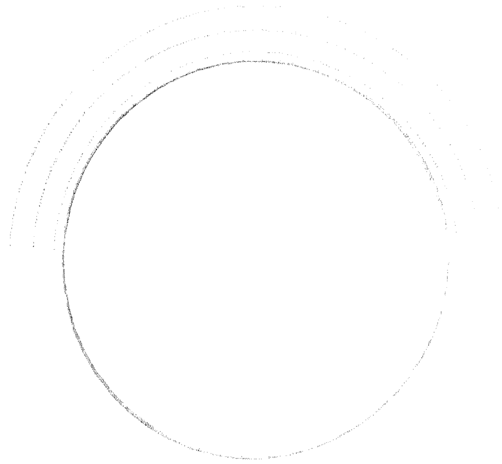

Figure 4.468

Isotherms for Re=10.0,n=0.5,and porosity 0.4 Pr=500.0(const heat flux)

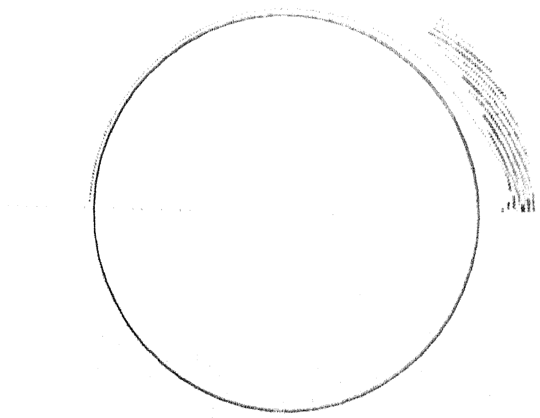

Figure 4.469

Isotherms for Re=100.0,n=0.5,and porosity 0.4 Pr=1.0(const heat flux)

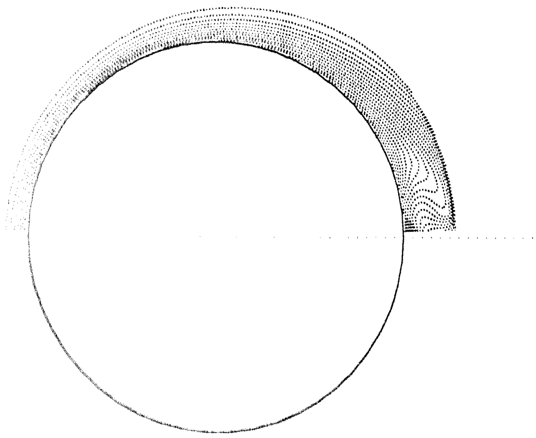

Figure 4.470

Isotherms for Re=100.0,n=0.5,and porosity 0.4 Pr=10.0(const heat flux)

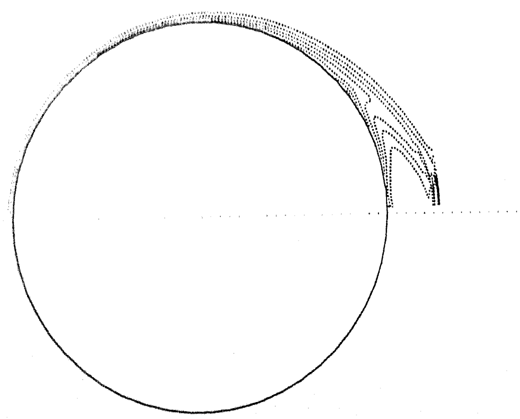

Figure 4.471

Isotherms for Re=100.0,n=0.5,and porosity 0.4 Pr=50.0(const heat flux)

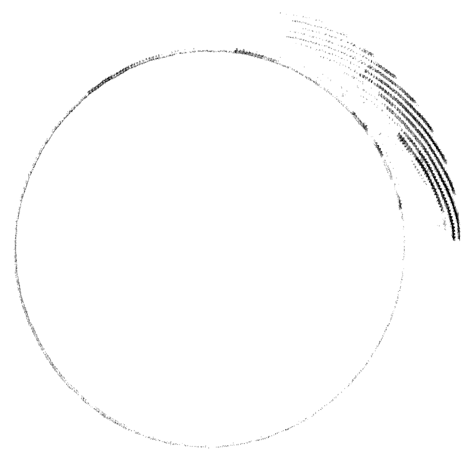

Figure 4.472

Isotherms for Re=100.0,n=0.5,and porosity 0.4 Pr=100.0(const heat flux)

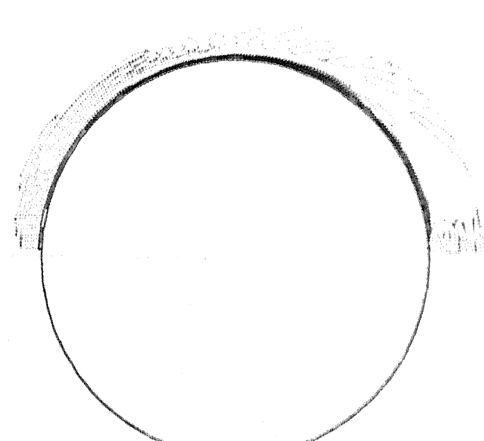

Figure 4.473

Isotherms for Re=100.0,n=0.5,and porosity 0.4 Pr=500.0(const heat flux)

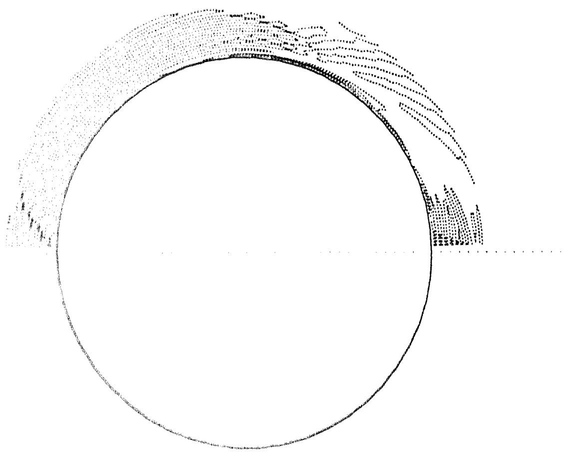

Figure 4.474

Isotherms for Re=1.0,n=0.8,and porosity 0.5 Pr=1.0(const heat flux)

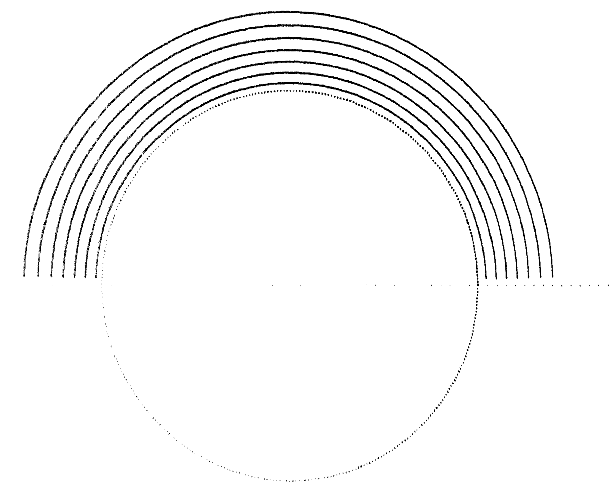

Figure 4.475

Isotherms for Re=1.0,n=0.8,and porosity 0.5 Pr=10.0(const heat flux)

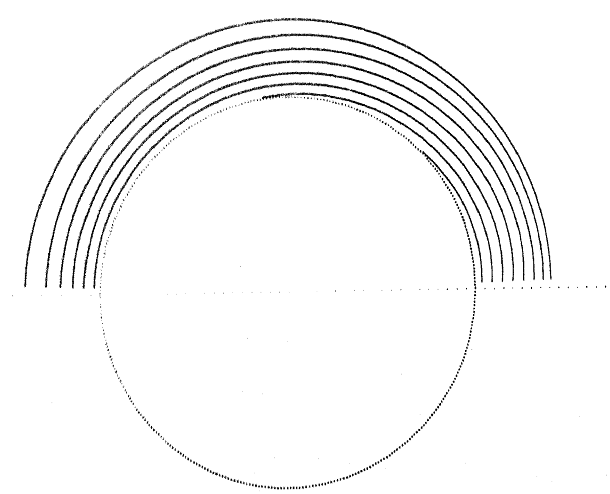

Figure 4.476

Isotherms for Re=1.0,n=0.8,and porosity 0.5 Pr=50.0(const heat flux)

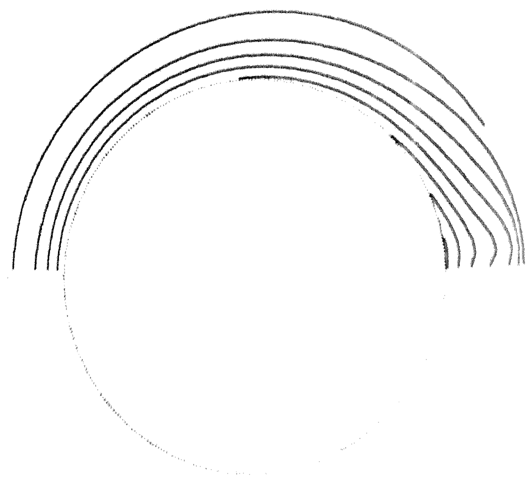

Figure 4.477

Isotherms for Re=1.0,n=0.8,and porosity 0.5 Pr=100.0(const heat flux)

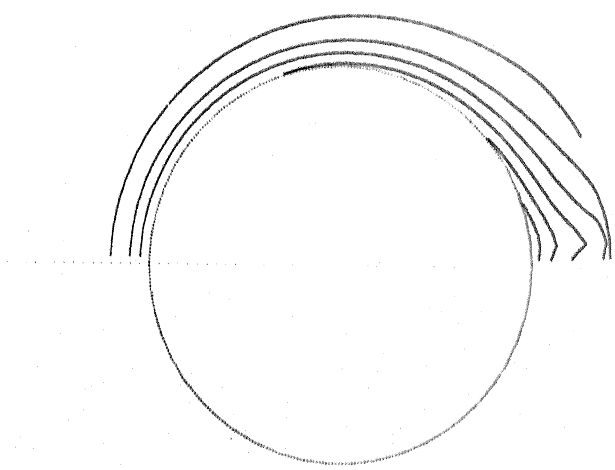

Figure 4.478

Isotherms for Re=1.0,n=0.8,and porosity 0.5 Pr=100.0(const heat flux)

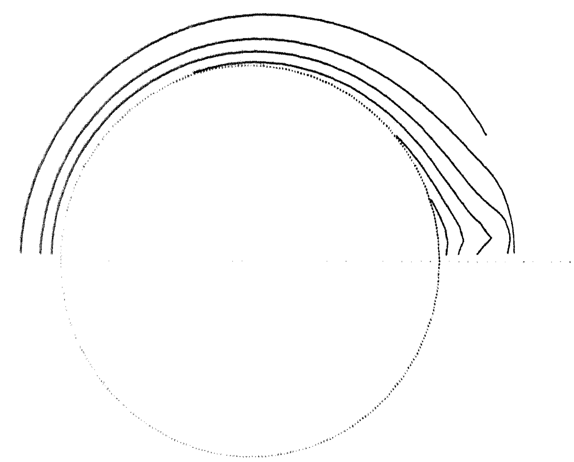

Figure 4.479

Isotherms for Re=1.0,n=0.8,and porosity 0.5 Pr=500.0(const heat flux)

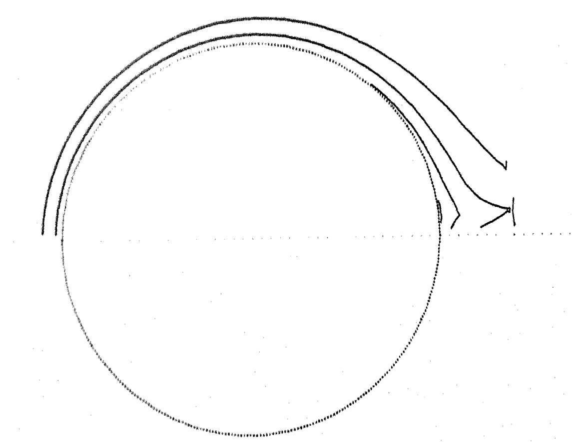

Figure 4.480

Isotherms for Re=10.0,n=0.8,and porosity 0.5 Pr=1.0(const heat flux)

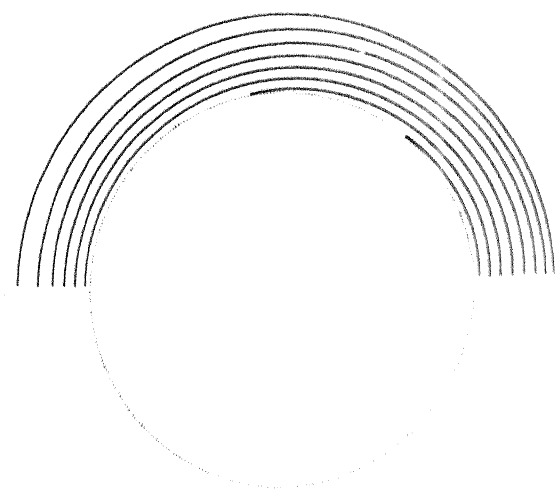

Figure 4.481

Isotherms for Re=10.0,n=0.8,and porosity 0.5 Pr=10.0(const heat flux)

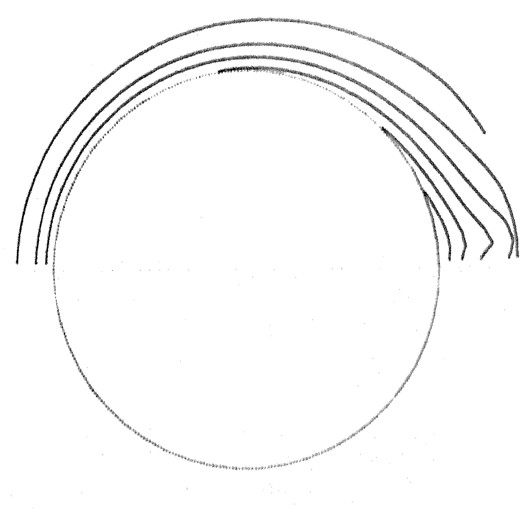

Figure 4.482

Isotherms for Re=10.0,n=0.8,and porosity 0.5 Pr=50.0(const heat flux)

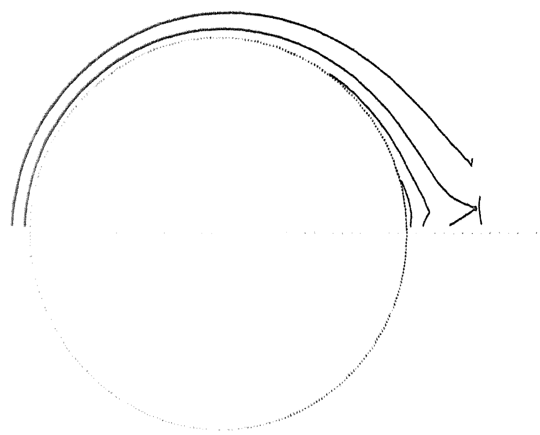

Figure 4.483

Isotherms for Re=10.0,n=0.8,and porosity 0.5 Pr=100.0(const heat flux)

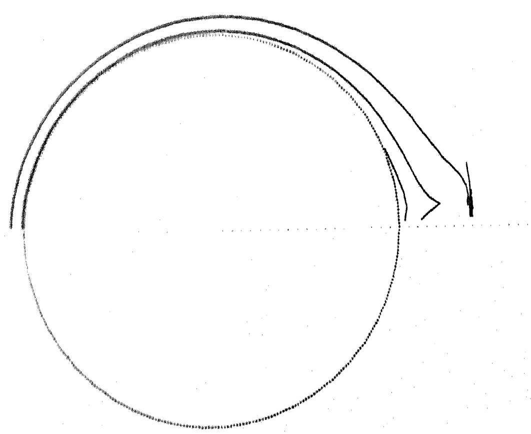

Figure 4.484

Isotherms for Re=10.0,n=0.8,and porosity 0.5 Pr=500.0(const heat flux)

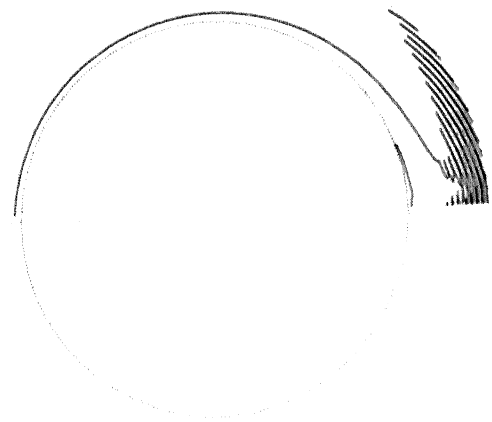

Figure 4.485

Isotherms for Re=100.0,n=0.8,and porosity 0.5 Pr=1.0(const heat flux)

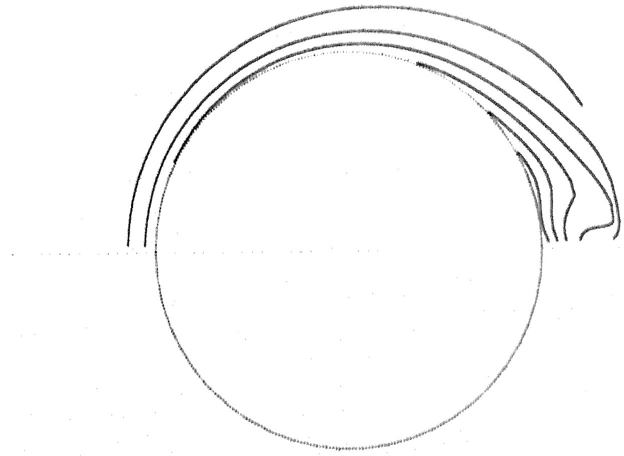

Figure 4.486

Isotherms for Re=100.0,n=0.8,and porosity 0.5 Pr=10.0(const heat flux)

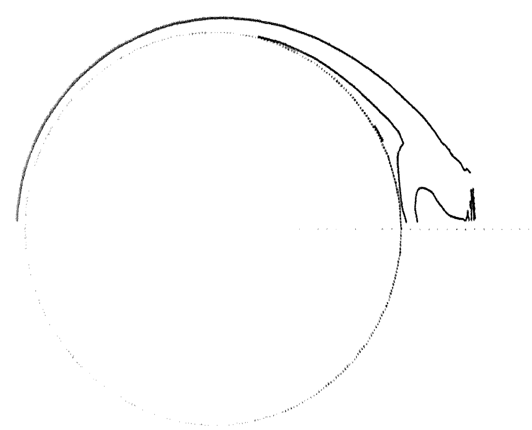

Figure 4.487

Isotherms for Re=100.0,n=0.8,and porosity 0.5 Pr=10.0(const heat flux)

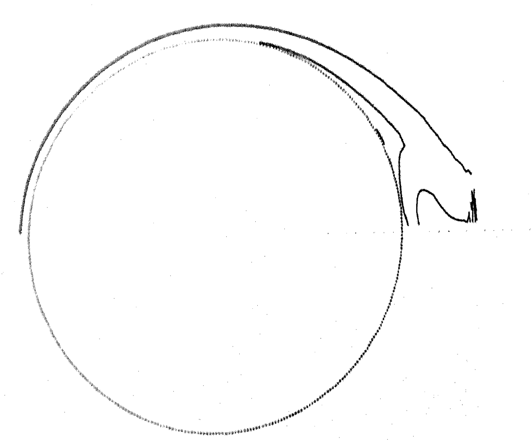

Figure 4.488

Isotherms for Re=100.0,n=0.8,and porosity 0.5 Pr=100.0(const heat flux)

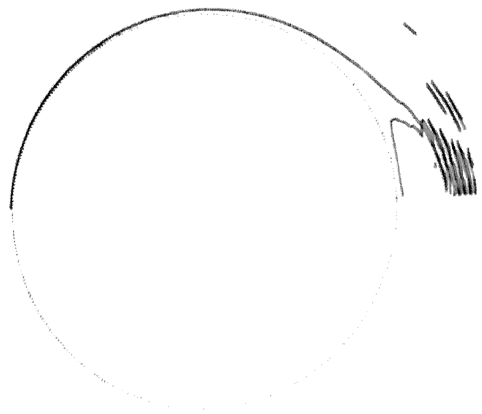

Figure 4.489

Isotherms for Re=100.0,n=0.8,and porosity 0.5 Pr=100.0(const heat flux)

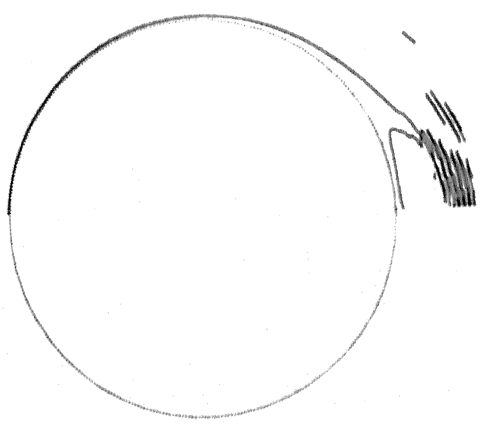

Figure 4.490

Isotherms for Re=200,n=0.8,and porosity 0.5 Pr=1.0(cont wall heat flux)

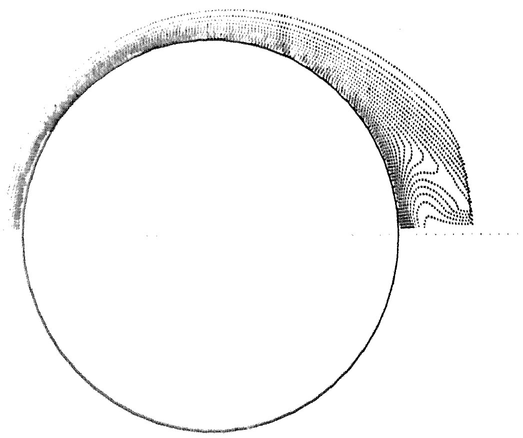

Figure 4.491

Isotherms for Re=200,n=0.8,and porosity 0.5 Pr=10.0(cont wall heat flux)

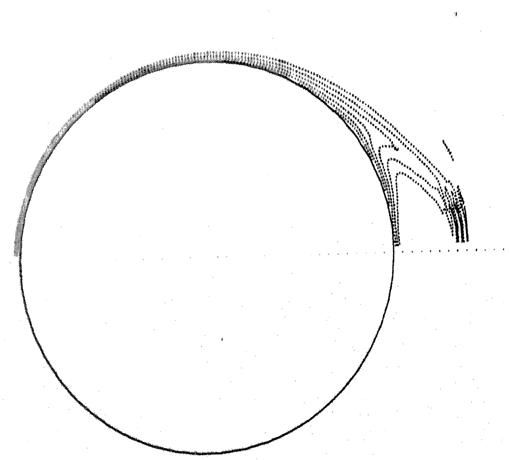

Figure 4.492

Isotherms for Re=200,n=0.8,and porosity 0.5 Pr=50.0(cont wall heat flux)

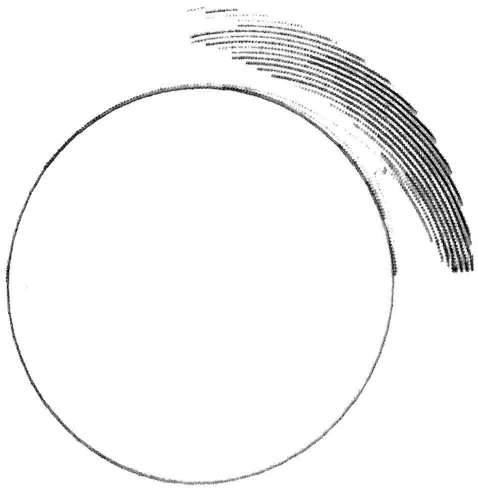

Figure 4.493

Isotherms for Re=200,n=0.8,and porosity 0.5 Pr=100.0(cont wall heat flux)

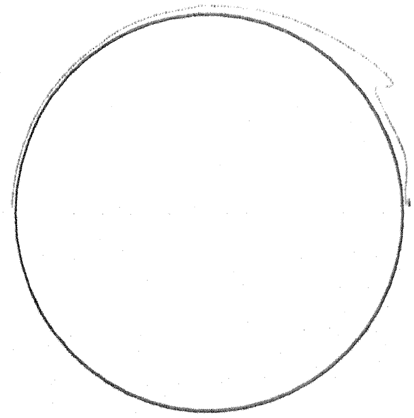

Figure 4.494

Isotherms for Re=200,n=0.8,and porosity 0.5 Pr=500.0(cont wall heat flux)

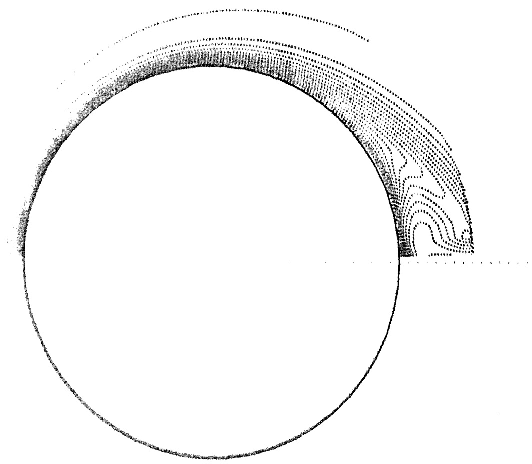

Figure 4.495

Isotherms for Re=500,n=0.8,and porosity 0.5 Pr=1.0(cont wall heat flux)

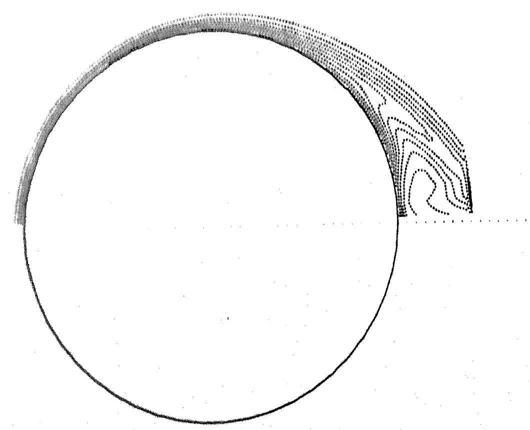

Figure 4.496

Isotherms for Re=500,n=0.8,and porosity 0.5 Pr=10.0(cont wall heat flux)

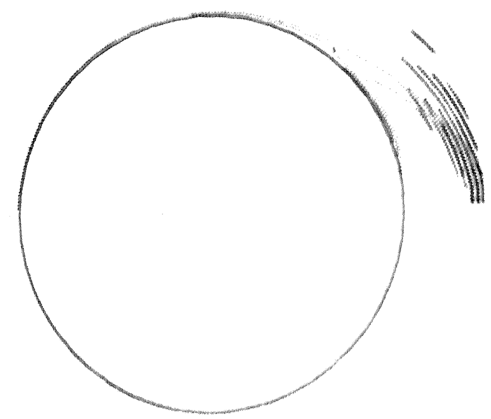

Figure 4.497

Isotherms for Re=500,n=0.8,and porosity 0.5 Pr=50.0(cont wall heat flux)

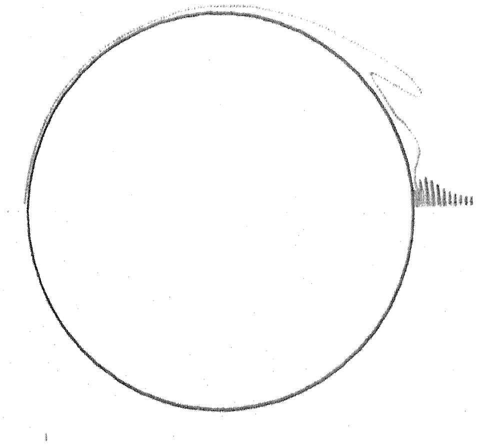

Figure 4.498

Isotherms for Re=500,n=0 8,and porosity 0.5 Pr=100.0(cont wall heat flux)

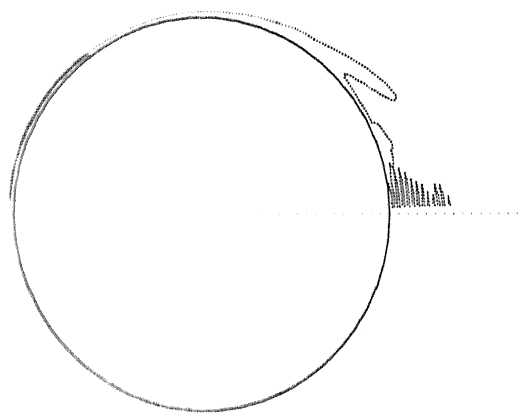

Figure 4.499

Isotherms for Re=1.0,n=0.6,and porosity 0.5 Pr=1.0(const heat flux)

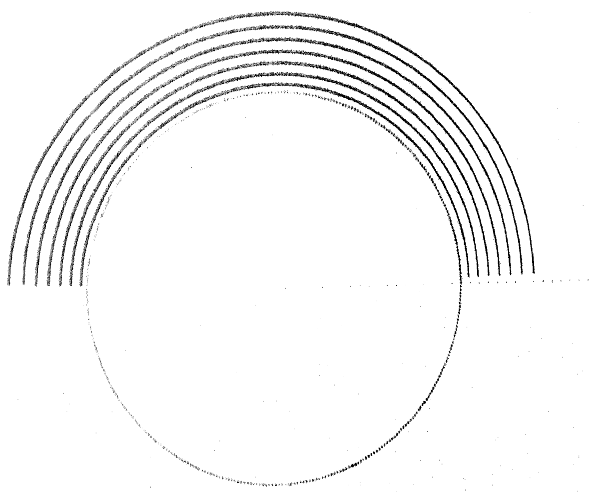

Figure 4.500

Isotherms for Re=1.0,n=0.6,and porosity 0.5 Pr=10.0(const heat flux)

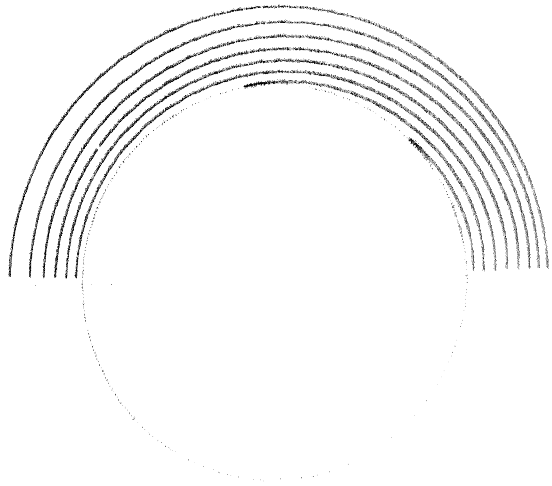

Figure 4.501

Isotherms for Re=1.0,n=0.6,and porosity 0.5 Pr=50.0(const heat flux)

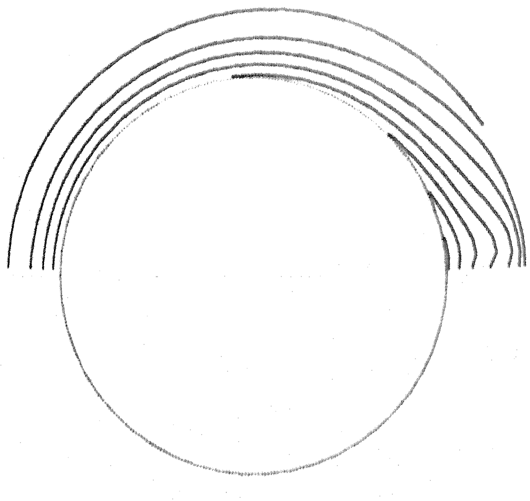

Figure 4.502

Isotherms for Re=1.0,n=0.6,and porosity 0.5 Pr=100.0(const heat flux)

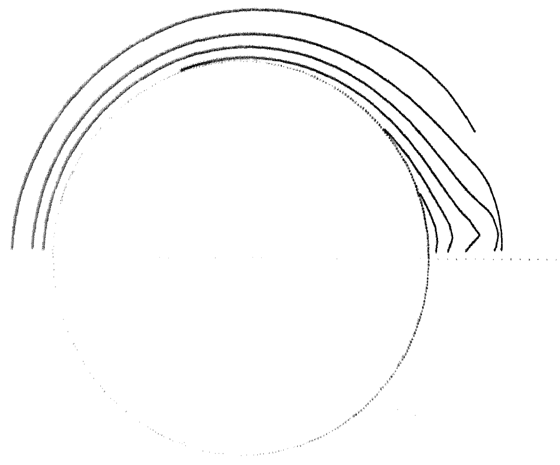

Figure 4.503

Isotherms for Re=1.0,n=0.6,and porosity 0.5 Pr=500.0(const heat flux)

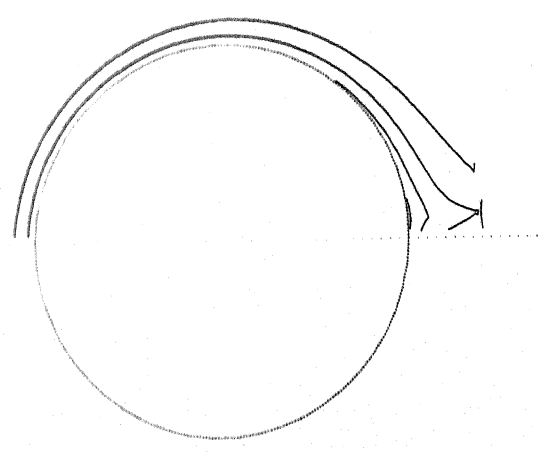

Figure 4.504

Isotherms for Re=10.0,n=0.6,and porosity 0.5 Pr=1.0(const heat flux)

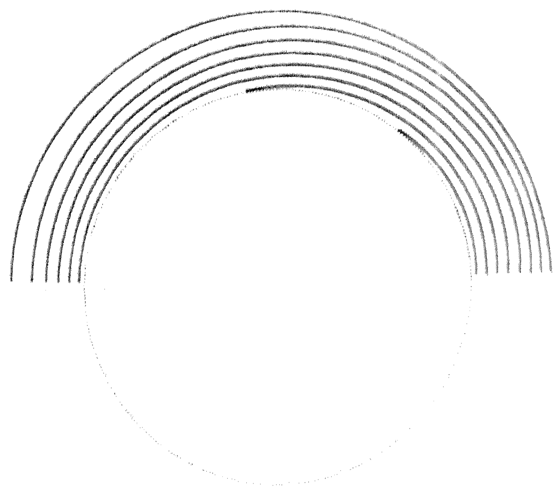

Figure 4.505

Isotherms for Re=10.0,n=0.6,and porosity 0.5 Pr=10.0(const heat flux)

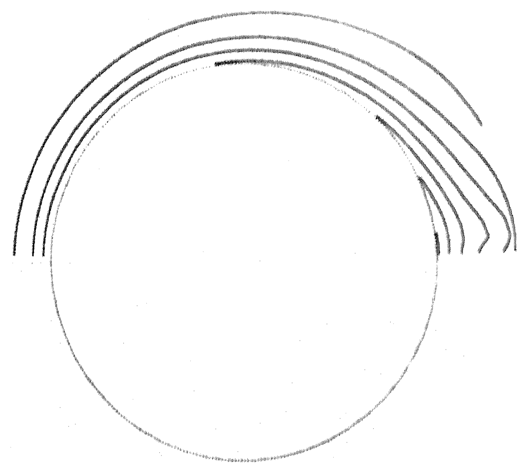

Figure 4.506

Isotherms for Re=10.0,n=0.6,and porosity 0.5 Pr=50.0(const heat flux)

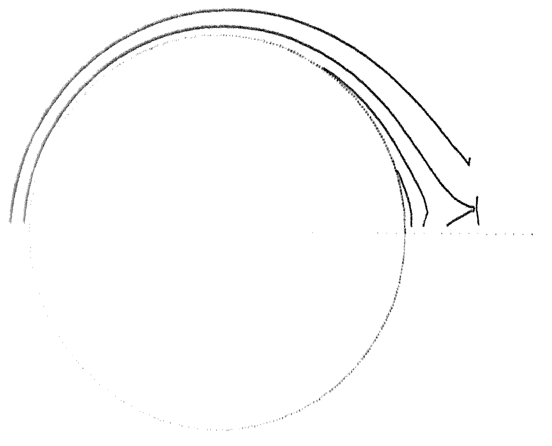

Figure 4.507

Isotherms for Re=10.0,n=0.6,and porosity 0.5 Pr=100.0(const heat flux)

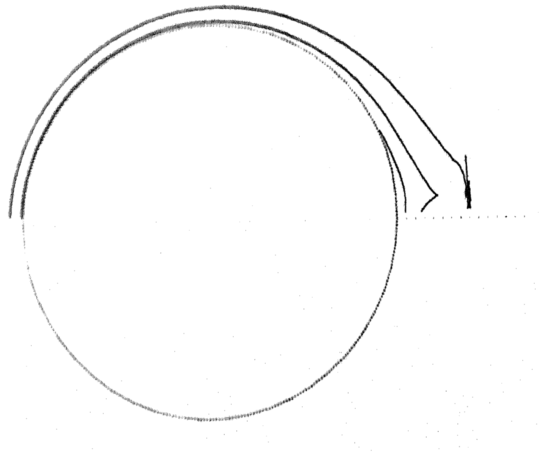

Figure 4.508

Isotherms for Re=10.0,n=0.6,and porosity 0.5 Pr=500.0(const heat flux)

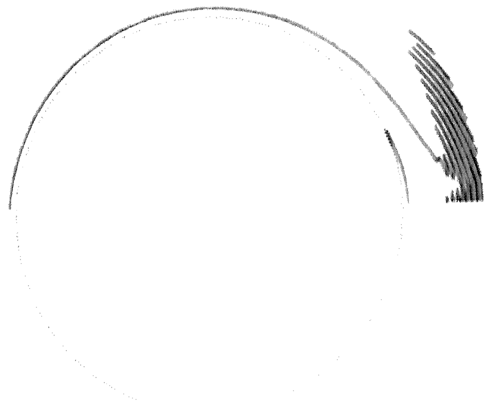

Figure 4.509

Isotherms for Re=100.0,n=0.6,and porosity 0.5 Pr=1.0(const heat flux)

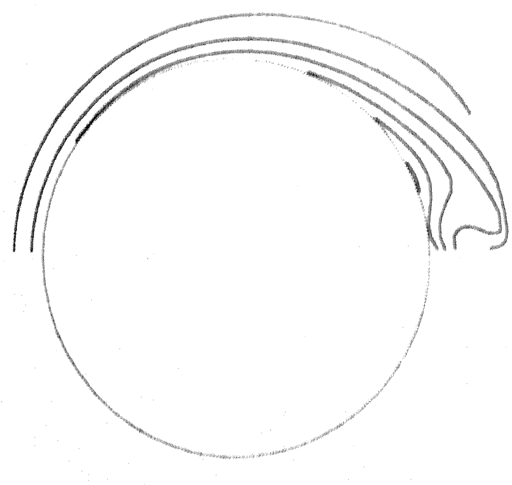

Figure 4.510

Isotherms for Re=100.0,n=0.6,and porosity 0.5 Pr=10.0(const heat flux)

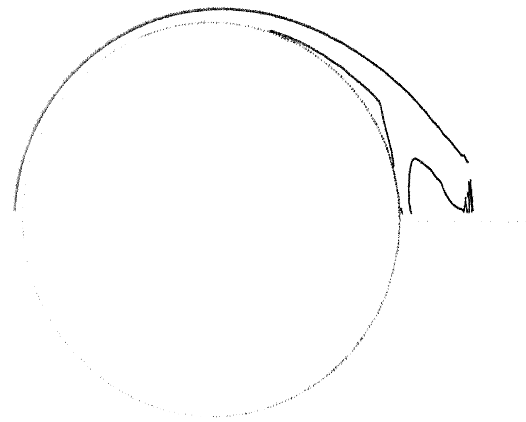

Figure 4.511

Isotherms for Re=100.0,n=0.6,and porosity 0.5 Pr=100.0(const heat flux)

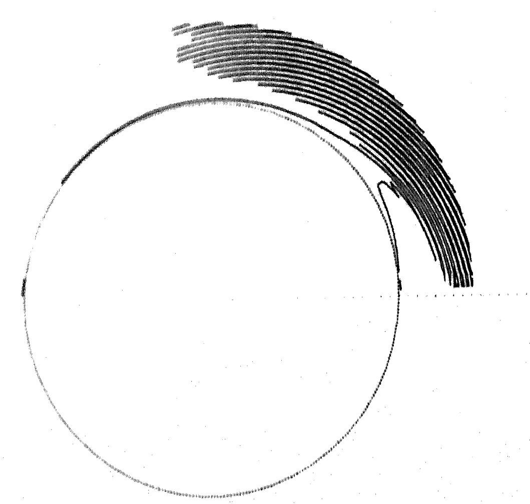

Figure 4.512

Isotherms for Re=100 0,n=0.6,and porosity 0.5 Pr=500.0(const heat flux)

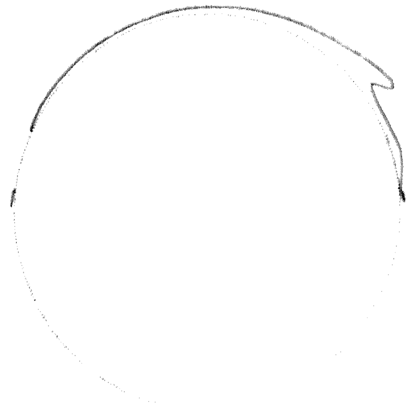

Figure 4.513

Isotherms for Re=200,n=0.6,and porosity 0.5 Pr=10.0(cont wall heat flux)

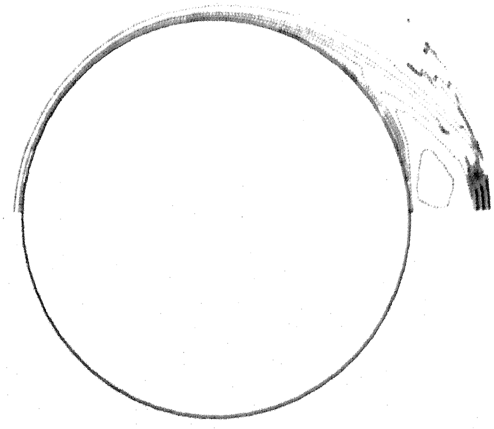

Figure 4.514

Isotherms for Re=200,n=0.6,and porosity 0.5 Pr=10.0(cont wall heat flux)

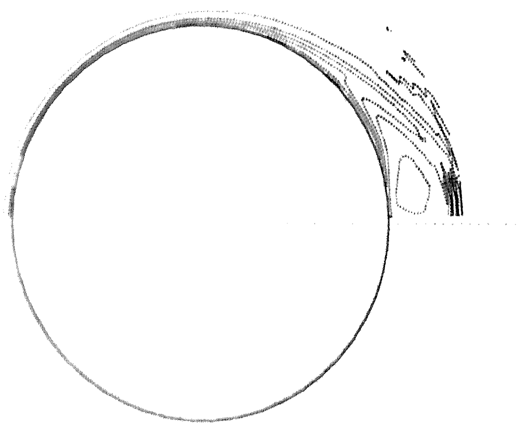

Figure 4.515

Isotherms for Re=200,n=0.6,and porosity 0.5 Pr=50.0(cont wall heat flux)

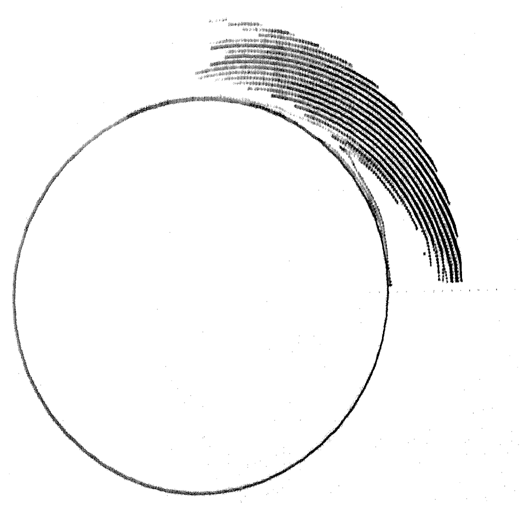

Figure 4.516

Isotherms for Re=200,n=0.6,and porosity 0.5 Pr=100.0(cont wall heat flux)

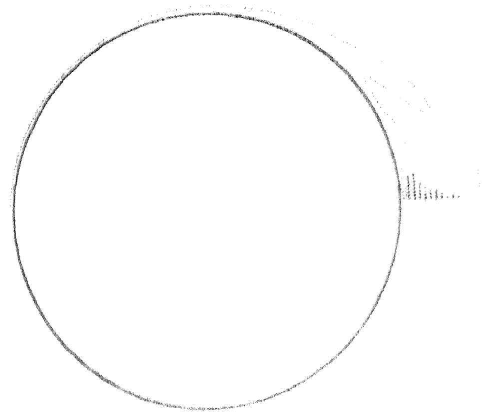

Figure 4.517

Isotherms for Re=200,n=0.6,and porosity 0.5 Pr=500.0(cont wall heat flux)

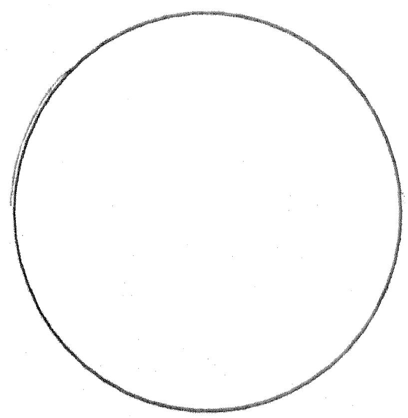

Figure 4.518

Isotherms for Re=500,n=0.6,and porosity 0.5 Pr=1.0(cont wall heat flux)

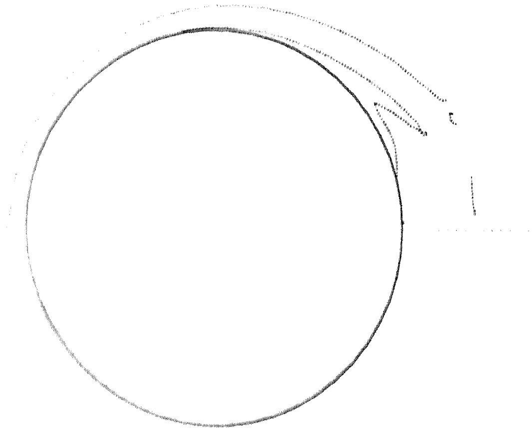

Figure 4.519

Isotherms for Re=500,n=0.6,and porosity 0.5 Pr=10.0(cont wall heat flux)

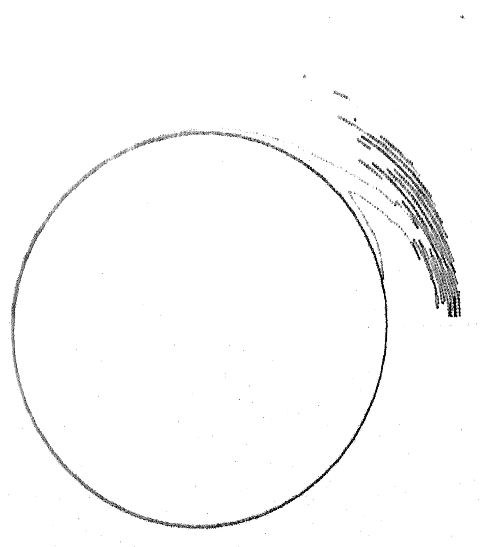

Figure 4.520

Isotherms for Re=500,n=0.6,and porosity 0.5 Pr=50.0(cont wall heat flux)

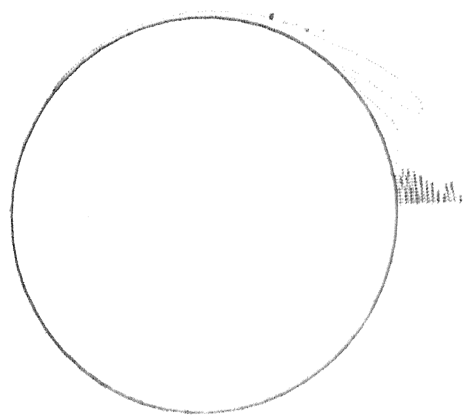

Figure 4.521

Isotherms for Re=500,n=0.6,and porosity 0.5 Pr=100.0(cont wall heat flux)

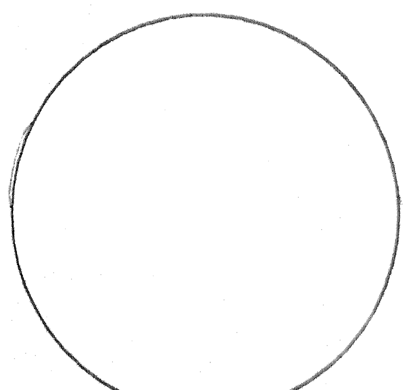

Figure 4.522

Isotherms for Re=1.0,n=0.5,and porosity 0.5 Pr=1.0(const heat flux)

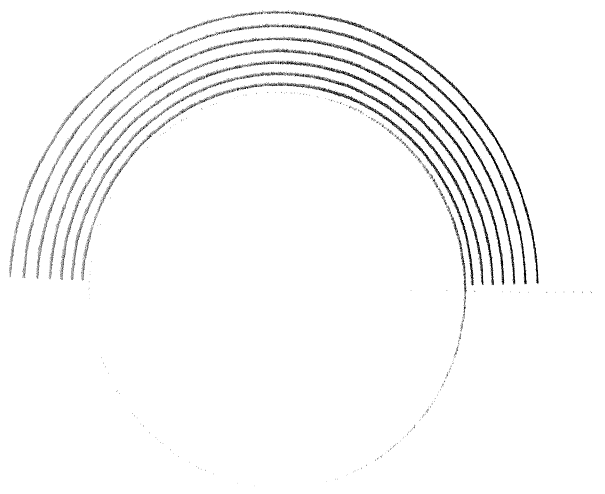

Figure 4.523

Isotherms for Re=1.0,n=0.5,and porosity 0.5 Pr=10.0(const heat flux)

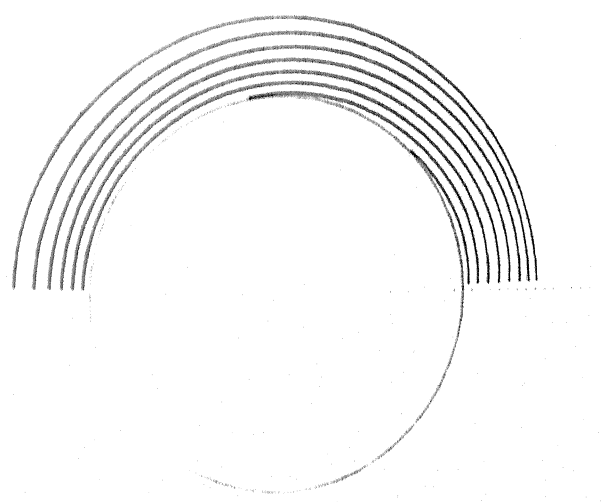

Figure 4.524

Isotherms for Re=1.0,n=0.5,and porosity 0.5 Pr=50.0(const heat flux)

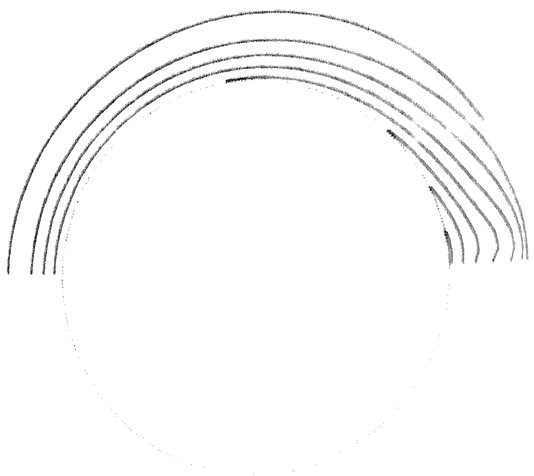

Figure 4.525

Isotherms for Re=1.0,n=0.5,and porosity 0.5 Pr=100.0(const heat flux)

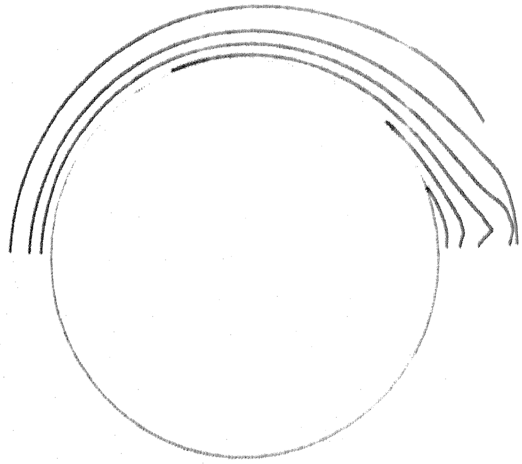

Figure 4.526

Isotherms for Re=1.0,n=0.5,and porosity 0.5 Pr=500.0(const heat flux)

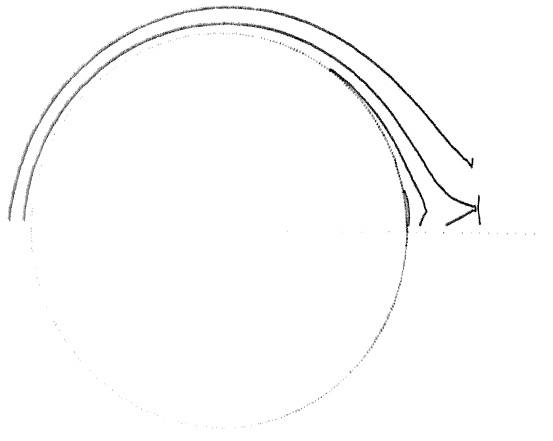

Figure 4.527

Isotherms for Re=10.0,n=0.5,and porosity 0.5 Pr=1.0(const heat flux)

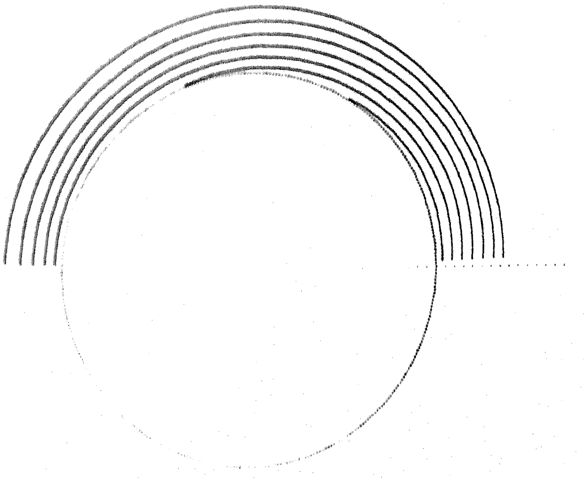

Figure 4.528

Isotherms for Re=10.0,n=0.5,and porosity 0.5 Pr=10.0(const heat flux)

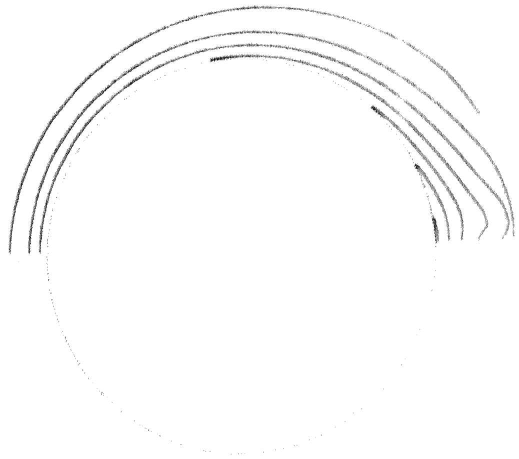

Figure 4.529

Isotherms for Re=10.0,n=0.5,and porosity 0.5 Pr=50.0(const heat flux)

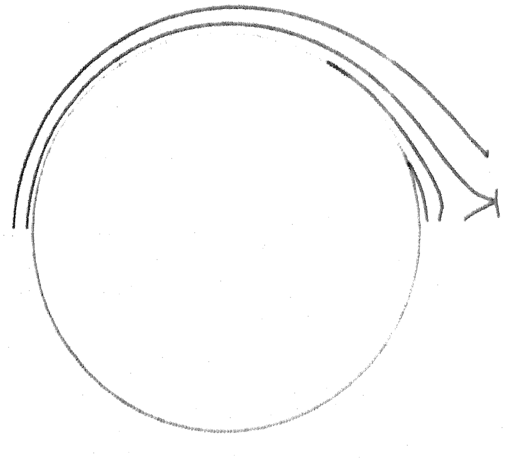

Figure 4.530

Isotherms for Re=10.0,n=0.5,and porosity 0.5 Pr=100.0(const heat flux)

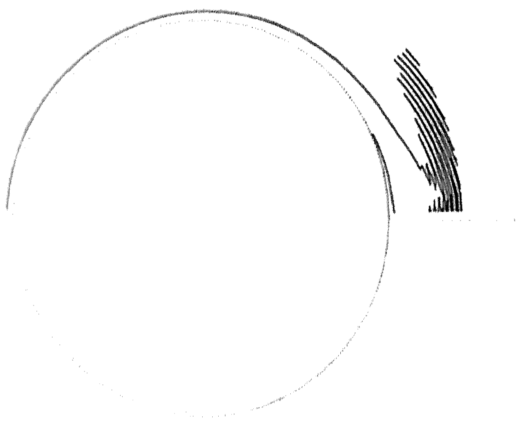

Figure 4.531

Isotherms for Re=100,n=0.5,and porosity 0.5 Pr=1.0(cont wall heat flux)

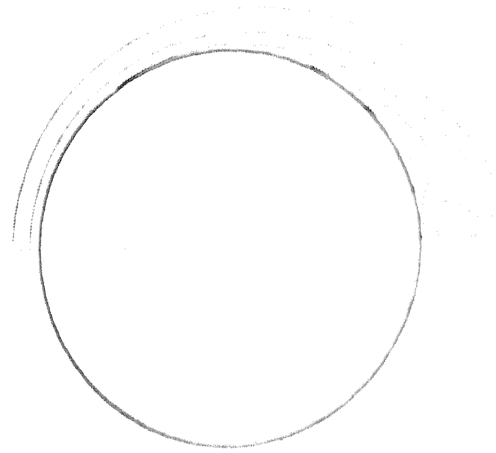

Figure 4.532

Isotherms for Re=100,n=0.5,and porosity 0.5 Pr=10.0(cont wall heat flux)

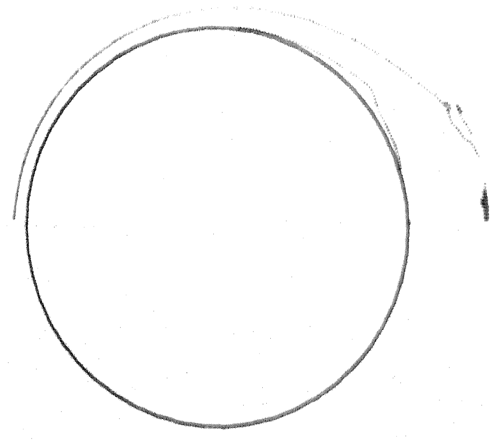

Figure 4.533

Isotherms for Re=100,n=0.5,and porosity 0.5 Pr=50.0(cont wall heat flux)

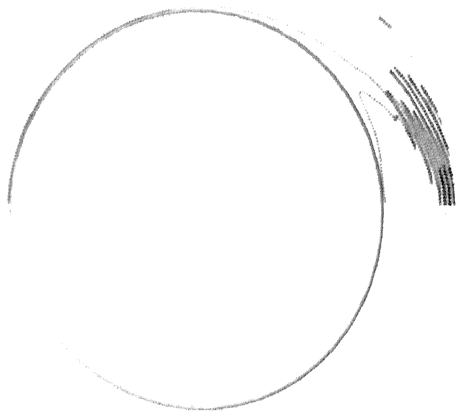

Figure 4.534

Isotherms for Re=100,n=0.5,and porosity 0.5 Pr=100.0(cont wall heat flux)

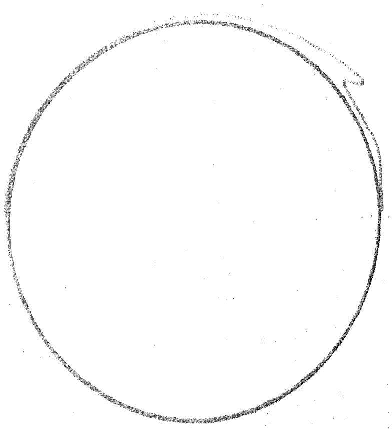

Figure 4.535

Isotherms for Re=100,n=0.5,and porosity 0.5 Pr=500.0(cont wall heat flux)

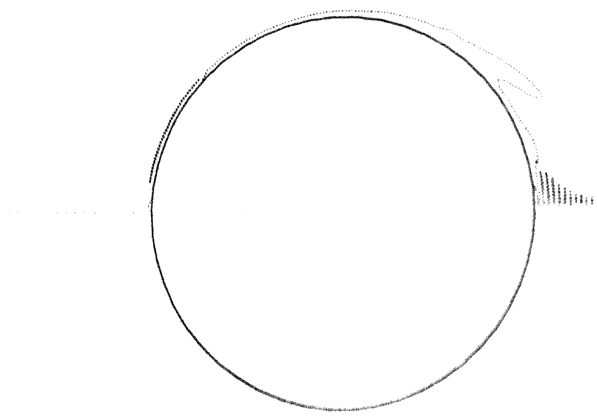

Figure 4.536

Isotherms for Re=200.0,n=0.5,and porosity 0.5 Pr=1.0(const heat flux)

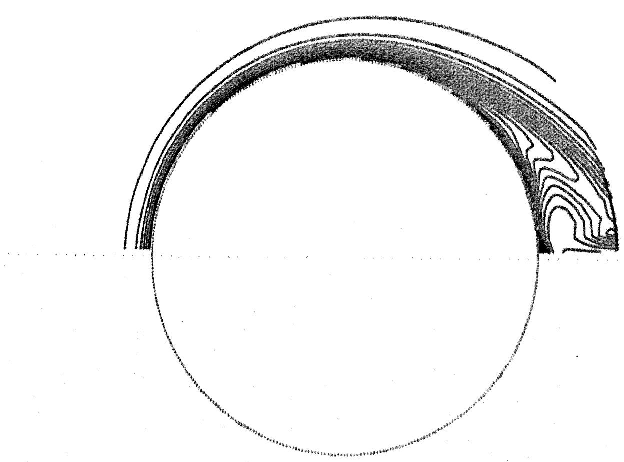

Figure 4.537

Isotherms for Re=200.0,n=0.5,and porosity 0.5 Pr=10.0(const heat flux)

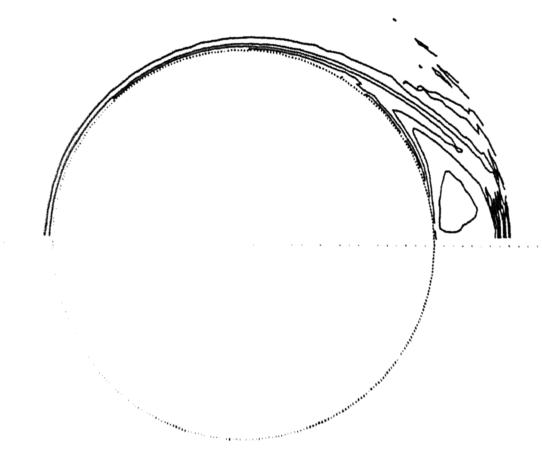

Figure 4.538

Isotherms for Re=200.0,n=0.5,and porosity 0.5 Pr=50.0(const heat flux)

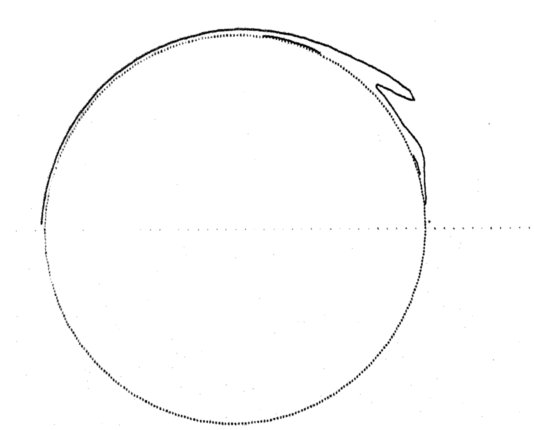

Figure 4.539

Isotherms for Re=200.0,n=0.5,and porosity 0.5 Pr=100.0(const heat flux)

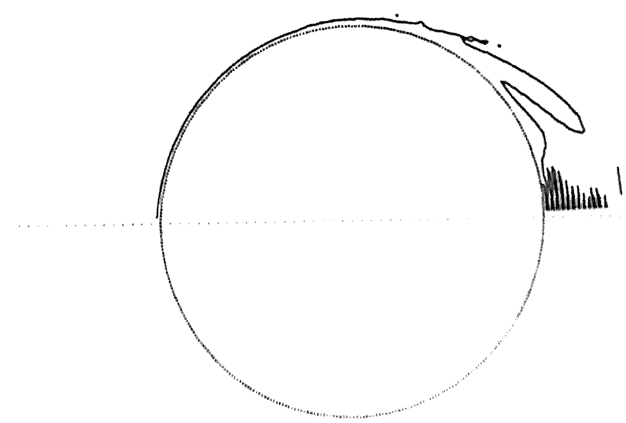

Figure 4.540

Isotherms for Re=200.0,n=0.5,and porosity 0.5 Pr=500.0(const heat flux)

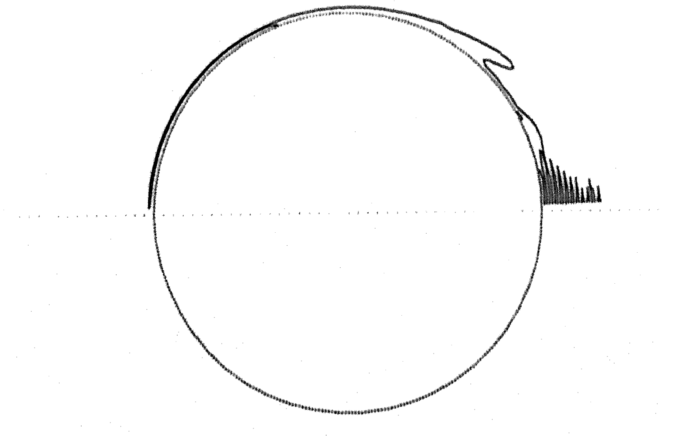

Figure 4.541

Isotherms for Re=500,n=0.5,and porosity 0.5 Pr=1.0(cont wall heat flux)

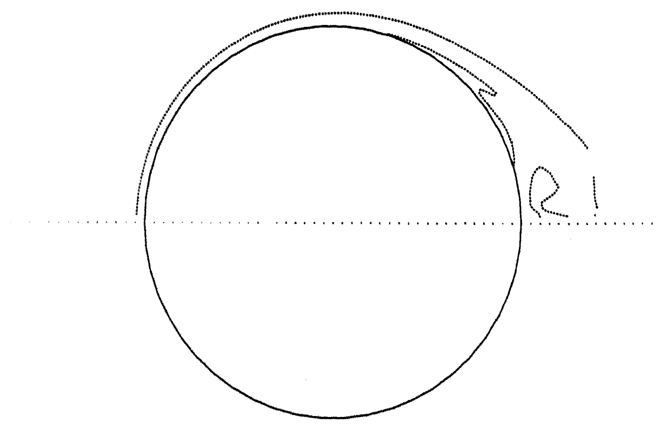

Figure 4.542

Isotherms for Re=500,n=0.5,and porosity 0.5 Pr=10.0(cont wall heat flux)

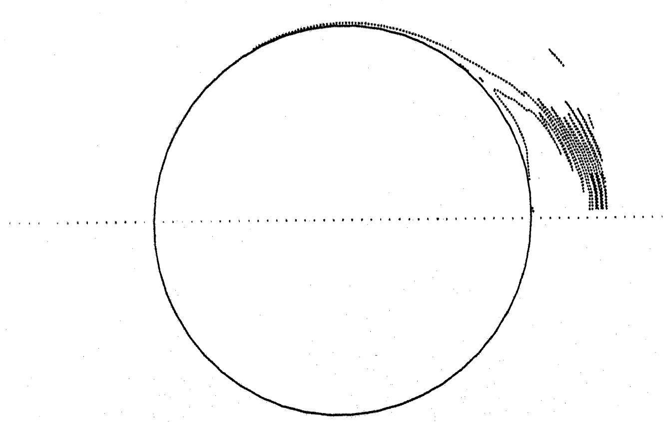

Figure 4.543

Isotherms for Re=500,n=0.5,and porosity 0.5 Pr=50.0(cont wall heat flux)

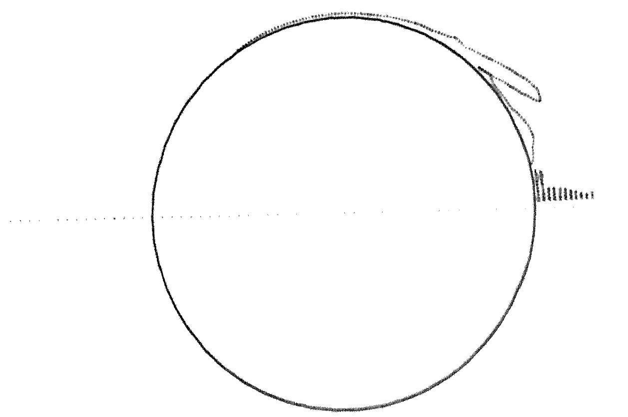

Figure 4.544

Isotherms for Re=500,n=0.5,and porosity 0.5 Pr=100.0(cont wall heat flux)

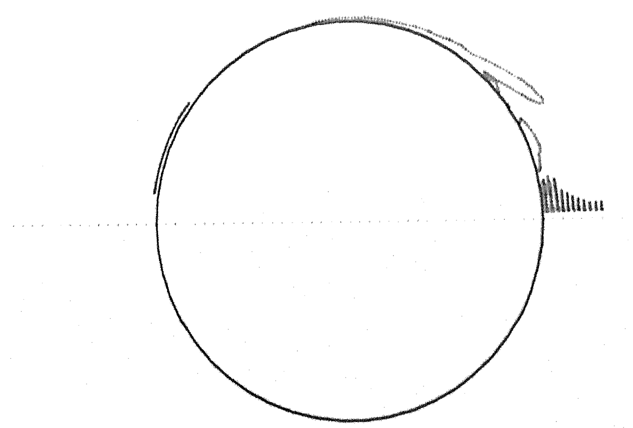

Figure 4.545

Isotherms for Re=1.0,n=1.0,and porosity 0.6 Pr=1.0(const heat flux)

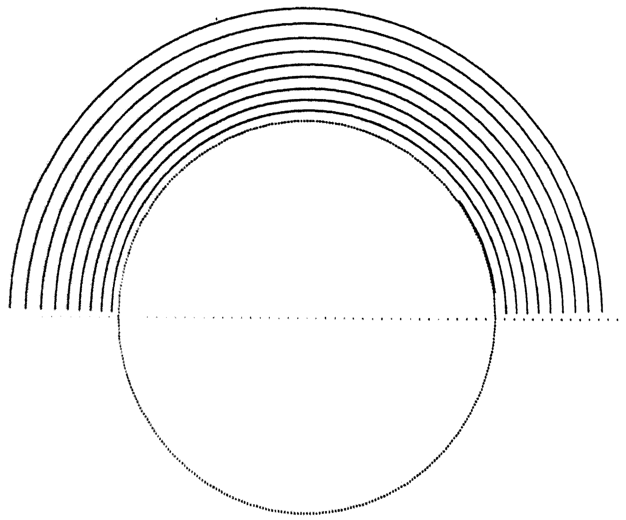

Figure 4.546

Isotherms for Re=1.0,n=1.0,and porosity 0.6 Pr=10.0(const heat flux)

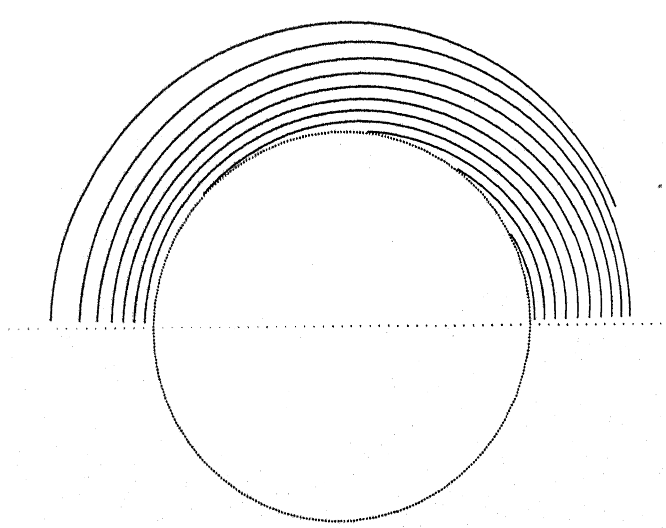

Figure 4.547

Isotherms for Re=1.0,n=1.0,and porosity 0.6 Pr=50.0(const heat flux)

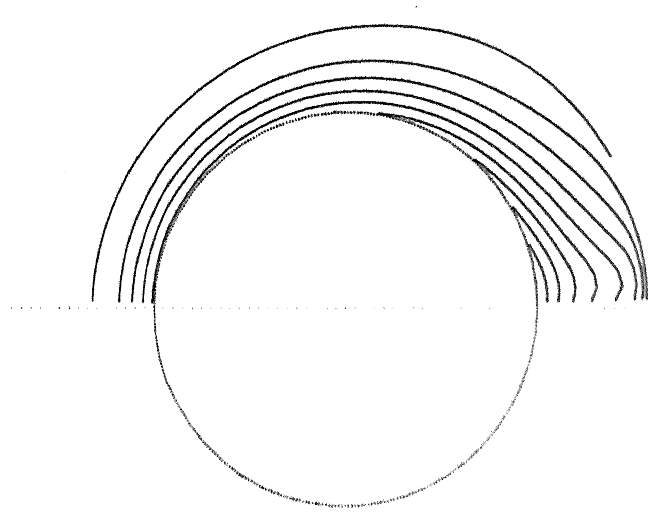

Figure 4.548

Isotherms for Re=1.0,n=1.0,and porosity 0.6 Pr=100.0(const heat flux)

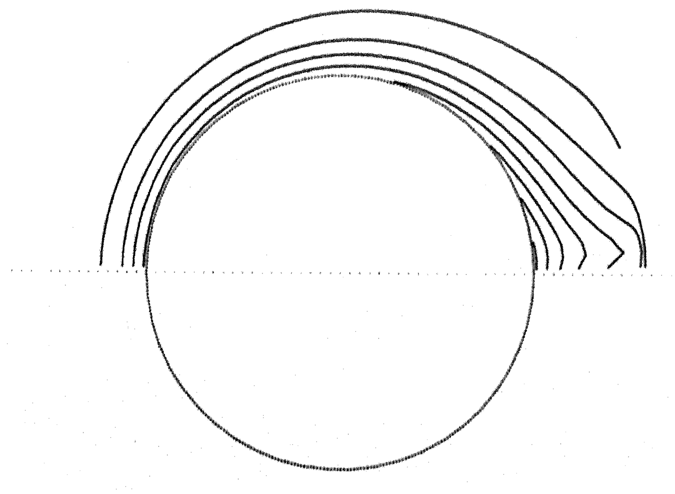

Figure 4.549

Isotherms for Re=1.0,n=1.0,and porosity 0.6 Pr=500.0(const heat flux)

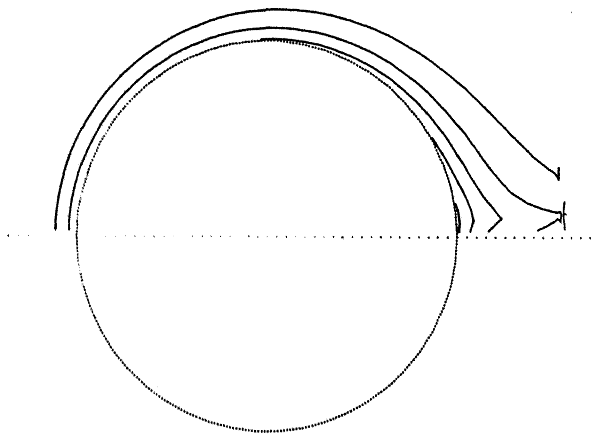

Figure 4.550

Isotherms for Re=10.0,n=1.0,and porosity 0.6 Pr=1.0(const heat flux)

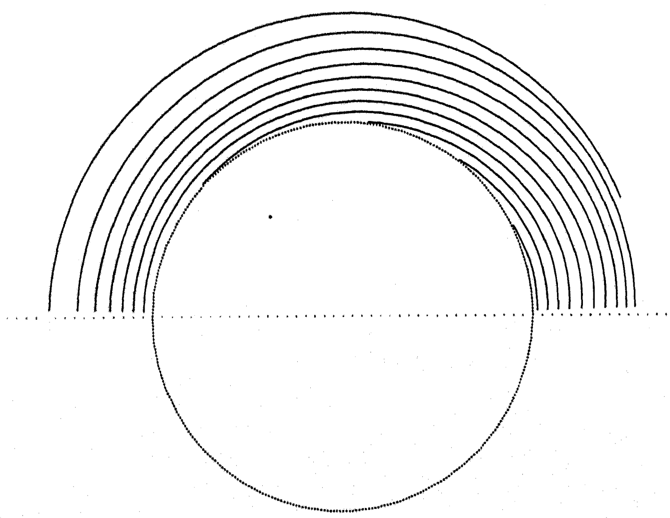

Figure 4.551

Isotherms for Re=10.0,n=1.0,and porosity 0.6 Pr=10.0(const heat flux)

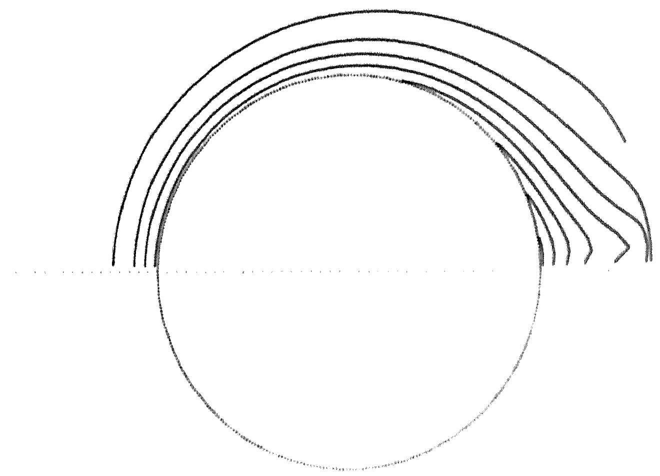

Figure 4.552

Isotherms for Re=10.0,n=1.0,and porosity 0.6 Pr=50.0(const heat flux)

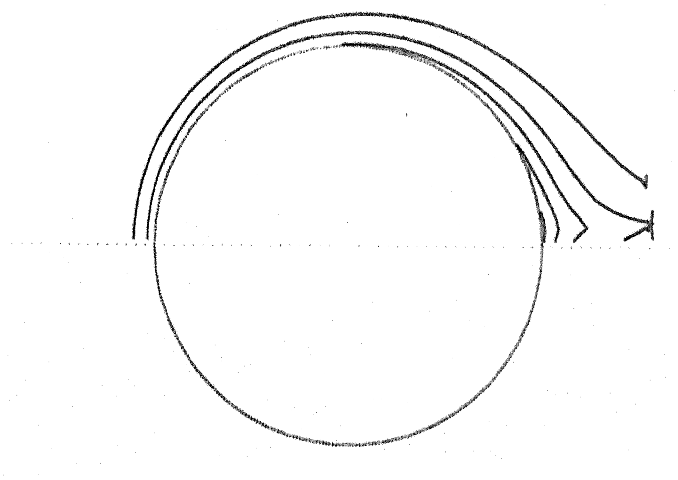

Figure 4.553

Isotherms for Re=10.0,n=1.0,and porosity 0.6 Pr=100.0(const heat flux)

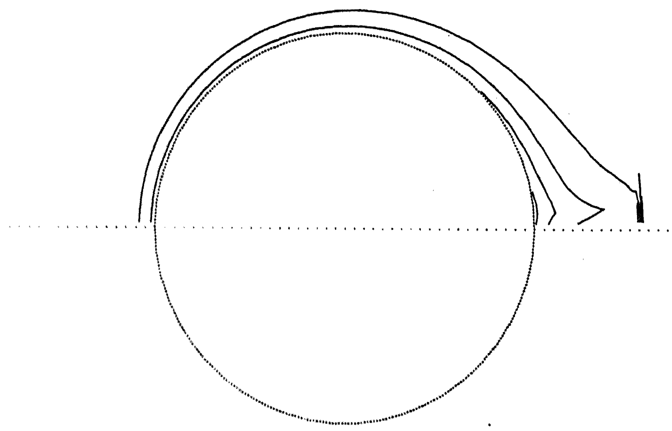

Figure 4.554

Isotherms for Re=10.0,n=1.0,and porosity 0.6 Pr=500.0(const heat flux)

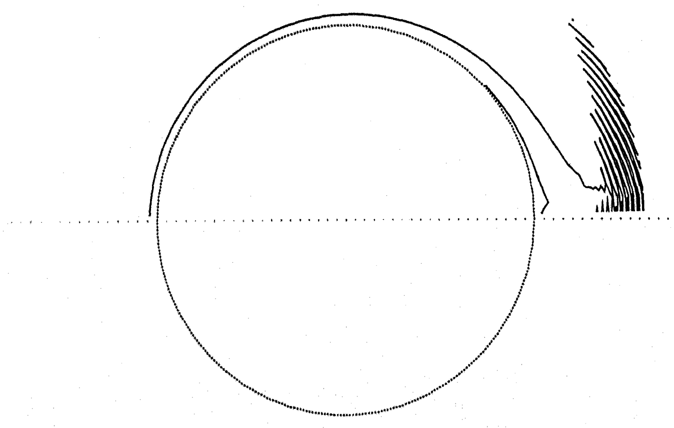

Figure 4.555

Isotherms for Re=100.0,n=1.0,and porosity 0.6 Pr=1.0(const heat flux)

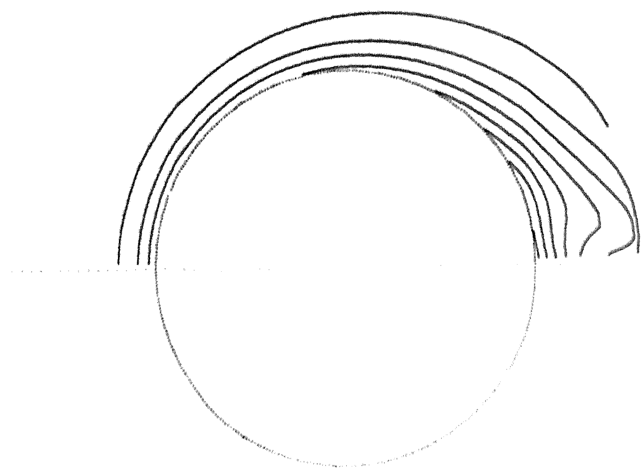

Figure 4.556

Isotherms for Re=100.0,n=1.0,and porosity 0.6 Pr=10.0(const heat flux)

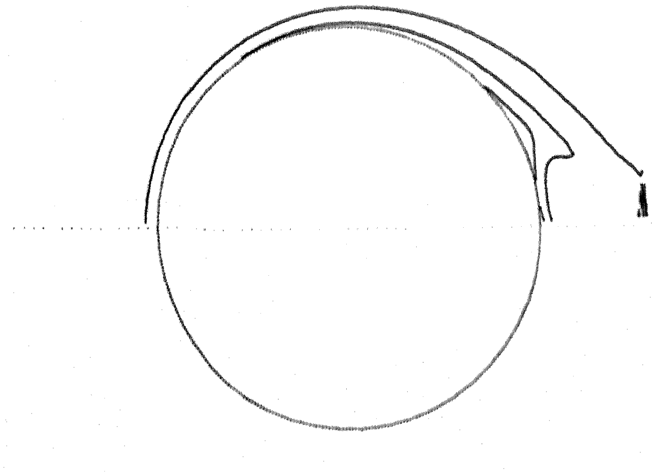

Figure 4.557

Isotherms for Re=100.0,n=1.0,and porosity 0.6 Pr=50.0(const heat flux)

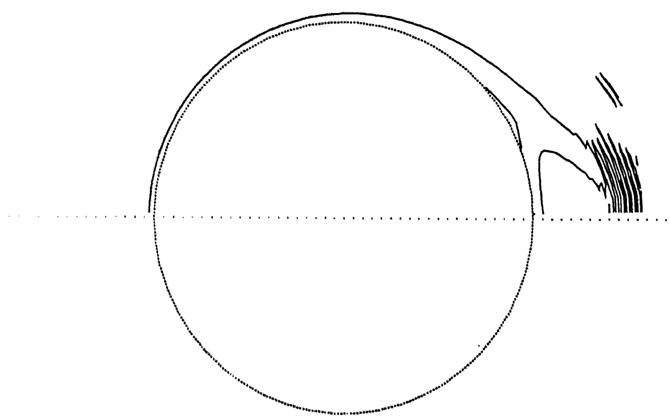

Figure 4.558

Isotherms for Re=100.0,n=1.0,and porosity 0.6 Pr=100.0(const heat flux)

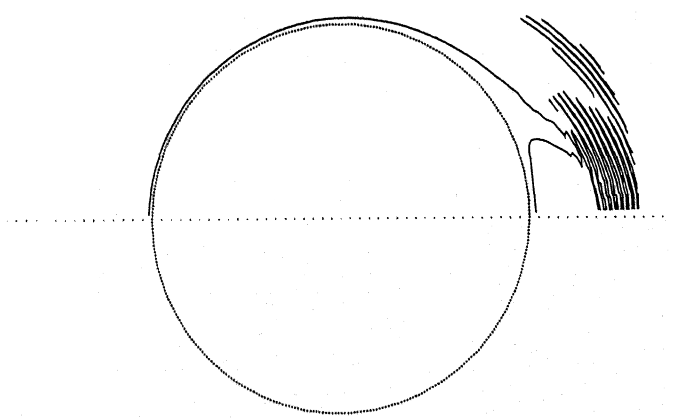

Figure 4.557

Isotherms for Re=100.0,n=1.0,and porosity 0.6 Pr=500.0(const heat flux)

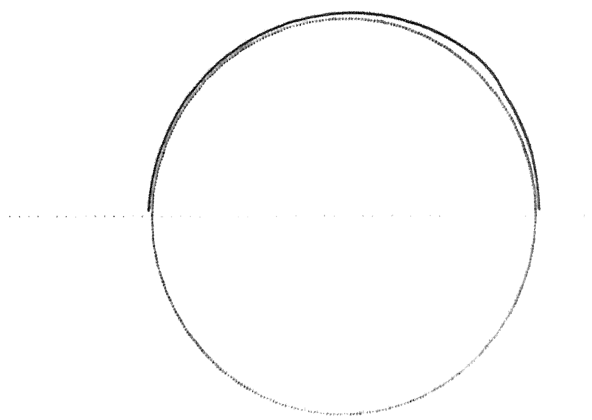

Figure 4.558

Isotherms for Re=200.0,n=1.0,and porosity 0.6 Pr=1.0(const heat flux)

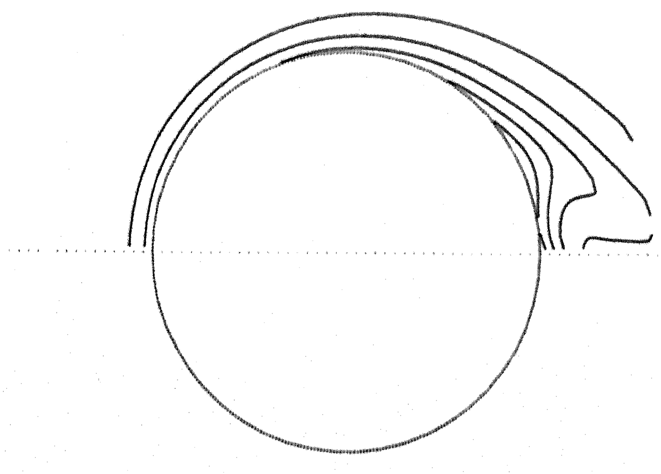

Figure 4.559

Isotherms for Re=200.0,n=1.0,and porosity 0.6 Pr=10.0(const heat flux)

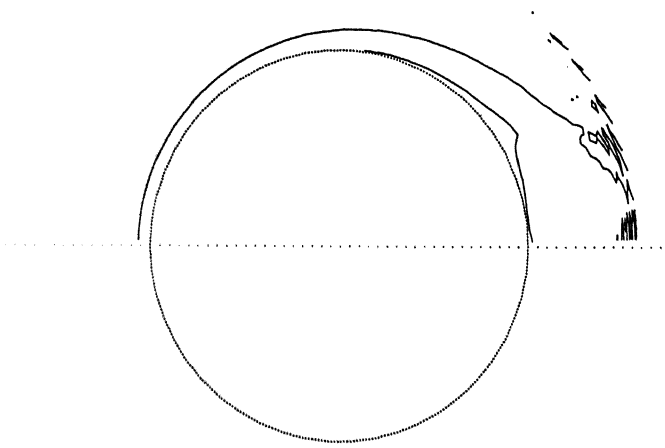

Figure 4.560

Isotherms for Re=200.0,n=1.0,and porosity 0.6 Pr=50.0(const heat flux)

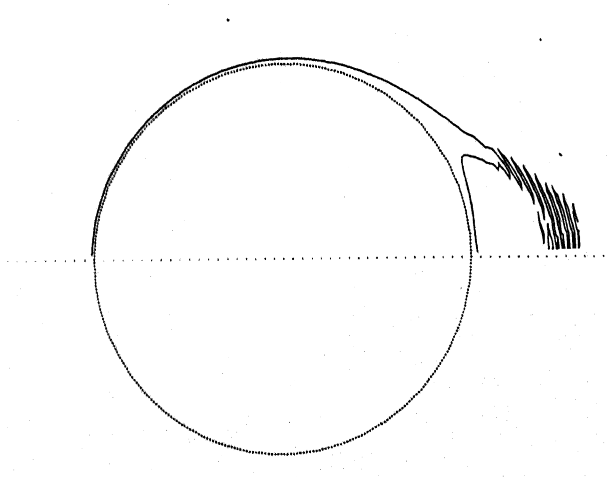

Figure 4.561

Isotherms for Re=200.0,n=1.0,and porosity 0.6 Pr=100.0(const heat flux)

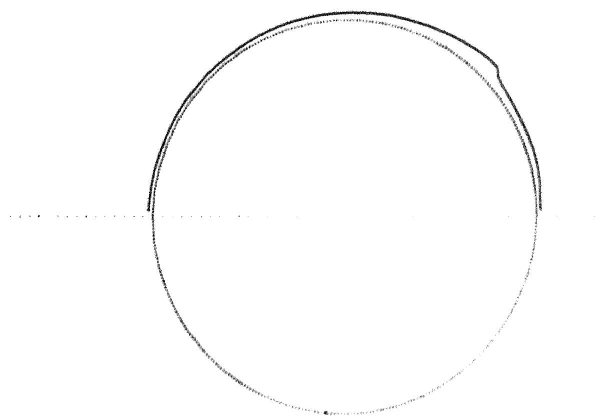

Figure 4.562

Isotherms for Re=200.0,n=1.0,and porosity 0.6 Pr=500.0(const heat flux)

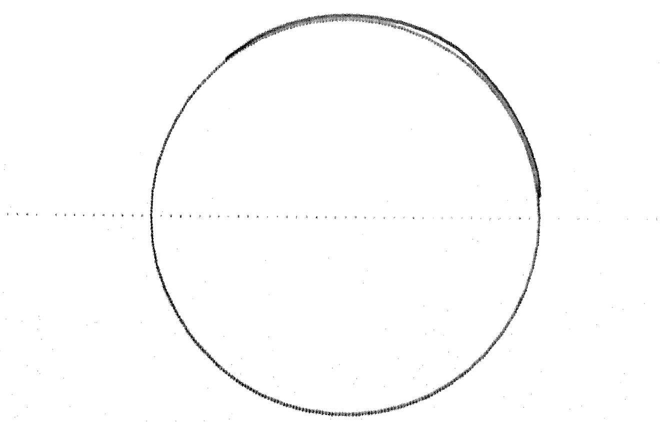

Figure 4.563

Isotherms for Re=500.0,n=1.0,and porosity 0.6 Pr=1.0(const heat flux)

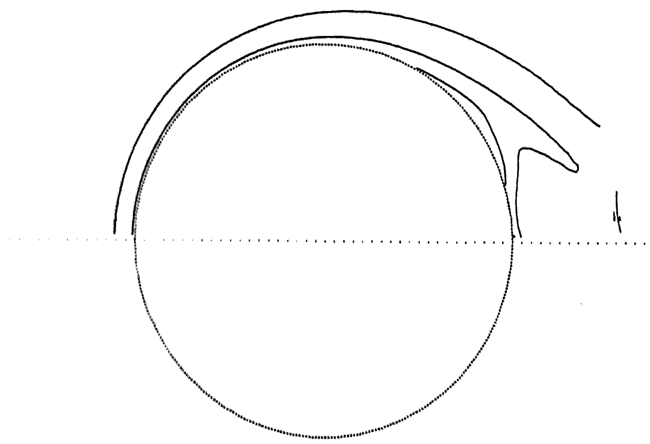

Figure 4.564

Isotherms for Re=500.0,n=1.0,and porosity 0.6 Pr=10.0(const heat flux)

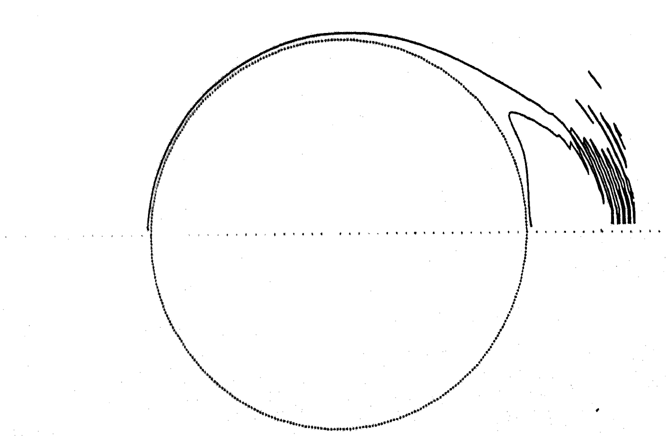

Figure 4.565

Isotherms for Re=500.0,n=1 0,and porosity 0 6 Pr=50 0(const heat flux)

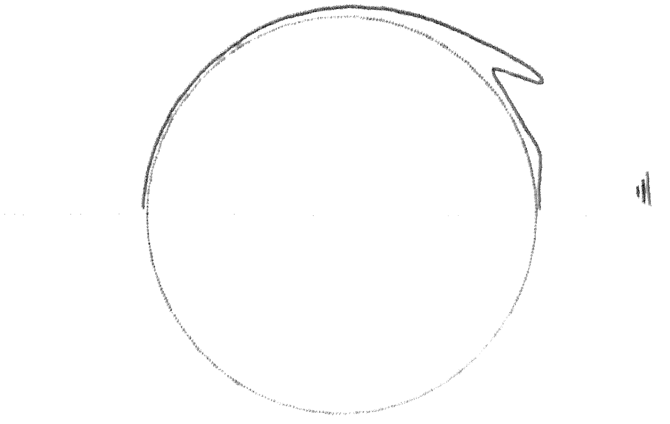

Figure 4.566

Isotherms for Re=500.0,n=1.0,and porosity 0.6 Pr=100.0(const heat flux)

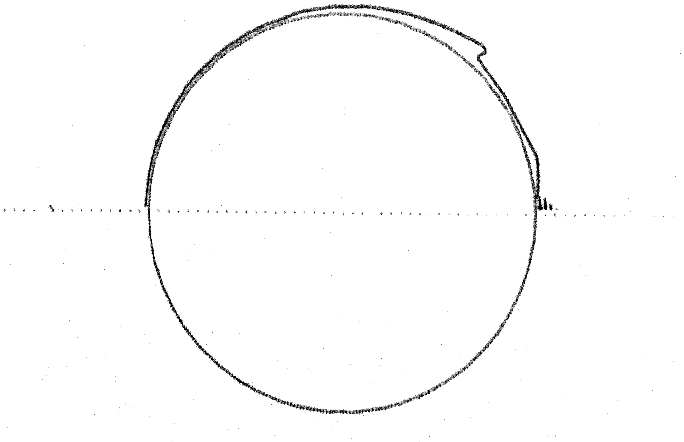

Figure 4.567

Isotherms for Re=1.0,n=0.8,and porosity 0.6,Pr=100.0(const heat flux)

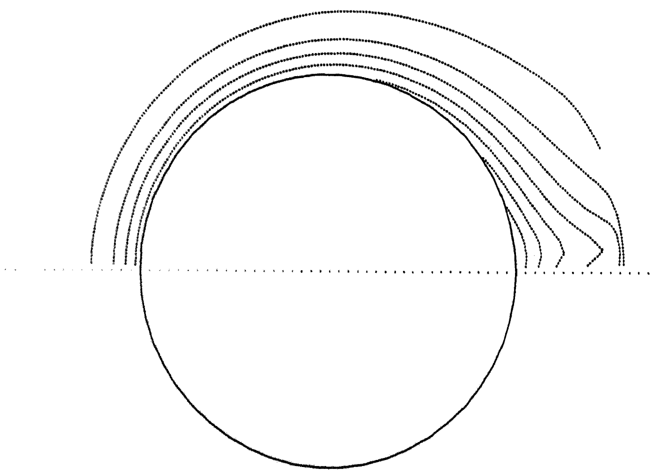

Figure 4.568

Isotherms for Re=1.0,n=0.8,and porosity 0.6,Pr=500.0(const heat flux)

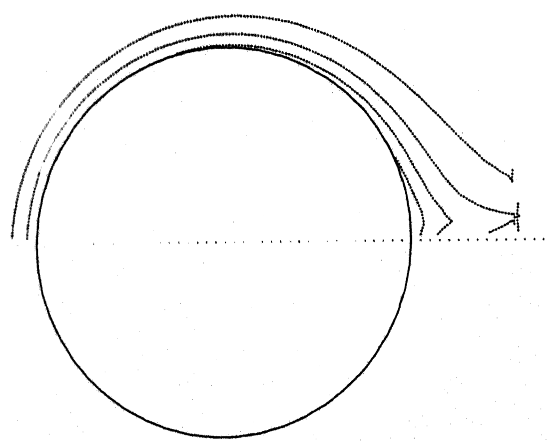

Figure 4.569

Isotherms for Re=1.0,n=0.8,and porosity 0.6,Pr=500.0(const heat flux)

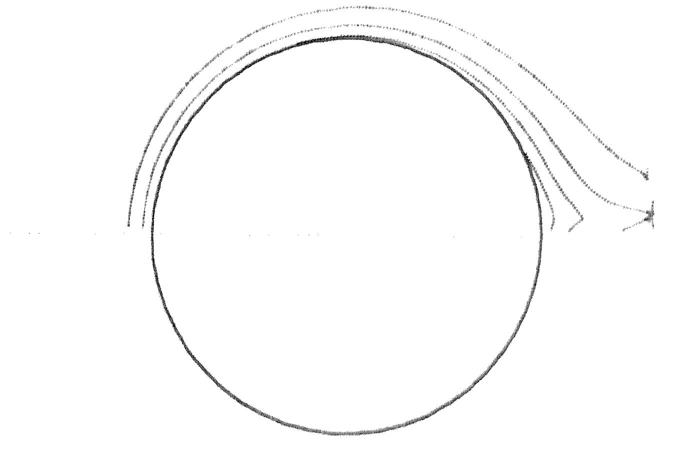

Figure 4.570

Isotherms for Re=10.0,n=0.8,and porosity 0.6 Pr=1.0(const heat flux)

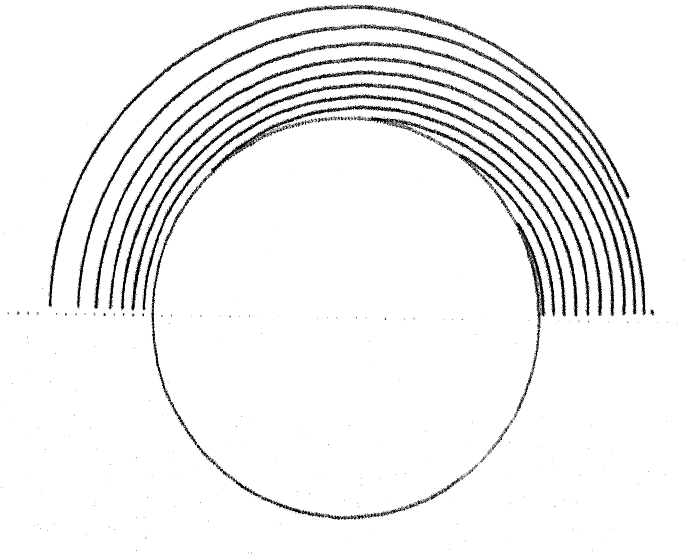

Figure 4.571

Isotherms for Re=10.0,n=0.8,and porosity 0.6 Pr=10.0(const heat flux)

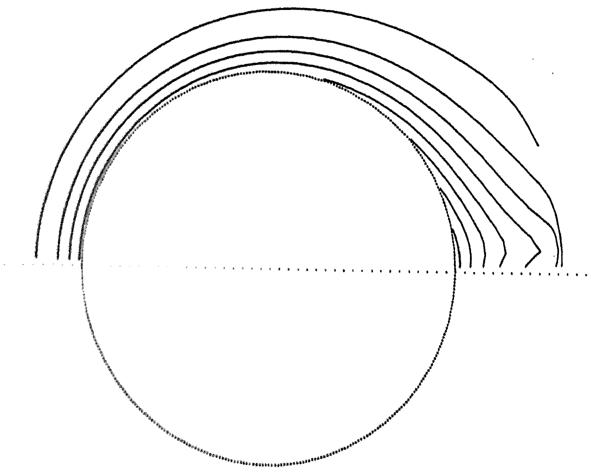

Figure 4.572

Isotherms for Re=10.0,n=0.8,and porosity 0.6 Pr=50.0(const heat flux)

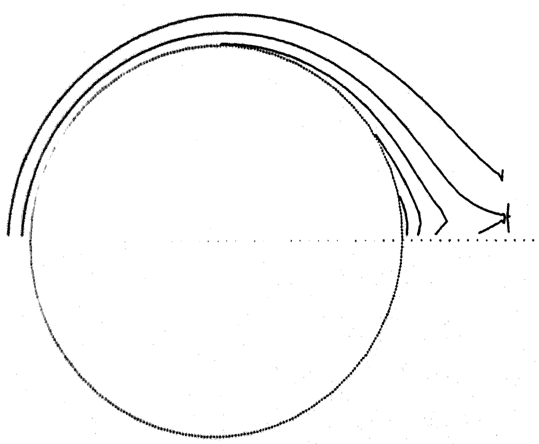

Figure 4.573

Isotherms for Re=10.0,n=0.8,and porosity 0.6 Pr=100.0(const heat flux)

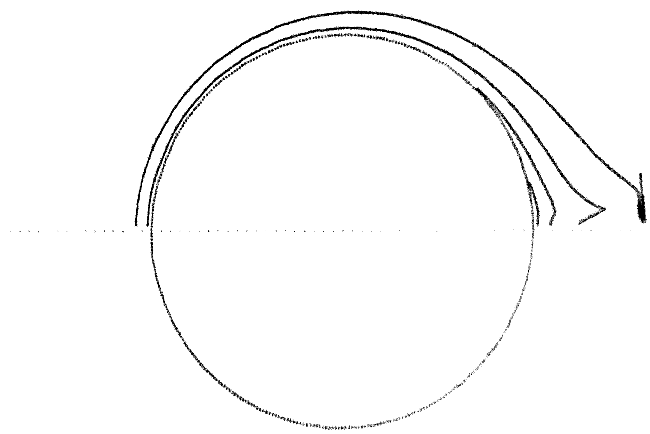

Figure 4.574

Isotherms for Re=10.0,n=0.8,and porosity 0.6 Pr=500.0(const heat flux)

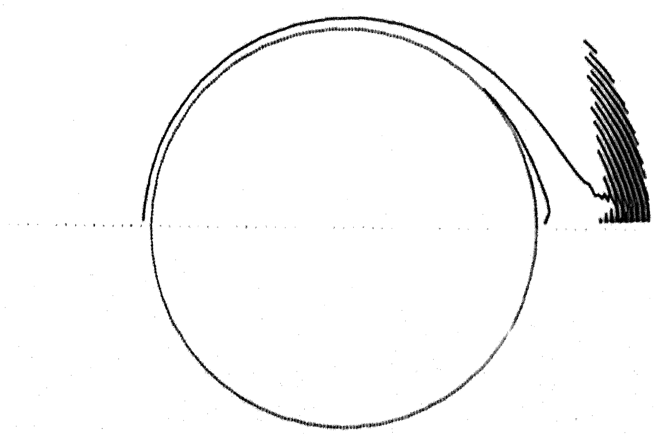

Figure 4.575

Isotherms for Re=100.0,n=0.8,and porosity 0.6,Pr=1.0(const heat flux)

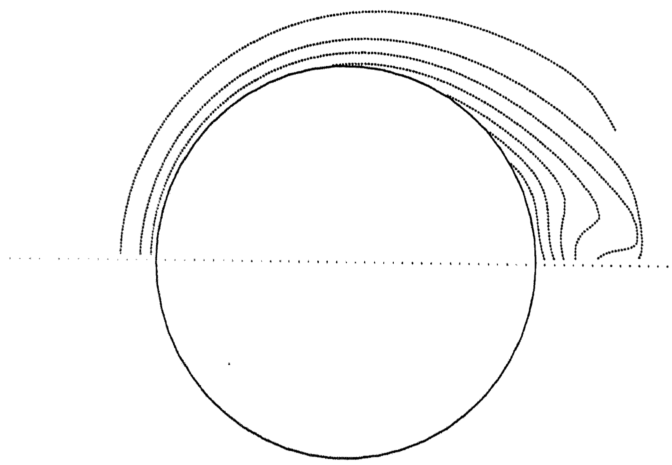

Figure 4.576

Isotherms for Re=100.0,n=0.8,and porosity 0.6,Pr=10.0(const heat flux)

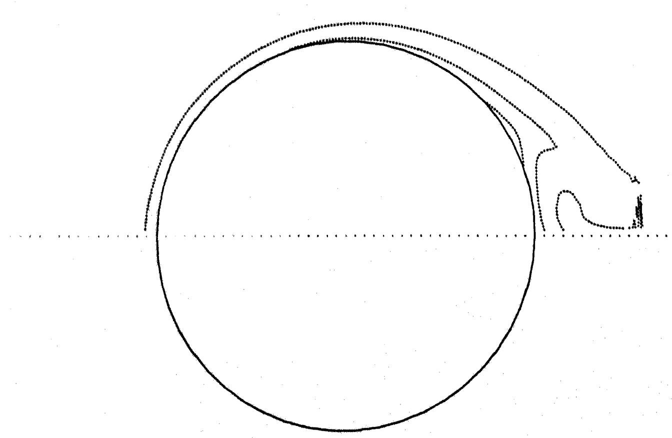

Figure 4.577

Isotherms for Re=100.0,n=0.8,and porosity 0.6,Pr=50.0(const heat flux)

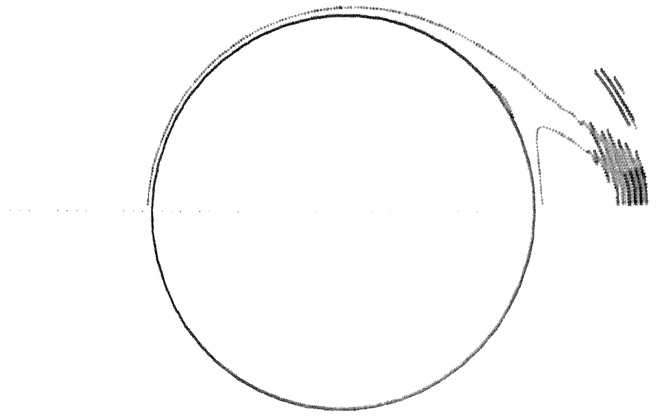

Figure 4.578

Isotherms for Re=100.0,n=0.8,and porosity 0.6,Pr=100.0(const heat flux)

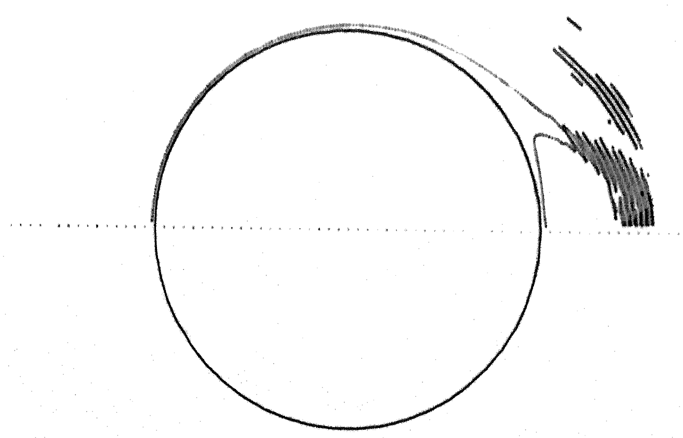

Figure 4.579

Isotherms for Re=100.0,n=0.8,and porosity 0.6,Pr=500.0(const heat flux)

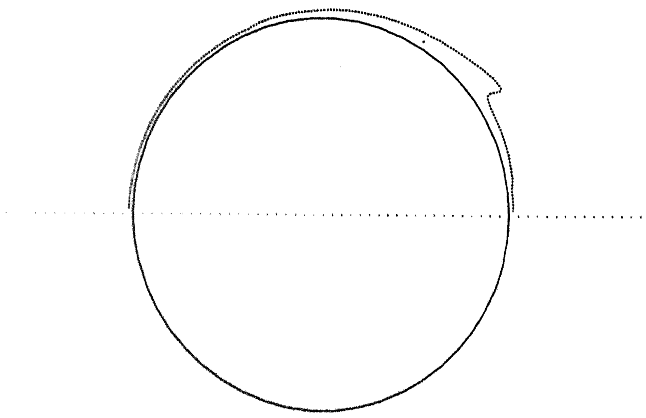

Figure 4.580

Isotherms for Re=500.0,n=0.8,and porosity 0.6 Pr=1.0(const heat flux)

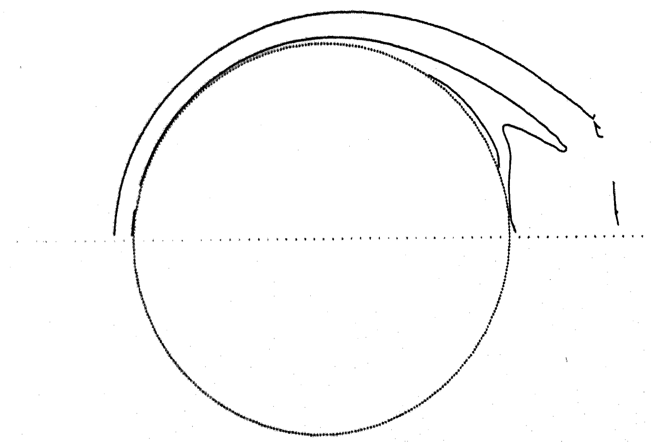

Figure 4.581

Isotherms for Re=500.0,n=0.8,and porosity 0.6 Pr=1.0(const heat flux)

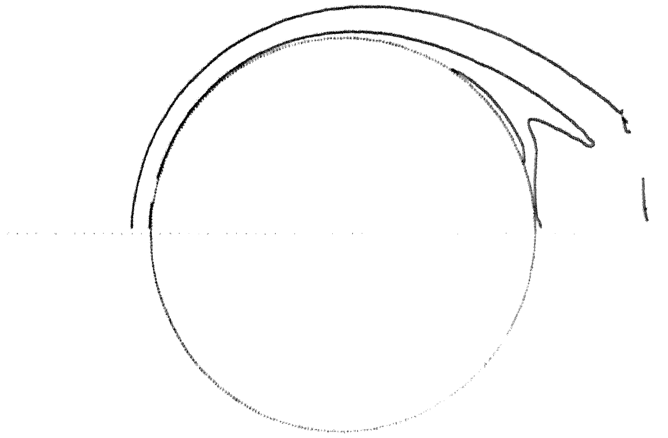

Figure 4.582

Isotherms for Re=500.0,n=0.8,and porosity 0.6 Pr=10.0(const heat flux)

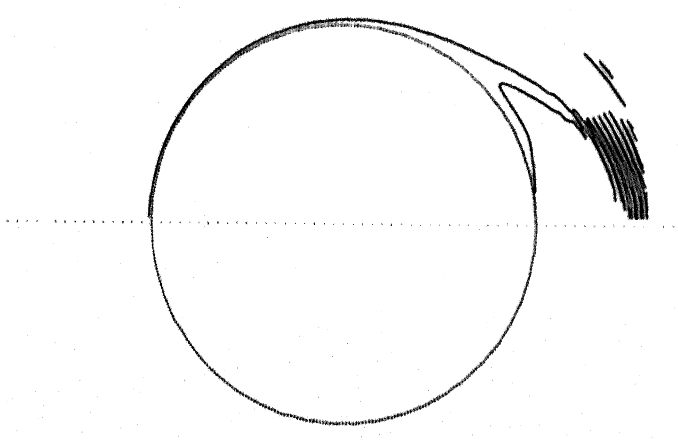

Figure 4.583

Isotherms for Re=500.0,n=0.8,and porosity 0.6 Pr=50.0(const heat flux)

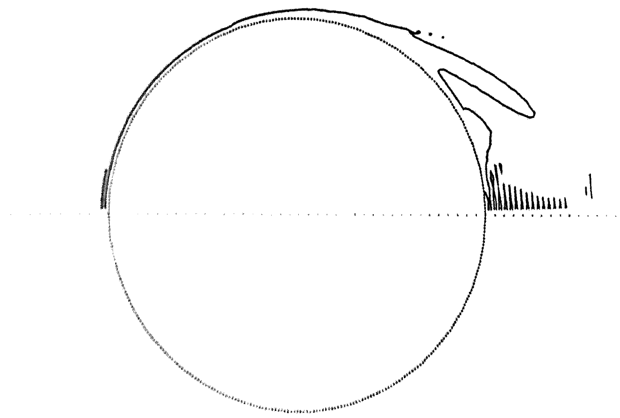

Figure 4.584

Isotherms for Re=500.0,n=0.8,and porosity 0.6 Pr=100.0(const heat flux)

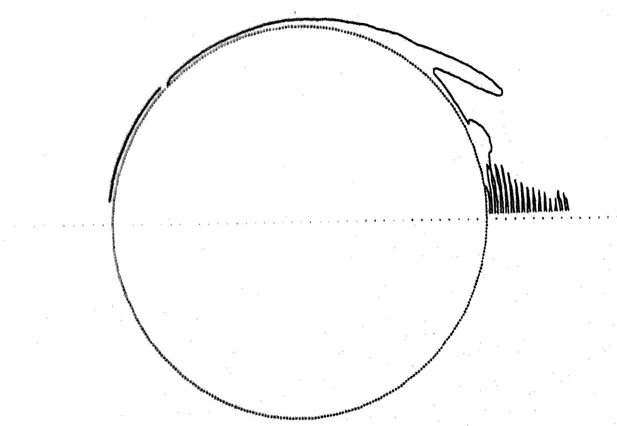

Figure 4.585

Isotherms for Re=1.0,n=0.6,and porosity 0.6 Pr=1.0(const heat flux)

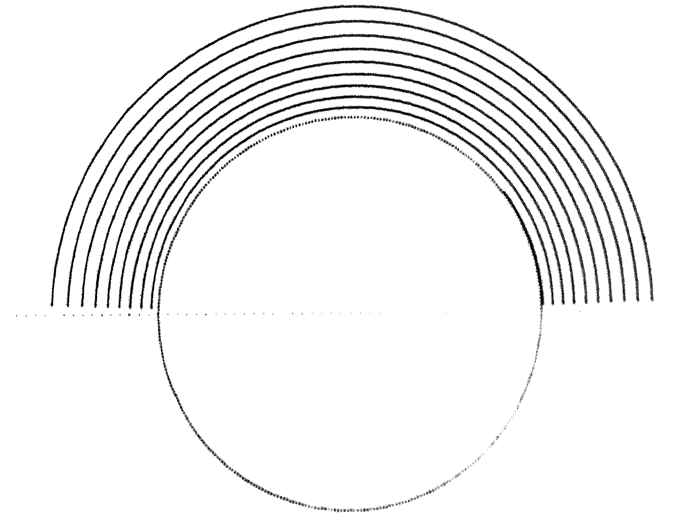

Figure 4.586

Isotherms for Re=1.0,n=0.6,and porosity 0.6 Pr=10.0(const heat flux)

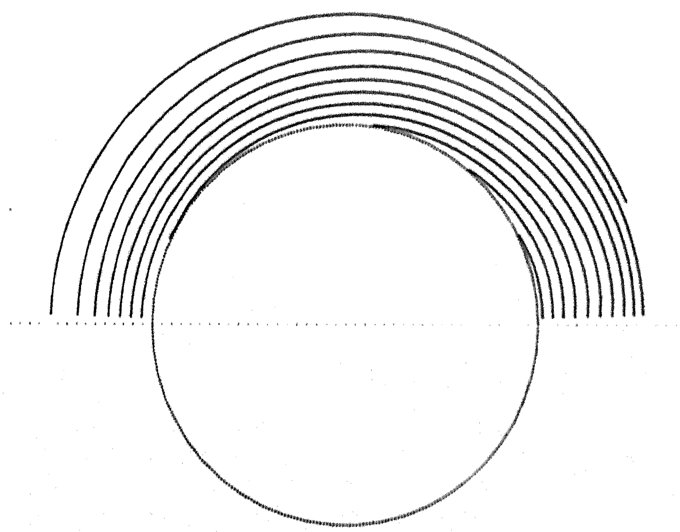

Figure 4.587

Isotherms for Re=1.0,n=0.6,and porosity 0.6 Pr=50.0(const heat flux)

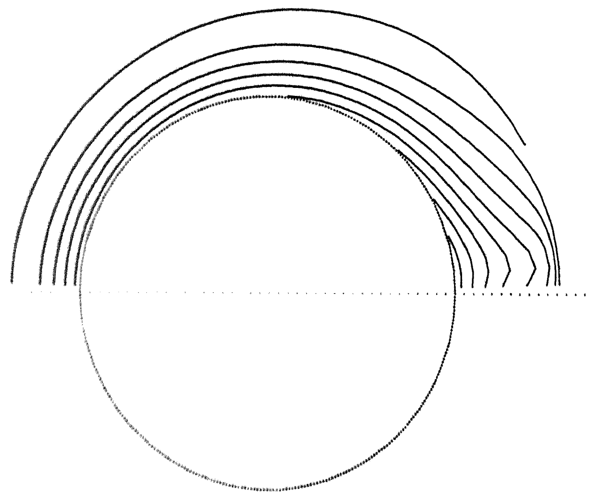

Figure 4.588

Isotherms for Re=1.0,n=0.6,and porosity 0.6 Pr=100.0(const heat flux)

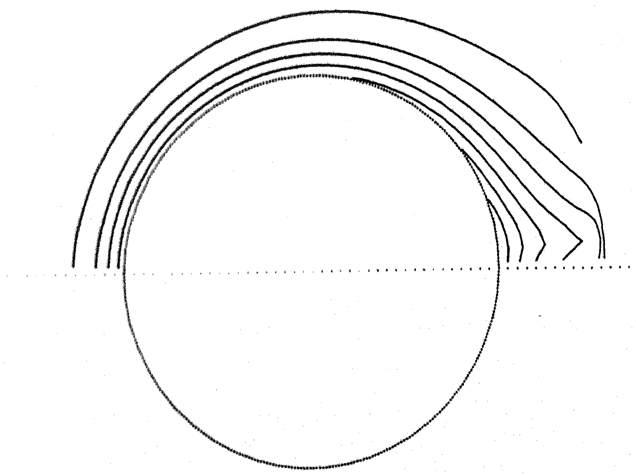

Figure 4.589

Isotherms for Re=1.0,n=0.6,and porosity 0.6 Pr=500.0(const heat flux)

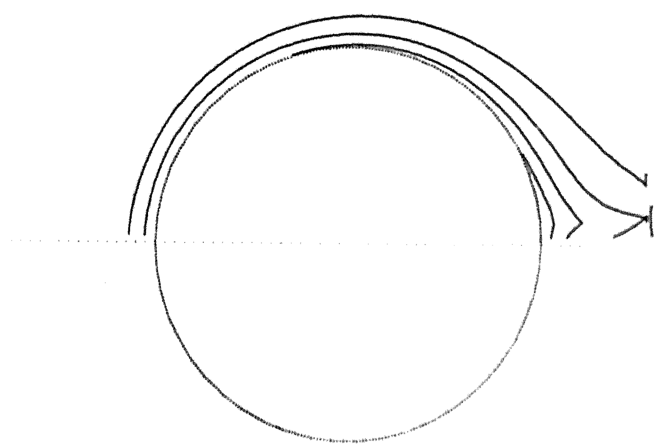

Figure 4.590

Isotherms for Re=10.0,n=0.6,and porosity 0.6 Pr=1.0(const heat flux)

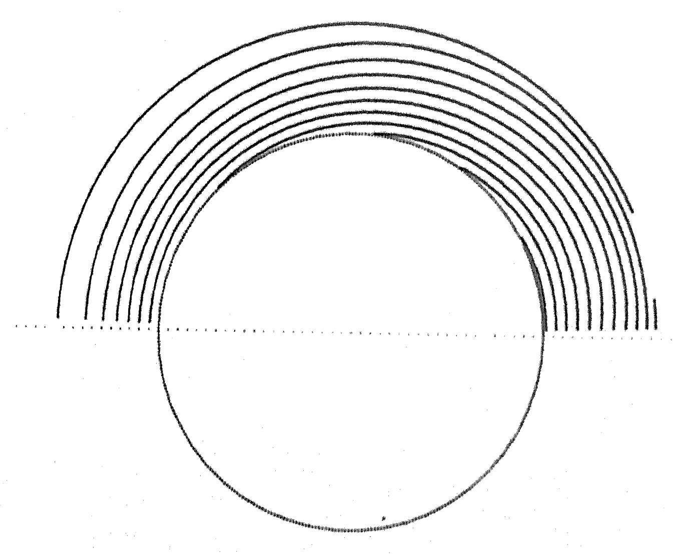

Figure 4.591

Isotherms for Re=10.0,n=0.6,and porosity 0.6 Pr=10.0(const heat flux)

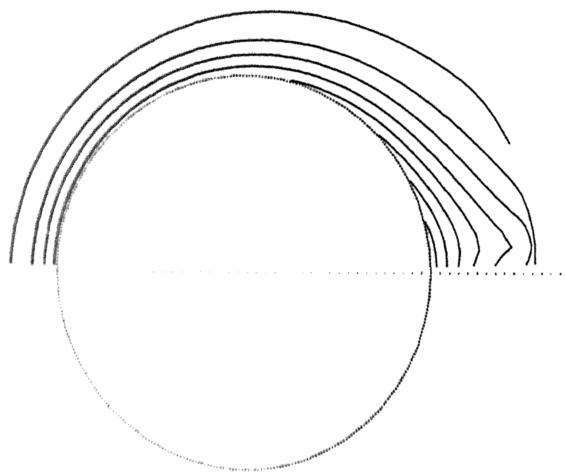

Figure 4.592

Isotherms for Re=10.0,n=0.6,and porosity 0.6 Pr=50.0(const heat flux)

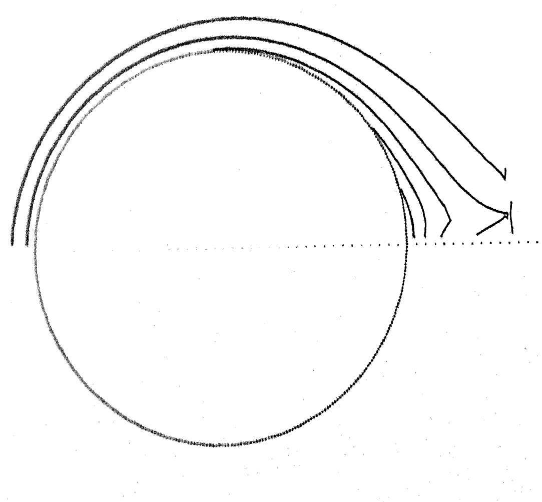

Figure 4.593

Isotherms for Re=10.0,n=0.6,and porosity 0.6 Pr=100.0(const heat flux)

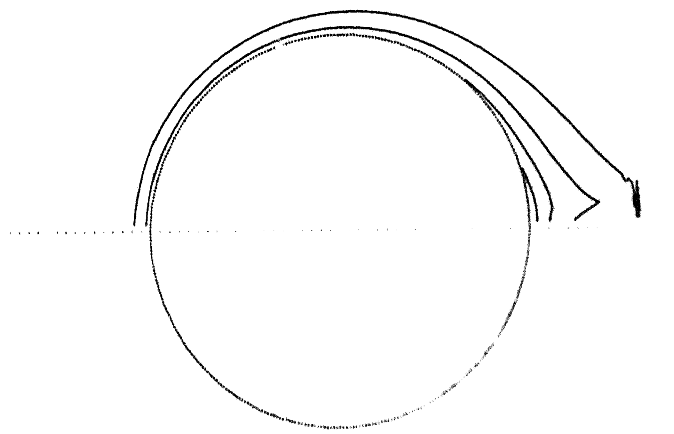

Figure 4.594

Isotherms for Re=10.0,n=0.6,and porosity 0.6 Pr=500.0(const heat flux)

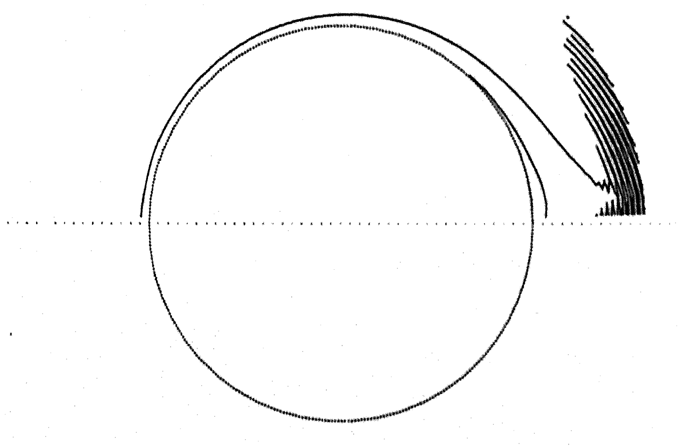

Figure 4.595

Isotherms for Re=100.0,n=0.6,and porosity 0.6 Pr=1.0(const heat flux)

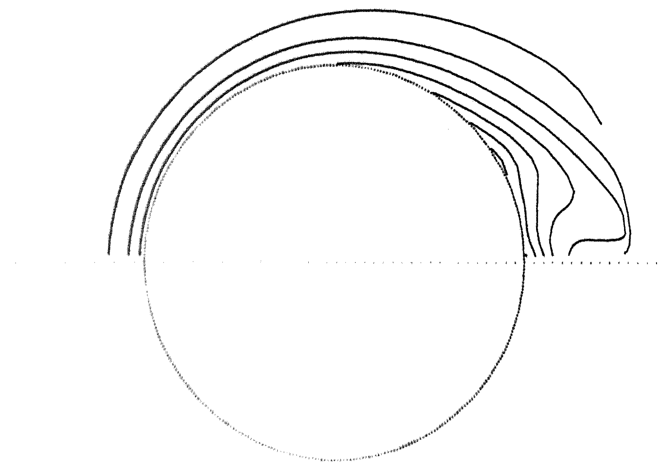

Figure 4.596

Isotherms for Re=100.0,n=0.6,and porosity 0.6 Pr=10.0(const heat flux)

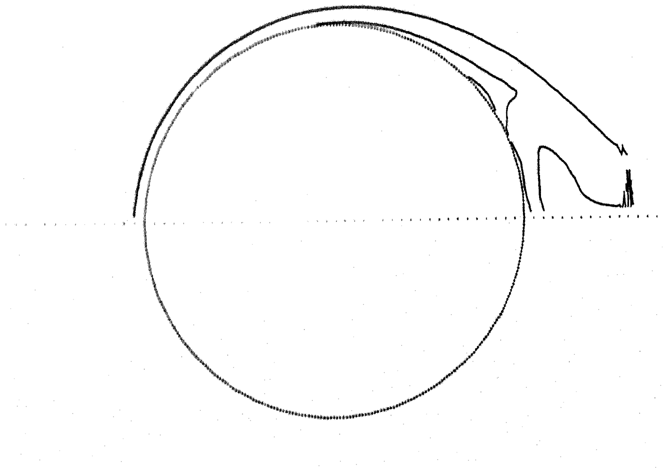

Figure 4.597

Isotherms for Re=100.0,n=0.6,and porosity 0.6 Pr=50.0(const heat flux)

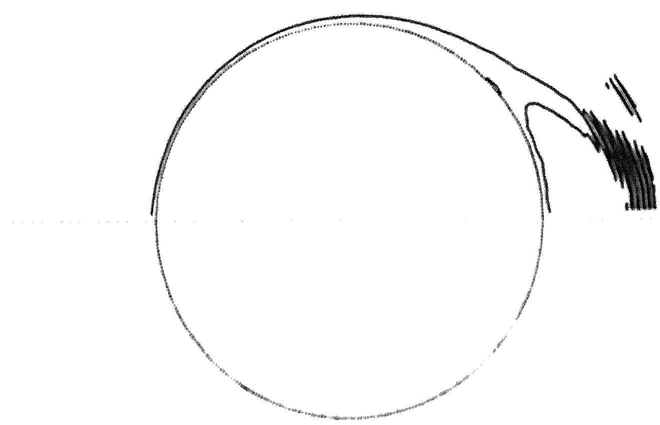

Figure 4.598

Isotherms for Re=100.0,n=0.6,and porosity 0.6 Pr=100.0(const heat flux)

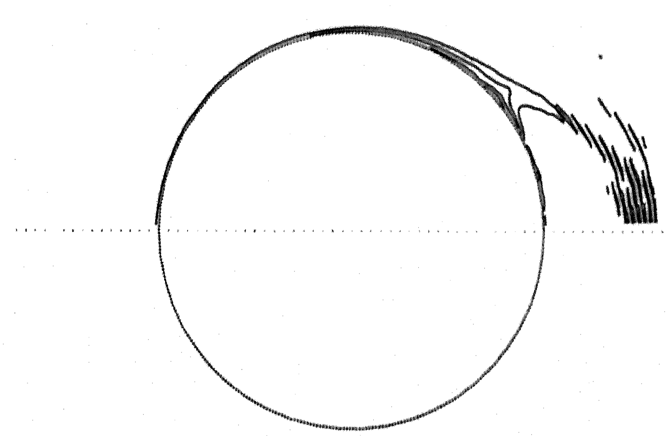

Figure 4.598

Isotherms for Re=100.0,n=0.6,and porosity 0.6 Pr=500.0(const heat flux)

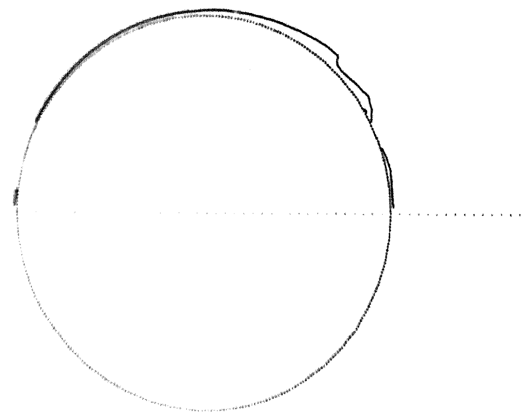

Figure 4.599

Isotherms for Re=200.0,n=0.6,and porosity 0.6 Pr=1.0(const heat flux)

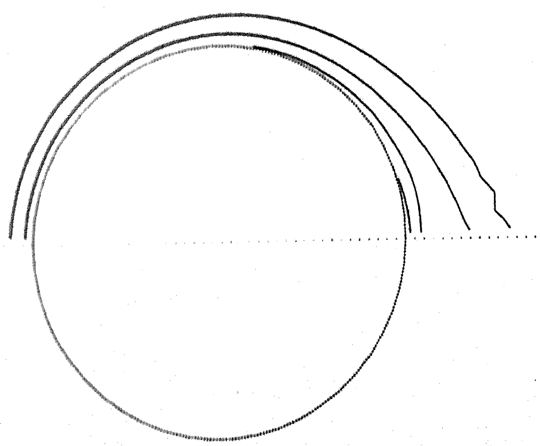

Figure 4.600

Isotherms for Re=200.0,n=0.6,and porosity 0.6 Pr=10.0(const heat flux)

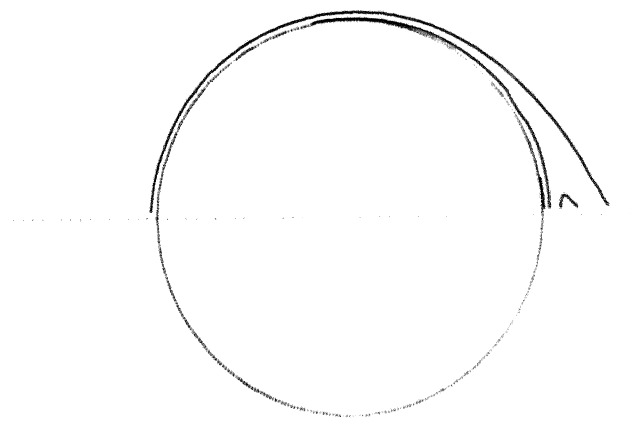

Figure 4.601

Isotherms for Re=200.0,n=0.6,and porosity 0.6 Pr=50.0(const heat flux)

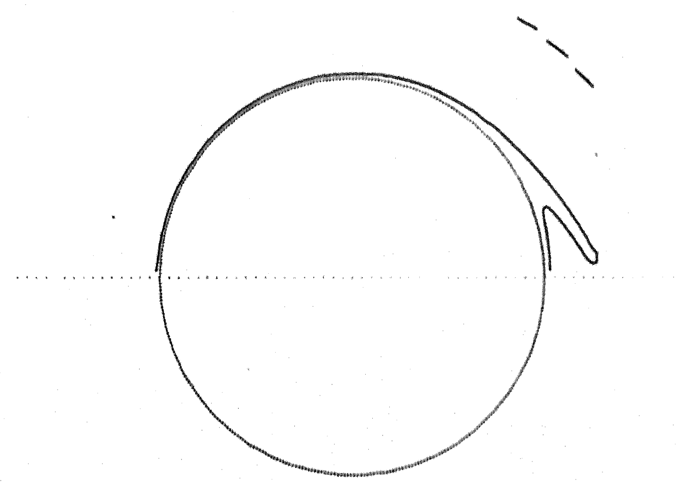

Figure 4.602

Isotherms for Re=200.0,n=0.6,and porosity 0.6 Pr=100.0(const heat flux)

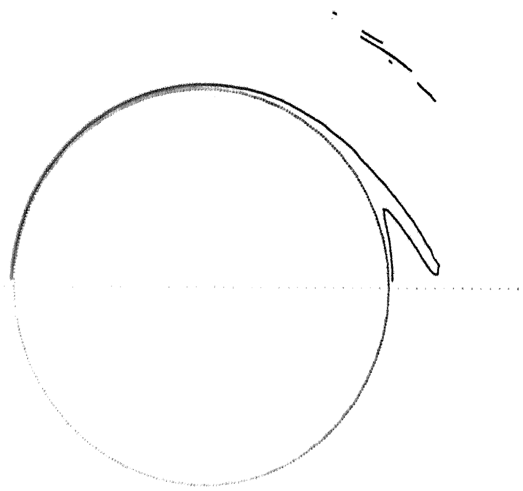

Figure 4.603

Isotherms for Re=200.0,n=0.6,and porosity 0.6 Pr=500.0(const heat flux)

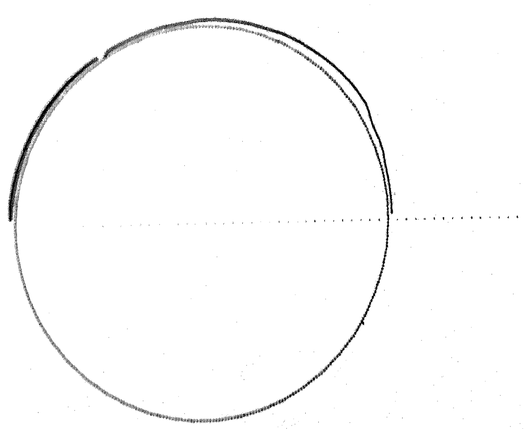

Figure 4.604

Isotherms for Re=500.0,n=0.6,and porosity 0.6 Pr=1.0(const heat flux)

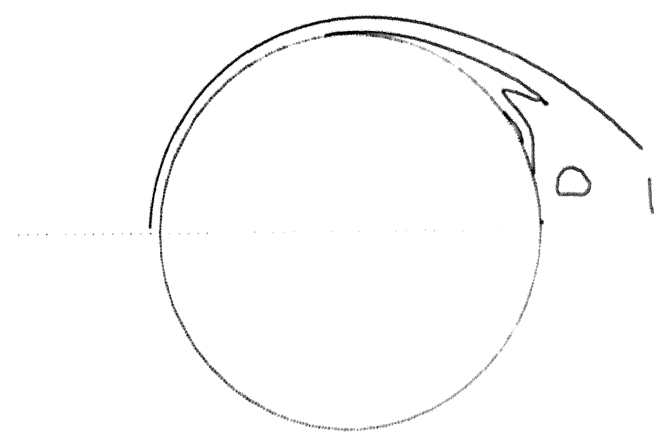

Figure 4.605

Isotherms for Re=500.0,n=0.6,and porosity 0.6 Pr=10.0(const heat flux)

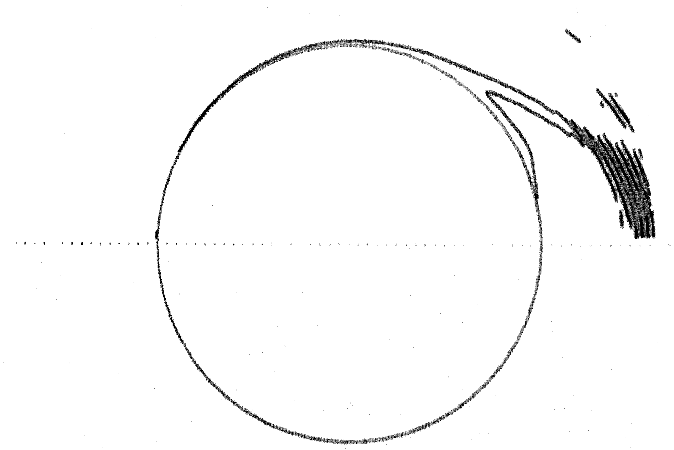

Figure 4.606

Isotherms for Re=500.0,n=0.6,and porosity 0.6 Pr=50.0(const heat flux)

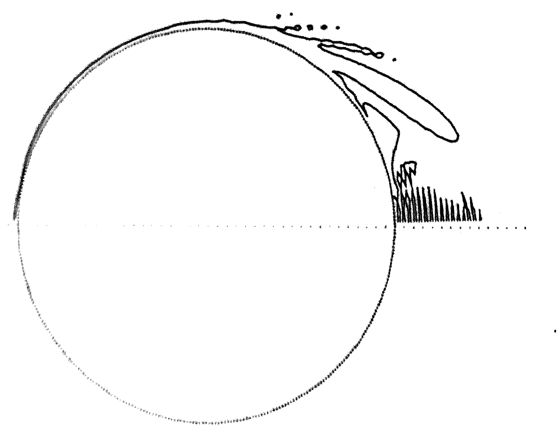

Figure 4.607

Isotherms for Re=500.0,n=0.6,and porosity 0.6 Pr=100.0(const heat flux)

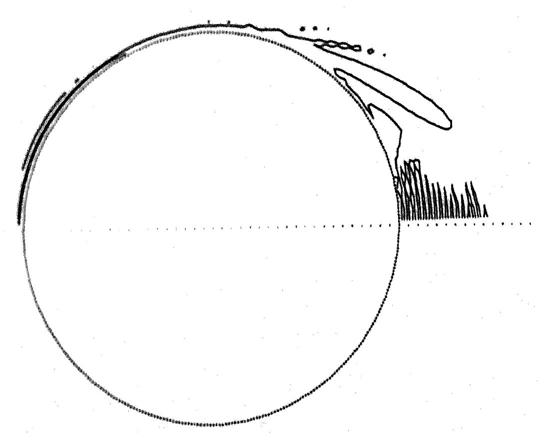

Figure 4.608

Isotherms for Re=1.0,n=0.5,and porosity 0.6 Pr=1.0(const heat flux)

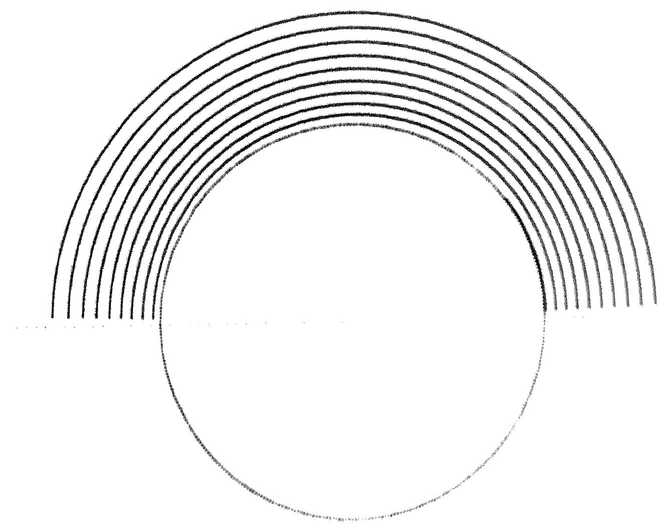

Figure 4.609

Isotherms for Re=1.0,n=0.5,and porosity 0.6 Pr=10.0(const heat flux)

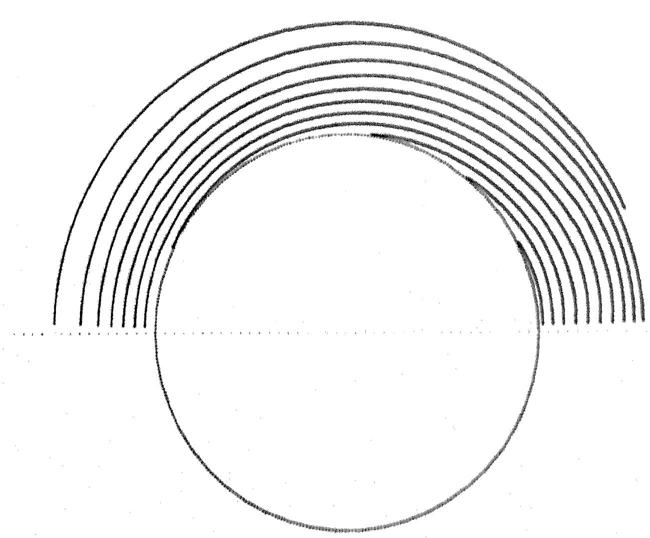

Figure 4.610

Isotherms for Re=1.0,n=0.5,and porosity 0.6 Pr=50.0(const heat flux)

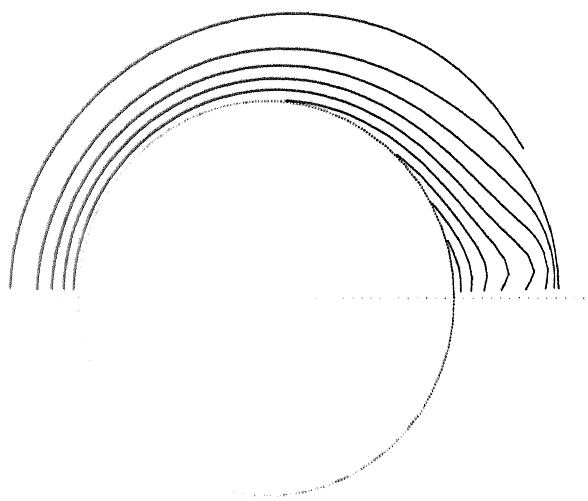

Figure 4.611

Isotherms for Re=1.0,n=0.5,and porosity 0.6 Pr=100.0(const heat flux)

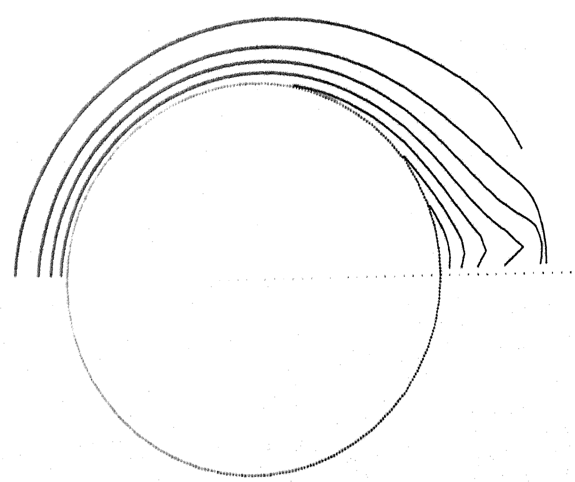

Figure 4.612

Isotherms for Re=1.0,n=0.5,and porosity 0.6 Pr=500.0(const heat flux)

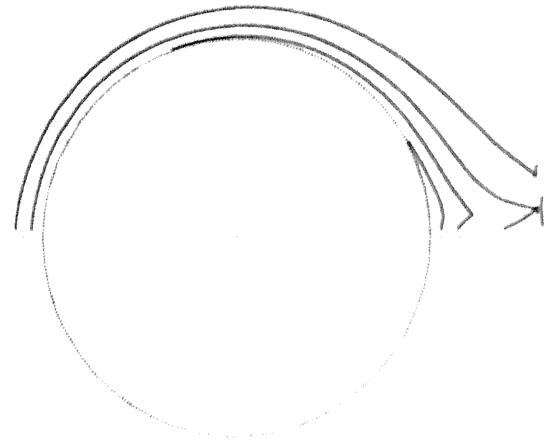

Figure 4.613

Isotherms for Re=10.0,n=0.5,and porosity 0.6 Pr=1.0(const heat flux)

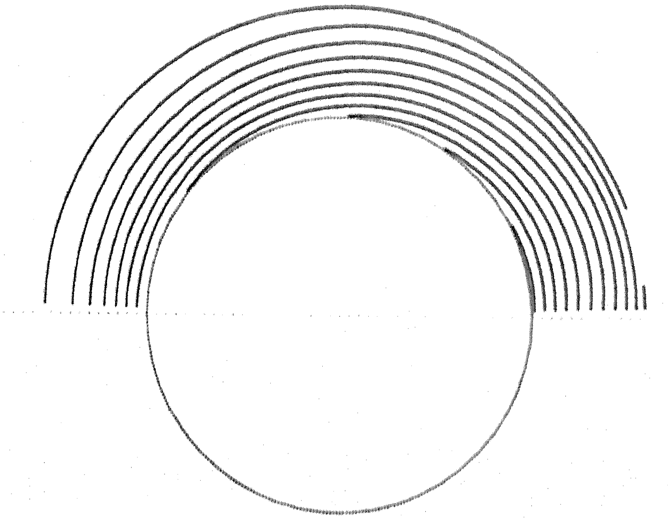

Figure 4.614

Isotherms for Re=10.0,n=0.5,and porosity 0.6 Pr=10.0(const heat flux)

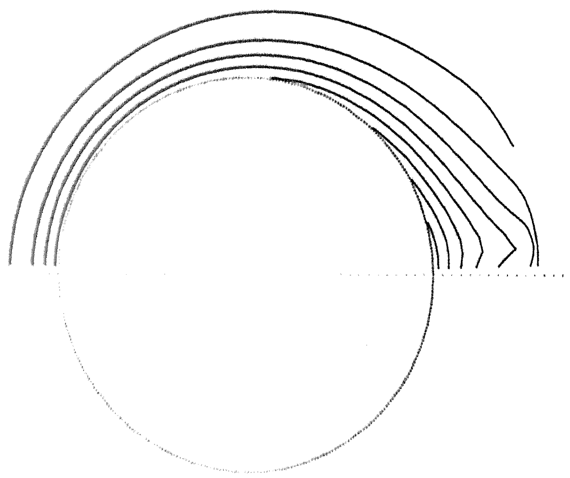

Figure 4.615

Isotherms for Re=10.0,n=0.5,and porosity 0.6 Pr=50.0(const heat flux)

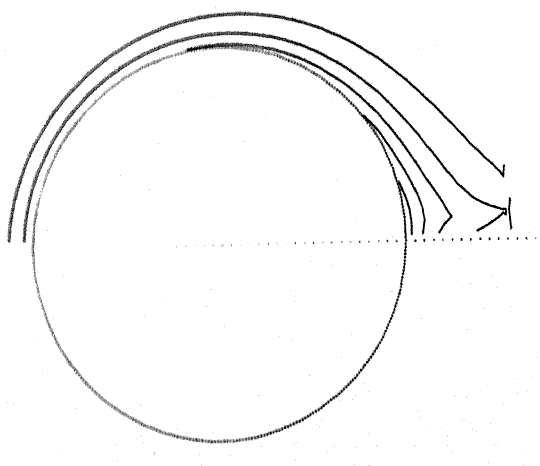

Figure 4.616

Isotherms for Re=10.0,n=0.5,and porosity 0.6 Pr=100.0(const heat flux)

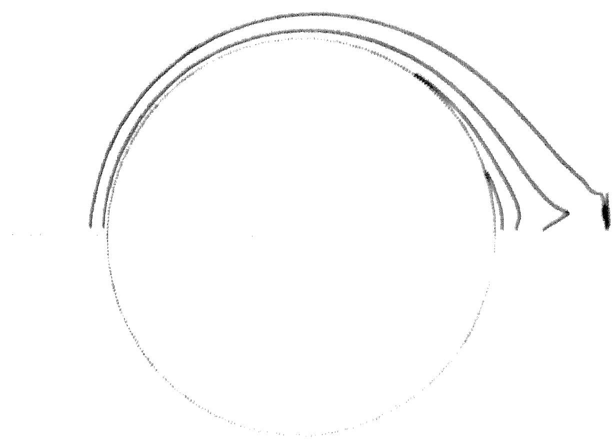

Figure 4.617

Isotherms for Re=10.0,n=0.5,and porosity 0.6 Pr=500.0(const heat flux)

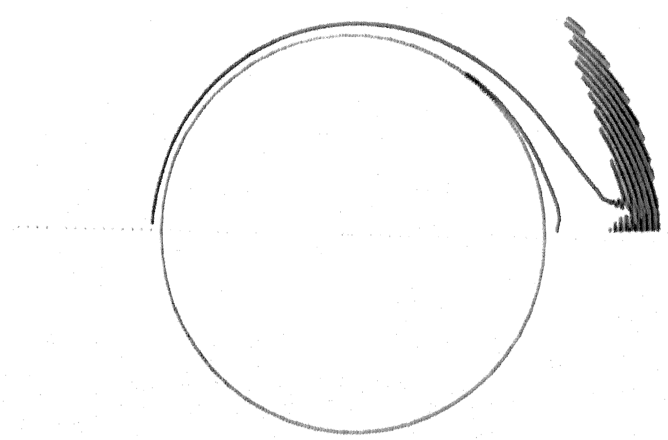

Figure 4.618

Isotherms for Re=100.0,n=0.5,and porosity 0.6 Pr=1.0(const heat flux)

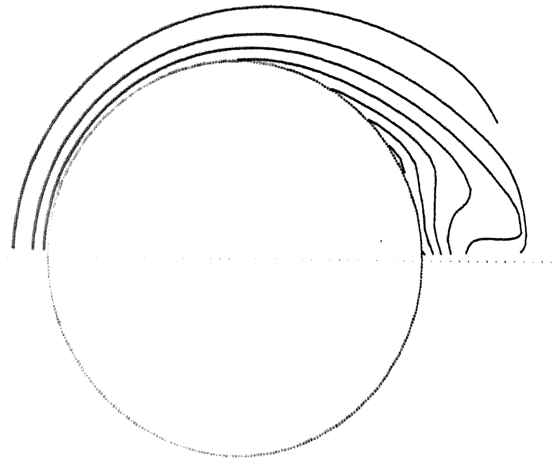

Figure 4.619

Isotherms for Re=100.0,n=0.5,and porosity 0.6 Pr=10.0(const heat flux)

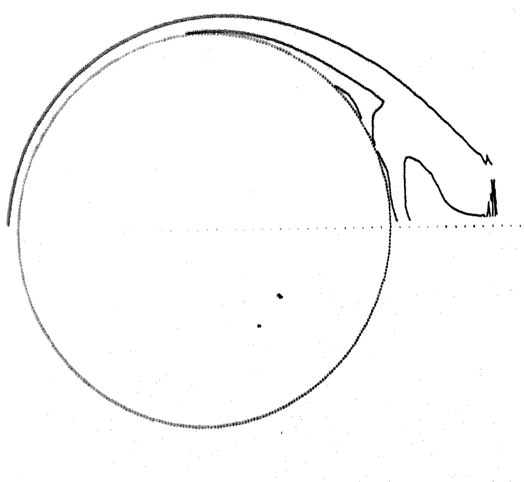

Figure 4.620

Isotherms for Re=100.0,n=0.5,and porosity 0.6 Pr=50.0(const heat flux)

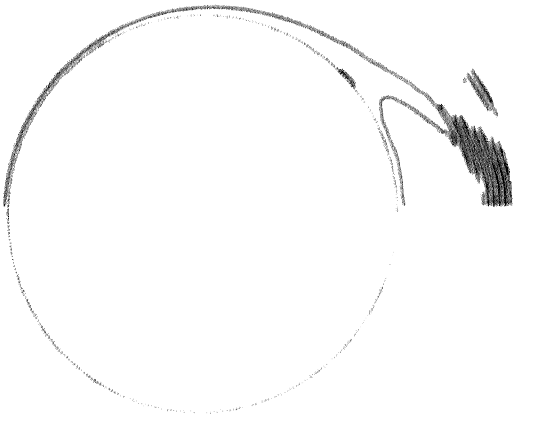

Figure 4.621

Isotherms for Re=100.0,n=0.5,and porosity 0.6 Pr=100.0(const heat flux)

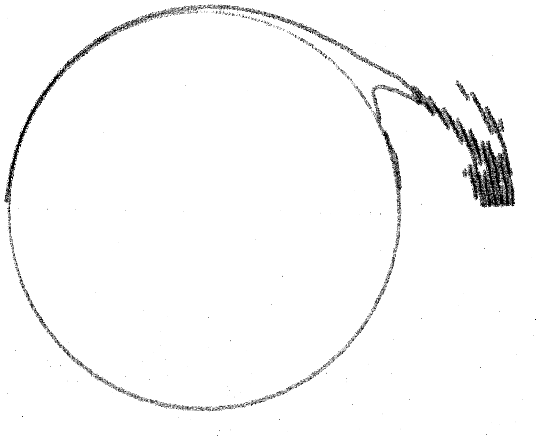

Figure 4.622

Isotherms for Re=100.0,n=0.5,and porosity 0.6 Pr=500.0(const heat flux)

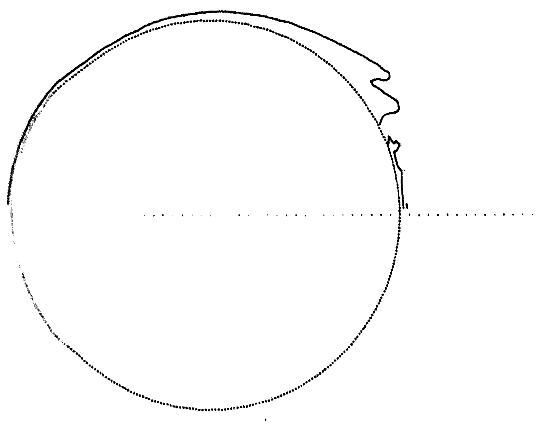

Figure 4.623

Isotherms for Re=200.0,n=0.5,and porosity 0.6 Pr=1.0(const heat flux)

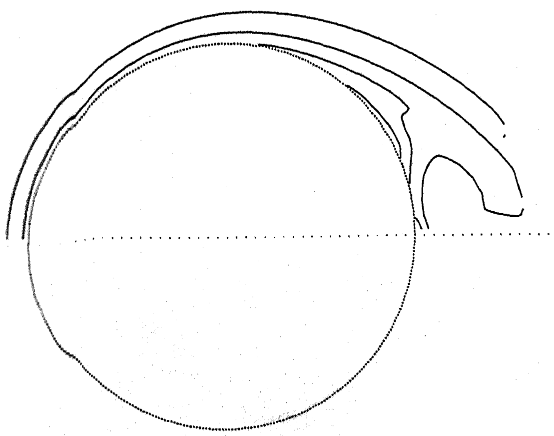

Figure 4.624

Isotherms for Re=200.0,n=0.5,and porosity 0.6 Pr=10.0(const heat flux)

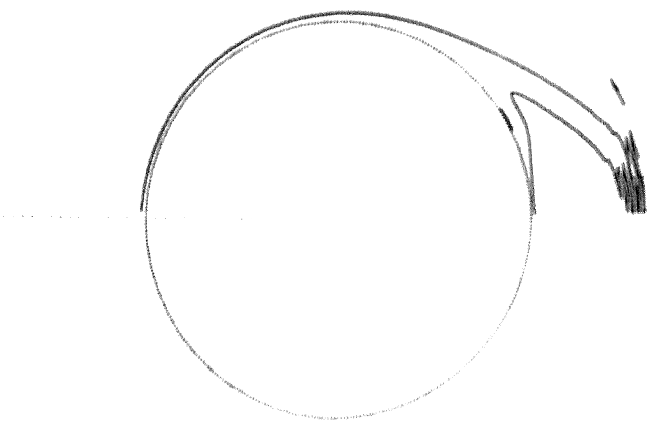

Figure 4.625

Isotherms for Re=200.0,n=0.5,and porosity 0.6 Pr=50.0(const heat flux)

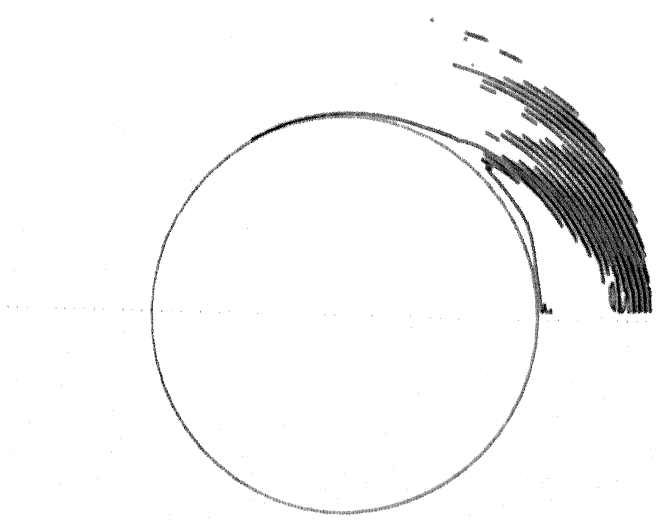

Figure 4.626

Isotherms for Re=200.0,n=0.5,and porosity 0.6 Pr=100.0(const heat flux)

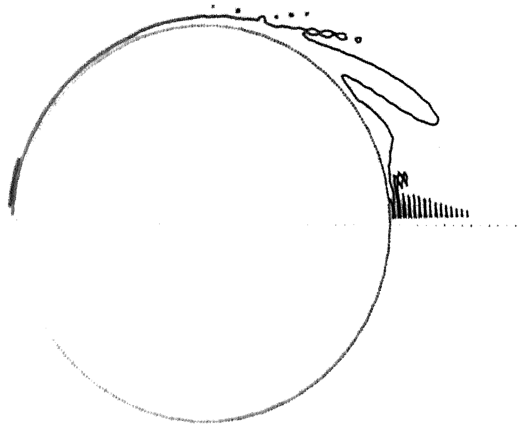

Figure 4.627

Isotherms for Re=200.0,n=0.5,and porosity 0.6 Pr=500.0(const heat flux)

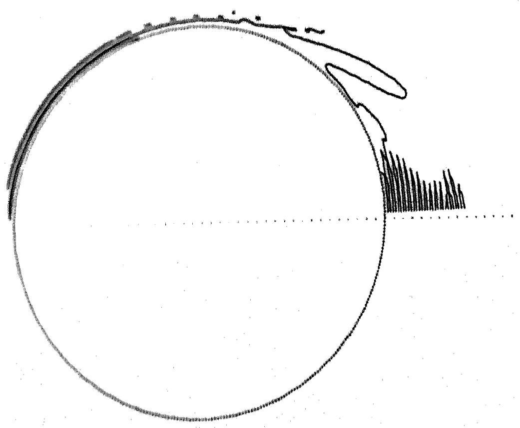

Figure 4.628

Isotherms for Re=500.0,n=0.5,and porosity 0.6 Pr=1.0(const heat flux)

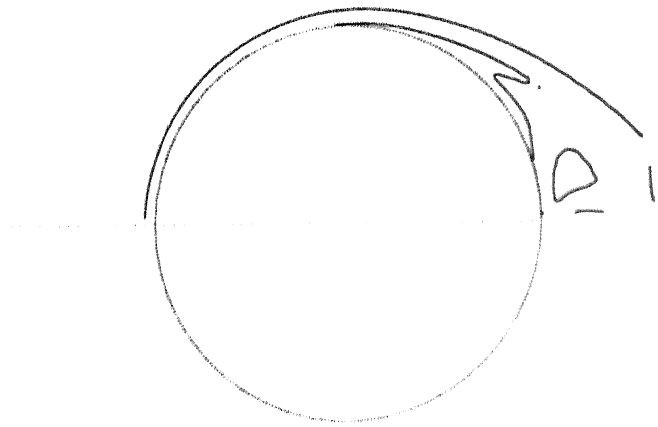

Figure 4.629

Isotherms for Re=500.0,n=0.5,and porosity 0.6 Pr=10.0(const heat flux)

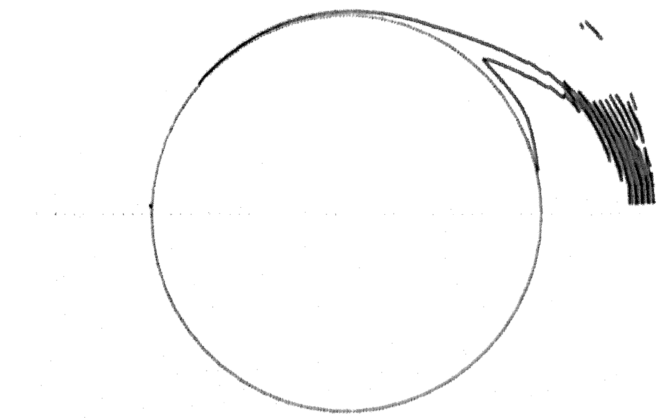

Figure 4.630

Isotherms for Re=500.0,n=0.5,and porosity 0.6 Pr=50.0(const heat flux)

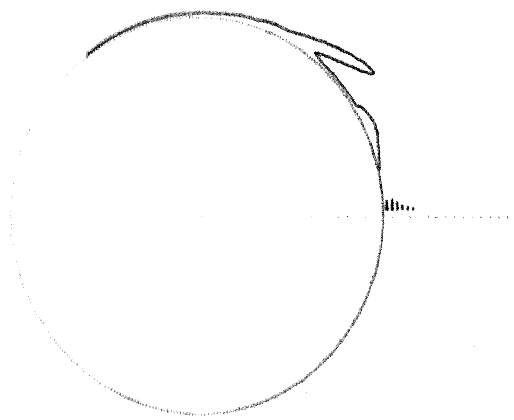

Figure 4.631

Isotherms for Re=500.0,n=0.5,and porosity 0.6 Pr=100.0(const heat flux)

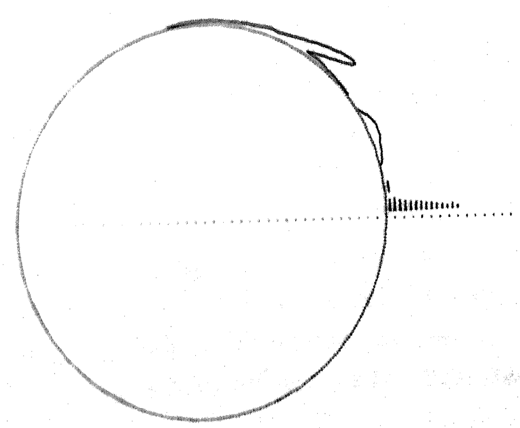

Chapter 5

CONCLUSIONS AND SUGGESTIONS FOR FUTURE WORK

5.1 Conclusions

In this work, the incompressible steady flow and heat transfer of power law fluid across a bank of circular cylinders has been studied numerically. The inter-cylinder interactions have been simulated using a simple cell model which does not exchange mass or energy with the neighboring cells. The resulting equations of continuity, momentum and energy have been solved using the finite difference method to obtain the velocity and temperature fields. These in turn have been further processed numerically to obtain the values of the local and average Nusselt number over a wide range of physical and kinematic parameters as : $0.5 \le n \le 1.0, 0.40 \le \varepsilon \le 0.60, 1 \le \mathrm{Re} \le 500$ and $1 \le \mathrm{Pr} \le 500$ for both boundary conditions, i.e., the constant wall temperature and constant heat flux at the surface of the cylinder. The solution procedure and computer code have been validated using the results for limiting conditions available in literature for both Newtonian and non-Newtonian fluids.

The observed dependencies of the Nusselt number on porosity, Reynolds number, Prandtl number , power law index and boundary conditions have been explained physically. As expected, the value of the Nusselt number is always higher in the case of constant heat flux condition than that for the isothermal case, though the extent of this enhancement is strongly dependent on the value of the porosity, Reynolds number , power law index and Prandtl number. At low Peclet numbers, the temperature field shows complete fore and aft symmetry which is progressively lost with the rising value of the Reynolds number and / or Prandtl number which indicates the increasing role of convective contribution to heat transfer.

The Nusselt number is influenced by the power law index, i.e. shearing action of fluid. As the value of the power law index decreases, the rate of heat transfer increases, because shear thinning lowers the resistance to heat flow and this facilitates heat transfer. Also the results, at low values of Reynolds number, are not much influenced by power law index. However, as the value of the Reynolds number progressively rises, shearing action influences the heat transfer rate.

The value of the Nusselt number is also strongly influenced by the value of porosity. The dependence is consistent with the intuitive feeling that owing to steeper velocity and temperature gradients in concentrated (low porosity) systems, the value of the Nusselt number shows an inverse dependence on the porosity. The present theoretical results have been validated using the scant experimental data available in the literature.

5.2 Suggestions for future work

Considerable scope exists to extend this work. Some of the possibilities are mentioned here.

1. Although the power law fluid model gives the simplest representation of shear-thinning non-Newtonian behavior, its inability to predict a constant value of viscosity at the outer surface, cast doubt about its appropriateness to describe flows with stagnation points. Thus one must use a more realistic model such as the Ellis or the Carreau equation.

2. Similar computations can be performed for more realistic non-isothermal processes of non-Newtonian fluids heat transfer from the cylinders.

BIBLIOGRAPHY

Adams, Don., and Bell, K.J., Fluid Friction and Heat Transfer For Flow of Sodium Carboxymethylcellulose Solutions Across Banks of Tubes, *Chem. Eng. Prog. Sym. Ser.* ,No. 82, Vol 64, 1968, pp.133-145

Ahmad, R.A., *Heat Transfer Engineering*, Vol 17, 1996, pp.31-81

Bailer, F., Tochon, P., Grilliot, J.M. and Mercier, P., *Rev. Gen. Therm.*, Vol 36, 1997, pp-744-754

Drummmond, J. E., and Tahir,M.I., *Int. Jl. Multiphase Flow*, 10,515, (1984)

Happel J., *Viscous flow relative to array of cylinders*. AIChE J. 5,p. 174, (1959).

Hsu, C.- J., *International jounal of Heat and Mass Transfer,* Vol 7, 1964, pp. 431-446

Kreith, F. (ed), The CRC Handbook of Thermal Engineering, CRC Press, Boca Raton, FL(U.S.A.) pp.3.26-3.46

Lange, C.F., Durst, F. and Breuer, M., *International Journal of Heat and Mass Transfer,* Vol 41, 1998, pp.3409-3430

Mandhani, V.K.,Chabbra, R.P and Eswaran, V., Forced Convection Heat Transfer in Tube Banks in Cross-Flow, *Chem. Engng. Sci.,* in press (2002).

Martin, A.R., saltiel, C. and Shyy, W., *International Journal of Heat and Mass Transfer*, Vol 41, 1998, pp.2383-2397

Metzner, A. B., and J.C. Reed, *AIChE J.*, Vol 1, 1955, pp.434-440

Metzner, A. B.,R. D. Vaughn, and G. L. Houghton., *AIChE J.*, Vol 3, 1957, pp.92-100

Nishimura, T., Itoh, H. and Miyashita, H., *International Journal of Heat and Mass Transfer*, Vol 36, 1993, pp.553-563

Sangani, A. and Acrivos, A., Saltiel, C. and Shyy, W. , *International Journal of Heat and Mass Transfer,* Vol 41, 1998, pp.3409-3430.

Shah, M. N., E. E. Petersen, and Andreas Acrivos., AIChE J., Vol 8, 1962, pp.542-549

Skartsis, L., Khomammi, B., and Kardos, J.L.,*Jl. Polymer. Eng. Sci.,* 23, 32, (1992)

Tripathi, A., and Chhabra, R.P., *Transverse laminar flow of non-Newtonian fluids over a bank of long cylinders*, Chem. Engg. Commm. Vol. 147, pp 197-212, (1996)

Tripathi, A., and Chhabra, R.P., Slow power law fluid flow relative to an array of infinite cylinders, Ind. Eng. Chem. Res. Vol 31, pp 2754-2759, (1992)

Zukaukas, A., Convective Heat Transfer in Cross-Flow in Handbook of Single-Phase Convective Heat Transfer (edited by S.Kakac.R.K.Shah, W.Aung) Wiley-Interscience , NewYork(1987).

APPENDIX – A

Adams and Bell(1968) work-relating the j_H factor with present parameters for a special cases of porosity 0.714,n=0.83 and Pr=740.56 (0.5% CMC solution) and porosity 0.75, n=0.748 and Pr=9921.36(1%CMC solution).

Fluid friction and heat transfer data are presented for flow of dilute sodium carboxymethylcellulose (CMC) solutions in water across the ideal tube banks containing an equilateral triangular tube layout and in-line square arrangement. The tube banks contained 0.375in. O.D. tubes in a 1.25 pitch ratio.

The Reynolds number used, for the calculation part, is

$$\mathrm{Re}_{A-B} = \frac{D^n V^{2-n} \rho}{\gamma} \quad \text{(A.1)}$$

where $$V = \frac{U}{(1-\sqrt{1-\varepsilon})} \quad \text{(A.2)}$$

$$\gamma = g_c 8^{n-1} m \left(\frac{3n+1}{4n} \right)^n \quad \text{(A.3)}$$

relating with the present Reynolds number, $\mathrm{Re} = \dfrac{D^n U^{2-n} \rho}{m}$

$$\mathrm{Re}_{A-B} = \mathrm{Re}\, F(n,\varepsilon) \quad \text{(A.4)}$$

where, $$F(n,\varepsilon) = \frac{1}{8^{n-1} \left(\frac{3n+1}{4n} \right)^n (1-\sqrt{1-\varepsilon})^{2-n}} \quad \text{(A.5)}$$

The Prandtl number used by Adams and Bell is

$$\mathrm{Pr}_{A-B} = \frac{C_p \gamma}{\kappa} \left(\frac{V}{D} \right)^{n-1} \quad \text{(A.6)}$$

relating with the present Prandtl number, $\mathrm{Pr} = \dfrac{C_p m}{\kappa} \left(\dfrac{U}{D} \right)^{n-1}$

$$\mathrm{Pr}_{A-B} = \mathrm{Pr}\ \mathrm{F}_1(n,\varepsilon) \quad \text{(A.7)}$$

Where, $$F_1(n,\varepsilon) = 8^{n-1} \left(\frac{3n+1}{4n} \right)^n \left\{ \frac{1}{1-\sqrt{1-\varepsilon}} \right\}^{n-1} \quad \text{(A.8)}$$

The heat transfer results are presented in plots of j_H factor vs. Reed-Metzner Reynolds number as,

$$j_H = \frac{h}{C_p G \Delta^{\frac{1}{3}}}\left[\frac{C_p \gamma}{\kappa}\left(\frac{V}{D}\right)^{n-1}\right]^{2/3} \qquad \text{(A.9)}$$

where $$\Delta^{1/3} = \left(\frac{3n+1}{4n}\right)^{1/3} = \frac{non-NewtonianfluidNusseltnumber}{NewtonianfluidNusseltnumber} \qquad \text{(A.10)}$$

Relating the j_H factor factor with Re ,Nu and Pr:

Using the difination of Nusselt number, $Nu = \dfrac{hD}{k}$
Re and Pr , the j_H factor can be written as

$$j_H = \frac{h}{C_p \rho V\left(\frac{3n+1}{4}\right)^{1/3}}\left[\frac{C_p \gamma}{\kappa}\left(\frac{V}{D}\right)^{n-1}\right]^{2/3} \qquad \text{(A.11)}$$

$$j_H = \frac{hD}{\kappa}\left(\frac{\kappa}{DC_p \rho V\left(\frac{3n+1}{4n}\right)^{1/3}}\right)\left[\Pr_{A-B}\right]^{2/3} \qquad \text{(A.12)}$$

$$j_H = Nu.\frac{\kappa}{C_p m\left(\frac{U}{D}\right)^{n-1}}.\frac{m\left(\frac{U}{D}\right)^{n-1}}{\rho VD\left(\frac{3n+1}{4n}\right)^{1/3}}\left[\Pr_{A-B}\right]^{2/3} \qquad \text{(A.13)}$$

$$j_H = \frac{Nu}{\Pr}.\frac{m}{\rho U^{2-n} D^n}\frac{(1-\sqrt{1-\varepsilon})}{\left(\frac{3n+1}{4n}\right)^{1/3}}\left[\Pr F_1(n,\varepsilon)\right]^{2/3} \qquad \text{(A.14)}$$

$$j_H = \left[\frac{Nu}{\operatorname{Re}\Pr^{1/3}}\right]F_2(n,\varepsilon) \qquad \text{(A.15)}$$

where, $$F_2(n,\varepsilon) = 8^{\frac{2(n-1)}{3}}\left(\frac{3n+1}{4n}\right)^{\frac{2n-1}{3}}\left(1-\sqrt{1-\varepsilon}\right)^{\frac{5-2n}{3}} \qquad \text{(A.16)}$$

A(a). Model 1 of the Adams and Bell (1968):

For the special case of porosity of 0.75(n=0.748) with the tube banks of an equilateral triangular arrangement and for 1% CMC solution(Pr=921.36), the above relations becomes

$$\mathrm{Re}_{A-B} = 3.78616\ \mathrm{Re} \qquad (A.17)$$

$$\mathrm{Pr}_{A-B} = 0.5282396\mathrm{Pr} \qquad (A.18)$$

$$j_H = 0.31804182 \frac{Nu}{\mathrm{Re}\,\mathrm{Pr}^{1/3}} \qquad (A.19)$$

The experimental j_H factor can be related by

$$j_H = 0.765\,\mathrm{Re}^{-0.667} - 0.0086 \qquad (A.20)$$

A(b). Model 2 of the Adams and Bell (1968):

For the special case of porosity of 0.712(n=0.83) with the tube banks of in-line square arrangement and for 0.5% CMC solution(Pr=740.56), the above relations becomes
the relations becomes

$$\mathrm{Re}_{A-B} = 3.3448\ \mathrm{Re} \qquad (A.21)$$

$$\mathrm{Pr}_{A-B} = 0.64265\ \mathrm{Pr} \qquad (A.22)$$

$$j_H = 0.22253 \frac{Nu}{\mathrm{Re}\,\mathrm{Pr}^{1/3}} \qquad (A.23)$$

The experimental j_H factor can be related by

$$j_H = 0.599\,\mathrm{Re}^{-0.667} + 0.003 \qquad (A.24)$$